

# **WIND POWER RESOURCE ASSESSMENT, DESIGN OF GRID- CONNECTED WIND FARM AND HYBRID POWER SYSTEM**

by

*Shafiqur Rehman*

**Submitted in partial fulfilment of the requirements for the degree Philosophiae Doctor  
in the Faculty of Engineering, Mechanical and Aerospace Engineering**



Supervisor: Dr. Md. Mahbub Alam

Co-supervisors: Prof. J. P. Meyer and Dr. Luai M. Al-Hadhrani

February 2012

# **WIND POWER RESOURCE ASSESSMENT, DESIGN OF GRID-CONNECTED WIND FARM AND HYBRID POWER SYSTEM**

by

**Shafiqur Rehman**

## **ABSTRACT**

An exponentially growing global population, power demands, pollution levels and, on the other hand, rapid advances in means of communication have made the public aware of the complex energy situation. The Kingdom of Saudi Arabia has vast open land, an abundance of fossil fuel, a small population but has always been among the front-runners where the development and utilisation of clean sources of energy are concerned. Several studies on wind, solar and geothermal sources of energy have been conducted in Saudi Arabia. Solar photovoltaic (pv) has been used for a long time in many applications such as cathodic protection, communication towers and remotely located oil field installations. Recently, a 2MW grid-connected pv power plant has been put online and much larger solar desalination plants are in planning stage.

Wind resource assessment, hub height optimisation, grid-connected wind farm and hybrid power system design were conducted in this study using existing methods. Historical daily mean wind speed data measured at 8 to 12metres above ground level at national and international airports in the kingdom over a period of 37 years was used to obtain long-term annual and monthly mean wind speeds, annual mean wind speed trends, frequency distribution, Weibull parameters, wind speed maps, hub height optimisation and energy yield using an efficient modern wind turbine of 2.75MW rated power. A further detailed analysis (such as estimation of wind shear exponent, Weibull parameters at different heights, frequency distribution at different heights, energy yield and plant capacity factor and wind speed variation with height) was conducted using wind speed measurements made at 20, 30 and 40metres above ground level.

As a first attempt, an empirical correlation was developed for the estimation of near-optimal hub height ( $HH = 142.035 * (\alpha) + 40.33$ ) as a function of local wind shear exponent ( $\alpha$ ) with

a correlation coefficient of 97%. This correlation was developed using the energy yield from a wind turbine of 1 000kW rated power and wind speed and local exponent for seven locations in Saudi Arabia. A wind-pv-diesel hybrid power system was designed and specifications were made for a remotely located village, which is being fed 100% by diesel power generating units. The proposed system, if developed, will offset around 35% of the diesel load and therefore will result in decreased air pollution by almost the same amount.

The developed wind speed maps, the frequency distributions and estimated local wind shear exponents for seven locations and energy yield will be of great help in defining the further line of action and policy-building towards wind power development and utilisation in the kingdom. The study also recommends conducting a wind measurement campaign using tall towers with wind measurements at more than one height and estimating the local wind shear exponents and developing a wind atlas for the kingdom. The study further states that a grid-connected wind farm of moderate capacity of 40MW should be developed using turbines of varying rated powers. The wind speed data was also analysed using wavelet transform and Fast Fourier Transform (FFT) to understand the fluctuation in wind speed time series for some of the stations. It is also recommended that policy-makers should take firm decision on the development of hybrid power systems for remotely located populations which are not yet connected with the grid. There are two challenges which need research: one is the effect of dust on the moving and structural elements of the wind turbines and the second is the effect of high prevailing temperatures on the performance and efficiency of the same.

**Keywords:** Wind power, resource assessment, wind maps, clean energy, wind frequency distribution, plant capacity factor, grid-connected wind farms, hybrid power system, wind shear exponent, wind rose diagram, hub height

Thesis supervisor: Dr. Md. Mahbub Alam

Thesis co-supervisors: Prof. JP Meyer and Dr. Luai M. Al-Hadhrami

Department of Mechanical and Aerospace Engineering

Degree: Doctor of Philosophy

Dedicated to my wife and children

## ACKNOWLEDGEMENTS

All praise be to God Almighty, for his limitless bounties, mercies, blessing and guidance showering on us twenty four seven. It is only because of his will and mercy that this thesis was made possible.

I would like to express my profound gratitude and appreciation to my supervisor, Dr. Md. Mahbub Alam and co-supervisor, Prof. J.P. Meyer of the University of Pretoria for their encouragement, guidance, patience, and sincere advice throughout this research work of which this thesis is the outcome. My sincerest thanks and appreciation are due to my local co-supervisor, Dr. Luai M. Al-Hadhrami, Director Centre for Engineering Research, King Fahd University of Petroleum and Minerals, Dhahran, Saudi Arabia for his continuous technical, administrative and management support during all the stages of this work. Last but not least, each moment I spent working with my supervisor and co-supervisors during this research work was enjoyable and exciting.

All my family members, especially my wife, Nayla Yusuf, and children, Imran, Aysha and Talha, deserve my personal and sincere gratitude for their co-operation and understanding during all these years of very busy days which I stole from their time.

The following articles and conference papers were produced during the completion of this thesis:

1. Alam MM, **Rehman S**, Meyer JP, and Al-Hadhrami LM, 2011. Review of 600kw to 2500kw sized wind turbines and optimization of hub height for maximum wind energy yield realization, **Renewable and Sustainable Energy Reviews**, Vol. 15(1), pp. 3839-3849. (**Journal Impact factor: 5.367-Five year average**)
2. **Rehman S**, Alam MM, Meyer JP, and Al-Hadhrami LM, 2012. Feasibility study of a wind-pv-diesel hybrid power system for a village, **Renewable Energy**, Vol. 38(1), pp. 258 – 268. (**Journal Impact factor: 2.79 Five year average**)
3. **Rehman S**, Alam MM, Meyer JP, and Al-Hadhrami LM, 2011. Wind speed characteristics and resource assessment using Weibull parameters, **International Journal of Green Energy**. (In press, **Journal Impact factor: 0.733**)
4. Alam MM, **Rehman S**, Meyer JP, Al-Hadhrami LM and Ahmad A, 2011. Optimal hub height for maximum wind power realization, **Renewable Energy Africa Conference & Expo 2011, 27 - 29 July 2011, Johannesburg, South Africa. (Presented)**
5. **Rehman S**, Alam MM., Meyer JP, and Al-Hadhrami LM, 2011. Analysis of a multi-megawatt grid connected wind farm, **8<sup>th</sup> International Conference on Heat Transfer, Fluid Mechanics and Thermodynamics (HEFAT2011), 11 – 13 July 2011, Pointe Aux Piments, Mauritius. (Presented)**
6. Alam MM, **Rehman S**, Meyer JP, Al-Hadhrami LM and Ahmad A, 2011. Optimal Hub Height for Maximum Wind Power Realization, **ASME Turbo Expo June 6 – 10, 2011, Vancouver Convention & Exhibition Centre Vancouver, Canada. (Presented)**
7. **Rehman S**, Alam MM, Meyer JP, and Al-Hadhrami LM, 2012. Long-term wind speed trends over Saudi Arabia, **World Congress on Water, Climate and Energy, International Water Association (IWA)**, The Convention Centre, Dublin, Ireland, May 13 – 18, 2012. (Accepted for presentation)

# CONTENTS

ABSTRACT .....	ii
ACKNOWLEDGEMENTS.....	v
LIST OF TABLES.....	xi
LIST OF FIGURES .....	xvi
LIST OF APPENDICES .....	xxiv
CHAPTER 1: INTRODUCTION .....	1
1.1 BACKGROUND TO THE STUDY .....	1
1.2 OBJECTIVES OF THE STUDY .....	4
1.3 APPROACH TO THE STUDY .....	4
1.4 CONTRIBUTION OF THE PRESENT WORK.....	5
1.5 ORGANISATION OF THE THESIS .....	5
CHAPTER 2: REGIONAL, NATIONAL AND GLOBAL POPULATION AND ENERGY PATTERNS .....	7
2.1 GLOBAL POPULATION AND ENERGY DEMAND PATTERNS .....	7
2.2 MIDDLE EAST POPULATION AND ENERGY DEMAND TRENDS.....	9
2.3 SAUDI ARABIAN POPULATION AND ENERGY DEMAND TRENDS .....	11
CHAPTER 3: LITERATURE REVIEW .....	15
3.1 GLOBAL WIND POWER SCENARIO.....	15
3.2 WIND POWER RESOURCE ASSESSMENT.....	20
3.3 WIND SPEED PREDICTION.....	23
3.4 WIND SHEAR EXPONENT (WSE).....	30
3.5 WEIBULL SHAPE AND SCALE PARAMETERS.....	33
3.6 WIND POWER TECHNOLOGY.....	36
3.6.1 <i>The working of a wind turbine</i> .....	36
3.6.2 <i>Commercial development</i> .....	37

3.6.3	<i>Wind monitoring</i> .....	37
3.6.4	<i>Wind farms</i> .....	38
3.6.5	<i>Transmission and distribution</i> .....	39
3.6.6	<i>Forecasting</i> .....	40
3.6.7	<i>Interconnectors</i> .....	40
3.6.8	<i>New wind farms and conceptual wind technologies</i> .....	40
3.7	HYBRID POWER SYSTEMS .....	41
CHAPTER 4:	SITES AND DATA DESCRIPTION .....	50
CHAPTER 5:	WIND SPEED DATA ANALYSIS FOR AIRPORTS .....	58
5.1	STATION-BASED LONG-TERM WIND SPEED SUMMARIES .....	58
5.2	ANNUAL VARIATION OF WIND SPEED.....	65
5.3	SEASONAL VARIATION OF WIND SPEED.....	78
5.4	WEIBULL PARAMETERS AND WIND FREQUENCY DISTRIBUTION.....	81
CHAPTER 6:	WIND DATA ANALYSIS AT DIFFERENT HEIGHTS .....	95
6.1	SITE AND DATA DESCRIPTION.....	96
6.2	STATION-BASED SUMMARIES .....	96
6.3	WIND ROSE AND FREQUENCY DISTRIBUTION ANALYSES.....	100
6.4	ANNUAL VARIATION OF MEAN WIND SPEED AT DIFFERENT HEIGHTS .....	108
6.5	SEASONAL VARIATION OF MEAN WIND SPEED AT DIFFERENT HEIGHTS .....	113
6.6	DIURNAL VARIATION OF MEAN WIND SPEED AT DIFFERENT HEIGHTS .....	117
6.7	LOCAL WIND SHEAR EXPONENT (WSE) ESTIMATION .....	121
6.7.1	<i>Wind shear exponent for Rawdat Ben Habbas</i> .....	122
6.7.2	<i>Wind shear exponent for Juaymah</i> .....	124
6.7.3	<i>Wind shear exponent for Dhahran</i> .....	126
6.7.4	<i>Wind shear exponent for Arar</i> .....	128

6.7.5	<i>Wind shear exponent for Gassim</i> .....	130
6.7.6	<i>Wind shear exponent for Yanbo</i> .....	133
6.7.7	<i>Wind shear exponent for Dhulom</i> .....	135
6.8	ANALYSIS OF WEIBULL SHAPE AND SCALE PARAMETERS .....	138
CHAPTER 7:	WIND TURBINE SELECTION AND WIND FARM ENERGY YIELD ANALYSES .....	146
7.1	ENERGY YIELD FROM SINGLE WIND TURBINE .....	148
7.2	ENERGY YIELD COMPARISON FOR WIND ELECTRIC CONVERSION SYSTEM FROM DIFFERENT MANUFACTURERS .....	157
7.3	HUB HEIGHT OPTIMISATION .....	160
7.4	PLANT CAPACITY FACTOR ANALYSIS .....	165
7.5	EMPIRICAL CORRELATION FOR THE ESTIMATION OF NEAR- OPTIMAL HUB HEIGHT .....	173
7.6	ENERGY YIELD ESTIMATION FROM WIND FARMS AT YANBO .....	180
7.7	ENERGY YIELD FROM VESTAS VT100 2.75MW WIND TURBINE AT ALL THE LOCATIONS .....	182
7.8	SUMMARY .....	186
CHAPTER 8:	WIND-PV-DIESEL HYBRID POWER SYSTEM .....	187
8.1	HYBRID POWER SYSTEM DESIGN TOOL .....	188
8.2	METEOROLOGICAL DATA USED AS INPUT TO HOMER MODEL .....	190
8.3	VILLAGE LOAD DATA USED AS INPUT TO HOMER MODEL .....	192
8.4	HYBRID SYSTEM INPUT PARAMETERS .....	194
8.5	DISCUSSION AND SPECIFICATIONS .....	196
8.5.1	<i>Energy yield analysis</i> .....	197
8.5.2	<i>Greenhouse gas (GHG) emissions</i> .....	199
8.5.3	<i>Economic analysis</i> .....	199
8.5.4	<i>Sensitivity analysis</i> .....	201
8.6	SUMMARY .....	203

CHAPTER 9:	WIND SPEED DATA ANALYSIS THROUGH WAVELETS AND FAST FOURIER TRANSFORM (FFT) .....	205
9.1	MATHEMATICAL DESCRIPTION OF WAVELET METHODOLOGY.....	206
9.2	WAVELET-BASED DECOMPOSITION OF WIND SPEED DATA.....	207
9.3	FAST FOURIER TRANSFORM POWER SPECTRUM OF WIND DATA .....	213
CHAPTER 10:	CONCLUSIONS AND RECOMMENDATIONS.....	220
10.1	SUMMARY OF FINDINGS .....	220
10.2	FUTURE WORK.....	224
	REFERENCES .....	226
APPENDICES	.....	FOLLOWING PAGE 242

## LIST OF TABLES

Table 4.1	Site-specific information on meteorological stations considered in this study. ....	52
Table 4.2	Site-specific information on 40-metre towers. ....	52
Table 4.3	Operating ranges and accuracies of various sensors used for data collection. ....	53
Table 5.1	Long-term statistics for daily mean wind speed. ....	59
Table 5.2	Long-term statistics for meteorological parameters. ....	63
Table 5.3	Best-fit regression lines for annual mean wind speed trend analysis. ....	69
Table 5.4	Long-term mean values of Weibull parameters over Saudi Arabia. ....	82
Table 5.5	Best-fit regression lines for annual shape parameter ( $k$ ). ....	90
Table 5.6	Best-fit regression lines for annual scale parameter ( $c$ ). ....	93
Table 6.1	Site-specific information. ....	95
Table 6.2	Annual mean values of meteorological parameters. ....	97
Table 6.3	Site-specific summary of wind shear exponent and related parameters. ....	122
Table 6.4	Seasonal values of Weibull shape parameter ( $k$ ) at 20metres AGL at seven locations. ....	141
Table 6.5	Seasonal values of Weibull shape parameter ( $k$ ) at 30metres AGL at all locations. ....	142
Table 6.6	Seasonal values of Weibull shape parameter ( $k$ ) at 40metres AGL at all locations. ....	142
Table 6.7	Seasonal values of Weibull scale parameter ( $c$ ) at 20metres AGL at all locations. ....	143
Table 6.8	Seasonal values of Weibull scale parameter ( $c$ ) at 30metres AGL at all locations. ....	144
Table 6.9	Seasonal values of Weibull scale parameter ( $c$ ) at 40metres AGL at all locations. ....	144
Table 7.1	Technical data of Nordex wind machines used in the analysis. ....	150
Table 7.2	Technical data of Vestas wind machines used in the analysis. ....	154
Table 7.3	Technical data of Ge wind machines used in the analysis. ....	154

Table 7.4	Technical data of DeWind wind machines used in the analysis.....	154
Table 7.5	Technical data of Bonus wind machines used in the analysis.....	154
Table 7.6	Technical data of Enercon wind machines used in the analysis.....	154
Table 7.7	Summary of wind energy yield (MWh/year) from single WECS at Yanbo.....	159
Table 7.8	Percentage increase in energy yield with increasing hub height for Yanbo.....	165
Table 7.9	Plant capacity factors for wind machines of different sizes at Yanbo.....	168
Table 7.10	PCF variation with increasing hub height for Yanbo.....	169
Table 7.11	Annual energy yield at different hub heights.....	175
Table 7.12	Percentage increase in annual energy yield with increase in hub height.....	176
Table 7.13	Total incremental cost of 1 000kW wind turbine.....	176
Table 7.14	Energy production (MWh/year) from wind farms of 20, 30, and 40MW Installed Capacities for Yanbo at 60metres hub height.....	182
Table 8.1	Optimal wind-pv-diesel hybrid power system for the village.....	197
Table 8.2	Energy contribution of different energy sources at annual mean wind speed and global solar radiation of 5.85m/s and 5.75kWh/m <sup>2</sup> /d, respectively.....	198
Table 8.3	Annual GHG emissions from diesel-only and hybrid power systems.....	199
Table 8.4	Summary of various costs related to the wind-pv-diesel hybrid system.....	200
Table 8.5	Summary of annualised cost of the hybrid power system.....	200
Table 8.6	Effect of annual mean wind speed (WS) on wind energy (WE) contribution, excess energy, COE, diesel consumed, REF achieved and total running hours for annual mean GSR of 5.75kWh/m <sup>2</sup> /d, annual mean solar energy of 1 653.48MWh and 9% contribution of solar energy in the wind-pv-diesel hybrid power system.....	201
Table 8.7	Effect of annual mean global solar radiation (GSR) on solar energy (SE) contribution, excess energy, COE, diesel consumed, REF achieved and total running hours for a diesel price of US\$ 0.2/l, annual mean WS of 5.85m/s, annual mean wind energy of 1 653.48MWh and 27% contribution of wind energy in the wind-pv-diesel hybrid power system.....	202
Table A-1	Information on 600kW wind machine.....	244
Table A-2	Information on 750kW wind machine.....	244
Table A-3	Information on 800kW wind machine.....	245

Table A-4	Information on 1 000kW wind machine. ....	245
Table A-5	Information on 1 300kW wind machine. ....	246
Table A-6	Information on 1 500kW wind machine. ....	246
Table A-7	Information on 2 000 kW wind machine. ....	247
Table A-8	Information on 2 500 kW wind machine. ....	247
Table C-1	Wind energy output from single Nordex WECS using wind data at 10metre for Yanbo. ....	251
Table C-2	Wind energy output from single Nordex WECS at 40-metre hub height for Yanbo wind data. ....	252
Table C-3	Wind energy output from single Nordex WECS at 50-metre hub height for Yanbo wind data. ....	253
Table C-4	Wind energy output from single Nordex WECS at 60-metre hub height for Yanbo wind data. ....	254
Table C-5	Wind energy output from single Nordex WECS at 70-metre hub height for Yanbo wind data. ....	255
Table C-6	Wind energy output from single Nordex WECS at 80-metre hub height for Yanbo wind data. ....	256
Table C-7	Wind energy output from single Vestas WECS using wind data at 10-metre for Yanbo. ....	257
Table C-8	Wind energy output from single Vestas WECS using wind data at 40-metre for Yanbo. ....	258
Table C-9	Wind energy output from single Vestas WECS using wind data at 50-metre for Yanbo. ....	259
Table C-10	Wind energy output from single Vestas WECS using wind data at 60-metre for Yanbo. ....	260
Table C-11	Wind energy output from single Vestas WECS using wind data at 70-metre for Yanbo. ....	261
Table C-12	Wind energy output from single Vestas WECS using wind data at 80-metre for Yanbo. ....	262
Table C-13	Wind energy output from single Ge WECS using wind data at 10-metre for Yanbo. ....	263
Table C-14	Wind energy output from single Ge WECS using wind data at 40- metre for Yanbo. ....	264

Table C-15	Wind energy output from single Ge WECS using wind data at 50-metre for Yanbo.....	265
Table C-16	Wind energy output from single Ge WECS using wind data at 60- metre for Yanbo.....	266
Table C-17	Wind energy output from single Ge WECS using wind data at 70-metre for Yanbo.....	267
Table C-18	Wind energy output from single Ge WECS using wind data at 80-metre for Yanbo.....	268
Table C-19	Wind energy output from single Dewind WECS using wind data at 10-metre for Yanbo. ....	269
Table C-20	Wind energy output from single Dewind WECS using wind data at 40-metre for Yanbo. ....	270
Table C-21	Wind energy output from single Dewind WECS using wind data at 50-metre for Yanbo. ....	271
Table C-22	Wind energy output from single Dewind WECS using wind data at 60-metre for Yanbo. ....	272
Table C-23	Wind energy output from single Dewind WECS using wind data at 70-metre for Yanbo. ....	273
Table C-24	Wind energy output from single Dewind WECS using wind data at 80-metre for Yanbo. ....	274
Table C-25	Wind energy output from single Bonus WECS using wind data at 10-metre for Yanbo. ....	275
Table C-26	Wind energy output from single Bonus WECS using wind data at 40-metre for Yanbo. ....	276
Table C-27	Wind energy output from single Bonus WECS using wind data at 50-metre for Yanbo. ....	277
Table C-28	Wind energy output from single Bonus WECS using wind data at 60-metre for Yanbo. ....	278
Table C-29	Wind energy output from single Bonus WECS using wind data at 70-metre for Yanbo. ....	279
Table C-30	Wind energy output from single Bonus WECS using wind data at 80-metre for Yanbo. ....	280
Table C-31	Wind energy output from single Enercon WECS using wind data at 10-metre for Yanbo. ....	281

Table C-32	Wind energy output from single Enercon WECS using wind data at 40-metre for Yanbo. ....	282
Table C-33	Wind energy output from single Enercon WECS using wind data at 50-metre for Yanbo. ....	283
Table C-34	Wind energy output from single Enercon WECS using wind data at 60-metre for Yanbo. ....	284
Table C-35	Wind energy output from single Enercon WECS using wind data at 70-metre for Yanbo. ....	285
Table C-36	Wind energy output from single Enercon WECS using wind data at 80-metre for Yanbo. ....	286

## LIST OF FIGURES

Figure 2.1	Global population growth trends.....	8
Figure 2.2	Global energy demand trend .....	9
Figure 2.3	Growth rates of global net energy generation and its consumption [13].....	9
Figure 2.4	Annual consumption of energy in Middle East countries. ....	10
Figure 2.5	Annual population of Saudi Arabia.....	11
Figure 2.6	Trend of per capita energy consumption in Saudi Arabia .....	12
Figure 2.7	Cumulative power installed capacity (MW) of Saudi Arabia .....	12
Figure 2.8	Annual peak load (MW) of Saudi Arabia .....	13
Figure 2.9	Annual energy production (GWh) in Saudi Arabia.....	13
Figure 2.10	Annual fuel consumed (thousand TOE) in Saudi Arabia .....	14
Figure 3.1	Global wind power cumulative installed capacity .....	18
Figure 3.2	Annual percentage wind power installed capacity .....	18
Figure 3.3	Regional cumulative share of wind power up to 2009 .....	18
Figure 3.4	Cumulative wind power installed capacity of top 10 countries up to 2009 .....	19
Figure 3.5	Percentage wind power contribution of top 10 countries up to 2009 .....	19
Figure 3.6	Wind power installed capacities for year 2009 for top 10 countries .....	19
Figure 3.7	Percentage wind power contribution in 2009 by top 10 countries .....	20
Figure 4.1	Geographical locations of meteorological stations .....	54
Figure 4.2	Geographical locations of 40-metre towers .....	55
Figure 4.3	Schematic diagram of placement of wind speed (WS) and wind direction (WD) sensors on a mast of 40 metres high .....	56
Figure 4.4	Erected wind tower at Juaymah .....	57
Figure 5.1	Long-term annual mean wind speed over Saudi Arabia .....	61
Figure 5.2	Wind speed contour map of Saudi Arabia .....	61
Figure 5.3	Monthly mean wind speed contour maps of Saudi Arabia.....	62

Figure 5.4	Long-term annual average values of temperature (°C) over Saudi Arabia.....	64
Figure 5.5	Long-term annual average values of surface pressure (mbar) over Saudi Arabia.....	64
Figure 5.7(a)	Annual mean wind speed trends for Abha, Al-Ahsa and Al-Baha.....	68
Figure 5.7(b)	Annual mean wind speed trends for Al-Jouf, Al-Wejh and Arar .....	70
Figure 5.7(c)	Annual mean wind speed trends for Bisha, Dhahran and Gassim.....	71
Figure 5.7(d)	Annual mean wind speed trends for Gizan, Guriat and Hafr-Al-Batin .....	72
Figure 5.7(e)	Annual mean wind speed trends for Hail, Jeddah and Khamis-Mushait.....	73
Figure 5.7(f)	Annual mean wind speed trends for Madinah, Makkah and Nejran .....	74
Figure 5.7(g)	Annual mean wind speed trends for Qaisumah, Rafha and Riyadh .....	75
Figure 5.7(h)	Annual mean wind speed trends for Sharourah, Sulayel and Tabouk .....	76
Figure 5.7(i)	Annual mean wind speed trends for Taif, Turaif and Wadi-Al-Dawasser .....	77
Figure 5.7(j)	Annual mean wind speed trends for Yanbo .....	78
Figure 5.8(a)	Seasonal variation of long-term mean wind speed at seven locations .....	79
Figure 5.8(b)	Seasonal variation of long-term mean wind speed at seven locations .....	79
Figure 5.8(c)	Seasonal variation of long-term mean wind speed at seven locations .....	80
Figure 5.8(d)	Seasonal variation of long-term mean wind speed at seven locations .....	80
Figure 5.9	Long-term mean Weibull shape parameter, $k$ .....	83
Figure 5.10	Long-term mean Weibull scale parameter, $c$ (m/s) .....	83
Figure 5.11	Frequency distribution .....	84
Figure 5.12	Frequency distribution .....	85
Figure 5.13	Frequency distribution .....	86
Figure 5.14	Frequency distribution .....	87
Figure 5.15(a)	Annual trend of shape parameter at Abha .....	88
Figure 5.15(b)	Annual trend of shape parameter at Al-Ahsa .....	89
Figure 5.15(c)	Annual trend of shape parameter at Al-Baha .....	89

Figure 5.16(a)	Annual trend of scale parameter at Abha .....	91
Figure 5.16(b)	Annual trend of scale parameter at Al-Ahsa .....	91
Figure 5.16(c)	Annual trend of scale parameter at Al-Baha .....	92
Figure 6.1	Comparison of mean wind speed at different heights .....	97
Figure 6.2	Comparison of wind shear exponent at measurement sites .....	98
Figure 6.3	Comparison of mean ambient temperature at measurement sites .....	98
Figure 6.4	Comparison of surface pressure at measurement sites .....	99
Figure 6.5	Comparison of relative humidity at measurement sites .....	99
Figure 6.6	Comparison of global solar radiation at measurement sites .....	99
Figure 6.7	Wind rose diagram of wind speed and direction data at Rawdat Ben Habbas .....	101
Figure 6.8	Wind rose diagram of wind speed and direction data at Juaymah .....	101
Figure 6.9	Wind rose diagram of wind speed and direction data at Dhahran .....	102
Figure 6.10	Wind rose diagram of wind speed and direction data at Arar .....	102
Figure 6.11	Wind rose diagram of wind speed and direction data at Yanbo .....	103
Figure 6.12	Wind rose diagram of wind speed and direction data at Dhulom .....	103
Figure 6.13	Frequency distribution at different heights for Rawdat Ben Habbas .....	105
Figure 6.14	Frequency distribution at different heights for Juaymah .....	106
Figure 6.15	Frequency distribution at different heights for Dhahran .....	106
Figure 6.16	Frequency distribution at different heights for Arar .....	106
Figure 6.17	Frequency distribution at different heights for Gassim .....	107
Figure 6.18	Frequency distribution at different heights for Yanbo .....	107
Figure 6.19	Frequency distribution at different heights for Dhulom .....	108
Figure 6.20	Annual mean wind speed at different heights at Rawdat Ben Habbas .....	109
Figure 6.21	Annual mean wind speed at different heights at Juaymah .....	109
Figure 6.22	Annual mean wind speed at different heights at Dhahran .....	110
Figure 6.23	Annual mean wind speed at different heights at Arar .....	111

Figure 6.24	Annual mean wind speed at different heights at Gassim .....	112
Figure 6.25	Annual mean wind speed at different heights at Yanbo.....	112
Figure 6.26	Annual mean wind speed at different heights at Dhulom .....	113
Figure 6.27	Monthly mean wind speeds in different years at Rawdat Ben Habbas .....	114
Figure 6.28	Monthly mean wind speeds in different years at Juaymah.....	114
Figure 6.29	Monthly mean wind speeds in different years at Dhahran .....	115
Figure 6.30	Monthly mean wind speeds in different years at Arar .....	115
Figure 6.31	Monthly mean wind speeds in different years at Gassim.....	116
Figure 6.32	Monthly mean wind speeds in different years at Yanbo .....	116
Figure 6.33	Monthly mean wind speeds in different years at Dhulom.....	117
Figure 6.34	Diurnal variation of mean wind speed at Rawdat Ben Habbas .....	118
Figure 6.35	Diurnal variation of mean wind speed at Juaymah .....	118
Figure 6.36	Diurnal variation of mean wind speed at Dhahran .....	119
Figure 6.37	Diurnal variation of mean wind speed at Arar .....	119
Figure 6.38	Diurnal variation of mean wind speed at Gassim.....	120
Figure 6.39	Diurnal variation of mean wind speed at Yanbo .....	120
Figure 6.40	Diurnal variation of mean wind speed at Dhulom .....	121
Figure 6.41	Wind shear exponent estimation using power and log law fit at Rawdat Ben Habbas .....	122
Figure 6.42	Annual variation of WSE at Rawdat Ben Habbas.....	123
Figure 6.43	Monthly mean WSE in different years at Rawdat Ben Habbas .....	123
Figure 6.44	Diurnal variation of WSE during different months of the year and over the entire data collection period at Rawdat Ben Habbas .....	123
Figure 6.45	Wind shear exponent estimation using power and log law fit at Juaymah .....	124
Figure 6.46	Annual variation of WSE at Juaymah .....	125
Figure 6.47	Monthly mean values of WSE in different years at Juaymah .....	125
Figure 6.48	Diurnal variation of WSE during different months of the year and over the entire data collection period at Juaymah .....	125

Figure 6.49	WSE estimation using power and log law fit at Dhahran .....	126
Figure 6.50	Annual variation of WSE at Dhahran .....	127
Figure 6.51	Monthly mean values of WSE in different years at Dhahran .....	127
Figure 6.52	Diurnal variation of WSE during different months of the year and over the entire data collection period at Dhahran.....	128
Figure 6.53	WSE estimation using power and log law fit at Arar .....	129
Figure 6.54	Annual mean values of WSE in different years at Arar .....	129
Figure 6.55	Monthly mean values of WSE in different years at Arar .....	130
Figure 6.56	Diurnal variation of WSE during different months of the year and over the entire data collection period at Arar .....	130
Figure 6.57	WSE estimation using power and log law fit at Gassim .....	131
Figure 6.58	Annual mean values of WSE in different years at Gassim .....	132
Figure 6.59	Monthly mean values of WSE in different years at Gassim .....	132
Figure 6.60	Diurnal variation of wind shear exponent during different months of the year and over entire data collection period at Gassim.....	133
Figure 6.61	WSE estimation using power and log law fit at Yanbo.....	134
Figure 6.62	Annual mean values of WSE in different years at Yanbo .....	134
Figure 6.63	Monthly mean values of WSE in different years at Yanbo .....	135
Figure 6.64	Diurnal variation of WSE during different months of the year and over the entire data collection period at Yanbo.....	135
Figure 6.65	WSE estimation using power and log law fit at Dhulom .....	136
Figure 6.66	Annual mean values of WSE in different years at Dhulom .....	137
Figure 6.67	Monthly mean values of WSE in different years at Dhulom .....	137
Figure 6.68	Diurnal variation of WSE during different months of the year and over the entire data collection period at Dhulom .....	138
Figure 6.69	Effect of $k$ on the nature of wind speed variations .....	139
Figure 6.70	Comparison of Weibull shape parameter at different heights and locations .....	140
Figure 6.71	Comparison of Weibull scale parameter at different heights and locations .....	140

Figure 7.1	View of a three-bladed wind turbine with rotor and nacelle unit.....	147
Figure 7.2	Layout drawing of nacelle unit of the Nordex N-60 wind turbine. ....	148
Figure 7.3	Wind power curves for WECSs of different sizes from Nordex .....	150
Figure 7.4	Wind rose diagram of hourly mean wind speed values at 10 metres above ground level for Yanbo.....	151
Figure 7.5	Wind rose diagram of hourly mean wind speed values at 40 metres above ground level for Yanbo.....	151
Figure 7.6	Wind rose diagram of hourly mean wind speed values at 50 metres above ground level for Yanbo.....	152
Figure 7.7	Wind rose diagram of hourly mean wind speed values at 60 metres above ground level for Yanbo.....	152
Figure 7.8	Wind rose diagram of hourly mean wind speed values at 70 metres above ground level for Yanbo.....	153
Figure 7.9	Wind rose diagram of hourly mean wind speed values at 80 metres above ground level for Yanbo.....	153
Figure 7.10	Wind power curves for WECSs of different sizes from Vestas .....	155
Figure 7.11	Wind power curves for WECSs of different sizes from GE .....	155
Figure 7.12	Wind power curves for WECSs of different sizes from DeWind .....	156
Figure 7.13	Wind power curves for WECSs of different sizes from Bonus.....	156
Figure 7.14	Wind power curves for WECSs of different sizes from Enercon.....	157
Figure 7.15	Effect of hub height on energy yield for Nordex wind machines at Yanbo.....	161
Figure 7.16	Effect of hub height on energy yield for Vestas wind machines at Yanbo .....	162
Figure 7.17	Effect of hub height on energy yield for GE wind machines at Yanbo.....	162
Figure 7.18	Effect of hub height on energy yield for DeWind wind machines at Yanbo.....	163
Figure 7.19	Effect of hub height on energy yield for Bonus wind machines at Yanbo.....	163
Figure 7.20	Effect of hub height on energy yield for Enercon wind machines at Yanbo.....	164
Figure 7.21	Comparison of percentage increase in energy yield due to increase in hub height at Yanbo for WECSs from different manufacturers.....	164

Figure 7.22	Effect of hub height on plant capacity factor for Nordex wind machines at Yanbo .....	170
Figure 7.23	Effect of hub height on plant capacity factor for Vestas wind machines at Yanbo .....	170
Figure 7.24	Effect of hub height on plant capacity factor for DeWind wind machines at Yanbo .....	171
Figure 7.25	Effect of hub height on plant capacity factor for GE wind machines at Yanbo.....	171
Figure 7.26	Effect of hub height on plant capacity factor for Bonus wind machines at Yanbo .....	172
Figure 7.27	Comparison of increase in plant capacity factor for Yanbo due to increase in hub height for WECSs from different manufacturers. ....	172
Figure 7.28	Wind power curve of an AAER 1 000kW wind turbine from Pioneer wind energy systems .....	175
Figure 7.29	Comparison of annual energy yields at different hub heights with wind shear exponents .....	175
Figure 7.30	Percentage increase in energy yield and the total cost of wind turbine installation with increasing hub height for Arar.....	176
Figure 7.31	Percentage increase in energy yield and the total cost of wind turbine installation with increasing hub height for Dhahran .....	177
Figure 7.32	Percentage increase in energy yield and the total cost of wind turbine installation with increasing hub height for Dhulom .....	177
Figure 7.33	Percentage increase in energy yield and the total cost of wind turbine installation with increasing hub height for Gassim .....	178
Figure 7.34	Percentage increase in energy yield and the total cost of wind turbine installation with increasing hub height for Juaymah.....	178
Figure 7.35	Percentage increase in energy yield and the total cost of wind turbine installation with increasing hub height for Rawdat Ben Habbas.....	179
Figure 7.36	Percentage increase in energy yield and the total cost of wind turbine installation with increasing hub height for Yanbo .....	179
Figure 7.37	Optimal hub height variation with wind shear exponent.....	180
Figure 7.38	Number of wind machines required for wind farms of 20, 30 and 40MW installed capacities .....	181
Figure 7.39	Wind power curve for Vestas VT100 2.75MW wind turbine .....	183

Figure 7.40	Wind speed at hub height of 100m at all the stations .....	184
Figure 7.41	Annual energy yield from Vestas 2.75MW wind turbine at all the stations .....	184
Figure 7.42	Annual mean plant capacity factor at all the locations.....	185
Figure 7.43	Percentages of rated and zero output at all the stations.....	185
Figure 8.1	Wind-pv-diesel hybrid model used in the study.....	188
Figure 8.2	Monthly mean and extreme wind speed at 40m AGL.....	190
Figure 8.3	Diurnal variation of hourly mean wind speed at 40m AGL.....	191
Figure 8.4	Frequency distribution of wind speed at 40m AGL .....	191
Figure 8.5	Monthly mean daily global solar radiation at the site .....	192
Figure 8.6	Diurnal variation of global solar radiation during different months .....	192
Figure 8.7	Typical summer's day load demand for the village (July 14, 2005) .....	193
Figure 8.8	Typical winter's day load demand for the village (January 03, 2005) .....	194
Figure 8.9	Diurnal variation of load during different months of the year .....	194
Figure 8.10	Monthly mean power contribution by wind, solar-pv and diesel systems .....	198
Figure 8.11	Cash flow summary of various components of the hybrid power system .....	200
Figure 8.12	Effect of diesel price on COE of hybrid power system at annual average wind speed of 5.85m/s and global solar radiation of 5.75kWh/m <sup>2</sup> /d .....	203
Figure 9.1	Decomposition of wind speed time series data for Abha using DB5 .....	208
Figure 9.2	Decomposition of wind speed time series data for Dhahran using DB5 .....	209
Figure 9.3	Decomposition of wind speed time series data for Gizan using DB5 .....	209
Figure 9.4	Decomposition of wind speed time series data for Guryat using DB5 .....	210
Figure 9.5	Decomposition of wind speed time series data for Hail using DB5.....	210
Figure 9.6	Decomposition of wind speed time series data for Jeddah using DB5 .....	211
Figure 9.7	Decomposition of wind speed time series data for Riyadh using DB5 .....	211
Figure 9.8	Decomposition of wind speed time series data for Turaif using DB5.....	212
Figure 9.9	Decomposition of wind speed time series data for Yanbo using DB5 .....	212

Figure 9.10	FFT power spectrum of wind speed data for Abha. ....	214
Figure 9.11	FFT power spectrum of wind speed data for Dhahran .....	215
Figure 9.12	FFT power spectrum of wind speed data for Gizan .....	215
Figure 9.13	FFT power spectrum of wind speed data for Guryat.....	216
Figure 9.14	FFT power spectrum of wind speed data for Hail.....	216
Figure 9.15	FFT power spectrum of wind speed data for Jeddah.....	217
Figure 9.16	FFT power spectrum of wind speed data for Riyadh .....	218
Figure 9.17	FFT power spectrum of wind speed data for Turaif.....	218
Figure 9.18	FFT power spectrum of wind speed data for Yanbo .....	219

## LIST OF APPENDICES

APPENDIX A	TECHNICAL INFORMATION RELATED TO WIND ENERGY CONVERSION SYSTEM FROM SELECTED MANUFACTURERS .....	244
APPENDIX B	DETAILED TECHNICAL INFORMATION ON WECS FROM NORDEX, VESTAS, DEWIND, GE, AND BONUS .....	249
APPENDIX C	ENERGY CALCULATIONS FROM SINGLE WIND MACHINES .....	251

# CHAPTER 1

## INTRODUCTION

The earth, home to approximately 7 billion inhabitants, is facing a severe threat from the continuous addition of dangerous unrequired gases and suspension of these into the atmosphere at all times. Are there people who think about a better and safer future for forthcoming generations? If so, will these thoughts be sufficient to make a difference to the extent that the addition of these poisonous gases, these days called greenhouse gases (GHG), is controlled or reduced to the required limit?

### 1.1 BACKGROUND TO THE STUDY

The mean global surface temperature has increased by  $0.74 \pm 0.18^{\circ}\text{C}$  ( $1.33 \pm 0.32^{\circ}\text{F}$ ) during the twentieth century as reported in the Intergovernmental Panel on Climate Change (IPCC) [1]. In general, the global scientific community is of the view that most of the temperature increase took place during the middle of the twentieth century and that it was caused by increasing concentrations of greenhouse gases (GHG) in the atmosphere, which resulted from human activities such as burning of fossil fuels and the cutting of trees. This increase in global mean temperatures is expected to cause sea levels to rise, change the amount and pattern of precipitation and expand the subtropical deserts [2]. The other adverse effects may include changes in the frequency and intensity of extreme weather events, species extinction and changes in agricultural yields. The magnitude of warming and subsequent changes will vary from region to region around the globe but the nature of these regional variations both in terms of magnitude and severity is uncertain [3].

In this modern world, more than 33% of people (about 2 billion) do not have access to electricity. Most of the unlucky ones live in developing and underdeveloped countries and a very few in the developed world. This is one side of the situation and the other side is that the increasing demand for energy puts an unnatural adverse burden on the atmosphere which results in unforeseen natural disasters such as earthquakes, thunderstorms and floods. The challenge now is two-fold. On the one hand, the energy demands have to be met and on the other hand, the atmosphere has to be kept clean. There are two options to facilitate these issues. One is to develop traditional power plants based on fossil fuels and to lay the grid network to reach to all parts of the country, region or world. This approach can resolve one issue, namely making power available to all people, but this will pollute the atmosphere with

an adverse effect on the climate. Moreover, the building of such power plants and the laying of the power grid network are both time and finance-intensive. Not all countries can afford these solutions.

The second approach, which is based on clean and renewable sources of energy such as solar (pv and thermal), wind, tidal, wave and geothermal, can resolve these issues in an efficient and economical manner. These sources are site-dependent and are available everywhere and have no political and geographical boundaries. There is no problem with fuel transport. The sources of energy are absolutely free, clean and are available in abundance. Of these sources, solar and wind resources have achieved commercial acceptability both in technological and economic terms. These sources can be tapped anywhere and do not require the national grid connectivity. They can be connected to isolated grids, to groups of houses, or to individual houses or installations.

Wind power is highly site-dependent and can be compared in terms of kilowatt of energy cost with the traditional-power-plant based cost of energy generation. Today, wind power plants can generate energy at 4 to 6 US cents/kWh with proven availability of wind. Wind turbines are now available from a few kilowatts to 5MW rated power and have been developed for both onshore and offshore applications. These modern wind turbines require minimal maintenance and hence a minimal attention of skilled manpower. Nowadays, the wind power technology has reached such a stage that wind power plants could be developed in less than a year at locations where wind resource assessment reports are available. The accurate and bankable wind power resource assessment reports are a must and are the basis for attracting the developers and financiers.

Wind power resource assessment (Wpra) is the key for fast-track development and implementation of wind power for both grid-connected and hybrid power plants. Countries such as Germany, Denmark, the USA, the UK, India, China, Spain, Morocco, Egypt, Tunisia and Syria, have first conducted wind power resource assessments and then moved towards installation of wind power plants and now have grid-connected wind power capacities in hundreds and thousands of MW. Wpra could be conducted using the available meteorological data for preliminary assessment and identification of windy sites in a region or country. The other approach, which is essential even on the availability of windy sites, is to conduct wind measurements at different heights over a period of at least one year to find out the local wind shear exponent. This wind shear exponent could provide the availability of

wind speed at higher altitudes with confidence and hence the energy yield using modern wind turbines of multimegawatt sizes and hub heights of 60 to 100metres.

The growing population on the earth and the fast-depleting reserves of fossil fuels have led researchers in the fields of engineering, hydrology, meteorology, economy, industry, and even politicians, to pursue the development and use of renewable energy resources such as solar energy, wind power, biomass and thermochemical recovery of energy. According to Winter [4], the population on this planet increases by about 2 million people every year. There were 5.5 billion people in 1992 and more than 8 billion were expected by 2010. Winter [4] also reports from Sadiq [5] that 60% of today's population lives in cities, and based on migration trends, the cities of the future will hold 80% of the world's population. Consequently, because of such a large number of inhabitants, the size of the cities, influx of supplies and outpouring of wastes produced, the energy supply must be increased in proportion.

Saudi Arabia has no threat of such an increase neither of population nor of an energy crisis, lack of basic supplies and outpouring of wastes produced. However, thinking in the direction of developing and using renewable energy resources for future use is indeed a good step towards clean energy. The Kingdom of Saudi Arabia did much work and invested a good amount of money on the development of wind and solar energy both experimentally and theoretically.

Usually, the airports are located at low windy sites; hence the wind measurements at these sites cannot be used for realistic wind power assessments. In order to make realistic wind power assessments in the Kingdom of Saudi Arabia, a nationwide wind speed measurement campaign should materialise. Furthermore, the wind speed measurements should be conducted at different heights to get the actual site-dependent wind power exponent. This exponent can then be used with confidence to estimate the wind speed at the hub height of modern wind turbines.

## **1.2 OBJECTIVES OF THE STUDY**

The overall objective of the present work is to understand the global wind power technological trends and apply them to local conditions in Saudi Arabia. The specific objectives are:

- statistical analysis of wind speed and other meteorological parameters;
- wind frequency and annual mean wind speed trend analysis;
- wind resource assessment of Saudi Arabia using both historical data from 28 stations and the data measured at different heights (20, 30 and 40 metres above ground level) at seven locations;
- development of wind speed and wind power density maps using long-term annual averages and the monthly means;
- hub height optimisation using wind data from one of the historical meteorological stations and wind turbines of varying plate capacity and from different manufacturers;
- design of grid-connected wind farms and wind-diesel hybrid power systems, and study of economical aspects of wind power utilisation in Saudi Arabia and estimation of cost of energy (COE) for a wind-pv-diesel hybrid power system.

## **1.3 APPROACH TO THE STUDY**

The present research work utilises long-term historical wind speed and direction data from 28 meteorological stations for preliminary assessment of wind power resources and identification of windy sites for potential usage of wind power development in Saudi Arabia. These meteorological stations are situated at national and international airports in the kingdom and wind measurements were made at 8 to 12metres above ground level. All of these stations are operated and maintained by the Presidency of Meteorology and Environment (PME) [6].

The WPRA was conducted using long-term, annual and monthly averages of the wind speed and of available energy using a wind turbine of 2.75MW from Vestas (Model VT100) for a hub height of 100 metres. The analysis also provided a frequency distribution for wind speed in different wind speed bins both on long-term and seasonal basis. The wind rose diagrams were also developed to find the prevailing wind directions for both long-term and seasonal periods. The hybrid wind-pv-diesel power system was designed for a village using HOMER,

the hybrid power plant designer tool, recommended by the National Renewable Energy Laboratory (NREL), USA.

#### **1.4 CONTRIBUTION OF THE PRESENT WORK**

The main contributions of the present work are as follows:

- The wind resource assessment was conducted using long-term wind speed data, for a period of 37 years from 1970 to 2006, from 28 meteorological stations maintained at national and international airports by the Presidency of Meteorology and Environment (PME, <http://www.pme.gov.sa>).
- Annual mean wind speed trends were estimated and linear best-fit equations with coefficient of determination were determined for all the meteorological stations used in the present work.
- Long-term annual and seasonal wind maps were developed and reported in this thesis. These could be used as starting point to locate potential sites for further detailed assessment and site-dependent wind measurements.
- Wind resource assessments were also accomplished for seven meteorological stations where wind speed measurements were made at 20, 30 and 40metres above ground level using 40metre wind masts. Local wind shear exponents, which are rarely available, were estimated and reported in this work.
- The optimal hub height for maximum energy yield from wind turbines was estimated using several wind turbines of varying rated power from various manufacturers.
- A techno-economic feasibility study was conducted to design an optimal wind-pv-diesel hybrid power system for a village using the measured wind speed at the site and the existing load data of the village. The study provided specifications for the designed hybrid power system for 25% renewable energy penetration.

#### **1.5 ORGANISATION OF THE THESIS**

The rest of the contents of this thesis are covered in another nine chapters with sub-sections in each chapter. Chapter 2 provides the background material related to global, Middle East and Saudi Arabian population and energy demand trends. A comprehensive literature review on global wind power scenario, wind power resource assessment, wind speed prediction,

wind shear exponent, Weibull shape and scale parameters, wind power technology and hybrid power systems is presented in Chapter 3. Data and site description are provided in Chapter 4 while Chapter 5 is devoted to wind data analysis of historical meteorological data obtained from airports. The wind speed data analysis of the data measured at different heights is given in Chapter 6. Chapter 7 provides wind farm design and energy yield estimation, hub height optimisation, plant capacity factor and rated and zero energy output analysis. Hybrid wind diesel power system design and its optimisation using HOMER software from NREL are covered in Chapter 8. The wavelet analysis of daily mean wind speed values for some chosen locations is reported in Chapter 9. Finally, the conclusions and recommendations are presented in Chapter 10 while references follow the last chapter.

## **CHAPTER 2**

### **REGIONAL, NATIONAL AND GLOBAL POPULATION AND ENERGY PATTERNS**

The regional, national and global population growth directly dictates the increasing trends of energy on respective scales. This chapter describes in detail the population growth and increasing power demands on regional, national and global levels in the following subsections.

#### **2.1 GLOBAL POPULATION AND ENERGY DEMAND PATTERNS**

As from 24 September 2010, the world population was estimated by the United States Census Bureau to be 6.871 billion [7]. According to papers published by the United States Census Bureau, the world population reached 6.5 billion (6,500,000,000) on 24 February 2006. The United Nations Population Fund designated 12 October 1999 as the approximate day on which world population reached 6 billion. This was about 12 years after the world population reached 5 billion in 1987, and six years after the world population reached 5.5 billion in 1993. However, the population of some countries, such as Nigeria and China, is not even known to the nearest million [8] so there is a considerable margin of error in such estimates [9]. Population growth increased significantly as the Industrial Revolution gathered pace from 1700 onwards [10]. The last 50 years have seen an even more rapid increase in the rate of population growth [10] due to medical advances and substantial increases in agricultural productivity, particularly beginning in the 1960s [11]. In 2007, the United Nations Population Division projected that the world population will likely surpass 10 billion in 2055 [12]. In the future, world population has been expected to reach a peak of growth; from there it will decline due to economic reasons, health concerns, land exhaustion and environmental hazards. The population growth trend is shown in Figure 2.1.

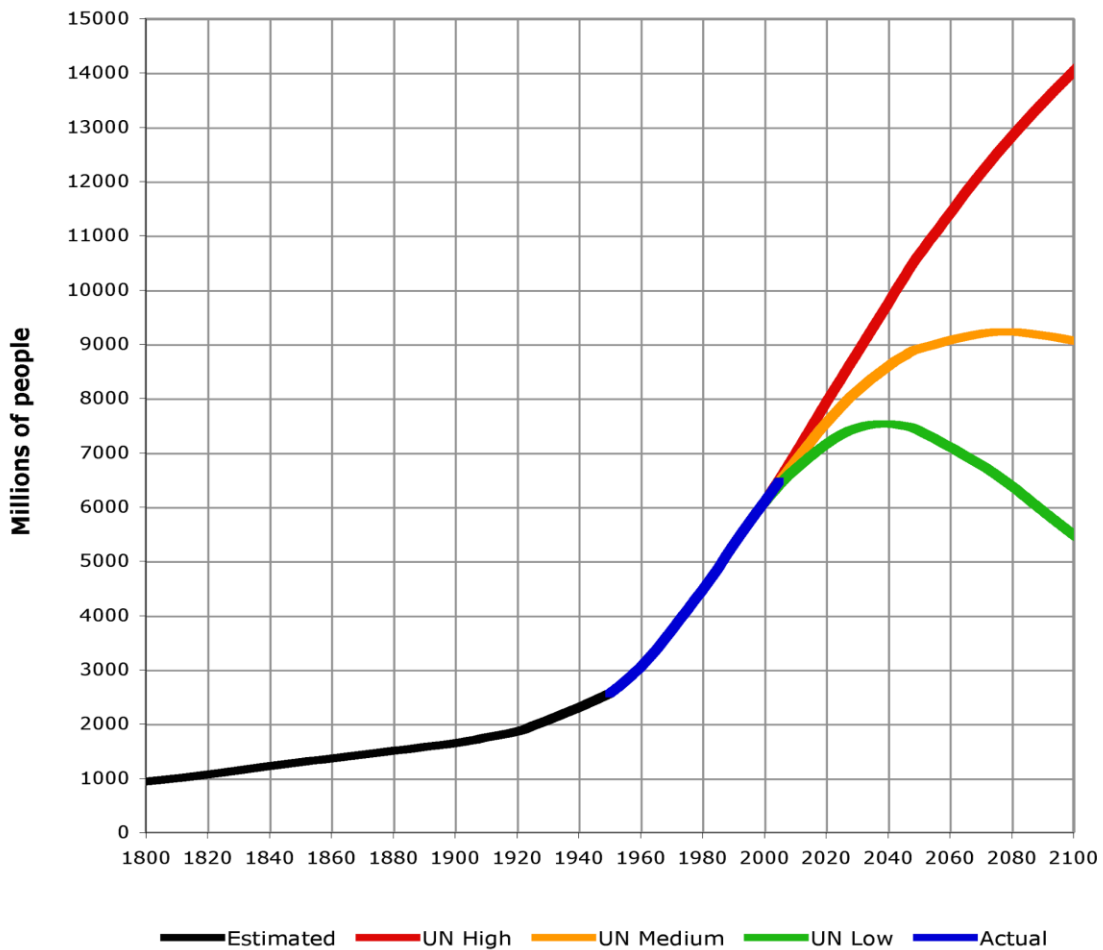


Figure 2.1 Global population growth trends

The global annual energy requirement is increasing continuously, as shown in Figure 2.2, [13]. From 2001 to 2010, the energy demand increased from 1 600terawatt hour (TWh) to 20 000 TWh, an increase of 25% in a time period of 10 years only. In terms of estimates, the energy consumption will increase to more than 25 000TWh by the end of year 2020. An annual increase of 1.5% to 2% in energy consumption is estimated by the experts as shown in Figure 2.3 [13]. The net energy generation is expected to be higher, as shown in Figure 2.3.

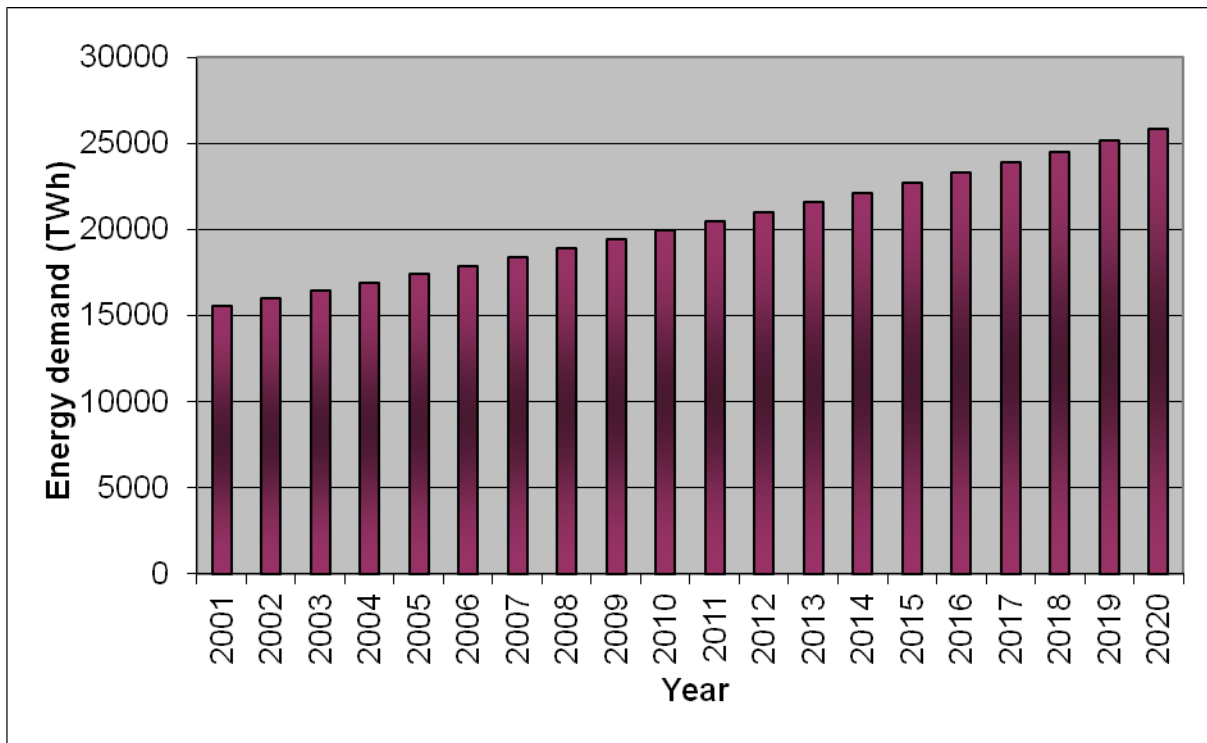


Figure 2.2 Global energy demand trend [13]

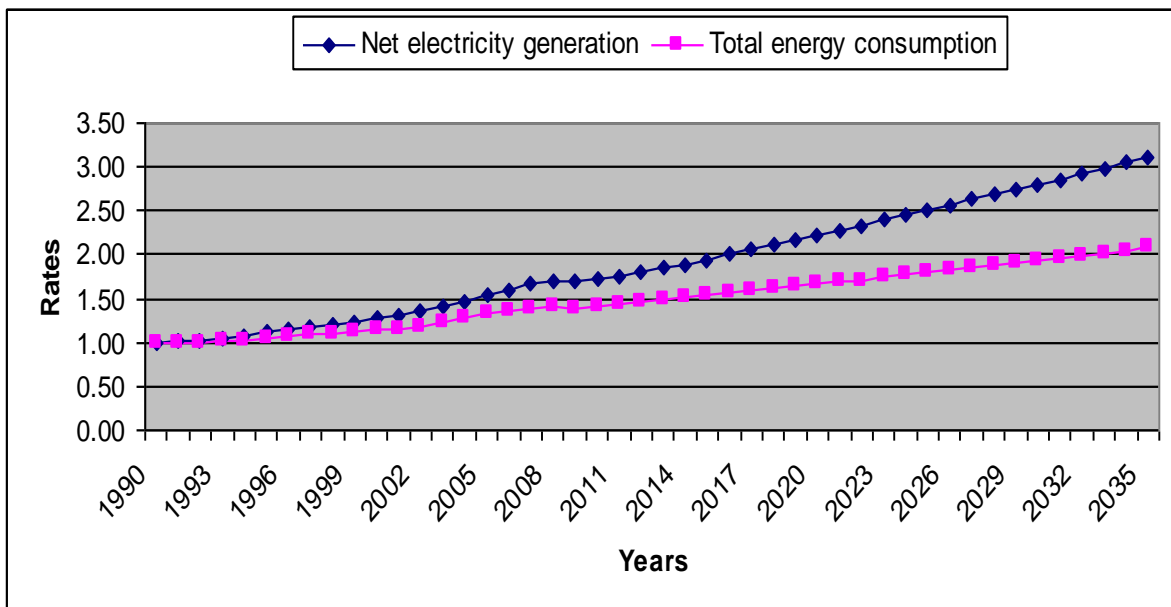


Figure 2.3 Growth rates of global net energy generation and its consumption [13]

## 2.2 MIDDLE EAST POPULATION AND ENERGY DEMAND TRENDS

The US Census Bureau estimates that the Middle East is a region where the population will nearly double between now and 2030. From 1950 to 2000, the Middle East experienced an explosive population growth. The region's population grew from 92 million to 349 million, a

3.8-fold increase, or 2.7% a year [14]. The total population of the Arabian Gulf has grown from 30 million in 1950 to 39 million in 1960, 52 million in 1970, 74 million in 1980, 109 million in 1990, and 139 million in 2000. Conservative projections put it at 172 million in 2010, 211 million in 2020, 249 million in 2030, 287 million in 2040, and 321 million in 2050 [15].

Rapid population growth in the Middle East and North Africa (MENA) carries serious implications for employment, access to services and the cost of subsidies. Population data for MENA is extremely sensitive and needs to be treated cautiously [16]. Nonetheless, it is clear that since the 1970s MENA has experienced a dramatic rise in population compared with other parts of the developing world. The result has been that the region's population has grown from 127 million in 1970 to 305 million in 2005. For example, in the 10 years between 1976 and 1986, the population of Iran grew by 50%.

The energy consumption in the Middle East was 366TWh in 1997 (see Figure 2.4), which reached to 614TWh in 2010 and it is expected to reach to more than 900TWh in 2020, an increase of about 50% within next 10 years. According to a report [17], in 2001 the respective total power installed capacity of Bahrain, Kuwait, Oman, Qatar, Saudi Arabia and the United Arab Emirates was 1.1, 8.5, 2.4, 1.5, 26.6 and 5.6GW and the energy consumption was reported as 6.19, 32.33, 8.05, 9.15, 126.01 and 36.54TWh; respectively. The energy demands are increasing at 3 to 5% per annum in Gulf Cooperation Council (GCC) countries.

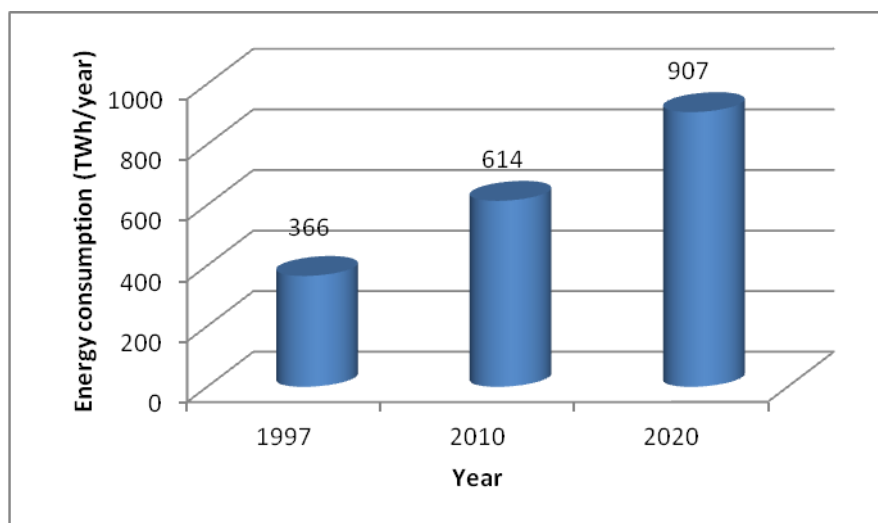


Figure 2.4 Annual consumption of energy in Middle East countries.

### 2.3 SAUDI ARABIAN POPULATION AND ENERGY DEMAND TRENDS

Saudi Arabia is a vast country with a total area of 2 149 690 square kilometre and having an international boundary of 4 431km (bordering countries: Iraq 814km, Jordan 744km, Kuwait 222km, Oman 676km, Qatar 60km, UAE 457km, Yemen 1,458km). Most of the cities and villages are either connected to the national electrical grid or to the isolated grids. Most of the remotely located villages get power through diesel power generating plants. It is really cumbersome to maintain a regular supply of fuel and to ensure the continuous electricity supply during breakdowns and scheduled shutdowns of the diesel units. The annual population trend of Saudi Arabia is depicted in Figure 2.5 [18]. In July 2006, the population was estimated to be over 27 million; including about 5.5 million resident foreigners. Until the 1960s, most of the population was nomadic or semi-nomadic; due to rapid economic and urban growth, more than 95% of the population now is settled. Some cities and oases have densities of more than 1 000 people per square kilometre. Saudi Arabia's population is characterised by rapid growth and a large cohort of youths. The estimated annual growth rate of the Saudi Arabian population is approximately 1.848%.

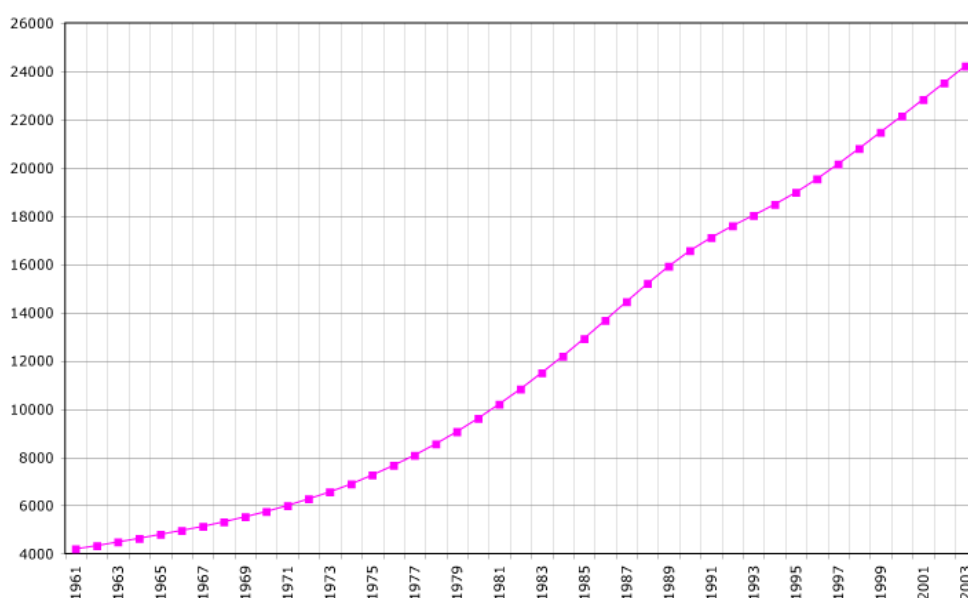


Figure 2.5 Annual population of Saudi Arabia

In Saudi Arabia, the per capita energy consumption has reached 20kWh/day in 2008 compared with 19.4kWh/day in 2007, i.e. a net increase of 3.1% in one year [19], as shown in Figure 2.6. A maximum of 10% increase in per capita energy was observed in 2004 compared with that in 2003. The average over a 25-year period from 1984 to 2008 of 4.1%

annual increase in per capita energy per day has been observed [19], which is really significant and needs to be resolved immediately. Moreover, the total installed capacity of the kingdom in year 2005 was 32 301MW, which increased to 34 825MW in 2006, an increase of 7.81% and then further increased by 6.1% and 6.21% in the years 2007 and 2008 compared with 2006 and 2007, respectively, as can be seen from Figure 2.7. A jump of 11.89% (i.e. from 31 240MW to 34 953MW) was observed in peak load in year 2007 compared with that in 2006, as shown in Figure 2.8. Again, in 2008, the peak load demand increased by another 8.72%, which shows a continuous increasing trend in peak load.

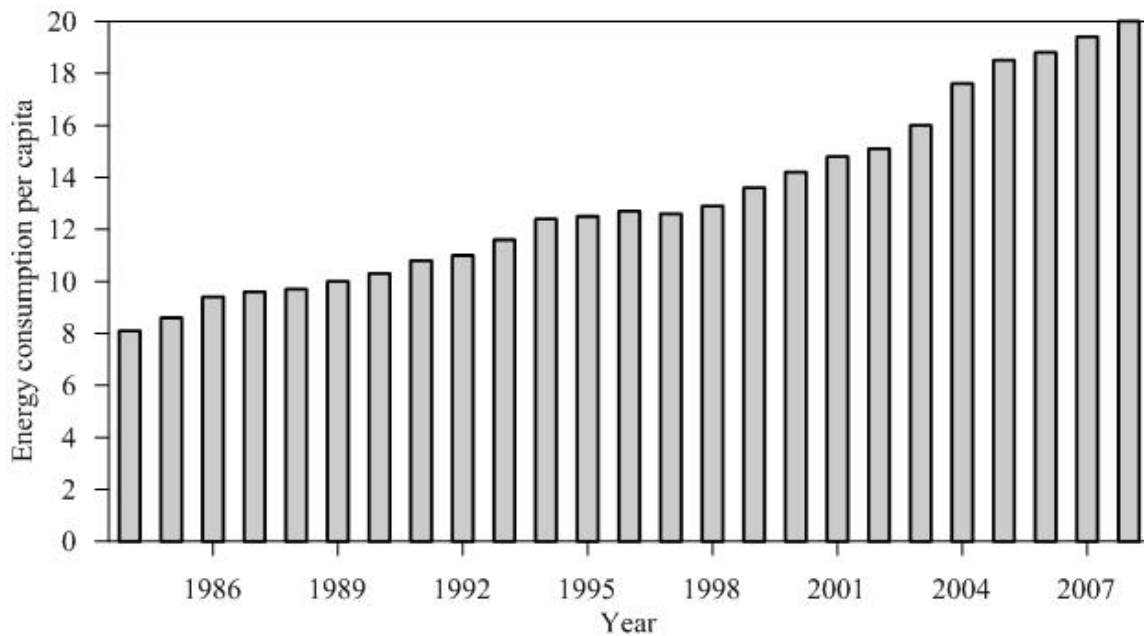


Figure 2.6 Trend of per capita energy consumption (kWh/d) in Saudi Arabia

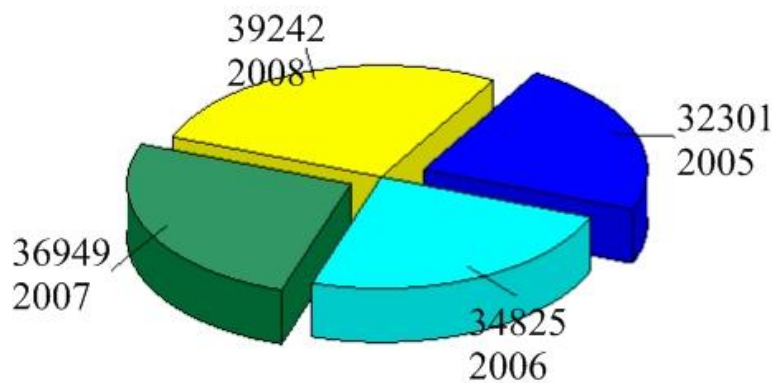


Figure 2.7 Cumulative power installed capacity (MW) of Saudi Arabia

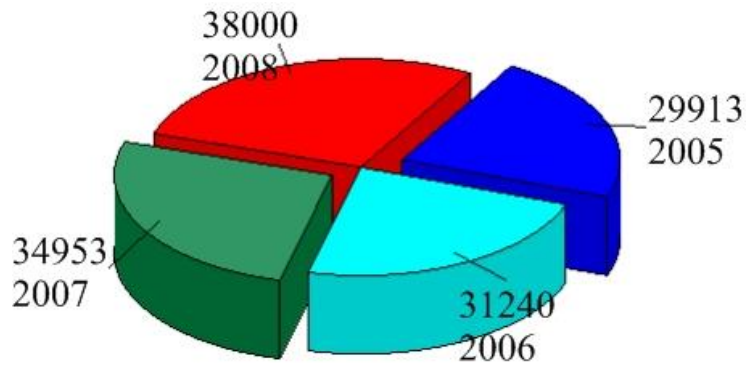


Figure 2.8 Annual peak load (MW) of Saudi Arabia

The annual energy production (as shown in Figure 2.9) from all conventional sources increased by 3.01%, 5.02% and 7.17% during 2006, 2007 and 2008 compared with 2005, 2006 and 2007, respectively. These numbers indicate a progressively increasing production of energy, which is reflective of growing energy demands. The total fuel consumption reached 49 740 thousand TOE in year 2008 compared with that of 45 760 TOE in 2007, a net increase of 8.7%, as can be seen from Figure 2.10. Around 3.5% increases were observed in the years 2007 and 2006 compared with those in 2005 and 2006, respectively. The Kingdom of Saudi Arabia has vast open land and is the largest producer and supplier of fossil fuels in the world but still encourages the utilisation of clean and renewable sources of energy.

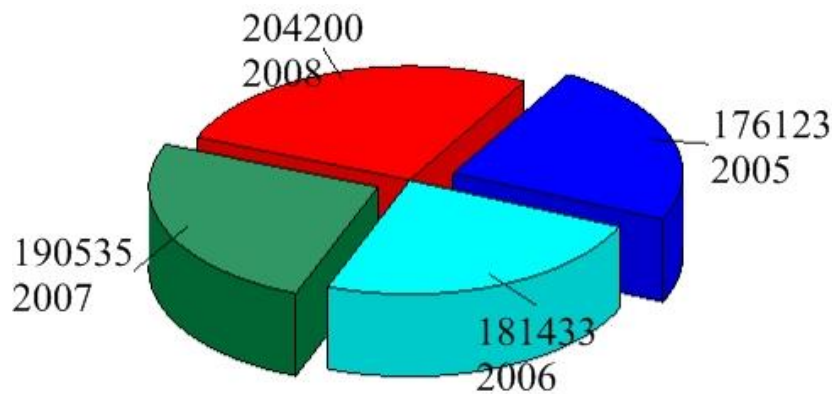


Figure 2.9 Annual energy production (GWh) in Saudi Arabia

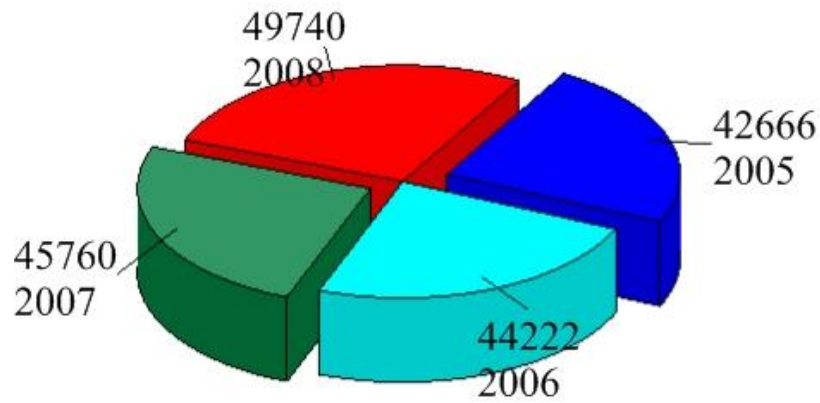


Figure 2.10 Annual fuel consumed (thousand TOE) in Saudi Arabia

The kingdom will experience higher demands of energy in the coming future and it has to meet these demands and at the same time keep the atmosphere clean. Therefore, to minimise the addition of pollutant gases into the atmosphere, new and renewable sources of energy are being sought to meet the increasing power demands. The power of the wind can be utilised to partially supplement the existing national grid. For wind power development, an accurate knowledge of the availability of wind and its intensity over the year is a must.

## SUMMARY

This chapter presented the review the population and electricity demand growth on global, Middle East and Saudi Arabian level. The percent increasing rates of population and energy are alarming on all scales and particularly on Middle East and Saudi Arabian level. These trends dictate the community to utilize and develop new and renewable sources of energy on all levels, Saudi Arabia is not an exception. This effort has to be extended to the point where we see some real time visible wind power working projects in Saudi Arabia.

## CHAPTER 3

### LITERATURE REVIEW

To understand the status of any research area, a comprehensive literature review has to be carried out to provide a handy guide to a particular topic. In the present case, a large number of research papers published in international journals have been consulted to understand the status of the art of wind power technology existing in the world. More specifically, the study sought answers to the following questions. What is grid-connected wind power? What are the meaning and technology of producing hybrid power? What are the design tools? What has been done? How has it been done? What is the cumulative global wind power installed capacity? Detailed literature reviews related to different topics are provided in the following sections.

#### 3.1 GLOBAL WIND POWER SCENARIO

The continued growth and expansion of the wind power industry in the face of a global recession *and* a financial crisis is a testament to the inherent attractiveness of the technology [20]. Wind power is clean, reliable and quick to install. It is the leading electricity generation technology in the fight against climate change, while it also enhances energy security, stabilises electricity prices, cleans up air and creates thousands of quality jobs in the manufacturing sector. The Global Wind Energy Council's (GWEC's) prediction of 12% growth in the wind sector was generally met with disbelief and derision but the global market grew by 41%, demonstrating that wind power is increasingly the power technology of choice. Wind power proved to be the leading power sector over all others by a substantial margin in the US and Europe, and with another fantastic year of more than 100% growth in China [20]. The short-term projections are once again cautious, but will increase to 200GW of installed wind power capacity at the end of 2010, doubling to 400GW by the end of 2014 [20].

The annual cumulative wind power installed capacities are shown in Figure 3.1. In fact, the annual market grew a staggering 41.5%, [compared with 2008]. More than 38GW of new wind power capacity was installed around the world in 2009, bringing the total installed capacity up to 158.5GW. This represents a year-on-year growth of 31.7%, as can be seen from Figure 3.2. One third of these additions were made in China, which doubled its installed capacity yet again. Since 2005, the global wind power growth has always been more than

25%. Wind energy is now an important player in the world's energy markets. The 2009 market for turbine installations was worth about € 45 billion or US\$ 63 billion and GWEC estimates that about half a million people are now employed by the wind industry around the world. The main markets driving this growth continue to be Asia, North America and Europe, each of which installed more than 10GW of new capacity in 2009. For the first time, Asia was the world's largest regional market for wind energy, with capacity additions amounting to 15.4GW. The regional wind power cumulative capacities are concentrated in Europe, Asia and North America, as shown in Figure 3.3.

**In Asia, China** was the world's largest market in 2009, more than doubling its capacity from 12.1GW in 2008 to 25.8GW, adding a staggering 13.0GW of capacity. China slipped past Germany to become the world's second largest wind power market by a very narrow margin. **India** also continued growing its wind market with 1.3GW of new installed capacity, bringing its total up to 10.9GW. The leading wind power state remains Tamil Nadu with 4.3GW installed, followed by Maharashtra and Karnataka. With the introduction of a national Generation Based Incentive at the end of 2009, and a real push by the government to support renewable energy development, substantial growth is expected in the near future, and the industry forecasts additions of at least 2.2GW for 2010. Other Asian countries with new capacity additions in 2009 include **Japan** (178MW, taking the total to 2.1GW), **South Korea** (112MW for a total of 348MW) and **Taiwan** (78MW for a total of 436MW).

**In North America**, the US wind energy market installed nearly 10 GW in 2009, maintaining its global leadership in installed capacity, increasing the country's installed capacity by 39% and bringing the total installed grid-connected capacity to 35GW. Texas remains the leading state with more than 9GW of total installed capacity, with Iowa in second place with 3 670MW, followed by California, Washington state and Minnesota. In terms of new capacity added in 2009, Texas again led the pack with 2 300MW, followed by Indiana, which got started in wind late in 2008, and installed more than 900MW in 2009. Oregon, Iowa and Illinois round out the top five in new capacity added in 2009. Canada also experienced a record year with 950MW of new capacity additions, bringing its total up to 3.3GW. For the first time, every province now has an operating wind farm, collectively generating enough electricity to power more than one million Canadian homes, or about 1.1% of Canada's total electricity production.

**In Europe**, once again, more wind power was installed than any other power technology, accounting for 39% of the total new generation capacity. A total of 10.5GW was installed in Europe last year, including 582MW offshore, taking the total wind power capacity up to 76.2GW. While the traditional wind markets in Germany and Spain continue to drive investment, other ‘second-wave’ countries are now firmly established, with new capacity additions of over 1 000MW in 2009 in Italy, France and the UK. Eleven out of the EU’s 25 member states now have more than 1GW of wind power capacity. Investment in new European wind farms in 2009 reached €13 billion, including €1.5 billion offshore. The wind capacity installed by the end of 2009 will in a normal year produce 163TWh of electricity, meeting 4.8% of total EU power demand. **Germany** continues to lead Europe, adding 1.9GW in 2009 for a total capacity of 25 777MW. In 2009, 38TWh of wind-generated electricity was generated in Germany. The German wind power sector now employs around 100 000 people.

The cumulative installed capacities of the top 10 wind power producers until the end of 2009, namely the United States of America, Germany, China, Spain, India, Italy, France, the United Kingdom, Portugal and Denmark, are depicted in Figure 3.4 and the respective percentage contribution of these nations is shown in Figure 3.5. China was the world’s largest market in 2009, nearly doubling its wind generation capacity from 12.1GW in 2008 to 25.1GW at the end of 2009 with new capacity additions of 13GW as can be seen from Figure 3.6. However, the US continues to have a comfortable lead in terms of total installed capacity. Against all expectations, the US wind energy market installed nearly 10GW in 2009, increasing the country’s installed capacity by 39% and bringing the total installed grid-connected capacity to 35GW. Europe, which has traditionally been the world’s largest market for wind energy development, continued to see strong growth, also exceeding expectations. In 2009, 10.5GW was installed in Europe, led by Spain (2.5GW) and Germany (1.9GW). Italy, France and the UK all added more than 1GW of new wind capacity each.

Wind energy is already making a significant contribution to saving CO<sub>2</sub> emissions. The 158GW of global wind capacity in place at the end of 2009 will produce 340TWh of clean electricity and save 204 million tons of CO<sub>2</sub> every year. In year 2009, more than 89% of the wind power capacities were added by the 10 countries mentioned above and the remaining by the rest of the world. Of this, China alone contributed 38.84% while the US, Spain, Germany, India, Italy, France, the UK, Canada, and Portugal added wind power capacities in decreasing order as shown in Figure 3.7.

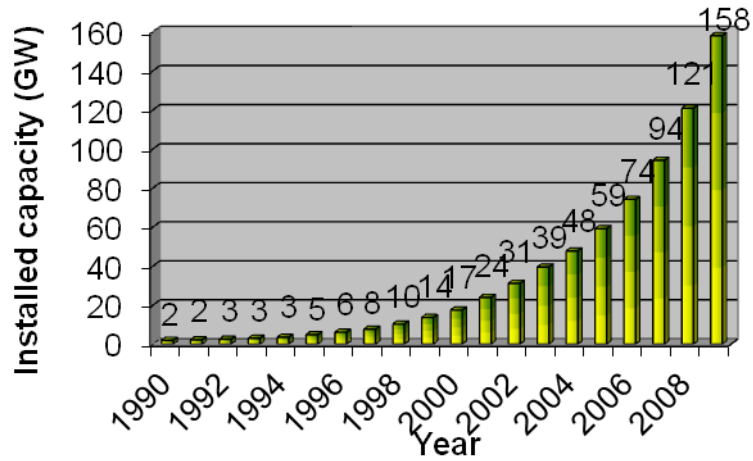


Figure 3.1 Global wind power cumulative installed capacity

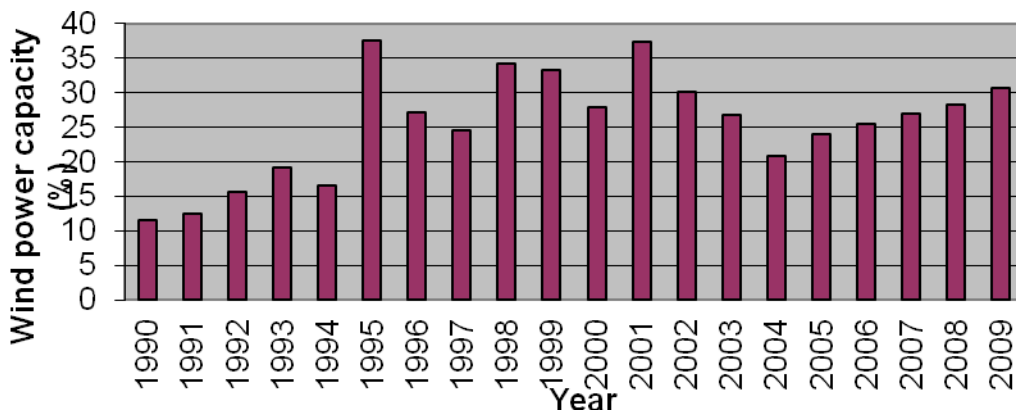


Figure 3.2 Annual (year to year) percentage wind power installed capacity

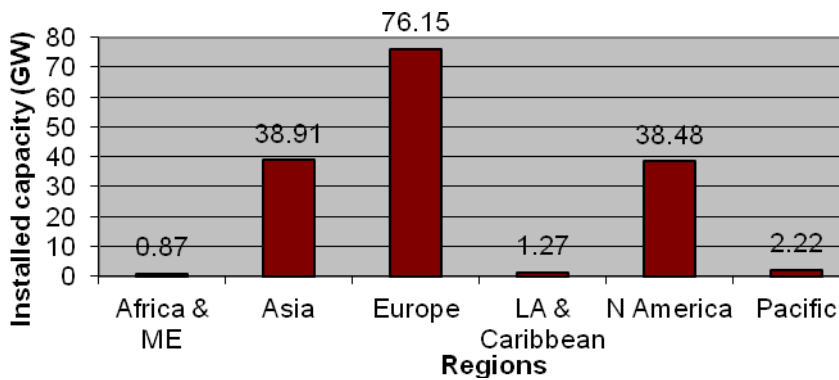


Figure 3.3 Regional cumulative share of wind power up to 2009

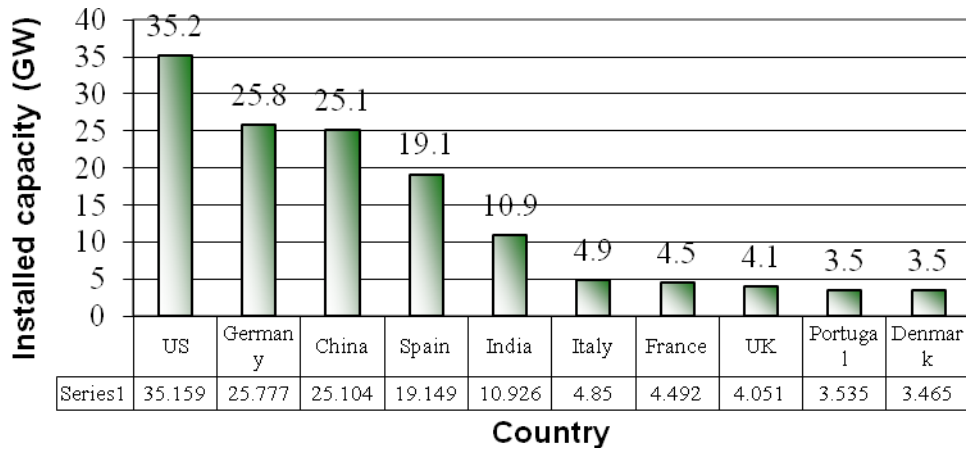


Figure 3.4 Cumulative wind power installed capacity of top 10 countries up to 2009

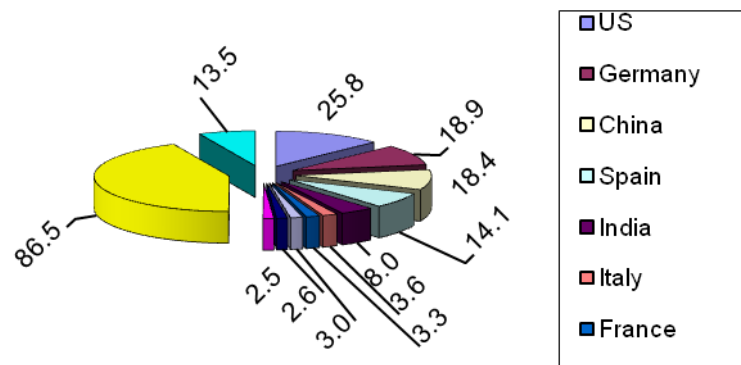


Figure 3.5 Percentage wind power contribution of top 10 countries up to 2009

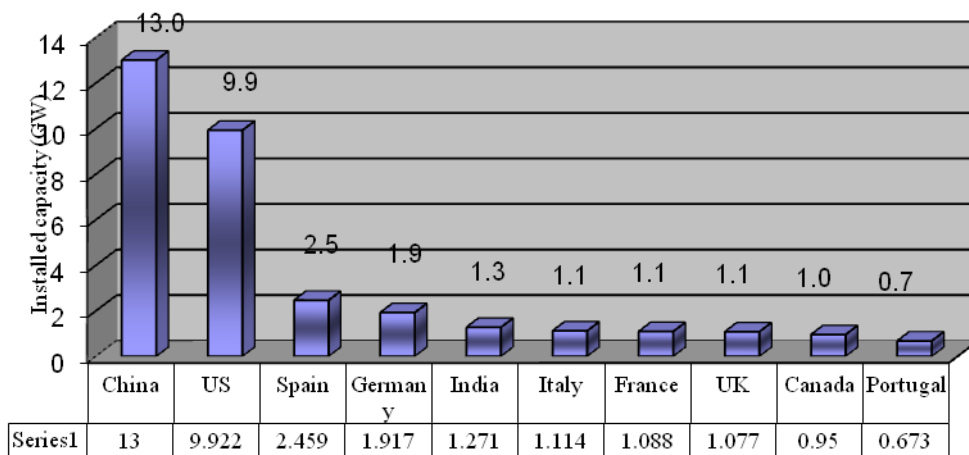


Figure 3.6 Wind power installed capacities for year 2009 for top 10 countries

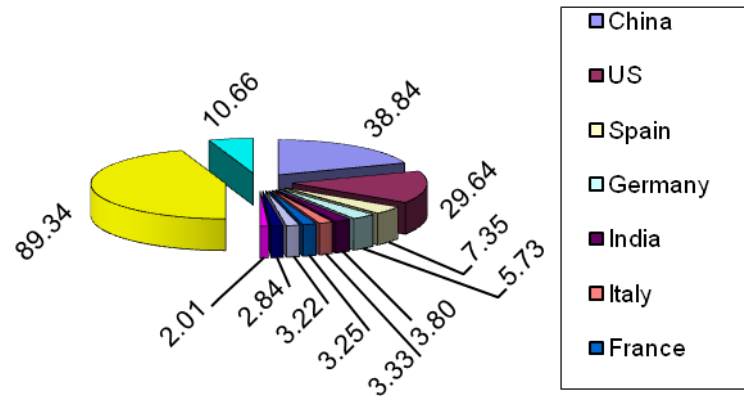


Figure 3.7 Percentage wind power contribution in 2009 by top 10 countries

### 3.2 WIND POWER RESOURCE ASSESSMENT

An accurate wind resource assessment is an important and critical factor to be well understood for harnessing the power of the wind. It is well known that an error of 1% in wind speed measurements leads to almost 2% error in energy output. The wind-power-based applications include grid-connected wind farms and hybrid power systems for isolated grids and remotely located small applications. The beauty of wind is that it is available everywhere 24 hours of the day. The question is how much for which duration? This question requires a perfect and accurate response which can be answered with confidence by conducting wind measurements at the sites of interest. As it is known that wind resources are seldom consistent and vary with time of day, season of the year, height above ground, type of terrain, and from year to year, hence these factors should be investigated carefully and completely. According to Tennis et al. [21], the wind resource assessment powering a wind farm project is as fundamental to the project's success as rainfall is to alfalfa production. Therefore, one who is interested in a wind farm development should know that how strong are the winds at the site of interest and how much energy will the wind farm produce in these winds. Potts et al. [22] performed the wind resources assessment of Western and Central Massachusetts using WindMap software which is based on geographic information systems (GIS). The authors utilised wind speed data from five locations and upper air data from one location as input to WindMap software to produce estimates of wind speed at 50metre. Brower [23] used GIS based tools to develop wind resource map for New Mexico using wind speed data from 67 stations and elevation data in the region.

In Saudi Arabia, a good deal of work is reported in the literature on various aspects of wind energy such as its measurements, conversion and utilisation. Rehman [24] presented the energy output and economical analysis of 30 MW installed capacity wind farms at five coastal locations in terms of unadjusted energy, gross energy, renewable energy delivered specific yield, and plant capacity factor using wind machines of 600, 1 000 and 1 500kW. In another study, Rehman [25] conducted a detailed analysis of wind speed in terms of energy yield, effect of hub height on energy yield, plant capacity factor, etc. for an industrial city situated on the north-west coast of Saudi Arabia. Rehman and Aftab [26] conducted a detailed wind data analysis of wind power potential assessment for five coastal locations in Saudi Arabia. Rehman et al. [27] computed the cost of energy generation at 20 locations in Saudi Arabia using the net present value approach. Al-Abbadi [28] utilised wind speed measurements taken at 20, 30 and 40 metres above ground level for five locations for wind power assessment. The author utilised the modern wind turbine of 600kW rated capacity and found annual energy yields of 1 080, 990, 730, 454 and 833MWh for Dhulom, Arar, Yanbo, Gassim and Dhahran, respectively. Earlier, in another study, Al-Abbadi et al. [29] and Alawaji [30] presented a wind resource assessment in Saudi Arabia.

Rehman and Halawani [31] presented the statistical characteristics of wind speed and its diurnal variation. The autocorrelation coefficients were found to match the actual diurnal variation of the hourly mean wind speed for most of the locations used in the study. Rehman et al. [32] calculated the Weibull parameters for 10 anemometer locations in Saudi Arabia and found that the wind speed was well represented by the Weibull distribution function. With growing global awareness of the usage of clean sources of energy, wind energy in particular, a lot of work is being carried out in different parts of the world, as can be seen from Jaramillo and Borja [33] for La Ventosa, Mexico; Kainkwa [34] for Basotu in Tanzania; Celik [35]; Ackermann and Soder [36]; Jebaraj and Iniyani [37]; Perez et al. [38]; Akpınar and Akpınar [39]; Acker et al. [40] for Arizona, USA; Shata and Hanitsch [41 and 42] for Egypt; Hrayshat [43] for Jordan; Bagiorgas and Assimakopoulos [44] for western Greece; Jiang et al. [45] for Inner Mongolia in China; Ulgen et al. [46] and Eskin et al. [47] for Turkey; El-Osta and Kalifa [48] for Libya; Omar [49] for Sudan; Himri et al. [50] for Algeria; and many others.

Chang and Tu [51] analysed monthly energy outputs and capacity factors of an existing medium-scale wind power station located in Mailiao, Taiwan and demonstrated that the

capacity factors calculated from the time series approach have better agreement with the actual capacity factors than the Weibull approach. In India, the wind power generation has gained a high level of attention and acceptability compared with other renewable energy technologies [52]. Mabel and Fernandez [52] presented a review of the development of wind energy in India and five potential Indian states. Ngala et al. [53] presented a statistical analysis of wind energy potential in Maiduguri using Weibull distribution and 10 years (1995–2004) of wind data. The study concluded that there is a good prospect of wind energy utilisation in Borno state, Nigeria. The wind speed was high enough to support wind power generation and supply. Elamouri and Ben Amar [54] used meteorological data from 17 stations in Tunisia to evaluate the wind speed characteristics and the wind power potential at a height of 10m above ground level and in an open area. An extrapolation of these characteristics with the height was also carried out. The results indicated a global vision of the distribution of the wind potential in Tunisia and defined the windy zones.

Mostafaeipour and Abarghoeei [55] analysed wind speed at different sites in Manjil and showed that these sites have a great potential for harnessing wind energy. The potential for wind power generation is estimated to be 6 500MW with the majority of the locations situated in the eastern and northern parts of the country. Manjil has winds that can result in as much as 1 609kWh/m<sup>2</sup> per year at the 40-metre elevation above ground. Mirza et al. [56] discussed the past, the present and the future of wind energy use in Pakistan. The efforts towards the utilisation of wind energy in the country were presented as well as the barriers to its development. It was concluded that the potential exists, but significant efforts are needed to effectively make use of this efficient renewable energy source. Tar [57] used statistical methods to analyse the time series of monthly average wind speed in the period between 1991 and 2000 measured on seven Hungarian meteorological stations. Empirical distribution of measured monthly average wind speeds was approximated by theoretical distributions to claim that certain distributions are universal, i.e. independent of orography.

Radics and Bartholy [58] studied the structure of the vertical wind profile and the relationships between atmospheric stability and different errors of empirical wind profile formulas using the data at different heights. The authors developed a wind energy map of Hungary using the Wind Atlas Analysis and Application Program. The most suitable region for wind energy utilisation was found to be the north-western part of the country; however, the south-eastern region of Hungary also possesses considerable wind energy resources. Dua

et al. [59] conducted a techno-economic feasibility study of installing utility-scale wind turbines on the Fox Islands, located 12 miles from the coast of Maine in the United States. They analysed three locations on the islands, as well as a near offshore site in detail as potential sites for wind turbine installations. As discussed in this work, the logistical problems of transporting and installing wind turbines on the island require innovative solutions. These include locally available amphibious vessels, which can land turbine components at suitable shallow spots on the island, self-erecting towers, which allow use of a smaller crane for installation, and a special turbine foundation suitable for the local ground conditions. In the economic analysis, in addition to standard life cycle parameters, renewable energy credits (RECs) were also included. Dua et al. [59] concluded that the installation of sub-megawatt wind turbines on the island is logistically possible and will lead to a reduction in the cost of electricity to the customers.

Dhanju et al. [60] described a method for assessing the electric production and value of wind resources, specifically for the offshore environment, and found year-round average output of over 5 200MW, or about four times the average electrical consumption of the state. On local wholesale electricity markets, this would produce just over \$2 billion/year in revenue. Marciukaitis et al. [61] reviewed a wind energy resource assessment experience as well as the current situation and the future prospective of wind energy usage in Lithuania. The main features of Lithuanian electrical system and issues related to wind energy integration in electrical networks are discussed.

### **3.3 WIND SPEED PREDICTION**

One of the major hurdles in the usage and development of wind power resources is the intermittent nature of the availability of wind during 24 hours of the day and seven days a week. Hence to assure a certain level of wind power penetration level into an existing conventional energy grid system, one has to determine the instant potential of the regions. Therefore, for an accurate wind power assessment, accurate wind speed measurements or estimates should be available at the site of wind farm development and also in future time domain. The wind velocity measurement network is still very sparse even in developed countries the more so in developing countries. In Saudi Arabia, there are around 30 meteorological stations, mostly at national and international airports, maintained by the Presidency of Meteorology and Environment (PME), a government organisation.

Short-term wind speed forecasting is of great importance for wind farm operations and the integration of wind energy into the power grid system. Adaptive and reliable methods and techniques of wind speed forecasts are urgently needed in view of the stochastic nature of wind resource varying from time to time and from site to site [43]. Gong et al. [62] used hourly average wind speed data from two North Dakota sites to demonstrate the effectiveness of the proposed approach. The results indicate that, while the performances of the neural networks are not consistent in forecasting one-hour-ahead wind speed for the two sites or under different evaluation metrics, the Bayesian combination method can always provide adaptive, reliable and comparatively accurate forecast results. Short-term wind speed forecasting is of great importance to control the dynamic aspects of a wind turbine so that the blades and electrical system can be quickly adjusted to respond to the predicted change in wind speed [63].

Integration of wind energy into power grid system is crucial for decision-making on the scheduling, maintenance and resource planning. For example, wind forecasts in the range of hours determine the issues of scheduling in a power system and forecasts in the range of days affect the maintenance and resource planning. Meanwhile, the electricity generated from wind power is still unsteady, comparatively high in cost, and difficult to integrate into traditional electricity systems, which is also mainly due to the stochastic nature of wind resource from time to time and from site to site. Along with the rapid development of wind power generation and the increasing integration of wind energy into power systems, reliable methods and techniques of wind speed forecasting are becoming more and more important and urgently needed for the characterisation and prediction of wind resource [64] as well as for the integration of wind energy into power systems [65].

To date, much research efforts have been made on developing effective methods for wind speed forecasting. The approaches in the literature to wind speed forecasting include physical methods, such as numerical weather forecast (NWF) and mesoscale models [66], conventional statistical methods such as BoxeJenkins or ARIMA models [67-69], hybrid physical and statistical models, and others [70 and 71]. In recent years, artificial intelligence techniques have been adopted for the purpose of wind speed forecasting, such as neural networks (NN) of multilayer perceptrons (MLP) [72 and 73], radial basis functions [74], recurrent neural networks [75 and 76] and fuzzy logic [77 and 78].

Damousis et al. [79] developed a fuzzy model to perform forecasting of wind speed and electrical power up to two hour ahead. Their model was trained with measured wind data from neighbouring meteorological stations at a radius of up to 30km. Their method provided significant improvement over the persistent method for a flat terrain. A recent paper by Alexiadis et al. [80] examined the contribution of data from local and remote sites to forecasting using neural network models, and suggested a possible way to improve prediction accuracy. A significant correlation of hourly or daily average speeds has been recognised for distances of 20 to 100km. However, it is to be noted that this correlation decreases with distance as pointed out by Corotis et al. [81] and topographical elevation difference as reported by Beyer et al. [82]. The correlation between the predicted and the measured wind speed values also decreases when the orientation of the distance vector differs from the wind direction [83]. The method presented by Bechrakis and Sparis [84] utilises wind speed at one particular site to simulate the wind speed at another, nearby site. Furthermore, the method takes into account the evolution of the sample cross correlation function (SCCF) of wind speed in time domain and uses an artificial neural network to perform the wind speed simulation. Tests showed that the higher the SCCF value between two sites, the better the simulation achieved.

Öztopal [85] used weighting factors of surrounding stations for the prediction of wind speed at a pivot station by an artificial neural network (ANN) technique. The author used daily wind velocity measurements in the Marmara region from 1993 to 1997 and found that the ANN model is more appropriate for winter period daily wind velocities prediction. Cadenas and Rivera [86] used autoregressive integrated moving average (ARIMA) and the artificial neural networks (ANN) methods for the prediction of wind speed and then assessment of available wind power. The authors used six years of data for the formulation of the models and the seventh year's data was utilised to validate and compare the effectiveness of the generated prediction by the two techniques mentioned above. Nevertheless, it was shown that both developed models can be used to predict in a reasonable way the monthly electricity production of the wind power stations in La Venta, Oaxaca, Mexico to support the operators of the Electric Utility Control Centre.

Bilgili et al. [87] applied artificial neural networks (ANNs) to predict the mean monthly wind speed of any target station using the mean monthly wind speeds of neighbouring stations, which are indicated as reference stations. Hourly wind speed data, collected by the Turkish

State Meteorological Service (TSMS) at eight measuring stations located in the eastern Mediterranean region of Turkey during the years 1992 to 2001, was used. Finally, the values determined by the ANN model were compared with the actual data. The maximum mean absolute percentage error was found to be 14.13% for the Antakya meteorological station and the best result was found to be 4.49% for the Mersin meteorological station. Artificial neural network (ANN) is a promising methodology in wind speed prediction as can be seen from references [88-92]. Lapedes and Farber [88] proposed an ANN along with feedforward and error back-propagation algorithm for wind speed prediction. Song [89] developed an ANN-based model to perform one-step-ahead prediction, which is found to be good when the wind data does not change rapidly. Alexiadis et al. [90] also found that the ANN predictor is about 10% better than persistence model for one-step-ahead prediction. Bechrakis and Sparis [91] applied the artificial neural network method for the prediction of wind speed variations at a given site utilising past values of wind speed as input. This method demonstrated optimum results for three-day period predictions. The forecasted mean wind speed, the standard deviation and the corresponding energy are compared with the actual values. The method proposed by Lopez et al. [92] uses only a few measurements taken at the selected site in a short time period and data collected at nearby fixed stations. The results obtained by simulating the annual average wind speed at the selected site based on data from nearby stations are satisfactory, with errors below 2%.

Multi-model techniques can provide consensus predictions by linearly combining individual model predictions according to different weighting strategies [93 and 94]. As one typical multi-model method, the Bayesian model averaging (BMA) has recently gained popularity in various fields because it can produce more adaptive and reliable predictions than other techniques [95-98]. In a previous study, the BMA approach demonstrated its capability of describing long-term wind speed distributions with high reliability and robustness [99]. Therefore, it is appealing to apply the Bayesian method to combine the short-term wind speed forecasts from different NN models. In view of this, this paper proposes to apply the BMA algorithm to combine one-hour-ahead wind speed forecasts from three competing NN-based models (ADALINE, BP, RBF), aiming to develop an adaptive and robust methodology for short-term wind speed forecasting.

Sancho et al. [100] presented the hybridisation of the fifth-generation mesoscale model (MM5) with neural networks in order to tackle a problem of short-term wind speed

prediction. The mean hourly wind speed forecast at wind turbines in a wind park is an important parameter used to predict the total power production of the park. This model for short-term wind speed forecast integrated a global numerical weather prediction model and observations at different heights (using atmospheric soundings) as initial and boundary conditions for the MM5 model. Then, the outputs of this model were processed using a neural network to obtain the wind speed forecast in specific points of the wind park. The results of the study were encouraging, and showed that the hybrid MM5 neural network approach is able to obtain good short-term predictions of wind speed at specific points. Lazar et al. [101] applied the regional atmospheric numerical weather prediction Eta model and described its performance in validation of the wind forecasts for wind power plants. Two sets of Eta model forecasts were made: one with a coarse resolution of 22km, and another with a nested grid of 3.5km, centred on the Nasudden power plants, (18.22°E, 57.07°N; 3metre) at Gotland island, Sweden. The Eta model is compared against the wind observed at the nearest surface station and against the wind turbine tower 10metre wind. Four common measures of accuracy relative to observations - mean difference (bias), mean absolute difference, root mean square difference and correlation coefficient are evaluated. In addition, scatter plots of the observed and predicted pairs at 10 and 96 m were generated. Average overall results of the Eta model 10 m wind fits to tower observations were: mean difference (bias) of 0.48 m/s, mean absolute difference of 1.14 m/s, root mean square difference of 1.38 m/s, and the correlation coefficient of 0.79. Average values for the upper tower observation levels were the mean difference (bias) of 0.40 m/s; mean absolute difference of 1.46 m/s; root mean square difference of 1.84 m/s and the correlation coefficient of 0.80.

Many research papers describe wind power forecasting systems using wind obtained from a numerical weather prediction (NWP) model. In their paper, Lei et al. [102] gave a bibliographical survey of the general background of research and developments in the fields of wind speed and wind power forecasting. Landberg et al. [103] provided an overview of the different methods used today for predicting the power output from wind farms on the one-to two-day time domain. They described the general set-up of such prediction systems and also gave examples of their performance. Landberg [104] described a model for prediction of the power produced by wind farms connected to the electrical grid. The physical basis of the model is the predictions generated from forecasts from the high-resolution limited area model (HIRLAM). Ramirez-Rosado et al. [105] presented a comparison of two new advanced statistical short-term wind-power forecasting systems developed by two independent research

teams. The input variables used in both systems were the same: forecasted meteorological variable values obtained from the NWP. Nutter and Manobianco [106] presented an objective verification of the 29km Eta model from May 1996 to January 1998. The evaluation was designed to assess the model's surface and upper-air point forecast accuracy at three selected locations during separate warm (May–August) and cool (October–January) season periods. O'Connor et al. [107] described the operation and verification of a surge warning system for lake Erie, showing a high correlation of the predicted wind speed by the Eta model and the observed water levels. Numerous studies are available concerning verification of the Eta model for different regions and different variables (e.g. [108–114]).

Kavasseri and Seetharaman [115] examined the use of fractional autoregressive integrated moving average (f-ARIMA) models to model, and forecast wind speeds on one-day-ahead (24h) and two-day-ahead (48h) horizons. The models were applied to wind speed records obtained from four potential wind generation sites in North Dakota. The forecasted wind speeds were used in conjunction with the power curve of an operational (NEG MICON, 750 kW) turbine to obtain corresponding forecasts of wind power production. The forecast errors in wind speed/power were analysed and compared with the persistence model. Results indicate that significant improvements in forecasting accuracy were obtained with the proposed models compared with the persistence method. Customarily, the persistence method is used to benchmark the accuracy of a newly proposed forecasting method. Both ARMA [116 and 117] and ARIMA models [118] have been applied in the past to predict hourly average wind speeds. As alternatives, the use of artificial neural networks [119 and 120], including a method that factors spatial correlations of wind speeds, has been proposed towards obtaining improved predictions compared with the persistence forecast.

Accurate forecasting of wind speed and wind power is important for the safety of renewable energy utilisation. Compared with physical methods, statistical methods are usually simpler and more suitable for small farms. Based on the methods of wavelet and classical time series analysis, a new short-term forecasting method is proposed. Simulation upon actual time data shows that: (1) the mean relative error in multistep forecasting based on the proposed method is small, which is better than the classical time series method and BP network method; (2) the proposed method is robust in dealing with jumping data; and (3) the proposed method is applicable to both wind speed and wind power forecasting [121]. Recently, researchers have proposed a number of methods to forecast wind speed and wind power, which can be

classified as physical methods and statistical methods. The physical methods have advantages in long-term prediction while statistical methods do well in short-term prediction. In the physical methods, physical models are used by considering terrains, obstacles, pressures and temperatures to estimate the future wind speed and generated power. The statistical methods use statistical models to predict the wind speed and wind power. Note that most newly proposed methods are combinations of physical methods and statistical methods [122–124]. Besides, many researchers have been studying spatial correlation models [125], which take the spatial relationship of the wind speed or the wind power of different sites into account. These kinds of models can usually attain higher prediction accuracy. Furthermore, various intelligent technologies have been used for such forecasting, including ANN [126], Kalman filter [127] and some hybrid methods [128].

Cadenas and Rivera [129] presented wind speed forecasting on the Isla de Cedros in Baja California, in the Cerro de la Virgen in Zacatecas and in Holbox in Quintana Roo. The time series utilised are average hourly wind speed data obtained directly from the measurements realised on the different sites during approximately one month. In order to do wind speed forecasting, hybrid models consisting of autoregressive integrated moving average (ARIMA) models and artificial neural network (ANN) models were developed. Statistical error measures such as the mean error (ME), the mean square error (MSE) and the mean absolute error (MAE) were calculated to compare the three methods. The results showed that the hybrid models predict the wind velocities with a higher accuracy than the ARIMA and ANN models on the three examined sites. Spatial correlation models take into account the spatial relationship of the wind speed on different sites. The wind speed time series of the predicted points and its neighbouring sites are employed to predict the wind speed on a new site. This kind of model has been used recently by a number of authors [130-132]. Lalarukh and Yasmin [133] used an ARMA model for wind speed forecasting using data of two years with non-Gaussian distribution and diurnal non-stationary. The conclusion was that forecast values of variance and wind speed with a confidence interval of 95% can be acceptable both for short-and long-term prediction. Sfetsos [134] presented a novel approach based on an ANN model for the forecasting of mean hourly wind speed time series. Ten minutes' data was used to carry out multistep forecasting, and the average results were used to generate the mean hourly predictions. It produced root mean square errors about four times lower than other models which were based on mean hourly data.

Hamzaçe [135] proposed an artificial neural network structure for four seasonal time series forecasting. The results obtained with the model were compared with the results of traditional statistical models and other ANN architectures. The comparison showed that the proposed model has a lower prediction error than other methods. It was concluded that the proposed model is especially convenient when the seasonality in time series is strong. Kalogirou [136] published a paper about various applications of neural networks mainly to renewable energy problems such as: solar steam generator, solar water heating systems, photovoltaic systems and solar radiation and wind speed prediction. The errors reported in the models were within acceptable limits, that is the reason why the author concluded that artificial neural networks can be used for modelling in other fields of renewable energy production and use. The intuitive technique, denominated as iterative method, has been used by several researchers to generate forecasting [137-139].

### **3.4 WIND SHEAR EXPONENT (WSE)**

Modern wind turbines are efficient and capable of producing more power as the height of the turbine rotor increases. Wind speed increases with height and hence the power output from the wind turbines. Therefore, for accurate assessment of wind power potential at a site, one should have precise knowledge of wind speed at different heights. This can be achieved either by measuring wind speed at the hub height of interest or by estimating using  $1/7^{\text{th}}$  wind power law. The wind power law cannot provide the actual estimation of wind speed at hub height and hence will result in inaccurate assessment of wind power. The best and economical way is to make wind speed measurements at two or three heights for a period of at least one year and then calculate the wind shear exponent (WSE) using measured values. This wind shear coefficient can then be used with confidence to estimate the wind speed at hub height.

Wind shear is the variation of wind speed with elevation and is highly site-dependent. It is a critical parameter and it directly affects the power output from wind turbines at different hub heights [140]. To cope with the higher hub heights of the order of 60 to 120 metres of modern today's wind turbines, the prior knowledge of wind shear has become very important [141]. Unfortunately, wind measurements are usually made at a height lower than the turbine hub height, e. g. 10-20 metres above ground level (AGL) vs. a hub height of 60-120 metres. This problem is generally solved by extrapolating surface wind speed to the hub height by using the well-known  $1/7^{\text{th}}$  wind power law. In fact, wind speed proved to increase with height by a

power factor known as wind shear exponent (WSE). WSE is highly affected by the site where measurements are made, as it depends on atmospheric stability, wind speed, terrain type (and thus surface roughness length), and the height interval [142 and 143]. In general, higher exponents are found in urban areas with tall buildings (0.40), small towns (0.30), or areas with many trees (0.24), whereas lowest values (0.10) occur over smooth hard ground, lake or ocean [144].

In principle, the  $1/7$  (0.143) value of WSE is only reasonable over smooth grass-covered terrain to describe wind profiles up to the first 100metres during near-neutral (adiabatic) conditions [145]. Therefore, it should be intended as a rough estimate to be used, at least at a pre-feasibility stage, only when upper-air data is missing. As a consequence, if the actual WSE is greater than 0.143, then wind power law will lead to an underestimation of actual wind speed and thus wind energy, otherwise an overestimation will result. Hence an accurate computation of WSE is essential for actual wind power estimates, which are generally made by measuring wind speed at two or three heights over at least a one-year period. Unfortunately, WSEs are rarely known because wind speed is usually measured at one height by most of the meteorological stations worldwide. There are few locations, mostly in developed countries, where wind speeds are measured at more than one height [146].

A number of massive measuring campaigns have been carried out through the years over several US states [147-151]. For example, Smith et al. [147] measured annual mean WSEs of 0.11 and 0.33 through the 25-40 and 25-50metres AGL height intervals, respectively, for two Midwest locations. Over a mountainous location in New Mexico [148], WSC was reported to be 0.24 between 25 and 40metres. WSCs were broadly measured based on long-term campaigns over a number of Minnesota sites [149]. In particular, between 10 and 40metres for sites located over treeless hills (i.e. Marshall and Chandler), values ranging from 0.19 to 0.22 were found. Through the 30-50 and 30-60metres height intervals, WSEs have been measured to be 0.17 and 0.26 over treeless hilly sites such as Currie and St. Killian, respectively, 0.29 in the treeless flat site of Hatfield, and 0.36 and 0.54 over forested locations such as Hillman and Isabella, respectively. For Brewster, Rogers [150] found an annual mean WSC of 0.38 between 38 and 49metres. Over Central Plains, Schwartz and Elliott [151] measured mean WSCs of 0.195 and 0.227 between 40 and 70metres, as well as values ranging from 0.170 to 0.254 through height intervals over 50metres.

As far as countries other than the US are concerned, over the Mediterranean island of Malta, using wind speed measured at 10 and 20metres through a six-year period, Farrugia [145] found an overall WSE mean value of 0.36. To calculate WSE over Saudi Arabia, Rehman and Al-Abbadi carried out two different studies, using wind measurements at 20, 30 and 40m. Over the coastal location of Dhahran, based on a five-year data sample, they found an annual mean WSC of 0.189 [146], while for the elevated, treeless flat site of Dhulom, based on a four-year data sample, they reported an overall value of 0.255 [141]. Again in Saudi Arabia at 20, 30 and 40metres, over an open and flat location, Rehman et al. [152] reported a mean WSE in the range of 0.319-0.348. In the coastal location of La Ventosa (Mexico), processing a 2.5-year wind data set, Jaramillo and Borja [153] measured an annual mean WSC of 0.166 through 15-32metres. In Hungary, based on a two-year data set, Tar [154] reported a remarkable mean WSC value of 0.45-0.50 between 20 and 50metres. Gualtieri and Secci [155] computed wind shear coefficients (WSCs) based on one-hour measured wind data for three stations located over coastal sites in southern Italy, namely Brindisi (BR), Portoscuso (PS) and Termini Imerese (TI). WSC overall mean values were found to be 0.271 at BR, 0.232 at PS and 0.15 at TI.

Rehman and Al-Abbadi [156] estimated realistic values of wind shear coefficients for Arar using measured values of wind speed at 20, 30 and 40metres above ground level, for the first time in Saudi Arabia in particular and to the best of the authors' knowledge in the Gulf region, in general. The paper also presents air density values calculated using the measured air temperature and surface pressure and effect of wind shear factor on energy production from wind machines of different sizes. The measured data used in the study covered a period of almost three years between June 17, 1995 and December 31, 1998. An overall mean value of wind shear coefficient of 0.194 can be used with confidence to calculate the wind speed at different heights if measured values are known at one height. The study showed that the wind shear coefficient is significantly influenced by seasonal and diurnal change. Hence for precise estimations of wind speed at a specific height, either monthly or seasonal and hourly or nighttime and daytime average values of wind shear coefficient must be used. It is suggested that the wind shear coefficients must be calculated using long-term average values of wind speed at different heights. Al-Abbadi and Rehman [157] used wind measurements at different heights for several years and recommended a value of WSE of 0.337 for the estimation of wind at different heights AGL for Gassim measurement site. Rehman and Al-Abbadi [158] used measured values of wind speed at 20, 30 and 40metres above ground level along with

other meteorological parameters to study the wind characteristics and wind energy yield. The measured data covered a period of almost 36 months between September 17, 1996 and October 21, 1999. Almost the same annual mean wind speeds were found at different heights with a very small value of wind shear exponent of 0.062.

Some of the studies which reported the WSE values include the study of Hall and Smith [159] for Midwest TVP site; Oklahoma Wind Power Initiative [160] and Smith et al. [161] for Big Spring, Ft. Davis, Iowa, Nebraska. According to Sisterton et al. [162], WSC of the order of 0.5 may be found between 30 and 150metres and in extreme cases may reach as high as 1.0. Michael et al. [163] calculated wind shear coefficients for 12 Minnesota sites, which have been in operation since 1995 or earlier. They found considerable variation (0.2 – 0.4) in the values of wind shear exponent from location to location. According to Brower [164], higher exponents are usually associated with rougher terrain and taller vegetation or other nearby obstacles. The wind shear coefficients were found to vary from 0.16 to 0.27 at all Iowa Wind Energy Research Institute sites and over all months with an overall average of 0.21 [164].

### **3.5 WEIBULL SHAPE AND SCALE PARAMETERS**

Weibull distribution is characterised by two parameters: the shape parameter  $k$  (dimensionless) and scale parameter  $c$  (m/s). The shape factor reflects the breadth of the distribution, with lower values corresponding to broader distributions where the wind speed tends to vary widely, whereas higher  $k$  values correspond to tighter distributions where the wind speed tends to stay within a narrower range. Weibull is a widely used distribution for the representation of wind speed frequency in different wind speed bins. Various methods have been developed for estimating the parameters of the Weibull probability distribution function. The most commonly used have been the method of moments [165-167], the maximum likelihood method [168], the least square method [169, 167 and 169] and the Chi-square method [167]. However, the maximum likelihood method has proved to be the most efficient [166 and 168] in determining the parameters of the Weibull probability distribution function.

Stevens and Smulders [170] obtained the values of  $k$  and  $c$  using five different methods: method of moments, method of energy pattern factor, maximum likelihood method, Weibull probability and the use of percentile estimators. The comparison of these analytical findings indicated that no significant discrepancies between the results from the different methods

were observed. Gupta [171] carried out work on estimating the annual and monthly Weibull parameters for five locations in India and these revealed two parameters which varied over a wide range. The values of the shape parameter could be used at hub height without any modification but the values of  $c$  required alteration that might be estimated from the usual power law, which generally holds good up to a height of 100metre. Justus et al. [172] applied the Weibull and log-normal distribution to wind speed data from more than a hundred stations of the US National Climatic Centre and concluded that the Weibull distribution rendered the best fit. Corotis et al. [173], however, preferred the Rayleigh distribution, a special case of Weibull distributions, for the wind data. Hennessey [174 and 175] used two parameter Weibull distribution function for wind speed representation and found that the energy output of WECS calculated by the Rayleigh distribution is within 10% of the output based on the Weibull distribution. Garcia et al. [176] carried out a case study on the performance of two different functions, the Weibull distribution and the log-normal distribution. The work indicated that both approaches fitted the data well. In particular, the Weibull distribution was pointed out to be the better distribution, which could provide a very useful model to estimate the potential wind energy.

Lysen [177], Justus and Mikhail [178], Darwish and Sayigh [179], Nfaoui et al. [180], Jamil et al. [181] and Khogali et al. [182] have all used different methods for the estimation of  $k$  and  $c$  parameters in different atmospheric conditions. Celik [183] reported that Weibull-representative data estimated the wind energy output very accurately with an overall error of 2.79%. Wind data for the years 2000 and 2001 was analysed to evaluate the wind potential at Mikra–Thessaloniki, Greece, by Vogiatzis et al. [184]. The polar diagrams of the mean monthly and annual wind speed profile and the Weibull distributions were presented. The Weibull distribution was found to be the best match to the actual probability distribution of wind data for most stations, according to Essa and Mubarak [185]. Rehman [186] presented the energy output and economical analysis of 30MW installed capacity wind farms at five coastal locations using wind machines of 600, 1 000 and 1 500 kW. With growing global awareness of the usage of clean sources of energy, wind energy in particular, a lot of work is being carried out in Saudi Arabia, as can be seen from Rehman and Aftab [187], Rehman and Halawani [188], Rehman et al. [189], Rehman [190], Rehman [191], Alawaji [192], Al-Abbadi et al. [193] and Al-Abbadi [194].

Recently, Safari and Gasore [195] conducted a statistical analysis of wind speed measured at five stations at 10metre above ground level in Rwanda. The authors used Weibull and Rayleigh distributions to evaluate the characteristics and the wind power potential at a height of 10metres above ground level. The results give a global picture of the distribution of the wind potential in different locations in Rwanda. Dahmouni et al. [196] performed a wind resource assessment for the Gulf of Tunis using wind speed measurements made at 20 and 30metres above ground level and Weibull distribution function and confirmed that the Gulf of Tunis has promising wind energy potential. Carta and Ramirez [197] used three most frequently used methods for the estimation of five parameters of the WW-pdf and the numerical methods. The authors used hourly mean wind speed data recorded at four weather stations located on the island of Gran Canaria (Spain) to analyse the estimation methods. The general conclusion is that if the sample data are independent then maximum likelihood (ML) estimators should be used due to their large sampling efficiency. The least-squares (LS) method provides a robust and computationally efficient alternative to the techniques currently in use. The method of moments has the disadvantage that it does not always supply a feasible result and lacks the desirable optimality properties of ML and LS estimators.

Ettoumi et al. [198] used Markov chains to model the wind speed and wind direction measured every three hours at the meteorological station of Es Senia (Oran), during the 1982/92 period. First-order nine-state Markov chains were found to fit the wind direction data well, whereas the related wind speed data fitted first-order three-state Markov chains well. The Weibull probability distribution function was found to fit the monthly frequency distributions of wind speed measurements [198]. According to Tuller and Brett [199], the two-parameter Weibull distribution (W-pdf) is the most widely used and accepted function in the specialised literature on wind energy and other renewable energy sources. To describe the statistical features of the wind speed at a given location, the usual method is to fit the experimental wind data with probability distributions as can be seen from references [200–203]. Eskin et al. [204] analysed wind data of four stations using Weibull probability density functions to find the wind speed distribution curves. Two Weibull parameters of the wind speed distribution function, namely shape parameter  $k$  (dimensionless) and scale parameter  $c$  (m/s) were calculated on monthly and yearly basis to find the wind profiles. Their results showed the general availability of wind energy potential across Gokceada island.

### 3.6 WIND POWER TECHNOLOGY

Wind is a form of solar energy. Winds are caused by the uneven heating of the atmosphere by the sun, the irregularities of the earth's surface and the rotation of the earth. Wind flow patterns are modified by the earth's terrain, bodies of water and vegetation. Humans use this wind flow, or motion energy, for many purposes: sailing, grinding grains, pumping water, flying a kite, and even generating electricity. The terms *wind energy* or *wind power* describes the process by which the wind is used to generate mechanical power or electricity. Wind turbines convert the kinetic energy in the wind into mechanical power. This mechanical power can be used for specific tasks (such as grinding grain or pumping water) or a generator can convert this mechanical power into electricity.

So how do wind turbines make electricity? A wind turbine works opposite to a fan. Instead of using electricity to make wind, like a fan, wind turbines use wind to make electricity. The wind turns the blades, which spin a shaft, which connects to a generator and makes electricity. Modern wind turbines fall into two basic groups: the horizontal-axis and the vertical-axis design. Horizontal-axis wind turbines typically either have two or three blades. These three-bladed wind turbines are operated "upwind," with the blades facing into the wind. Utility-scale turbines range in size from tens of kilowatts to as large as several megawatts. Larger turbines are grouped together into wind farms, which provide bulk power to the electrical grid. Single small turbines, below 100kW, are used for homes, telecommunications dishes, or water pumping. Small turbines are sometimes used in connection with diesel generators, batteries and photovoltaic systems. These systems are called hybrid power systems and are typically used in remote, off-grid locations, where a connection to the utility grid is not available

#### 3.6.1 *The working of a wind turbine*

In contrast to the windmills common in the nineteenth century, a modern power generating wind turbine is designed to produce high quality, network frequency electricity whenever enough wind is available. Wind turbines can operate continuously, unattended and with low maintenance with some 120 000 hours of active operation in a design life of 20 years. The rotors of modern wind turbines generally consist of three blades, with their speed and power controlled by either stall or pitch regulation. Stall regulation involves controlling the mechanical rotation of the blades and pitch regulation involves changing the angle of the

blades themselves. Rotor blades are manufactured from composite materials using fibreglass and polyester or fibreglass and epoxy, sometimes in combination with wood and carbon.

Energy captured by the steadily rotating blades is transferred to an electrical generator via a gearbox and drive train. Alternatively, the generator can be coupled directly to the rotor in a “direct drive” arrangement. Turbines able to operate at varying speeds are increasingly common, a characteristic which improves compatibility with the electricity grid. The gearbox, generator and other control equipment are housed within a protective nacelle. Tubular towers supporting the nacelle and rotor are usually made of steel, and taper from their base to the top. The entire nacelle and rotor are designed to move around, or “yaw”, in order to face the prevailing wind.

### **3.6.2 Commercial development**

Manufacturing of commercial wind turbines started in the 1980s, with Danish technology leading the way. From units of 20-60kW with rotor diameters of around 20 metres, wind turbine generators have increased in capacity to 2MW and above, with rotor diameters of 60-90metres [186]. The largest machine being manufactured now has a capacity of 4 500kW and a rotor diameter of 112metres. Some prototype designs for offshore turbines have even larger generators and rotors. Improvements are continuously being made in the ability of wind turbines to capture as much energy as possible from the wind. These include more powerful rotors, larger blades, improved power electronics, better use of composite materials and taller towers. One result is that fewer turbines are required to achieve the same power output, saving land use. Depending on its siting, a 1MW turbine can produce enough electricity for up to 650 households. Since the beginning of the 1980s, the power of a wind turbine has increased by a factor of more than 200. Wind turbines are highly reliable, with operating availabilities (the proportion of the time in which they are available to operate) of 98%. No other electricity generating technology has a higher availability [205].

### **3.6.3 Wind monitoring**

The wind resource is the fuel for a wind power station, and just small changes have a large impact on the commercial value of a farm. Every time the average wind speed doubles, the power in the wind increases by a factor of eight, so even small changes in average speed can produce large changes in performance. If the average wind speed at a given site increases from 6 m/s to 10 m/s, for example, the amount of energy produced by a wind farm will

increase by over 130%. Detailed and reliable information about how strongly, from which direction and how regularly the wind blows, is therefore vital for any prospective development [205].

At regional and national level, European wind atlases which record the wind speed to be expected in particular areas have been produced. For specific sites, a more detailed assessment is required using data from nearby weather stations and specialist computer software to model the wind resource. Finally, site-specific measurements are carried out using an anemometry mast on which a number of anemometers measure the wind speed and direction at different heights above ground. Overall, the exploitable onshore wind resource for the European Union (EU-25) is conservatively estimated to be capable of generating an output of 600TWh. The wind resource in offshore waters has been assessed at up to 3 000TWh. This alone would exceed Europe's entire current electricity consumption [205].

#### **3.6.4 Wind farms**

A number of constraints affect the siting of a cluster of wind turbines, usually described as a wind farm or park. These include land ownership, positioning in relation to buildings and roads, and avoidance of sites of special environmental importance. Once these constraints have been determined, the layout of the wind turbines themselves can be planned. The overall aim is to maximise electricity production while minimising infrastructure, operation and maintenance (O&M) costs, and environmental impacts. Specialist software has been developed to produce visualisations of how the turbines will appear in the landscape, enabling developers and planners to choose the best visual impact solutions before the project is constructed [205].

Apart from the turbines themselves, the other principal components of a wind farm are the foundations to support the turbine towers, access roads and the infrastructure to export the electrical output to the grid network. A 10MW wind farm can easily be constructed in two months, producing enough power to meet the consumption of over 5 000 average European households. Once operating, a wind farm can be monitored and controlled remotely. A mobile team carries out maintenance work, with roughly two personnel for every 20 to 30 turbines. Typical maintenance time for a modern wind turbine is about 40 hours per year. Wind farms can vary in size from a few megawatts up to the largest so far - 300MW in the western United States.

### 3.6.5 *Transmission and Distribution*

A key strategic element in the successful penetration of wind power is its efficient integration into the electricity transmission and distribution network. The increase in the penetration of wind power production into the grid raises a number of issues. Most are matters of utility attitude rather than engineering imperative [205]. The issues are:

- The output from a wind farm fluctuates to a certain degree according to the weather.
- Wind farms are often located at the end of the distribution networks. Most grids have been designed for large-scale electricity generation from a relatively small number of large plants, sending power outwards towards the periphery, rather than in the opposite direction.
- The technical characteristics of wind generation are different from those of conventional power stations, around which the existing systems have evolved.

The requirement for grid network operators to handle an increasing proportion of such “distributed generation” is coming not only from wind energy. Environmental considerations and the liberalisation of the electricity market have increased interest in small-scale commercial generation; a shift in both the attitude of utilities, and grid operation, is required to accommodate this development. Intermittency issues require an understanding of variability and predictability. Wind prediction techniques are at an early stage of development, and improvements can help firm up wind power for system operators by reducing and specifying forecast error. Because of its intermittency, it has been suggested that grid stability issues might arise with the penetration of wind power above a certain level. Such concerns need to be weighed against the potential benefits, including local reinforcement of grids and the ability of variable speed turbines to contribute to grid stability. As more wind farms are connected to the system across a wide geographical area, their aggregate output is likely to even up the overall pattern of generation, resulting in fewer requirements for backup use of conventional power stations.

In balancing a system to accommodate the fluctuating input from wind power, a range of techniques are available to the grid operator. In a situation where a lot of wind is available, for example, the operator can maintain other types of generation plants at a low output. Other solutions are likely to become increasingly significant as the penetration of wind energy expands. These include forecasting and the use of interconnectors to neighbouring electricity networks, as described below. Using such techniques, as well as reinforcement of the grid

network itself and increased geographical dispersion of wind power, it is feasible to have a very high level of wind penetration in the electricity systems without affecting the quality of supply.

### **3.6.6 Forecasting**

Much progress has been made in recent years in forecasting the energy output from wind farms. It has generally been found that with short measurement periods on a site, it is possible to predict output very accurately using a correlation with measured meteorological data from nearby weather stations [205].

### **3.6.7 Interconnectors**

An essential element in establishing wind energy is to ensure that the electricity generated can feed into the grid system, and reach electricity consumers. Experience has shown that combining a diverse mix of creative demand and supply solutions allows large wind power penetration in an electricity grid without adverse effect. In the Eltra system in western Denmark, for example, the use of interconnectors to the large hydropower generators in Norway to the north and Germany to the south has allowed 30% wind energy penetration, with minor adjustments in grid operation [205]. The variability of the wind has produced far fewer problems for electricity grid management than sceptics had anticipated. On a few windy winter nights, wind turbines can account for up to 100% of power generation in the western part of Denmark, for example, but the grid operators have managed it successfully. The majority of wind farms in Europe are presently connected to the local distribution system.

### **3.6.8 New wind farms and conceptual wind technologies**

As the world discovers new ways to meet its growing energy needs, energy generated from the sun, which is better known as solar power, and energy generated from the wind called wind power, are being considered as a means of generating power [205]. Though these two sources of energy have attracted the scientists for a very long time, it is still not clear which of the two is the better source to generate power. Now scientists are looking at a third option as well. Scientists at Washington State University have now combined solar power and wind power to produce enormous energy called solar-wind power, which will satisfy all energy requirements of humankind.

### 3.7 HYBRID POWER SYSTEMS

The exponentially increasing global population, even faster-growing energy demands and consequently rapidly depleting fixed reserves of fossil fuel have become the concern of all human beings. The depletion of fossil fuel is one challenge and increasing environmental pollution as a result of burning of these fuels is another threat to the life of present and future generations. Therefore, for a safe globe and better life of all living beings on this planet new, clean and renewable sources of energy and related technologies are being sought, developed and implemented worldwide. These alternative sources of energy include wind, solar, geothermal, tidal, wave and biofuels. These fuels are clean, renewable, environmental friendly, absolutely free and have enough potential to meet the global energy needs. The applications of these sources include the very small to large isolated, grid-connected and hybrid power systems.

Hybrid power systems (HPS) are combinations of two or more energy conversion devices (e.g. electricity generators or storage devices), or two or more fuels for the same device, which when integrated, overcome limitations that may be inherent in either. Hybrid systems can produce synergistic benefits in which the “whole is greater than the sum of its parts”. System efficiencies are typically higher than those of the individual technologies used separately, and higher reliability can be accomplished with redundant technologies and/or energy storage. Some hybrid systems include both, which can simultaneously improve the quality and availability of power. In general, well-designed hybrid systems will substantially reduce diesel fuel consumption while increasing system reliability. In addition to the diesel generator and the renewable energy generator, hybrid systems consist of a battery bank for energy storage, a control system and particular system architecture that allows optimal use of all components. Hybrid power systems can consist of any combination of wind, photovoltaics, diesel and batteries. Such flexibility has obvious advantages for customising a system to a particular site's energy resources, costs and load requirements. In the present case, a wind-pv-diesel hybrid power system and a power converter are used to design and meet the load requirements of the village under investigation.

The grid extension to populations living in remote or rough terrain areas is neither cost-effective nor feasible. In such situations, decentralised renewable energy-based power generating options can provide feasible alternative options. These alternatives may include hybrid power systems like wind-pv-diesel, wind-diesel, pv-diesel and others with and without

battery backup option. With continuous research and development efforts, it has been established that the hybrid systems, if optimised properly, are both cost-effective and reliable compared with single power source systems. In this period of time, the electrification of rural areas has become an effective instrument for the sustainable development of such regions in both developing and developed countries. During the last couple of decades, an increasing interest has been observed in the deployment of medium-to large-scale wind-diesel, pv-diesel and wind-pv-diesel hybrid power systems for rural electrification in various countries around the globe. There are many indications that there is a large potential market for such systems, and though there are an increasing number of demonstration projects, a true market for such systems has yet to emerge [208]. Baring-Gould [209] outlined the foundations for hybrid power systems architecture and design and presented hybrid systems as an optimum approach for stand-alone power supply options for remote area applications. Moreover, the hybrid power systems exhibit higher reliability and lower cost of generation than those that use only one source of energy [208 and 209].

Yang et al. [210] recommended an optimal design model for a hybrid solar-wind system which, employed battery banks to calculate the system's optimum configurations in China. In another study, Yang et al. [211] recommended an optimal sizing method to optimise the configurations of a hybrid solar-wind system with battery banks. The authors used a genetic algorithm (GA) to calculate the optimum system configuration that could achieve the customers' required loss of power supply probability (LPSP) with minimum annualised cost of system (ACS).

Wichert et al. [212] studied the techno-economic characteristics of hybrid power systems and outlined the expected future directions for the development of hybrids. According to the authors, the hybrid power systems were found to be more favourable when the cost of diesel fuel transportation was incorporated into the analysis. Hunter and Elliot [213] studied in detail the technical and operational characteristics of wind-diesel hybrid systems and found that among various disadvantages of diesel-only generation in remote areas, there has to be a stand-by diesel generator to be used only when repairs or maintenance is being performed. According to Hunter [213], this could be handled by introducing wind energy generation to the existing diesel-only system. Mahmoud and Ibrik [214] reported that the utilisation of pv systems for rural electrification in Palestine is economically more feasible than using diesel generators or extension of the high-voltage electric grid.

The hybrid power systems exhibit higher reliability and lower cost of generation than those that use only one source of energy [215 and 216]. Bakos and Soursos [216] conducted a techno-economic assessment of an autonomous pv-diesel hybrid power system installed in a bungalow complex in Elounda, Crete. In remote areas which are far from the grids, the electric energy is supplied either by diesel generators or small hydroelectric plants. Under such circumstances, the supply of diesel fuel becomes so expensive that hybrid diesel-photovoltaic generation becomes competitive with diesel-only generation [217]. Schmid et al. [218] reported that pv systems with energy storage connected to existing diesel generators, allowing them to be turned off during the day, provide the lowest energy costs. The authors suggested that in northern Brazil, it is economical to convert diesel systems up to 50kW peak power into hybrid systems.

According to Wies et al. [219] and Dufo-Lopez and Bernal-Agustin [220], the solar pv-diesel hybrid power systems provide a reduction in operation and maintenance costs and air pollutants emitted into the local atmosphere compared with that of a diesel-only system. Nfah et al. [221] studied a solar-diesel-battery hybrid power system to meet the energy requirements of a typical rural household in the range 70–300kWh/yr and found that a hybrid power system comprising of a 1 440Wp solar pv array and a 5kW single-phase generator operating at a load factor of 70% could meet the required load. Bala and Siddique [222] presented an optimal design of a solar-pv-diesel hybrid mini-grid system for a fishing community in an isolated island, Sandwip in Bangladesh. Their study revealed that the major share of the cost was for solar panels and batteries. In future, the technological development in solar-pv technology and economic production of batteries would make rural electrification on the isolated islands more promising and demanding.

Hrayshat [223] presented a detailed techno-economic analysis of an optimal autonomous hybrid pv-diesel-battery system to meet the load of an off-grid house, located in a remote Jordanian settlement. The hybrid system with 23% of photovoltaic energy penetration and consisting a 2kW pv array, a 4kW diesel generator and two storage batteries in addition to 2kW converter was found to be the optimal system and economically feasible for diesel prices greater than 0.15 \$/L. Dhrab and Sopian [224] proposed a hybrid power system to generate power for grid-connected applications in three cities in Iraq. Results showed that it is possible for Iraq to use solar and wind energy to generate enough power for villages in the desert and rural areas. Furthermore, small off-grid stand-alone hybrid power systems provide

an important option for decreasing the electricity gap in remote areas of the developing and developed world, where progress in grid extension remains slower than population growth [225 and 226]. According to Celik [227], these small-scale systems generate relatively little power but can significantly improve quality of life in remote areas. Cavello and Grubb [229] state that 1kWh of electricity provides 10 times more electricity services in India than in Indiana and further added that two small wind generators, which would supply only two homes with electric heating in the United States, could pump water for 4 000 people in Morocco [228].

Ekren et al. [229] designed and developed an optimum sizing procedure of wind-pv-diesel hybrid system for small applications in Turkey. Saheb-Koussa et al. [230] designed a wind-pv-diesel hybrid energy system with battery backup and conducted its techno-economic feasibility for remote applications in Algeria. Their simulation results indicated that the hybrid system is the best option for all the sites considered, provides higher system performance than photovoltaic or wind-alone systems, the reliability of the system is enhanced, and finally it was revealed that the energy cost depends largely on the renewable energy potential. Jose et al. [231] presented a comprehensive techno-economic analysis of wind-pv hybrid power system for the production of hydrogen and that the selling price of hydrogen produced by means of electrolysis should be high in order to recover the initial investment of a pv-wind system in a reasonable lapse of time (10 years). Arribas et al. [232] presented the guidelines suitable for long-term assessment hybrid power systems with different combinations and also for the assessment of components and of the short-term performance of the systems necessary at the actual stage of development. The study also recommended that, at least for demonstration projects, the monitoring activity should be used not only for long-term assessment, but also for the characterisation of components and for the analysis of the system, in order to gain a better understanding of hybrid systems. Sopian et al. [233] presented the performance of an integrated pv-wind hydrogen energy production system. Their system was capable of producing 130-140 ml/min of hydrogen, for an average global solar radiation and wind speed ranging between 200 and 800 W/m<sup>2</sup> and 2.0 and 5.0 m/s, respectively.

To meet the energy requirement of seawater greenhouse desalination plant in the Oman, Mahmoudi et al. [234] used hourly wind speed and solar radiation data and designed a wind-solar power system. Dufo-Lopez et al. [235], for the first time, presented a triple multi-

objective design of isolated hybrid systems minimising, simultaneously, the total cost throughout the useful life of the installation, pollutant emissions (CO<sub>2</sub>) and unmet load. To achieve the task, the authors used a multi-objective evolutionary algorithm (MOEA) and a genetic algorithm (GA) to find the best combination of components of the hybrid system and control strategies. Shakya et al. [236] studied the feasibility of stand-alone hybrid wind-pv system incorporating compressed hydrogen gas storage in Australia. Tina et al. [237] assessed the long-term performance of a hybrid solar-wind power system for both standalone and grid-connected applications. Kalantar and Mousavi [238] presented dynamic behaviour and simulation results in a stand-alone hybrid power generation system of wind turbine, microturbine, solar array and battery storage. The hybrid system consisted of a 195kW wind turbine, an 85kW solar array; a 230kW microturbine and a 2.14kAh lead acid battery pack optimised based on economic analysis using genetic algorithm (GA). The authors developed a supervisory controller for the management of energy between generated and consumed energies. The proposed system can be used in the isolated rural and mountainous areas far from the power generation networks.

Lau et al. [239] analysed the potential use of hybrid photovoltaic pv-diesel energy system in remote locations in Malaysia. The National Renewable Energy Laboratory's (NREL) HOMER software was used to perform the techno-economic feasibility of hybrid pv-diesel energy system. The investigation demonstrated the impact of pv penetration and battery storage on energy production, cost of energy and number of operational hours of diesel generators for the given hybrid configurations. The study demonstrated that the use of hybrid pv-diesel system with battery (one unit of 60kW pv array, two units of 50kW diesel generator, with 12 units of battery) can significantly reduce the dependence on solely available diesel resource. Although utilisation of a hybrid pv-diesel system with battery might not significantly reduce the total net present cost (NPC) and cost of energy (COE), it has been able to cut down the dependence on diesel. In addition, it also helped to reduce pollutants, such as carbon emission, thus reducing the greenhouse effect. On the other hand, it was also proved that the use of hybrid pv-diesel system with battery would be more economical if the price of diesel increased significantly. With a projection period of 25 years and 6% annual real interest rate, it was found that the use of hybrid pv-diesel system with battery could achieve significantly lower NPC and COE as compared with a stand-alone diesel system. As a conclusion, the hybrid PV/diesel system has potential use in remote areas, especially in replacing or upgrading existing standalone diesel systems in Malaysia.

Diaf et al. [240] studied the impact of the renewable energy potential quality on the system size, the optimum dimensions of system were defined for five sites on the island Corsica. The authors developed a complete sizing model able to predict the optimum system configuration on the basis of levelised cost of energy (LCE). Their simulation results indicated that the hybrid system was the best option for all the sites considered in this study, yielding lower LCE. The study showed that the LCE depends largely on the renewable energy potential quality. At high wind potential sites, more than 40% of the total production energy is provided by the wind generator, while at low wind potential sites, less than 20% of total production energy is generated by the wind generator. Ekren and Ekren [241] showed the use of the response surface methodology (RSM) in size optimisation of an autonomous pv-wind integrated hybrid energy system with battery storage. The case study was conducted using ARENA 10.0, commercial simulation software, for satisfaction of electricity consumption of the global system for mobile communications (GSM) base station at the Izmir Institute of Technology Campus Area, Urla, Turkey. As a result, the optimum pv area, wind turbine rotor swept area and battery capacity were obtained to be  $3.95\text{m}^2$ ,  $29.4\text{m}^2$  and  $31.92\text{kWh}$ , respectively. The optimum result obtained by RSM is confirmed using loss of load probability (LLP) and autonomy analysis.

Dalton et al. [242] presented an analysis of the technical and financial viability of grid-only, RES-only and grid-RES hybrid power supply configurations for a large-scale grid-connected hotel (over 100 beds). The results demonstrated that RES, in principle, has the potential to supply significant power for a large-scale tourist accommodation, in conjunction with the grid-electricity supply. Optimisation modelling demonstrated that, at 2004 prices, the NPC of the grid-RES hybrid configuration is comparable with the grid-only supply and resulted in an RF of 73%, a payback time of 14 years and a reduction in greenhouse gas emissions of 65%.

Iqbal [243] presented a feasibility study of a wind energy conversion system based zero energy home in Newfoundland. The investigation indicated the feasibility of a wind energy system-based zero energy home in Newfoundland. A zero net energy home is designed and constructed to generate all of the energy it requires through a combination of energy efficiency and renewable energy generation technologies [244]. Kamel and Dahl [244] used optimisation software to assess the economics of hybrid power systems versus the present diesel generation technology in a remote agricultural development area. The authors also considered the emission reduction advantages of using hybrid systems. Interestingly enough,

optimisation results showed that hybrid systems were less costly than diesel generation from a net present cost perspective even with the high diesel fuel price subsidies.

A number of zero energy homes and buildings have been built, tested and reported throughout the world [245-251]. In almost all of such demonstrations, the renewable energy sources consist of photovoltaic cells, solar water heaters and geothermal heat pumps. While on the energy demand-side, passive solar design techniques such as passive solar heating, insulation, controlled windows, shading, interior space planning and landscaping have been tried. In zero energy houses, high efficiency lighting and appliances also contribute to energy savings. Studies of successful renewable energy system (RES) installations have been carried out on many non-tourist enterprises and the installations may be split into two configuration categories, namely RES in hybrid combinations with grid power, for example, photovoltaics pv-grid [252-257], wind energy conversion systems (WECS-grid [258-260] and pv-WECS-grid [257, 261 and 262]. RES for complete autonomous supply, such as photovoltaic-only configurations [263], wind energy conversion systems (WECS-only) [264] and combinations of pv-WECS-only [265-267].

It is well understood that neither a stand-alone solar nor a wind energy system can provide a continuous supply of energy due to seasonal and periodical variations. Therefore, to satisfy the load demand, hybrid energy systems which combine solar and wind energy conversion units with battery storage are implemented. A great deal of research [268–279] has been carried out on hybrid energy systems with respect to performance and optimisation, and other related parameters of significance. Borowy and Salameh [268] developed an algorithm to optimise a photovoltaic-array with battery bank for a stand-alone hybrid pv-wind system. The model proposed was based on a long-term hourly solar irradiance and peak load demand data of the site chosen. However, the direct cost of the pv-wind systems was not considered for optimising the hybrid energy system. Later, Borowy and Salameh [269] optimised a similar system taking into account the cost of the pv modules and battery systems. A graphic construction technique to optimise the size of the pv-wind energy system was presented by Markvart [270] considering the monthly average solar and wind energy values. On the other hand, unlike the methods based on hourly, daily and monthly average, a statistical approach for optimising the size of pv arrays and the number of batteries for a stand-alone pv-wind hybrid system was presented by Bagul et al. [271]. Ashok [272] proposed a model based on different system components of a hybrid energy system and developed a general model to

find an optimal combination of energy components for a typical rural community, minimising the life cycle cost.

Photovoltaic solar and wind energy conversion systems have been widely used for electricity supply in isolated locations far from the distribution network. If such systems are designed properly, they can provide a reliable service and operate in an unattended manner for extended periods of time. However, they suffer from the fluctuating characteristics of available solar and wind energy sources, which must be resolved in the design stage. The degree of desired reliability from a solar and wind process to meet a particular load can be fulfilled by a combination of properly sized wind turbine, PV panel, storage unit and auxiliary energy. Because the storage unit and auxiliary energy are needed to provide high reliability and avoid gross overdesign of the solar and wind system [273 and 275], proposed in this system, the use of battery storage and auxiliary energy is proposed. Hybrid energy system studies in the past [273–274 and 276-279] have been based upon a particular design scenario with a certain set of design values yielding the optimum design solution only.

Carlos and Calros [279] performed an economic analysis on a hybrid pv-diesel system and demonstrated that the system has advantages over a stand-alone diesel system. With cost analysis over a 20-year period, the hybrid system was found to reduce fuel consumption, operation and maintenance costs while improving the quality of service. This is exceptionally true for small villages with up to 100 families. The application of the hybrid pv-diesel system has seen its successful implementation in Malaysia with the Langkawi Cable Car Resort Facilities Project [280]. The project has proved to be successful in offering solutions to off-grid power generation in terms of reduced operation, maintenance and logistics problem and cost, providing 24-hours, reliable supply at an effective cost as well as preserving the nature. Another successful implementation of a hybrid PV-diesel project in Malaysia was described in [281]. The authors conducted studies on the alternative energy design scheme for an Information and Communication Technologies (ICT) Telecenter. The authors concluded that the hybrid PV-diesel energy system was more practical than a stand-alone diesel generator.

## **SUMMARY**

A little less than 300 research papers and technical project reports published on different aspects of wind power development and utilization were reviewed and recorded. Specifically, long-term wind speed, shape parameter and scale parameter trend analysis, wind power

resource assessment, wind measurements, local wind shear exponent estimation, grid connected wind farm and hybrid power systems (wind-diesel and wind-photovoltaic-diesel with and without battery backup options) design, energy yield estimation from chosen wind turbines, optimal hub height estimation, and wavelet based analysis of wind speed data topics were considered. It was observed that no comprehensive and dependable work has been reported in the literature on all of these aspects with respect to Saudi Arabia. Being a major energy supplier of the world, Saudi Arabia has to look in future energy outlook to partially cater its domestic and global energy demands through new and renewable sources of energy. Hence the present scope of the work will help the nation in building its future energy infrastructure ahead of time when it becomes necessary.

## CHAPTER 4

### SITES AND DATA DESCRIPTION

The Kingdom of Saudi Arabia lies between latitudes 31°N and 17.5°N and longitudes 50°E and 36.6°E. The land elevation varies from 0 m to 2 600metres above mean sea level. Complex terrain is found in the south-west region of the kingdom. The east and the west coasts of the kingdom are located on the Arabian Gulf and Red Sea, respectively. Mainly two seasons, winter and summer, are observed during the year. The historical meteorological data collected at national and international airports in the kingdom shows a long-term annual wind speed of about 4 to 4.5m/s at different locations at about 10m above ground level (AGL).

The latitude, longitude, altitude and data collection period for national and international airports are summarised in Table 4.1. In general, the data collection period varied from 1970 to 2006 for most of the data collection stations. However, for some stations, the daily mean values were available and at a few stations, the data was available from 1985. The data was missing for the year 1976 and 1984 for almost all the stations. At all of these stations, the hourly values of all the parameters such as wind speed (WS), wind direction (WD), dry bulb temperature (T), wet bulb temperature ( $T_w$ ), station pressure (P), sea level pressure ( $P_{sl}$ ), relative humidity (RH), vapour pressure ( $V_p$ ), total rainfall (R), and others are recorded manually and then daily average, maximum and minimum values are saved on the computer. The meteorological stations at Al-Wejh, Yanbo, Jeddah, Gizan and Dhahran are situated near the coast. Hence these stations could be considered as representative of coastal locations. The physical locations of these meteorological stations are depicted in Figure 4.1.

All of these stations could be grouped into five regions, viz. northern (Rafha, Arar, Turaif, Guriat, Al-Jouf and Tabouk); western (Yanbo, Al-Wejh, Madina, Jeddah, Makkah and Taif); central (Hail, Gassim and Riyadh); southern (Al-Baha, Bisha, Wadi Al-Dawasser, Sulayel, Khamis-Mushait, Abha, Gizan, Nejran and Sharourah) and eastern (Al-Ahsa, Dhahran, Qaisumah and Hafr Al-Batin). The northern region is blessed with flat land and a gentle topography. From Rafha to Arar, there is a change of only 100metres in elevation while Guriat is situated at around 500 metres above mean sea level (AMSL). Turaif, Jouf and Tabouk are around 800 metres AMSL. The southern area has a complex terrain with high mountains and layers of mountains. Abha and Khamis-Mushait are situated at around 2 100 m AMSL while Al-Baha, Bisha and Nejran at 1 000 to 1 200metres AMSL. The central

stations Gassim and Riyadh are situated at 600metres while Hail at around 1 000metres AMSL. In the western region, most of the meteorological stations are near sea shore and represent a flat area. The eastern region south and north of Dhahran increases in elevation.

For detailed and more accurate wind power resources assessment, the present work utilised wind speed and direction data from seven stations where measurements were made at 20, 30 and 40metres above ground level for a period of two to four years. Five of these stations or towers (Dhahran, Arar, Yanbo, Gassim and Dhulom) were erected by King Abdulaziz City for Science and Technology (KACST) and two (Rowdat Ben Habbas and Juaymah) by King Fahd University of Petroleum and Minerals (KFUPM). The site-dependent details and data measurement periods are given in Table 4.2. The locations of these wind masts are shown in Figure 4.2 and the schematic diagram of the mast is given in Figure 4.3. At each height, two sensors were installed (opposite to each other of the mast) and recorded data was tagged as WS1 and WS2 at 20metres, WS3 and WS4 at 30metres, and WS5 and WS6 at 40metres. The wind direction data was recorded at 30 and 40metres as WD1 and WD2, respectively. A schematic diagram showing the positions of all the sensors on the mast is shown in Figure 4.3. The surface air temperature ( $^{\circ}\text{C}$ ), relative humidity (%), surface station pressure (in. of Hg), and global solar radiation ( $\text{W}/\text{m}^2$ ) data was collected at 1.5m above the ground surface. The operating ranges and accuracies of various sensors used for the measurements are given in Table 4.3.

The data collection site at Rawdat Ben Habbas was an open area from all directions except a couple of warehouse shades and diesel storage tanks in the far vicinity of the wind mast. The area around the wind mast in Juaymah was surrounded by government and private industries and power plants which are connected to the national electric grid. At Rawdat Ben Habbas and Juaymah stations, the data was scanned every three seconds and was recorded every 10 minutes on a removable data storage card as mean, maximum and minimum. The wind mast at Dhahran was surrounded by a single-storey building of about 4metres high in the south, gulf sea-shore on its west and the highway to the north of the tower. The Arar meteorological data measurement site was an open area from all directions. The land surface was consisted of small rocks. The Gassim site was an open area from three directions, east, south and west. There were some trees of about 5metres tall about 150metres north of the tower. The soil was consisted mostly of desert sand.

Table 4.1 Site-specific information on meteorological stations considered in this study

Location	From	To	Latitude (°N)	Longitude (°E)	Altitude (m)
Abha	01/09/1983	31/12/2006	18.20	42.70	2084
Al-Ahsa	01/01/1990	30/11/2006	25.30	49.50	172
Al-Baha	01/09/1983	31/12/2006	20.00	41.50	1021
Al-Jouf	05/08/1970	31/12/2006	29.80	39.90	771
Al-Wejh	01/01/1970	31/12/2006	26.20	36.50	16
Arar	07/04/1970	30/11/2006	30.90	41.10	552
Bisha	01/01/1970	31/12/2006	20.00	42.60	1157
Dhahran	01/01/1970	31/12/2006	26.30	50.20	17
Gassim	01/01/1973	31/12/2006	26.30	43.80	650
Gizan	01/01/1970	31/12/2006	16.90	42.60	3
Guriat	01/01/1984	31/12/2006	31.40	37.30	499
Hafr-Al-Batin	01/01/1990	31/12/2006	28.30	46.10	355
Hail	01/01/1990	30/11/2006	27.40	41.70	1013
Jeddah	01/01/1970	31/12/2006	21.70	39.20	12
Khamis Mushait	01/01/1970	31/12/2006	18.30	42.80	2054
Madinah	01/01/1970	31/12/2006	24.60	39.70	631
Makkah	03/05/1984	31/12/2006	21.50	39.80	310
Nejran	04/09/1973	31/12/2006	17.60	44.40	1203
Qaisumah	01/01/1970	31/12/2006	28.30	46.10	355
Rafha	01/01/1970	31/12/2006	29.60	43.50	447
Riyadh	01/04/1984	31/12/2006	24.70	46.70	612
Sharourah	01/01/1990	30/11/2006	17.50	47.10	722
Sulayel	10/05/1970	28/02/1990	20.46	45.64	612
Tabuk	01/01/1970	31/12/2006	28.40	36.60	770
Taif	01/01/1970	31/12/2006	21.50	40.60	1449
Turaif	03/08/1970	31/12/2006	31.70	38.70	813
Wadi-Al-Dawasser	03/03/1990	31/12/2006	20.52	45.19	627
Yanbo	22/02/1977	31/12/2006	24.20	38.10	14

Table 4.2 Site-specific information on 40metre tall towers

Location	Latitude	Longitude	Altitude, m	Data Period
Rawdat Ben Habbas	29.14°N	44.33°E	443	Sep. 2005 to Apr. 2010
Juaymah	26.80°N	49.90°E	20	Jul. 2006 to Apr. 2009
Dhahran	26.10°N	50.10°E	3	Oct. 1995 to Nov. 2000
Arar	30.80°N	41.30°E	550	Jun. 1995 to Dec. 1998
Gassim	26.30°N	43.97°E	648	Dec. 1995 to Oct. 1998
Yanbo	23.90°N	38.30°E	11	Sep. 1996 to Oct. 1999
Dhulom	22.74°N	42.18°E	1117	Nov. 1998 to Oct. 2002

The surrounding areas had small hilly sand dunes with vegetation of short grasses. In general, the tower site was an open site and the tower was not obstructed by any building or elevated structure. The 40metre wind mast at Dhulom site was installed inside a fenced area owned by Western SCECO. The west anchors were located 5metres from the north to the south of the fence. There were no barriers or obstacles about 200metres around the tower. There were some buildings that housed the diesel generators about 300metres away and west of the tower. At the Dhahran, Arar, Gassim, Yanbo and Dhulom sites, the data was scanned every

three seconds and was recorded as average, maximum and minimum every 30 minutes on a removable data card. A photograph of the wind mast at Juaymah site is shown in Figure 4.4.

Table 4.3 Operating ranges and accuracies of various sensors used for data collection

Item Description	Technical Information
Wind speed sensor, NRG#40 Three-cup anemometer	AC sine wave, Accuracy: 0.1 m/s, Range: 1-96 m/s Output: 0-125 HZ, Threshold: 0.78 m/s
Wind direction vane, NRG#200P Potentiometer	Accuracy: 1%, Range: 360° Mechanical, Output: 0-Exc. Voltage, Threshold: 1 m/s, Dead band: Max - 8° and Typical 4°
Temperature sensor #110S Integrated circuit	Accuracy: $\pm 1.1$ °C, Range: -40 °C to 52.5 °C, Output: 0 – 2.5 volts DC, Operating temperature range: -40 °C to 52.5 °C
Barometric pressure sensor BP20	Accuracy: $\pm 15$ mb, Range: 150 – 1150 mb, Output: Linear voltage
Relative humidity sensor RH-5 Polymer resistor	Accuracy: $\pm 5\%$ , Range: 0 – 95 % Output: 0 – 5 volts, Operating temperature range: -40 °C to 54 °C
Pyranometer Li-Cor #LI-200SA Global solar radiation	Accuracy: 1%, Range: 0 – 3000 W/m <sup>2</sup> , Output: Voltage DC, Operating temperature range: -40 °C to 65 °C



Figure 4.1 Geographical locations of meteorological stations



Figure 4.2 Geographical locations of 40-metre towers

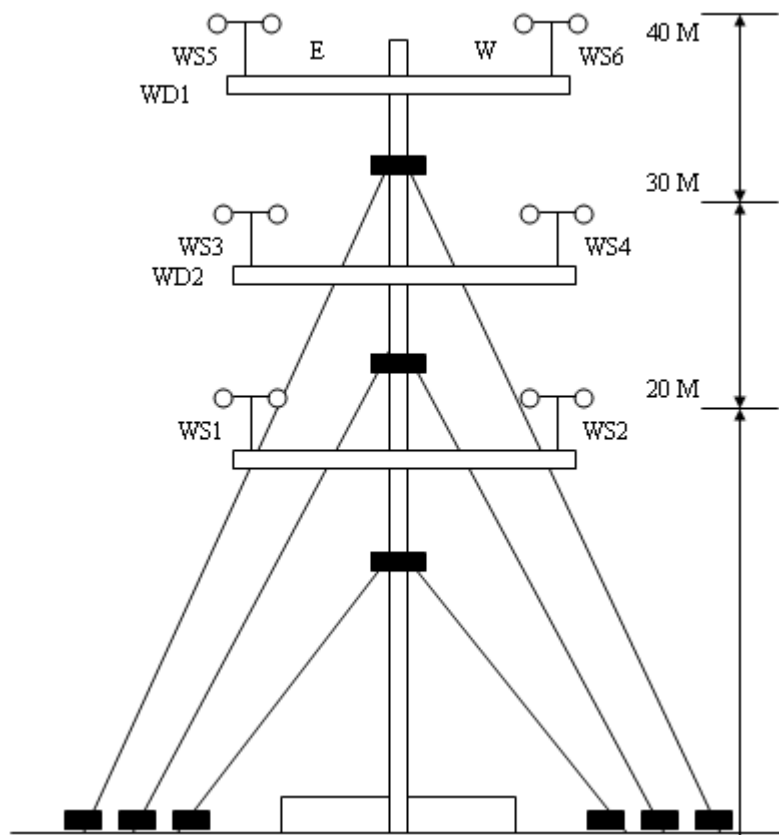


Figure 4.3 Schematic diagram of placement of wind speed (WS) and wind direction (WD) sensors on a mast of 40 metres high



Figure 4.4 Erected wind tower at Juaymah

## CHAPTER 5

### WIND SPEED DATA ANALYSIS FOR AIRPORTS

An accurate wind resource assessment is an important and critical factor to be well understood for harnessing the power of the wind. It is well known that an error of 1% in wind speed measurements leads to an almost 2% error in energy output. Hence precise measurements of wind speed at a site minimise the risk of huge investments. Moreover, the wind measurements are usually made at a height different from the hub height of the wind machine. The wind speed is extrapolated to the hub height by using the well-known  $1/7^{\text{th}}$  wind power law. In fact, the wind speed, at a given site, increases with height by a power factor known as wind shear factor or coefficient or exponent. This coefficient is highly dependent on the site where the measurements are made. So, if the wind shear coefficient is greater than  $1/7$  then wind power law will lead to over-estimation of wind speed and hence the wind energy overestimation. Hence accurate knowledge of wind shear exponent is essential for actual wind power estimates. The other important parameter that directly affects the energy production estimates is the air density. The air density depends on the air temperature and the surface pressure of the site of interest. So an assumed value of air density will result in either under- or over-estimation of energy production. Hence actual air density at the specific site should be obtained using the local temperature and pressure measurements to facilitate accurate energy estimation.

This chapter provides an in-depth analysis of historical wind speed and other meteorological parameters while Chapter 6 will be devoted to a more precise and accurate analysis of wind measurements made at different heights at seven locations in the Kingdom of Saudi Arabia. The analysis will provide station-based long-term wind data summaries, annual and seasonal trends of wind speed, wind rose and frequency distribution and finally, the variation of Weibull shape and scale parameters.

#### 5.1 STATION-BASED LONG-TERM WIND SPEED SUMMARIES

The long-term average, maximum and standard deviation values of wind speed (along with Weibull parameters) for all the stations under investigation are summarised in Table 5.1. The highest annual average wind speed of 4.4m/s was observed at Dhahran while the lowest of 1.59m/s at Makkah as can be seen from Figure 5.1. Promising long-term annual means of

more than 4m/s were observed at Al-Wejh, Guriat, Turaif and Yanbo. A contour map of wind speed variation over Saudi Arabia developed using long-term mean wind speed values given in Table 5.1, is shown in Figure 5.2. This map clearly indicates the high and low windy regions. The seasonal wind maps are shown in Figure 5.3.

Table 5.1 Long-term statistics for daily mean wind speed

Location	Possible Records	Valid Records	Mean (m/s)	Median (m/s)	Max (m/s)	Std. Dev. (m/s)
Abha	6,209	6,186	2.96	2.57	14.92	1.26
Al-Ahsa	6,209	6,167	3.41	3.09	11.83	1.72
Al-Baha	8,035	6,190	3.34	3.09	13.91	1.45
Al-Jouf	12,053	9,247	3.94	3.61	15.97	1.82
Al-Wejh	13,514	10,683	4.26	4.12	14.92	1.38
Arar	13,498	10,229	3.83	3.61	24.21	1.87
Bisha	13,482	10,656	2.61	2.57	12.35	1.19
Dhahran	13,514	11,067	4.40	4.12	12.86	1.70
Gassim	12,418	9,601	2.87	2.57	19.03	1.42
Gizan	13,514	10,685	3.42	3.09	13.89	1.00
Guriat	8,035	6,209	4.21	4.12	16.46	1.99
Hafr-Al-Batin	6,209	6,201	3.33	3.09	12.86	1.64
Hail	6,209	6,171	3.22	3.09	10.80	1.30
Jeddah	13,514	10,953	3.66	3.60	12.35	1.30
Khamis-Mushait	13,514	10,686	3.12	3.09	12.86	1.28
Madinah	13,514	10,670	3.33	3.09	10.29	1.16
Makkah	8,035	6,192	1.59	1.54	22.12	0.81
Nejran	11,322	8,635	2.23	2.06	8.75	1.03
Qaisumah	13,498	10,662	3.92	3.60	14.40	1.98
Rafha	13,514	10,240	3.77	3.60	17.49	1.78
Riyadh	13,514	10,664	3.23	3.09	9.77	1.51
Sharourah	6,209	6,146	3.23	3.09	16.46	1.37
Sulayel	7,305	3,619	3.50	3.09	13.89	1.63
Tabuk	13,514	10,640	2.85	2.57	15.43	1.38
Taif	13,514	10,677	3.73	3.60	10.29	1.43
Turaif	12,417	9,575	4.18	4.12	19.03	1.87
Wadi-Al-Dawasser	6,209	6,130	3.50	3.09	12.35	1.53
Yanbo	13,514	10,701	4.19	4.12	18.01	1.79

The windy regions (Dhahran, Guriat, Turaif, Al-wejh and Yanbo) are well indentified by contour map shown in Figure 5.2. The long-term annual mean wind speed is observed to be more than 4.2m/s at 10m AGL in all of these regions. The annual WS was found to be greater than 3.5m/s in the northern territory and along the east and west coasts of Saudi Arabia. According to historical available data from airports, the central, southern and south-western regions could be classified as low windy regions but need to be revisited by making new

measurements at different heights and up to 100metres AGL before excluding these regions for a wind power development programme.

The seasonal shifting of windy regions and higher intensities of wind speeds are well explained by long-term monthly mean WS contour maps shown in Figure 5.3. In January, the windiest regions were spotted as Dhahran, Turaif and Al-Wejh while the least windy were Nejran and Abha as seen from extreme top left map in Figure 5.3. In February, the higher winds of more than 4.4m/s covered a wider region in the northern territory and on the west coast south of Al-Wejh and west of Yanbo. Still the least winds were noticed in the Nejran and Abha regions. The situation remained almost the same in March as can be seen from top most extreme right contour map in Figure 5.3 with the exception that the WS magnitude reached 4.5m/s. The long-term monthly mean WS reached a further high (>4.6m/s) in the same regions but higher winds were dominant in the Guriat, Turaif, Al-Jouf and Arar areas. This is clearly indicated in the first map in the second row of Figure 5.3. From May to September, the windy regions were confined in the vicinity of Dhahran, Guriat and Yanbo but the overall magnitude indicated WS of 5.4m/s, 5.8m/s and 5.0m/s in June, July and August, respectively. From September onwards, the WS magnitude decreased to 4.0m/s but the high windy regions were found again to be widespread.

The long-term summaries of annual mean temperature, surface pressure and air density are provided in Table 5.2. The air density ( $\rho$ ), given in the last column of Table 5.2, was calculated using the following relationship:

$$\rho = \frac{P}{R \times T} \quad (\text{kg/m}^3) \quad (5.1)$$

where  $P$  = the air pressure (Pa or N/m<sup>2</sup>);  $R$  = the specific gas constant for air (287J/kg<sup>o</sup>K); and  $T$  = the air temperature in degrees Kelvin ( $^{\circ}\text{C}+273$ ).

The highest values of long-term annual temperatures ( $\geq 30^{\circ}\text{C}$ ) were observed at Gizan and Makkah and the lowest of  $12.2^{\circ}\text{C}$  at Abha. The relative comparison of long-term temperature over Saudi Arabia is shown in Figure 5.4. The knowledge of temperature magnitude and its frequency of occurrence in different temperature bins is important for wind turbine energy output and the functioning of different components of wind turbine. The variation of surface pressure and the air density at different locations in the kingdom are shown in Figures 5.5 and 5.6, respectively. The long-term air density was observed to be more than 1.0 at all the

stations except at Abha, Al-Baha and Khamis-Mushait where it was a little less than 1.0. The lower values of air density at these locations could be attributed to low air pressure at high altitudes.

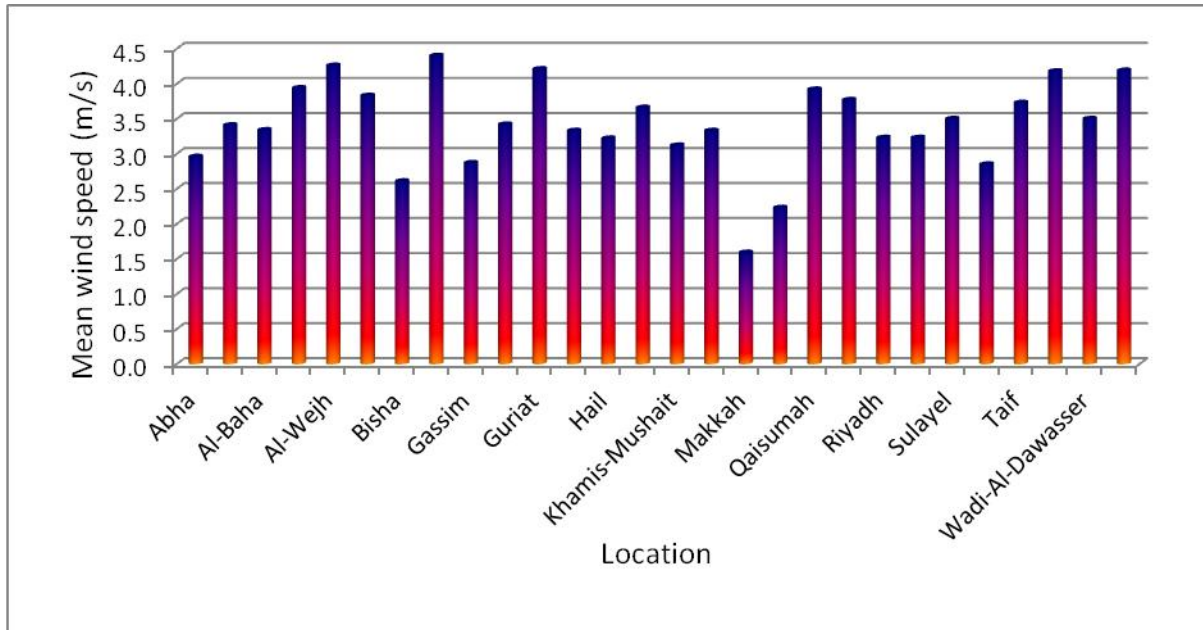


Figure 5.1 Long-term annual mean wind speed over Saudi Arabia

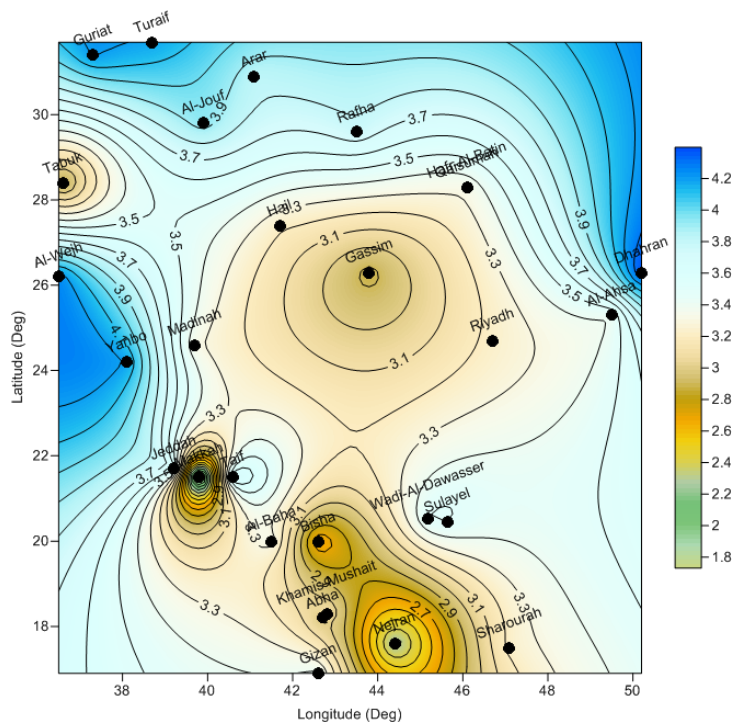
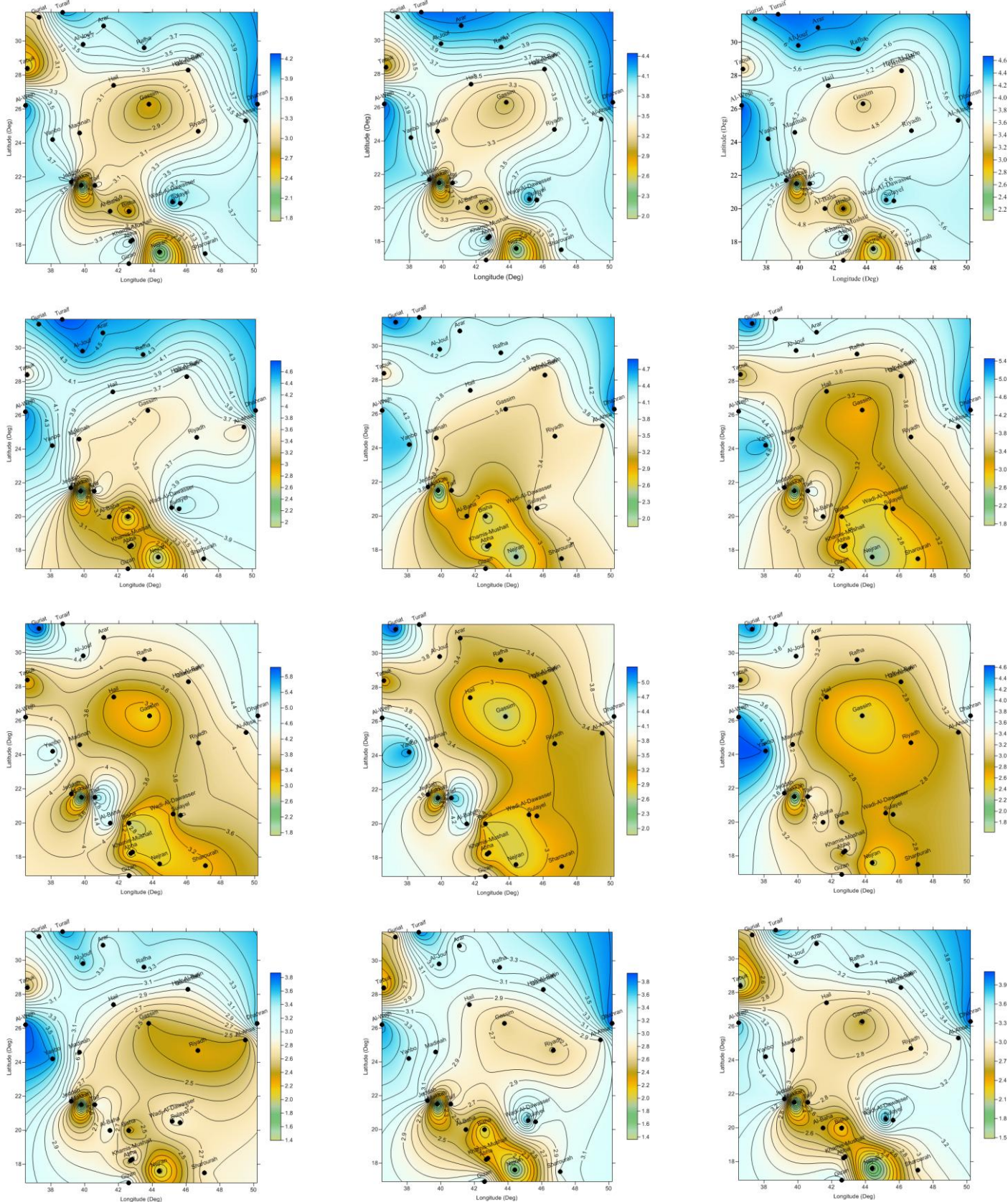


Figure 5.2 Wind speed contour map of Saudi Arabia



Jan, Apr, Jul and Oct

Feb, May, Aug and Nov

Mar, Jun, Sep and Dec

Figure 5.3 Monthly mean wind speed contour maps of Saudi Arabia

Table 5.2 Long-term Statistics for meteorological parameters

Location	Latitude (°N)	Longitude (°E)	Altitude (m)	Temperature (°C)	Pressure (mbar)	Density (kg/m <sup>3</sup> )
Abha	18.2	42.7	2084	18.7	794	0.97
Al-Ahsa	25.3	49.5	172	19.6	99.27	1.182
Al-Baha	20	41.5	1021	22.8	836.2	0.986
Al-Jouf	29.8	39.9	771	22	92.45	1.096
Al-Wejh	26.2	36.5	16	24.8	1008	1.182
Arar	30.9	41.1	552	22.2	949.5	1.126
Bisha	20	42.6	1157	25.7	883.8	1.035
Dhahran	26.3	50.2	17	26.2	1007	1.176
Gassim	26.3	43.8	650	24.8	937.6	1.102
Gizan	16.9	42.6	3	30.3	1008	1.162
Guriat	31.4	37.3	499	19.5	954.8	1.137
Hafr-Al-Batin	28.3	46.1	355	25.2	964	1.127
Hail	27.4	41.7	1013	22.8	901.3	1.062
Jeddah	21.7	39.2	12	28.2	1007	1.168
Khamis Mushait	18.3	42.8	2054	19.3	800.6	0.947
Madinah	24.6	39.7	631	28.3	938.7	1.091
Makkah	21.5	39.8	310	30.7	981.4	1.125
Nejran	17.6	44.4	1203	25.5	879.4	1.031
Qaisumah	28.3	46.1	355	25.7	969.6	1.136
Rafha	29.6	43.5	447	23.4	960.4	1.134
Riyadh	24.7	46.7	612	26.3	942.3	1.102
Sharourah	17.5	47.1	722	28.6	929	1.074
Sulayel	20.46	45.64	612	27.7	941.7	1.114
Tabuk	28.4	36.6	770	21.9	926	1.098
Taif	21.5	40.6	1449	22.8	855.1	1.011
Turaif	31.7	38.7	813	19	918.5	1.099
Wadi-Al-Dawasser	20.52	45.19	627	28.5	939.7	1.087
Yanbo	24.2	38.1	14	27.5	1008	1.172

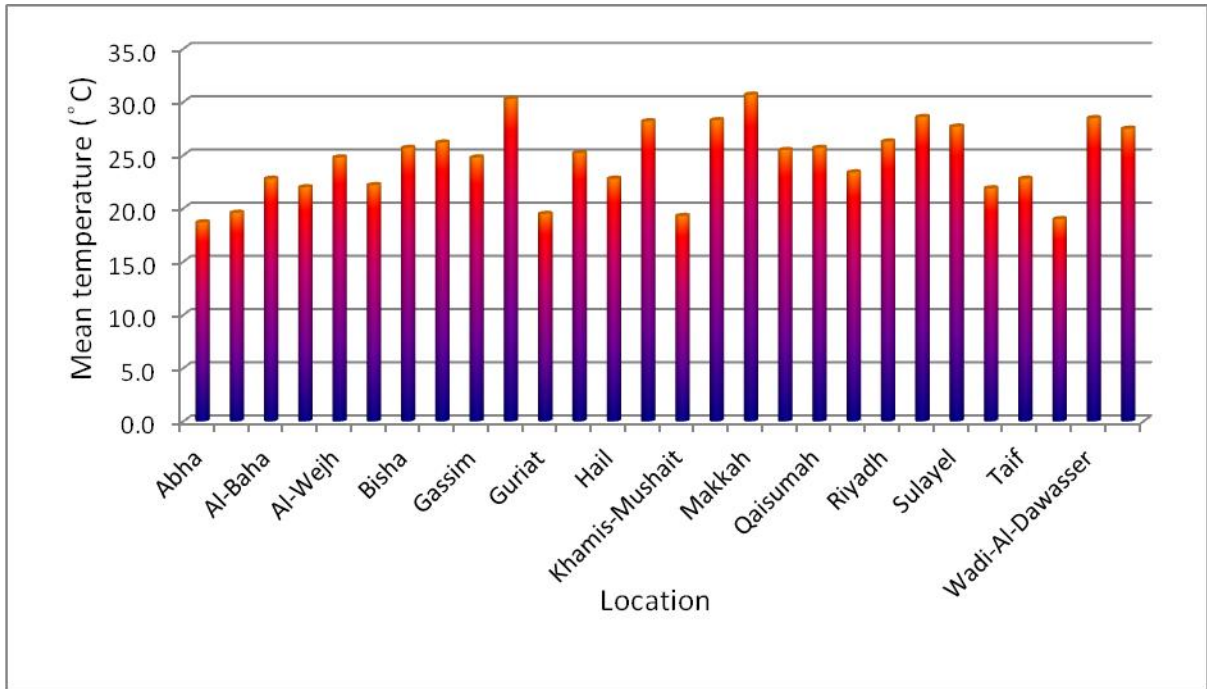


Figure 5.4 Long-term annual average values of temperature (°C) over Saudi Arabia

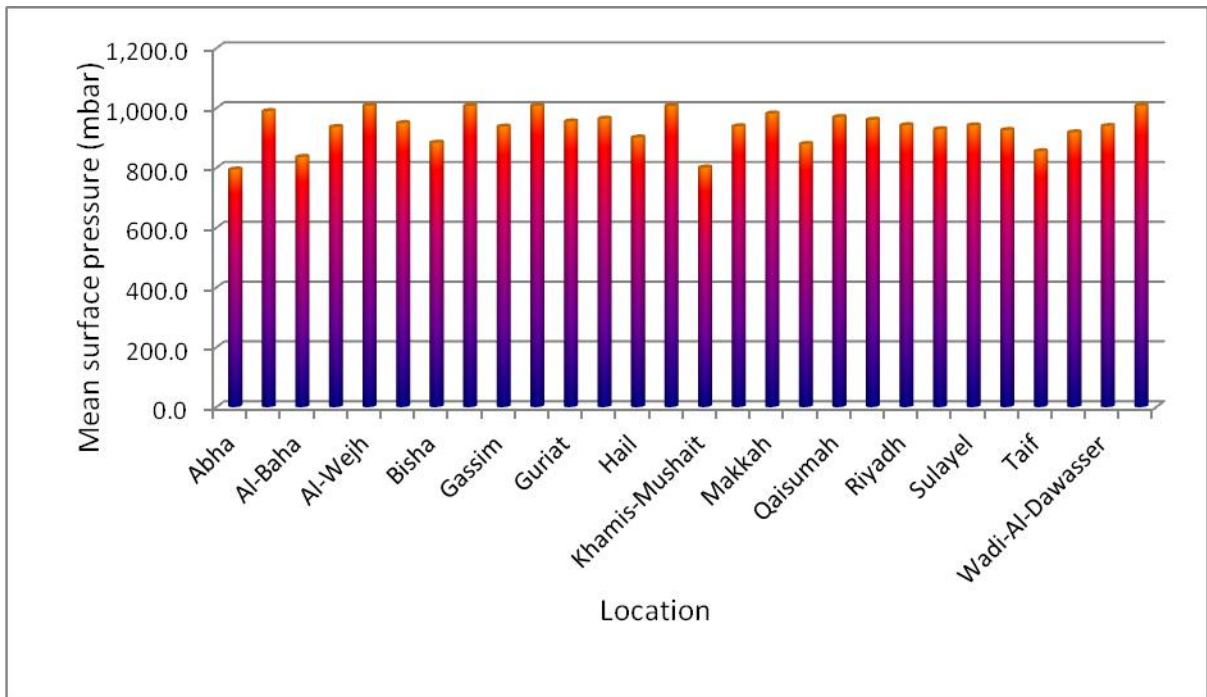


Figure 5.5 Long-term annual average values of surface pressure (mbar) over Saudi Arabia

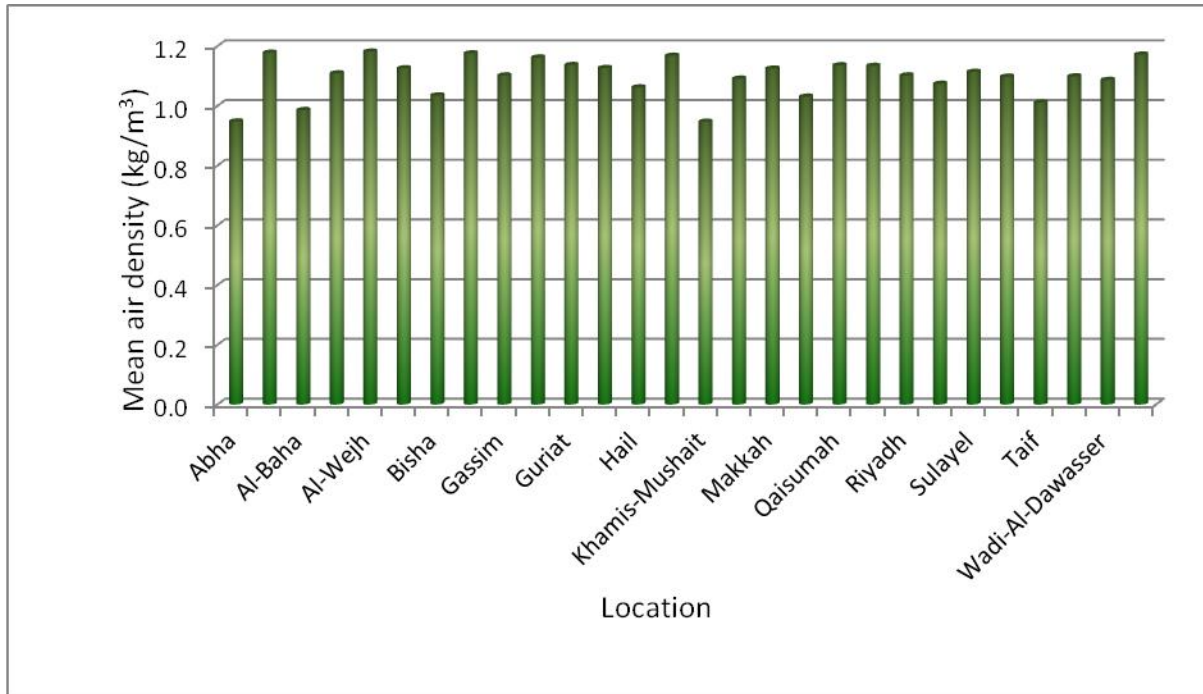


Figure 5.6 Long-term annual average values of air density (kg/m<sup>3</sup>) over Saudi Arabia

## 5.2 ANNUAL VARIATION OF WIND SPEED

Annual variation of mean wind speed provides confidence on the availability of wind intensity over a long period and thus supports getting accurate estimates of wind energy from wind turbines. Moreover, the annual trends of wind speed are also repeated after a decade or so, which could also be understood from this analysis and could be helpful in planning and managing the energy output from future wind farms.

Regression lines can be used as a way of visually depicting the relationship between the independent (x) and dependent (y) variables in the graph. A straight line depicts a linear trend in the data. Regression analysis is used to find equations that fit the data, in our case the wind speed data. Once the best fit regression equation has been obtained, it could be used in statistical model to make predictions. One type of regression analysis is linear analysis. When a correlation coefficient shows that data is likely to be able to predict future outcomes and a scatter graph of the data appears to form a straight line, statisticians may use linear regression to find a predictive function. Recalling from elementary algebra, the equation for a line is given by

$$y = ax + b \tag{5.2}$$

where y is the dependent variable, x is the independent variable (wind speed in the present case), a is the slope of the linear line and b the intercept. The best fit line coefficients a and b are obtained using the following equations:

$$a = \frac{(\sum y)(x^2) - (\sum x)(\sum xy)}{n(\sum x^2) - (\sum x)^2} \quad (5.3)$$

$$b = \frac{n(\sum xy) - (\sum x)(\sum y)}{n(\sum x^2) - (\sum x)^2} \quad (5.4)$$

Furthermore, the correlation coefficients are used in statistics to measure how strong a relationship is between two variables. There are several types of correlation coefficient: Pearson's correlation is a correlation coefficient commonly used in linear regression. The coefficient of determination,  $R^2$  is the square of the sample correlation coefficient between outcomes and predicted values. The coefficient of determination is calculated using the following equation:

$$R = \frac{n(\sum xy) - (\sum x)(\sum y)}{\sqrt{[n\sum x^2 - (\sum x)^2][n\sum y^2 - (\sum y)^2]}} \quad (5.5)$$

The annual mean wind speeds for all the locations were plotted and best regression line coefficients (a and b) and the corresponding values of coefficient of determination ( $R^2$ ) were obtained as shown in Figure 5.7(a) for Abha, Al-Ahsa and Al-Baha. The linear regression line coefficients for all the stations are summarised in Table 5.3. Based on regression line analysis, decreasing trends of annual mean wind speed were found at Al-Ahsa, Al-Baha, Bisha, Dhahran, Gizan, Guriat, Hail, Khamis-Mushait, Madina, Makkah, Nejran, Qasumah, Riyadh, Sharourah, Tabouk, Taif and Yanbo and increasing at remaining locations namely Abha, Al-Jouf, Al-Wejh, Gassim, Hafr-Al-Batin, Jeddah, Rafha, Sulayel, Turaif and Wadi-Al-Dawasser. Overall, a decreasing trend of 0.01852m/s per year was observed in annual mean wind speed values based on the algebraic average of the trend coefficient (a) of all the stations used in the present work. The best-fit trend lines for remaining stations are shown in Figures 5.7(b) to 5.7(j).

At Sharourah, in southern Saudi Arabia, a significantly high rate of decrease of 0.0999m/s in annual mean wind speed was observed from 1990 to 2006. Al-Ahsa was the next station where an annual decrease of 0.0876m/s was estimated and similar magnitude of rate of

decrease was followed at Al-Baha (0.0656m/s per year), Qaisumah (0.0513 m/s per year), Nejran (0.0495m/s per year), Guriat (0.0477m/s per year) and Yanbo (0.0405m/s per year). At Hafr-Al-Batin, Taif, Turaif and Al-Wejh, the rate of increase of annual wind speed of 0.0391, 0.0154, 0.0151 and 0.014m/s per year was observed, respectively. These trends need to be verified using more accurate wind speed measurements but could be used as preliminary indicators of the future wind regime in Saudi Arabia.

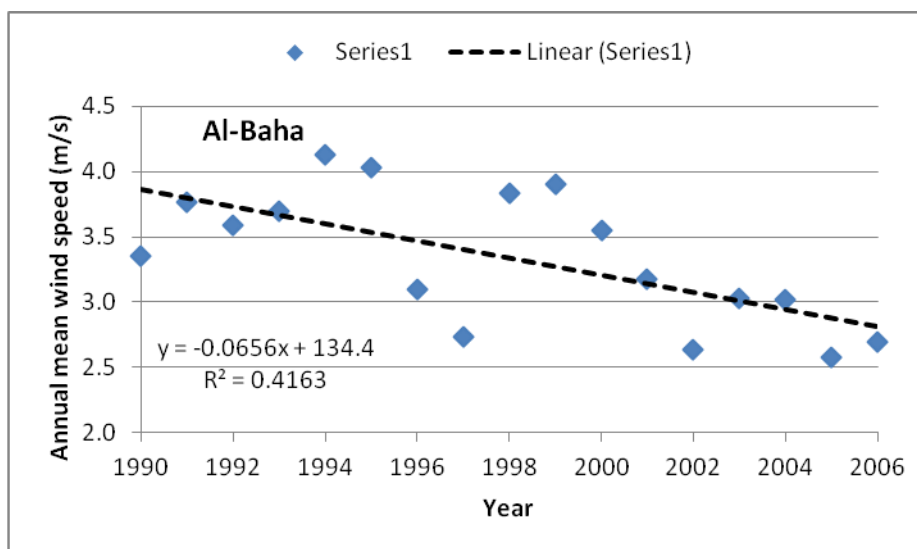
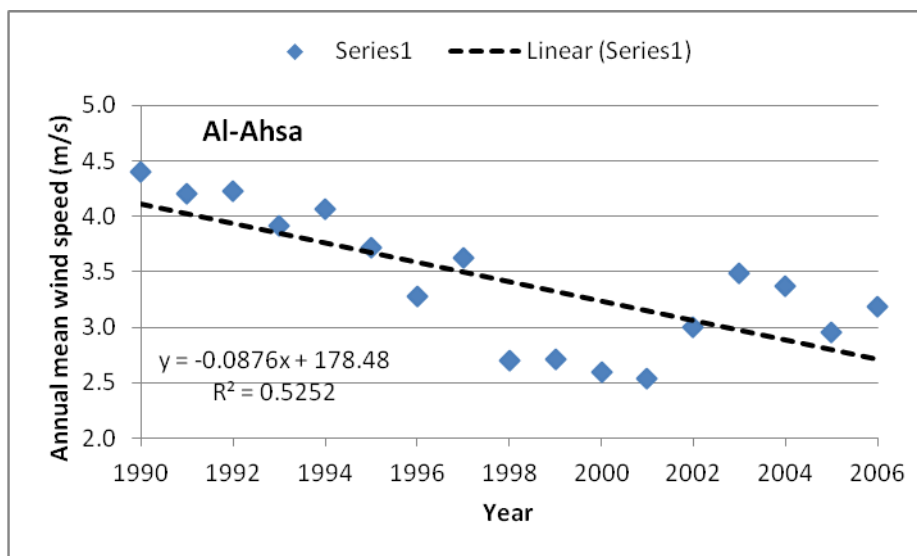
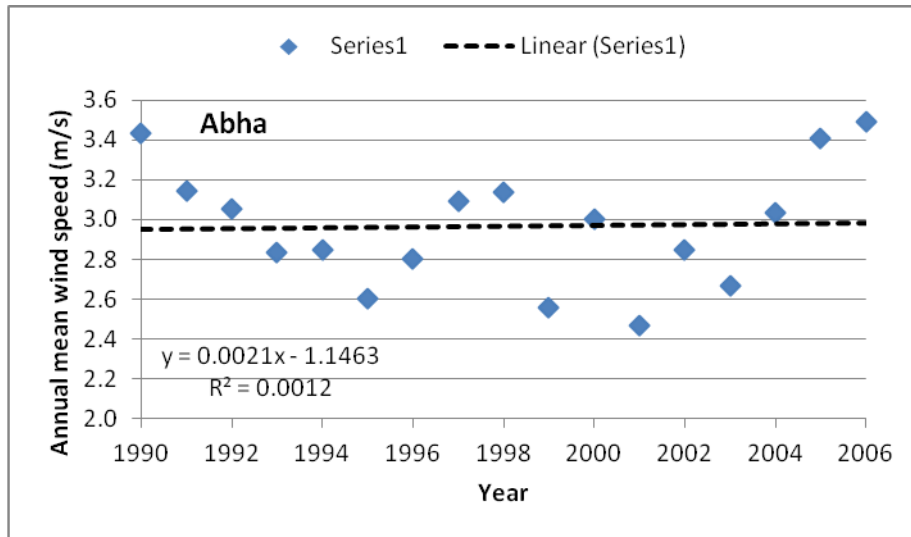


Figure 5.7(a) Annual mean wind speed trends for Abha, Al-Ahsa and Al-Baha

Table 5.3 Best-fit regression lines for annual mean wind speed trend analysis

Location	Regression coefficients		R <sup>2</sup>
	a	b	
Abha	0.0021	-1.1463	0.0012
Al-Ahsa	-0.0876	178.48	0.5252
Al-Baha	-0.0656	134.4	0.4163
Al-Jouf	0.0105	-16.926	0.1216
Al-Wejh	0.014	-23.694	0.1476
Arar	-0.0003	4.3872	5.00E-05
Bisha	-0.0241	50.499	0.2349
Dhahran	-0.013	30.28	0.08
Gassim	0.0058	-8.6893	0.0152
Gizan	-0.0321	67.239	0.5074
Guriat	-0.0477	99.475	0.484
Hafr Al-Batin	0.0391	-74.757	0.2563
Hail	-0.0265	56.177	0.1126
Jeddah	0.0016	0.4082	0.0044
Khamis-Mushait	-0.008	19	0.0442
Madinah	-0.0265	55.98	0.4414
Makkah	-0.0078	17.112	0.037
Nejran	-0.0495	100.77	0.6234
Qaisumah	-0.0513	105.96	0.5849
Rafha	0.0064	-8.9633	0.0159
Riaydh	-0.0174	37.932	0.2311
Sharourah	-0.0999	202.89	0.4922
Sulayel	0.0004	2.7283	3.00E-05
Tabouk	-0.0185	39.588	0.3946
Taif	-0.0126	28.889	0.2631
Turaif	0.0151	-25.85	0.1112
Wadi Al-Dawasser	0.0154	-27.207	0.0903
Yanbo	-0.0405	84.624	0.3275

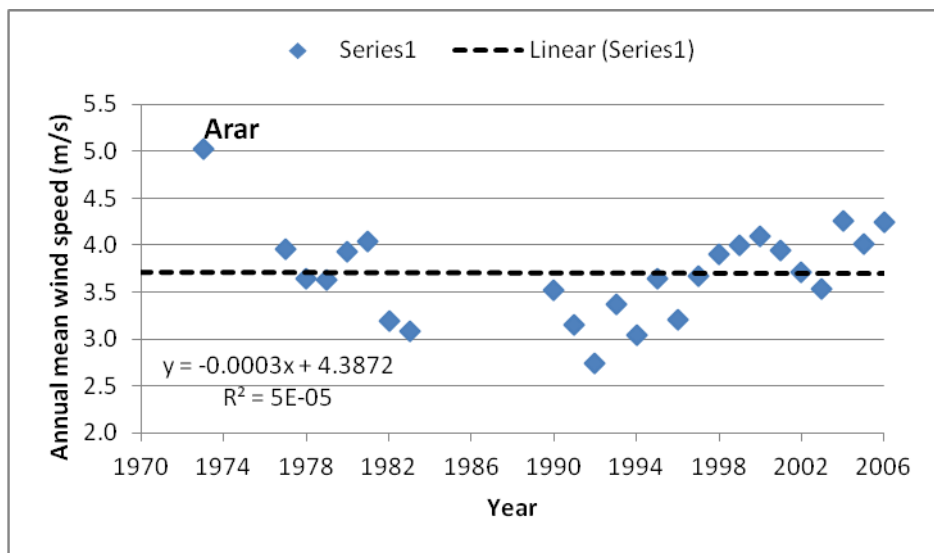
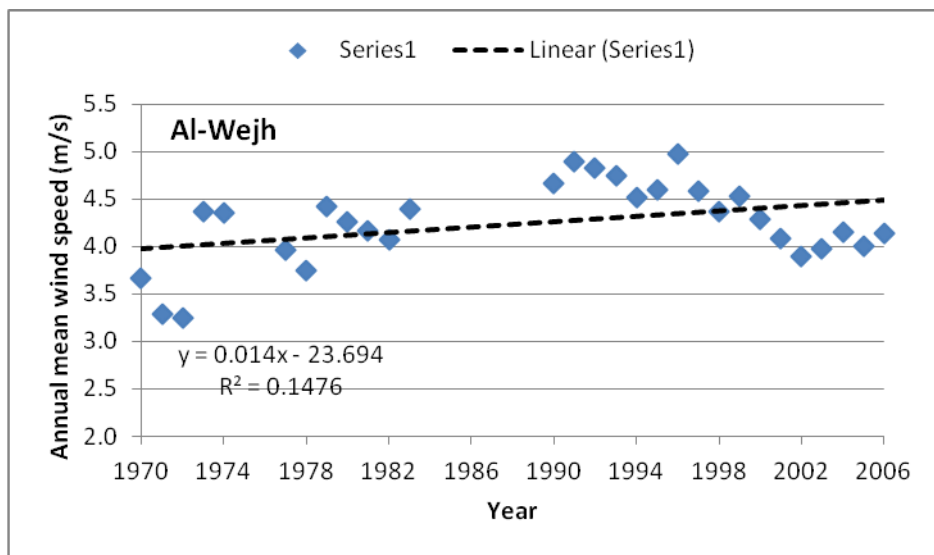
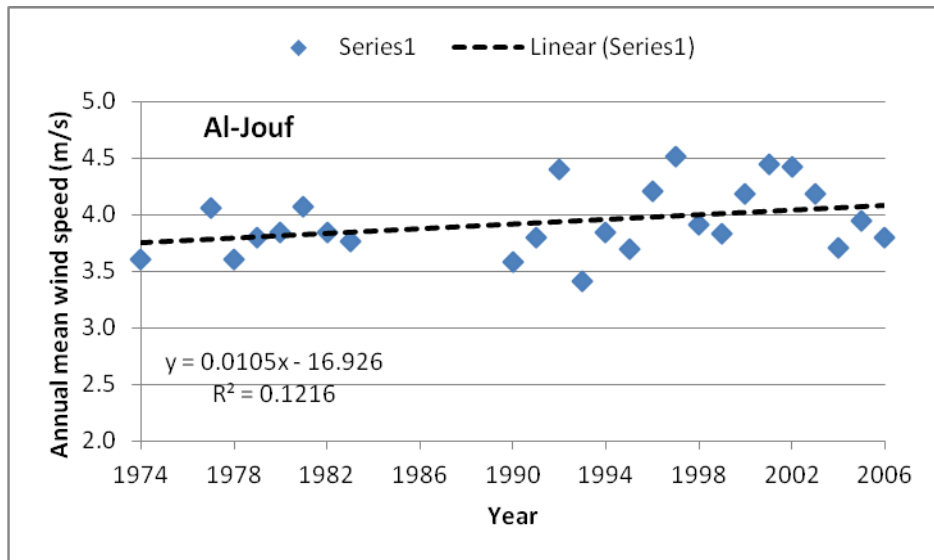


Figure 5.7(b) Annual mean wind speed trends for Al-Jouf, Al-Wejh and Arar

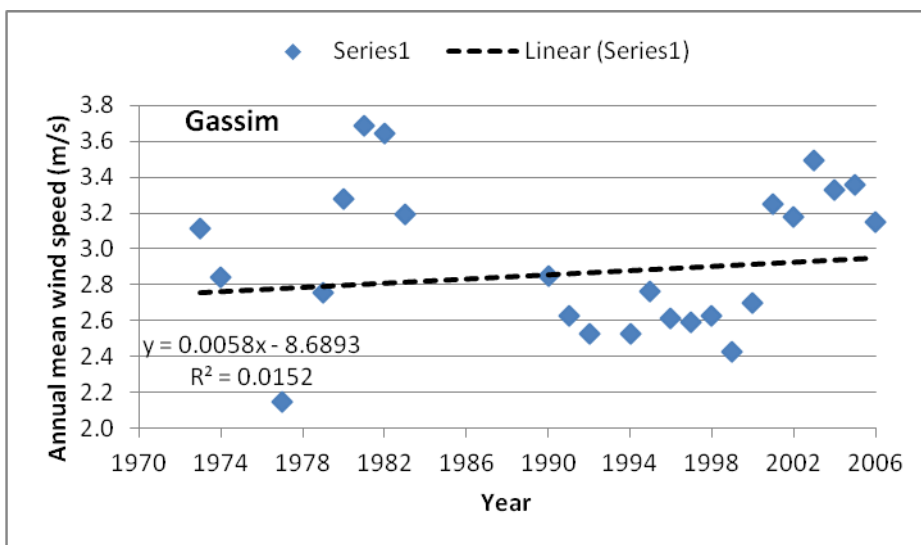
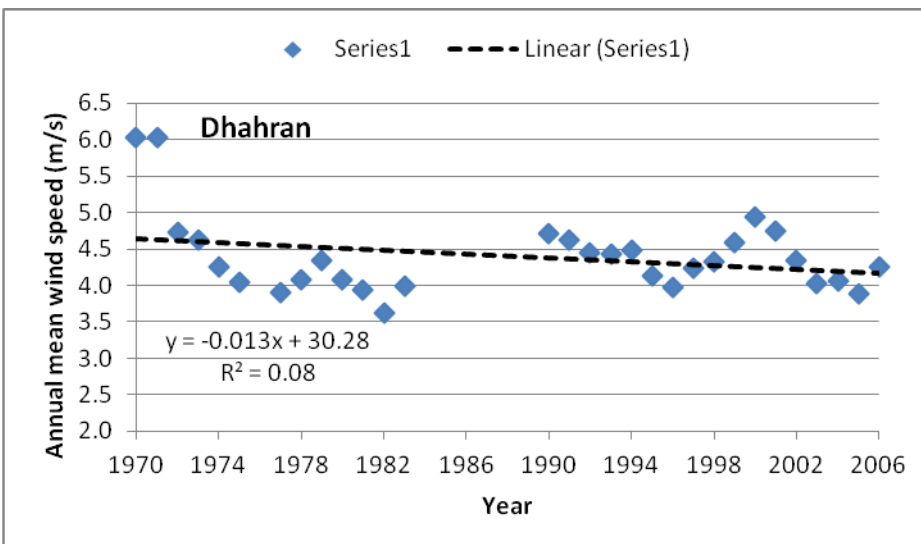
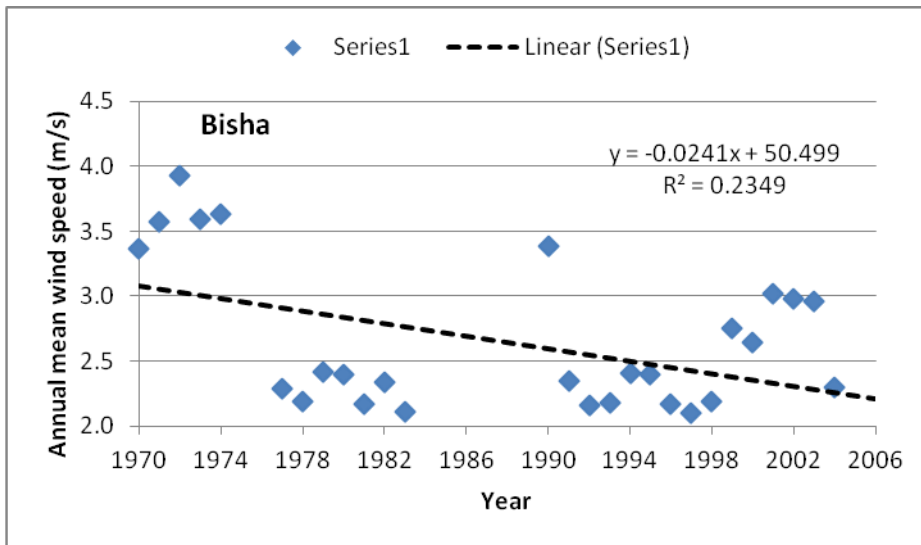


Figure 5.7(c) Annual mean wind speed trends for Bisha, Dhahran and Gassim

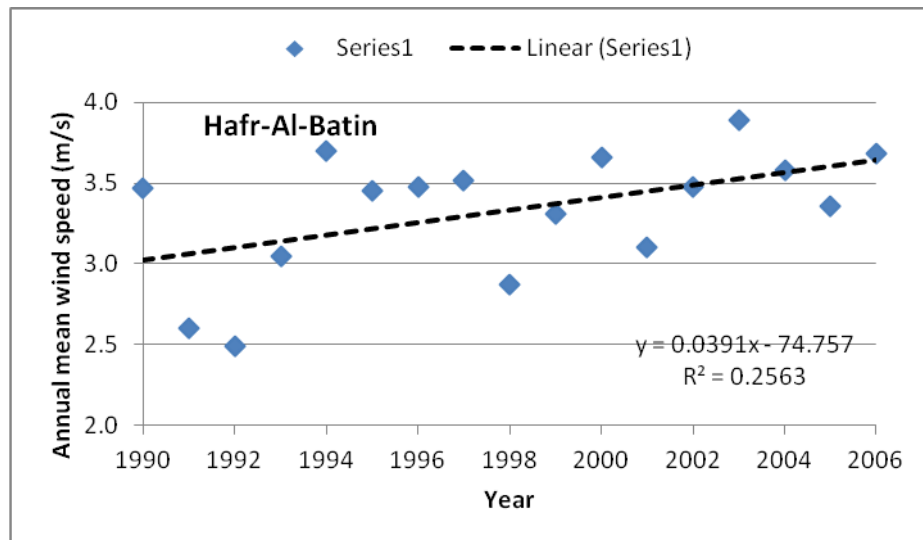
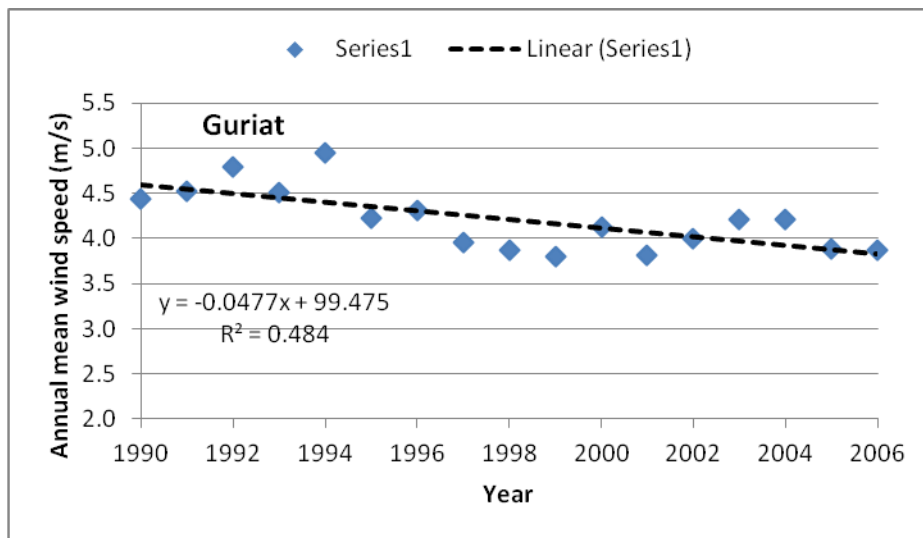
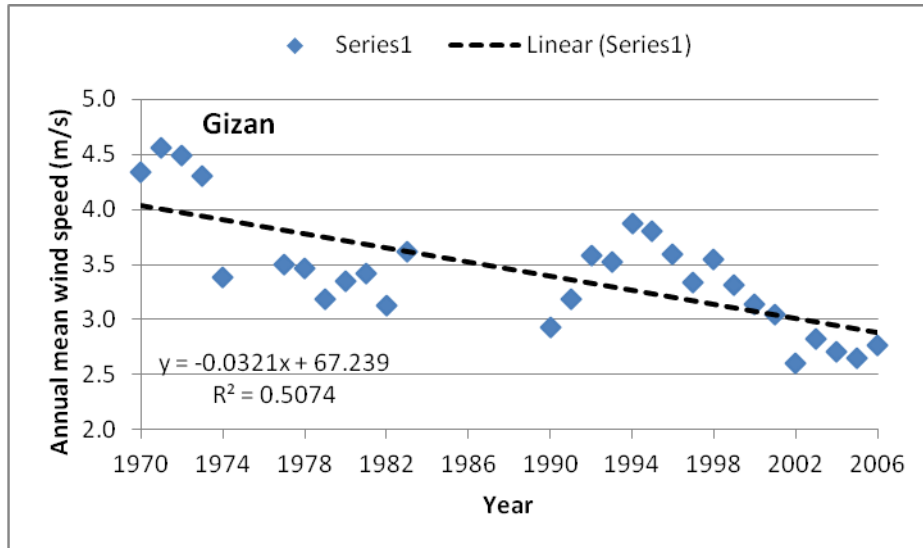


Figure 5.7(d) Annual mean wind speed trends for Gizan, Guriat and Hafr-Al-Batin

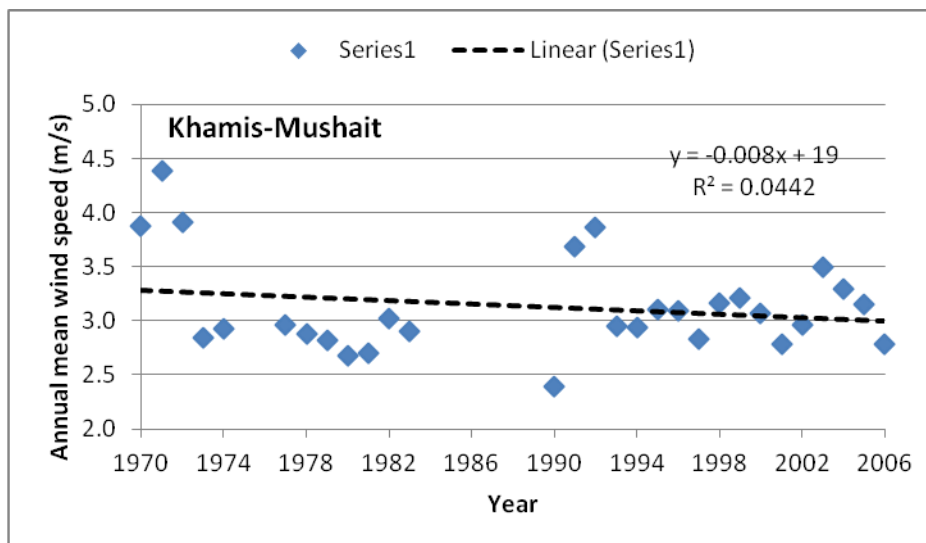
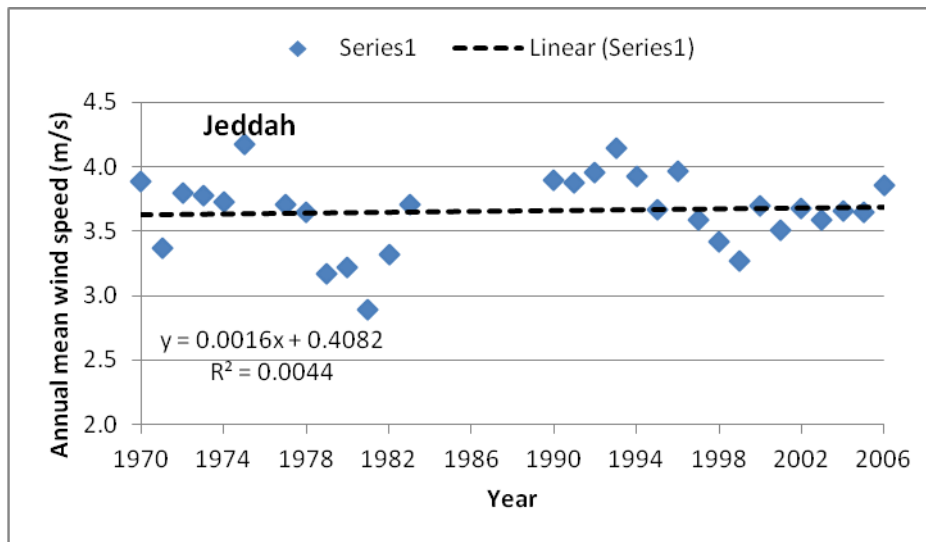
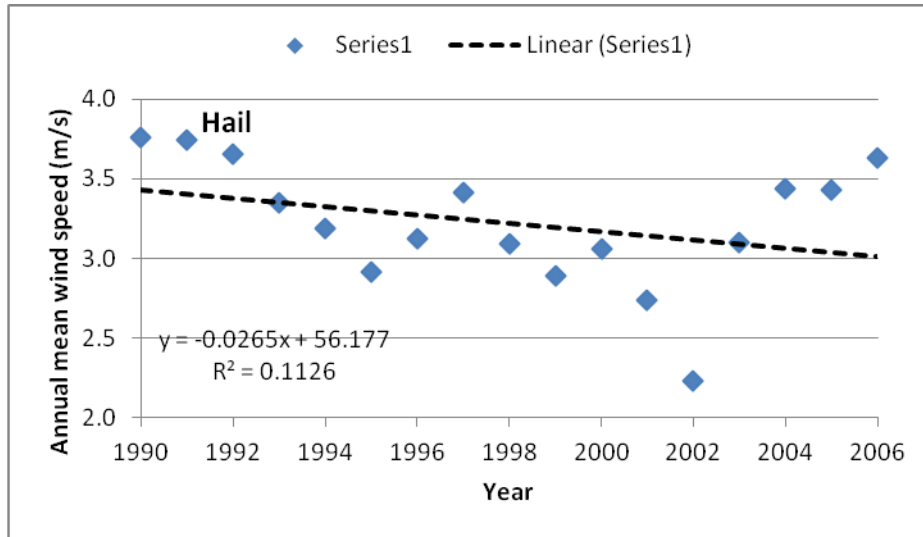


Figure 5.7(e) Annual mean wind speed trends for Hail, Jeddah and Khamis-Mushait

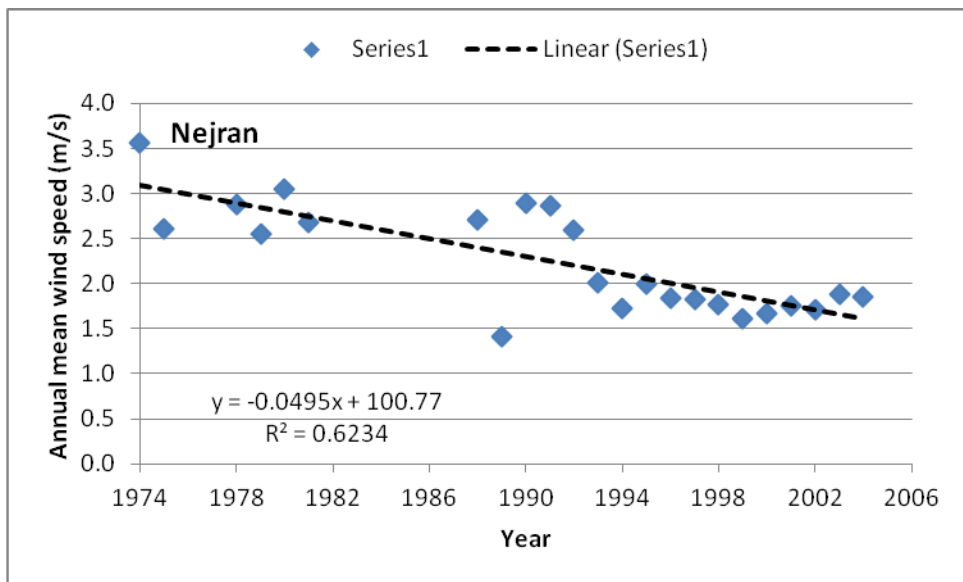
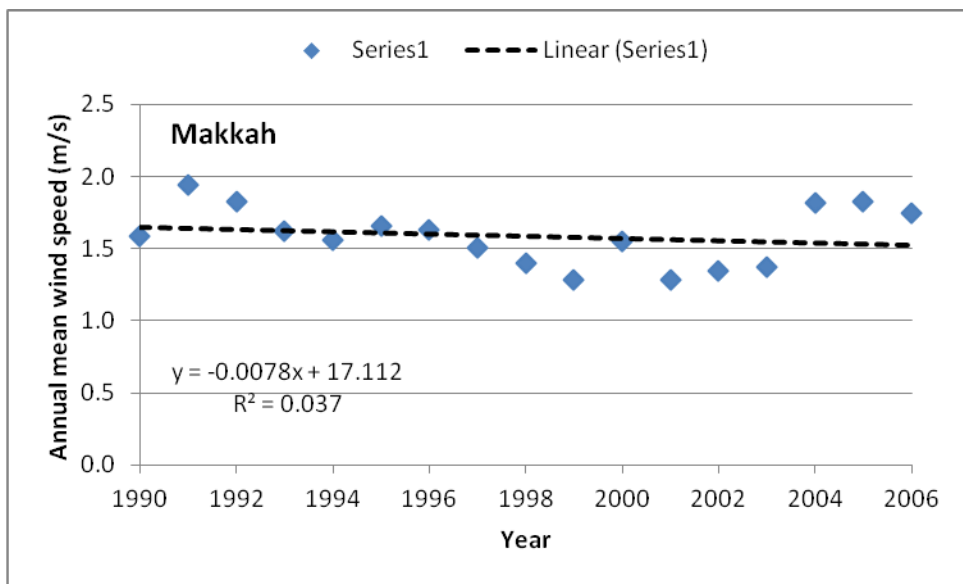
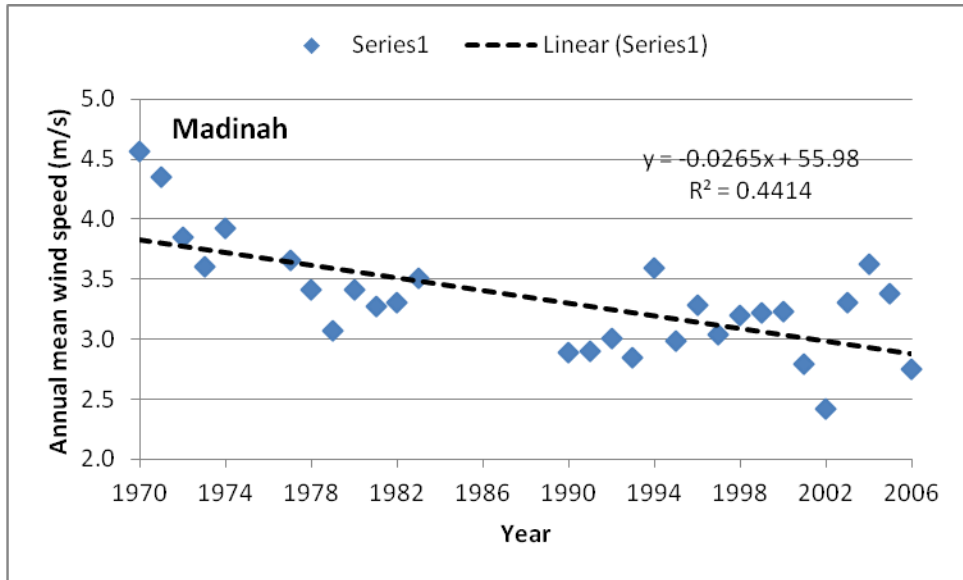


Figure 5.7(f) Annual mean wind speed trends for Madinah, Makkah and Nejran

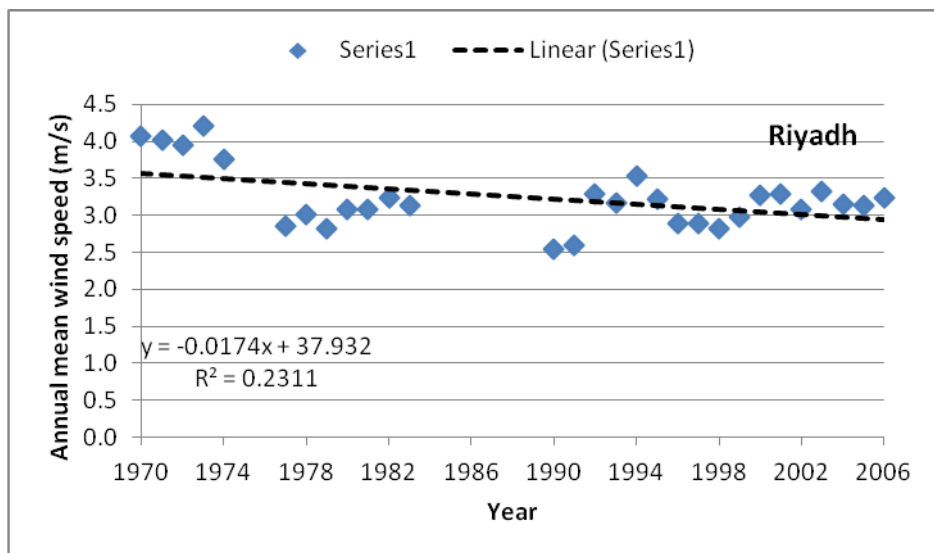
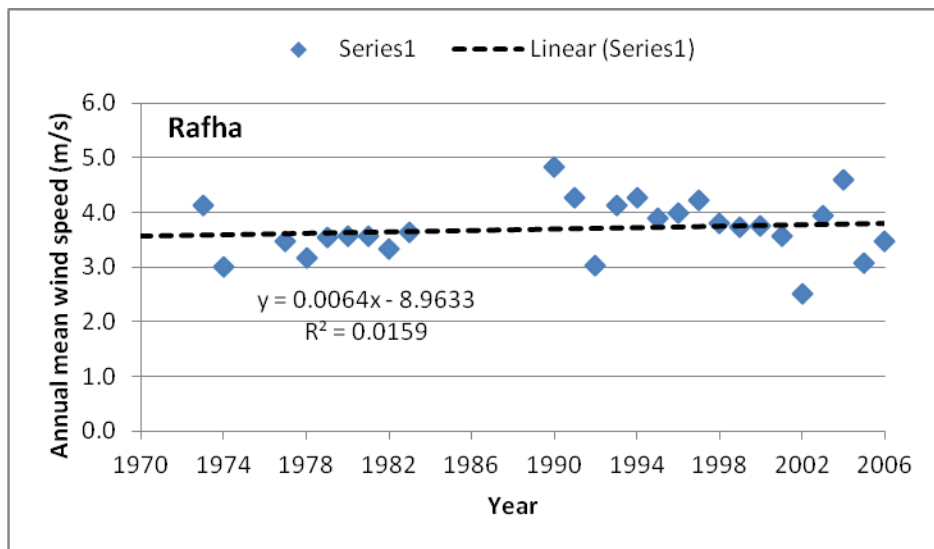
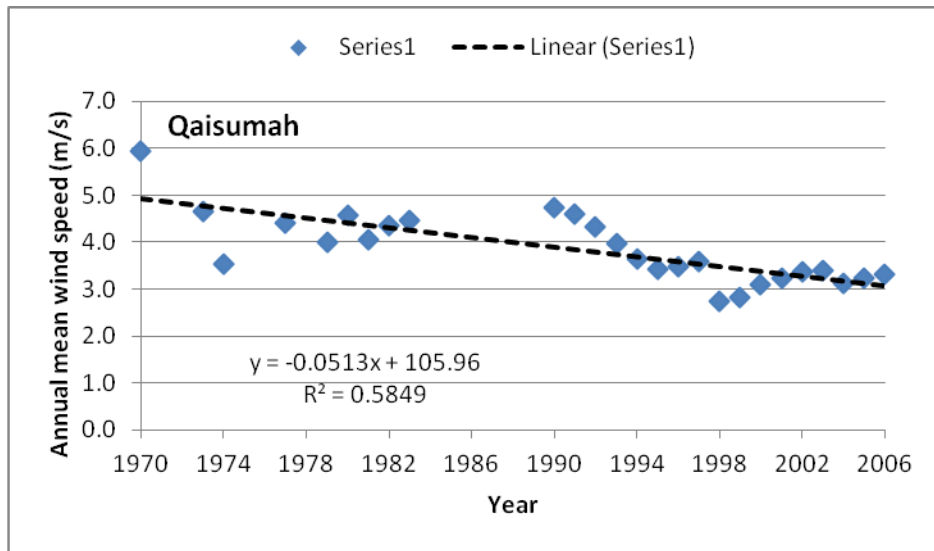


Figure 5.7(g) Annual mean wind speed trends for Qaisumah, Rafha and Riyadh

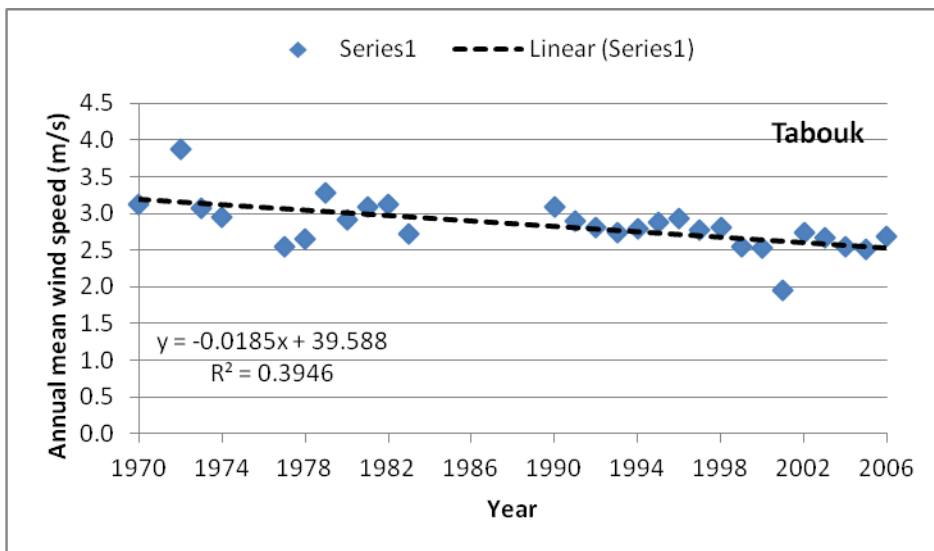
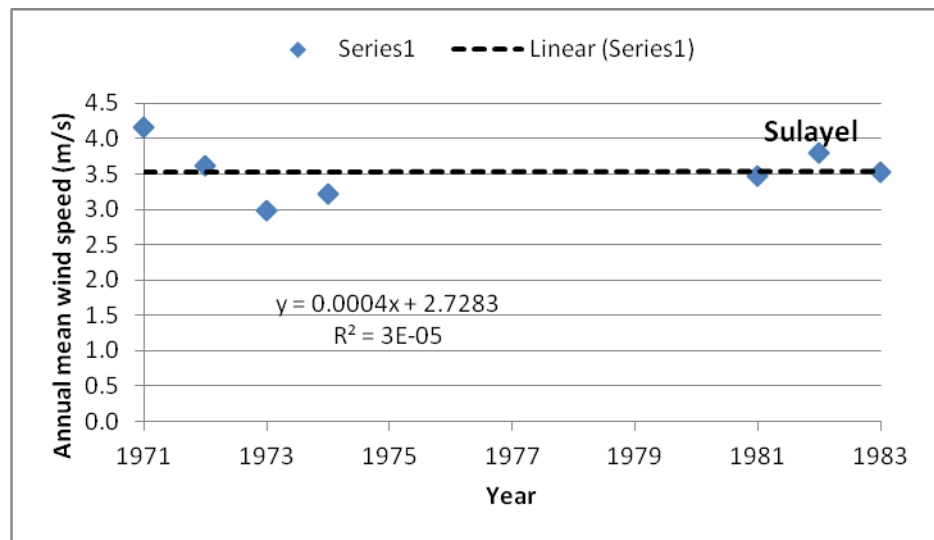
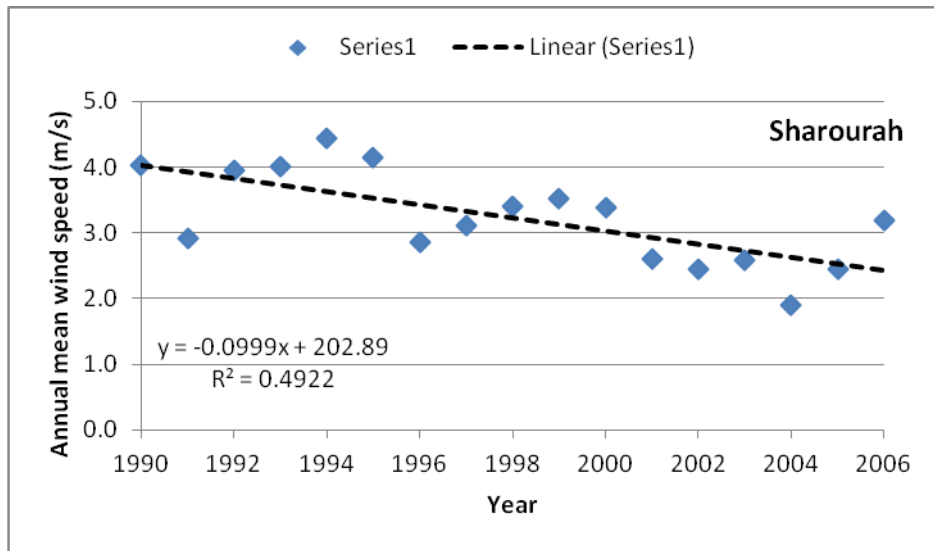


Figure 5.7(h) Annual mean wind speed trends for Sharourah, Sulayel and Tabouk

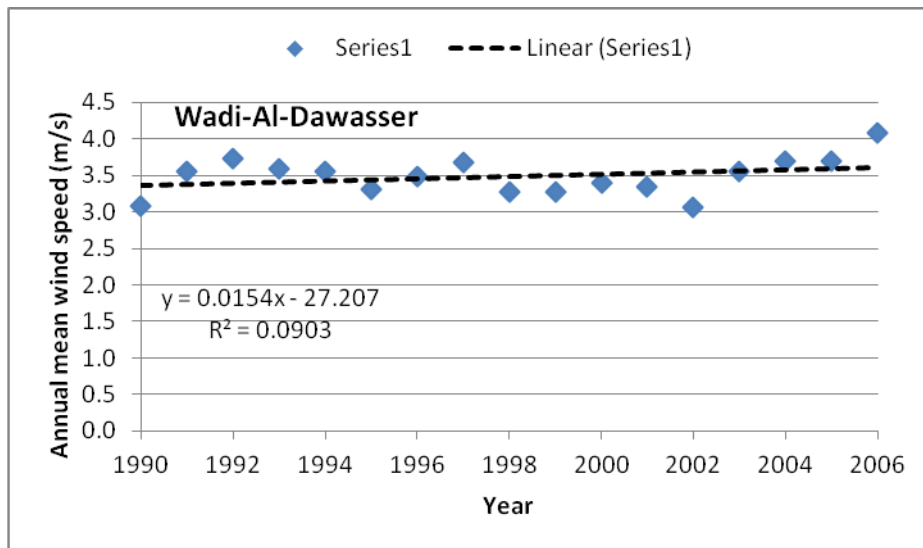
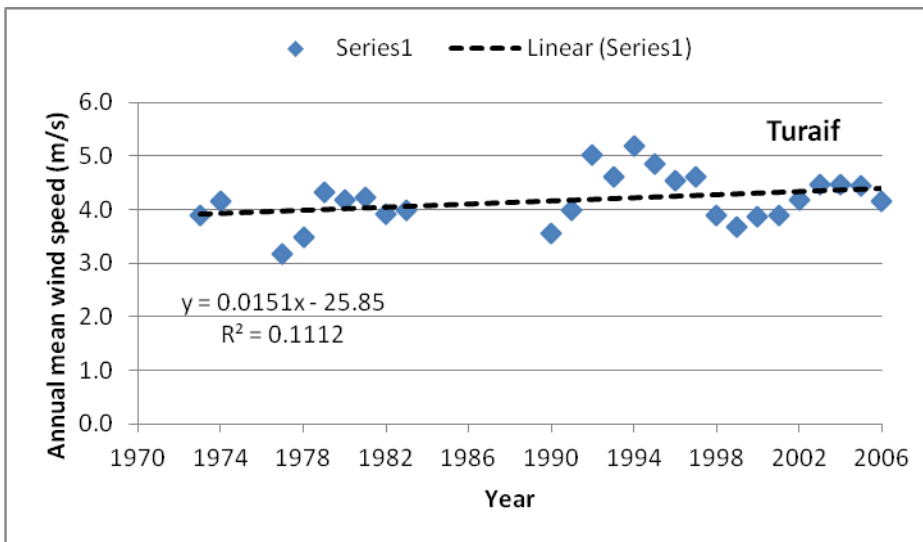
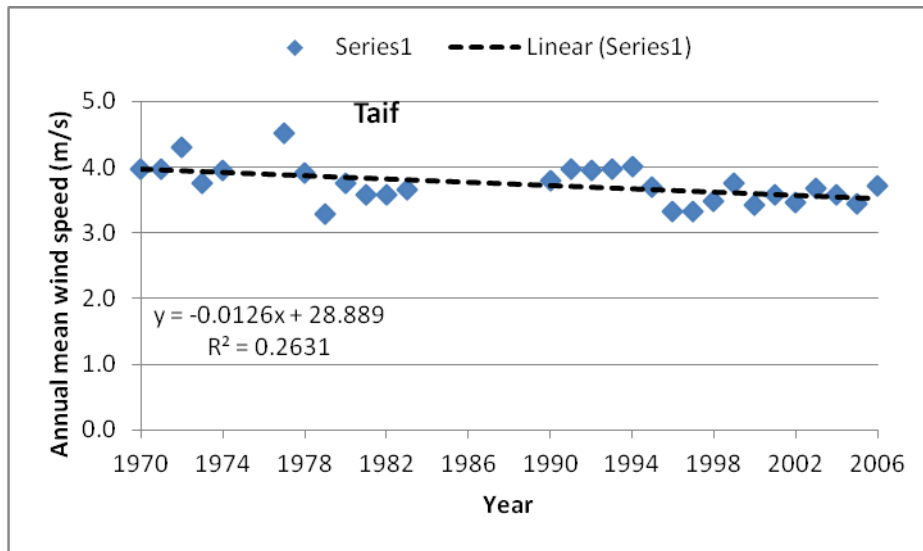


Figure 5.7(i) Annual mean wind speed trends for Taif, Turaif and Wadi-Al-Dawasser

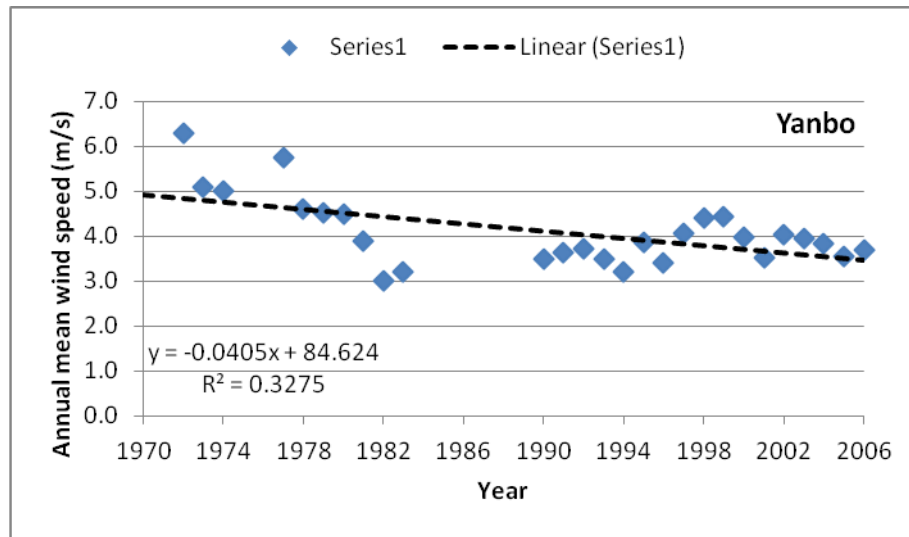


Figure 5.7(j) Annual mean wind speed trends for Yanbo

### 5.3 SEASONAL VARIATION OF WIND SPEED

The study of seasonal trends of wind speed is required to manage the electricity production from wind during different months of the year and then to integrate it with the grid and the load centres. The monthly mean values of wind speed were calculated over the entire period of data collection and for all the locations. The monthly mean wind speed at Abha was higher during January to March and varied between 2.5 to 3m/s during rest of the months as can be seen in Figure 5.8(a). At Al-Ahsa and Al-Baha, the wind speed was the highest in July and the lowest in October and November. At Al-Ahsa, the wind speed varied between 2.5 and 4m/s while at Al-Baha, from 2.5 to 4.75m/s. At Al-Jouf, Al-Wejh and Arar, the wind speed values were always above 3m/s while at Bisha, it remained between 2.5 and 3m/s, as depicted in Figure 5.8(a).

The highest mean wind speed at Dhahran was observed in June and the lowest in October, as shown in Figure 5.8(b). Larger seasonal variations were observed at Dhahran and Guriat while smaller seasonal ranges (2.5 to 4m/s) were seen at Gassim, Gizan, Hafr-Al-Batin, Hail and Jeddah. At Kahmis-Mushait, Madinah, Qaisumah, Rafha and Riyadh, relatively higher monthly mean wind speeds were observed compared to Makkah and Nejran, as given in Figure 5.8(c). At Sulayel and Wadi-Al-Dawasser, higher values were observed during the winter months with lower values during summer time, as observed from Figure 5.8(d). It is evident from this analysis that at most of the stations, the wind speed values were higher during summer months and lower during winter months with the above exception.

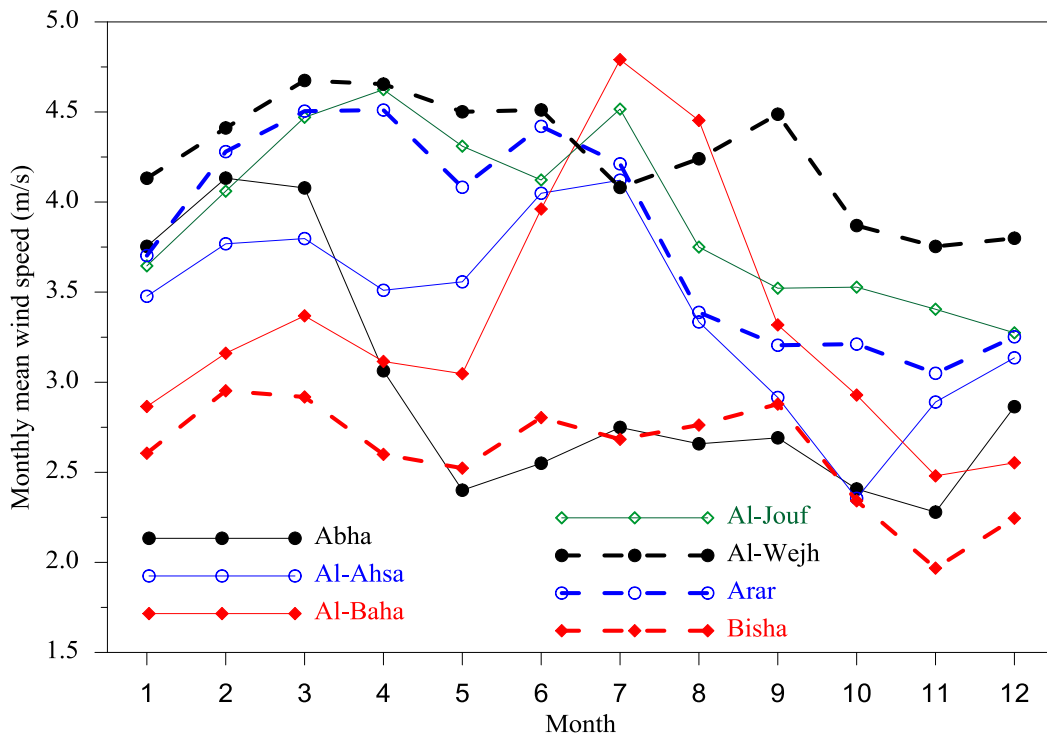


Figure 5.8(a) Seasonal variation of long-term mean wind speed at seven locations

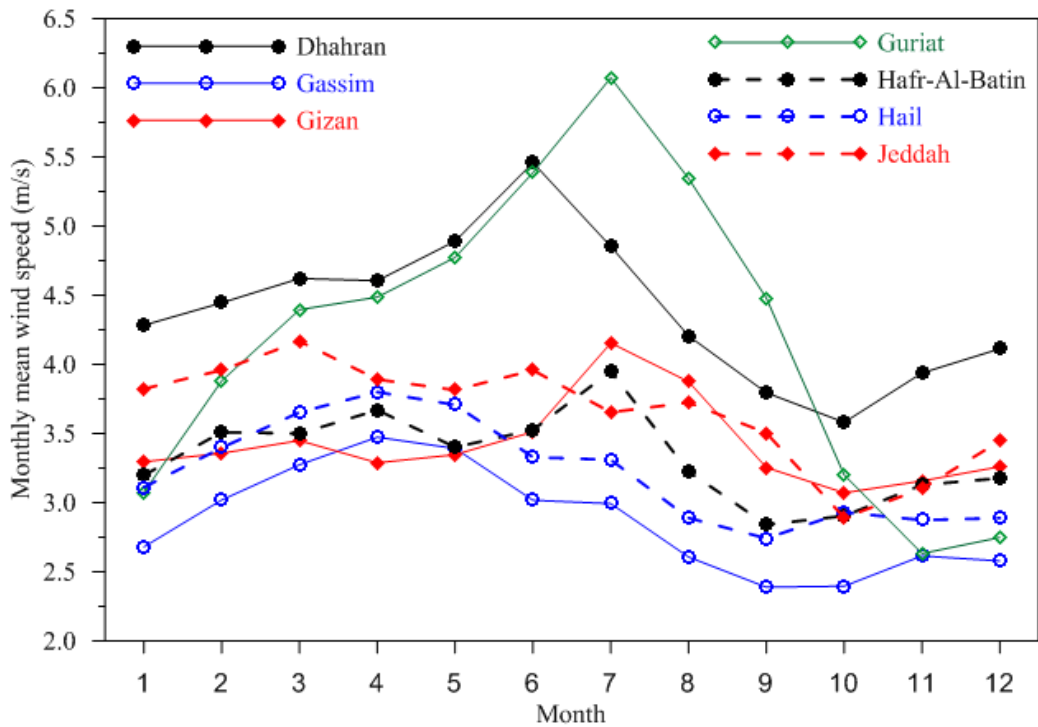


Figure 5.8(b) Seasonal variation of long-term mean wind speed at seven locations

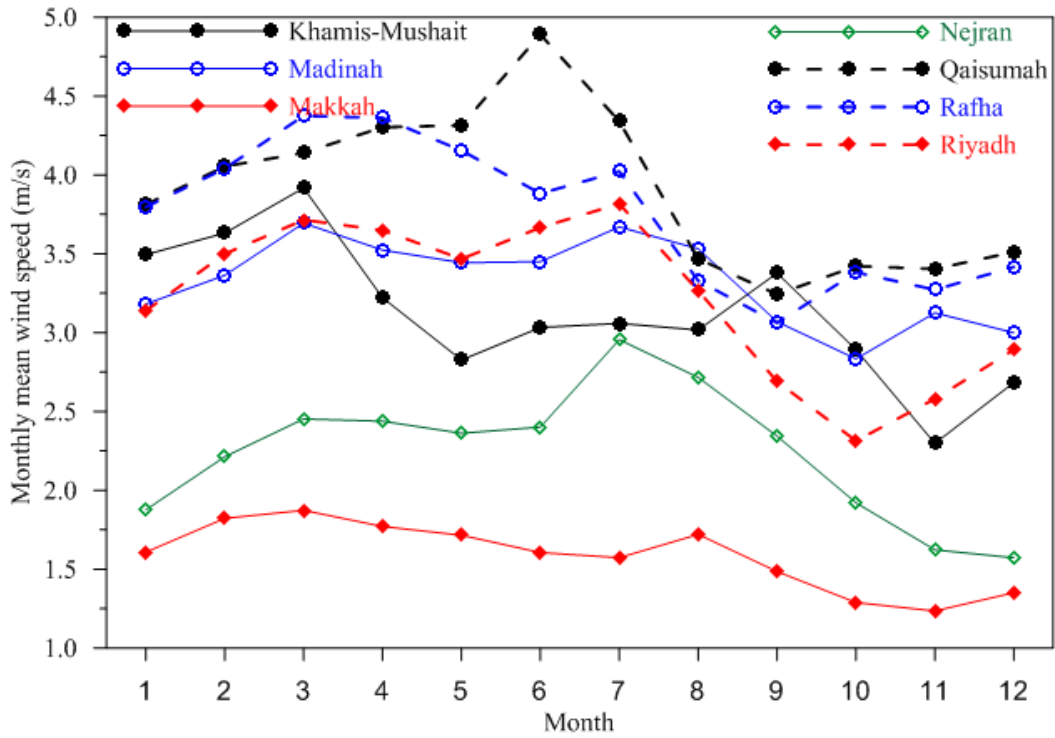


Figure 5.8(c) Seasonal variation of long-term mean wind speed at seven locations

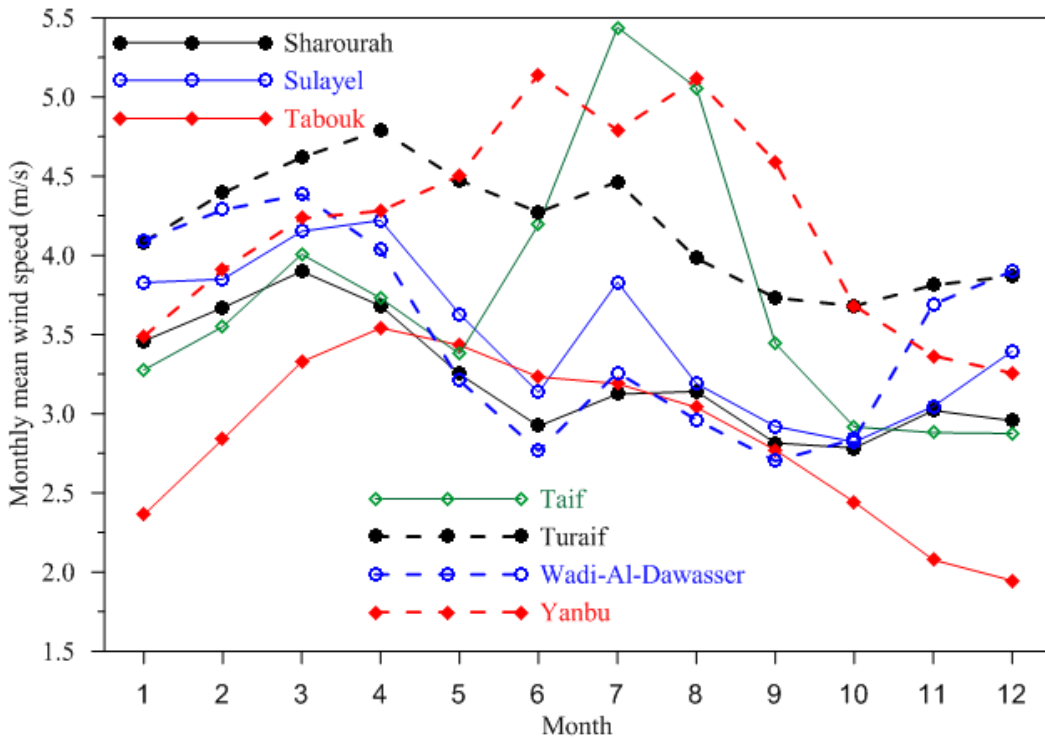


Figure 5.8(d) Seasonal variation of long-term mean wind speed at seven locations

#### 5.4 WEIBULL PARAMETERS AND WIND FREQUENCY DISTRIBUTION

It is a well-understood fact that Weibull distribution gives a good match with the measured wind speed data. This distribution is characterised by two parameters: the shape parameter  $k$  (dimensionless) and scale parameter  $c$  (m/s). The shape parameter reflects the breadth of the distribution, with lower values corresponding to broader distributions where the wind speed tends to vary widely, whereas higher  $k$  values correspond to tighter distributions where the wind speed tends to stay within a narrower range. The Weibull distribution is expressed mathematically as:

$$f(v) = \left(\frac{k}{c}\right) \left(\frac{V}{c}\right)^{k-1} \exp \left[ -\left(\frac{V}{c}\right)^k \right] \quad (5.6)$$

$$F(v) = 1 - \exp \left[ -\left(\frac{v}{c}\right)^k \right] \quad (5.7)$$

where  $V$  is the measured wind speed. To solve for  $k$  and  $c$ , the principle of maximum likelihood method was applied. This results in the following non-linear equations for shape and scale parameters  $k$  and  $c$ , respectively:

$$k = \left[ \frac{\sum v_i^k (\ln v_i)}{\sum v_i^k} - \frac{\sum \ln v_i}{n} \right]^{-1} \quad (5.8)$$

$$c = \left( \frac{\sum \ln v_i^k}{n} \right)^{1/k} \quad (5.9)$$

Where  $v_i (i=1,2,3,\dots,n)$  is the observed mean monthly or annual wind speeds. The annual values of Weibull shape and scale parameters calculated using the above-mentioned method are summarised in Table 5.4. The Weibull shape parameter values were found to be highest of 3.0 at Madinah and lowest of 0.37 at Makkah, as can be seen from Figure 5.8 and data provided in Table 5.4. The Weibull scale parameter values followed the same trend as that of wind speed, which is very evident from Table 5.4 and Figure 5.10. At Abha, Al-Wejh, Gizan and Makkah the  $k$  values were less than 1, which is indicative of a broader distribution and

simply means a wider range or large variation. In Makkah, with a least value of  $k = 0.37$ , the highest variation in annual mean wind speed values was observed. This characteristic of small values of shape parameter  $k$  at the Al-Wejha, Abha, Gizan and Makkah stations is very well represented in Figures 5.11(a), (b), 5.12(d) and 5.13(b), respectively. At all other stations, the  $k$  values were greater than 2 and hence tight frequency distributions were observed.

Table 5.4 Long-term mean values of Weibull parameters over Saudi Arabia

Location	Latitude (°N)	Longitude (°E)	Weibull k	Weibull c, (m/s)
Abha	18.2	42.7	0.64	2.88
Al-Ahsa	25.3	49.5	2.11	3.86
Al-Baha	20	41.5	2.42	3.77
Al-Jouf	29.8	39.9	2.30	4.46
Al-Wejh	26.2	36.5	0.95	4.24
Arar	30.9	41.1	2.14	4.32
Bisha	20	42.6	2.30	2.94
Dhahran	26.3	50.2	2.74	4.95
Gassim	26.3	43.8	2.09	3.23
Gizan	16.9	42.6	0.80	3.39
Guriat	31.4	37.3	2.24	4.75
Hafr-Al-Batin	28.3	46.1	2.15	3.77
Hail	27.4	41.7	2.58	3.62
Jeddah	21.7	39.2	2.95	4.09
Khamis-Mushait	18.3	42.8	2.55	3.52
Madinah	24.6	39.7	3.03	3.71
Makkah	21.5	39.8	0.37	1.48
Nejran	17.6	44.4	2.29	2.53
Qaisumah	28.3	46.1	2.09	4.43
Rafha	29.6	43.5	2.23	4.26
Riyadh	24.7	46.7	2.27	3.65
Sharourah	17.5	47.1	2.48	3.63
Sulayel	20.46	45.64	2.28	3.96
Tabuk	28.4	36.6	2.16	3.22
Taif	21.5	40.6	2.77	4.20
Turaif	31.7	38.7	2.32	4.71
Wadi-Al-Dawasser	20.52	45.19	2.43	3.95
Yanbo	24.2	38.1	2.45	4.73

Wind speed frequency distribution is useful in estimating the number of hours in different wind speed bins, which then could be used to calculate the energy yield from a chosen wind turbine. In the present case, daily mean values of wind speed are used instead of hourly mean values, which are less accurate. The frequency distribution of daily mean values of wind speed is shown in Figures 5.11 to 5.14 for all the stations. All of these stations were well

represented by Weibull scale and shape parameters with the exception of Abha, Al-Wejh, Gizan and Makkah where  $k$  values were less than 1.0 and the distribution became wide open.

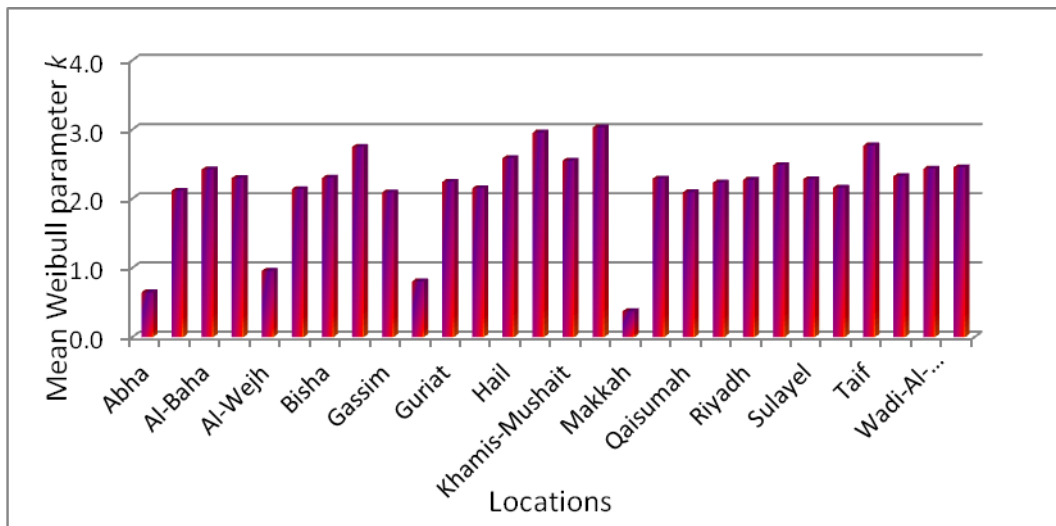


Figure 5.9 Long-term mean Weibull shape parameter,  $k$

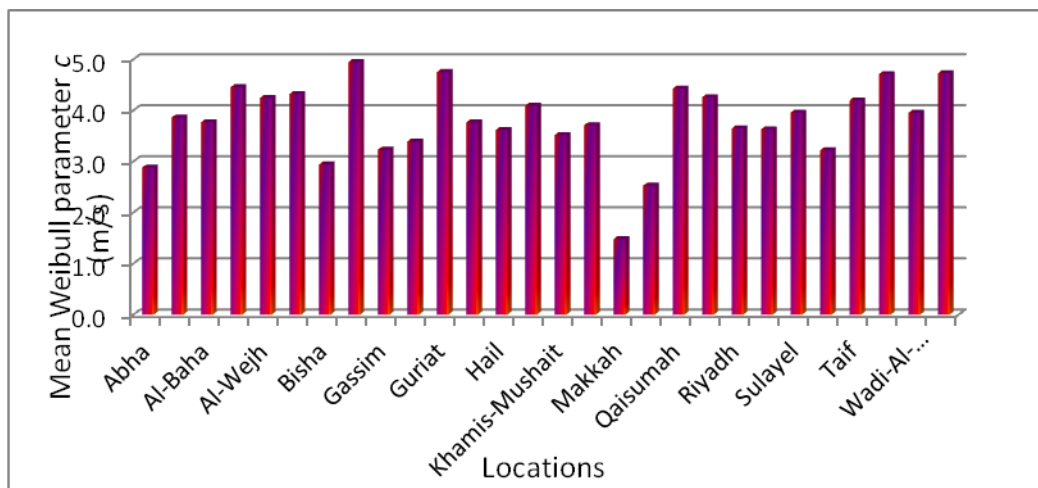


Figure 5.10 Long-term mean Weibull scale parameter,  $c$ (m/s)

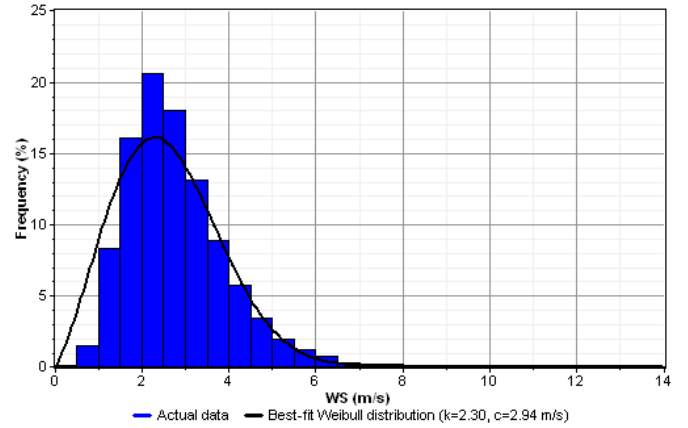
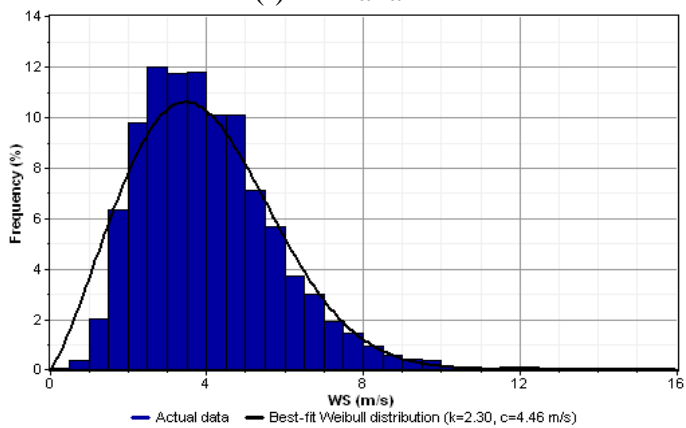
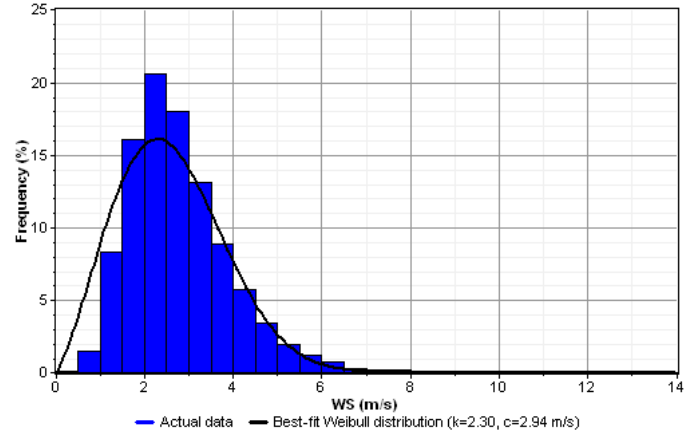
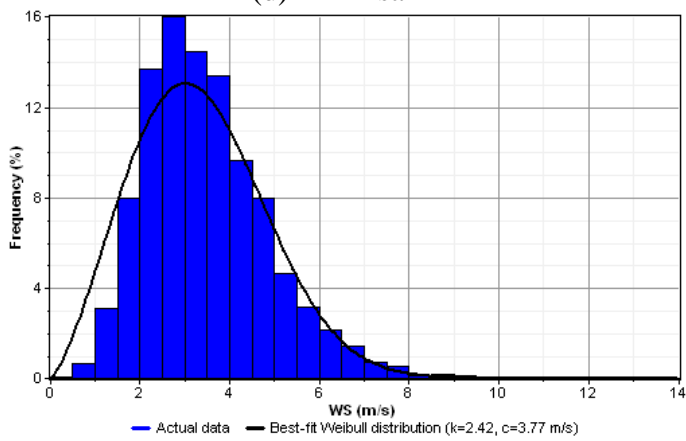
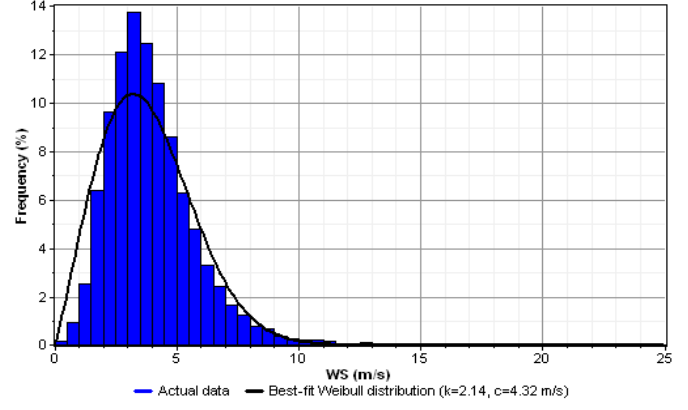
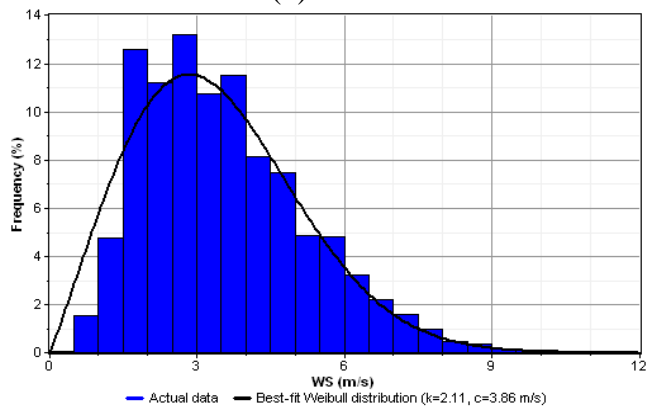
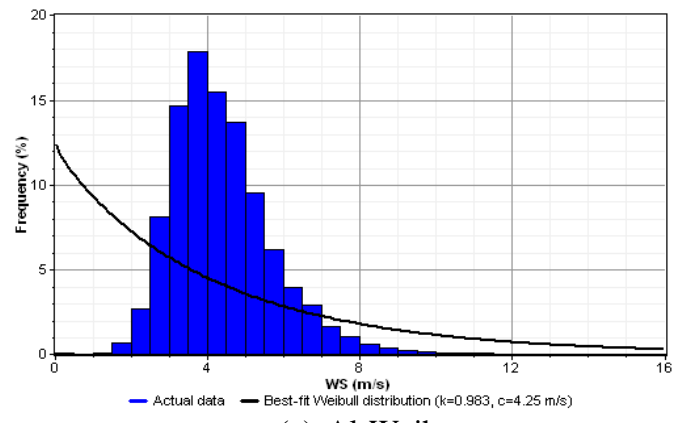
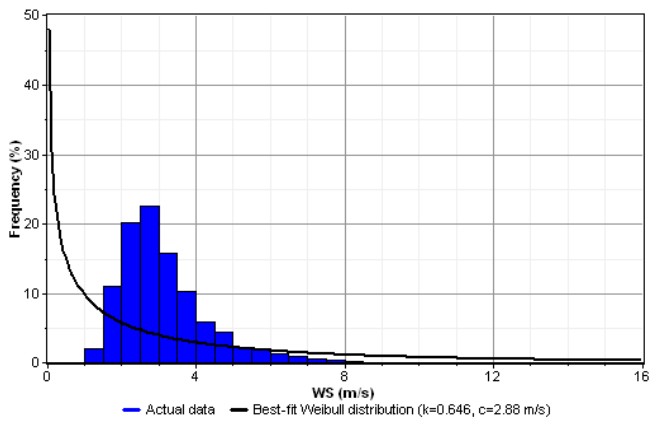
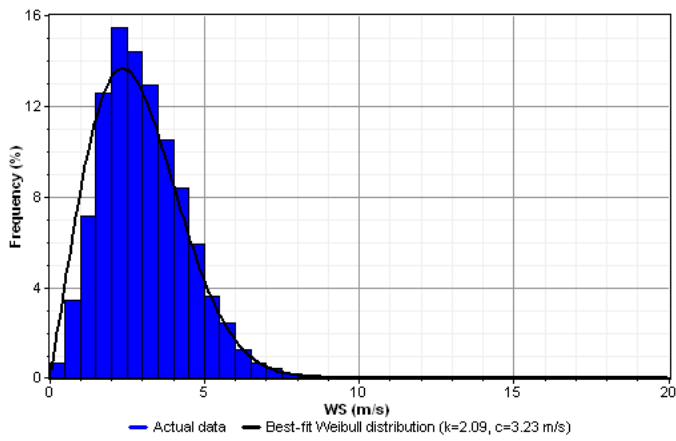
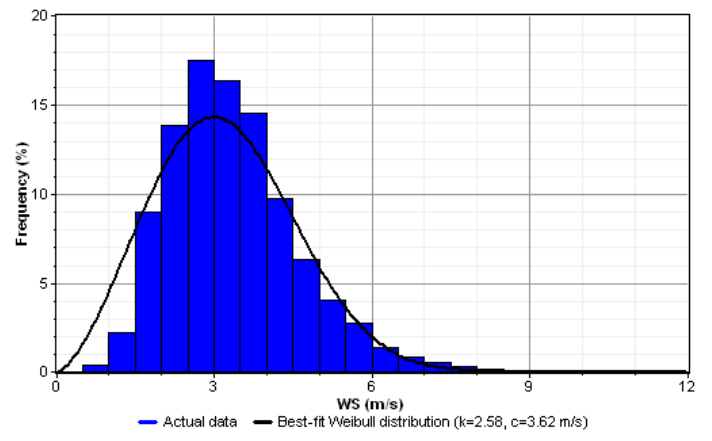


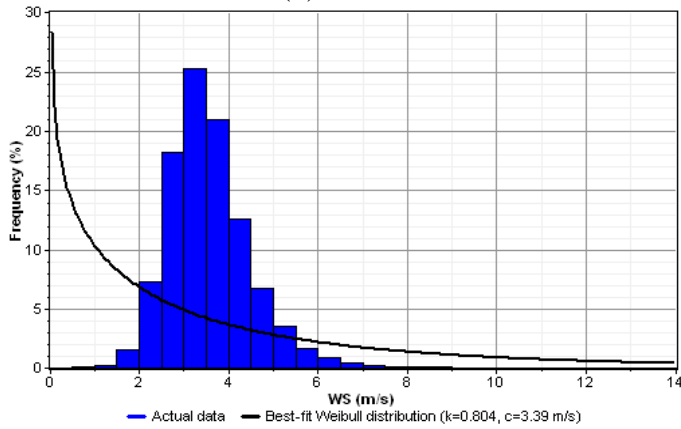
Figure 5.11 Frequency distribution



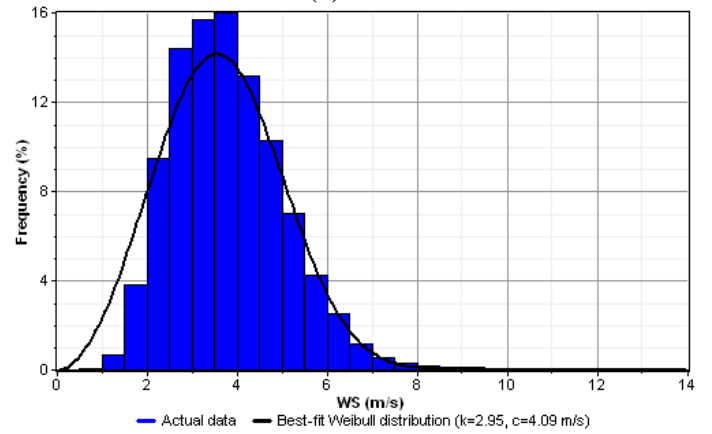
(b) Gassim



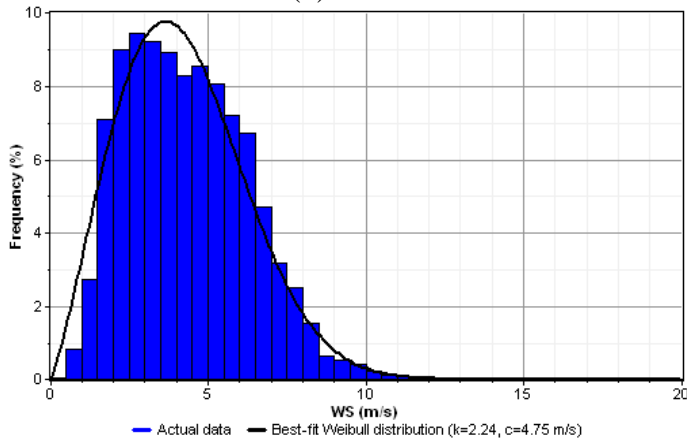
(a) Hail



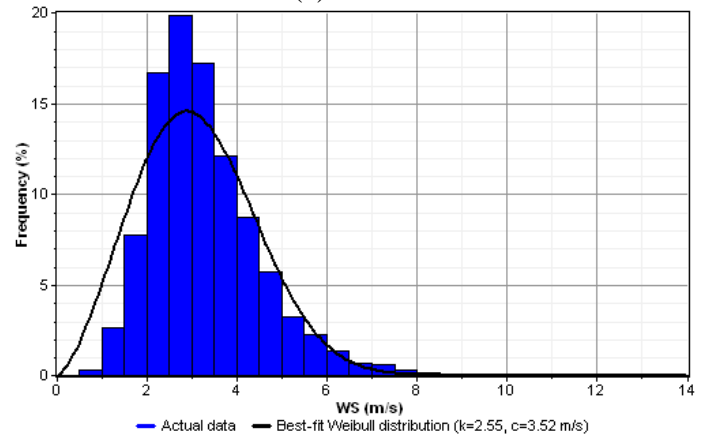
(d) Gizan



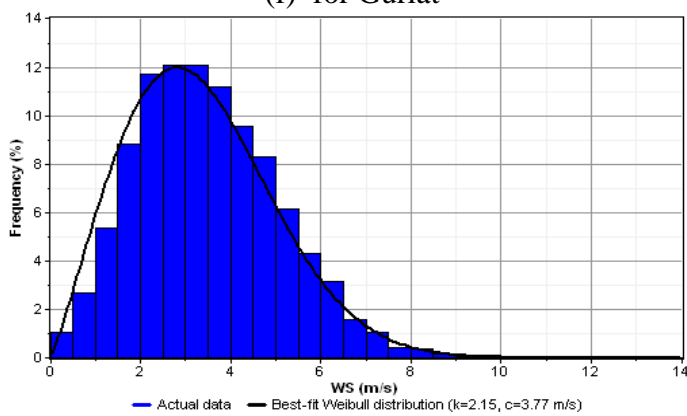
(c) Jeddah



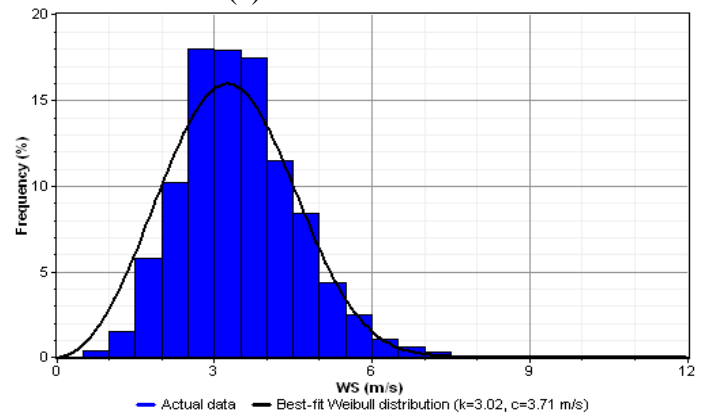
(f) for Guriat



(e) Khamis-Mushait

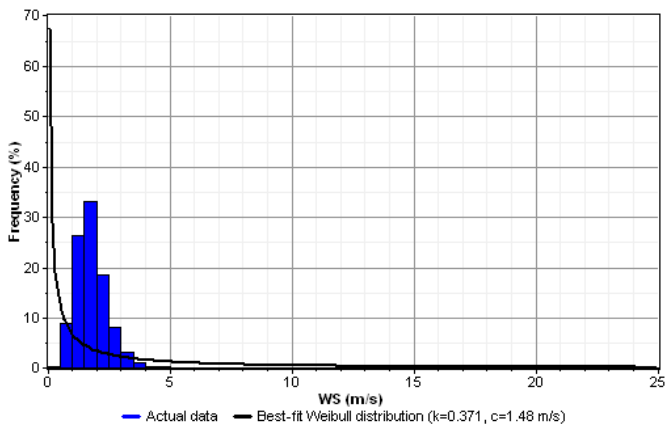


(g) Hafr Al-Batin

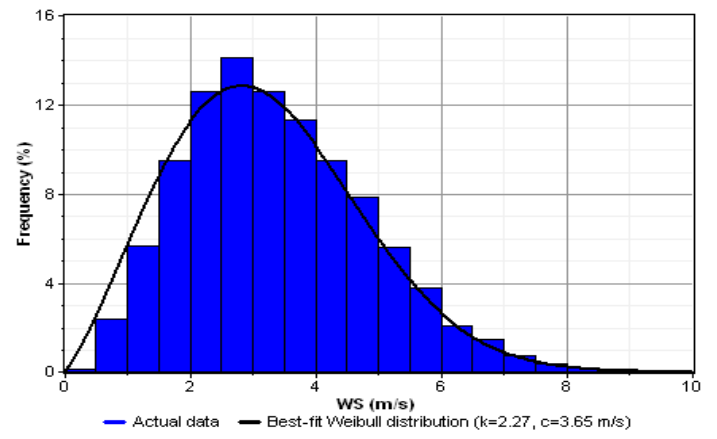


(h) Madinah

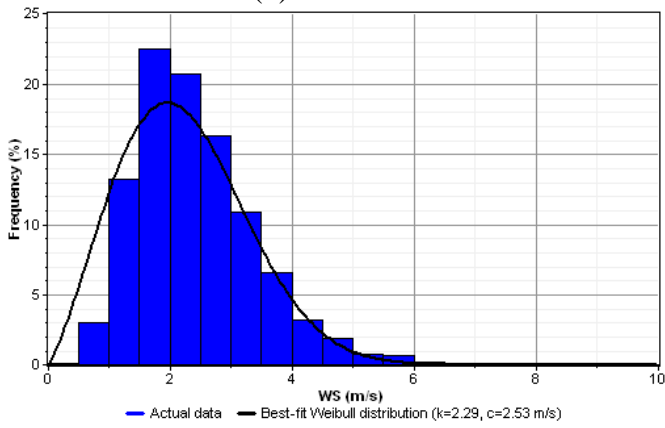
Figure 5.12 Frequency distribution



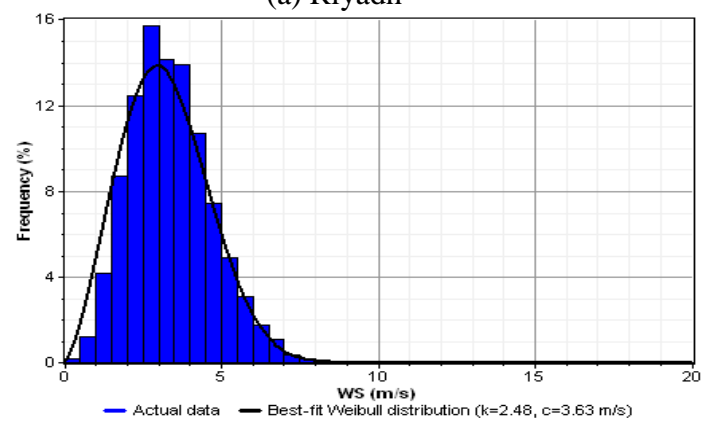
(b) Makkah



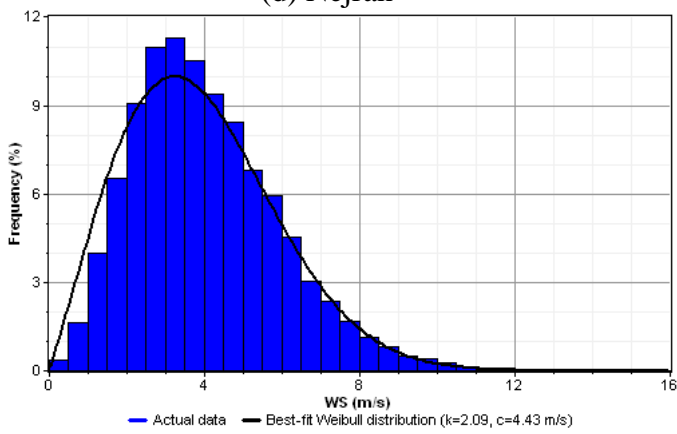
(a) Riyadh



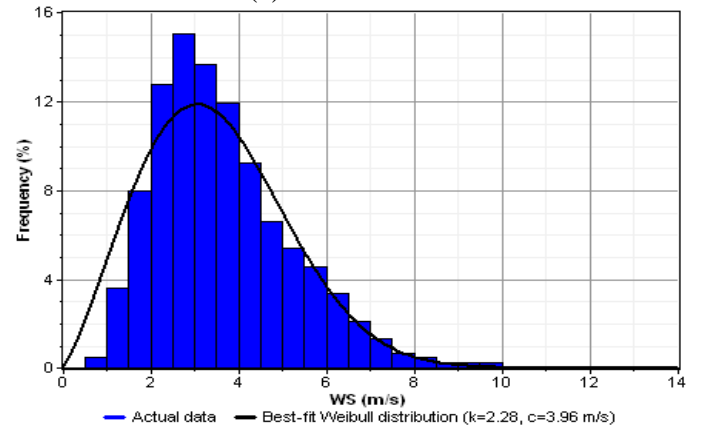
(d) Nejran



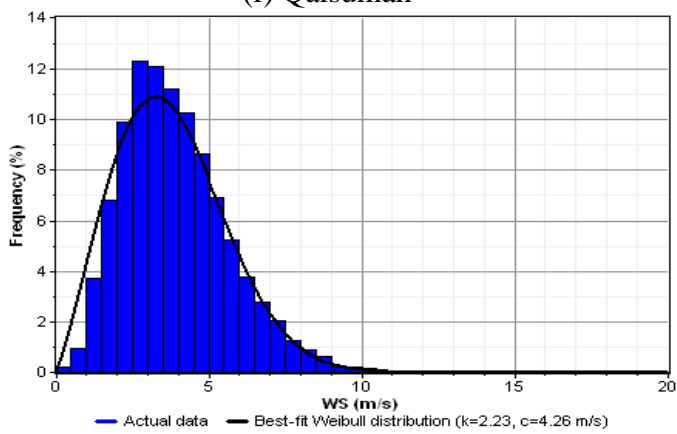
(c) Sharourah



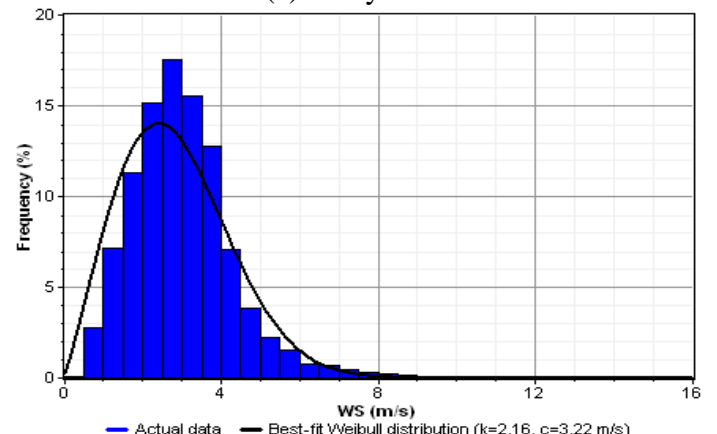
(f) Qaisumah



(e) Sulayl

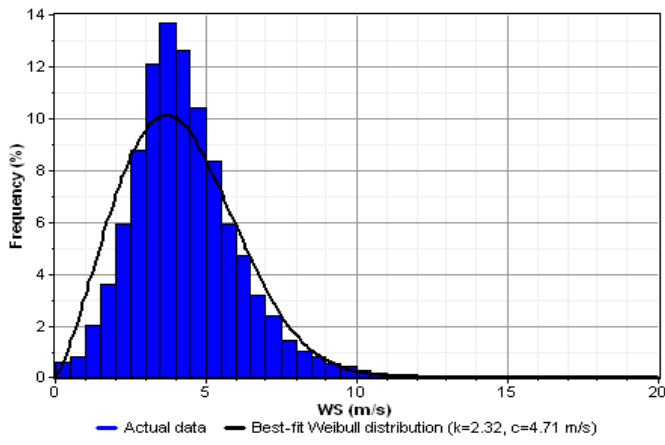


(h) Rafha

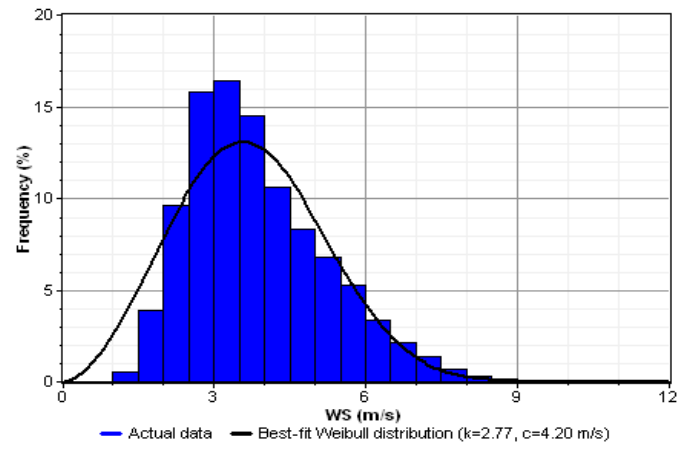


(g) Tabuk

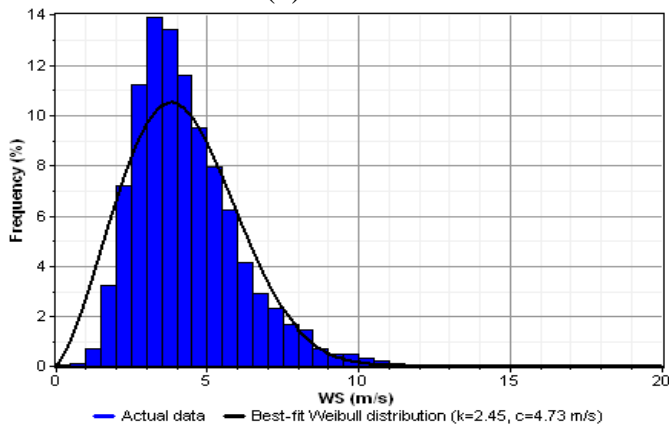
Figure 5.13 Frequency distribution



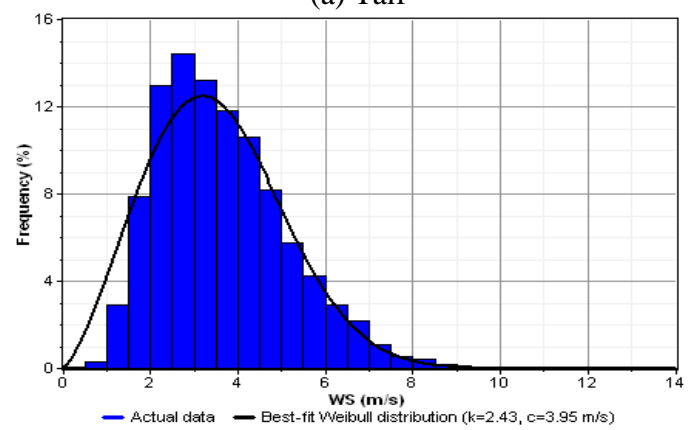
(b) Turaif



(a) Taif



(d) Yanbo



(b) Wadi-Al-Dawasser

Figure 5.14 Frequency distribution

The annual trends of Weibull shape and scale parameters were studied in depth by finding best-fit linear line coefficients and the corresponding values of  $R^2$ . As an example, such linear regression lines for Abha, Al-Ahsa and Al-Baha for shape parameter  $k$  are shown in Figures 5.15(a) – 5.15(c) and for scale parameter in Figures 5.16(a) – 5.16(c), respectively. At Abha, the shape parameter trend line showed an increasing trend of 0.0388 per year while at Al-Ahsa and Al-Baha, a decreasing trend of 0.0151 and 0.041 per year, as can be seen from Figures 5.15(b) and 5.15(c), respectively. The regression line coefficients for remaining stations along with the above are summarised in Table 5.5. As observed from this table, the annual  $k$  values were found to be decreasing at Bisha, Guriat, Madinah, Taif and Yanbo and increasing for the rest of the stations. On the other hand, the scale parameter regression lines for Abha, Al-Ahsa and Al-Baha showed decreasing trends of 0.0004, 0.0988 and 0.0688 m/s per year, as observed from Figures 5.16(a) to 5.16(c), respectively. The annual scale parameter trends were found to be decreasing for most of the stations with the exception of Al-Jouf, Gassim, Hafr-Al-Batin, Jeddah, Rafha, Sulayel, Turaif and Wadi-Al-Dawasser with an increasing rate of 0.0117, 0.0065, 0.0442, 0.0036, 0.0297, 0.001, 0.0125 and 0.0161 m/s per year, respectively, as summarised in Table 5.6.

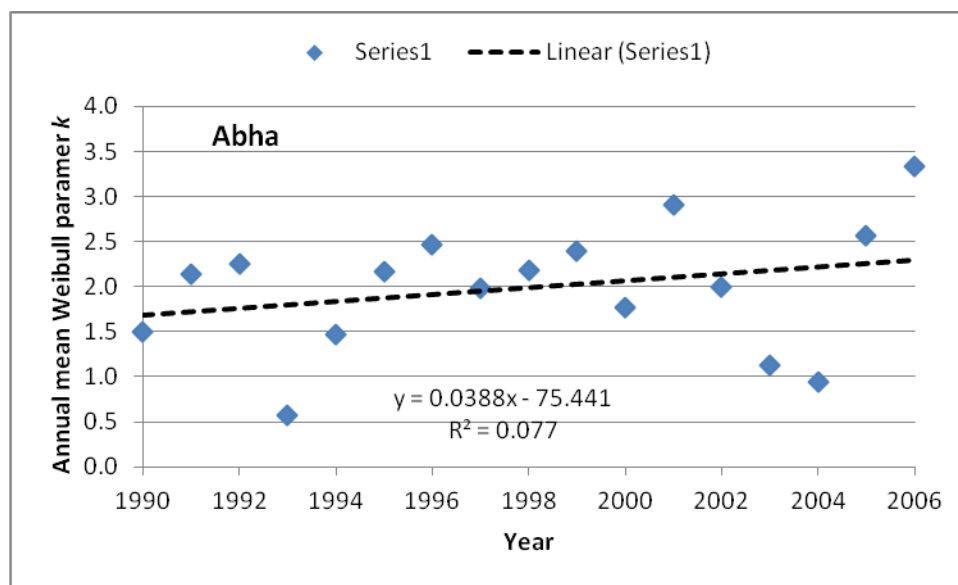


Figure 5.15(a) Annual trend of shape parameter at Abha

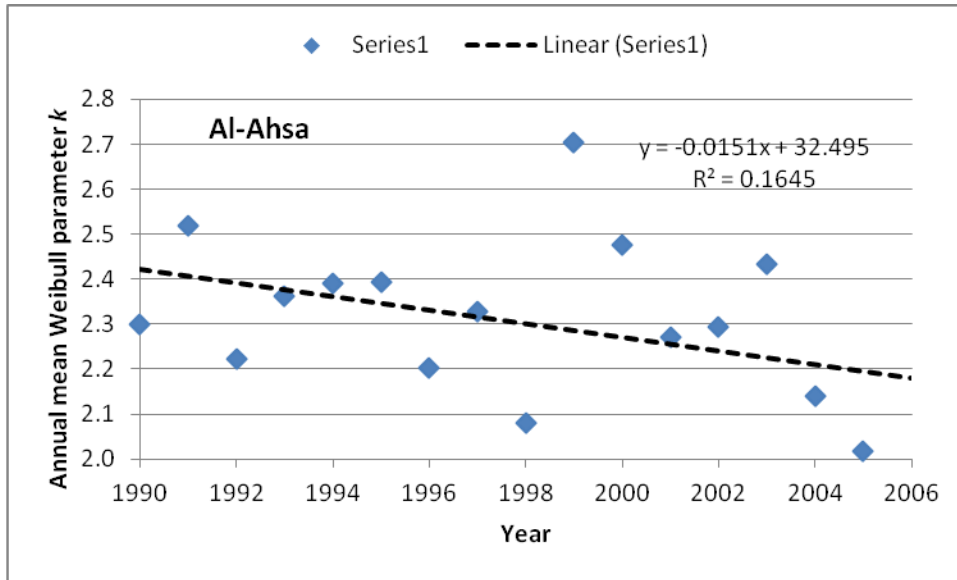


Figure 5.15(b) Annual trend of shape parameter at Al-Ahsa

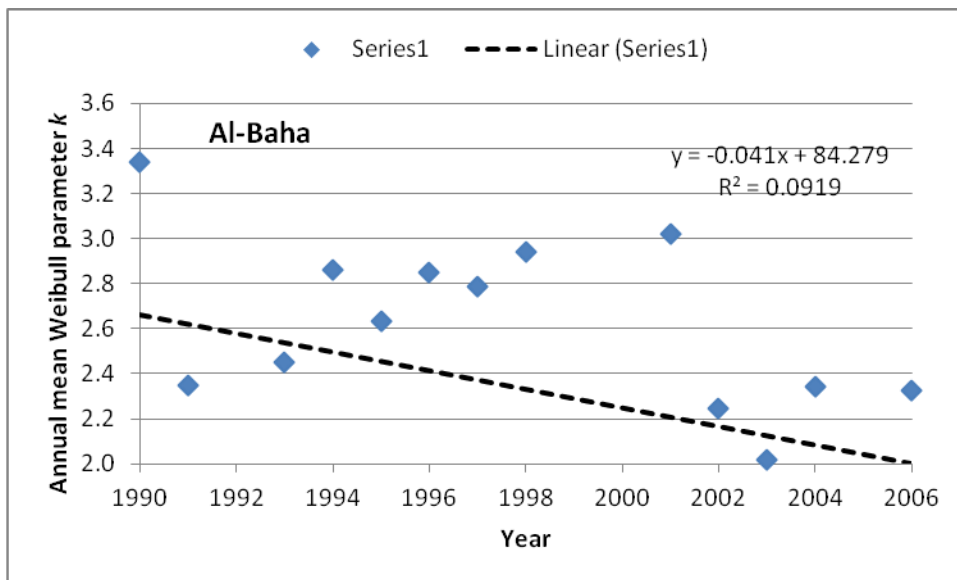


Figure 5.15(c) Annual trend of shape parameter at Al-Baha

Table 5.5 Best-fit regression lines for annual shape parameter ( $k$ )

Location	Regression coefficients		$R^2$
	a	b	
Abha	0.0388	-75.4	0.08
Al-Ahsa	-0.0151	32.5	0.16
Al-Baha	-0.0410	84.3	0.09
Al-Jouf	0.0070	-11.5	0.11
Al-Wejh	0.0391	-75.4	0.16
Arar	0.0073	-12.1	0.02
Bisha	-0.0041	10.7	0.01
Dhahran	0.0123	-21.5	0.22
Gassim	0.0051	-7.9	0.01
Gizan	0.0288	-54.0	0.06
Guriat	-0.0209	44.1	0.29
Hafr-Al-Batin	0.0380	-73.7	0.37
Hail	0.0420	-81.5	0.15
Jeddah	0.0274	-51.7	0.17
Khamis-Mushait	0.0066	-10.7	0.01
Madinah	-0.0292	61.2	0.16
Makkah	0.2911	-578.7	0.16
Nejran	0.0078	-13.1	0.01
Qaisumah	0.0010	0.3	0.00
Rafha	0.0382	-73.4	0.10
Riyadh	0.0034	-4.4	0.02
Sharourah	0.0376	-71.9	0.02
Sulayel	0.0063	-10.1	0.01
Tabouk	0.0152	-27.8	0.02
Taif	-0.0172	37.1	0.35
Turaif	0.0284	-54.1	0.17
Wadi-Al-Dawasser	0.0164	-30.3	0.18
Yanbo	-0.0202	42.9	0.15

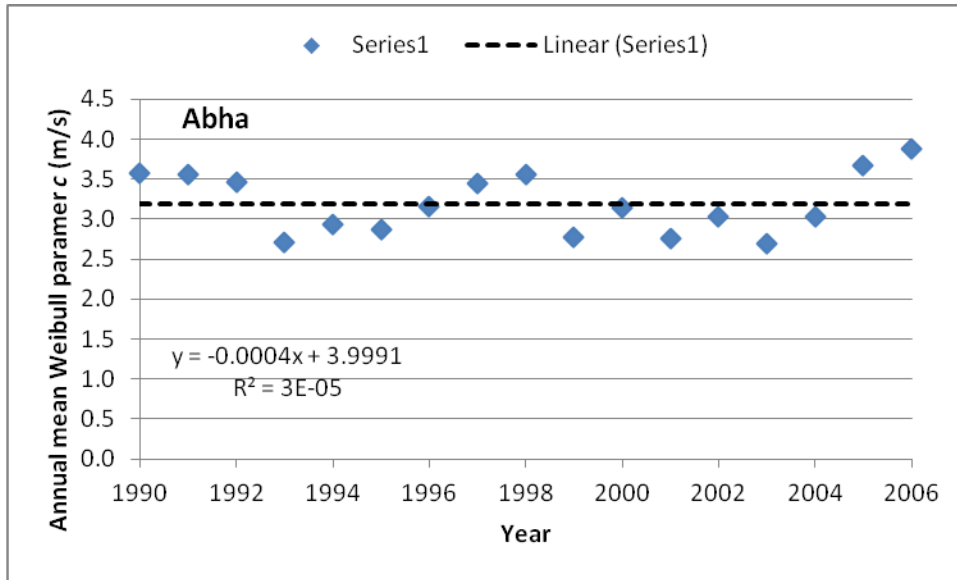


Figure 5.16(a) Annual trend of scale parameter at Abha

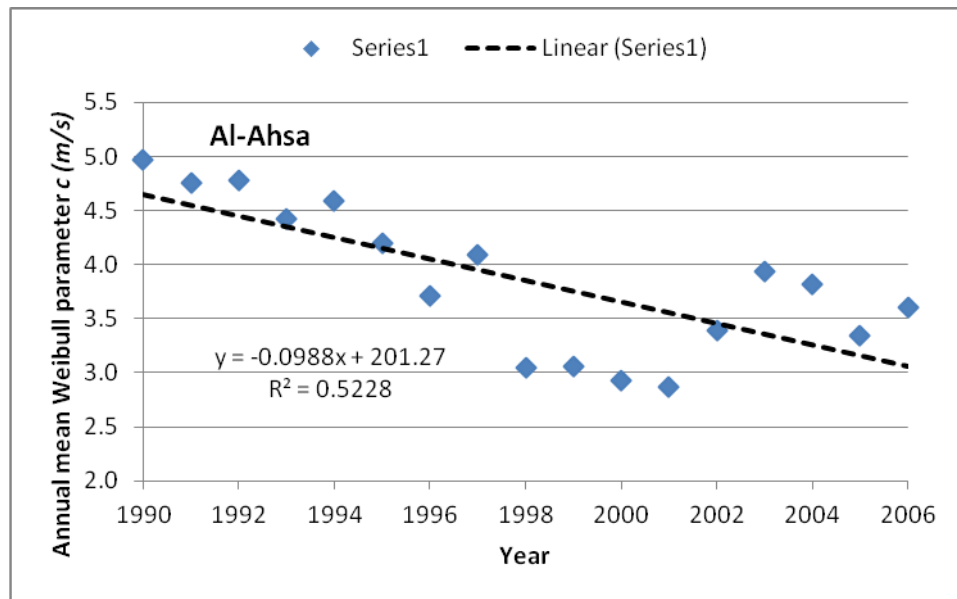


Figure 5.16(b) Annual trend of scale parameter at Al-Ahsa

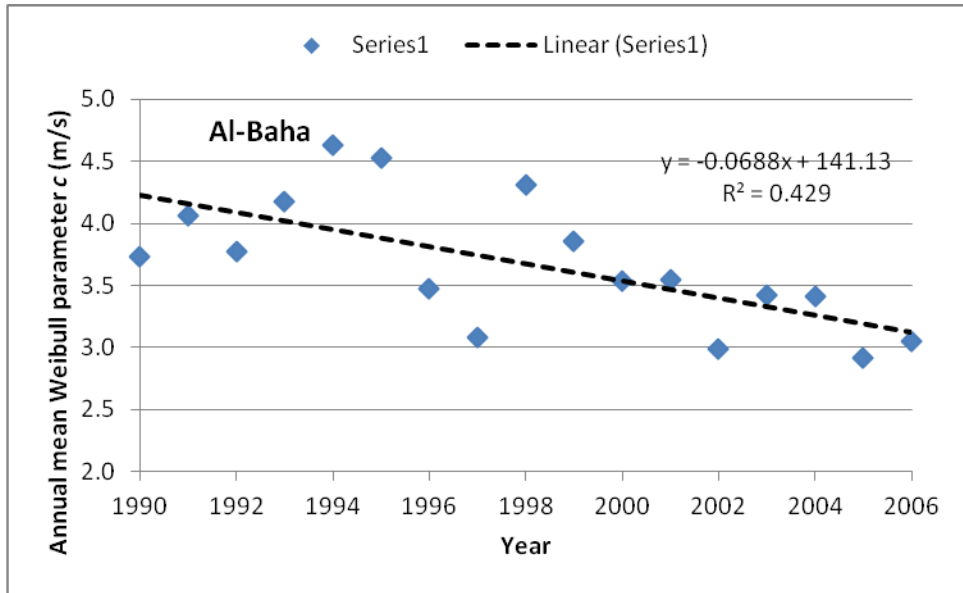


Figure 5.16(c) Annual trend of scale parameter at Al-Baha

Table 5.6 Best fit regression lines for annual scale parameter (c)

Location	Regression coefficients		R <sup>2</sup>
	a	b	
Abha	-0.0004	4.0	0.00
Al-Ahsa	-0.0988	201.3	0.52
Al-Baha	-0.0688	141.1	0.43
Al-Jouf	0.0117	-18.8	0.12
Al-Wejh	0.0224	-40.0	0.24
Arar	-0.0048	13.6	0.01
Bisha	-0.0270	56.6	0.25
Dhahran	-0.0158	36.3	0.10
Gassim	0.0065	-9.7	0.01
Gizan	-0.0317	66.6	0.44
Guriat	-0.0535	111.6	0.49
Hafr-Al-Batin	0.0442	-84.5	0.26
Hail	-0.0166	36.7	0.05
Jeddah	0.0036	-3.1	0.02
Khamis-Mushait	-0.0106	24.5	0.05
Madinah	-0.0283	59.9	0.41
Makkah	0.3284	-654.2	0.22
Nejran	-0.0527	107.4	0.59
Qaisumah	-0.0574	118.6	0.59
Rafha	0.0297	-54.7	0.10
Riyadh	-0.0196	42.6	0.23
Sharourah	-0.0264	56.6	0.01
Sulayel	0.0010	2.1	0.00
Tabouk	-0.0025	8.4	0.00
Taif	-0.0129	29.9	0.24
Turaif	0.0125	-20.2	0.06
Wadi-Al-Dawasser	0.0161	-28.3	0.08
Yanbo	-0.0595	123.0	0.39

## SUMMARY

Based on regression line analysis, decreasing trends of annual mean wind speed were found at Al-Ahsa, Al-Baha, Bisha, Dhahran, Gizan, Guriat, Hail, Khamis-Mushait, Madina, Makkah, Nejran, Qasumah, Riyadh, Sharourah, Tabouk, Taif and Yanbo and increasing at remaining locations namely Abha, Al-Jouf, Al-Wejh, Gassim, Hafr-Al-Batin, Jeddah, Rafha, Sulayel, Turaif and Wadi-Al-Dawasser. Overall, a decreasing trend of 0.01852 m/s per year was observed in annual mean wind speed values based on the algebraic average of the trend

coefficient ( $a$ ) of all the stations used in the present work. At Hafr-Al-Batin, Taif, Turaif and Al-Wejh, the rate of increase of annual wind speed of 0.0391, 0.0154, 0.0151 and 0.014 m/s per year was observed, respectively. These trends need to be verified using more accurate wind speed measurements but could be used as preliminary indicators of the future wind regime in Saudi Arabia.

Larger seasonal variations were observed at Dhahran and Guriat while smaller seasonal ranges (2.5 to 4 m/s) were seen at Gassim, Gizan, Hafr-Al-Batin, Hail and Jeddah. At Kahmis-Mushait, Madinah, Qaisumah, Rafha and Riyadh, relatively higher monthly mean wind speeds were observed compared to Makkah and Nejran. At Sulayel and Wadi-Al-Dawasser, higher values were observed during the winter months with lower values during summer time. It is evident from this analysis that at most of the stations, the wind speed values were higher during summer months and lower during winter months with the above exception.

The annual trends of Weibull shape and scale parameters were studied in depth by finding best-fit linear line coefficients and the corresponding values of  $R^2$ . The annual  $k$  values were found to be decreasing at Bisha, Guriat, Madinah, Taif and Yanbo and increasing for the rest of the stations. On the other hand, the scale parameter regression lines for Abha, Al-Ahsa and Al-Baha showed decreasing trends of 0.0004, 0.0988 and 0.0688 m/s per year. The annual scale parameter trends were found to be decreasing for most of the stations with the exception of Al-Jouf, Gassim, Hafr-Al-Batin, Jeddah, Rafha, Sulayel, Turaif and Wadi-Al-Dawasser with an increasing rate of 0.0117, 0.0065, 0.0442, 0.0036, 0.0297, 0.001, 0.0125 and 0.0161 m/s per year, respectively.

## CHAPTER 6

### WIND DATA ANALYSIS AT DIFFERENT HEIGHTS

The wind speed data at different height is the key for accurate wind power resource assessment at a site and it is recommended by experts to conduct at least one-year wind measurements at a site of interest before any sort of installation or wind farm development. The reason for making measurements of wind speed at different heights is that today's wind turbines have hub heights of more than 60m and wind measurements are usually available at 10 to 12metres above ground level. Therefore, in order to calculate the wind speed at hub height, the local wind shear exponent (WSE) is required. To calculate the local WSE, wind measurements at two heights at least are needed. Under this task, the wind measurements made at 20, 30 and 40metres above ground level and temperature, pressure, relative humidity and global solar radiation near ground surface at seven locations in Saudi Arabia are analysed.

The latitude, longitude, altitude and data collection starting and ending dates of these stations are summarised in Table 6.1 and the locations are identified in the map shown in Figure 4.2. The photograph of an actual wind mast installed at one of these locations is shown in Figure 4.4. Two anemometers were installed at 20, 30 and 40metres above ground level (AGL) each and one wind vane each at 30 and 40metres as shown in the schematic diagram (Figure 4.3). The meteorological sensors for temperature, pressure, relative humidity and global solar radiation were installed at 1.5 AGL. The analysis includes the overall, annual and monthly statistical summaries of all the measured parameters; annual, seasonal and diurnal variation of wind speed and other parameters; estimation and variation of WSE; wind rose diagrams on overall and monthly basis; air density and atmospheric turbulence intensity variation.

Table 6.1 Site-specific information

Location	Latitude	Longitude	Altitude, m	Data Period
Rawdat Ben Habbas	29.14°N	44.33°E	443	Sep 2005 to Apr 2010
Juaymah	26.80°N	49.90°E	20	Jul 2006 to Apr 2009
Dhahran	26.10°N	50.10°E	3	Oct 1995 to Nov 2000
Arar	30.80°N	41.30°E	550	Jun 1995 to Dec 1998
Gassim	26.30°N	43.97°E	648	Dec 1995 to Oct 1998
Yanbo	23.90°N	38.30°E	11	Sep 1996 to Oct 1999
Dhulom	22.74°N	42.18°E	1117	Nov 1998 to Oct 2002

## **6.1 SITE AND DATA DESCRIPTION**

The wind mast at Rawdat Ben Habbas was installed inside a diesel power plant fenced on all four sides. The surrounding area was open from all sides and could be considered as flat land for all practical purposes. The Juaymah data collection site was also located inside a gas power plant and the whole area was fenced. There were other buildings and Saudi Aramco facilities within a kilometre or two and hence the site could not be used for wind farm development. In Dhahran, the wind tower was installed near the gate of KFUPM beach and was about 200metres away from the seashore on the west. The surrounding soil was sandy with 2 to 5metres high trees. There was a sand dune of roughly 70 to 80metres high to the north-western side of the tower and a security office building to the south.

The Arar data collection station was situated on flat land and consisted of hard rocky soil. The Gassim site was an open area from three directions, east, south and west while 4 to 5metres tall trees were found 150metres north of the tower. The soil consisted mostly of desert sand. The surrounding areas had small sand dunes with vegetation of short grasses. The data collection station at Yanbo was near the highway connecting Yanbo and Jeddah. About 15metres north-east of the tower there was a weather and environmental data collection station housed in a 6metre high cargo container. The station was open from other sides and could be considered flat land. The wind data collection tower at Dhulom was installed inside a fenced area owned by Saudi Electricity Company (SEC). The site was open from all sides having flat land. On the western side, about 300m away from the tower, there was a small power station consisting of a few diesel generating sets.

## **6.2 STATION-BASED SUMMARIES**

The annual averages of wind speeds at 20, 30 and 40metres AGL along with the WSE and other meteorological parameters are summarized in Table 6.2. It is evident that wind speed increases with height and hence it is essential to make wind measurements at a site where wind farms are being planned to be developed to get the local wind exponent. The highest wind was observed at Dhulom while the lowest at Gassim with good wind regimes at Rawdat Ben Habbas, Juaymah and Dhahran with more than 5m/s annual average wind speed. The site-based mean wind speeds at different heights are compared in Figure 6.1. The WSE was the highest for Gassim and lowest for Yanbo as can be seen from Figure 6.2. The overall mean temperature was found to be the highest at Yanbo and the lowest at Arar, as can be seen from Column 6 of Table 6.2 and Figure 6.3. At other locations, the overall mean temperature

was found to be greater than 20°C. The variation of surface pressure, relative humidity and global solar radiation values is compared in Figures 6.4 to 6.6, respectively. The prevailing wind direction at all the above sites was found to be from the north with some seasonal variation.

Table 6.2 Annual mean values of meteorological parameters

Location	Wind speed, (m/s)			WSE	T	P	RH	GSR
	20m	30m	40m		(°C)	(mb)	(%)	(kWh/m <sup>2</sup> /d)
Rawdat Ben Habbas	4.76	5.36	5.74	0.286	24.24	941	21.7	5.66
Juaymah	4.87	5.37	5.69	0.274	26.58	1014	13.5	4.90
Dhahran	4.17	5.13	5.37	0.151	28.90	1021	52.0	4.90
Arar	5.00	5.50	5.75	0.182	23.40	1009	34.0	4.51
Gassim	3.50	4.10	4.30	0.241	28.50	0992	41.0	5.10
Yanbo	4.51	4.71	4.82	0.081	29.70	----	49.9	4.70
Dhulom	5.10	5.50	5.90	0.193	24.70	0919	38.0	4.94

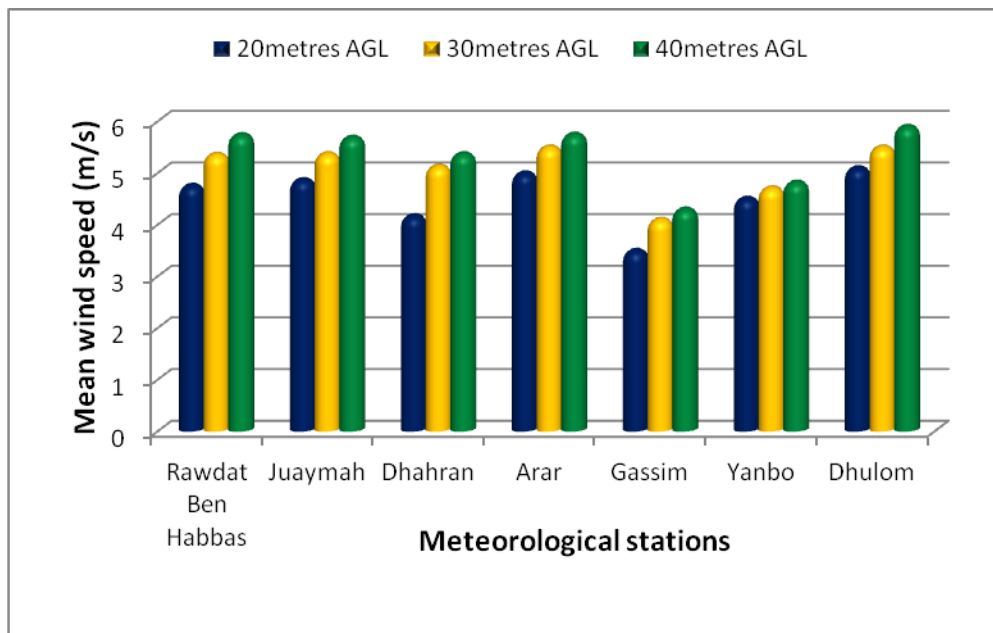


Figure 6.1 Comparison of mean wind speed at different heights

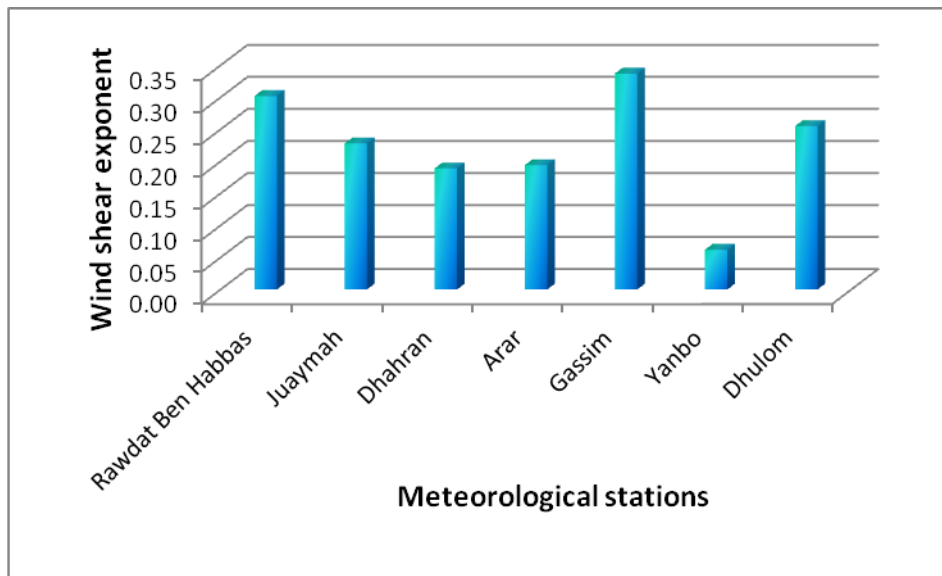


Figure 6.2 Comparison of wind shear exponent at measurement sites

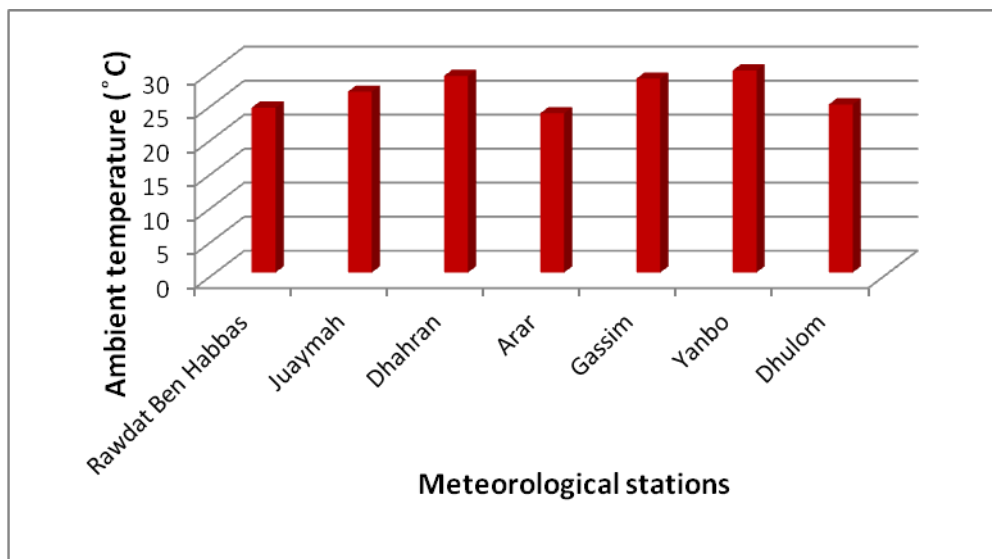


Figure 6.3 Comparison of mean ambient temperature at measurement sites

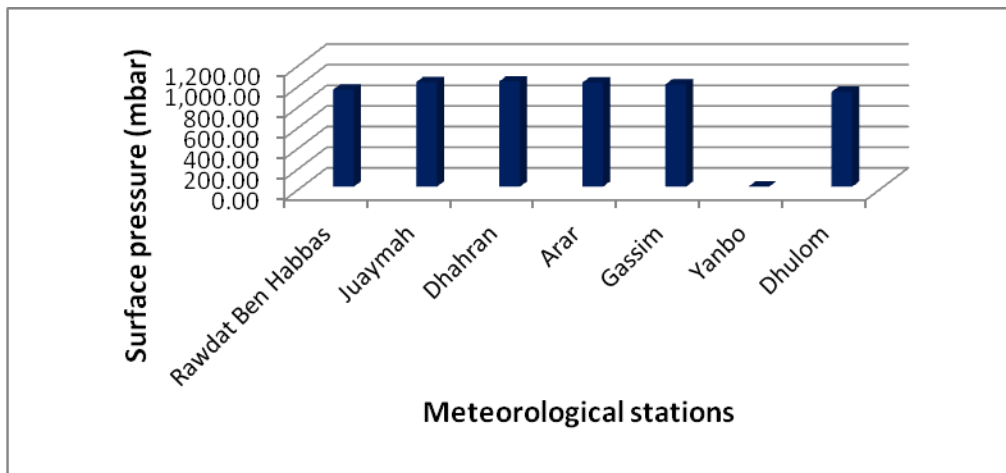


Figure 6.4 Comparison of surface pressure at measurement sites

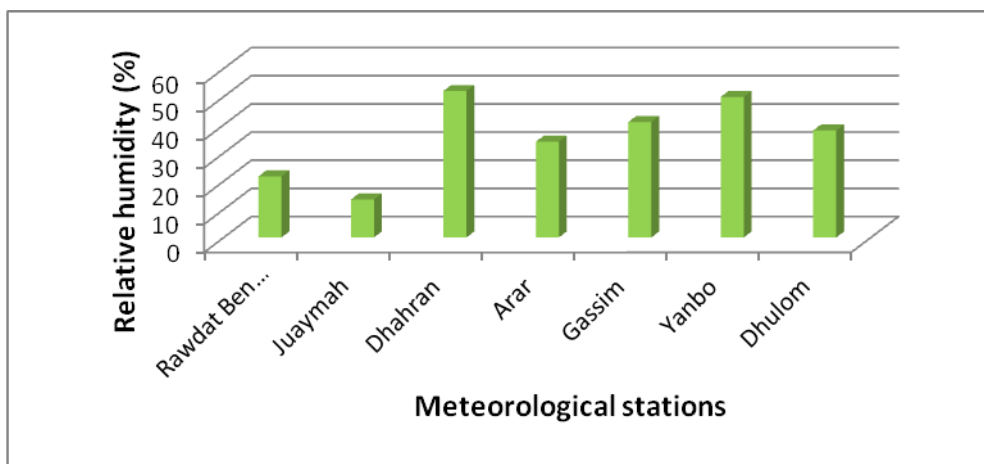


Figure 6.5 Comparison of relative humidity at measurement sites

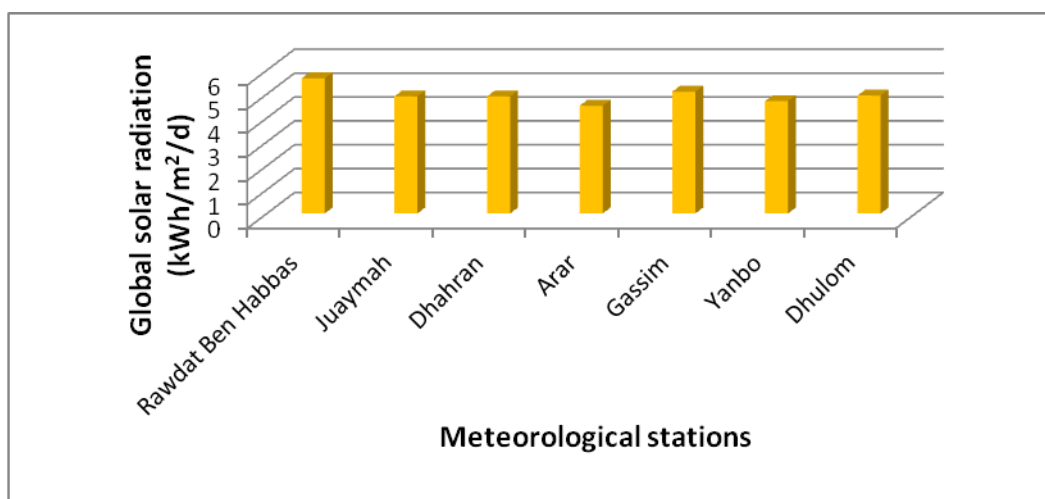


Figure 6.6 Comparison of global solar radiation at measurement sites

### 6.3 WIND ROSE AND FREQUENCY DISTRIBUTION ANALYSES

The wind rose diagrams were obtained for all the sites using the mean wind speed at 40 metres and the wind direction at the same height and are shown in Figures 6.7 to 6.12. The wind rose diagram provides useful information on the prevailing wind direction and availability of directional wind speed in different wind speed bins. Like wind speed, wind roses also vary from one location to another and are known as a form of meteorological fingerprint. Hence, a close look at the wind rose and understanding its message correctly are extremely important for siting wind turbines. Therefore, if a large share of wind comes from a particular direction then the wind turbines should be put against this direction. Figure 6.7 show the wind rose diagram constructed using hourly mean wind speed and wind direction at 40metres AGL for Rawdat Ben Habbas. At Rawdat Ben Habbas, most of the wind blows from NNE-N-NNW (~25%), NW (~13%) and around 11% from WWN and 13% from NE and EEN. Wind was also found to be blowing from the south, east, west and in between directions for short periods of time as can be observed from Figure 6.7.

At the Juaymah wind measurement site, the wind was found to be blowing for more than 60% of the times from WWN, NW, NNW, N and NNE directions as can be seen from Figure 6.8. For the rest of the period at Juaymah, the wind was found to be blowing over a broad range of directions. At Dhahran (Figure 6.9), the wind was found to be blowing from the south, east and in between directions for about 32% of the time while around more than 45% of the time from WN, NW, NNW, NNE, and N directions. The wind rose frequency diagram of Figure 6.10 for Arar clearly shows that the most of the times (>60%) the wind blows from N(15%), NNW(10.5%), NW(11.5%), WN(6%), NNE(10%) and NE(6%) and from other directions for the rest of the time. At Yanbo, which is situated on the north-west coast of Saudi Arabia, the wind was found to be blowing from the east, west and in between directions for more than 55% of the time while merely 30% from N, NNE, NE, NNW and NW directions as indicated in Figure 6.11. At Dhulom, a similar wind frequency distribution was observed as that at Yanbo (Figure 6.12) with 20% contribution from all the north directions and around 60% from the south, east and in between directions.

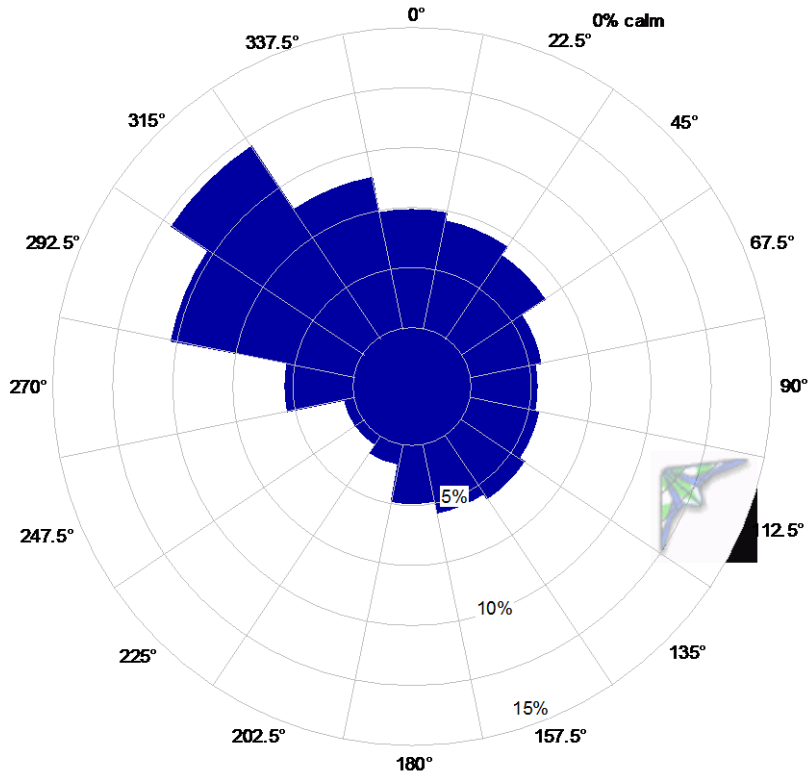


Figure 6.7 Wind rose diagram of wind speed and direction data at Rawdat Ben Habbas

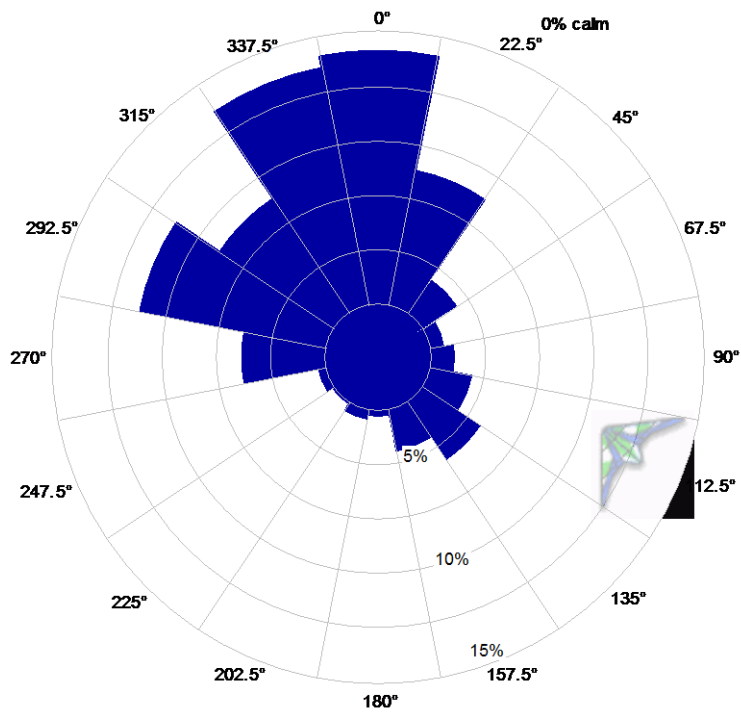


Figure 6.8 Wind rose diagram of wind speed and direction data at Juaymah

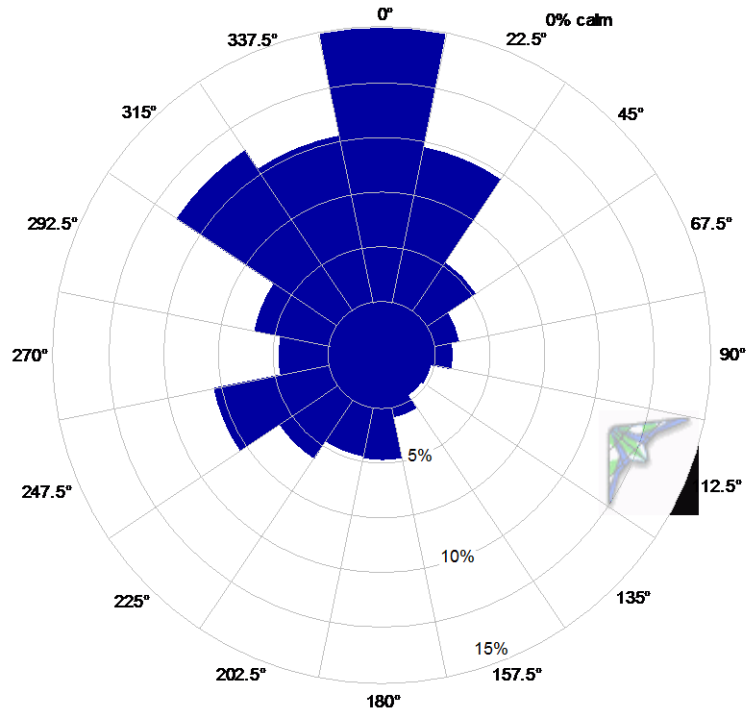


Figure 6.9 Wind rose diagram of wind speed and direction data at Dhahran

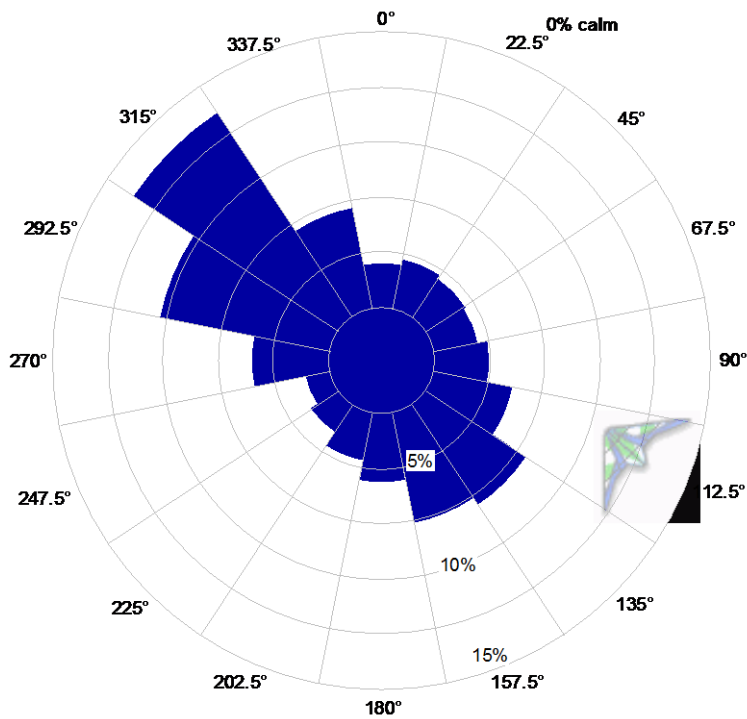


Figure 6.10 Wind rose diagram of wind speed and direction data at Arar

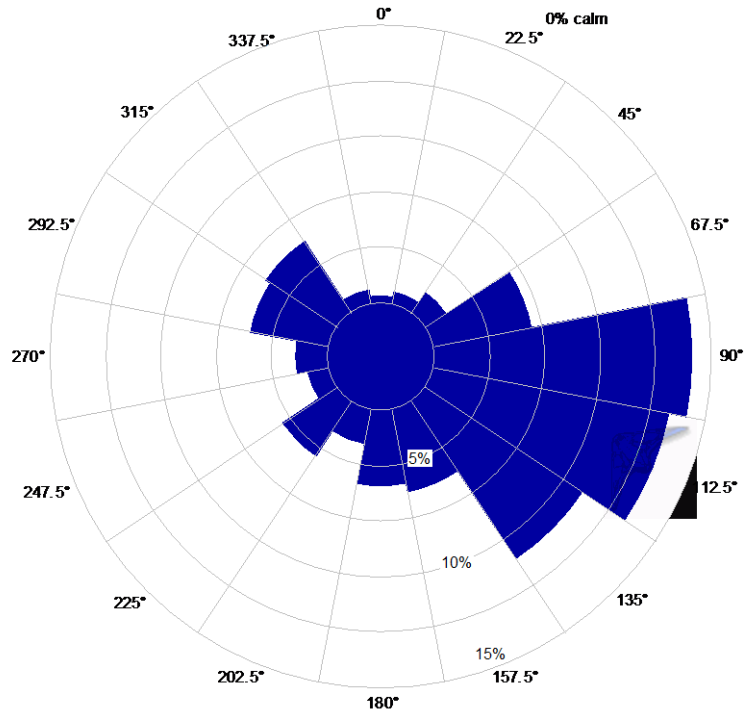


Figure 6.11 Wind rose diagram of wind speed and direction data at Yanbo

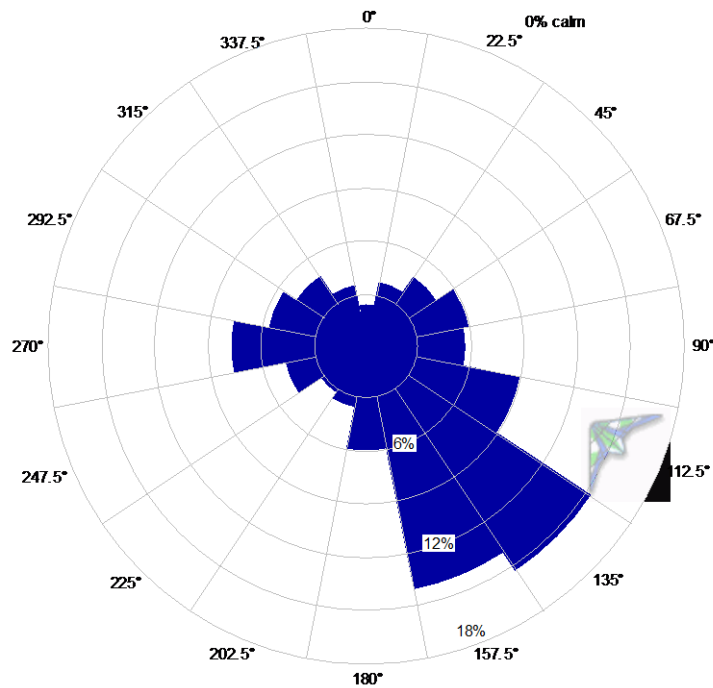


Figure 6.12 Wind rose diagram of wind speed and direction data at Dhulom

The frequency distribution of hourly mean wind speed plays an important role in estimating the energy yield from a particular wind turbine in conjunction with the wind power curve of

the turbine being used for the purpose. In this process, the number of hours during which the wind speed remained in certain wind speed bin is obtained from the wind data series and then multiplied by the power available from the wind turbine at corresponding wind speed. For example if the frequency at 4-5 m/s wind speed bin is 70 and the wind turbine power output at this wind speed is 95kW then the energy yield from this wind turbine at this wind speed will be  $95 \times 70 = 6650 \text{ kWh}$ . In this sub-section, the percentages of hourly mean wind speed in different wind speed bins such as 0-1, 1-2, ..., 14-15m/s were determined at measurement heights and are compared in Figures 6.13 to 6.19 for Rawdat Ben Habbas, Juaymah, Dhharan, Arar, Gassim, Yanbo and Dhulom, respectively. At Rawdat Ben Habbas, the wind was found to be above 4m/s for 62%, 71%, and 74% of the time at 20, 30, and 40 m above ground level, respectively. This simply meant that any wind turbine with 3.5m/s cut-in speed can produce power for a minimum of 74% of the time because the modern wind turbines have much higher hub heights than 40 m. Furthermore, the wind was found to blow above 8m/s and 10m/s for 18.7% and 5.2% of the time, respectively, at Rawdat Ben Habbas. Since wind speed increases with height, much higher frequencies of speed in higher wind speed bins are expected, this in other words means higher energy yields.

At the Juaymah wind data collection site, the wind was found to be above 4m/s for 47%, 62%, 70% and 75% of the time at 10, 20, 30 and 40 m above ground level (AGL), respectively, see Figure 6.14 for details. This simply meant that any wind turbine with 3.5m/s cut-in speed can produce power for a minimum of 75% of the time. Furthermore, the wind was found to blow above 8m/s and 10m/s for 17.7% and 5.5% of the time, respectively at Juaymah. At Dhahran, where the wind mast was located near the coast, the wind was found to be above 4m/s for 58%, 66% and 68% of the time at 20, 30, and 40 m AGL, respectively, as can be observed from Figure 6.15. The wind was observed to be blowing above 8m/s and 10m/s for 9.8, 11.8 and 13.3% and 3.3, 4.2 and 5.1% of the time at 20, 30, and 40 m AGL at Dhahran.

At Arar, Gassim, Yanbo and Dhulom, the wind was found to be above 4m/s for 71%, 52%, 55% and 72% of the time at 40 m AGL, as can be understood from Figures 6.16 to 6.19, respectively. This implies that any wind turbine with cut-in speed of 3.5m/s and hub height of 60 to 100 m can produce power for a bigger percentage of the time than indicated above because higher and smoother winds are expected at higher altitudes. At 30 m AGL, in the same order as above, the wind was found to be available for 67%, 45%, 54% and 69% of the

time while at 20 m AGL these numbers reduced to 62%, 34%, 51% and 60%, respectively. In general, the wind frequency analysis indicated lesser-rated power yield at most of these stations but higher yields. Finally, the wind data collection sites can be prioritised as best, second-best etc. in order as Juaymah, Rawdat Ben Habbas, Dhulom, Arar, Dhahran, Yanbo, and Gassim with having wind frequencies of around 75%, 74%, 72%, 71%, 68%, 55% and 52% above 4 m/s at 40 m AGL, respectively.

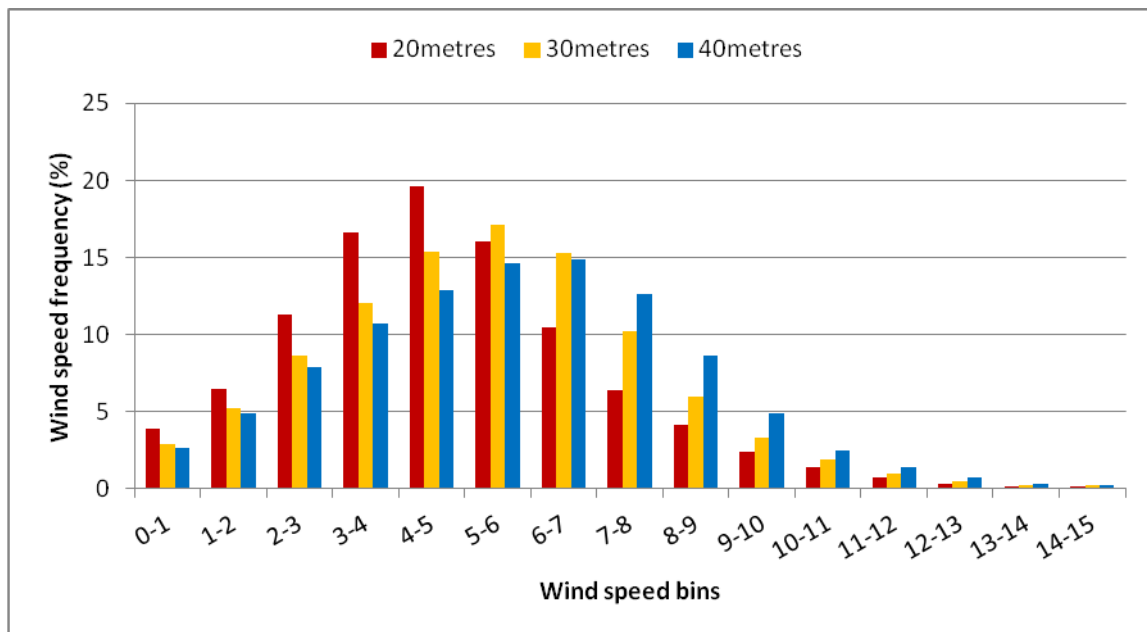


Figure 6.13 Frequency distribution at different heights for Rawdat Ben Habbas

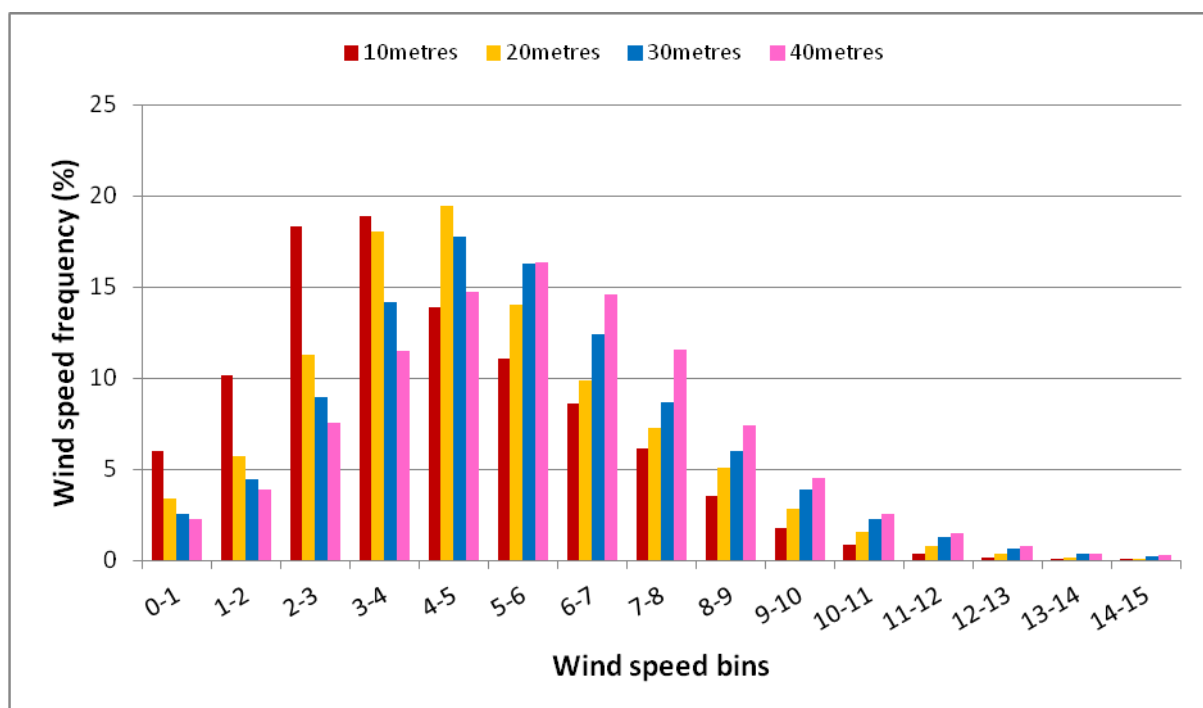


Figure 6.14 Frequency distribution at different heights for Juaymah

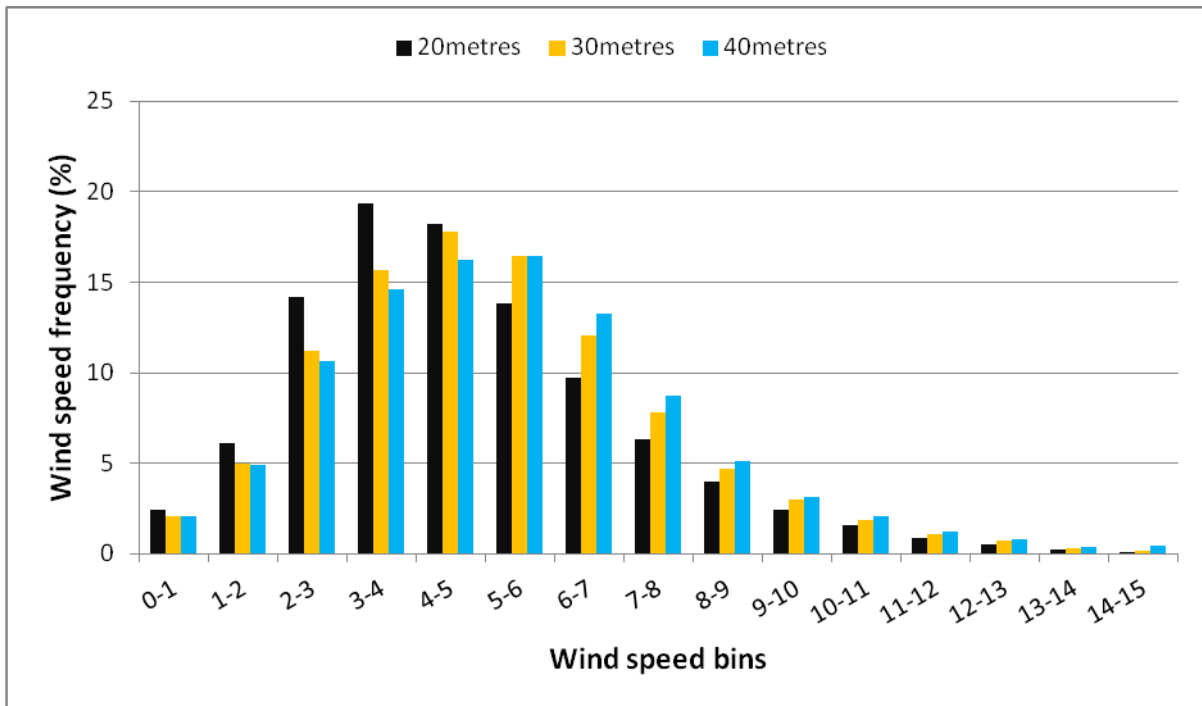


Figure 6.15 Frequency distribution at different heights for Dhahran

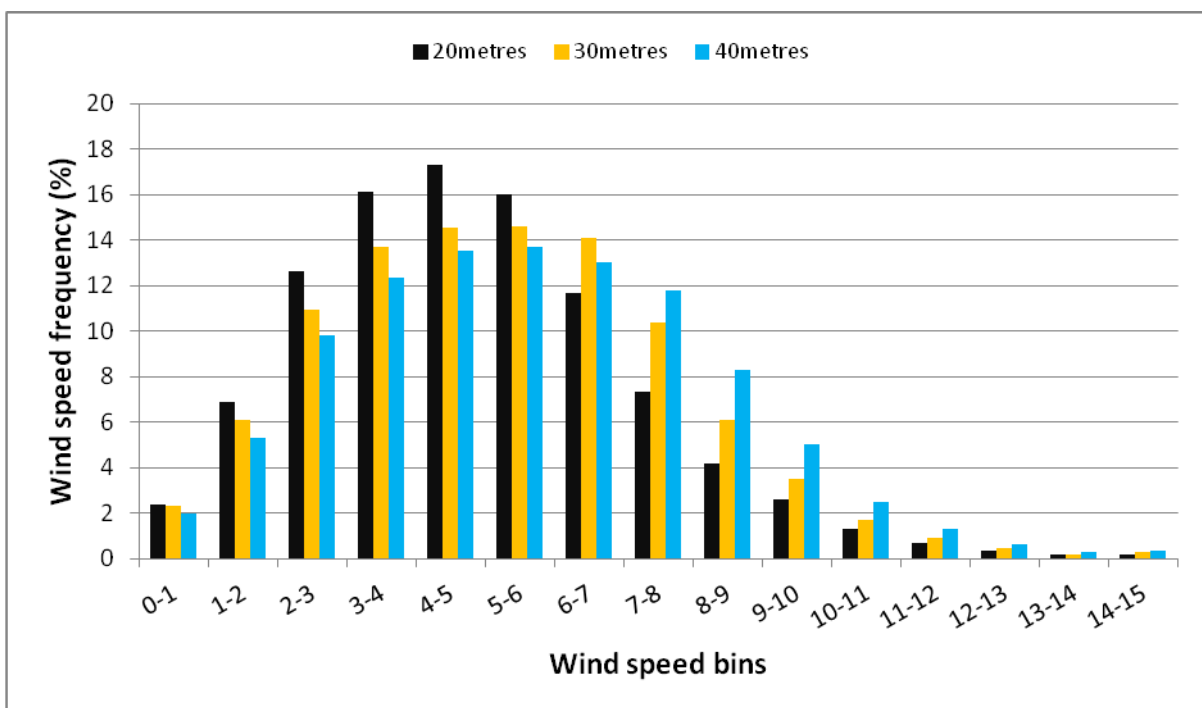


Figure 6.16 Frequency distribution at different heights for Arar

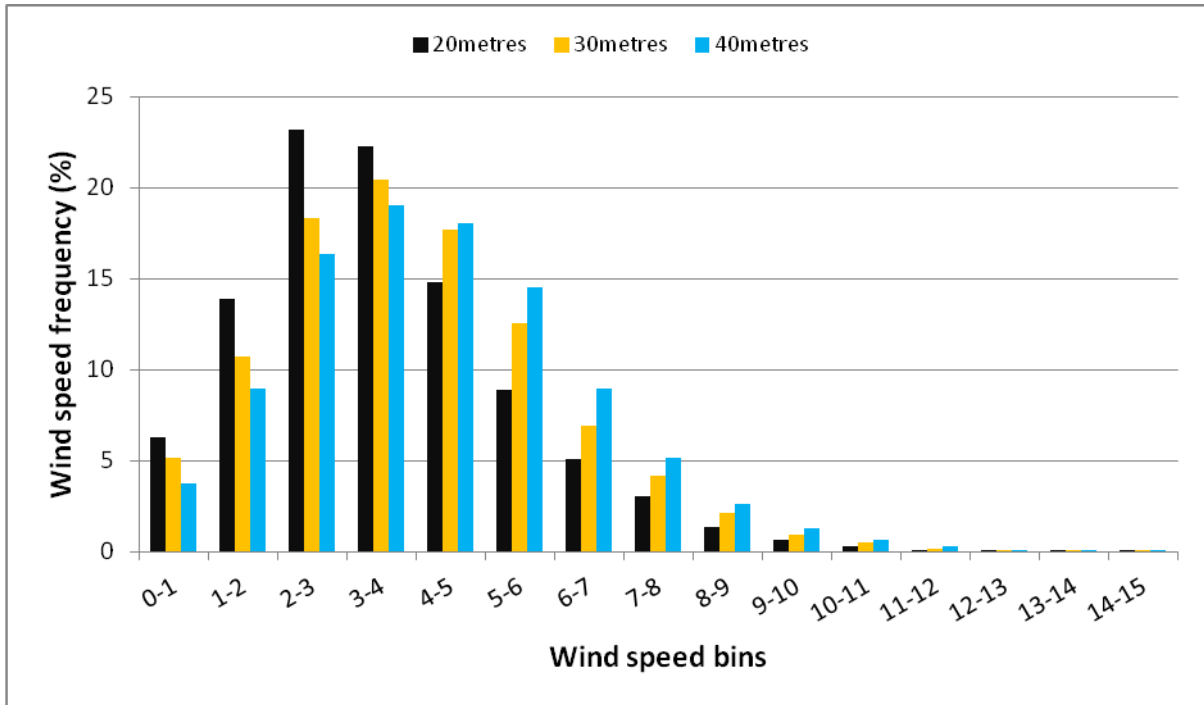


Figure 6.17 Frequency distribution at different heights for Gassim

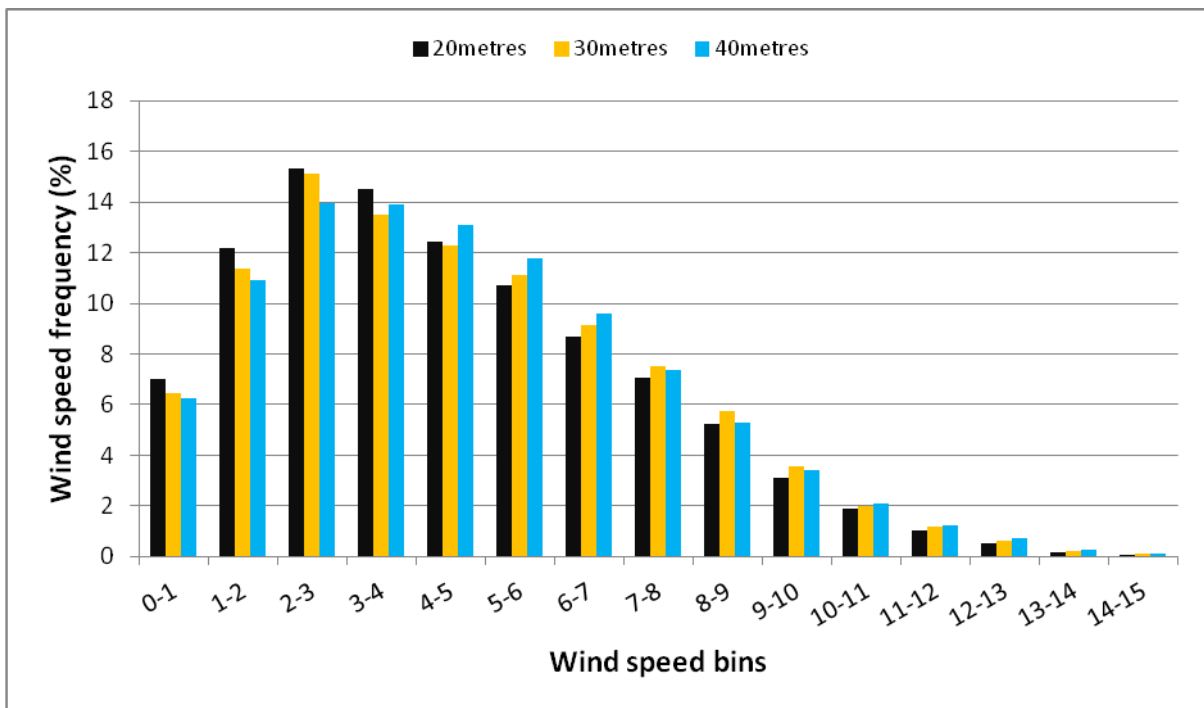


Figure 6.18 Frequency distribution at different heights for Yanbo

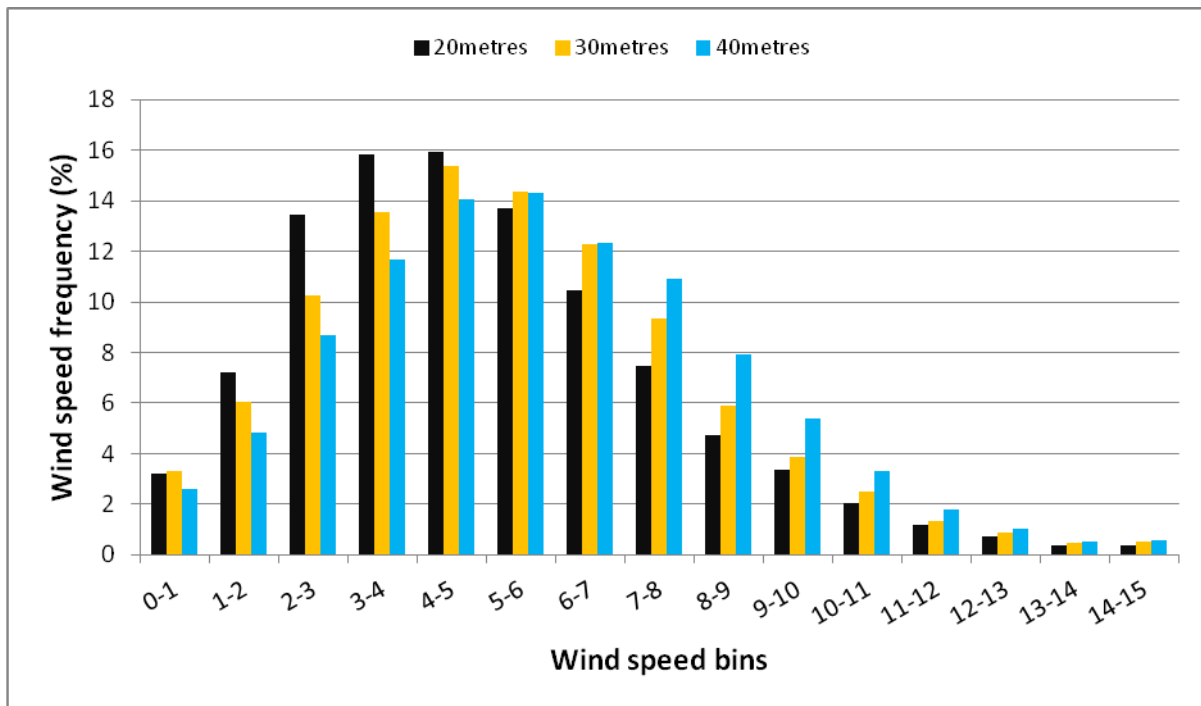


Figure 6.19 Frequency distribution at different heights for Dhulom

#### 6.4 ANNUAL VARIATION OF MEAN WIND SPEED AT DIFFERENT HEIGHTS

Annual variation of wind speed provides an insight into the availability and intensity of the wind during different years, which, in turn, facilitates the estimation of energy yield from the wind turbines or wind farms in the vicinity of the measurements. The annual trends of the wind speed also provide information about the increase or decrease in annual mean wind speed with upcoming years. In the present case, the annual mean wind speeds were calculated for complete years, which mean that the years with missing values even for five days were not considered in the analysis.

The annual mean wind speed variation over the data collection period from 2006 to 2009 at Rawdat Ben Habbas is shown in Figure 6.20. The annual mean wind speed was observed to increase by 3% in 2007 compared with that in 2006 but decreased by 3%, 4%, and 1% in 2008 compared with that in 2007 at 20, 30 and 40 m measurement heights, respectively. With respect to height, the annual mean wind speed increased by 13.1% and 6.3% at 30 m and 40 m AGL compared with that at 20 m and 30 m respectively. At Juaymah, the wind speed data was available for only two complete years, namely 2007 and 2008, as shown in Figure 6.21. As seen from this figure, the annual mean wind speed increased from 4.13 m/s to 4.81 m/s (16.6%) due to increase in measurement height from 10 m to 20 m. Similarly, an increase of

10.3% and 6.6% was noticed in annual mean wind speed values at 30 and 40 m compared with those at 20 and 30 m AGL, respectively. The annual mean wind speed increased by 2.1% to 2.7% in year 2008 compared with that in 2007.

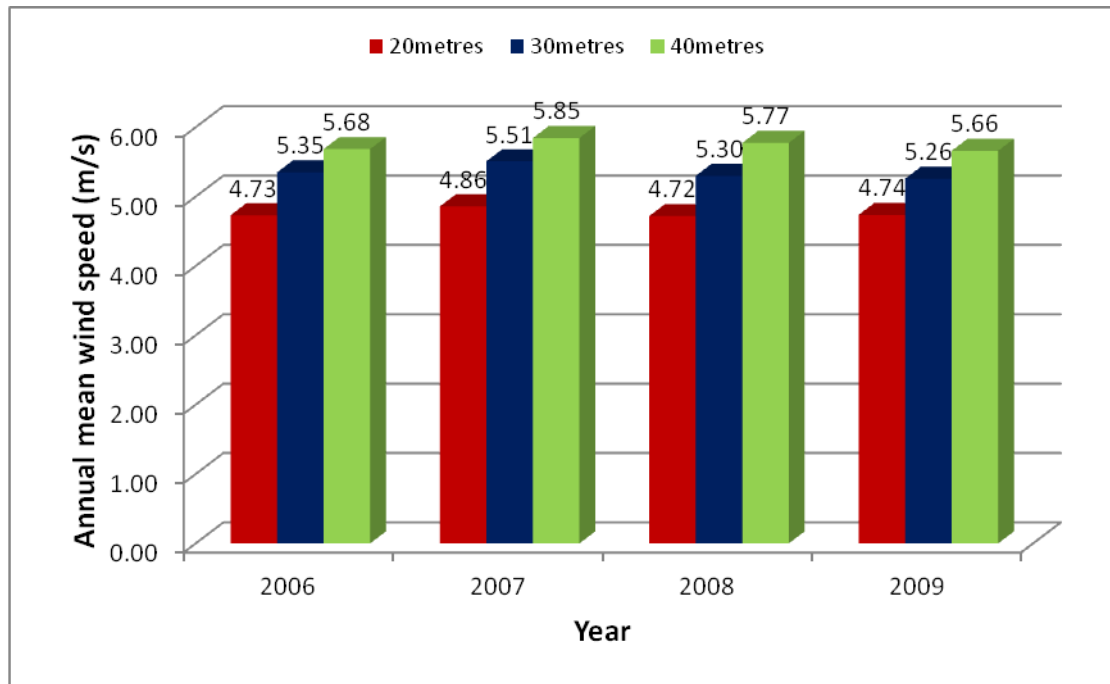


Figure 6.20 Annual mean wind speed at different heights at Rawdat Ben Habbas

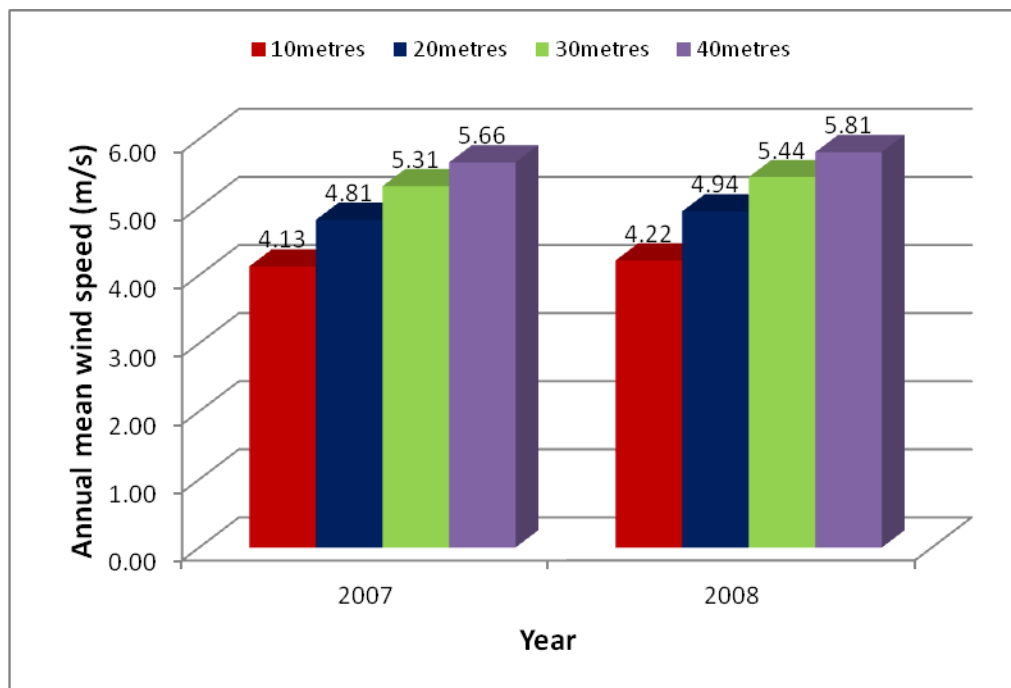


Figure 6.21 Annual mean wind speed at different heights at Juaymah

At Dhahran, the annual mean values of wind speed were available for four years from 1996 to 1999 at 20, 30 and 40 m AGL as shown in Figure 6.22. An increase of 6.8% was observed in wind speed values at 30m compared with those at 20 m and of 2.1% at 40m compared with those at 30 m in 1996. In 1997, 1998 and 1999, increases of 7.1%, 8.6% and 8.9% were found at 30 m compared with those at 20 m and of 4.1%, 1.7% and 3.3% at 40 m compared with those at 30 m, respectively. With respect to year-to-year change, an increase of 6%, 6.3% and 8.4% was found in 1997 compared with that in 1996 while in 1998 decreases of 7.6%, 6.4% and 8.5% were noticed compared with those of year 1997. Again in 1999, increases of 5.6%, 5.9% and 7.6% were observed in the values of mean wind speed at 20, 30 and 40m AGL, respectively. At Arar, the annual wind speed values were available for 1996 and 1997, as shown in Figure 6.23. The wind speed increased to 5.42m/s at 30m from 4.92m/s at 20m (an increase of 10.3%) and 5.65m/s at 40m from 5.42m/s at 30m (an increase of 4.2%) in the year 1996 while in 1997 these increases were 9.9% and 4.6%. From a year-to-year perspective, the annual mean wind speed increased by almost 4.5% at all the heights of measurements.

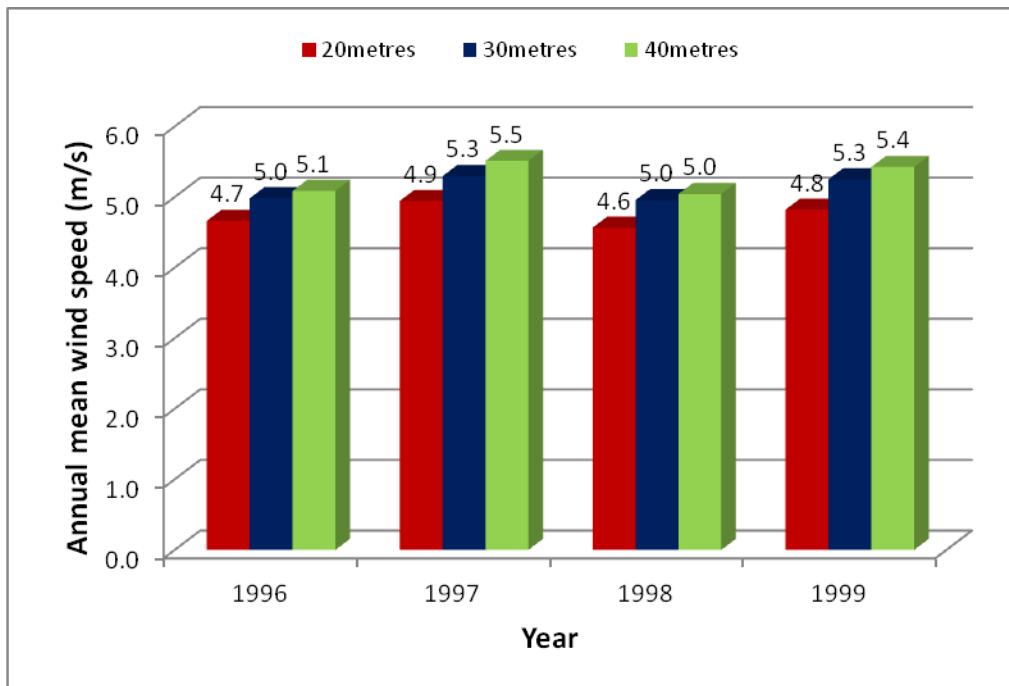


Figure 6.22 Annual mean wind speed at different heights at Dhahran

The annual mean wind speeds were found for two years only, i.e. 1996 and 1997 at Gassim and 1997 and 1998 at Yanbo, respectively. An increase of approximately 15% was found in wind speed values at 30 m (4.29 m/s) height compared with those at 20 m (3.72 m/s) in both

the years at Gassim, as shown in Figure 6.24. For a further increase of 10 m in measurement height, i.e. from 30 m to 40 m, the wind speed increased by 2.5% (from 4.29 to 4.39 m/s) in the year 1996 and by 4.6% (from 4.09 to 4.28 m/s) in the year 1997. As seen from Figure 6.25, the annual mean wind speed at Yanbo remained almost the same (increase of less than 1%) in both the years 1997 and 1998. The wind speed did increase by 4.8% and 3.9% at 30 m compared with that at 20 m in the years 1997 and 1998, respectively. A less than 2% increase in annual mean wind speed was observed for a height increase of 10 m, i.e from 30 m to 40 m at Yanbo.

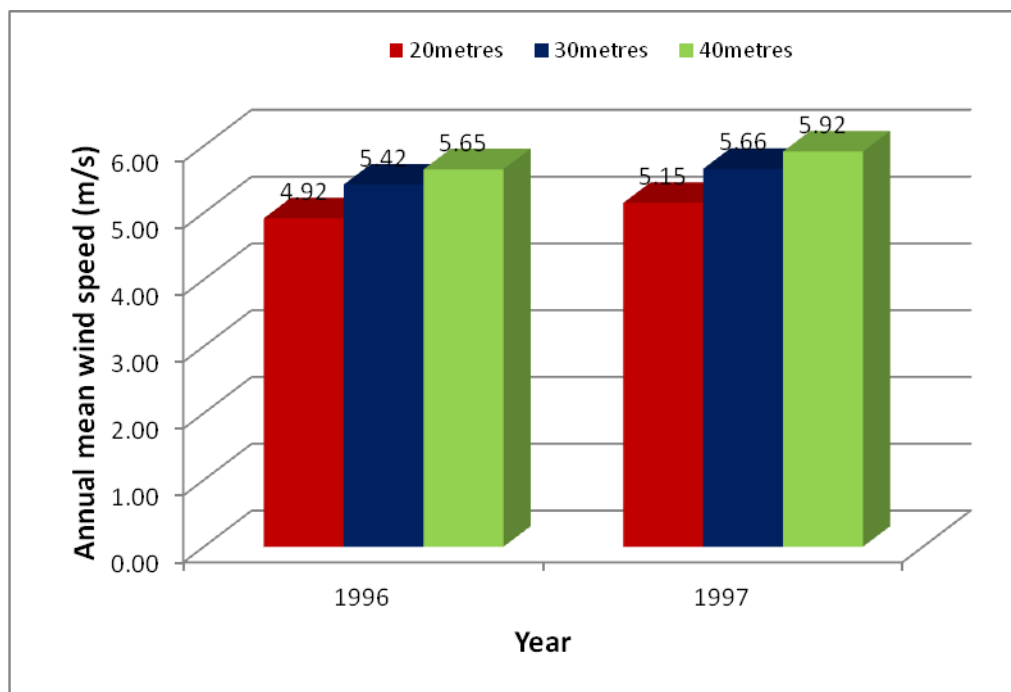


Figure 6.23 Annual mean wind speed at different heights at Arar

At 20 m AGL, the annual mean wind speed at Dhulom increased from 4.92 m/s in year 1999 to 5.25 m/s in year 2000 (an increase of 6.7%) while it decreased to 4.57 m/s in 2001 compared with 5.25 m/s in 2000 (a decrease of 12.9%) and then again increased to 5.14 m/s (12.3% jump) compared with the previous year's value of 4.57 m/s, as can be observed from Figure 6.26. Similar types of increasing and then decreasing and then again increasing trends were observed in wind speed values at 30 and 40 m AGL. With a respective increase in measurement height from 20 to 30 m, the annual mean wind speed values increased by 8.2%, 3.9%, 12.1% and 8.3% in the years 1999 to 2002, respectively. For a further increase of 10m in measurement heights, the mean wind speed values increased by 7.1%, 9.6%, 6.5% and 6% for respective years.

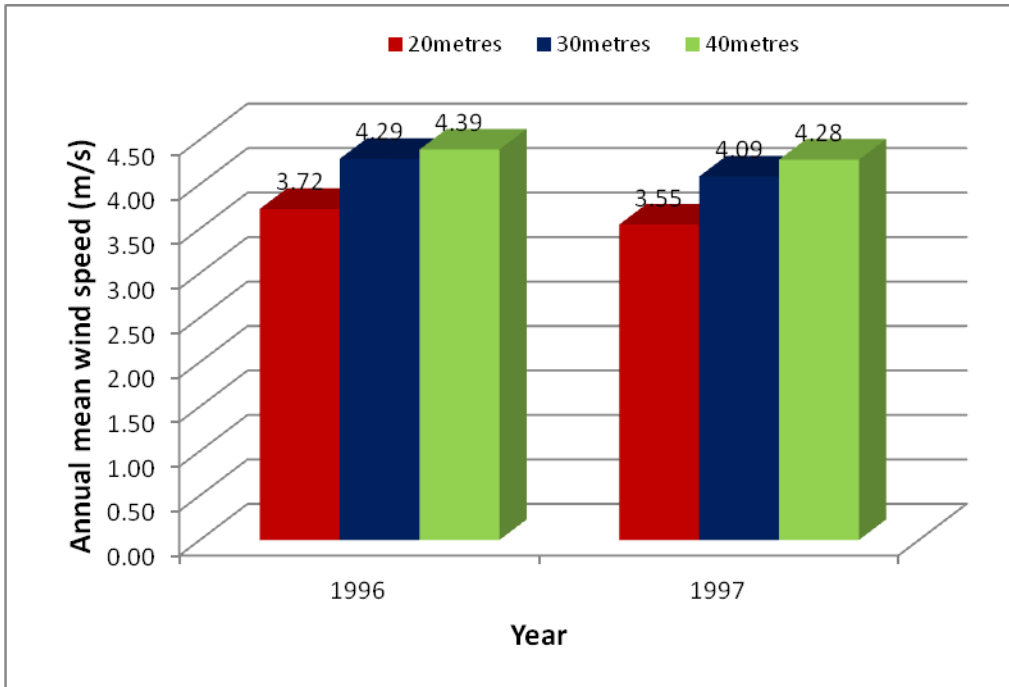


Figure 6.24 Annual mean wind speed at different heights at Gassim

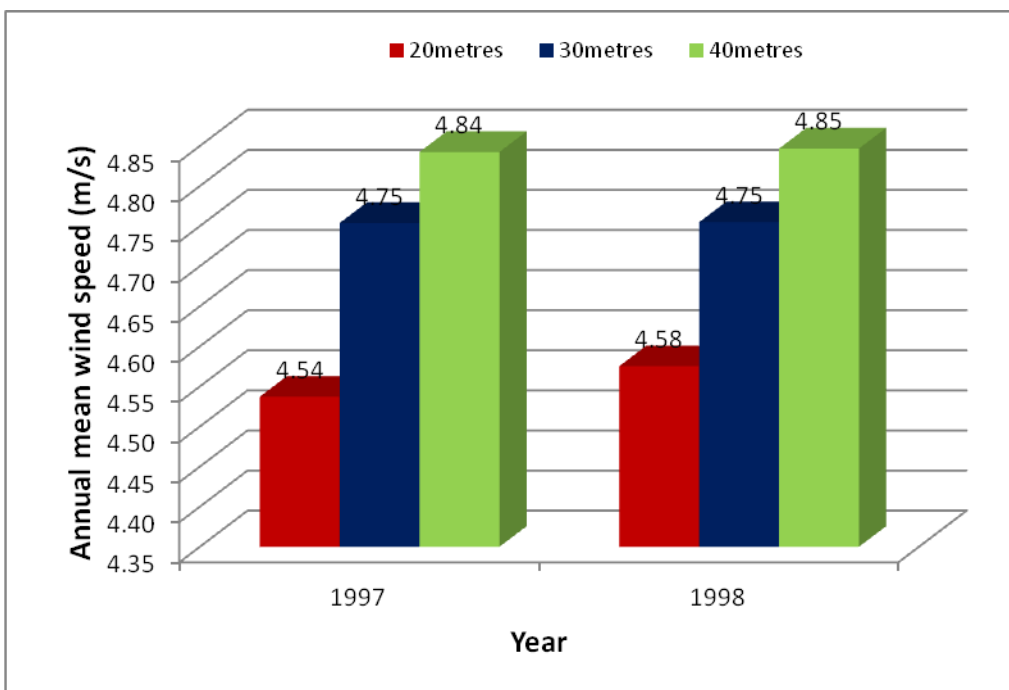


Figure 6.25 Annual mean wind speed at different heights at Yanbo.

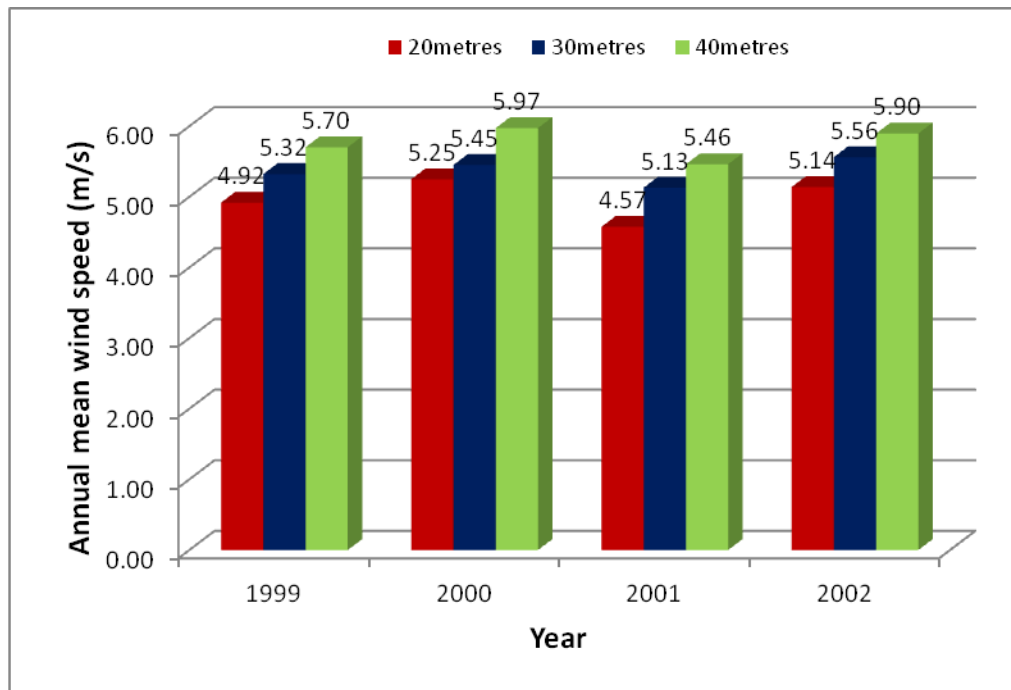


Figure 6.26 Annual mean wind speed at different heights at Dhulom

## 6.5 SEASONAL VARIATION OF MEAN WIND SPEED AT DIFFERENT HEIGHTS

The knowledge of seasonal variation of monthly mean wind speed is critical from an energy management point of view due to the fluctuating nature of the electrical load requirements during different months of the year. For example, in Saudi Arabia, the demand increases tremendously during summer months due to the increased air-conditioning load. The seasonal trends of monthly mean wind speed values at 20, 30 and 40 m AGL for Rawdat Ben Habbas are depicted in Figure 6.27. In general, higher values were seen in summer time and lower values in winter season during all the years of measurements but a slowly decreasing trend was also observed from year to year, which is in compliance with the trend discussed earlier in Chapter 6.4. In year 2006, peak winds were observed in March and June; in 2007, it shifted to April and June while in 2008 and 2009, the peaks were found in March and July. In Juaymah, higher values of monthly mean wind speeds were observed during summer months, as can be seen from Figure 6.28. These figures clearly indicate the effect of measurement heights on the measured mean wind speed values. The seasonal patterns are also observed repeating during different upcoming years. Similar types of repetitive patterns were observed at other locations such as Dhahran, Arar, Gassim, Yanbo and Dhulom as shown in Figures 6.29 to 6.33, respectively.

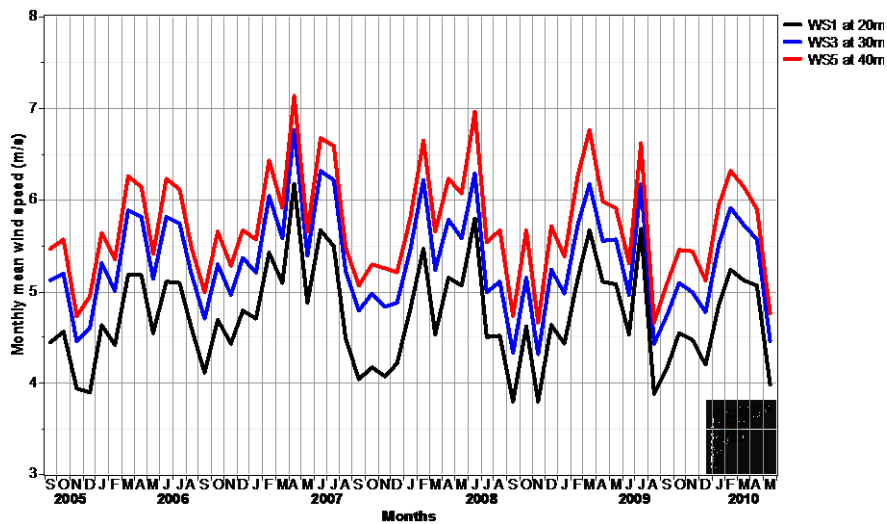


Figure 6.27 Monthly mean wind speeds in different years at Rawdat Ben Habbas

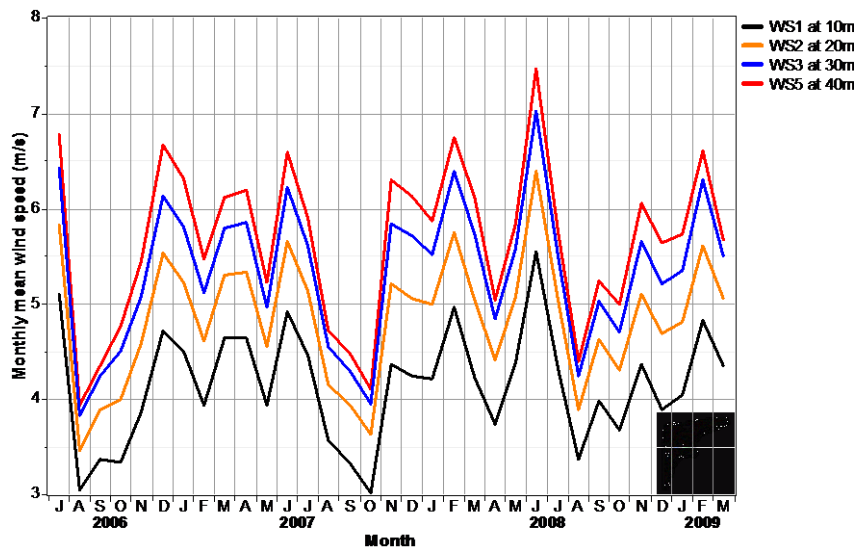


Figure 6.28 Monthly mean wind speeds in different years at Juaymah

Higher values of monthly mean wind speeds were observed at Dhahran (see Figure 6.29) in April, February and August, July, June, and March and May in the years 1996, 1997, 1998, 1999, and 2000, respectively. Year 1997 saw the highest winds while an upward trend was observed from 1998 towards the year 2000 as can be seen from Figure 6.29. At Arar (Figure 6.30), peak wind speeds were observed in April and July, March and July and July in the years 1996, 1997 and 1998, respectively. Year 1997 was a bit more turbulent compared with other years.

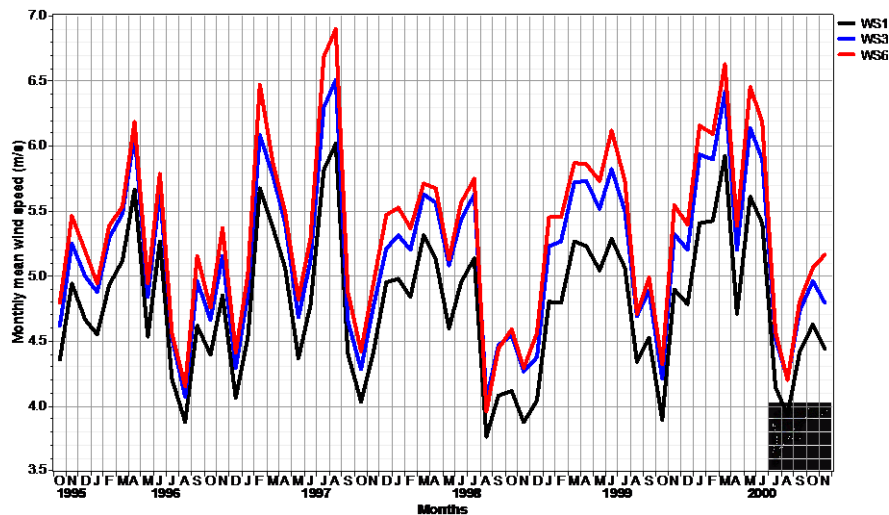


Figure 6.29 Monthly mean wind speeds in different years at Dhahran

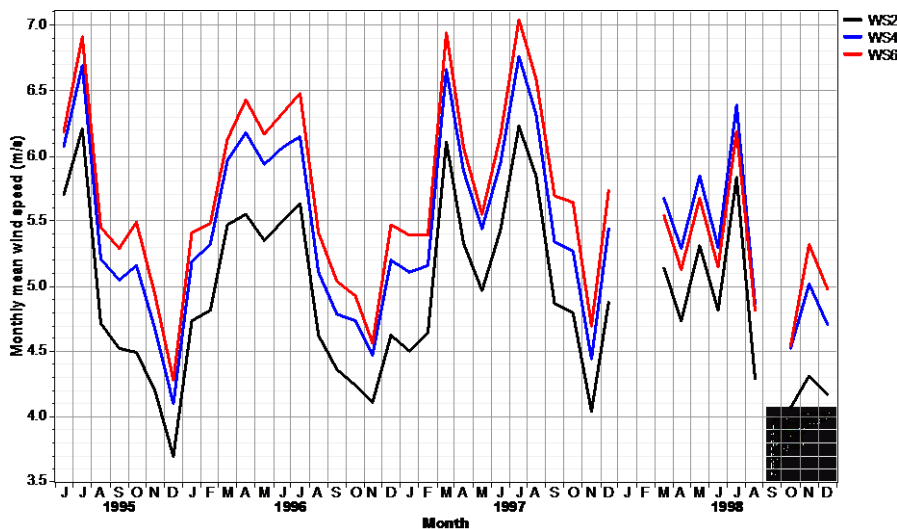


Figure 6.30 Monthly mean wind speeds in different years at Arar

Higher values of monthly mean wind speeds were observed at Gassim in the years 1996 and 1998 compared with those in 1997, as shown in Figure 6.31. Peak monthly mean winds occurred in April and July in 1996, February in 1997, and May in 1998. At Yanbo, the measured data was available during 1997 and 1998, as shown in Figure 6.32 with peaks occurring in the months of February and May in the respective years. At Dhulom (see Figure 6.33), higher monthly mean wind speeds occurred in March, March and July, and February and July in the years 1999, 2000 and 2002, respectively.

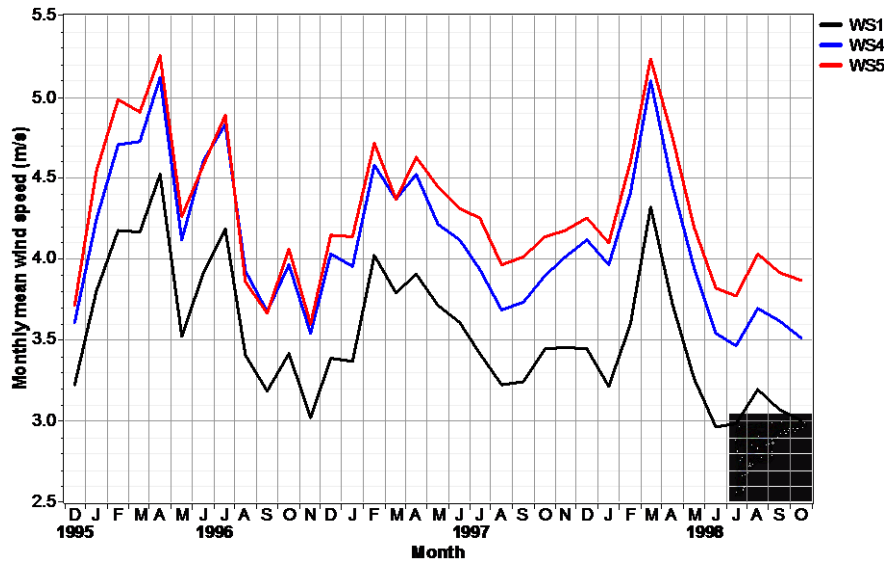


Figure 6.31 Monthly mean wind speeds in different years at Gassim

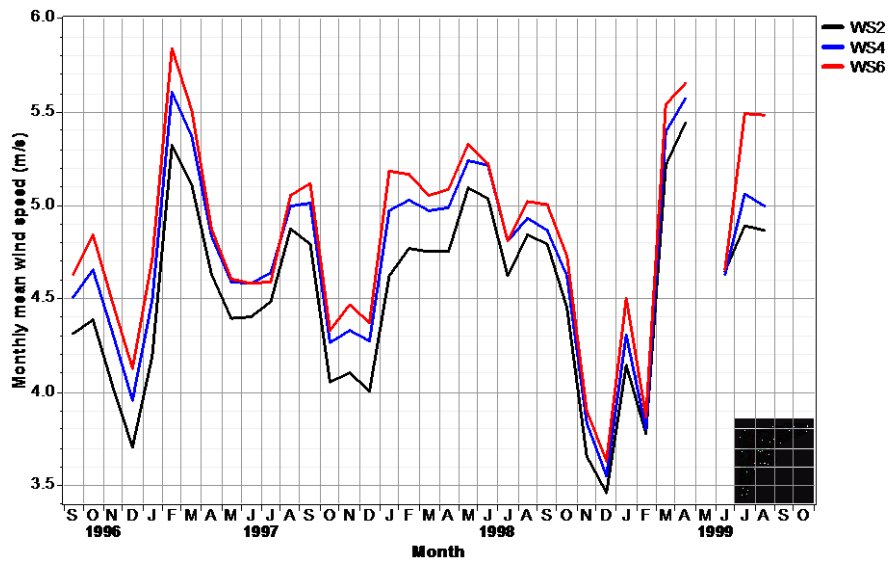


Figure 6.32 Monthly mean wind speeds in different years at Yanbo

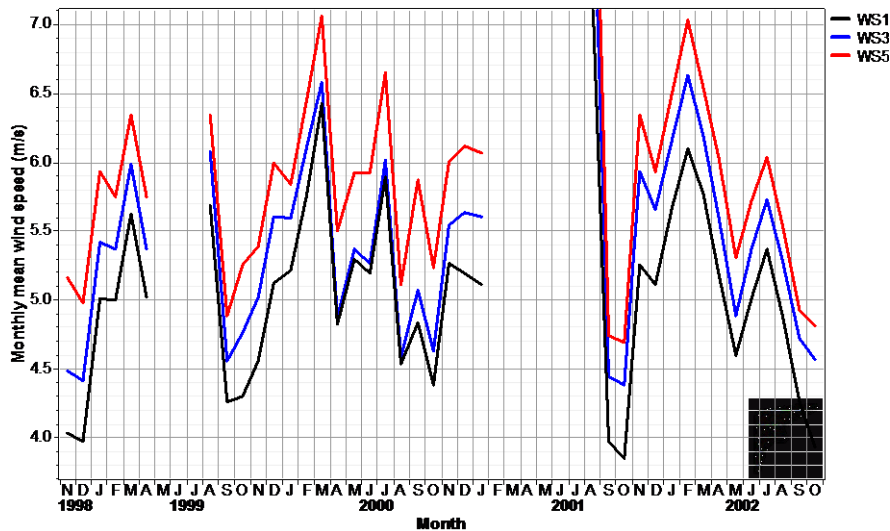


Figure 6.33 Monthly mean wind speeds in different years at Dhulom

## 6.6 DIURNAL VARIATION OF MEAN WIND SPEED AT DIFFERENT HEIGHTS

The diurnal variation of hourly or half-hourly mean wind speed provides an insight into the availability of wind during different hours of the day and helps in planning the utilisation of the power of wind in conjunction with the regular fossil-fuel-based power generation. This knowledge is used to make optimal usage of the intermittent source of energy to offset the greenhouse gases (GHG) by minimising the running of fossil-fuel-based power plants. In this study, the hourly and half-hourly mean wind speed values at all measurement heights and from all the anemometers were obtained using Windographer software and are shown for all the stations in Figures 6.34 to 6.40.

At Rawdat Ben Habbas, the lower wind speed values were observed during night-time and early morning hours but this diurnal range decreased at 30 m and then again started increasing with a further increase as can be observed from Figure 6.34. At 20 m, the difference between the maximum and minimum wind speed, i.e the range, was 1.3m/s while it reduced to 0.97 at 30m and again increased to 1.2 m/s at 40 m and kept on increasing with increasing heights. The wind speeds above 40 m were extrapolated using the local wind shear exponent. It is important to note that the extrapolated wind speeds were higher during night-time and lower during daytime, which shows a reversed pattern relative to wind speeds at lower heights.

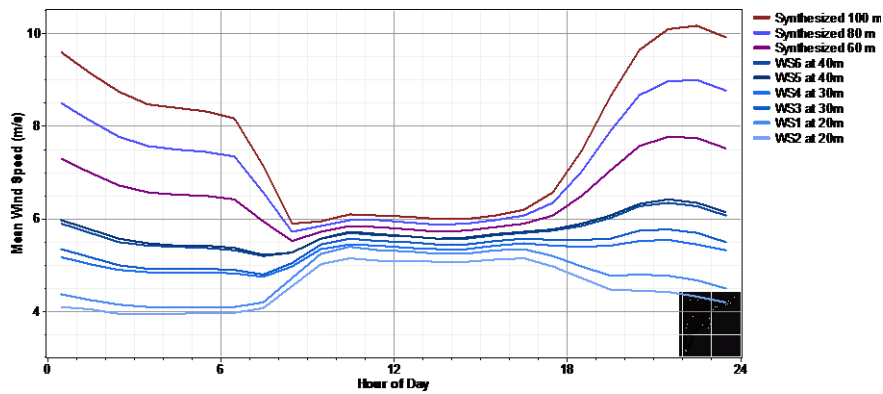


Figure 6.34 Diurnal variation of mean wind speed at Rawdat Ben Habbas

At Juaymah, the wind measurements were taken at four heights and the resulting diurnal variation is shown in Figure 6.35. Lower values were observed during night-time and higher values during daytime, which matches the load pattern of most of the cities in Saudi Arabia. The maximum range, i.e. the difference between maximum and minimum diurnal wind speed, was 3.3 m/s at 10 m while at 20, 30 and 40 m, the ranges decreased to 3 m/s, 2.71 m/s and 2.41 m/s, respectively. The peak values of wind speeds were observed between 14:00 to 15:00 hours. This shows that at Juaymah, the turbulence intensity or fluctuation in wind speed decreases with height, which simply means more stable winds above.

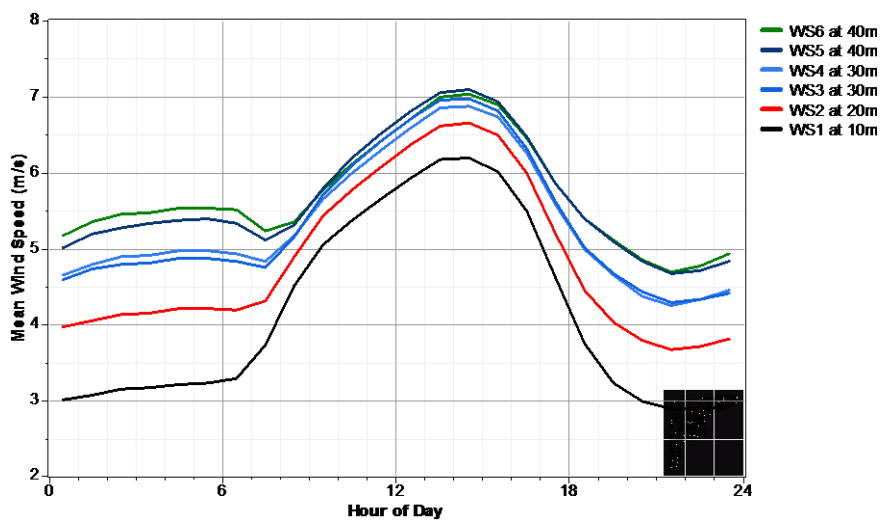


Figure 6.35 Diurnal variation of mean wind speed at Juaymah

Almost similar diurnal patterns were observed at Dhahran with the peak occurring between 15:00 to 16:00 hours, as shown in Figure 6.36. The ranges of diurnal cycle at Dhahran were found to be decreasing from 3.05m/s at 20m to 2.55m/s at 40m with 2.74m/s at 30m AGL. In Arar, a reversed diurnal pattern of wind speed with higher values during night-time and lower

values during daytime were observed as can be seen from Figure 6.37. This figure also includes the synthesised diurnal wind speeds at 50 m and 60 m, estimated using local wind shear exponent. The highest hourly mean winds were observed at 00:00 hours while the lowest between 11:00 to 12:00 hours. At Arar, the ranges were found to be increasing with height as 0.52 m/s at 20 m, 0.99 m/s at 30 m and 1.51 m/s at 40 m AGL but with further increase in height, the range remained almost 1.5 m/s up to 60 m AGL.

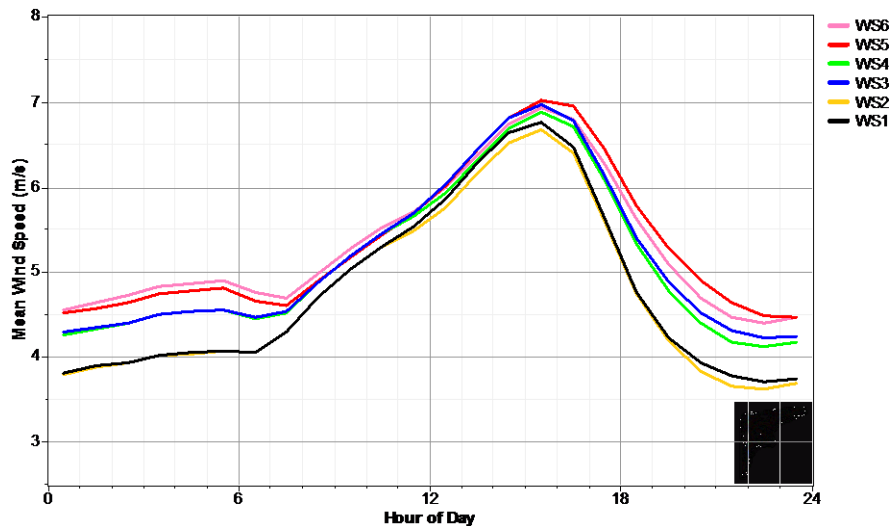


Figure 6.36 Diurnal variation of mean wind speed at Dhahran

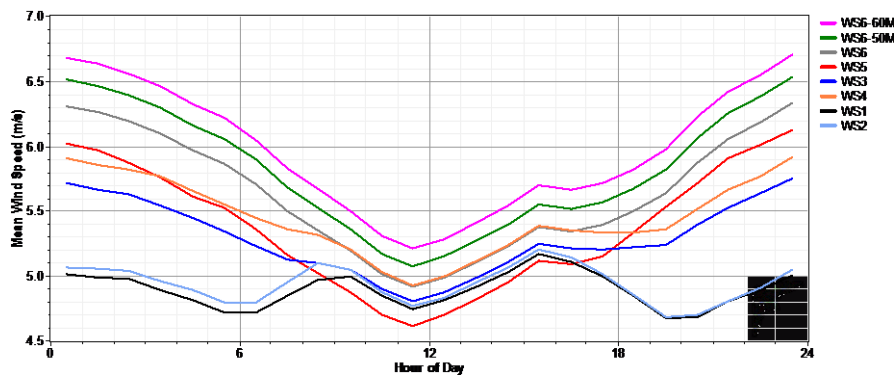


Figure 6.37 Diurnal variation of mean wind speed at Arar

The measured (at 20, 30 and 40 m AGL) and estimated (at 60, 80 and 100 m AGL) values of diurnal patterns of hourly mean wind speeds at Gassim are shown in Figure 6.38. Higher winds were observed during night-time and lower winds during daytime with a smaller range of less than 1 m/s corresponding to measurement heights but crossed 1 m/s at 60 m and above. At Yanbo, as shown in Figure 6.39, a steep diurnal change (range > 4.5 m/s) was observed at all the measurement heights. At 20 m AGL, the diurnal wind varied between a minimum of 2.92m/s and a maximum of 7.56m/s and at 30m between 3.14m/s and 7.78m/s.

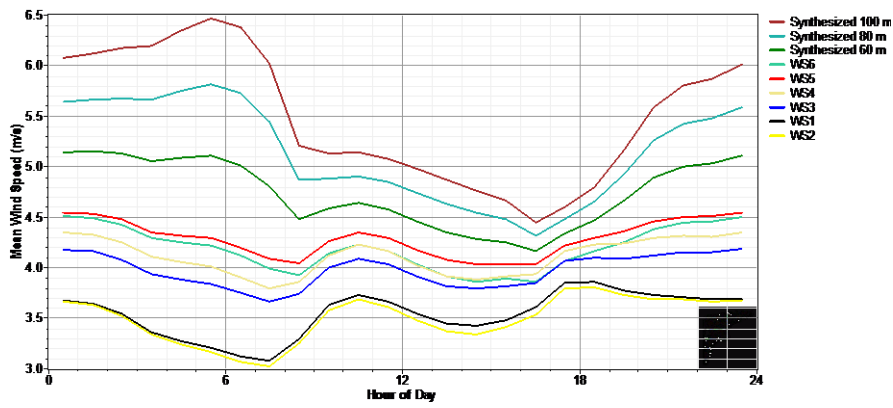


Figure 6.38 Diurnal variation of mean wind speed at Gassim

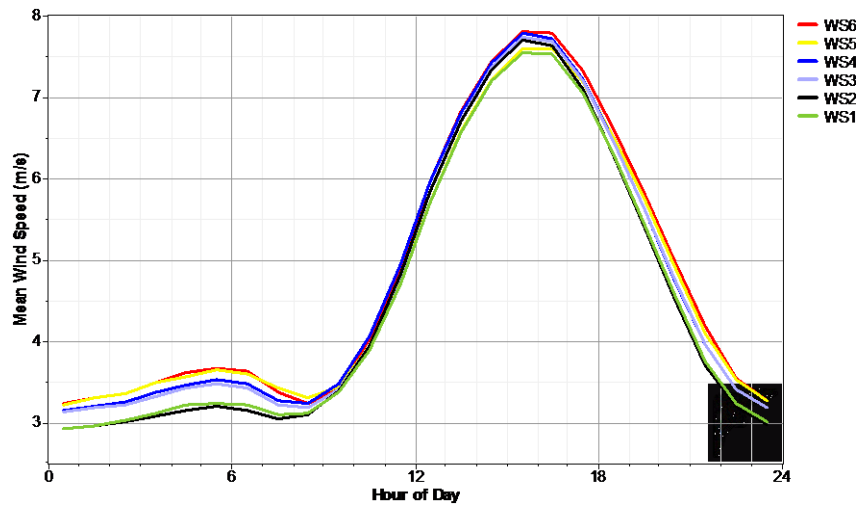


Figure 6.39 Diurnal variation of mean wind speed at Yanbo

The hourly mean winds were found to be decreasing from 00:00 hours to 06:00 hours and then an increasing trend for a short duration of 3-4 hours and then again a decreasing trend upto 17:00 hours at Dhulom as given in Figure 6.40. Higher ranges of 2.58m/s, 2.13m/s and 1.79m/s were obtained at 20, 30 and 40m measurement levels.

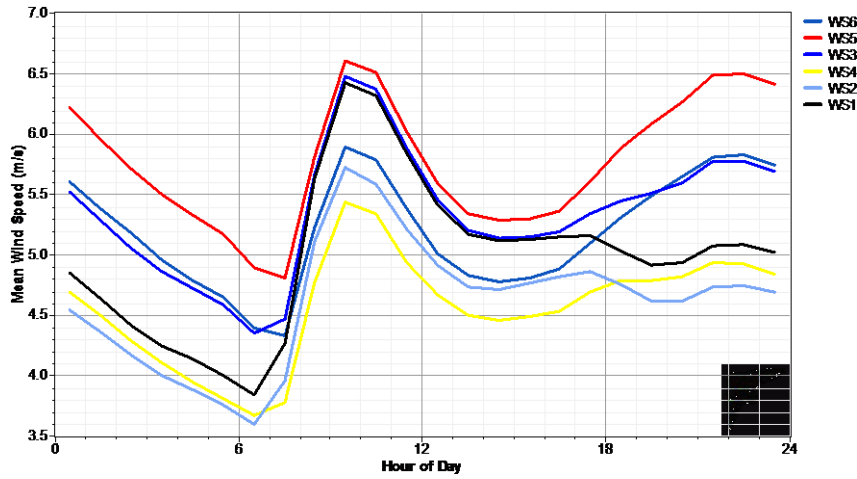


Figure 6.40 Diurnal variation of mean wind speed at Dhulom

### 6.7 LOCAL WIND SHEAR EXPONENT (WSE) ESTIMATION

The wind shear exponent (WSE) is a number that characterises the wind shear, which is the change in wind speed with height above ground. For data sets from Rawdat Ben Habbas, Juaymah, Dhahran, Arar, Gassim, Yanbo and Dhulom, the WSE were calculated using the observed wind data profile by best-curve fitting method given in the software (Windographer, 2008), as shown in Figure 6.13. The wind shear exponent values may also be calculated using the following equation:

$$\alpha = \frac{\ln(V_2) - \ln(V_1)}{\ln(Z_2) - \ln(Z_1)} \quad (6.1)$$

where  $V_1$  and  $V_2$  are the wind speeds at heights  $Z_1$  and  $Z_2$ , respectively. These values of WSE calculated using Equation 6.1, were used to find the annual, seasonal, and hourly and half-hourly means. The site-specific values of WSE, surface roughness, roughness class and roughness description are summarised in Table 6.3. The highest WSE value of 0.286 was obtained for Rawdat Ben Habbas while the lowest of 0.081 for Yanbo. These WSE values should be used to extrapolate the wind speed above measurement height to get accurate wind speed values. This table also includes the roughness length, class and description of each site. According to this classification, Rawdat Ben Habbas and Gassim were classified as suburban areas while Arar and Dhulom as areas having a few trees in the surroundings. Juaymah, Dhahran and Yanbo were classified as areas having many trees, crops and smooth land, respectively.

Table 6.3 Site-specific summary of wind shear exponent and related parameters

Location	Wind shear exponent	Roughness length, m	Roughness class	Roughness description
Rawdat Ben Habbas	0.286	1.81	4.41	Suburban
Juaymah	0.274	0.239	2.72	Many trees
Dhahran	0.151	0.056	1.52	Crops
Arar	0.182	0.138	2.27	Few trees
Gassim	0.241	1.070	3.97	Suburban
Yanbo	0.081	0	0	Smooth
Dhulom	0.193	0.134	2.25	Few trees

### 6.7.1 Wind shear exponent for Rawdat Ben Habbas

The wind shear exponent was estimated using the power and log law fit for Rawdat Ben Habbas station as shown in Figure 6.41. The annual mean values of WSE decreased slightly by 0.72% and 0.85% in the years 2007 and 2008 compared with 2006 and 2007 while an insignificant decrease of 0.18% was obtained in 2009 compared with 2008 (see Figure 6.42). Overall, a decreasing seasonal pattern was seen starting from January to June and then again an increasing trend towards the end of the year, as shown in Figure 6.43. A well-defined diurnal change was noticed in the values of WSE during different months of the year for the entire data collection period with higher values during night-time and lower values during daytime and with transitions between 06:00 and 09:00 and 18:00 and 21:00 hours, as seen from Figure 6.44. Almost flat or constant WSE values were observed between 09:00 and 18:00 hrs. Higher values during night-time may be referred to as stable, less hot, higher humid and relatively calm conditions and lower values during daytime may be referred to as relatively higher turbulent atmosphere, high temperatures and relatively lower humidity.

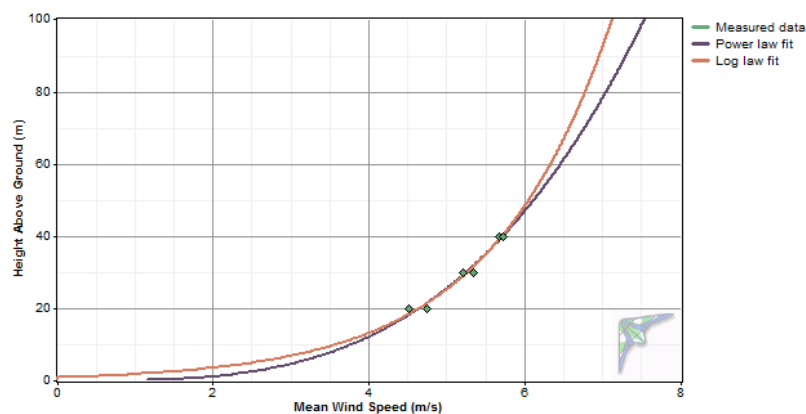


Figure 6.41 Wind shear exponent estimation using power and log law fit at Rawdat Ben Habbas

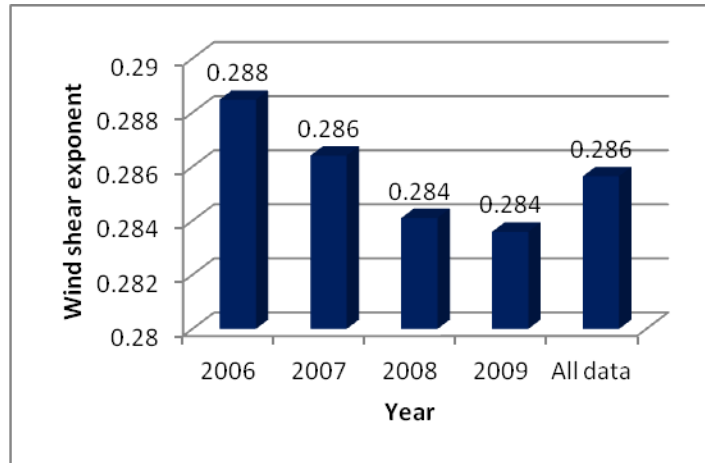


Figure 6.42 Annual variation of WSE at Rawdat Ben Habbas

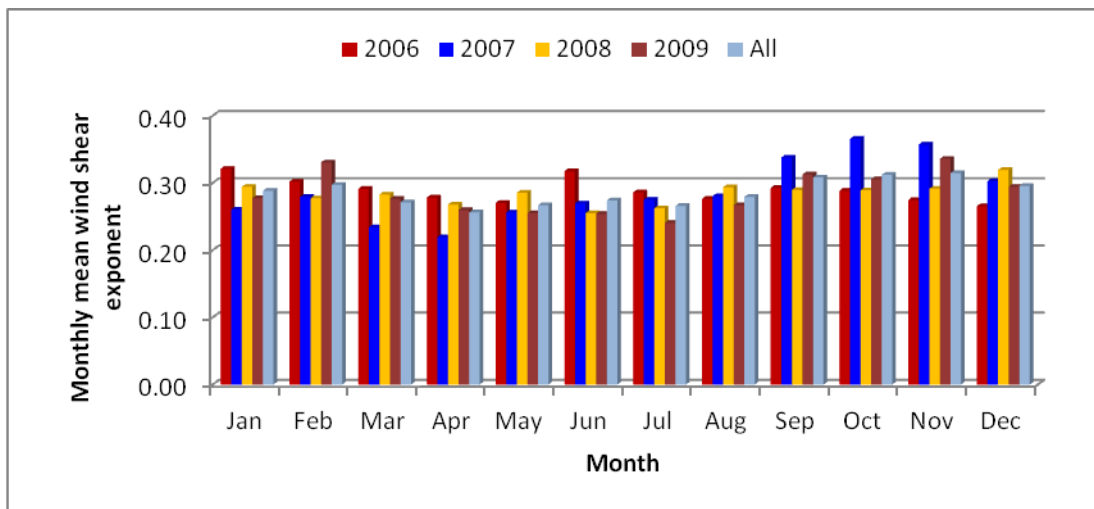


Figure 6.43 Monthly mean WSE in different years at Rawdat Ben Habbas

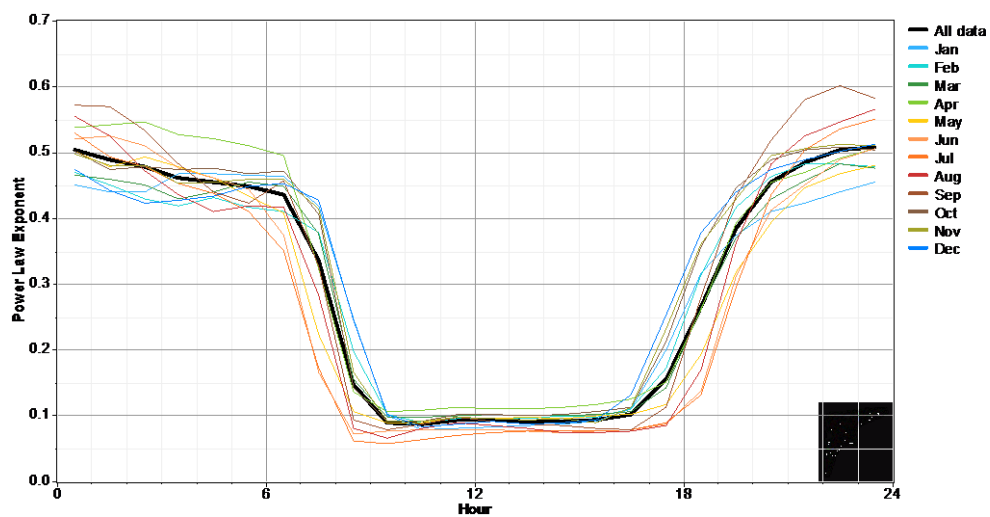


Figure 6.44 Diurnal variation of WSE during different months of the year and over the entire data collection period at Rawdat Ben Habbas

### 6.7.2 Wind shear exponent for juaymah

For data sets that contain wind speed data for two or more different heights above ground, Windographer calculates the power law exponent from the observed wind shear profile by best-curve-fitting method, as shown in Figure 6.45. The WSEs obtained using the entire data set were 0.273 with 0.269 and 0.279 for the data of years 2007 and 2008, respectively, as shown in Figure 6.46. Higher values of WSE ( $\sim 0.25$ ) were observed from October to January and relatively lower values ( $\sim 0.245$ ) during the rest of the months with the lowest value in August as can be seen from Figure 6.47. In general a decreasing trend was observed from January to August and then an increasing towards the end of the year, which is evident from Figure 6.47. The WSE values are very much dependent on the meteorological changes that take place during 24 hours of the day as demonstrated in Figure 6.48. It is clear from this figure that higher values of WSE ( $\sim 0.35 - 0.4$ ) were observed from 20:00 to 06:00 hours and lower values ( $\sim 0.1$ ) from 08:00 to 17:00 hours. For precise estimation of wind speed at higher altitudes, different values of WSE during day- and night-time could be used. The overall surface roughness estimated was 1.124m with the highest of 1.386metres in October and the lowest of 0.995metres in June.

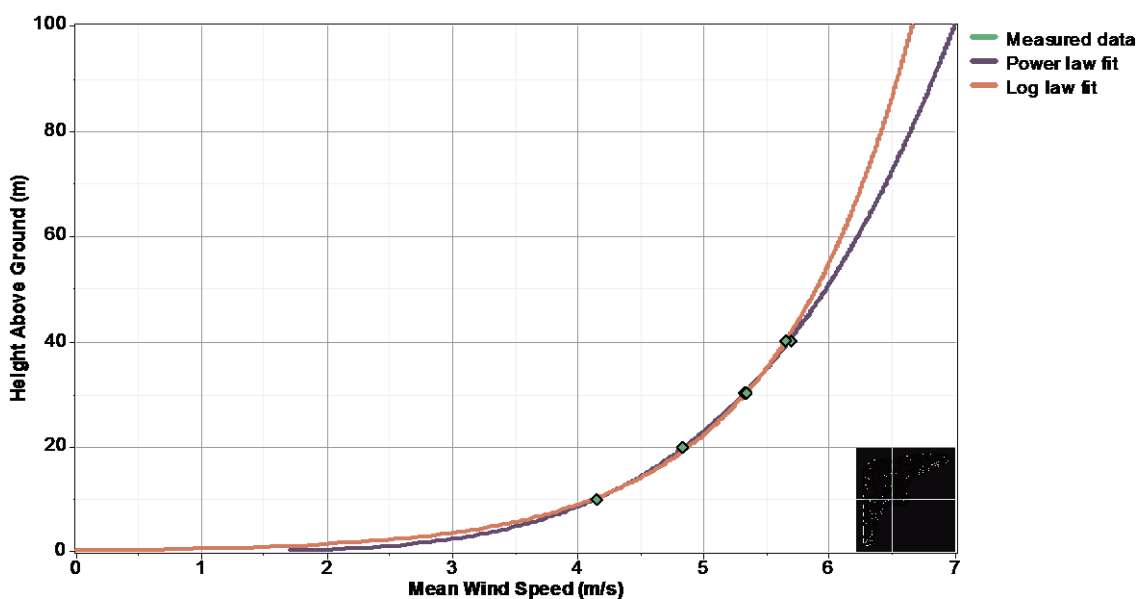


Figure 6.45 Wind shear exponent estimation using power and log law fit at Juaymah

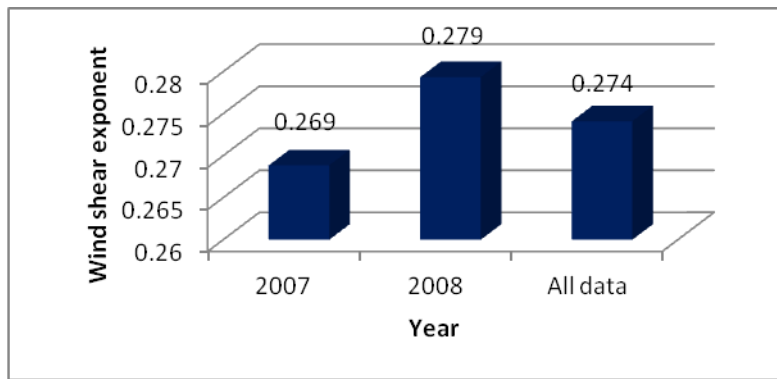


Figure 6.46 Annual variation of WSE at Juaymah

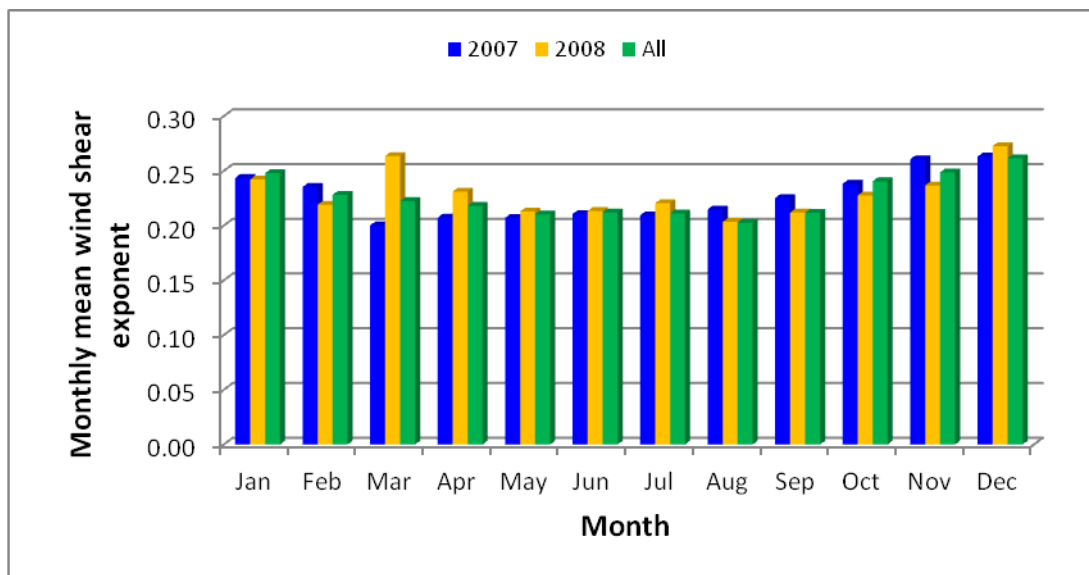


Figure 6.47 Monthly mean values of WSE in different years at Juaymah

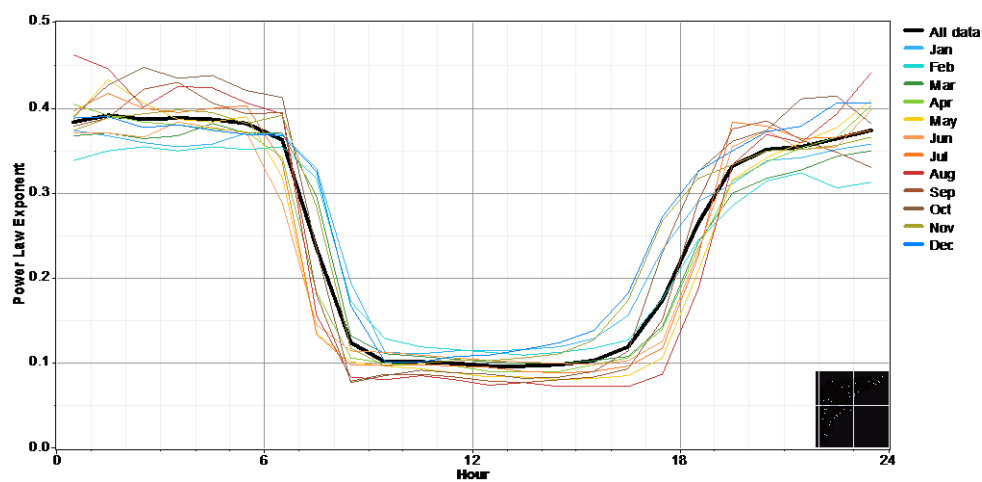


Figure 6.48 Diurnal variation of WSE during different months of the year and over the entire data collection period at Juaymah

### 6.7.3 Wind shear exponent for dhahran

The wind shear coefficients were calculated using pairs of wind speeds, three on each side of the wind measurement mast and the resulting vertical variation of measured wind speed along with the best-curve-fitting line is shown in Figure 6.49. As seen from Figure 6.50, the maximum value of WSE of 0.174 was observed in the year 1998 and a minimum of 0.118 in 1999, while the overall mean during all years was found to be 0.151. No definite seasonal trend could be observed in WSE values at Dhahran during individual years and also for the entire data set. The WSE values were found to be decreasing from January to March and then increasing until June and again falling back until August. Finally, higher values were observed towards the end of the year as can be seen from Figure 6.51.

It is evident from Figure 6.52 that the heating and cooling cycle of the air adjacent to the earth during 24 hours of the day influences the wind shear coefficients. During the early hours of the day i.e. between 00:00 and 06:00 hours, higher and almost constant values of WSE (~0.25) were observed while from 06:00 hours onwards, as heating of the ground surface and the air above it took place, these values started decreasing and after reaching a minimum (~0.05) at 08:00 hours, remained almost constant up to 16:00 hours. After 16:30 hours, the values again started increasing and after reaching a maximum at 19:00 hours showed a decreasing pattern during the rest of the night hours. The decrease may be the result of cooling of the ground surface and the air above it.

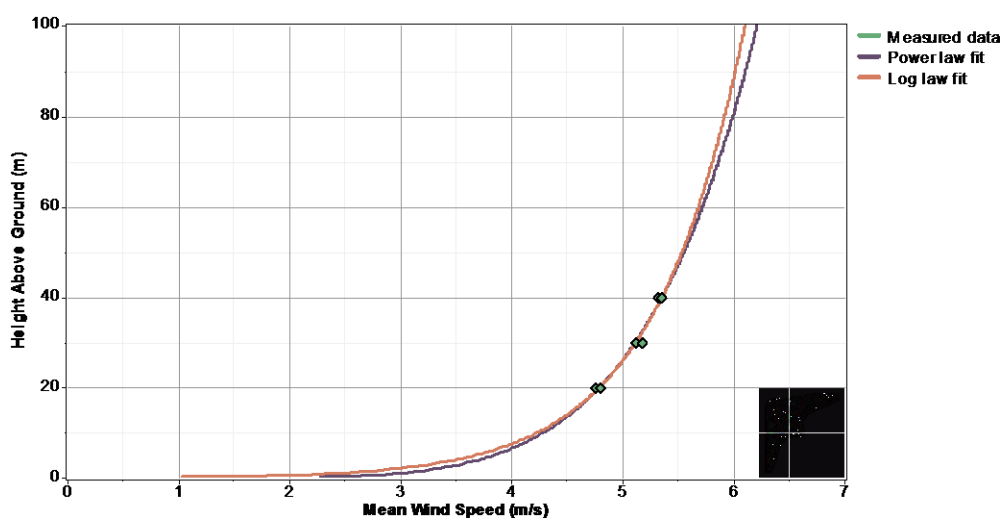


Figure 6.49 WSE estimation using power and log law fit at Dhahran

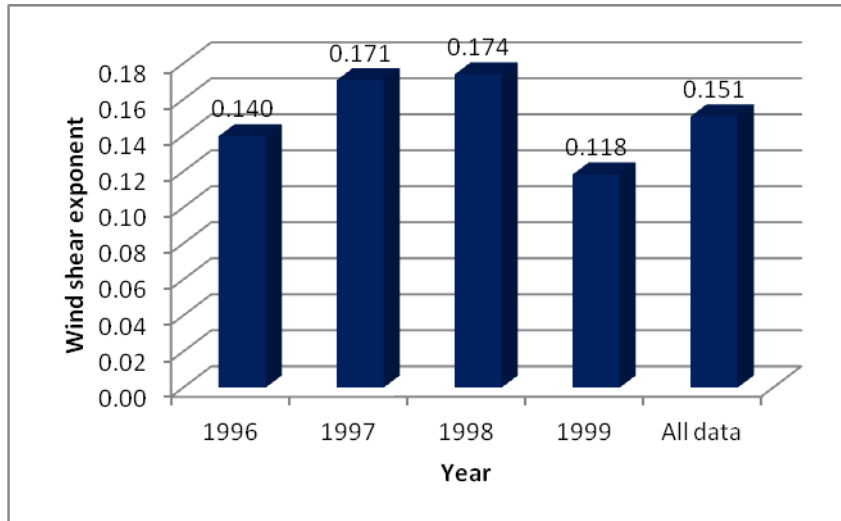


Figure 6.50 Annual variation of WSE at Dhahran

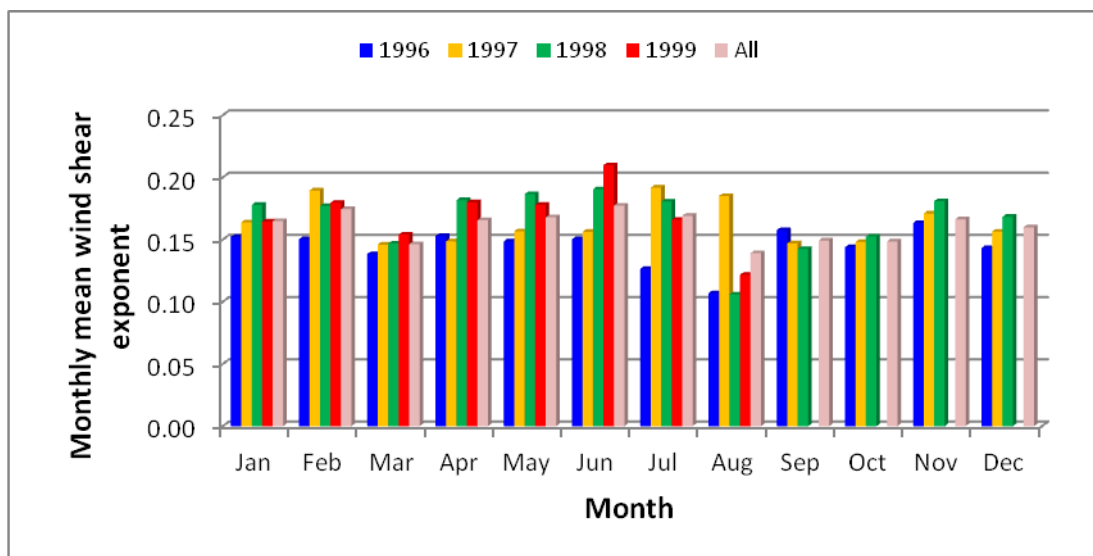


Figure 6.51 Monthly mean values of WSE in different years at Dhahran

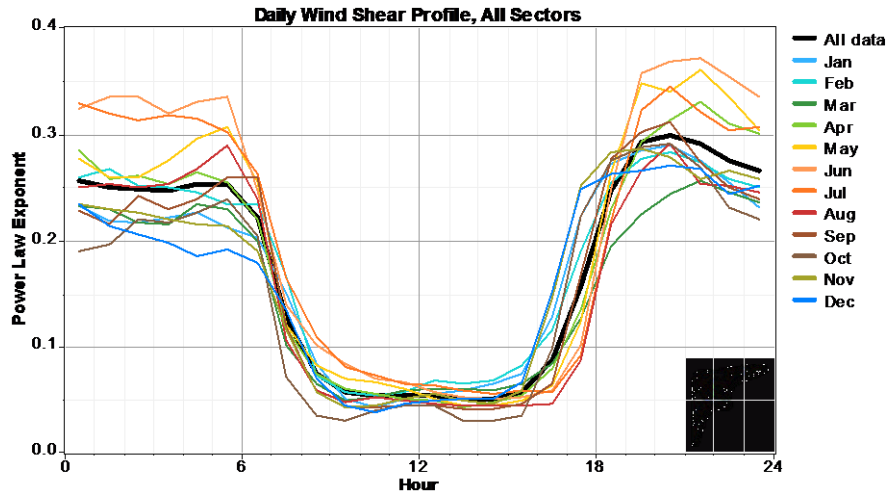


Figure 6.52 Diurnal variation of WSE during different months of the year and over the entire data collection period at Dhahran

#### 6.7.4 Wind shear exponent for Arar

The wind shear exponents were calculated by curve-fitting using Windographer software as shown in Figure 6.53. The annual mean values of WSE and overall mean during 1995 to 1997 are compared in Figure 6.54. The annual mean values for the years 1995 and 1996 were close ( $\sim 0.179$ ) while a relatively high value of 0.186 was found in 1997. The overall mean WSE value was 0.182. A decreasing trend was observed in monthly mean values WSE from January till October with least values in April and May, as can be seen from Figure 6.55. In general, higher values of WSE were observed in winter months and lower values in summer months. This conforms to the physical reasoning that during summer time, the temperatures are higher and hence better mixing of the air takes place above the ground, which results into smaller values of shear coefficients. On the other hand, during winter time, the air above the ground experiences less mixing due to lower temperatures and hence higher values of wind shear coefficients.

In order to study the diurnal pattern, half-hourly mean values of wind speeds were used to obtain the WSEs and the resulting trends for individual months are shown in Figures 6.56. It is evident from this figure that the heating and cooling cycle of the air adjacent to the earth during 24 hours of the day influences the WSE. During the early hours of the day, i.e. between 00:00 and 06:00 hours, higher and almost constant values of 0.25 to 0.28 were observed while from 07:00 hours onwards, as heating of the ground surface and the air above it took place, these values started decreasing and after reaching a minimum at 09:00 hours

remained constant (~0.075) up to 16:00 hours. After 16:00 hours, the WSE again started increasing and after reaching a maximum value of 0.25 to 0.28, remained constant during the rest of the night hours, which may be the result of cooling of the ground surface and the air above it. Hence it is recommended that the wind coefficients should be calculated using the long-term averages of wind speeds at different heights instead of half-hourly or hourly mean values of wind speeds.

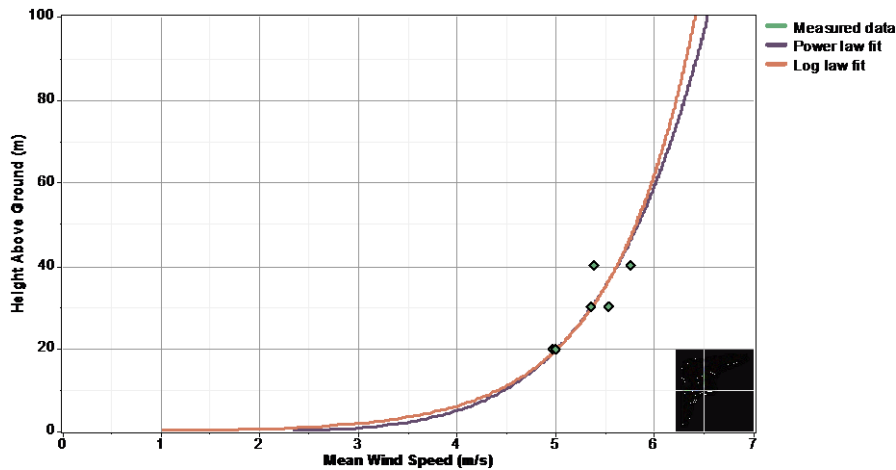


Figure 6.53 WSE estimation using power and log law fit at Arar

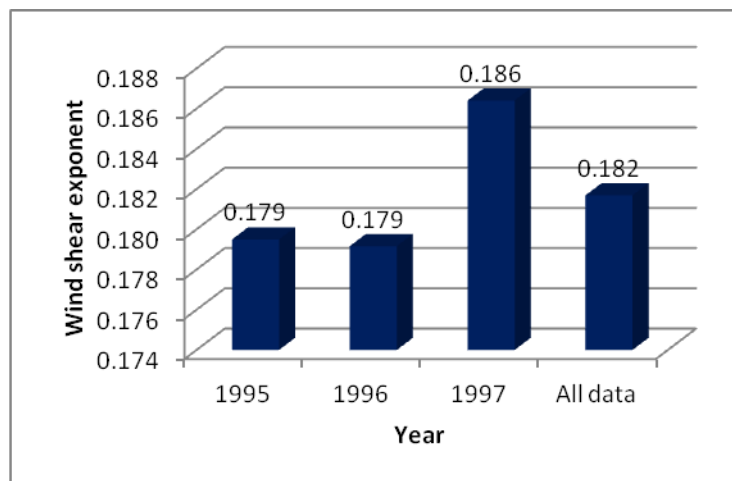


Figure 6.54 Annual mean values of WSE in different years at Arar

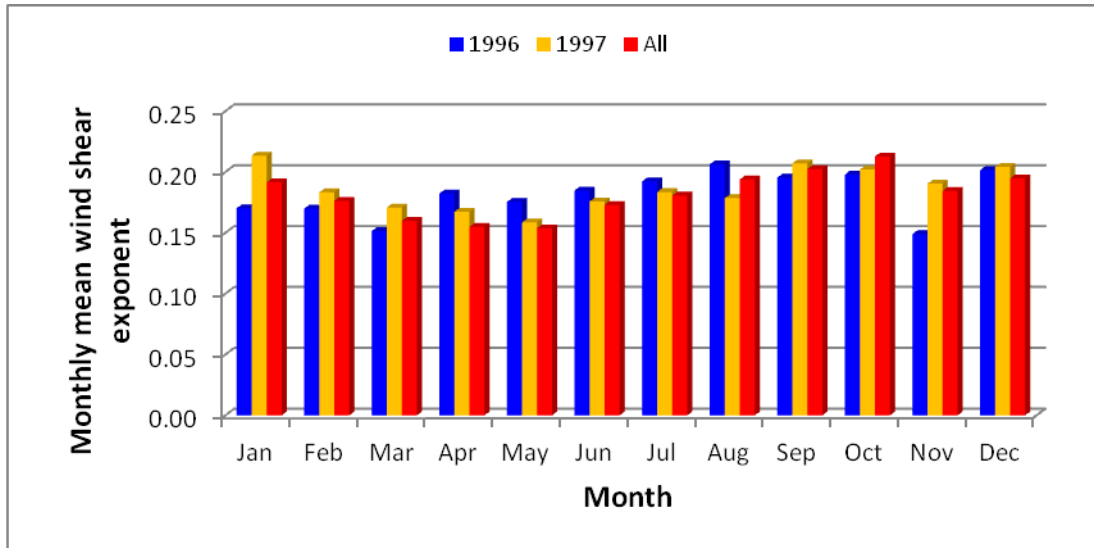


Figure 6.55 Monthly mean values of WSE in different years at Arar

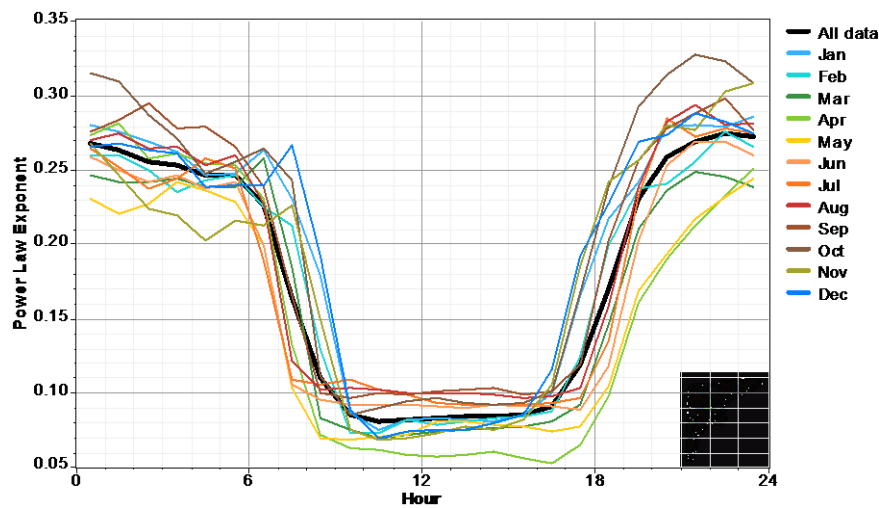


Figure 6.56 Diurnal variation of WSE during different months of the year and over the entire data collection period at Arar

### 6.7.5 Wind shear exponent for Gassim

The power law exponent is a number that characterises the wind shear, which is the change in wind speed with height above ground. For data sets that contain wind speed data for two or more different heights above ground, the software (Windographer) calculates the power law exponent from the observed wind shear profile by the best-curve-fitting method, as shown in Figure 6.57. The WSE obtained using all the data values was 0.241 while 0.218, 0.220 and 0.298 corresponded to the years 1996, 1997 and 1998, respectively as shown in Figure 6.58.

The WSE value for year 1995 is based on an incomplete data set due to some missing values during this particular year. The shape of the wind shear profile typically depends on several factors, most notably the roughness of the surrounding terrain and the stability of the atmosphere. Since the atmospheric stability changes with season, time of day, and meteorological conditions, the power law exponent also tends to change in time.

The seasonal variation of WSE for two years, i.e. 1996 and 1997, and the complete data set are shown in Figure 6.59. It is evident that the values of WSE had lesser range in 1996 (with minimum in August and maximum in December) compared with those in 1997 (with minimum in March and maximum in January). This simply indicates that higher values of WSE are observed during winter time and lower values during summer time, in general. Furthermore, no definite seasonal trend could be noticed in the values of WSE during the years under investigation. The overall values of WSE were found to be closer to those of 1997 both in terms of pattern and magnitude. The WSE values are very much dependent on the meteorological changes that take place during 24 hours of the day as demonstrated in Figure 6.60. The WSE values touched its minimum during daylight hours between 09:00 and 18:00 hours when the temperature is relatively higher and the air in different layers above ground surface is more turbulent and very well mixed. The diurnal patterns during 1997 and 1998 were almost the same in nature and also closer to the overall pattern shown in Figure 6.60.

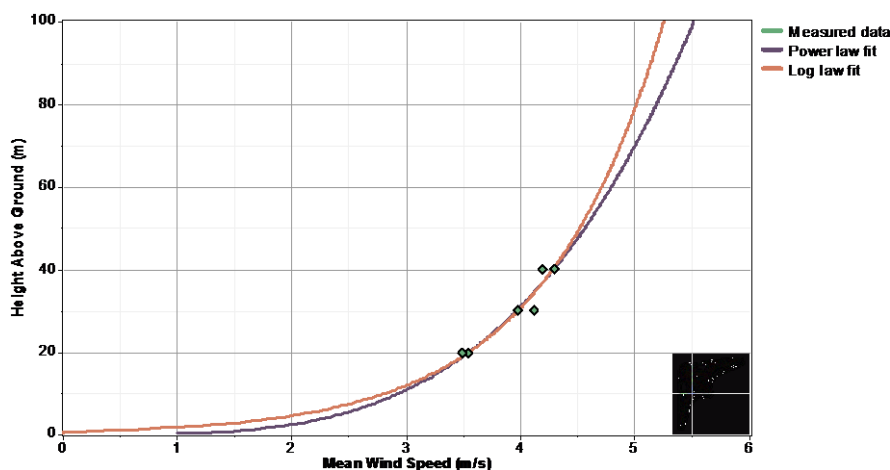


Figure 6.57 WSE estimation using power and log law fit at Gassim

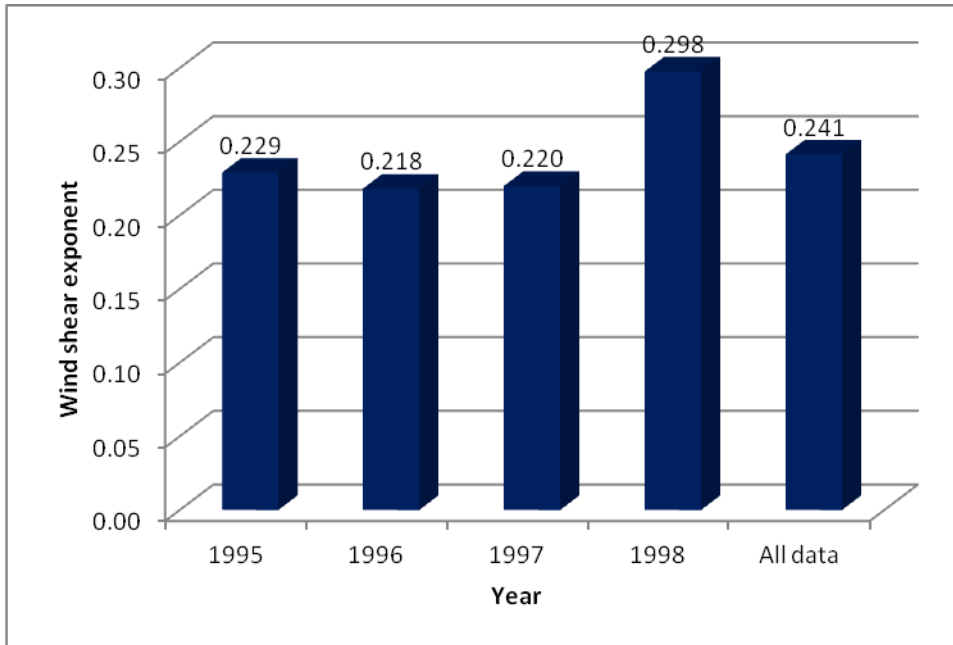


Figure 6.58 Annual mean values of WSE in different years at Gassim

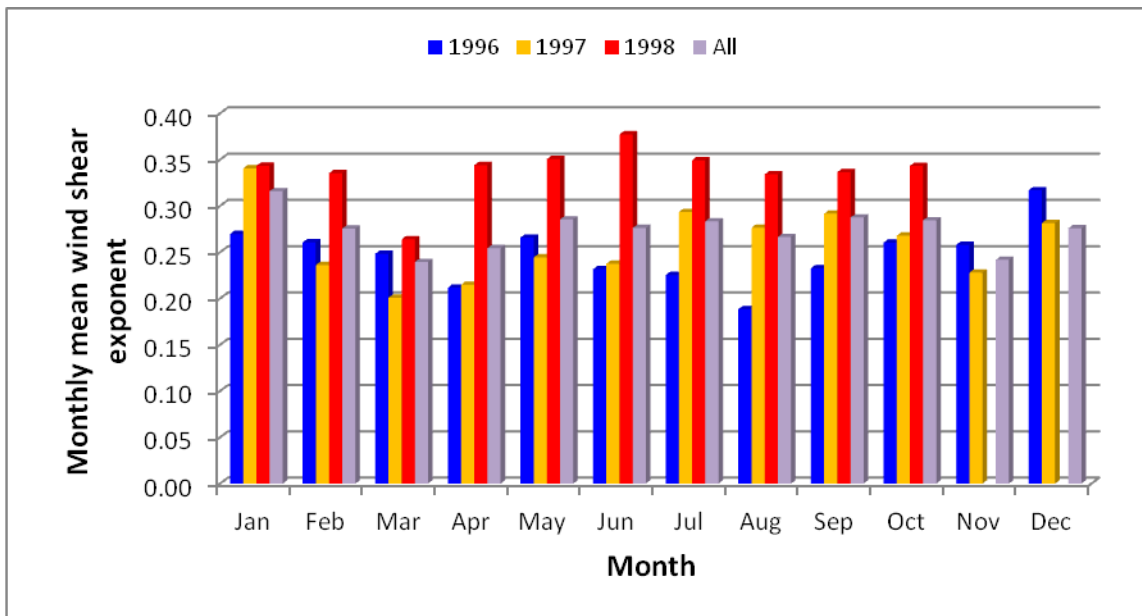


Figure 6.59 Monthly mean values of WSE in different years at Gassim

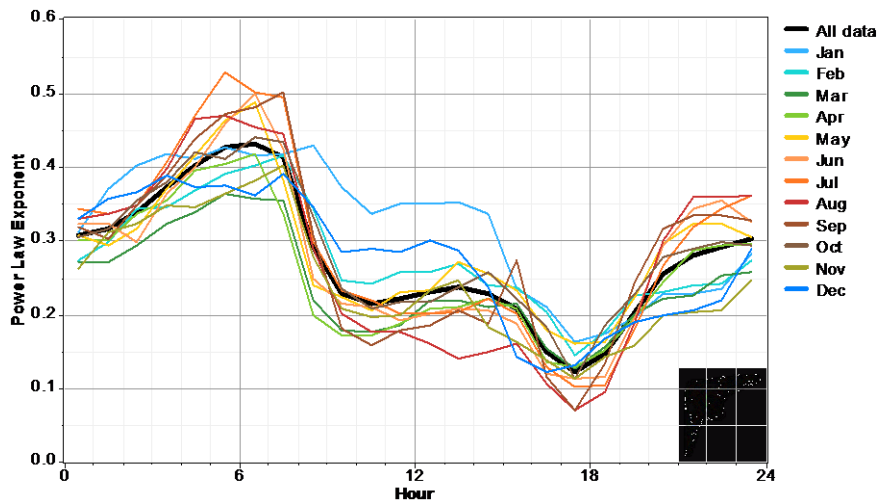


Figure 6.60 Diurnal variation of wind shear exponent during different months of the year and over entire data collection period at Gassim

#### 6.7.6 Wind shear exponent for Yanbo

The power law exponent is a number that characterises the wind shear, which is the change in wind speed with height above ground. For data sets that contain wind speed data for two or more different heights above ground, the software (Windographer, 2008) calculates the power law exponent from the observed wind shear profile by the best-curve-fitting method, as shown in Fig. 6.61. The WSE obtained using the complete data set was 0.081. The annual mean values of WSE were 0.111, 0.072 and 0.061 corresponding to years 1996, 1997 and 1998, respectively. A decreasing trend was observed in annual mean WSE values from 1996 to 1998, as can be seen from Figure 6.62. The shape of the wind shear profile typically depends on several factors, most notably the roughness of the surrounding terrain and the stability of the atmosphere. Since the atmospheric stability changes with season, time of day and meteorological conditions, the power law exponent also tends to change in time.

Very well-defined seasonal trends were observed for both years 1996 and 1997, for which complete data was available, as shown in Figure 6.63. The highest WSE values were observed in January and then a decreasing trend towards the middle of the year and after a minimum in June, an increasing trend was observed towards the end of the year. Where diurnal values of WSE are concerned at Yanbo, large variations were observed from one month to another and the average values were found to be higher in the early hours and the night-time and small values during daytime with transitions at both the ends, as given in Figure 6.64.

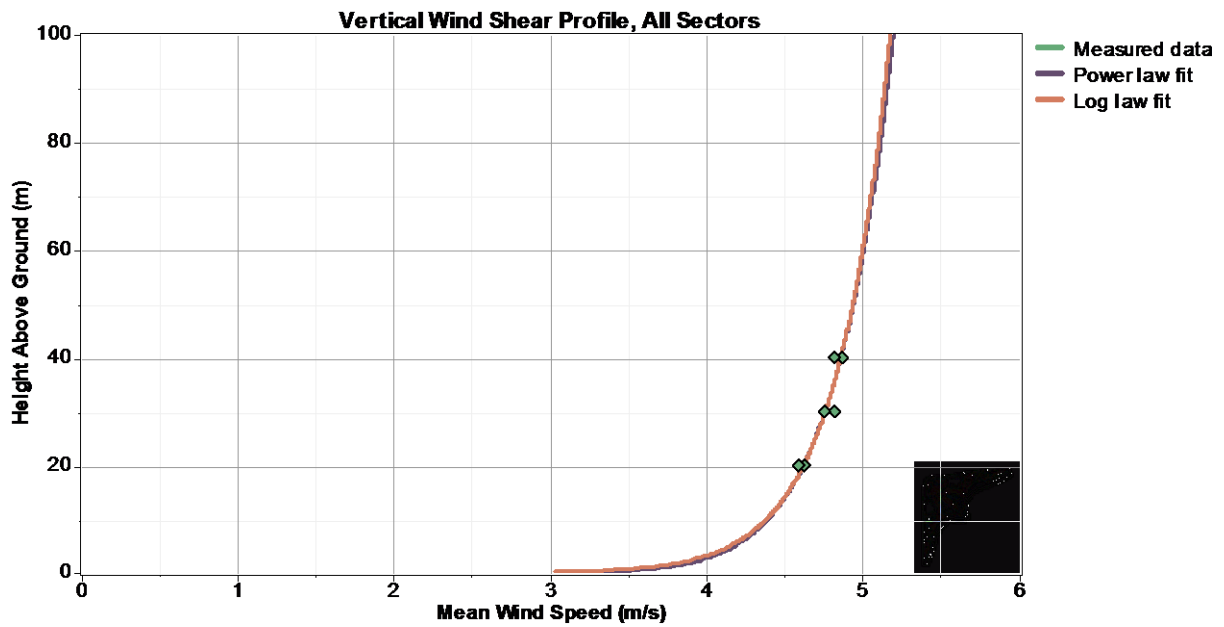


Figure 6.61 WSE estimation using power and log law fit at Yanbo

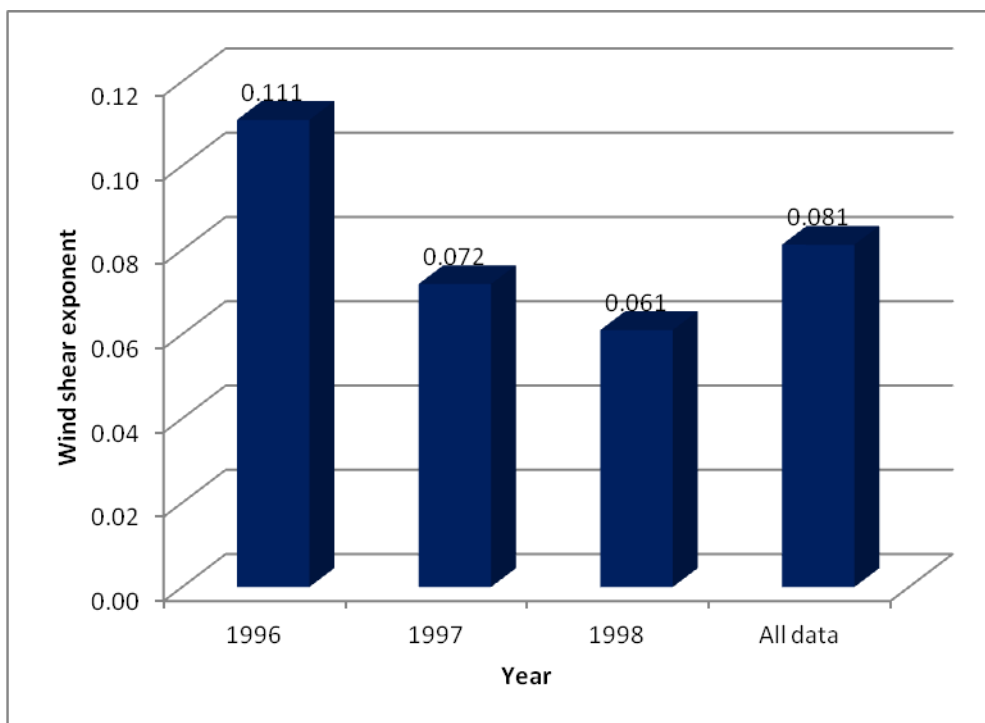


Figure 6.62 Annual mean values of WSE in different years at Yanbo

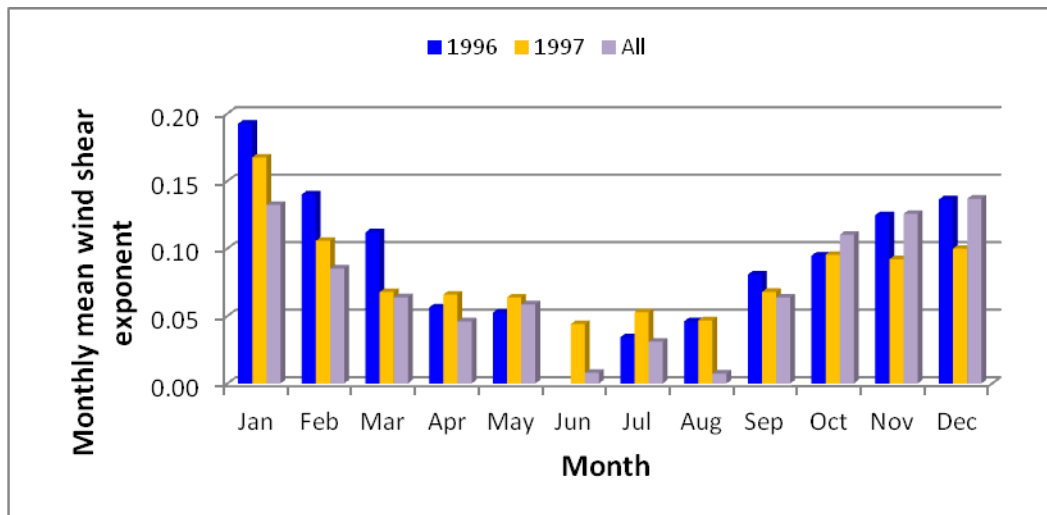


Figure 6.63 Monthly mean values of WSE in different years at Yanbo

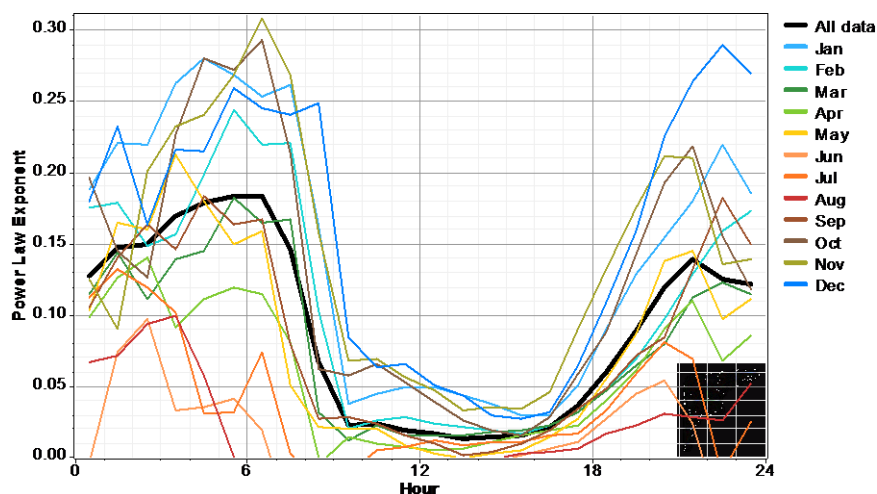


Figure 6.64 Diurnal variation of WSE during different months of the year and over the entire data collection period at Yanbo

### 6.7.7 Wind shear exponent for Dhulom

The WSE calculated using the wind speed measurements made at 20, 30 and 40metres by power law best-fit method deployed in Windographer software is shown in Figure 6.65. The WSE values obtained using annual mean wind speeds at different height are compared in Figure 6.66. The annual mean values of WSE were found to vary from 0.011 to 0.351 corresponding to years 2000 and 2001, respectively, while the value obtained based on all measured wind speeds was 0.193, as can be seen from Figure 6.66. The seasonal variation of

wind shear exponent showed a decreasing trend from January until middle of the year and then again an increasing trend towards the end of the year as can be seen from Figure 6.67. Relatively higher WSEs were observed from September to December.

To understand the diurnal pattern of wind shear coefficient, half-hourly mean values of wind speeds were used to obtain the WSEs. The diurnal variation of WSE is shown in Figure 6.68. From this figure, it is evident that the heating and cooling cycle of the air adjacent to the earth during 24 hours of the day influences the wind shear exponent. During early hours of the day, i.e. between 00:00 and 06:00 hours, higher and almost constant values of WSE were observed while from 06:00 hours onwards, as heating of the ground surface and the air above it took place, these values started decreasing and after reaching a minimum at 09:00 hours remained almost constant up to 17:00 hours. After 17:00 hours, these values again started increasing and after reaching a maximum at 20:00 hours showed a constant pattern during the rest of the night hours, which may be the result of cooling of the ground surface and the air above it.

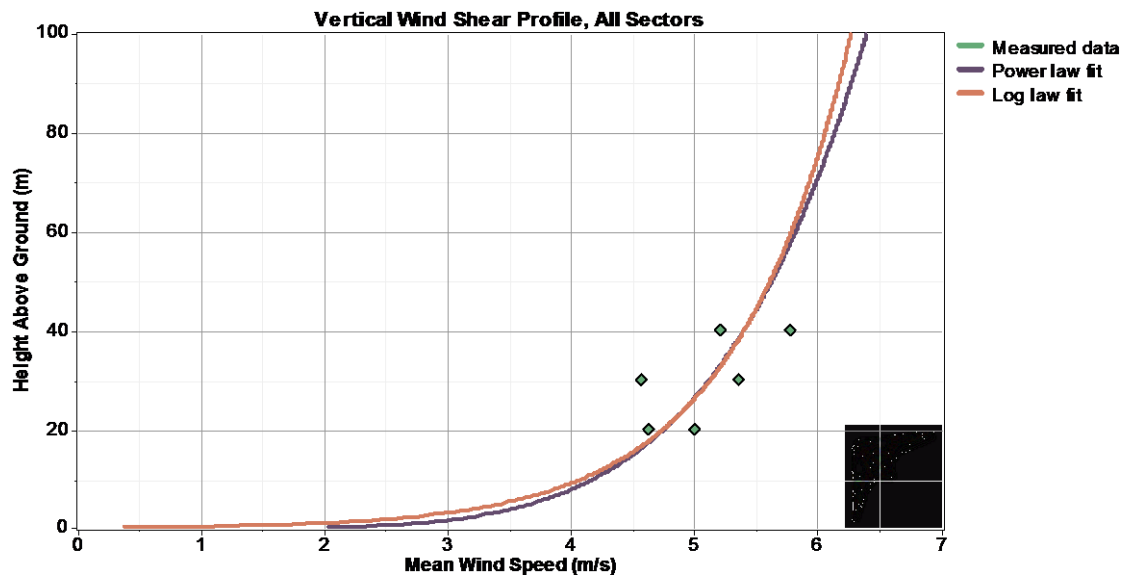


Figure 6.65 WSE estimation using power and log law fit at Dhulom

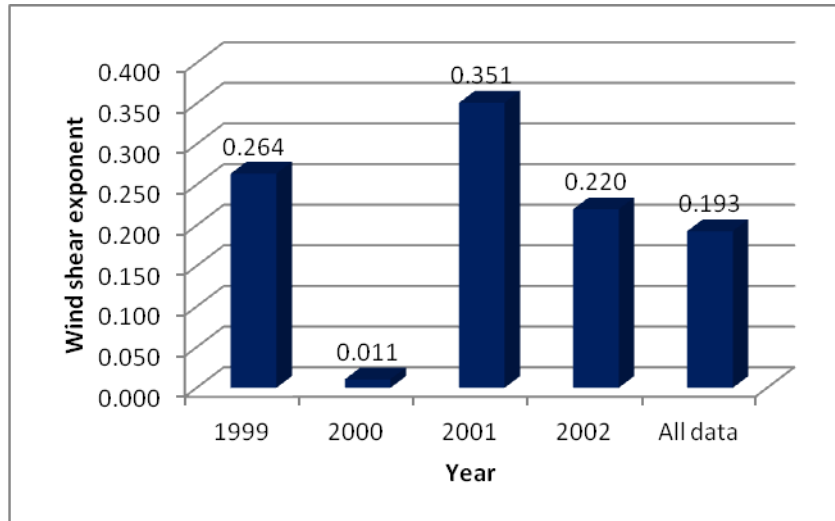


Figure 6.66 Annual mean values of WSE in different years at Dhulom

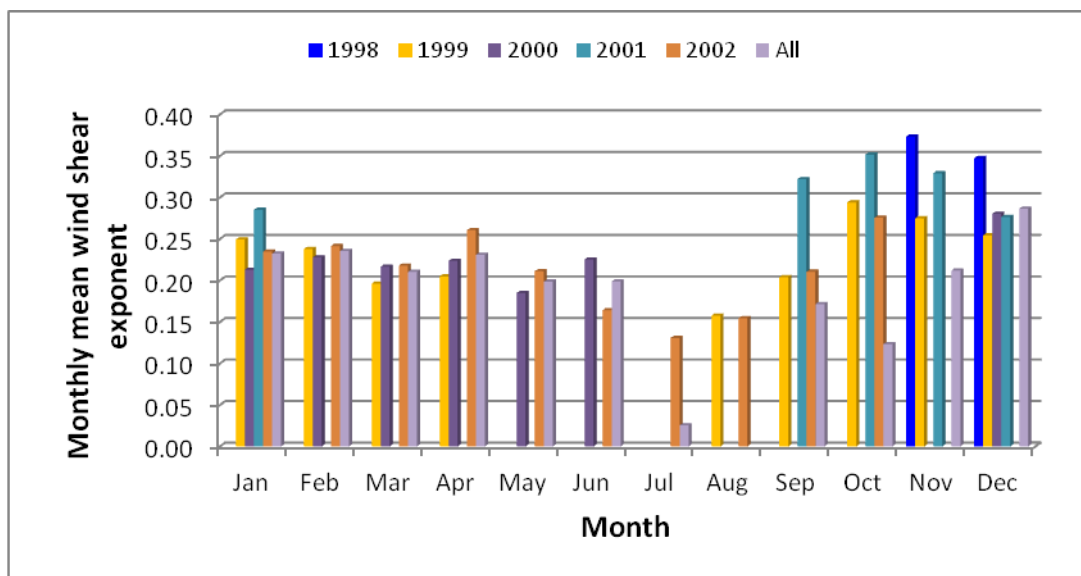


Figure 6.67 Monthly mean values of WSE in different years at Dhulom

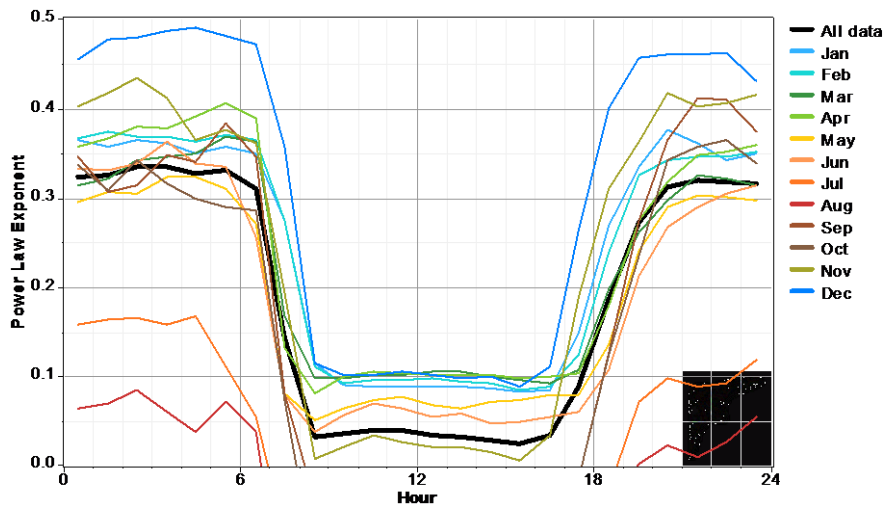


Figure 6.68 Diurnal variation of WSE during different months of the year and over the entire data collection period at Dhulom

## 6.8 ANALYSIS OF WEIBULL SHAPE AND SCALE PARAMETERS

Weibull distribution is characterised by two parameters: the shape parameter  $k$  (dimensionless) and scale parameter  $c$  (m/s). The shape factor reflects the breadth of the distribution, with lower values corresponding to broader distributions where the wind speed tends to vary widely, whereas higher  $k$  values correspond to tighter distributions where the wind speed tends to stay within a narrower range, as shown in Figure 6.69. Weibull is a widely used distribution for the representation of wind speed frequency in different wind speed bins. In the present case, the maximum likelihood algorithm was used to fit a Weibull distribution to a measured wind speed distribution.

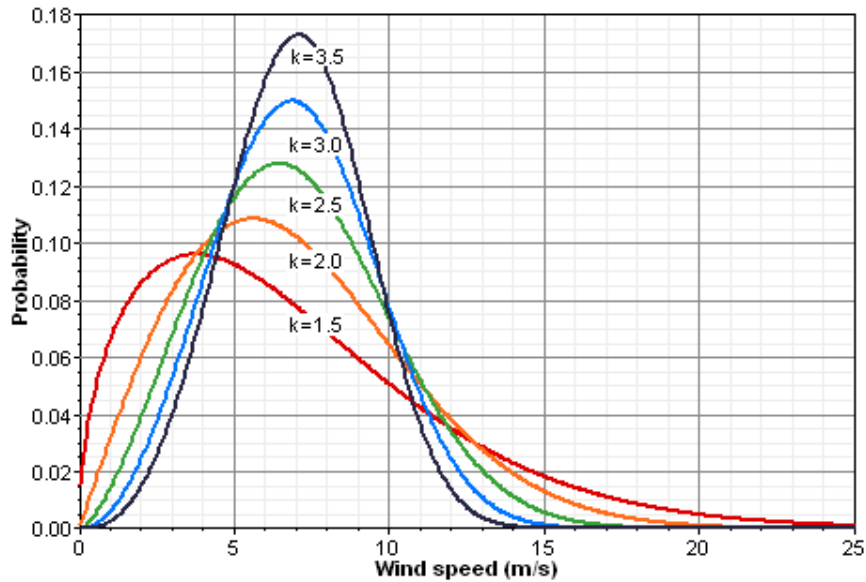


Figure 6.69 Effect of  $k$  on the nature of wind speed variations

The Weibull shape and scale parameters value calculated using the Windographer software and resulting site-dependent means over respective data collection periods at different heights are shown in Figures 6.70 and 6.71, respectively. In most of the cases, the  $k$  values were found to be increasing with height with the exception of Dhahran and Yanbo where lower values were found at 40metre. Shape parameter values were always greater than 2 at all heights of measurements with the exception of Yanbo and Gassim. The highest value of  $k = 2.31$  was found at Rawdat Ben Habbas, 2.26 at Arar and 2.23 at Juaymah. The scale parameter values were always above 5.0m/s even at 20metre with the exception of Gassim where these values were less than 5.0m/s. Moreover, an increasing trend with height, as expected, was also observed and scale parameter was always greater than 6.0 at 40metre AGL at Arar, Dhahran, Dhulom, Juaymah, Rawdat Ben Habbas and Yanbo. The highest value of  $c = 6.51\text{m/s}$  was found at Dhulom while Rawdat Ben Habbas, Arar and Juaymah followed with  $c = 6.42\text{m/s}$  and  $6.36\text{m/s}$ , respectively.

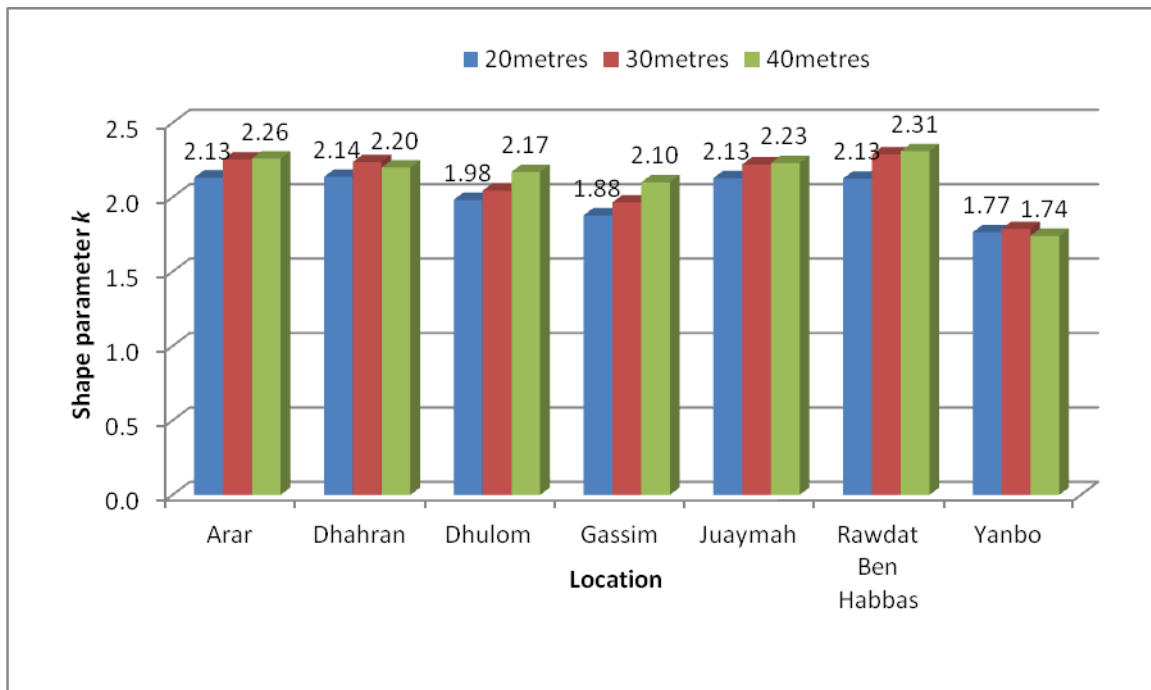


Figure 6.70 Comparison of Weibull shape parameter at different heights and locations

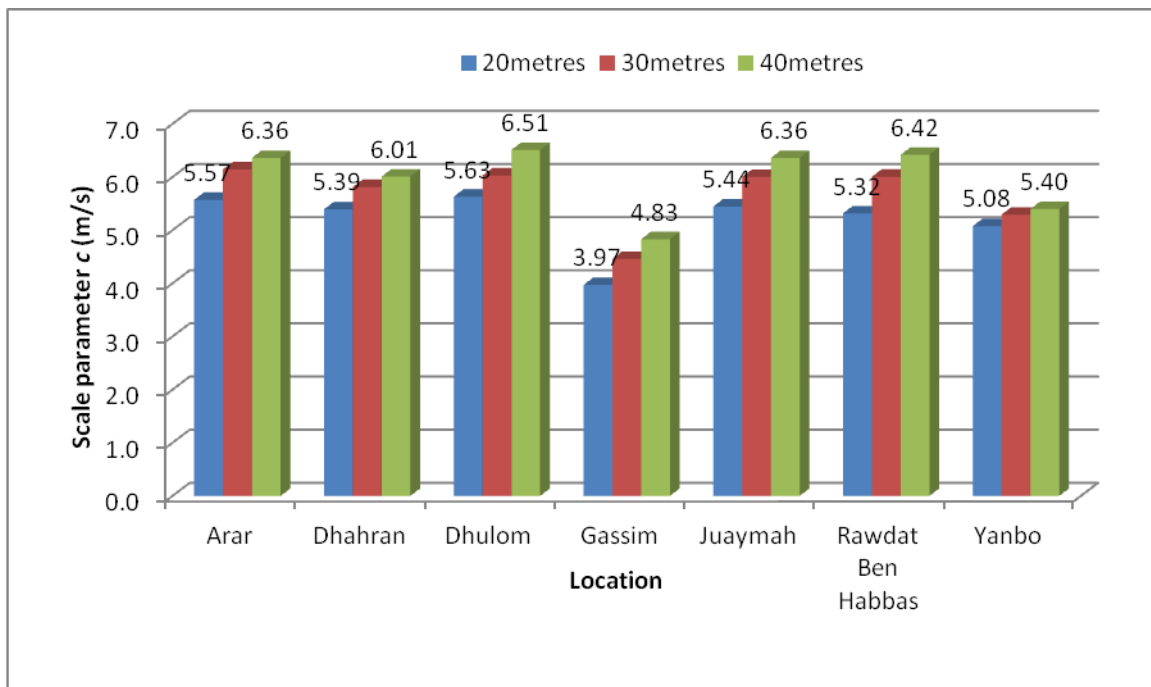


Figure 6.71 Comparison of Weibull scale parameter at different heights and locations

The monthly mean values of  $k$  at 20, 30 and 40metres AGL and for all the wind mast sites are summarised in Tables 6.4 to 6.6 and those of  $c$  in Tables 6.7 to 6.9, respectively. At Arar, a

seasonal trend with increasing  $k$  values from January until July and then a decreasing trend towards the end of the year, were observed as given in Table 6.4, Column 2. The maximum value of 2.82 was obtained in the month of July and the minimum of 1.9 in February. The  $k$  values were always  $>2$  at Arar except in February and March when it was  $<2.0$ . At Dhahran, higher values were seen during winter months and lower values during summer time with a minimum of 1.91 in July and a maximum of 2.59 in December. At Dhahran, the  $k$  values were  $<2.0$  from May to August and  $>2.0$  during the rest of the months. The seasonal trend at Dhahran was almost opposite compared with that at Arar. At Dhulom, again the same seasonal pattern was observed as the one at Arar with its maximum of 2.38 in June and minimum of 1.82 in December. The shape parameter values at Dhulom were  $<2.0$  during April, November and December and  $> 2.0$  during the rest of the months.

Table 6.4 Seasonal values of Weibull shape parameter ( $k$ ) at 20metre AGL at seven locations

Month	Arar	Dhahran	Dhulom	Gassim	Juaymah	Rawdat Ben Habbas	Yanbo
Jan	2.22	2.40	2.06	1.92	2.12	2.14	1.89
Feb	1.90	2.42	2.12	<b>2.09</b>	1.75	2.11	1.76
Mar	1.99	2.28	2.02	1.88	1.88	2.02	1.72
Apr	2.03	2.11	1.90	1.81	2.29	2.17	1.67
May	2.05	1.99	2.18	1.76	2.82	2.14	1.73
Jun	2.39	1.93	<b>2.38</b>	2.04	2.50	2.37	1.66
Jul	<b>2.82</b>	1.91	2.25	1.97	<b>3.07</b>	2.34	1.73
Aug	2.38	1.95	2.29	1.95	2.13	<b>2.48</b>	1.76
Sep	2.22	2.06	2.05	1.94	2.31	2.17	1.80
Oct	2.13	2.39	2.03	1.93	2.39	2.19	<b>2.15</b>
Nov	2.06	2.45	1.83	1.86	2.09	2.11	1.86
Dec	2.21	<b>2.59</b>	1.82	1.89	2.23	2.05	1.91
All	2.13	2.14	1.98	1.88	2.13	2.13	1.77

Relatively higher values of  $k$  were observed during summer months and lower values during winter months at Gassim but no definite increasing or decreasing trend could be seen. The highest value of 2.09 was found in February and the lowest of 1.76 in May, as can be seen from Table 6.4, column 5 above. At Juaymah, the highest  $k$  value of 3.07 was observed in July and the lowest of 1.75 in February. Values of  $k$  always remained  $>2.0$  at Juaymah with the exception of February and March when it was  $<2.0$ . At Juaymah, the highest value of  $k$  was found compared with all stations under investigation, however, no definite seasonal trend could be observed at this station. At Rawdat Ben Habbas, also no definite decreasing or increasing trend was observed but the highest value of 2.48 was found corresponding to the

month of August and the lowest of 2.02 in March but  $k$  was always  $>2.0$  without exception. At Yanbo, the situation was reversed relative to Rawdat Ben Habbas where  $k$  was always  $<2.0$  except in the month of October when it was 2.15. It is worth mentioning that a seasonal trend with decreasing values from January to June and then an increasing pattern towards the end of the year was seen at Yanbo. At 30 and 40metres AGL, almost the same trends were observed as discussed at 20metre height with few exceptions and relatively higher magnitudes, as can be observed from Tables 6.5 and 6.6, respectively.

Table 6.5 Seasonal values of Weibull shape parameter ( $k$ ) at 30metre AGL at all locations

Month	Arar	Dhahran	Dhulom	Gassim	Juaymah	Rawdat Ben Habbas	Yanbo
Jan	2.44	2.46	2.14	2.07	2.24	2.27	1.89
Feb	2.10	2.52	2.11	<b>2.26</b>	1.94	2.26	1.76
Mar	2.21	2.37	2.01	1.97	1.98	2.13	1.77
Apr	2.24	2.24	1.90	1.91	2.41	2.34	1.70
May	2.19	2.11	2.11	1.74	2.99	2.27	1.77
Jun	2.48	2.08	<b>2.33</b>	2.09	2.67	2.64	1.69
Jul	<b>2.93</b>	2.06	<b>2.33</b>	2.09	<b>3.26</b>	2.63	1.75
Aug	2.42	2.04	2.29	2.05	2.16	<b>2.76</b>	1.73
Sep	2.27	2.16	2.15	2.01	2.32	2.33	1.84
Oct	2.21	2.47	2.18	1.96	2.57	2.32	<b>2.16</b>
Nov	2.09	2.55	1.97	1.95	2.20	2.26	1.85
Dec	2.34	<b>2.64</b>	1.97	2.11	2.39	2.20	1.90
All	2.25	2.24	2.04	1.97	2.22	2.29	1.79

Table 6.6 Seasonal values of Weibull shape parameter ( $k$ ) at 40metre AGL at all locations

Month	Arar	Dhahran	Dhulom	Gassim	Juaymah	Rawdat Ben Habbas	Yanbo
Jan	2.43	2.35	2.27	2.20	2.23	2.32	1.86
Feb	2.07	2.38	2.27	<b>2.35</b>	1.89	2.34	1.73
Mar	2.21	2.30	2.17	2.02	1.88	2.21	1.73
Apr	2.20	2.27	2.02	2.02	2.40	2.42	1.65
May	2.17	2.09	2.16	1.92	2.96	2.30	1.73
Jun	2.43	2.05	2.31	2.26	2.71	<b>2.79</b>	1.61
Jul	<b>2.92</b>	2.09	2.32	2.30	<b>3.42</b>	2.64	1.66
Aug	2.42	2.01	<b>2.34</b>	2.25	2.20	2.64	1.70
Sep	2.29	2.16	2.17	2.20	2.32	2.27	1.81
Oct	2.18	2.47	2.30	2.12	2.67	2.32	<b>2.08</b>
Nov	2.04	2.45	2.18	2.08	2.23	2.28	1.82
Dec	2.38	<b>2.49</b>	2.18	2.18	2.47	2.22	1.84
All	2.26	2.20	2.17	2.10	2.23	2.31	1.74

The monthly mean values of Weibull scale parameter,  $c$  in cm/s, calculated using the method given in Windographer software and described above are summarised in Tables 6.7 to 6.9 for

wind speed measurements made at 20, 30, and 40metres AGL at seven locations used in the present work, respectively. The monthly mean values of  $c$  at Arar varied between a minimum of 4.63m/s and a maximum of 6.69m/s corresponding to November and July, respectively, as given in Column 2, Table 6.7. The maximum values of scale parameter of 6.1, 6.69 and 4.61m/s occurred in the month of March at Dhahran, Gassim and Juaymah while the minimum of 4.77, 4.68 and 3.62m/s in the months of October and November, respectively. At the Juaymah wind mast site, the maximum value of  $c$  (6.56m/s) was obtained during January with the minimum of 3.88m/s in February, while at Rawdat Ben Habbas and Yanbo the maximum was found in June and March, respectively. At all of these sites, no definite seasonal trends were observed. In general, higher values were found during winter time and lower values during summer time. Almost similar trends were noticed at 30m and 40m measurement heights as can be seen from Tables 6.8 and 6.9.

Table 6.7 Seasonal values of Weibull scale parameter ( $c$ ) at 20metre AGL at all locations

Month	Arar	Dhahran	Dhulom	Gassim	Juaymah	Rawdat Ben Habbas	Yanbo
Jan	5.20	5.47	6.05	3.87	<b>6.56</b>	5.31	4.88
Feb	5.33	5.78	6.32	4.42	3.88	5.74	5.20
Mar	6.50	<b>6.10</b>	<b>6.69</b>	<b>4.61</b>	4.37	5.56	<b>5.64</b>
Apr	5.88	5.83	5.65	4.53	4.50	6.20	5.46
May	5.88	5.46	5.58	3.93	5.13	5.44	5.32
Jun	5.97	5.80	5.75	3.93	6.24	<b>6.22</b>	5.27
Jul	<b>6.69</b>	5.49	6.33	3.96	5.82	5.65	5.16
Aug	5.65	4.95	5.53	3.67	5.19	5.09	5.46
Sep	5.16	4.97	4.78	3.54	5.99	4.56	5.29
Oct	4.97	4.77	4.68	3.70	6.00	5.07	4.83
Nov	4.63	5.15	5.38	3.62	5.12	4.46	4.44
Dec	4.84	5.06	5.44	3.75	6.36	4.85	4.15
All	5.57	5.39	5.63	3.97	5.44	5.32	5.08

Table 6.8 Seasonal values of Weibull scale parameter ( $c$ ) at 30metre AGL at all locations

Month	Arar	Dhahran	Dhulom	Gassim	Juaymah	Rawdat Ben Habbas	Yanbo
Jan	5.79	5.90	6.54	4.42	<b>7.24</b>	5.98	5.18
Feb	5.92	6.24	6.77	5.00	4.30	6.48	5.40
Mar	7.10	<b>6.55</b>	<b>7.02</b>	5.11	4.77	6.27	<b>5.90</b>
Apr	6.53	6.32	5.94	<b>5.08</b>	5.06	<b>6.89</b>	5.68
May	6.48	5.93	5.78	4.40	5.67	6.04	5.52
Jun	6.54	6.31	5.99	4.42	6.91	6.88	5.44
Jul	<b>7.27</b>	5.96	6.61	4.51	6.45	6.33	5.35
Aug	6.20	5.30	5.81	4.11	5.76	5.79	5.57
Sep	5.69	5.35	5.22	3.93	6.54	5.27	5.46
Oct	5.56	5.11	5.16	4.09	6.57	5.80	5.06
Nov	5.10	5.54	5.90	4.00	5.59	5.12	4.69
Dec	5.42	5.41	5.98	4.28	7.00	5.57	4.37
All	6.14	5.81	6.03	4.46	6.00	6.01	5.29

Table 6.9 Seasonal values of Weibull scale parameter ( $c$ ) at 40metre AGL at all locations

Month	Arar	Dhahran	Dhulom	Gassim	Juaymah	Rawdat Ben Habbas	Yanbo
Jan	6.08	5.91	6.90	4.79	<b>7.61</b>	6.37	5.41
Feb	6.14	6.39	7.19	5.36	4.41	6.91	5.56
Mar	7.32	6.54	<b>7.47</b>	5.45	4.88	6.69	<b>6.01</b>
Apr	6.64	<b>6.67</b>	6.49	<b>5.49</b>	5.36	7.32	5.75
May	6.54	5.90	6.33	4.84	6.08	6.43	5.56
Jun	6.66	6.49	6.55	4.77	7.49	<b>7.42</b>	5.43
Jul	<b>7.45</b>	6.42	7.15	4.85	6.99	6.82	5.32
Aug	6.49	5.69	6.23	4.44	6.15	6.21	5.72
Sep	6.02	5.46	5.60	4.33	6.89	5.64	5.59
Oct	5.83	5.26	5.66	4.52	6.95	6.23	5.22
Nov	5.33	5.68	6.45	4.37	5.89	5.48	4.82
Dec	5.69	5.50	6.47	4.55	7.40	5.94	4.49
All	6.36	6.01	6.51	4.83	6.36	6.42	5.40

## SUMMARY

The highest wind was observed at Dhulom while the lowest in Gassim with good wind regimes at Rawdat Ben Habbas, Juaymah and Dhahran with more than 5 m/s annual average wind speed. The prevailing wind direction at all of these sites was found to be from North with some seasonal variation. The local wind shear exponent (WSE) was highest for Gassim and lowest for Yanbo. The wind data collection sites can be prioritized as first, second etc. best in order as Juaymah, Rawdat Ben Habbas, Dhulom, Arar, Dhahran, Yanbo, and Gassim with having wind frequencies of around 75%, 74%, 72%, 71%, 68%, 55%, and 52% above 4 m/s at 40m AGL, respectively. The highest WSE value of 0.286 was obtained for Rawdat

Ben Habbas while the lowest of 0.081 for Yanbo. Following WSE values should be used to extrapolate the wind speed above measurement heights to get accurate wind speed values at higher altitudes.

Rawdat Ben Habbas	0.286
Juaymah	0.274
Dhahran	0.151
Arar	0.182
Gassim	0.241
Yanbo	0.081
Dhulom	0.193

## CHAPTER 7

### WIND TURBINE SELECTION AND WIND FARM ENERGY YIELD ANALYSES

The selection of wind machine size will depend on the existing worldwide standard sizes, commercial availability, high energy yield and capacity factor, local adoptability, ease of transportation to the installation site, etc. The choice of manufacturer will include the interest of the manufacturer for providing services in Saudi Arabia, competitive cost, technical support during installation phase, training of the operation and maintenance staff, terms and conditions for maintenance of the wind machines and the supply of spare parts during project life time and re-powering provision of the plant after the expiry of designed life.

The placement of the right turbine at the right place is very important and critical from an optimal energy production point of view. The other important aspects are its rated power, cut-in speed, transportability, life span, capital cost, corrosion resistivity and harsh weather resistance. Wind turbines are now available in multimegawatt rated capacities and are being used successfully worldwide. The manufacturing technology is well developed and has a proven record. A wind machine consists of a nacelle unit, a tower and blades. The nacelle unit is the main unit of the whole assembly and houses the gearbox, the cooling system, the generator and other control systems. A schematic view of a typical wind turbine or wind energy conversion system (WECS) and nacelle unit is shown in Figures 7.1 and 7.2. The following guidelines should be considered when selecting wind turbines:

- In order to optimise energy production, wind machines with high rated power should be chosen.
- A wind turbine with larger rotor diameter considerably increases the output in low wind regions. The knowledge of annual mean wind speed at the site is important for size selection.
- The choice of the tower is also important from a foundation and crane availability point of view. For example, a particular type of tower may not be suitable for a particular type of soil or cranes of required capacity may not be available. Therefore, before proceeding with the selection of wind turbine, soil conditions and information on the availability of crane and wide roads with spacious bands should be at hand.
- Basically, the choice of wind turbine is limited by the wind turbine's maximum mean wind speed at hub height.

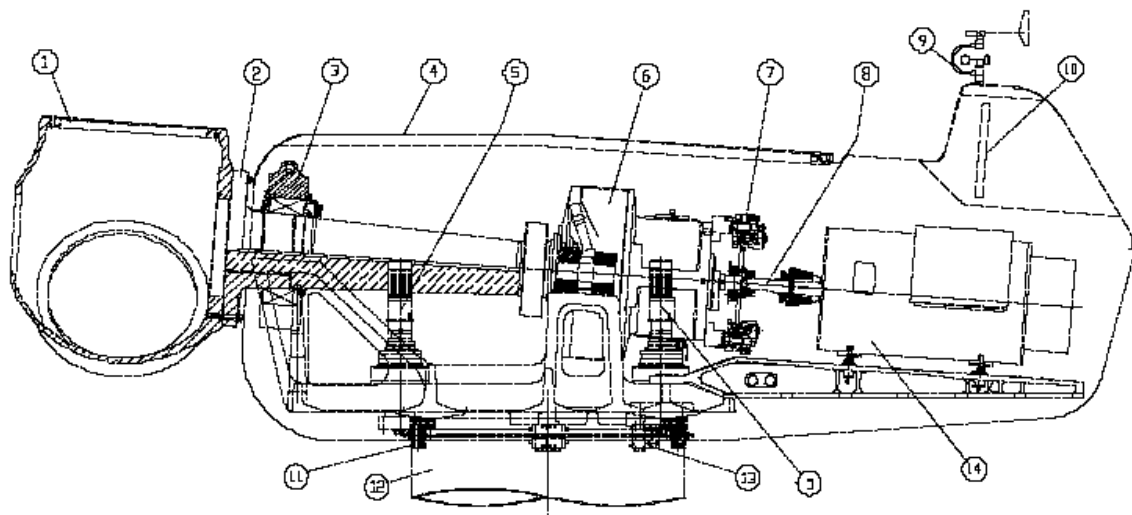
- The maximum total height of the wind turbine may be restricted if the wind park site is in the proximity of airports or monuments.
- The maximum admissible noise emission values at the site may restrict the choice of a particular type of wind machine.
- In reference to Saudi Arabia, where the temperature reaches 50 °C and more, and relative humidity up to 90% is experienced during summer season, the wind turbine blades, nacelle unit and the tower should withstand these weather conditions. Moreover, the wind turbine material should be corrosion-resistant because in Saudi Arabia there is a severe corrosion problem.
- The materials of the wind turbine blade and tower should be resistant towards sand storms, which are common in Saudi Arabia.
- While selecting the wind turbine it should be agreed with the manufacturer that wind turbine towers must be manufactured locally. The technical knowledge will be transferred by the manufacturer and the manpower will also be trained by the manufacturer.

To further understand the workability and other characteristics of the wind electricity conversion systems, a number of major manufacturers were identified, contacted, and technical specifications on different sizes of the WECSs were obtained. Tables A-1 to A-8, in Appendix – A, summarise the specifications of wind machines of sizes between 600 and 2 500kW from different WECS manufacturers.



Figure 7.1 View of a three-bladed wind turbine with rotor and nacelle unit

Layout drawing of the NORDEX N-60



1 Hub	5 Yaw drive	9 Wind sensors	13 Yaw brakes
2 Main shaft	6 Gearbox	10 Cooler	14 Generator
3 Main bearing	7 Disc brake	11 Yaw bearing	
4 Nacelle cover	8 Generator coupling	12 Tower	

Figure 7.2 Layout drawing of nacelle unit of the Nordex N-60 wind turbine.

## 7.1 ENERGY YIELD FROM SINGLE WIND TURBINE

Energy production from a single WECS was obtained from wind power curves of the wind machines and the frequency distribution of number of hours during which the wind remained in certain wind speed intervals. To perform energy calculations, several wind machines with different sizes were chosen from the list of WECSs given in Tables A-1 to A-8 in Appendix-A, on the basis of generally used sizes in the wind power sector. According to Bolinger and Wiser [282], the average size of utility-scale wind turbines installed in the US was 686kW in 2000 while it was 327kW in 1995. In the year 2001, the average size of utility turbines reached 893kW. In Europe, the trend of higher capacity wind machines has become a deciding factor in wind farm development projects due to scarcity of land. The developers are embarking on 1.5 to 2.5MW size of wind machines with 80- to 90-metre high tower. Larger wind machines produce more power and require less space, so they are becoming popular in Europe. For energy production and plant capacity factor (PCF) analysis, wind machines of 600, 800, 850, 900, 1 000, 1 300, 1 500, 1 800, 2 000, 2 300 and 2 500kW sizes from manufacturers Nordex, Vestas, GE, DeWind, Bonus and Enercon were chosen. The detailed

technical information like ratings, weight of different components, control system, breaking system, tower type, and other specifications for all the wind machines chosen for the study from the above manufacturers are included in Appendix-B.

Table 7.1 summarises the technical information of wind machines of sizes 600, 800, 1 000, 1 300, 1 500, 2 300 and 2 500kW from Nordex. As seen from Table 7.1, the cut-in speed of most machines is 3 m/s while the cut-out speed is 25 m/s. The hub height varies between 40 and 80metre for the whole range (600 to 2 500kW) of wind machines listed in Table 7.1. The technical information on Nordex wind machines and the wind power curves were obtained from references [283 – 289]. The wind power curves for all the WECSs from Nordex are shown in Figure 7.3. The frequency distribution obtained by constructing the wind rose using hourly average wind data at 10 metres above ground level, the wind power curve, and the energy production calculations performed are summarised in Table C-1, in Appendix-C. The wind rose diagram constructed using hourly average data at 10 metres above ground is shown in Figure 7.4. The wind rose diagram provides valuable information about the predominant wind direction and the availability of wind in different wind speed bins and wind directions. Usually, the wind turbines are erected against the prevailing wind direction.

To obtain the wind energy production at 40, 50, 60, 70 and 80metres above ground level, the wind speed was calculated at these heights using the 1/7 wind power law. Next, wind roses were developed to obtain the frequency distribution at different heights and finally, the wind energy production was obtained. The wind roses constructed using wind data at above-mentioned heights are shown in Figures 7.5 to 7.9. The wind power production details at 40, 50, 60, 70 and 80metres above ground level or at these hub heights are given in Tables C-2 to C-6. Similar types of detailed calculations were also made for wind machines from Vestas, GE, DeWind, Bonus and Enercon. The technical information for Vestas, GE, DeWind, Bonus and Enercon WECSs is summarised in Tables 7.2 to 7.6 and wind power curves for wind machines from these manufacturers are shown in Figures 7.10 to 7.14, respectively. The technical information and wind power curves for wind machines were obtained from references [290-301]. The following chapters focus on the comparison of energy production from WECSs of same sizes but from different manufacturers, the effect of hub height on energy production, plant capacity factor analysis and energy production from a wind farm of installed capacities of 20, 30 and 40MW.

Table 7.1 Technical data of Nordex wind machines used in the analysis

Wind Machine	Cut-in speed (m/s)	Cut-out speed (m/s)	Rated speed (m/s)	Rated output (kW)	Hub Height (metre)	Rotor Diameter (metre)	Expected Life (Years)
N80/2500	4	25	14	2500	60	80	20
N90/2300	4	25	13	2300	80	90	20
S70/1500	3	25	13	1500	65	70	20
N60/1300	3	25	15	1300	60	60	20
N54/1000	4	25	14	1000	60	54	20
N50/800	3	25	15	800	50	50	20
N43/600	3	25	13.5	600	40	43	20

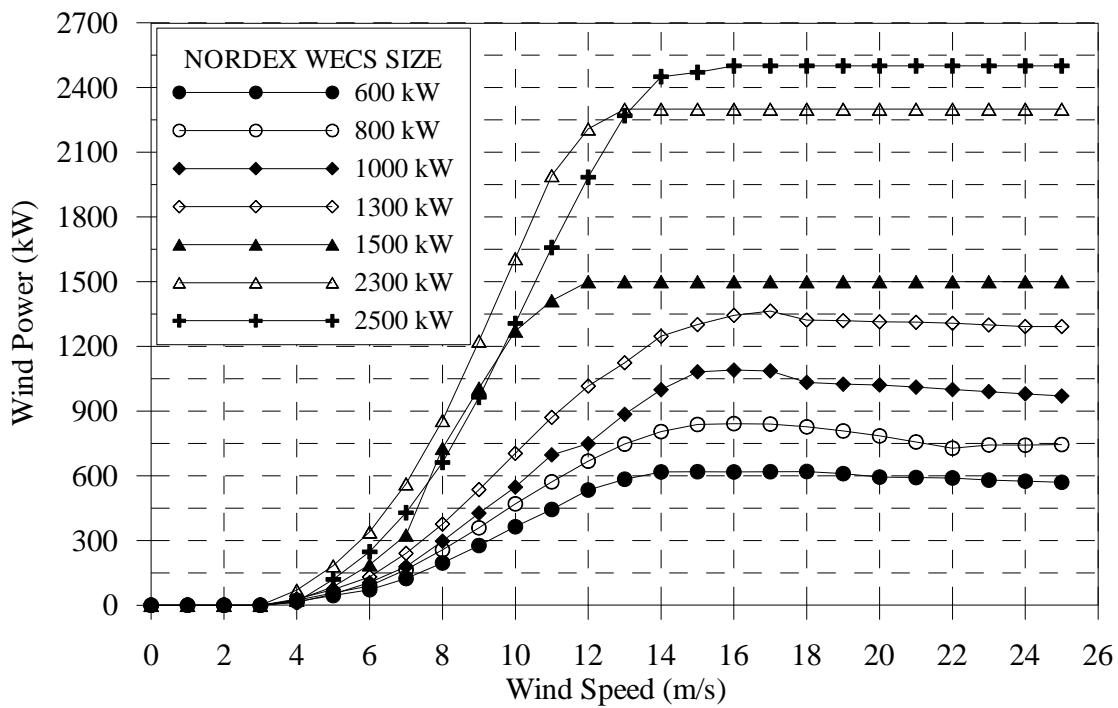


Figure 7.3 Wind power curves for WECSs of different sizes from Nordex

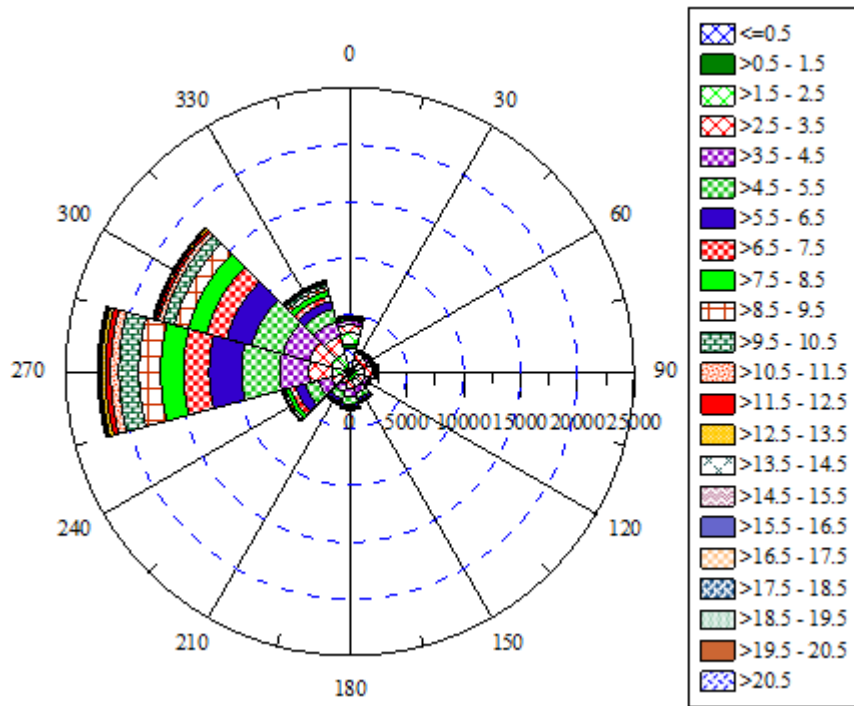


Figure 7.4 Wind rose diagram of hourly mean wind speed values at 10metres above ground level for Yanbo

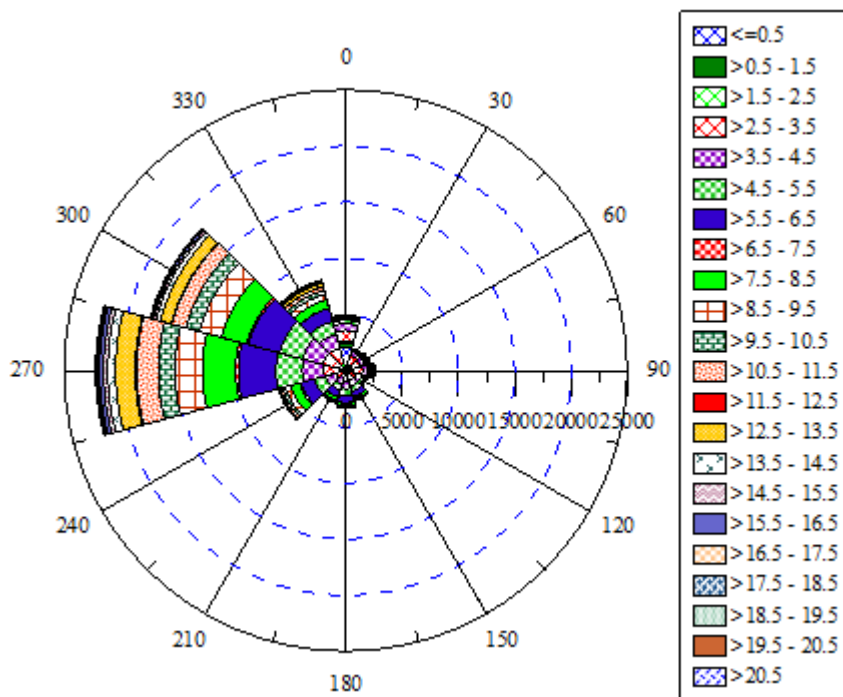


Figure 7.5 Wind rose diagram of hourly mean wind speed values at 40metres above ground level for Yanbo

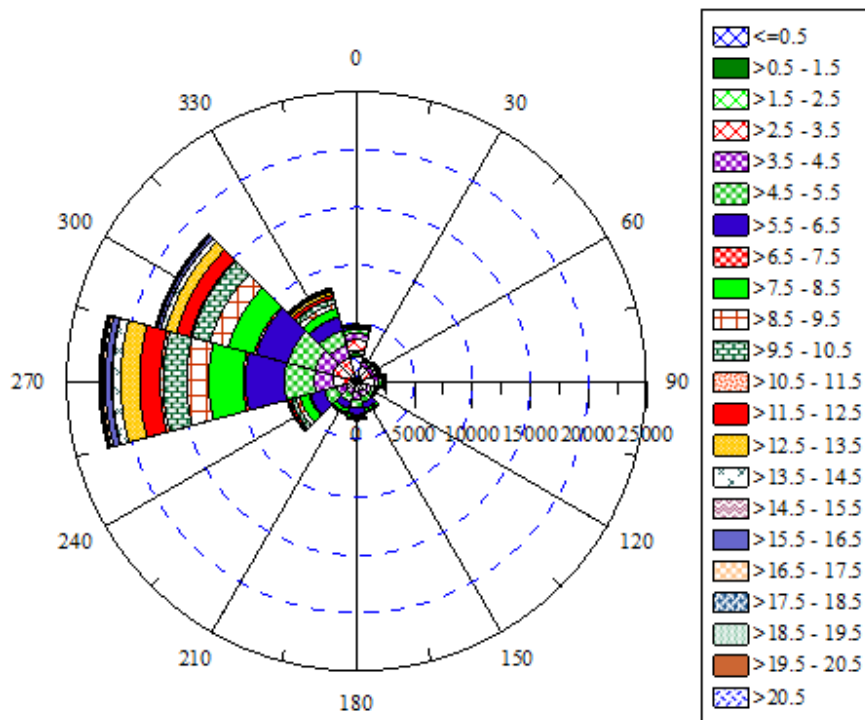


Figure 7.6 Wind rose diagram of hourly mean wind speed values at 50metres above ground level for Yanbo

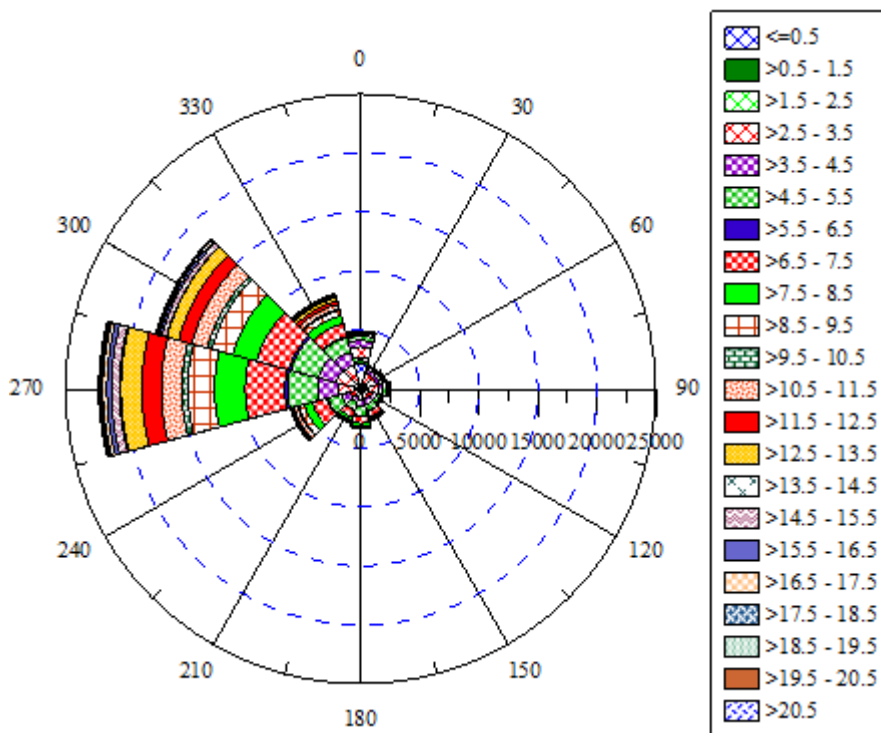


Figure 7.7 Wind rose diagram of hourly mean wind speed values at 60metres above ground level for Yanbo

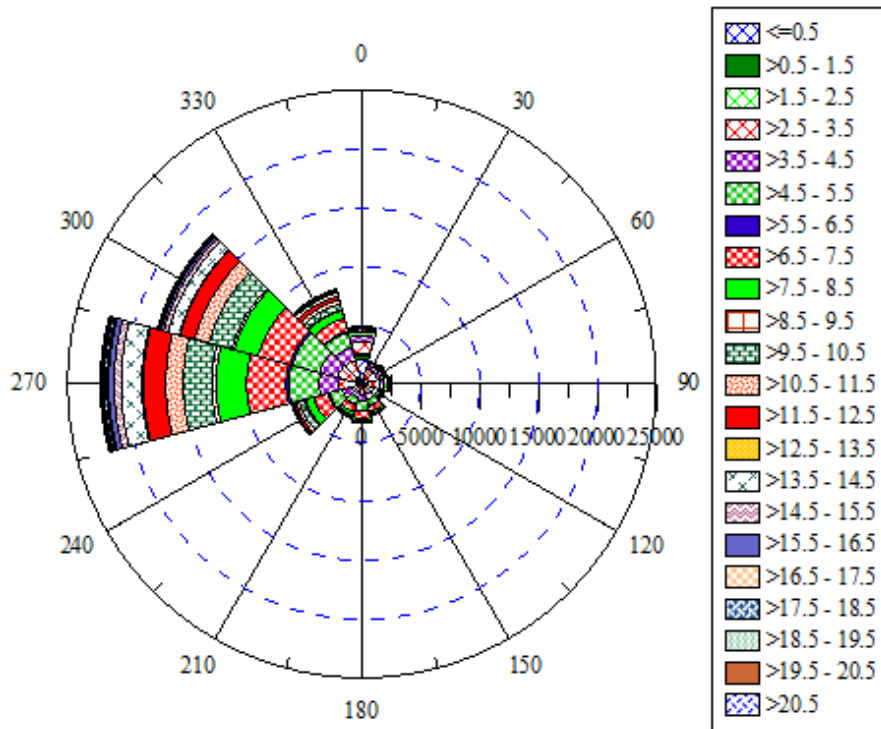


Figure 7.8 Wind rose diagram of hourly mean wind speed values at 70metres above ground level for Yanbo

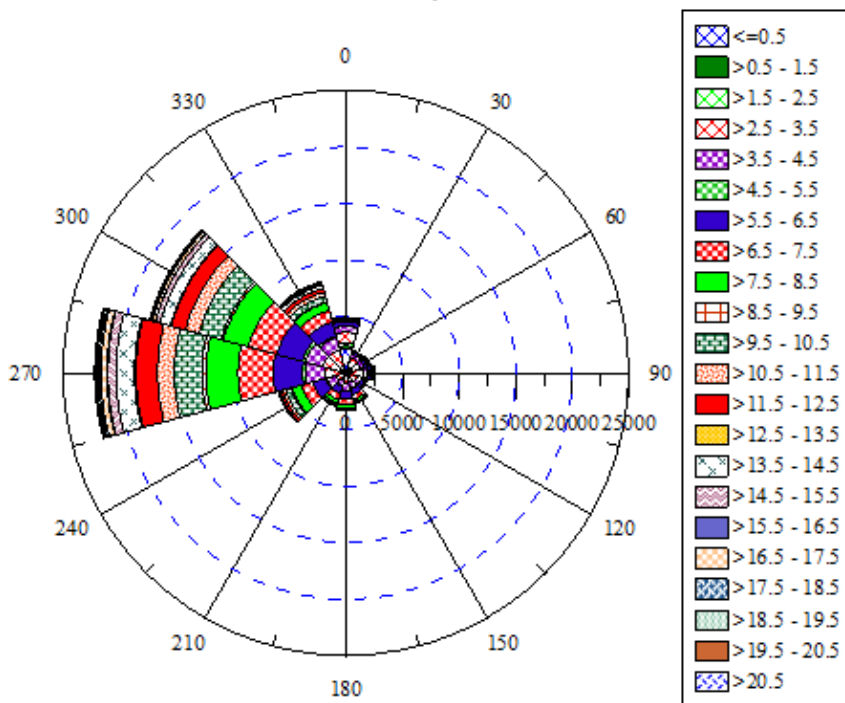


Figure 7.9 Wind rose diagram of hourly mean wind speed values at 80metres above ground level for Yanbo

Table 7.2 Technical data of Vestas wind machines used in the analysis

Wind Machine	Cut-in speed (m/s)	Cut-out speed (m/s)	Rated speed (m/s)	Rated output (kW)	Hub Height (metre)	Rotor Diameter (metre)	Expected Life (Years)
V42	4	25	17	600	35,40, 50	42	20
V52	4	25	16	850	44, 60,65	52	20
V63	4.5	25	16	1500	58, 60	63	20
V80	4	25	15	2000	60, 78,100	80	20

Table 7.3 Technical data of GE wind machines used in the analysis

Wind Machine	Cut-in speed (m/s)	Cut-out speed (m/s)	Rated speed (m/s)	Rated output (kW)	Hub Height (metre)	Rotor Diameter (metre)	Expected Life (Years)
GE/900s	3	25	13	900	60	55	20
GE/1.5SL	4	20	14	1500	65, 80	77	20
GE45.7	3	25	14	2300	80 to 95	94	20
GE42.7	4	25	15	2500	70 to 90	88	20

Table 7.4 Technical data of DeWind wind machines used in the analysis.

Wind Machine	Cut-in speed (m/s)	Cut-out speed (m/s)	Rated speed (m/s)	Rated output (kW)	Hub Height (metre)	Rotor Diameter (metre)	Expected Life (Years)
D4/48	3	22	11.5	600	55, 60, 70	48	20
D6/60	3	23	11.5	1000	60, 65, 91	60	20
D8/80	3	None	13.5	2000	80, 95	80	20

Table 7.5 Technical data of Bonus wind machines used in the analysis.

Wind Machine	Cut-in speed (m/s)	Cut-out speed (m/s)	Rated speed (m/s)	Rated output (kW)	Hub Height (metre)	Rotor Diameter (metre)	Expected Life (Years)
Bonus/44	3	25	13	600	40, 50,60	44	20
Bonus/54	3	25	15	1000	45, 50,60	54.2	20
Bonus	3	25	15	1300	45 - 68	62	20

Table 7.6 Technical data of Enercon wind machines used in the analysis.

Wind Machine	Cut-in speed (m/s)	Cut-out speed (m/s)	Rated speed (m/s)	Rated output (kW)	Hub Height (metre)	Rotor Diameter (metre)	Expected Life (Years)
E-40-6.44	2.5	28	12	600	50, 65	44	20
E-58-10.58	2.5	28	12	1000	70, 89	58	20
E-66-15.66	2.5	28	12	1500	85, 98	66	20
E-66-18.70	2.5	28	12	1800	65, 98	70	20

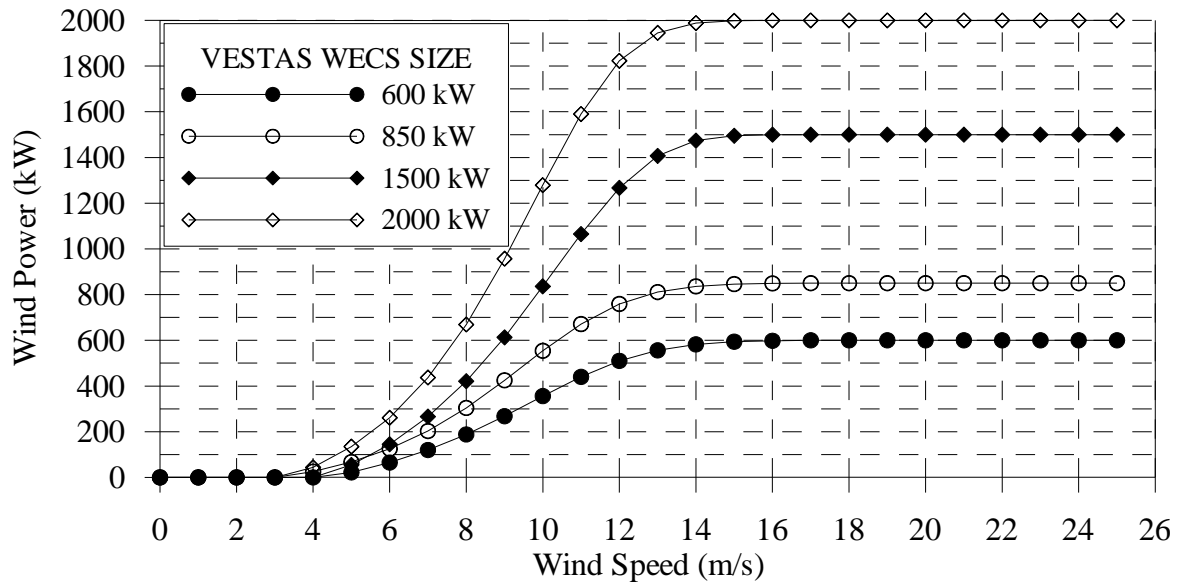


Figure 7.10 Wind power curves for WECSs of different sizes from Vestas

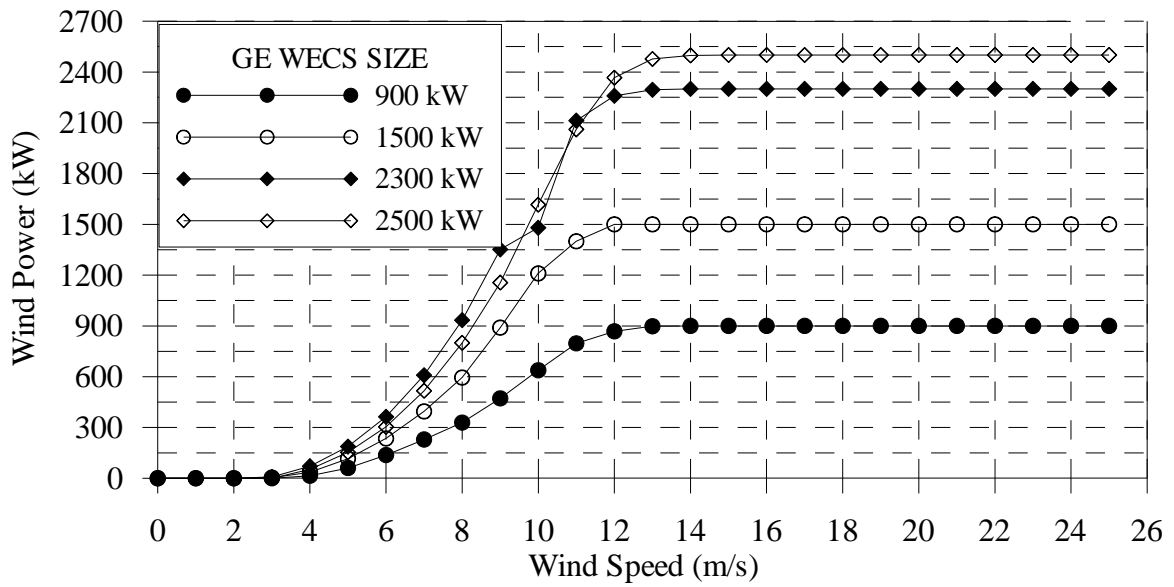


Figure 7.11 Wind power curves for WECSs of different sizes from GE

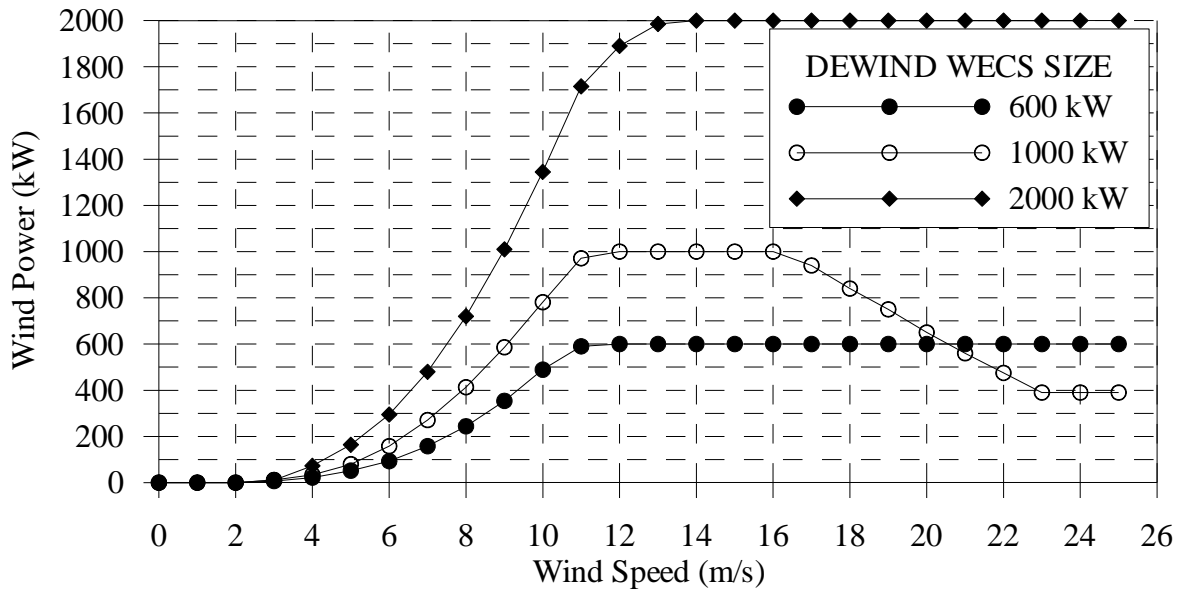


Figure 7.12 Wind power curves for WECSs of different sizes from DeWind

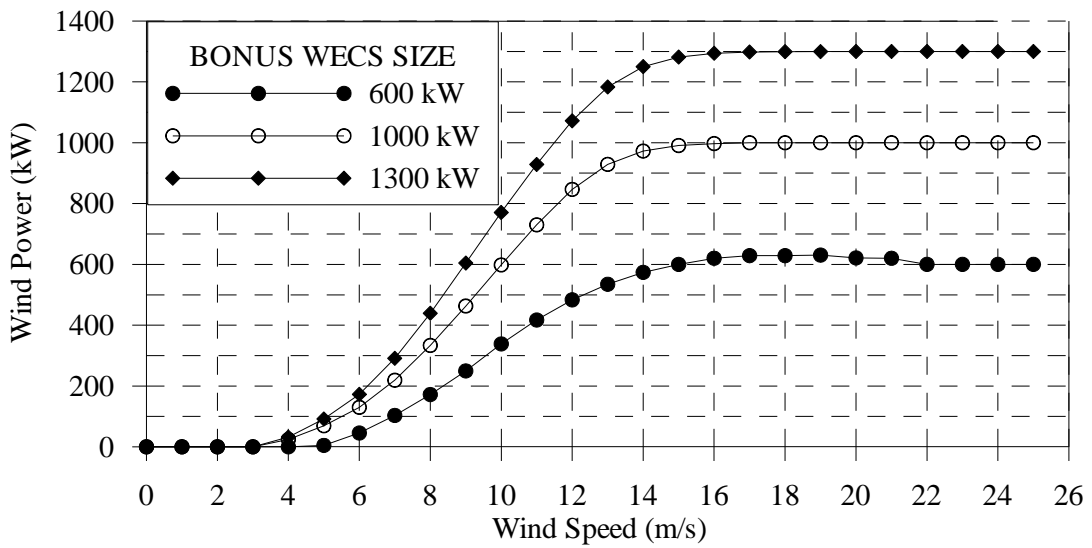


Figure 7.13 Wind power curves for WECSs of different sizes from Bonus

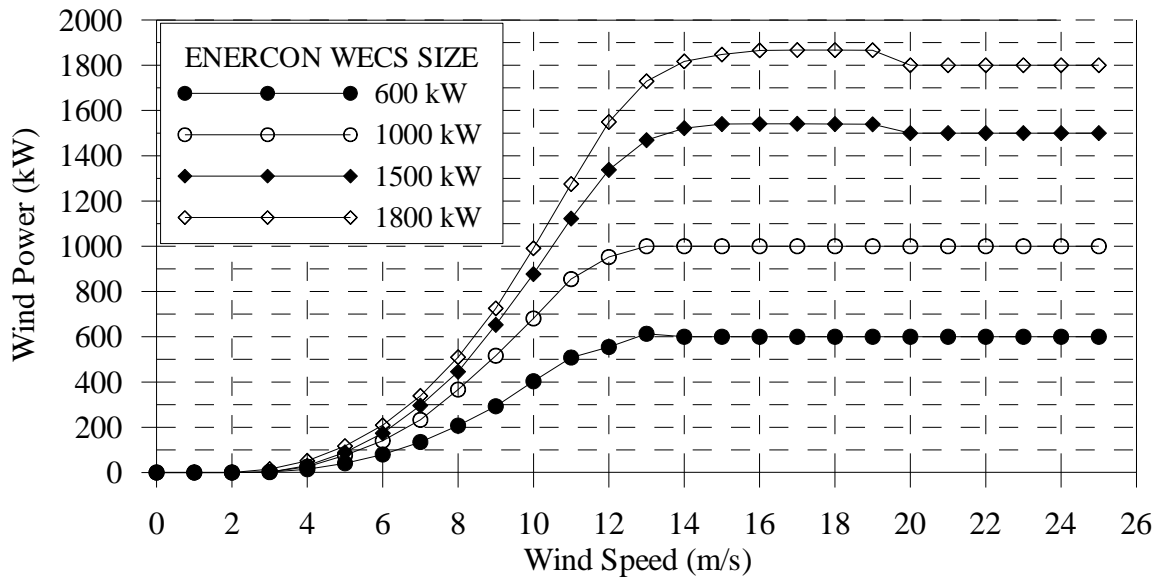


Figure 7.14 Wind power curves for WECSs of different sizes from Enercon

## 7.2 ENERGY YIELD COMPARISON FOR WIND ENERGY CONVERSION SYSTEMS FROM DIFFERENT MANUFACTURERS

The annual production of energy (MWh/year), from different WECSs presented in Tables C-1 to C-36 of Appendix-C, is summarised in Table 7.7. It is observed that the maximum energy production of 981.90MWh was obtained from DeWind machines while the minimum of 626.17MWh from the Vestas machine of 600kW capacity using wind speed data at 10 metres above ground level. The second-highest producer of wind energy of 830.3MWh was Enercon while the Nordex production stood at third place with 782.03MWh of electricity. GE does not produce 600kW machines at present. Similar types of wind energy production trends were followed at other heights, as observed from the data in Table 7.7.

Wind machines of 800, 850 and 900kW rated power were available only from one manufacturer each, namely Nordex, Vestas and GE, respectively. The performance of these WECSs will be compared for wind farm production of certain installed capacity. The sixth column of Table 7 shows that the DeWind machine of 1 000kW rated power produces the maximum energy of 1 618.85MWh, Enercon with 1 436.09MWh of energy stood at second place, and Bonus with 1 297.64MWh energy output at the third place. The Nordex wind machine produces the least energy among the compared WECSs.

The WECSs with rated power of 1 300kW were available from Nordex and Bonus, as shown in Table 7.7, Column 7. In this case, the Bonus WECS performed better than the Nordex

machine. The Nordex wind machine with 1 500kW rated power produced the maximum energy of 2 383.54MWh compared with WECSs from Vestas, GE and Enercon. The GE WECS was found to be the next best producer of energy with an annual energy production of 2 376.0MWh. Table 7.7 shows the energy production from WECS of 2 000kW rated power from sole manufacturer DeWind in Column 9. The GE wind machines of rated power 2 300 and 2 500kW produced maximum energy of 3 536.94 and 3 269.88MWh compared with others. Based on the energy production from a single wind machine, the following is the rating of different sizes of WECSs according to the manufacturer:

WECS Size	First	Second	Third	Fourth
600 kW	DeWind	Enercon	Nordex	Vestas
1000 kW	DeWind	Enercon	Bonus	Nordex
1500 kW	Nordex	GE	Enercon	Vestas
2300 kW	GE	Nordex	Vestas	-
2500 kW	GE	Nordex	-	-

Table 7.7 Summary of wind energy yield (MWh/year) from single WECS at Yanbo

Manufacturer ▼	Size of Wind Energy Conversion System (WECS – kW) ▼									
	600	800	850	900	1000	1300	1500	2000	2300	2500
<b>NORDEX</b>										
10 metres	782.03	1011.67	-	-	1146.98	1487.79	<b>2383.54</b>	-	3397.49	<b>2688.1</b>
40 metres	1326.0	1717.92	-	-	2021.51	2569.90	<b>3988.60</b>	-	5611.64	<b>4776.8</b>
50 metres	1377.9	1777.54	-	-	2068.24	2663.62	<b>4068.64</b>	-	5765.07	<b>4972.9</b>
60 metres	1477.6	1918.38	-	-	2237.79	2880.49	<b>4308.23</b>	-	6210.01	<b>5358.5</b>
70 metres	1542.6	2004.98	-	-	2345.97	3023.97	<b>4458.38</b>	-	6432.01	<b>5630.0</b>
80 metres	1577.0	2047.26	-	-	2413.92	3098.80	<b>4600.79</b>	-	6622.39	<b>5784.4</b>
<b>VESTAS</b>										
10 metres	706.43	-	1198.54	-	-	-	1652.36	-	2671.22	-
40 metres	1234.7	-	1977.95	-	-	-	2952.01	-	4509.22	-
50 metres	1278.6	-	2037.13	-	-	-	3071.85	-	4659.07	-
60 metres	1385.1	-	2186.75	-	-	-	3325.71	-	5015.48	-
70 metres	1446.7	-	2271.52	-	-	-	3483.77	-	5220.91	-
80 metres	1498.2	-	2341.04	-	-	-	3591.92	-	5373.40	-
<b>DEWIND</b>										
10 metres	<b>981.9</b>	-	-	-	<b>1618.85</b>	-	-	2918.29	-	-
40 metres	<b>1589.6</b>	-	-	-	<b>2613.85</b>	-	-	4815.18	-	-
50 metres	<b>1616.6</b>	-	-	-	<b>2656.21</b>	-	-	4943.31	-	-
60 metres	<b>1741.3</b>	-	-	-	<b>2870.28</b>	-	-	5331.79	-	-
70 metres	<b>1815.6</b>	-	-	-	<b>2974.39</b>	-	-	5530.96	-	-
80 metres	<b>1866.1</b>	-	-	-	<b>3061.88</b>	-	-	5689.26	-	-
<b>GE</b>										
10 metres	-	-	-	1310.12	-	-	2376.00	-	<b>3536.94</b>	<b>3269.9</b>
40 metres	-	-	-	2176.49	-	-	3874.27	-	<b>5817.59</b>	<b>5588.8</b>
50 metres	-	-	-	2233.86	-	-	3969.33	-	<b>5908.69</b>	<b>5786.5</b>
60 metres	-	-	-	2416.42	-	-	4255.13	-	<b>6482.65</b>	<b>6243.9</b>
70 metres	-	-	-	2512.14	-	-	4435.76	-	<b>6564.76</b>	<b>6521.1</b>
80 metres	-	-	-	2600.71	-	-	4578.24	-	<b>6778.03</b>	<b>6704.0</b>
<b>BONUS</b>										
10 metres	626.17	-	-	-	1297.64	<b>1690.54</b>	-	-	-	-
40 metres	1140.4	-	-	-	2179.16	<b>2822.51</b>	-	-	-	-
50 metres	1182.4	-	-	-	2251.62	<b>2913.10</b>	-	-	-	-
60 metres	1291.7	-	-	-	2422.52	<b>3133.95</b>	-	-	-	-
70 metres	1358.4	-	-	-	2519.08	<b>3257.66</b>	-	-	-	-
80 metres	1408.2	-	-	-	2593.25	<b>3356.36</b>	-	-	-	-
<b>ENERCON</b>										
<b>1800 kW</b>										
10 metres	830.3	-	-	-	1436.09	-	1846.06	2173.36	-	-
40 metres	1402.2	-	-	-	2394.18	-	3193.42	3745.28	-	-
50 metres	1439.3	-	-	-	2462.27	-	3318.76	3902.29	-	-
60 metres	1553.6	-	-	-	2652.54	-	3580.83	4191.63	-	-
70 metres	1612.3	-	-	-	2748.50	-	3735.31	4384.59	-	-
80 metres	1659.3	-	-	-	2827.82	-	3836.75	4496.34	-	-

### 7.3 HUB HEIGHT OPTIMISATION

In order to study the effect of hub height on energy yield, the wind power curves for individual wind machines and wind duration data in different wind speed bins and at different heights were used. To obtain the wind duration or wind speed frequency distribution at different heights, the wind speed data at different heights was calculated using the 1/7 wind power law. For this analysis, hourly average values of wind speed for Yanbo were used for a period of 14 years between 1970 and 1983. The energy production from different WECSs at 40, 50, 60, 70 and 80metres hub heights is also tabulated in Table 7.7 and graphical variation for these machines from Nordex, Vestas, DeWind, Ge, Bonus and Enercon is shown in Figures 7.15 to 7.20, respectively. It is clear from these figures that taller towers lead to increased energy production.

Table 7.8 summarises the percentage increase in energy production due to increase in hub height for all the WECSs from chosen manufacturers. The first column provides the name of the manufacturer and size of wind machine and the second column gives the percentage increase in energy production as a result of using wind data at 40metres instead of at 10 metres above ground. Similarly, the third, fourth, fifth and sixth columns provide percentage increase in energy production when hub heights are changed from 40 to 50, 50 to 60, 60 to 70, and 70 to 80metres, respectively. This table also includes the mean values of percentage increase in energy production for each hub height change for wind machines from different manufacturers.

The percentage increase in energy production with corresponding increase in hub height for WECSs from different manufacturers is compared in Figure 7.21. As can be seen from this figure, a change of hub height from 40 to 50metres causes an increase of 3.17% in energy production for the WECS from Nordex, with a change of 3.48% for the WECS from Vestas, and so on. The minimum increase of 1.99% in energy production was noticed for the WECS from DeWind, for this change in hub height, i.e. 40 to 50 metres. The overall mean increase in energy production was found to be 2.92% while changing the hub height from 40 to 50 metres.

A further increase of 10metres in hub height from 50 to 60 metres showed an increase of 7.55%, 7.90%, 7.88%, 8.25%, 8.14% and 7.75% for WECSs from Nordex, Vestas, DeWind, GE, Bonus and Enercon, respectively, as shown in Figure 7.21. The maximum increase of

8.25% in energy production was obtained from the GE wind machines with the next highest increase from Bonus wind machines. The overall mean increase in energy production was found to be 7.91% for this change of hub height from 50 to 60 metres. An overall mean increase of 4.09% in energy production was obtained when the hub height was changed from 50 to 60 metres. Similarly, an increase of 3.02% in energy production was obtained for an additional 10 metres' increase in hub height i.e. from 70 to 80 metres. This analysis can be summarised as follows:

- On the average the maximum increase in energy production of 7.94% was obtained while changing the hub height from 50 to 60metres. It is therefore recommended to use 60metres of hub height for further energy calculations and also for actual wind farm development.
- The next higher increase of 4.09% in energy production was obtained when hub height was increased to 70metres from 60.
- The percentage increase in energy production was observed to be of the order of 3% in the case of change of hub heights from 40 to 50 and 70 to 80metres.

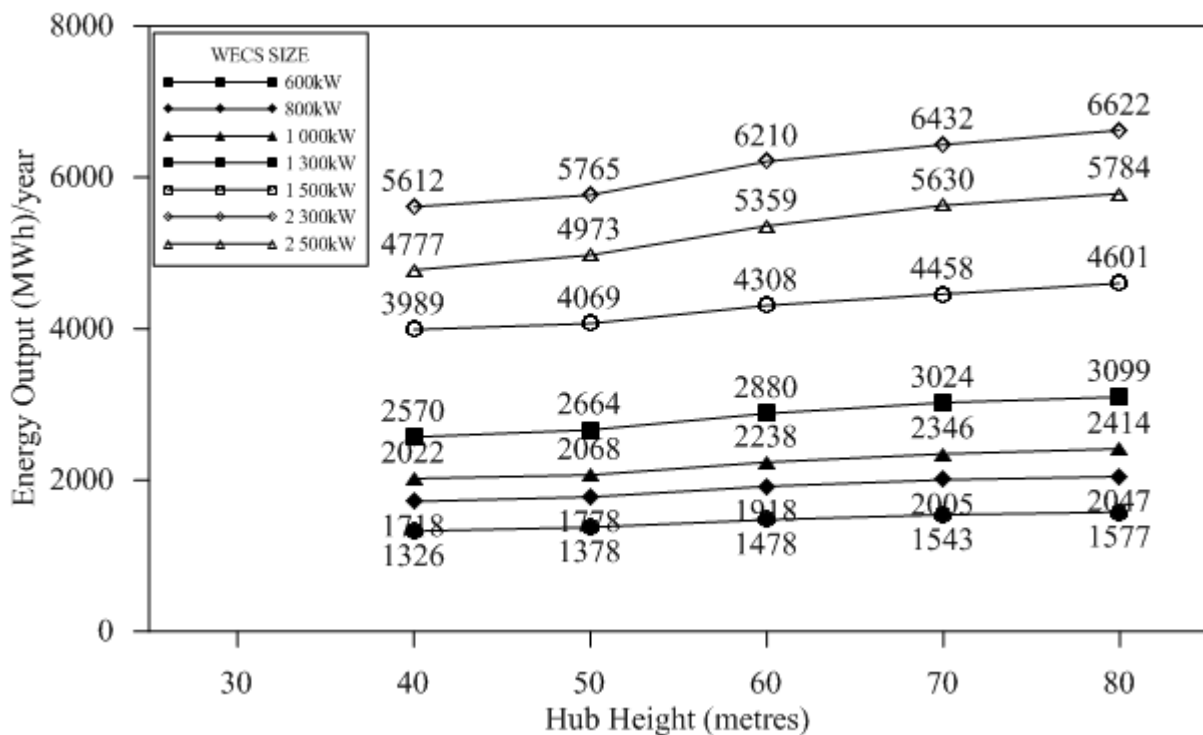


Figure 7.15 Effect of hub height on energy yield for Nordex wind machines at Yanbo

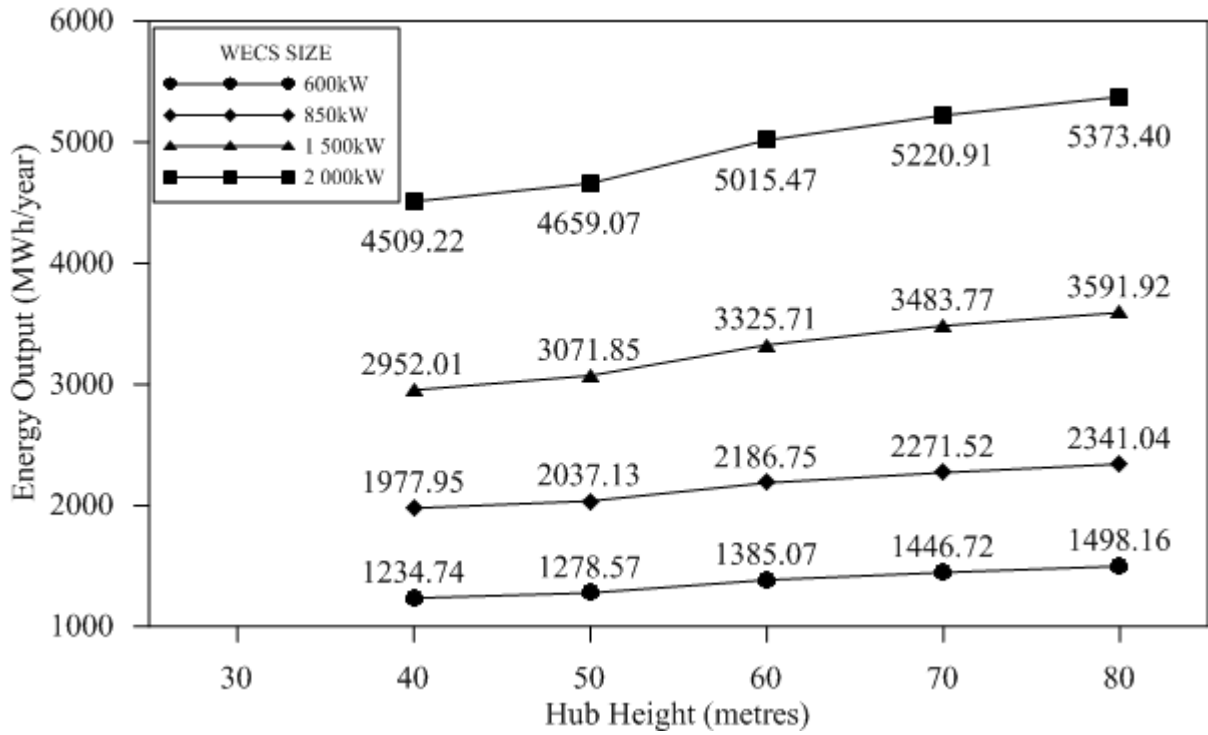


Figure 7.16 Effect of hub height on energy yield for Vestas wind machines at Yanbo

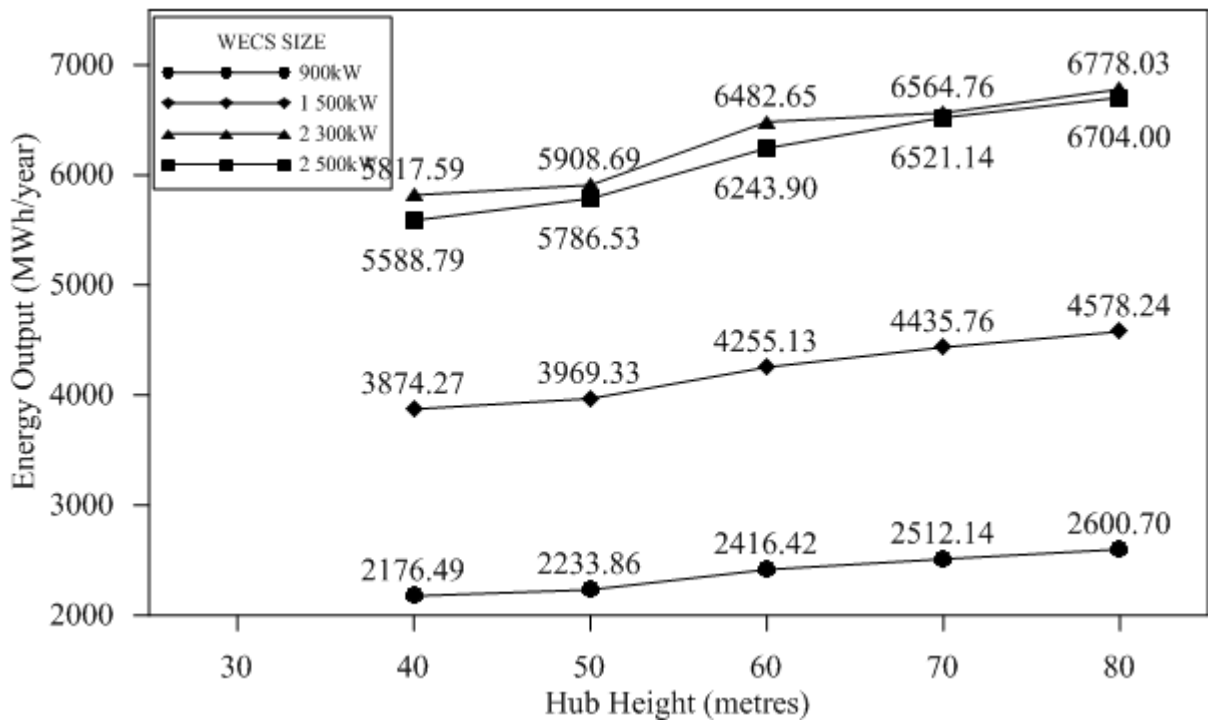


Figure 7.17 Effect of hub height on energy yield for GE wind machines at Yanbo

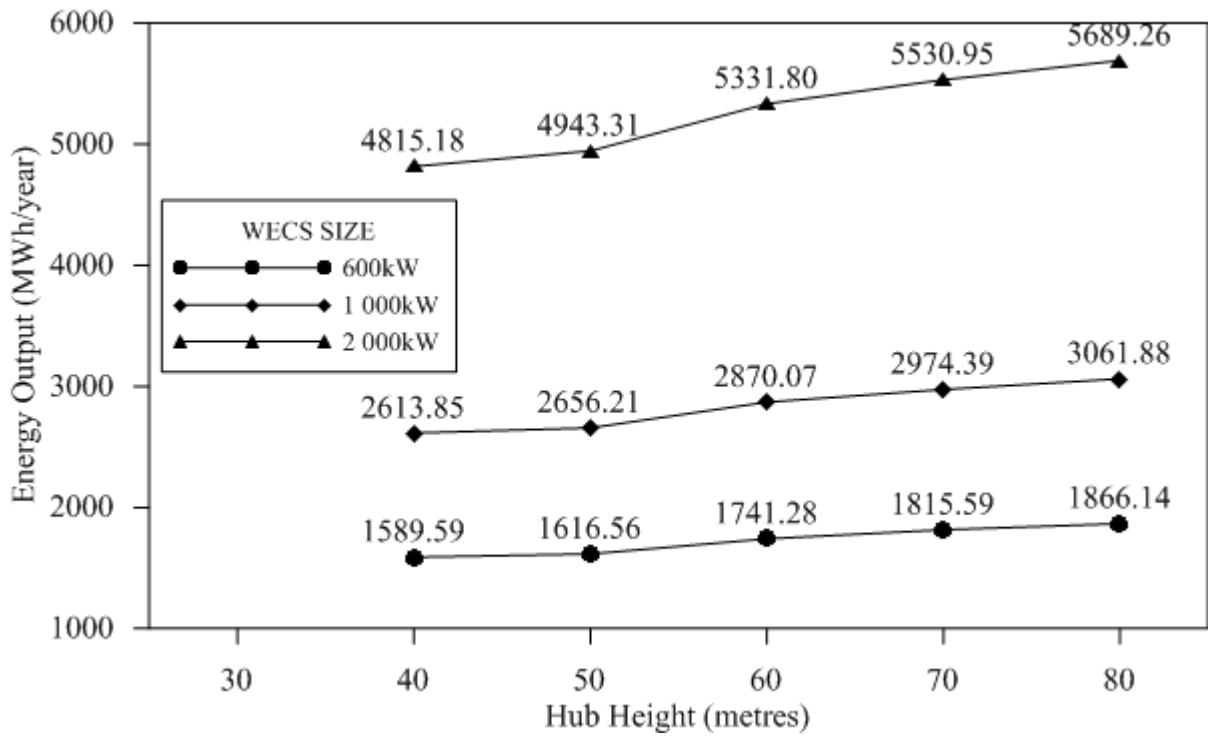


Figure 7.18 Effect of hub height on energy yield for DeWind wind machines at Yanbo

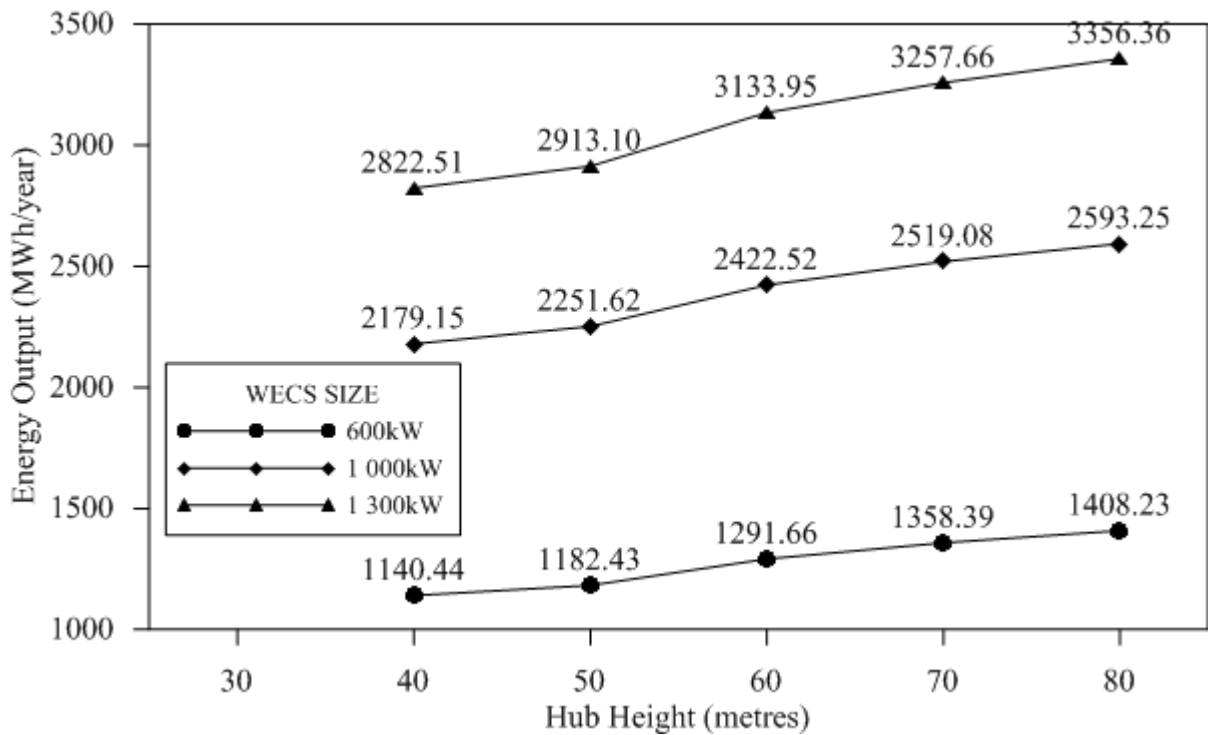


Figure 7.19 Effect of hub height on energy yield for Bonus wind machines at Yanbo

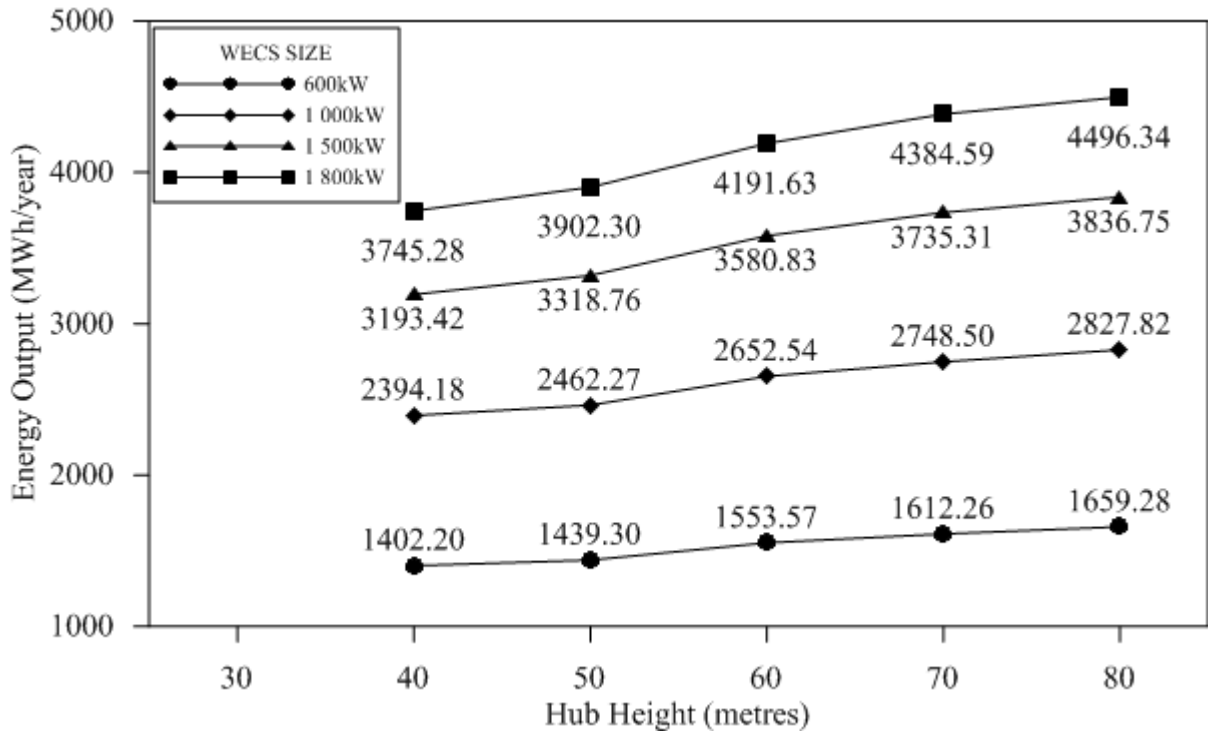


Figure 7.20 Effect of hub height on energy yield for Enercon wind machines at Yanbo

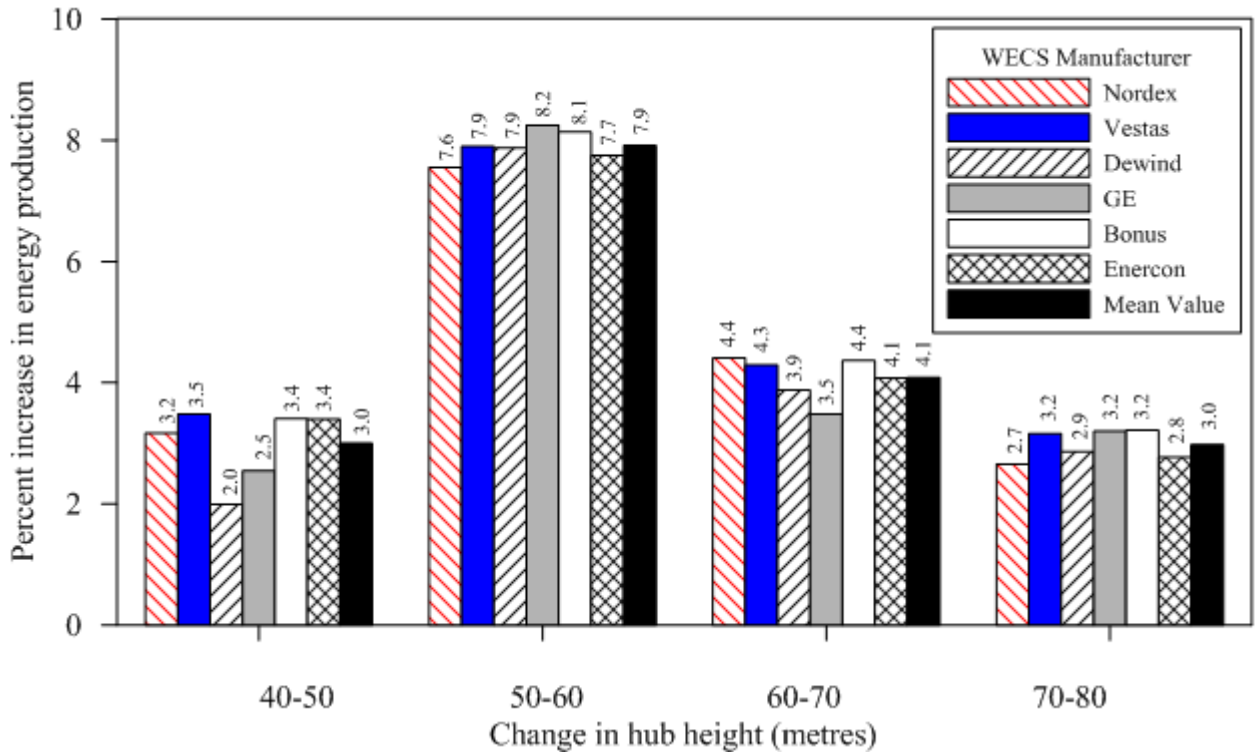


Figure 7.21 Comparison of percentage increase in energy yield due to increase in hub height at Yanbo for WECSs from different manufacturers

Table 7.8 Percentage increase in energy yield with increasing hub height for Yanbo

Manufacturer ▼ WECS Size (kW)	Percentage increase in energy production due to change in hub height				
	10-40	40-50	50-60	60-70	70-80
<b>NORDEX</b>					
600	69.56	3.91	7.24	4.40	2.23
800	69.81	3.47	7.92	4.51	2.11
1000	76.25	2.31	8.20	4.83	2.90
1300	72.73	3.65	8.14	4.98	2.47
1500	67.34	2.01	5.89	3.48	3.19
2300	65.17	2.73	7.72	3.57	2.96
2500	77.70	4.11	7.75	5.07	2.74
<b>Mean (%)</b>	<b>71.22</b>	<b>3.17</b>	<b>7.55</b>	<b>4.41</b>	<b>2.66</b>
<b>VESTAS</b>					
600	74.79	3.55	8.33	4.45	3.56
850	65.03	2.99	7.34	3.88	3.06
1500	78.65	4.06	8.26	4.75	3.10
2300	68.81	3.32	7.65	4.10	2.92
<b>Mean (%)</b>	<b>71.82</b>	<b>3.48</b>	<b>7.90</b>	<b>4.29</b>	<b>3.16</b>
<b>DEWIND</b>					
600	61.88	1.70	7.72	4.27	2.78
1000	61.46	1.62	8.05	3.63	2.94
2000	65.00	2.66	7.86	3.74	2.86
<b>Mean (%)</b>	<b>62.78</b>	<b>1.99</b>	<b>7.88</b>	<b>3.88</b>	<b>2.86</b>
<b>GE</b>					
900	66.13	2.64	8.17	3.96	3.53
1500	63.06	2.45	7.20	4.25	3.21
2300	64.48	1.57	9.71	1.27	3.25
2500	70.92	3.54	7.90	4.44	2.80
<b>Mean (%)</b>	<b>66.15</b>	<b>2.55</b>	<b>8.25</b>	<b>3.48</b>	<b>3.20</b>
<b>BONUS</b>					
600	82.13	3.68	9.24	5.17	3.67
1000	67.93	3.33	7.59	3.99	2.94
1300	66.96	3.21	7.58	3.95	3.03
<b>Mean (%)</b>	<b>72.34</b>	<b>3.41</b>	<b>8.14</b>	<b>4.37</b>	<b>3.21</b>
<b>ENERCON</b>					
600	68.88	2.64	7.94	3.78	2.92
1000	66.72	2.84	7.73	3.62	2.89
1500	72.99	3.92	7.90	4.31	2.72
1800	72.33	4.19	7.41	4.60	2.55
<b>Mean (%)</b>	<b>70.23</b>	<b>3.40</b>	<b>7.75</b>	<b>4.08</b>	<b>2.77</b>
<b>Overall Mean (%)</b>	<b>69.09</b>	<b>3.00</b>	<b>7.91</b>	<b>4.09</b>	<b>2.98</b>

#### 7.4 PLANT CAPACITY FACTOR ANALYSIS

The plant capacity factor (PCF) is a measure of the actual energy production compared with the installed capacity or rated power of a wind energy conversion system (WECS). The larger the PCF, the better the wind energy conversion system is. The PCF generally varies from 25 to 45%. The PCF is calculated by dividing the actual energy production by the rated capacity

of the WECS and number of hours in a year i.e. 8 760. For plant capacity factor analysis, wind machines of 600, 800, 850, 900, 1 000, 1 300, 1 500, 2 000, 2 300 and 2 500kW sizes were chosen from different manufacturers. The capacity factors calculated for all the WECSs under investigation are summarised in Table 7.9.

In general, it was noticed that smaller machines have relatively higher capacity factors. For example, DeWind machines of 600kW rated power has the highest PCF compared with 1 000 and 2 000kW rated power wind machines at all hub heights. In the case of Nordex machines, the 600kW machine has the highest PCF compared with other sizes except for wind machines of 1 500 and 2 300kW rated power, which have higher PCF than a 600kW machine due to very large rotor diameters. In the case of the WECSs from Vestas, the 850kW machines showed the highest PCF while the 1 500kW the least. The 600kW wind machines from DeWind attained the maximum PCF compared with 1 000 and 2 000kW machines. The 1 500kW wind machine from GE showed the maximum PCF while the 2 500kW the minimum.

While comparing the PCF for the 600kW WECS, the DeWind machine attained the maximum PCF of 30.2% at 40m hub height while the Nordex machine the next highest PCF of 25.2%. The Vestas machine was placed at third place with PCF of 23.5% while Bonus stood at fourth place with PCF of 21.7%. The DeWind machine of 1 000kW rated power attained the maximum PCF of 29.8% while Bonus with 24.9% and Nordex with 23.1% PCF were placed at second and third place, respectively. The Nordex 1 500kW machine performed the best with PCF of 30.4% while GE and Vestas stood at second and third place with PCF of 29.5 and 22.5%, respectively. The GE wind machine of 2 300kW rated power performed the best with PCF of 28.9%, Nordex next best with PCF of 27.9%, and next best was the Vestas machine with PCF of 25.7%.

The effect of increase in hub height on capacity factor was also studied and the increase in capacity factors for WECSs from different manufacturers is summarised in Table 7.10. The values in Columns 2 to 6 show the simple difference between the PCF values at 50 and 40m. Figures 7.22-7.26 show the effect of hub height on capacity factor for the WECSs from Nordex, Vestas, DeWind, GE and Bonus, respectively. It is clearly understood that the PCF increases with height as shown in these figures and in Table 7.9. The change in PCF for WECSs from different manufacturers is also compared in Figure 7.27.

As seen from Column 3 of Table 7.10 and Figure 7.27, the highest mean change in PCF of 0.85% was observed for the WECS from Vestas while the next highest mean change of 0.81% for Bonus machines. In this class (40-50 metres) of hub height change, an overall mean increase of 0.74% in PCF was noticed. For an increase of hub height from 50 to 60 m, a maximum mean increase of 2.36% was noticed for GE machines with the mean minimum of 1.93% for WECS from Nordex. The DeWind machines showed to be the second best with a mean increase of 2.34% in PCF and Vestas with 2.0% increase, the third best. In case of increase of hub height from 60 to 70m, a maximum of 1.25% change in PCF was noticed for DeWind machines while a minimum of 1.07% for GE machines. In this class of hub height change, an overall of 1.17% increase in PCF was observed. For further increase of hub height from 70 to 80m, an overall of 0.91% increase in PCF was found.

This analysis shows that a maximum increase of 2.12% in PCF was found when increasing the hub height from 50 to 60 m. In the case of change of the hub-heights from 40 to 50 and 70 to 80 m, the increase in PCF was less than 1% and in the case of increase from 60 to 70 m, the increase in PCF was a little more than 1%. The effect of hub height on PCF matches with the hub height effect on energy production presented in the previous sub-section. Hence it is recommended to install the wind machines at 60 m hub height to obtain the optimal PCF.

Table 7.9 Plant capacity factors for wind machines of different sizes at Yanbo

Manufacturer	Size of Wind Energy Conversion System (WECS – kW)									
	600	800	850	900	1000	1300	1500	2000	2300	2500
<b>NORDEX</b>										
10 metres	14.9	14.4	-	-	13.1	13.1	<b>18.1</b>	-	16.9	12.3
40 metres	25.2	24.5	-	-	23.1	22.6	<b>30.4</b>	-	27.9	21.8
50 metres	26.2	25.4	-	-	23.6	23.4	<b>31.0</b>	-	28.6	22.7
60 metres	28.1	27.4	-	-	25.5	25.3	<b>32.8</b>	-	30.8	24.5
70 metres	29.3	28.6	-	-	26.8	26.6	<b>33.9</b>	-	31.9	25.7
80 metres	30.0	29.2	-	-	27.6	27.2	<b>35.0</b>	-	32.9	26.4
<b>VESTAS</b>										
10 metres	13.4	-	16.1	-	-	-	12.6	-	15.2	-
40 metres	23.5	-	26.6	-	-	-	22.5	-	25.7	-
50 metres	24.3	-	27.4	-	-	-	23.4	-	26.6	-
60 metres	26.4	-	29.4	-	-	-	25.3	-	28.6	-
70 metres	27.5	-	30.5	-	-	-	26.5	-	29.8	-
80 metres	28.5	-	31.4	-	-	-	27.3	-	30.7	-
<b>DEWIND</b>										
10 metres	<b>18.7</b>	-	-	-	<b>18.5</b>	-	-	16.7	-	-
40 metres	<b>30.2</b>	-	-	-	<b>29.8</b>	-	-	27.5	-	-
50 metres	<b>30.8</b>	-	-	-	<b>30.3</b>	-	-	28.2	-	-
60 metres	<b>33.1</b>	-	-	-	<b>32.8</b>	-	-	30.4	-	-
70 metres	<b>34.5</b>	-	-	-	<b>34.0</b>	-	-	31.6	-	-
80 metres	<b>35.5</b>	-	-	-	<b>35.0</b>	-	-	32.5	-	-
<b>GE</b>										
10 metres	-	-	-	16.6	-	-	18.1	-	<b>17.6</b>	<b>14.9</b>
40 metres	-	-	-	27.6	-	-	29.5	-	<b>28.9</b>	<b>25.5</b>
50 metres	-	-	-	28.3	-	-	30.2	-	<b>29.3</b>	<b>26.4</b>
60 metres	-	-	-	30.6	-	-	32.4	-	<b>32.2</b>	<b>28.5</b>
70 metres	-	-	-	31.9	-	-	33.8	-	<b>32.6</b>	<b>29.8</b>
80 metres	-	-	-	33.0	-	-	34.8	-	<b>33.6</b>	<b>30.6</b>
<b>BONUS</b>										
10 metres	11.9	-	-	-	14.8	<b>14.8</b>	-	-	-	-
40 metres	21.7	-	-	-	24.9	<b>24.8</b>	-	-	-	-
50 metres	22.5	-	-	-	25.7	<b>25.6</b>	-	-	-	-
60 metres	24.6	-	-	-	27.7	<b>27.5</b>	-	-	-	-
70 metres	25.8	-	-	-	28.8	<b>28.6</b>	-	-	-	-
80 metres	26.8	-	-	-	29.6	<b>29.5</b>	-	-	-	-

Table 7.10 PCF variation with increasing hub height for Yanbo

Manufacturer ▼ WECS Size (kW)	Percentage increase in energy production due to change in hub height				
	10-40	40-50	50-60	60-70	70-80
<b>NORDEX</b>					
600	10.35	0.99	1.90	1.24	0.66
800	10.08	0.85	2.01	1.24	0.60
1000	9.98	0.53	1.94	1.24	0.78
1300	9.50	0.82	1.90	1.26	0.66
1500	12.22	0.61	1.82	1.14	1.08
2300	10.99	0.76	2.21	1.10	0.94
2400	9.54	0.90	1.76	1.24	0.71
<b>Mean (%)</b>	<b>10.38</b>	<b>0.78</b>	<b>1.93</b>	<b>1.21</b>	<b>0.77</b>
<b>VESTAS</b>					
600	10.05	0.83	2.03	1.17	0.98
850	10.47	0.79	2.01	1.14	0.93
1500	9.89	0.91	1.93	1.20	0.82
2300	10.49	0.86	2.03	1.17	0.87
<b>Mean (%)</b>	<b>10.23</b>	<b>0.85</b>	<b>2.00</b>	<b>1.17</b>	<b>0.90</b>
<b>DEWIND</b>					
600	11.56	0.51	2.37	1.41	0.96
1000	11.36	0.48	2.44	1.19	1.00
2000	10.83	0.73	2.22	1.14	0.90
<b>Mean (%)</b>	<b>11.25</b>	<b>0.58</b>	<b>2.34</b>	<b>1.25</b>	<b>0.95</b>
<b>GE</b>					
900	10.99	0.73	2.32	1.21	1.12
1500	11.40	0.72	2.18	1.37	1.08
2300	11.32	0.45	2.85	0.41	1.06
2500	10.59	0.90	2.09	1.27	0.83
<b>Mean (%)</b>	<b>11.07</b>	<b>0.70</b>	<b>2.36</b>	<b>1.07</b>	<b>1.03</b>
<b>BONUS</b>					
600	9.78	0.80	2.08	1.27	0.95
1000	10.06	0.83	1.95	1.10	0.85
1300	9.94	0.80	1.94	1.09	0.87
<b>Mean (%)</b>	<b>9.93</b>	<b>0.81</b>	<b>1.99</b>	<b>1.15</b>	<b>0.89</b>
<b>Overall Mean (%)</b>	<b>10.57</b>	<b>0.74</b>	<b>2.12</b>	<b>1.17</b>	<b>0.91</b>

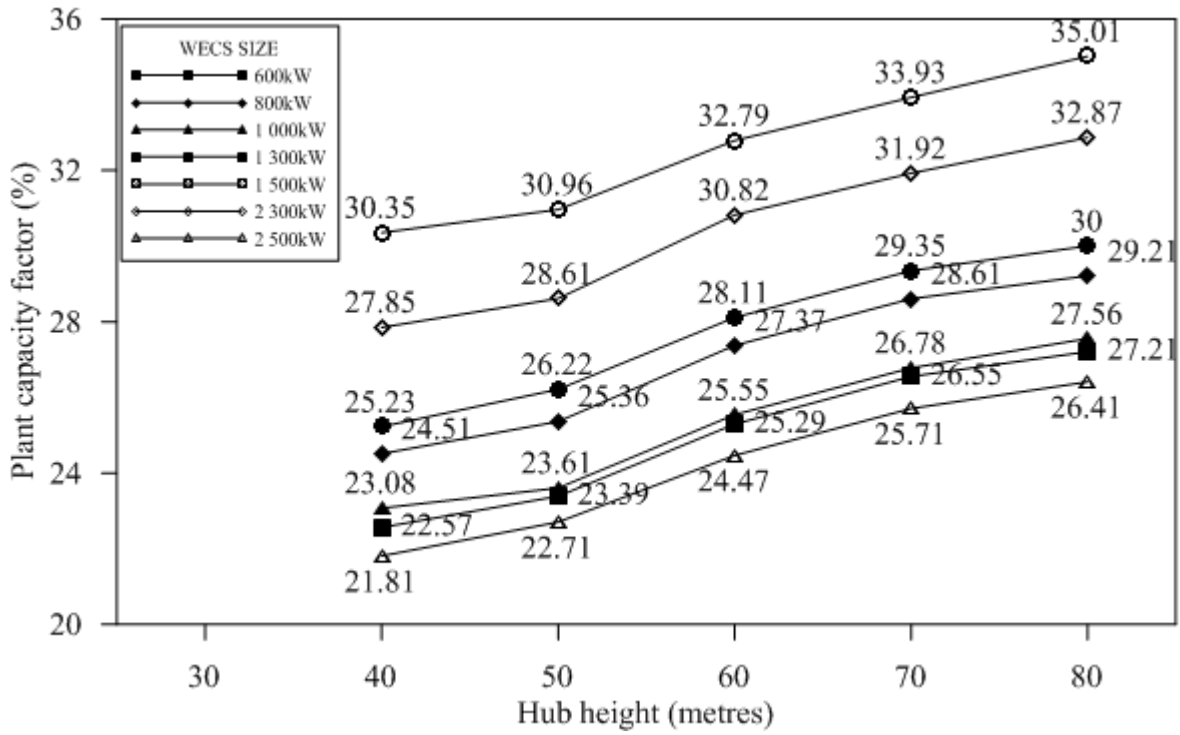


Figure 7.22 Effect of hub height on plant capacity factor for Nordex wind machines at Yanbo

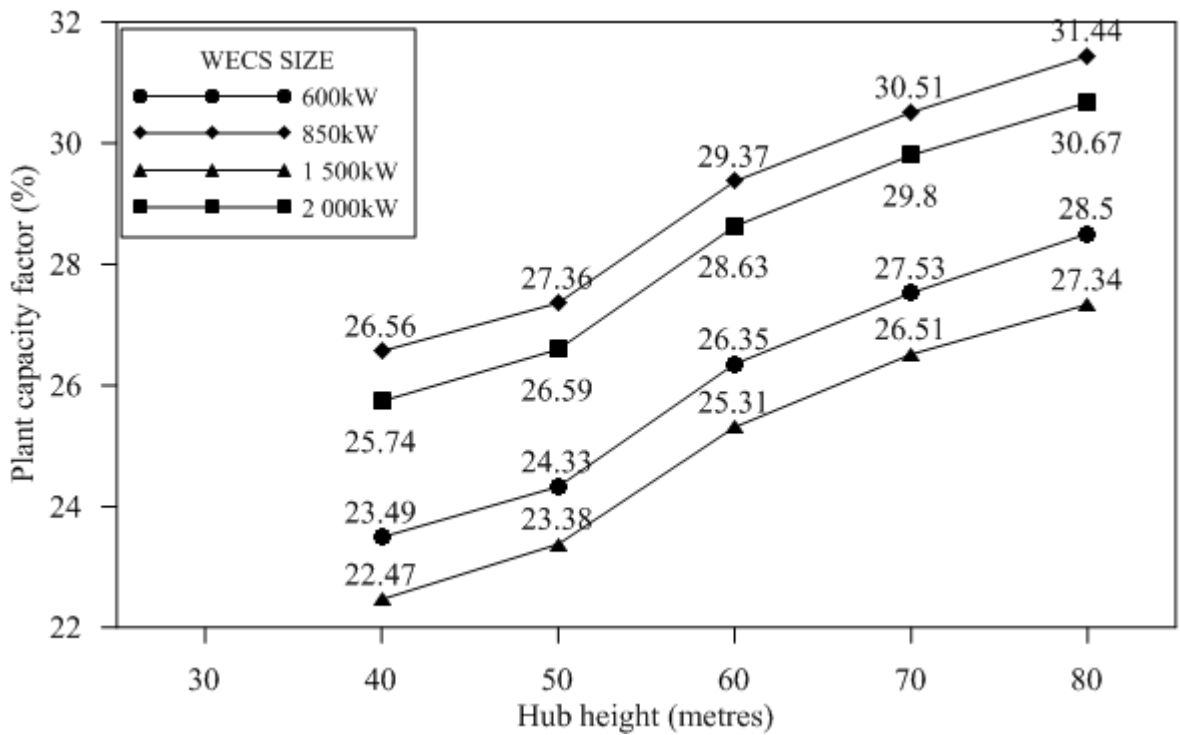


Figure 7.23 Effect of hub height on plant capacity factor for Vestas wind machines at Yanbo

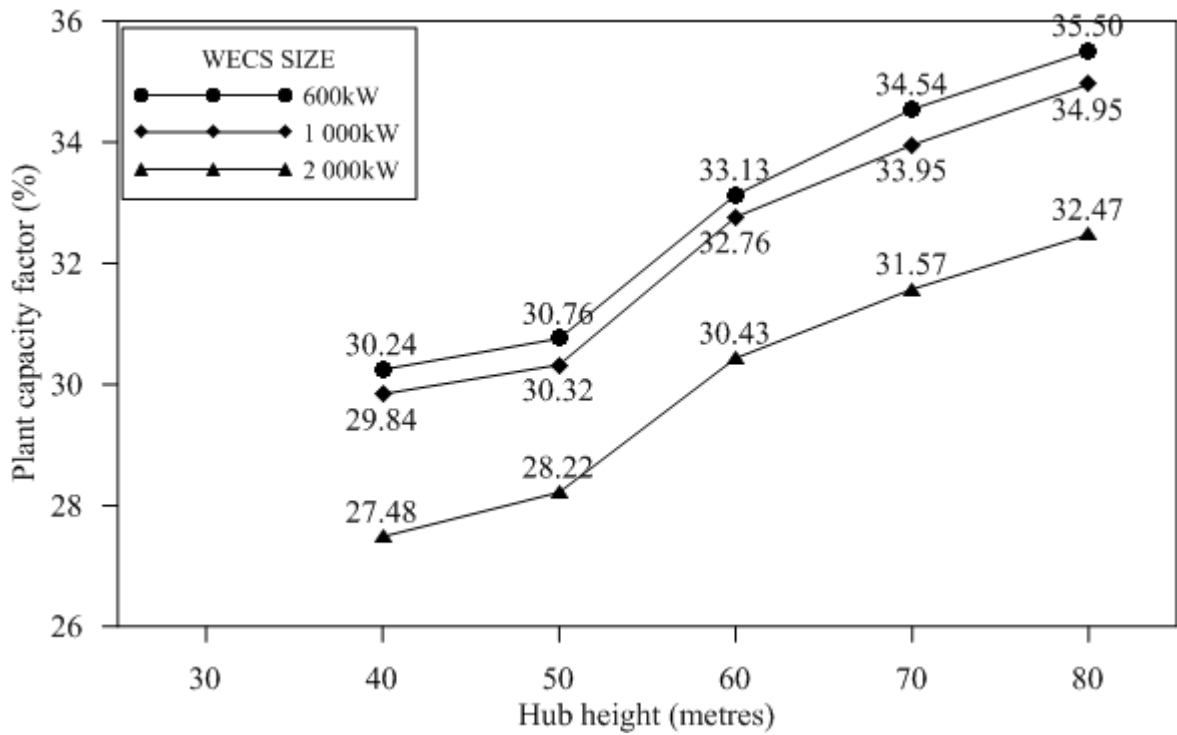


Figure 7.24 Effect of hub height on plant capacity factor for DeWind wind machines at Yanbo

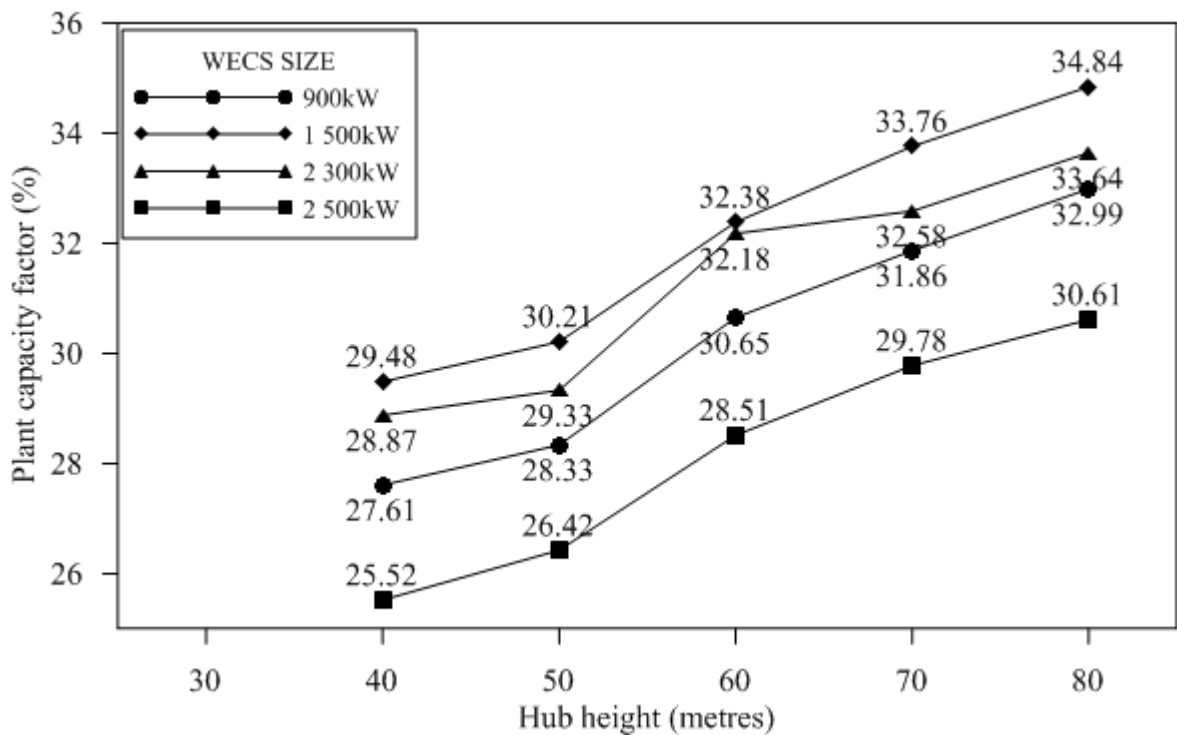


Figure 7.25 Effect of hub height on plant capacity factor for GE wind machines at Yanbo

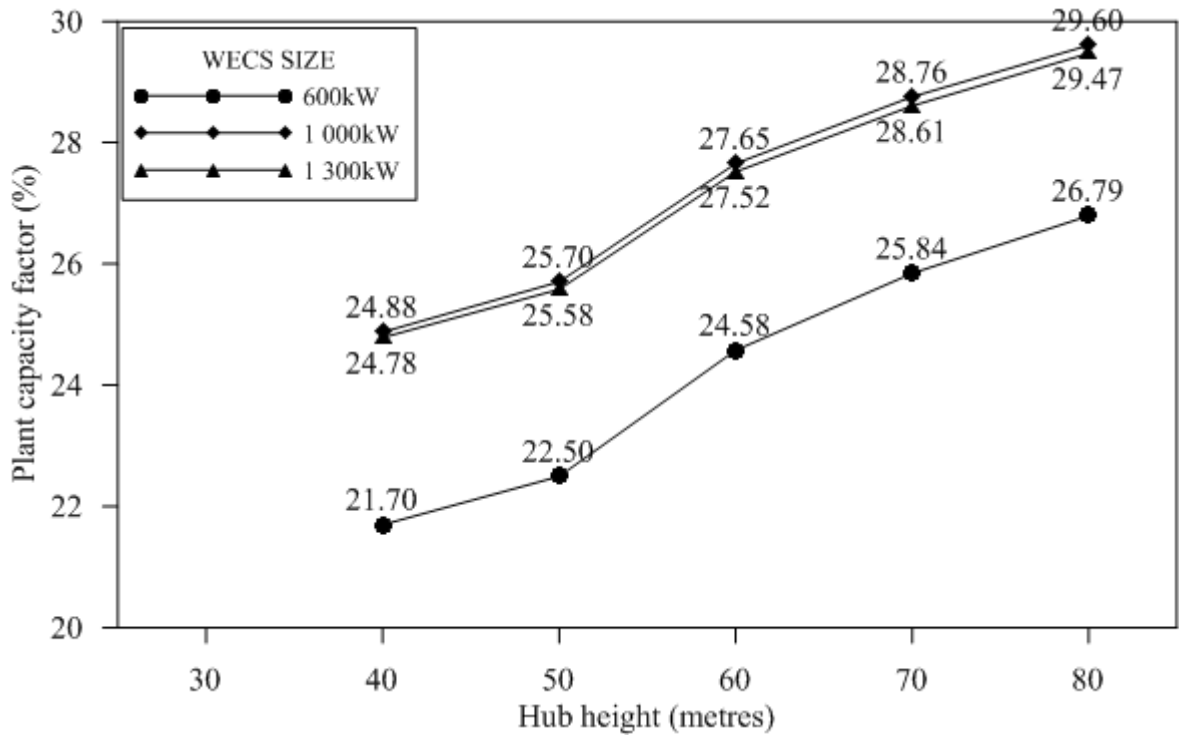


Figure 7.26 Effect of hub height on plant capacity factor for Bonus wind machines at Yanbo

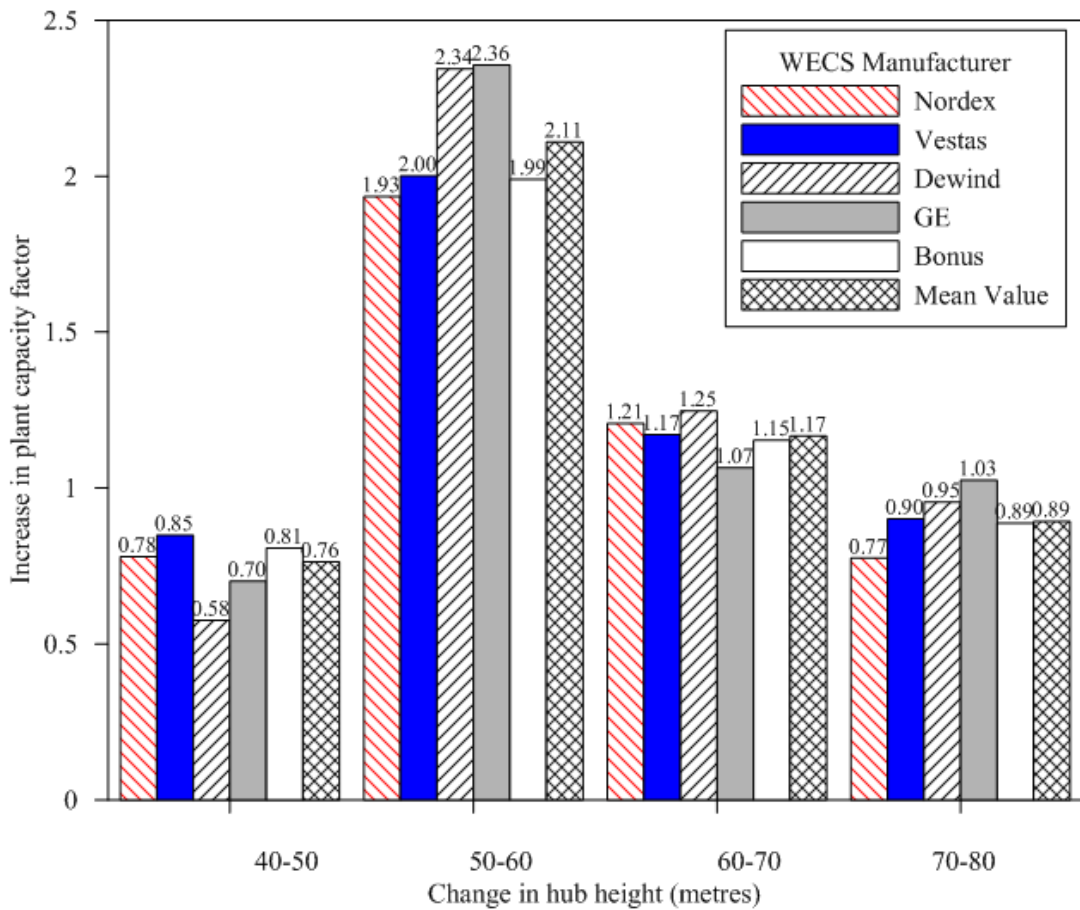


Figure 7.27 Comparison of increase in plant capacity factor for Yanbo due to increase in hub height for WECSs from different manufacturers.

## 7.5 EMPIRICAL CORRELATION FOR THE ESTIMATION OF NEAR-OPTIMAL HUB HEIGHT

To author's knowledge, hub-height optimization has not been reported in the literature and being demonstrated for the first time in the present work. We have followed the following procedure to reach near optimal hub-height:

- Energy yield estimation from wind turbine for incremental increase of 10metre
- Percent increase estimation in energy yield for each 10meter increase in hub-height
- Cost of wind turbine including the capital cost, installation cost, operation & maintenance cost, and additional cost of each 10meter increase in hub-height
- Estimation of percent increase in total cost for each 10metre increase in hub-height
- Finally, plotting the percent increases in energy and cost on the same scale. The point where the two curves cross each other is expected to be the near optimal hub-height.
- To prove this concept, on site measurements of energy output from wind turbines having different hub-heights need to be carried out which is out of the scope of the present work.
- Similarly, actual cost of wind turbine with incremental change in hub-height will also be needed.

To establish empirical correlations of optimum hub height (HH) with wind shear exponents, 10 minutes average wind speed data from seven stations viz. Arar, Dhahran, Dhulom, Gassim, Juaymah, Rawdat Ben Habbas (RBH) and Yanbo was used. The measured wind speed data at 20, 30 and 40metres above ground level was first used to estimate the wind shear exponent, as stated earlier in this thesis. The wind shear exponent ( $\alpha$ ) values for Arar, Dhahran, Dhulom, Gassim, Juaymah, Rawdat Ben Habbas and Yanbo were found to be 0.181, 0.161, 0.185, 0.269, 0.228, 0.302 and 0.0731 respectively. Next, these wind shear exponent values were used to estimate wind speed at 50, 60, 70, 80, 90 and 100metres AGL. As third step, these extrapolated wind speed values were used in conjunction with the wind power curve of an AAER 1 000kW wind turbine from Pioneer Wind Energy System to estimate annual energy yield. The wind power curve of the chosen wind turbine is shown in Figure 7.28. The resulting annual wind energy yield at different heights for all the stations is summarised in Table 7.11 and is also compared in Figure 7.29. It is evident from the data

given in Table 7.11 and Figure 7.29 that the energy yield increases with increasing hub height.

The corresponding increases in annual energy yield with increase in hub height are summarised in Table 7.12. As can be seen from Table 7.12, maximum increase in annual energy is observed with increasing hub height from 40 to 50metres. In order to find out the optimal hub height, the cost of wind turbine including the capital and installation cost was obtained from Morthorst [302] to be € 900/kW for a hub height of 40metres. The increase in hub height of a turbine adds the civil construction and installation cost, which varies from 6 to 20% of the total investment cost. Based on initial cost and incremental cost, the total cost of the wind turbine with incremental hub height was worked out to be as summarised in Table 7.13. As the next step, the percentage increase in energy yield and the total wind turbine cost with increasing hub height are plotted for each station, as shown in Figures 7.30 to 7.36 for Arar, Dhahran, Dhulom, Gassim, Juaymah, Rawdat Ben Habbas (RBH) and Yanbo, respectively. The hub height is defined as the height where two curves cross each other. For Arar, as seen from Figure 7.30, the two curves cross each other at a point where the hub height is 68metres. Similarly, the optimal hub heights for Dhahran, Dhulom, Gassim, Juaymah and Raddat Ben Habbas were found to be 64, 66, 81, 70 and 82metres, respectively as can be seen from Figures 7.31 to 7.35. In the case of Yanbo, the two curves did not cross each other due to the abnormally small value of wind shear exponent, therefore the optimal hub height is assumed to be 50metres in this case.

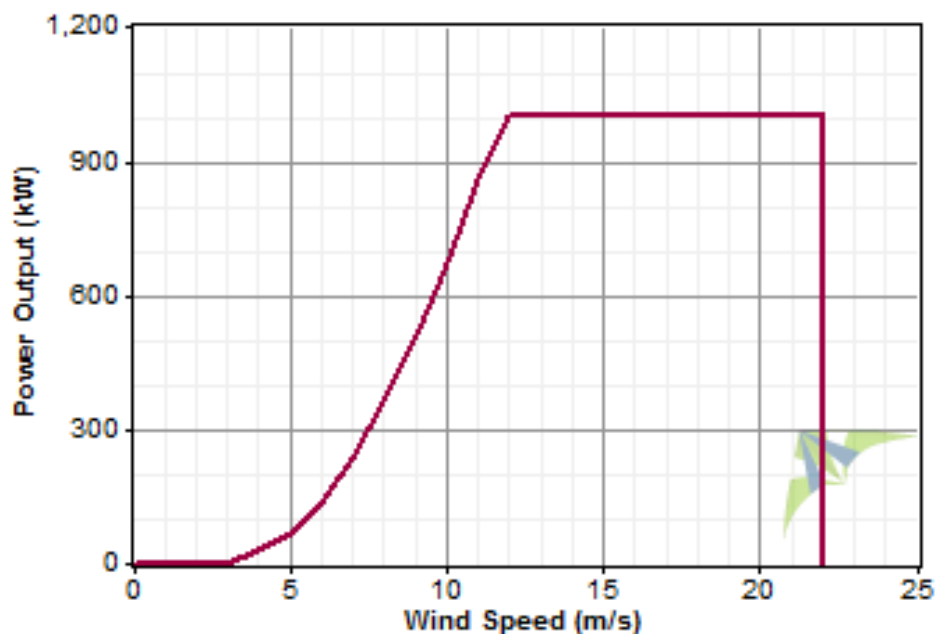


Figure 7.28 Wind power curve of an AAER 1 000kW wind turbine from Pioneer wind energy systems

Table 7.11 Annual energy yield at different hub heights

HH	Annual energy yield (MWh)						
	Arar	Dhahran	Dhulom	Gassim	Juaymah	Rawdat	Yanbo
40	1225.4	1137.9	1162.5	635.2	1338.0	1256.8	988.4
50	1353.3	1252.9	1451.9	758.6	1530.3	1533.7	1029.6
60	1467.4	1355.4	1585.2	880.4	1703.1	1774.9	1067.9
70	1594.9	1446.3	1703.5	996.0	1858.4	2008.9	1101.0
80	1700.1	1528.0	1810.1	1109.1	2008.8	2251.2	1130.2
90	1796.5	1602.5	1907.0	1206.1	2125.9	2409.8	1156.3
100	1884.9	1670.7	1995.8	1324.9	2243.4	2664.5	1180.0

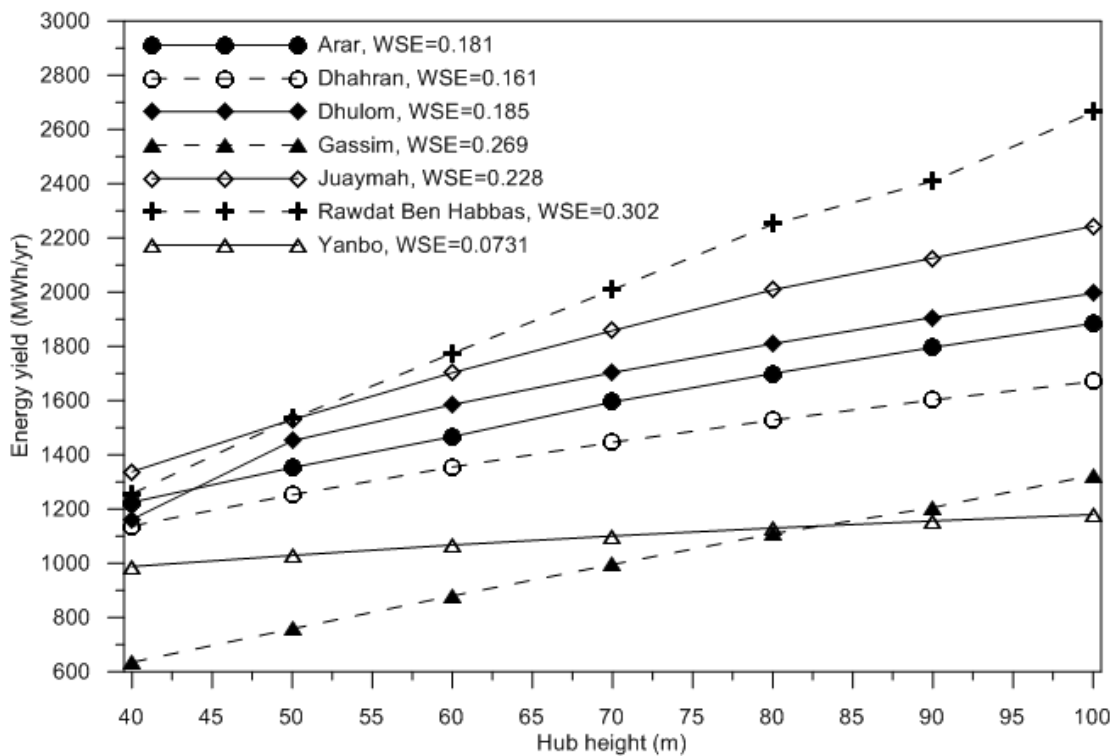


Figure 7.29 Comparison of annual energy yields at different hub heights with wind shear exponents

Table 7.12 Percent increase in annual energy yield with increase in hub height

HH	Percentage increase in annual energy yield with change in hub height						
	Arar	Dhahran	Dhulom	Gassim	Juaymah	Rawdat	Yanbo
40	-	-	-	-	-	-	-
50	10.4	10.1	24.9	19.4	14.4	22.0	4.2
60	8.4	8.2	9.2	16.1	11.3	15.7	3.7
70	8.7	6.7	7.5	13.1	9.1	13.2	3.1
80	6.6	5.7	6.3	11.3	8.1	12.1	2.6
90	5.7	4.9	5.4	8.7	5.8	7.0	2.3
100	4.9	4.3	4.7	9.8	5.5	10.6	2.0

Table 7.13 Total incremental cost of 1 000kW wind turbine

HH	Total capital and installation cost of 1 000kW wind turbine (euro)	Percentage increase in total cost
40	900,000	-
50	954,000	6
60	1,020,780	7
70	1,112,650	9
80	1,235,000	11
90	1,395,600	13
100	1,618,900	16

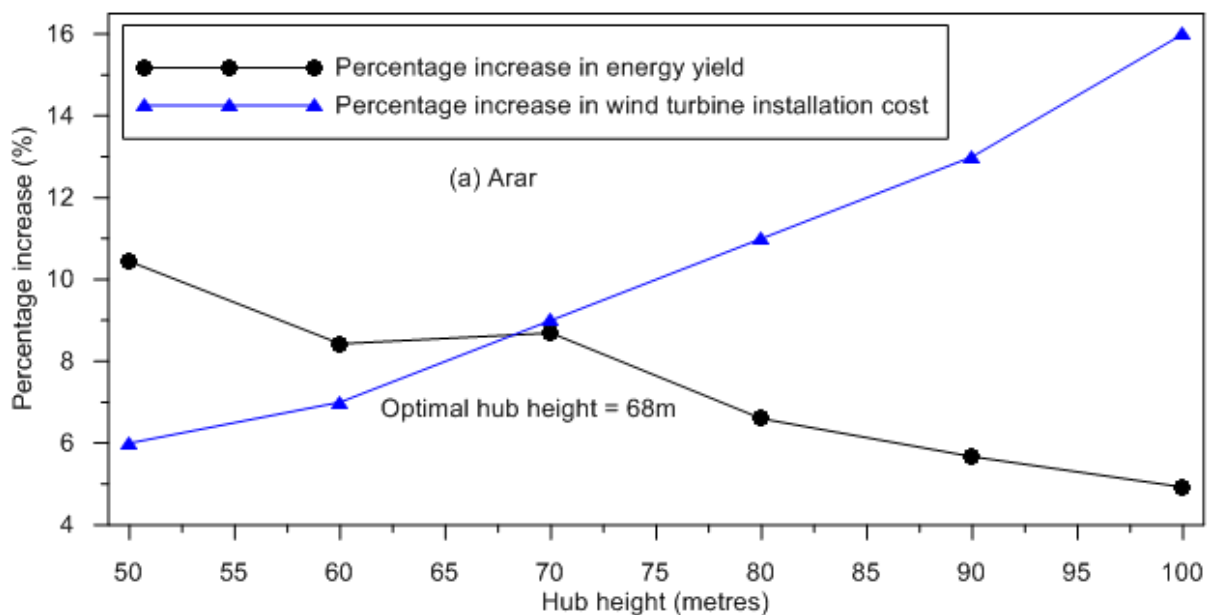


Figure 7.30 Percentage increase in energy yield and the total cost of wind turbine installation with increasing hub height for Arar

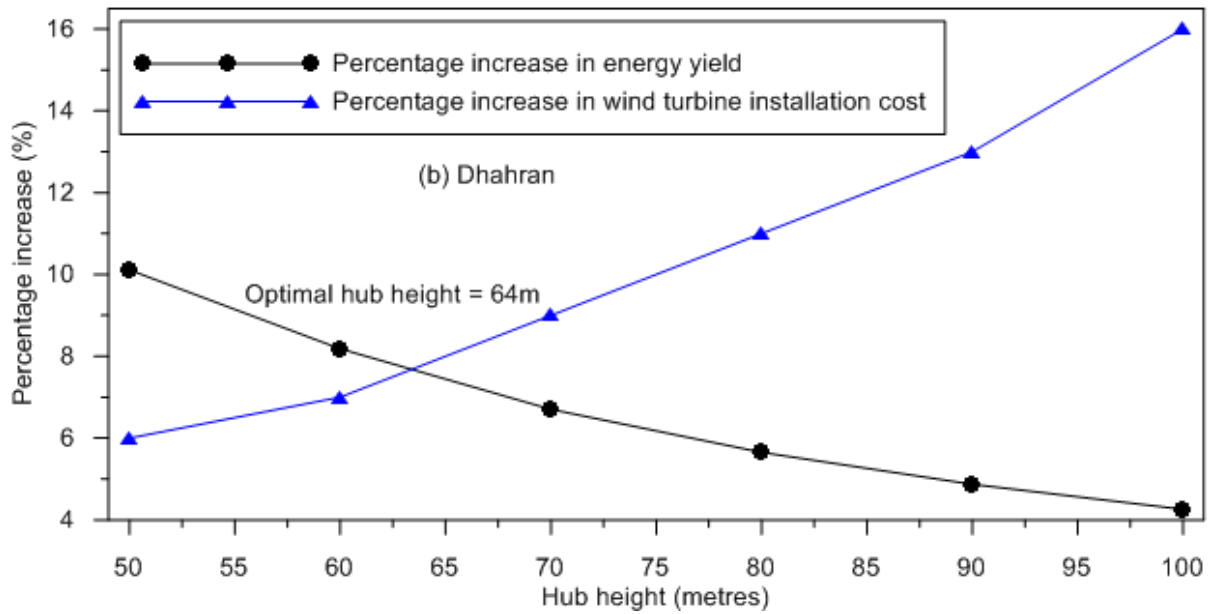


Figure 7.31 Percentage increase in energy yield and the total cost of wind turbine installation with increasing hub height for Dhahran

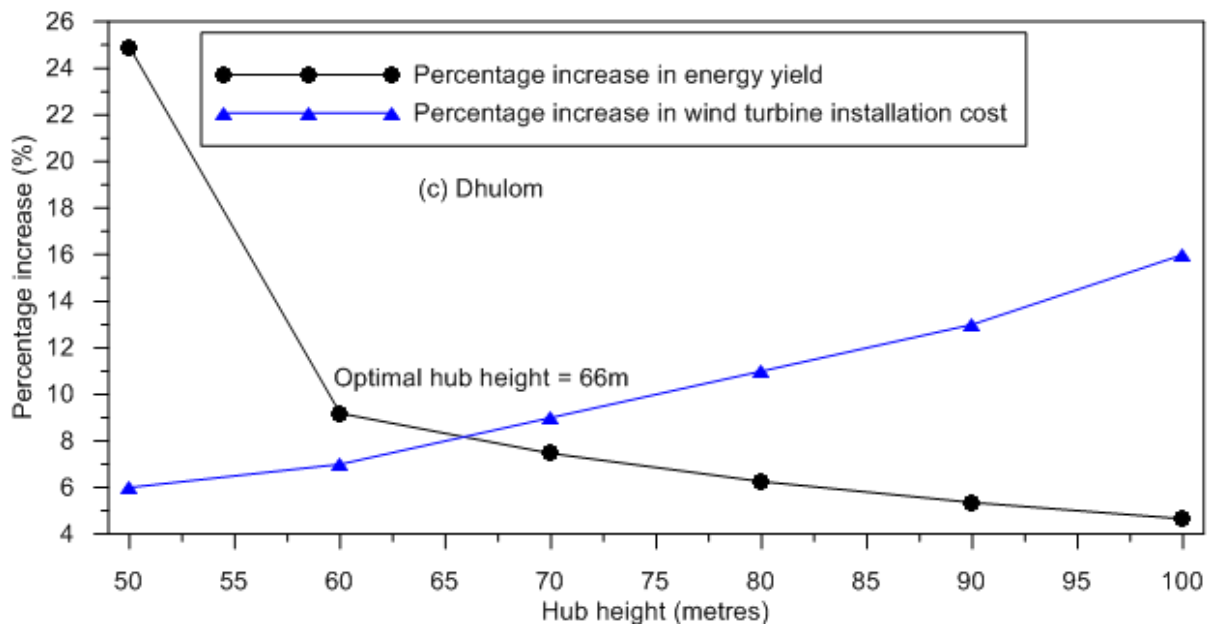


Figure 7.32 Percentage increase in energy yield and the total cost of wind turbine installation with increasing hub height for Dhulom

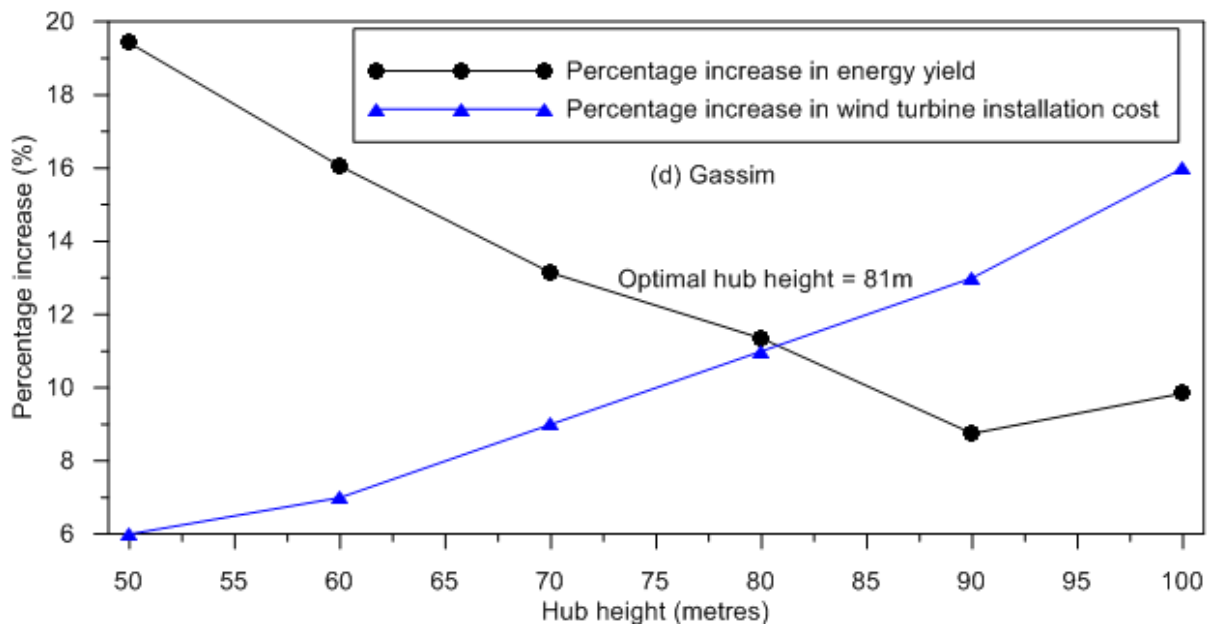


Figure 7.33 Percentage increase in energy yield and the total cost of wind turbine installation with increasing hub height for Gassim

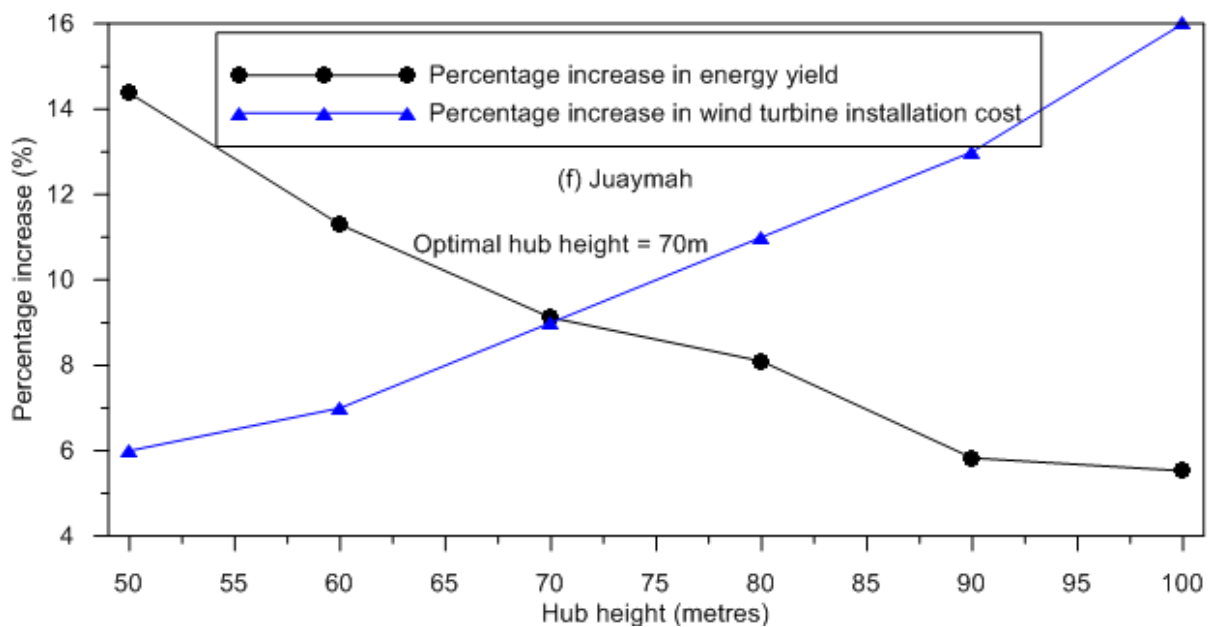


Figure 7.34 Percentage increase in energy yield and the total cost of wind turbine installation with increasing hub height for Juaymah

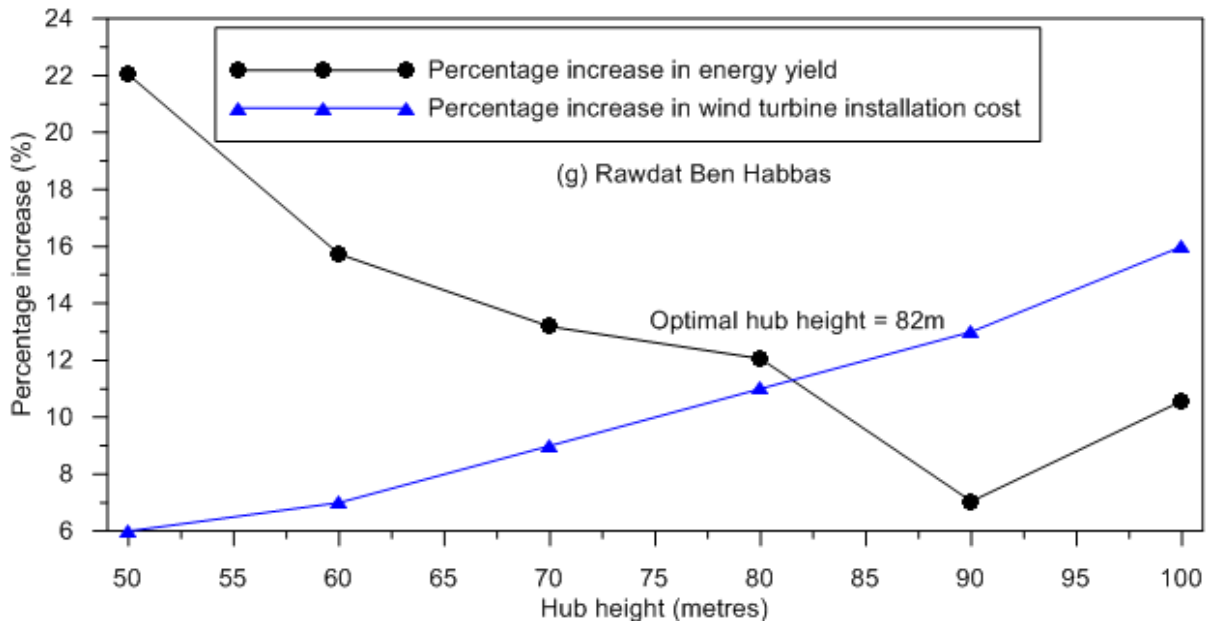


Figure 7.35 Percentage increase in energy yield and the total cost of wind turbine installation with increasing hub height for Rawdat Ben Habbas

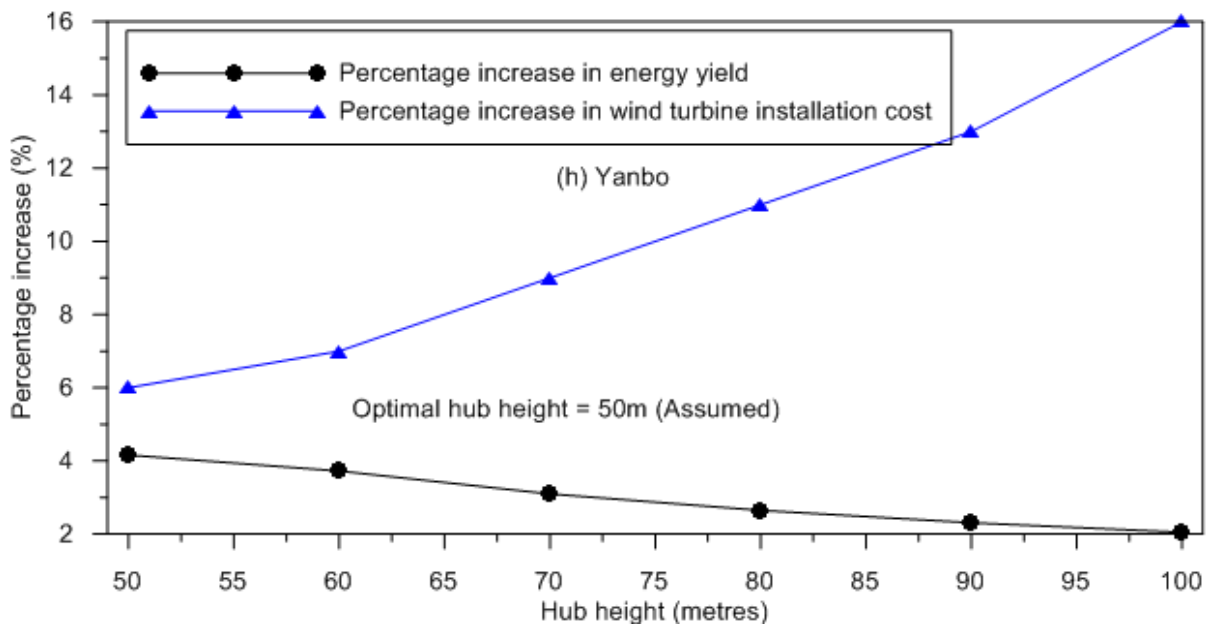


Figure 7.36 Percentage increase in energy yield and the total cost of wind turbine installation with increasing hub height for Yanbo

Finally, in order to find an empirical relation between optimal hub height and the wind shear exponent ( $\alpha$ ), the two are plotted in Figure 7.37 and best-fit curves were obtained. Three types of best-fit curves were obtained, viz. linear fit (Equation 7.1), log fit (Equation 7.2) and power fit (Equation 7.3). The values of the coefficient of determination for the three best-fit curves were found to be 0.97, 0.94 and 0.97, respectively. The linear and power fit equations

were found to be the best approximation of optimal hub height with wind shear exponent given by Equations 7.1 and 7.3.

Linear fit equation:

$$HH = 142.035 * (\alpha) + 40.33 \quad (7.1)$$

Residual sum of squares = 20.30                      Coef of determination, R-squared = 0.97

Residual mean square, sigma-hat-sq'd = 4.06

Log fit equation:

$$HH = 22.533 * \ln(\alpha) + 106.79 \quad (7.2)$$

Residual sum of squares = 46.357                      Coef of determination, R-squared = 0.94

Residual mean square, sigma-hat-sq'd = 9.27

Power fit equation:

$$\ln(HH) = 0.35 * \ln(\alpha) + 4.81 \quad (7.3)$$

Alternate (HH) =  $[(\alpha)^{0.3501}] * 122.7449$

Residual sum of squares = 0.0055                      Coef of determination, R-squared = 0.97

Residual mean square, sigma-hat-sq'd = 0.0011

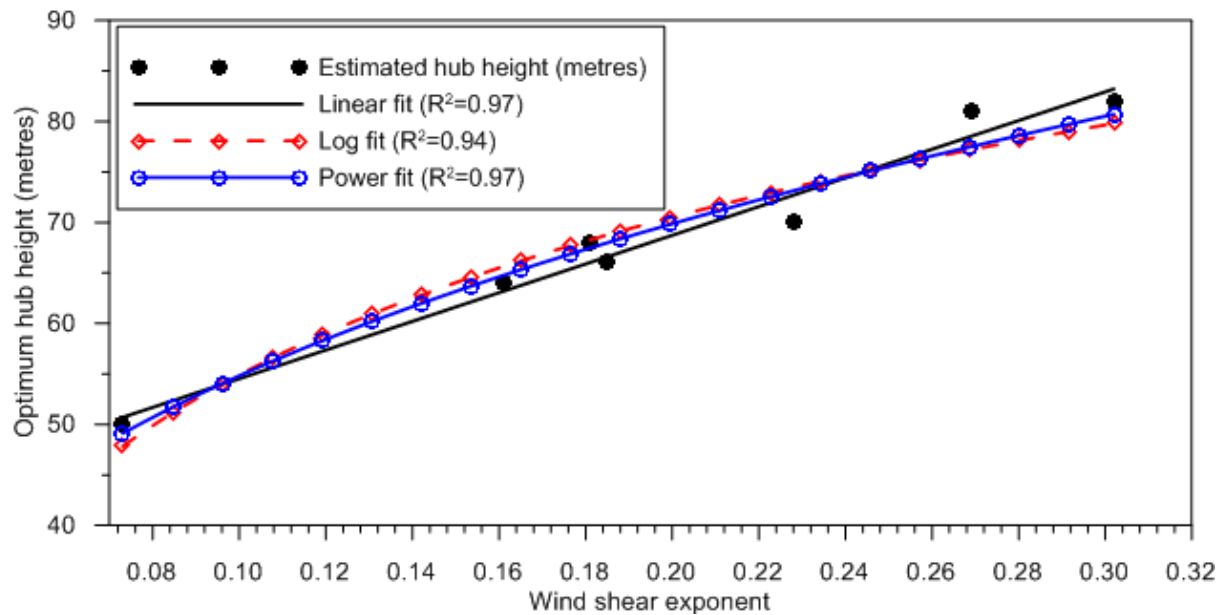


Figure 7.37 Optimum hub height variation with wind shear exponent

## 7.6 ENERGY YIELD ESTIMATION FROM WIND FARMS AT YANBO

To further study the energy production for wind energy conversion systems from different manufacturers, wind farms of 20, 30 and 40MW installed capacities were analysed. The number of wind machines shown in Figure 7.38 was approximated to the nearest whole numbers wherever found in fractions. The energy produced using different sizes of wind machines for wind farms is summarised in Table 7.14. The wind energy presented in Table 7.14 was calculated for a hub height of 60metre. It is observed from this table that for a

20MW wind farm, the maximum energy of 58 344MWh/year was produced by 9 GE machines of 2 300kW rated power. The DeWind machines of 600kW rated power produced 57 463MWh of electricity while 1 000kW rated power WECS, from the same manufacturer, produced 57 406MWh. For wind farms of 30 and 40MW installed capacities, WECS of 600kW rated power from DeWind produced the maximum electricity of 87 065 and 116 667MWh each year on an average, respectively. The Nordex wind machines of 1 500kW rated power produced 86 165 and 116 322MWh of electricity from wind farms of 30 and 40MW installed capacities, respectively.

Among 600kW machines, DeWind performed the best from an energy production point of view while Nordex machines the next best. Vestas machines were placed at number three with Bonus at number four. The wind machines of 850kW from Vestas and 900kW from GE produced almost the same amount of energy for all three sizes of wind farms considered here. The DeWind machines of 1 000kW size produced the maximum electricity compared with wind machines from Nordex and Bonus.

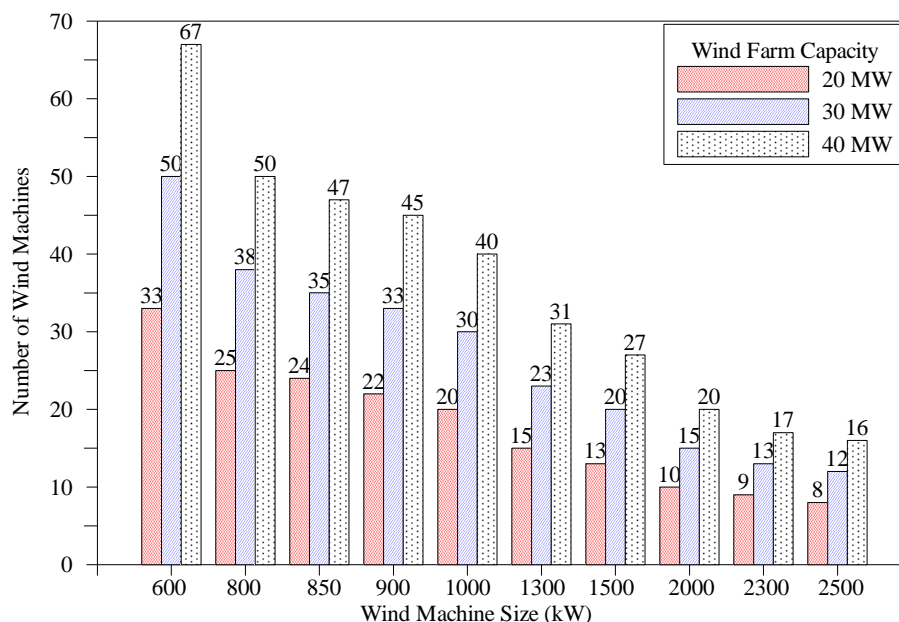


Figure 7.38 Number of wind machines required for wind farms of 20, 30 and 40MW installed capacities

Table 7.14 Energy production (MWh/year) from wind farms of 20, 30 and 40MW installed capacities for Yanbo at 60metres hub height

Manufacturer ▼	Size of Wind Energy Conversion System (WECS – kW) ▼									
	600	800	850	900	1000	1300	1500	2000	2300	2500
<b>NORDEX</b>	Energy Production From Wind Farms (MWh/Year)									
20 MW	48,761	47,960	-	-	44,756	43,207	56,007	-	55,890	42,868
30 MW	73,880	72,898	-	-	67,134	66,251	<b>86,165</b>	-	80,730	64,302
40 MW	98,999	95,919	-	-	89,512	89,295	<b>116,322</b>	-	105,570	85,737
<b>VESTAS</b>										
20 MW	45,708	-	52,482	-	-	-	43,234	-	45,139	-
30 MW	69,255	-	76,536	-	-	-	66,514	-	65,201	-
40 MW	92,802	-	102,777	-	-	-	89,794	-	85,263	-
<b>DEWIND</b>										
20 MW	<b>57,463</b>	-	-	-	<b>57,406</b>	-	-	53,318	-	-
30 MW	<b>87,065</b>	-	-	-	<b>86,108</b>	-	-	79,977	-	-
40 MW	<b>116,667</b>	-	-	-	114,811	-	-	106,636	-	-
<b>GE</b>										
20 MW	-	-	-	53,161	-	-	55,317	-	<b>58,344</b>	49,951
30 MW	-	-	-	79,742	-	-	85,103	-	84,274	74,927
40 MW	-	-	-	108,739	-	-	<b>114,889</b>	-	110,205	99,902
<b>BONUS</b>										
20 MW	42,626	-	-	-	48,450	47,009	-	-	-	-
30 MW	64,585	-	-	-	72,676	72,081	-	-	-	-
40 MW	86,544	-	-	-	96,901	97,152	-	-	-	-

Note: Green, blue, and red colours indicate maximum, second maximum and third maximum energy production from wind farms of different installed capacities.

## 7.7 ENERGY YIELD FROM VESTAS VT100 2.75MW WIND TURBINE AT ALL THE LOCATIONS

In order to have an idea of energy yield at all the locations under investigation, an efficient wind turbine VT100 of 2.75MW from Vestas with 100m diameter and 100m hub height was used to get the annual energy yield. The cut-in-wind speed of this turbine was 2m/s and the cut-out speed was 25m/s. The wind power curve of the chosen wind turbine is shown in Figure 7.39. The wind speed at hub height was obtained using the 1/7 wind power law and is compared in Figure 7.40 for all the stations. The long-term annual mean wind speed was between 5 and 6m/s at Al-Jouf, AL-Wejh, Arar, Guriat, Rafha, Turaif and Qaisumah in the northern region and Jeddah, Taif and Yanbo in the western region and Dhahran on the east coast. At the rest of the stations, the annual mean wind speed at hub height was more than 4m/s with the exception of Bisha, Makkah and Nejran where it was less than 4m/s, as can be seen from Figure 7.40.

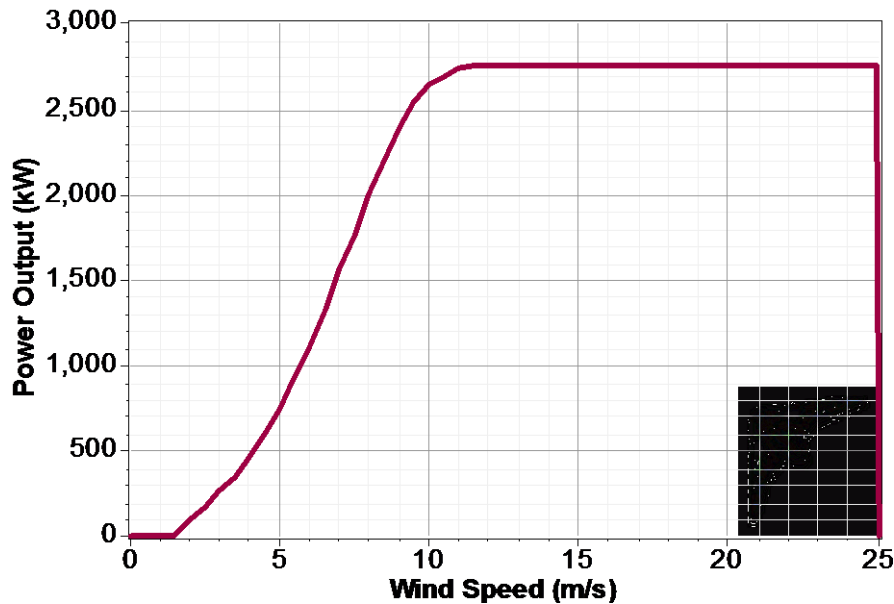


Figure 7.39 Wind power curve for Vestas VT100 2.75MW wind turbine

The net (after losses, i.e. downtime = 6%, array = 5%, icing = 4%, and others = 4%) annual energy yield from the chosen wind turbine at a hub height of 100m was more than 7 000MWh at Al-Wejh, Guriat, Qaisumah, Turaif, Dhahran and Yanbo, as shown in Figure 7.41. Most of these stations are in the north-eastern region and Al-Wejh and Yanbo in the north-western coastal region. At Al-Jouf, Arar, Rafha and Jeddah the net annual energy yield was little more than 6 000MWh. At Al-Ahsa, Gizan, Hafr, Sulayel, Taif and Wadi-Al-Dawasser, the annual energy yield was found to be between 5 000 and 6 000MWh. The plant capacity factor (PCF) was found to vary between a minimum of 4% and a maximum of 35% corresponding to Makkah and Dhahran, respectively, as shown in Figure 7.42. At Al-Wejh, Guriat, Turaif and Yanbo the annual mean PCF was between 30 and 35% while it varied from 25 to 30% at Al-Jouf, Arar, Jeddah, Qaisumah and Rafha. The PCF was found to vary from 20 to 25% at Al-Ahsa, Gizan, Hafr Al-Batin, Riyadh, Sulayel, Taif and Wadi-Al-Dawasser.

The percentage duration during which the wind turbine remained idle or with zero energy yield was always much less than 5% for most of the locations but between 5 to 10% at Al-Ahsa, Bisha, Gassim, Hafr Al-Batin, Qaisumah, Rafha, Riyadh, Sharourah and Tabouk, as shown in Figure 7.43. The percentage duration during which the wind turbine produced the rated output was almost negligible, as can be seen from Figure 7.43.

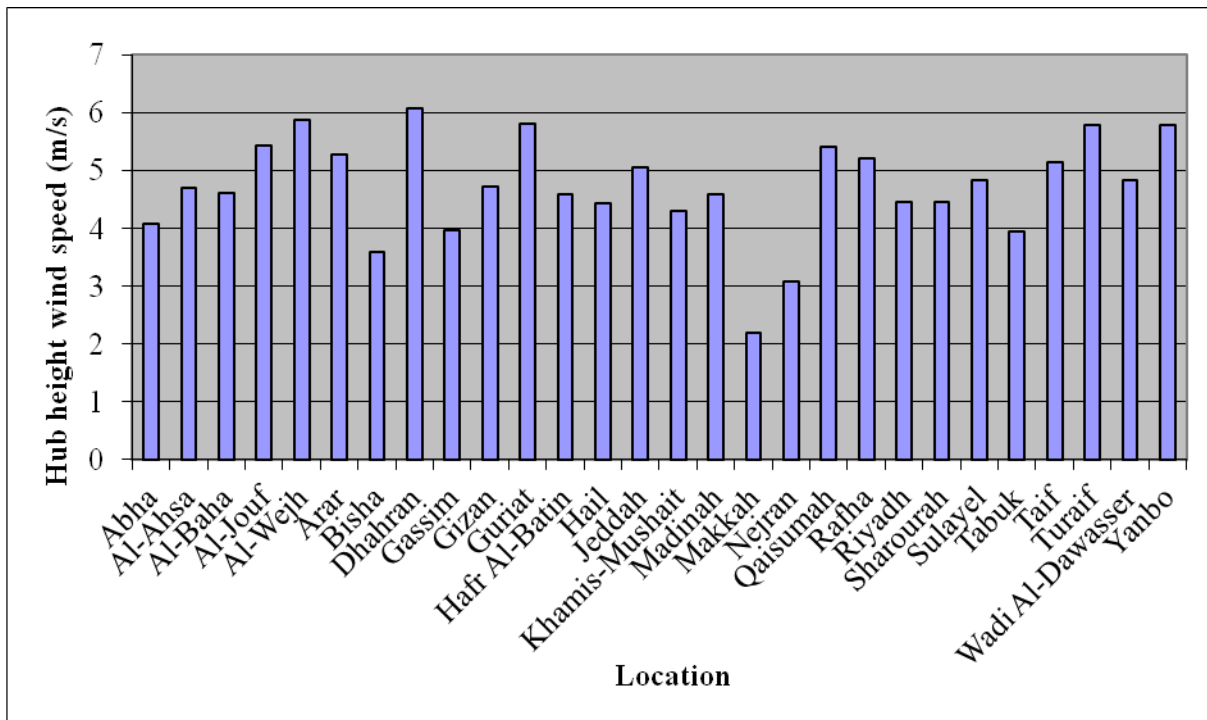


Figure 7.40 Wind speed at hub height of 100m at all the stations

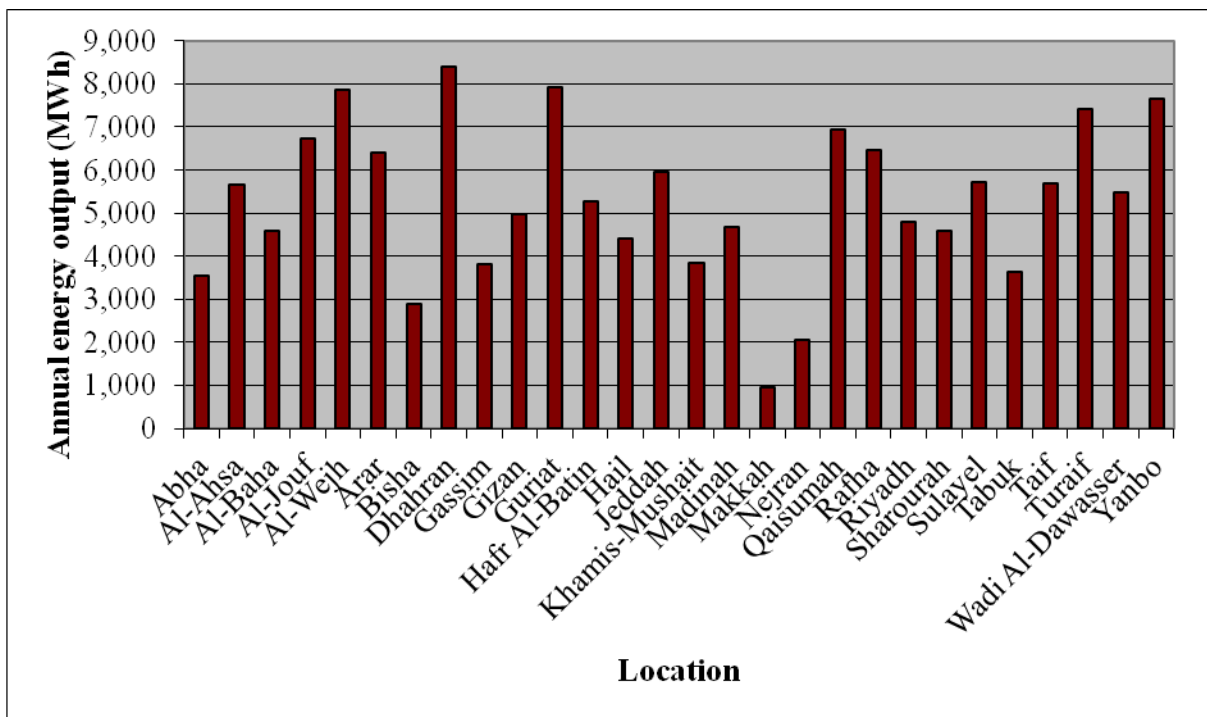


Figure 7.41 Annual energy yield from Vestas 2.75MW wind turbine at all the stations

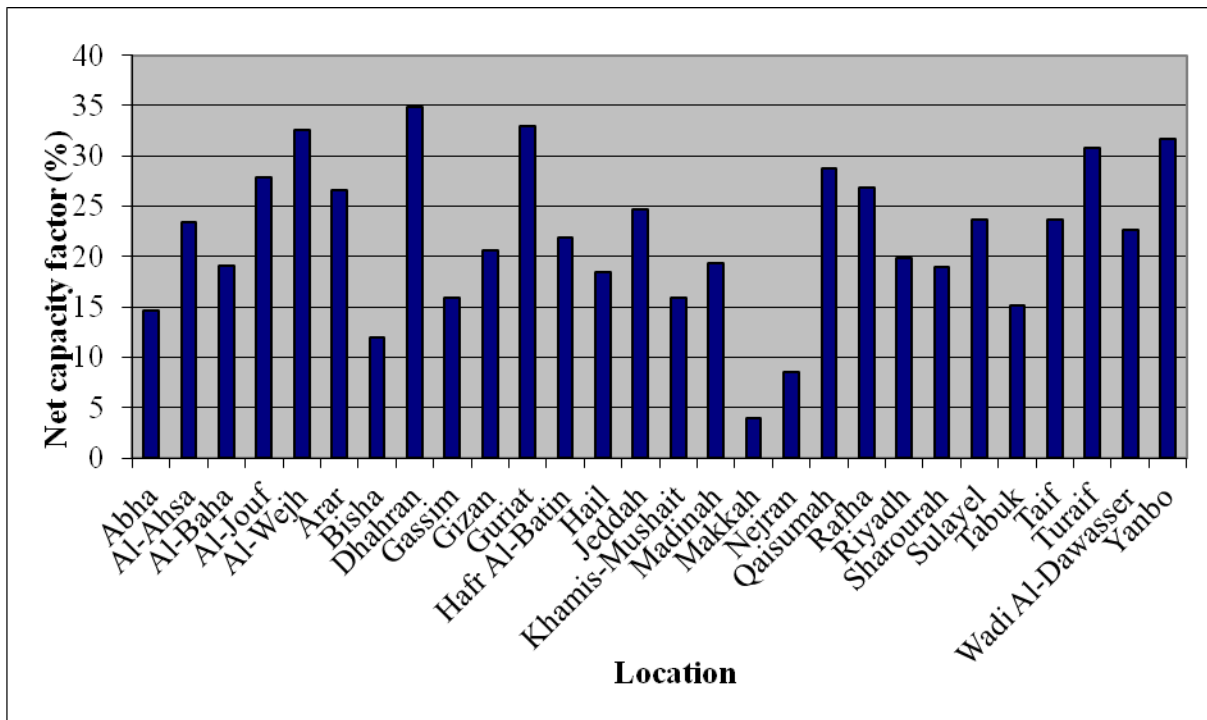


Figure 7.42 Annual mean plant capacity factor at all the locations

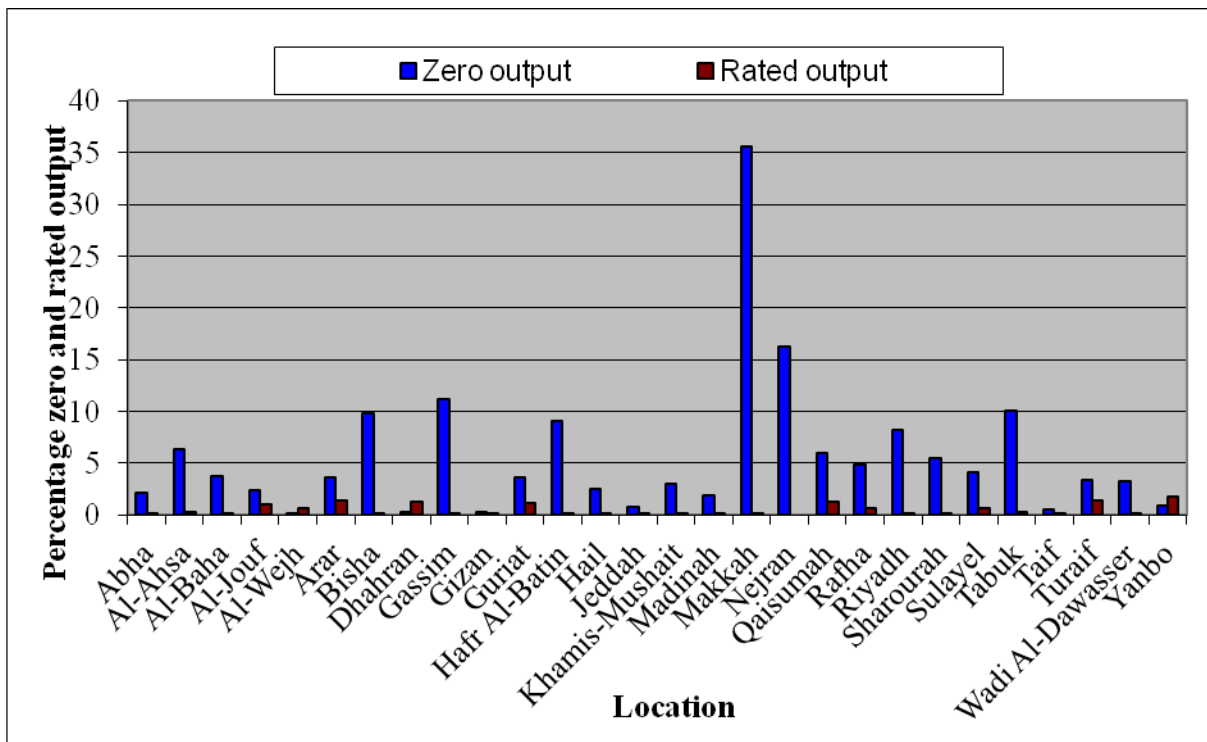


Figure 7.43 Percentages of rated and zero output at all the stations

## 7.8 SUMMARY

The analysis presented in this chapter can be summed up as follows:

1. Based on energy yield from a single machine, it is recommended that wind machines of sizes ranging between 600 and 1 000kW should be used for wind farm development if commercially available. In case of unavailability, WECSs of 1 300 or 1 500 may be considered.
2. Based on the hub height effect on energy production, it is recommended that a maximum of 60m of hub-height should be used for wind farm development. The maximum increase of about 8% was obtained for a change of hub height from 50 to 60metre while further increase in hub-height from 60 to 70metre produced only 4% more of electricity. The increase in energy production was found to be only 3% for a further increase of 10metre in hub height.
3. An empirical correlation was proposed for the estimation of near-optimal hub height using local wind shear exponent for a chosen wind turbine of 1 000kW rated capacity. This correlation could be used for other locations and wind turbine sizes but it is advisable to repeat this exercise for each turbine size.
4. Relatively higher values of PCF were obtained for WECSs of smaller sizes. The plant capacity analysis also showed that a maximum increase of 2.12% in PCF was found for an increase in hub height from 50 to 60metre while less than 1% in other cases except for a 60 to 70metre increase in hub height where it was 1.17%.
5. The net annual energy yield from the chosen wind turbine at a hub height of 100m was more than 7 000MWh at Al-Wejh, Guriat, Qaisumah, Turaif, Dhahran and Yanbo. At Al-Jouf, Arar, Rafha and Jeddah, the net annual energy yield was little more than 6 000MWh. At Al-Ahsa, Gizan, Hafr, Sulayel, Taif and Wadi-Al-Dawasser, the annual energy yield was found to be between 5 000 and 6 000MWh.
6. The plant capacity factor (PCF) was found to vary between a minimum of 4% and a maximum of 35% corresponding to Makkah and Dhahran, respectively. At Al-Wejh, Guriat, Turaif and Yanbo the annual mean PCF was between 30 and 35% while it varied from 25 to 30% at Al-Jouf, Arar, Jeddah, Qaisumah and Rafha. The PCF was found to vary from 20 to 25% at Al-Ahsa, Gizan, Hafr-Al-Batin, Riyadh, Sulayel, Taif and Wadi-Al-Dawasser.

## CHAPTER 8

### WIND-PV-DIESEL HYBRID POWER SYSTEM

Saudi Arabia is a vast country and the population is spread all over. All the villages and remotely located populations are not connected to the national electricity grid. Electricity is provided to these dwellings through small isolated power generation systems based on diesel generators. These units are maintained and operated by local contractors. In order to maintain the regular power supply, additional units are kept for usage during breakdowns and sufficient quantities of diesel are also stored. It is difficult to provide skilled manpower in such remote areas and maintain a regular and sufficient supply of diesel fuel. Therefore, in order to reduce the dependency on diesel generating sets and offset some of the green house gases, hybrid power systems are being sought for such areas. The present study is a unique and pioneering attempt to design an optimal wind-pv-diesel (WPVD) hybrid power system (HPS) for a village known as Rawdat Ben Habbas (RBH).

This village is located in the north on the Jordan highway and is almost 700km away from Dammam, the major city in the region. The latitude, longitude and the altitude of the village are 29.14°N, 44.33°E and 443m above mean sea level, respectively. There are around 600 houses in the village, two schools, a primary health centre, police office and other public amenities. The population of the village is around 4 500 which keeps on varying depending upon the public holidays. Most of the people from this village work in military and other government sectors and hence live away from the village. The village is connected through a local isolated grid fed by a power station consisting of six diesel generators each of 1MW plate capacity. The Saudi Electricity Company (SEC), the major electric utility in Saudi Arabia, has embarked on partially powering such dwellings through wind and solar power. For RBH, SEC opted for a wind-pv-diesel hybrid option and gave the responsibility to the King Fahd University of Petroleum and Minerals to conduct the techno-economic feasibility study of such a hybrid system. The university took the responsibility and conducted wind measurements at 20, 30 and 40metres AGL using a 40-metre tower for around four years between September 2005 and April 2010.

The diesel power plant at RBH also provided hourly load data of the village for one complete year. The load data, the wind speed data, the technical data of wind turbines and the diesel generators, etc. were used as input into the HOMER software for the optimal design of a

hybrid power system for the village. The details of the HOMER, the input data, the hybrid power system components and finally the economic aspects are discussed in the next paragraphs. The schematic diagram of the proposed WPVD HPS is shown in Figure 8.1.

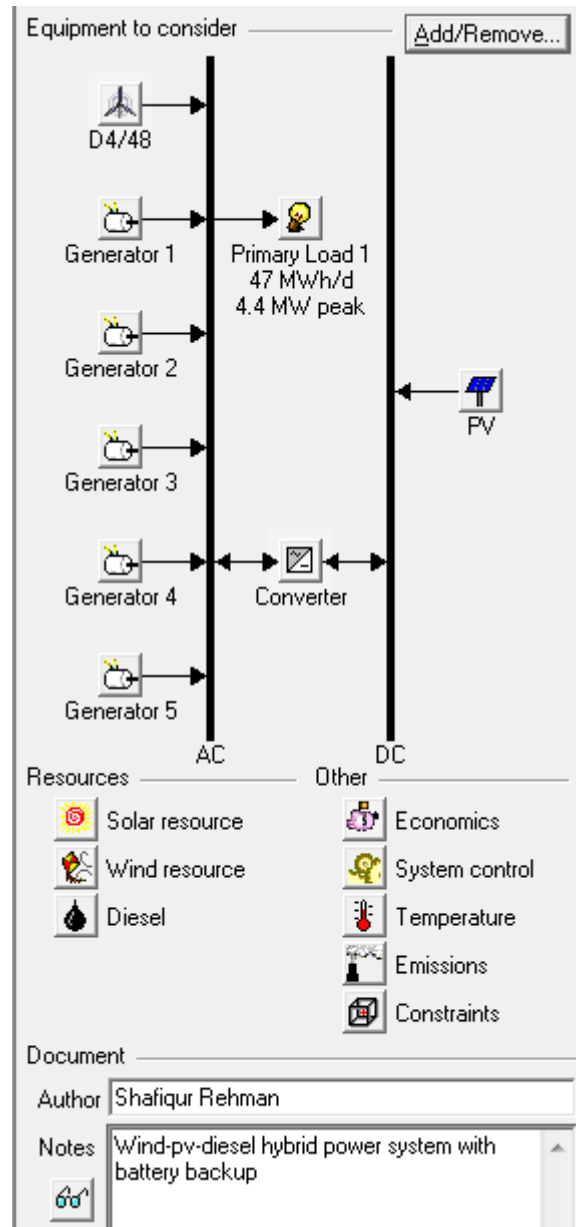


Figure 8.1 Wind-pv-diesel hybrid model used in the study

## 8.1 HYBRID POWER SYSTEM DESIGN TOOL

HOMER [303] is primarily an optimisation software package, which simulates varied renewable energy sources (RES) system configurations and scales them on the basis of net present cost (NPC). Net present cost is the total cost of installing and operating the system

over its lifetime. It firstly assesses the technical feasibility of the RES system (i.e. whether the system can adequately serve the electrical and thermal loads and any other constraints imposed by the user). Secondly, it estimates the NPC of the system. HOMER models each individual system configuration by performing an hourly time-step simulation of its operation for the duration of one year. The available renewable power is calculated and is compared with the required electrical load. Following calculations of one-year duration, any constraints on the system imposed by the user are then assessed, e.g. the fraction of the total electrical demand served or the proportion of power generated by renewable sources.

The calculation assesses all costs occurring within the project lifetime, including initial set-up costs (IC), component replacements within the project lifetime, maintenance and fuel. Future cash flows are discounted to the present. HOMER calculates NPC according to the following equation [303]:

$$\text{NPC} = \text{TAC}/\text{CRF} \quad (8.1)$$

where TAC is the total annualised cost (\$). The capital recovery factor (CRF) is given by [303]:

$$\text{CRF} = i(1+i)^N / ((1+i)^N - 1) \quad (8.2)$$

where N is the number of years and ‘i’ is the annual real interest rate (6% in the present case). HOMER assumes that all prices escalate at the same rate, and applies an ‘annual real interest rate’ rather than a ‘nominal interest rate’. NPC estimation in HOMER also takes into account salvage cost, which is the residual value of power system components at the end of the project lifetime. The equation to calculate salvage value (S) is

$$S(\$) = \text{Crep} (\text{Rrem}/\text{Rcomp}) \quad (8.3)$$

where Crep is the replacement cost of the component (\$), Rrem is the remaining life of the component (t) and Rcomp is the lifetime of the component (t). Annual savings are estimated by subtracting the annualised costs for each supply method from each other, giving the overall saving or loss for each year. Year 0 will have a negative figure because the initial cost (IC) of the hybrid RES exceeds that of the grid-only system. Finally, the annual savings are cumulatively summed to provide the cash flow for the duration of the project. Published

payback times for grid-connected small-scale systems range from seven years (IC aided by large rebates) [304] to 11.2 years [305], 15 years [306] and as high as 30 years [307].

## 8.2 METEOROLOGICAL DATA USED AS INPUT TO HOMER MODEL

Data was recorded every 10 minutes on a removable data storage card. The wind speed data was measured at 20, 30 and 40 metres' height above the ground. At each height, two sensors were installed. The surface air temperature ( $^{\circ}\text{C}$ ), relative humidity (%), surface station pressure (mbar), and global solar radiation (GSR,  $\text{W}/\text{m}^2$ ) data was also measured at 2 metres above ground surface level. The monthly mean wind speed was always above 6 m/s at 40m AGL except during September to November, as shown in Figure 8.2. The diurnal pattern of hourly mean wind speed in different months, especially during summer, coincides with the peak load demand of the village, as can be seen from Figure 8.3. Furthermore, the frequency distribution of wind speed in different wind speed bins confirmed the availability of wind above 4m/s at 40m AGL for 76% of the time during the year, see Figure 8.4. The monthly mean values of the GSR obtained using daily totals during each month are shown in Figure 8.5. April to September higher radiation intensities were observed with the highest in June and the lowest in December. Similarly, the monthly average diurnal profiles of GSR showed peak intensity around 12:00 during all the months of the year as can be seen from Figure 8.6.

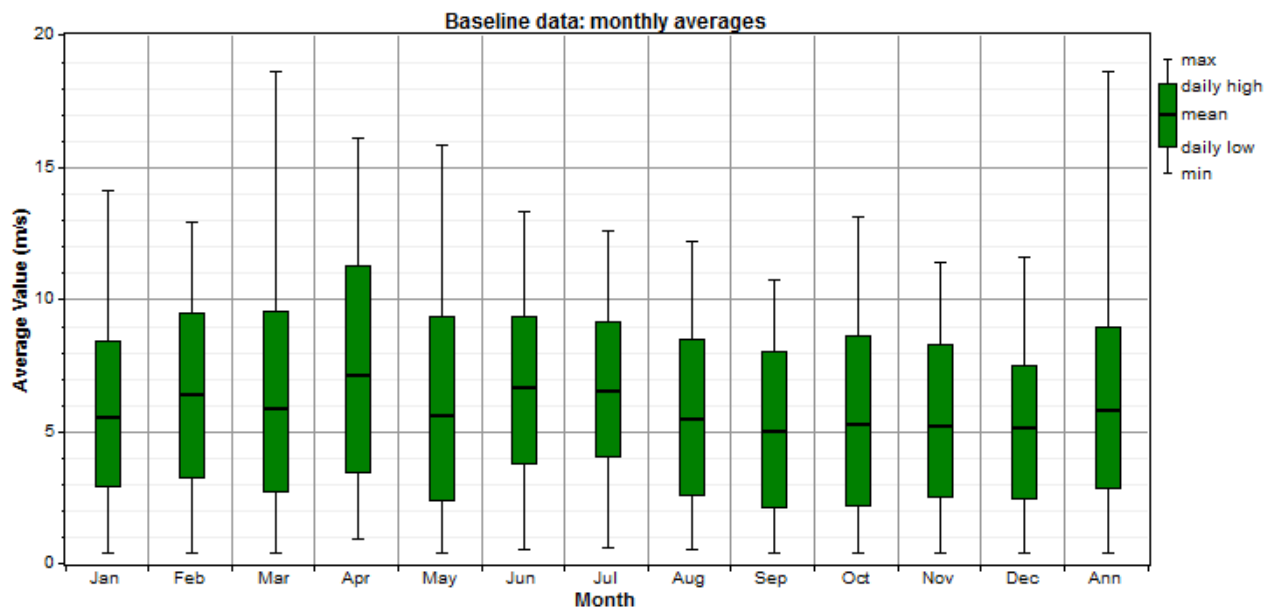


Figure 8.2 Monthly mean and extreme wind speed at 40metre AGL

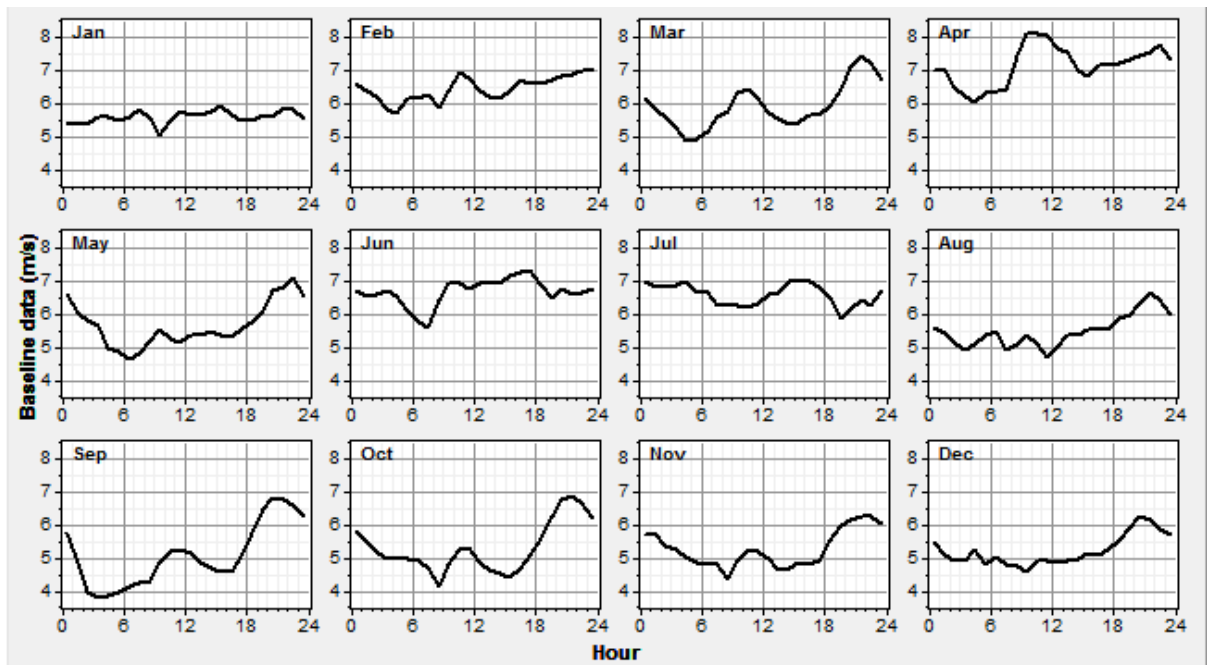


Figure 8.3 Diurnal variation of hourly mean wind speed at 40metre AGL

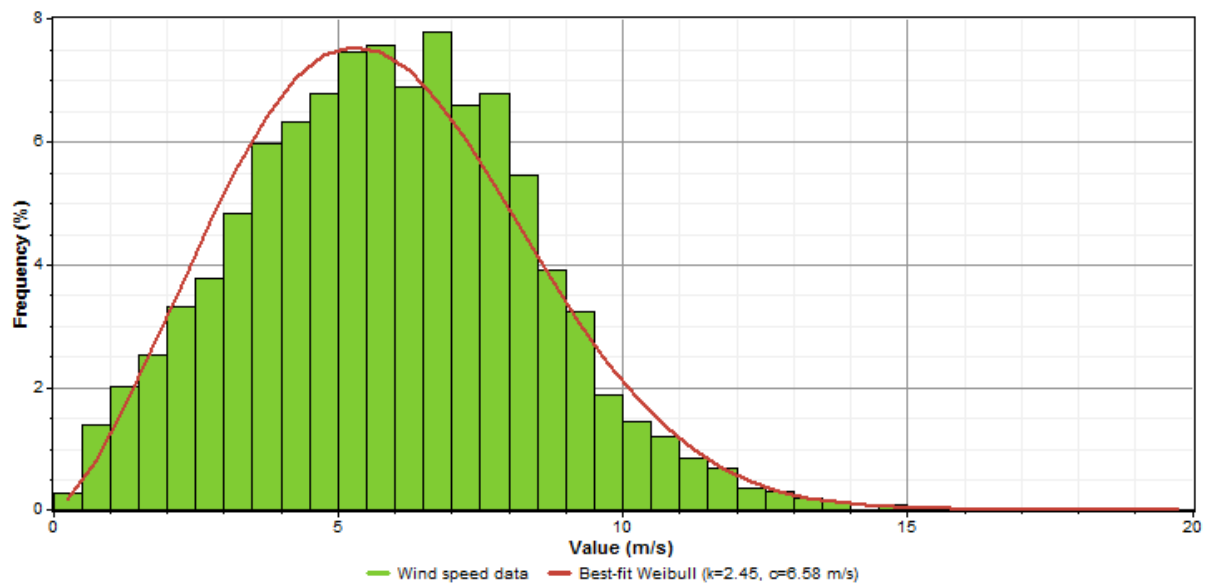


Figure 8.4 Frequency distribution of wind speed at 40metre AGL

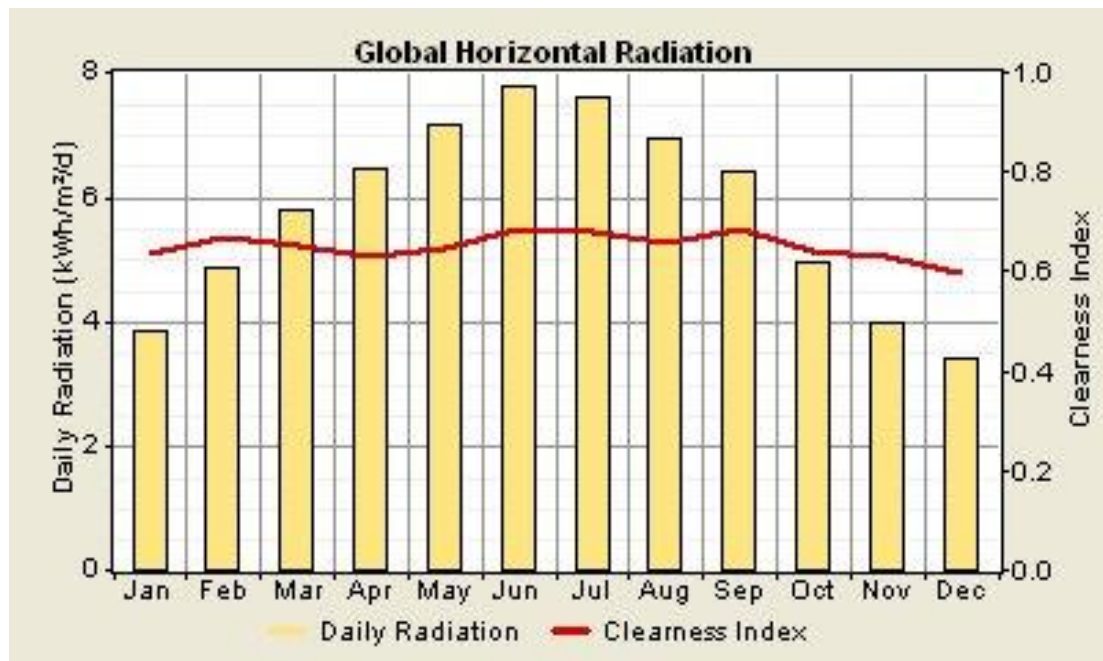


Figure 8.5 Monthly mean daily global solar radiation at the site

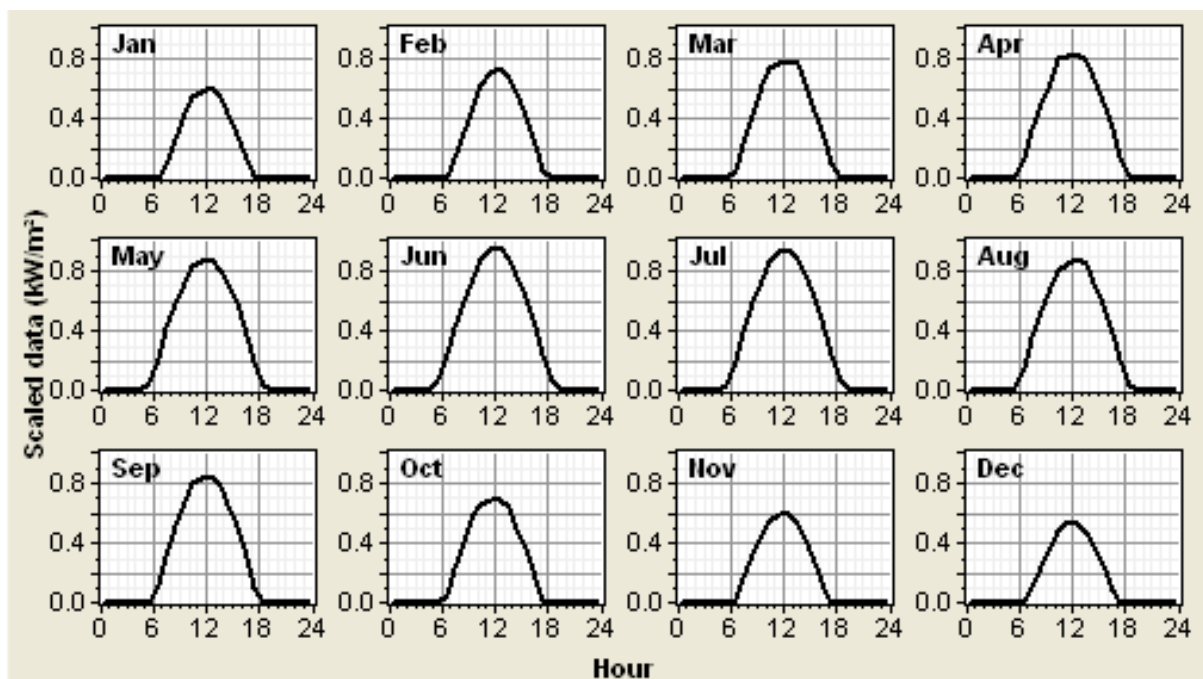


Figure 8.6 Diurnal variation of global solar radiation during different months

### 8.3 VILLAGE LOAD DATA USED AS INPUT TO HOMER MODEL

The hourly electrical load data for the year 2005 was obtained for the village and load analysis was conducted. The maximum value of the load recorded was 4.370MW and occurred on 14 July, 21 July, 31 July and 18 August 2005. The peak was recorded at 15:00

hours. The annual load factor for this area was 0.45. However, the monthly load factor varied between 0.49 in April (low demand) and 0.71 in August (high demand). Figure 8.7 shows the hourly load demand for the peak summer day (July 14, 2005). As evident from the graph, the demand increased during the daytime due to higher air-conditioning load. The average demand for the day was approximately 3.3MW. The load variation for a typical winter's weekday (January 03, 2005) is shown in Figure 8.8. As shown, the demand was much lower than that for the summer's day. The peak value for the day was only 1.8MW and was recorded in the evening. During January to February and November to December, the peak load appeared at around 18:00 hours while two peaks were observed during March and April at 00:00 and 14:00 hours, as shown in Figure 8.9. From June to October, the peak load was found to be around 14:00 with the highest load of more than 4 000kW during the month of August.

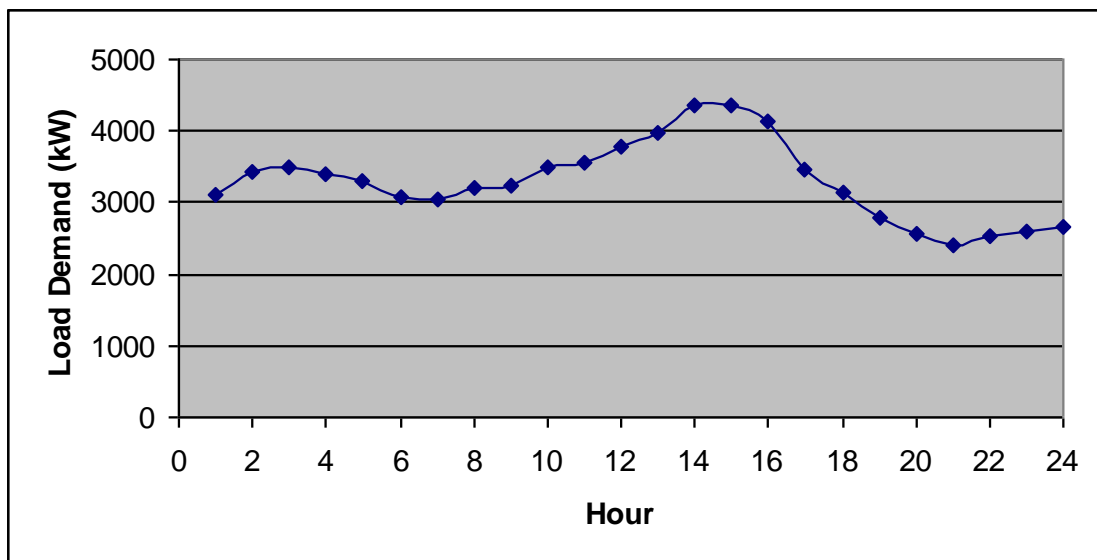


Figure 8.7 Typical summer's day load demand for the village (July 14, 2005)

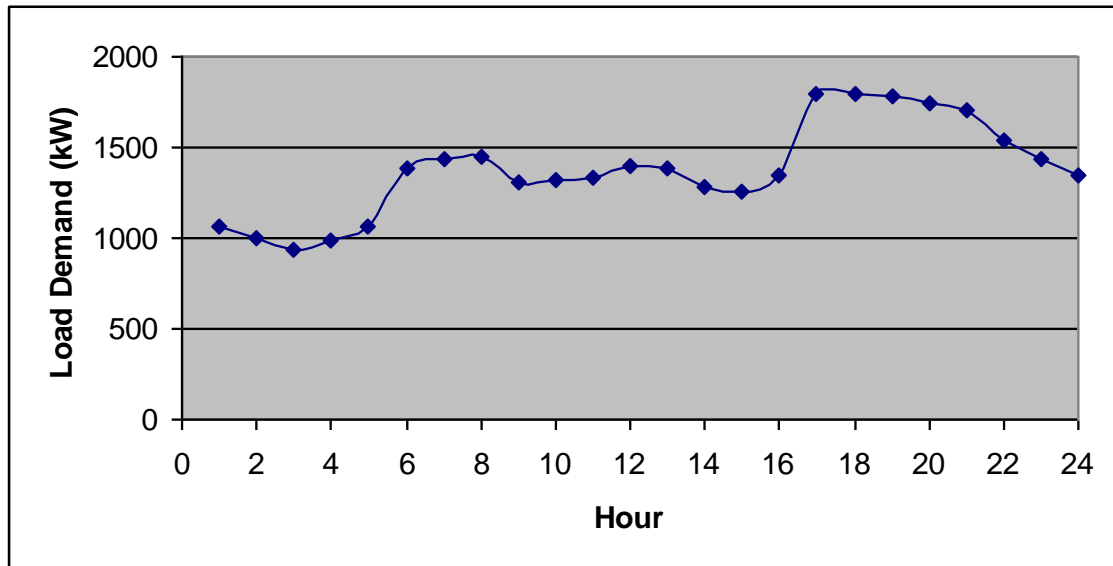


Figure 8.8 Typical winter's day load demand for the village (January 03, 2005)

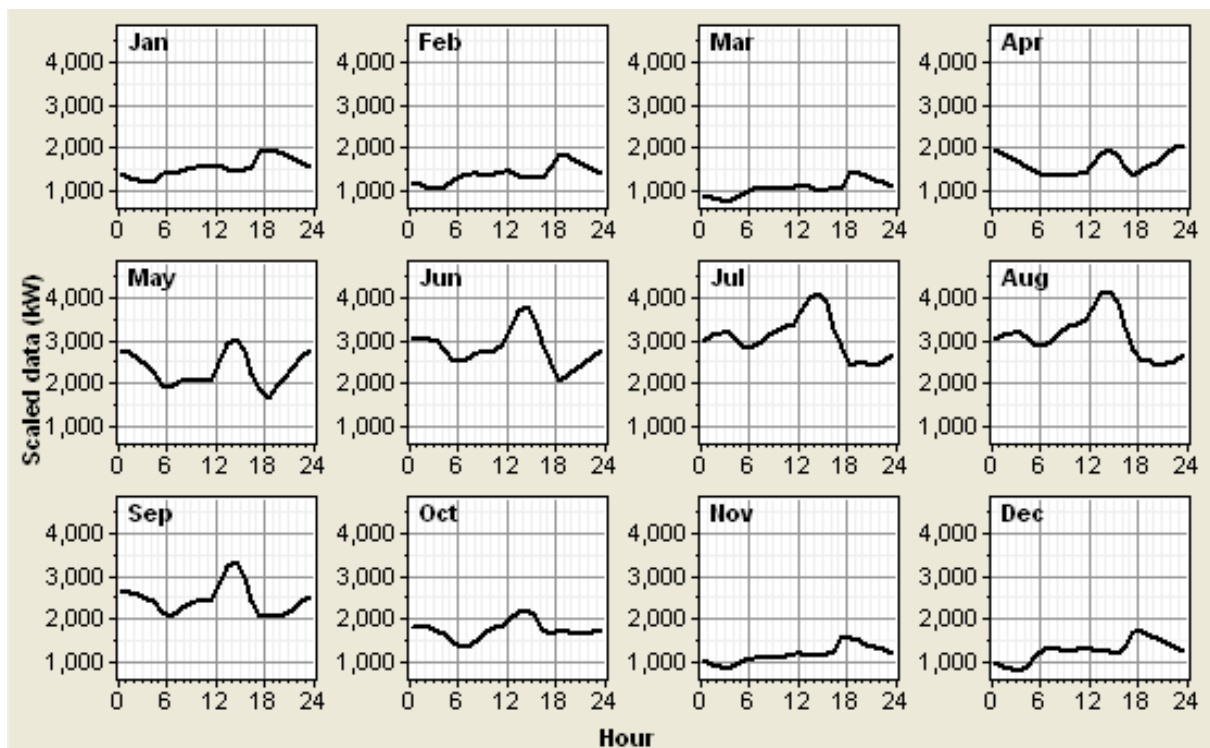


Figure 8.9 Diurnal variation of load during different months of the year

#### 8.4 HYBRID SYSTEM INPUT PARAMETERS

The main input data includes the hourly mean wind speed, hourly total solar radiation and load data, technical specifications and cost data of diesel generators, wind turbines, photovoltaic modules, power converters, system controls, economic parameters and system

constraints. The details of solar radiation and load data have been given above in the preceding paragraphs and the values of remaining data are given below:

### **Control parameters**

Minimum renewable energy fractions (MRF) considered = 0%, 20% and 40%

Annual real interest rate = 6%

Plant working lifespan = 20 years

Diesel price considered (US\$/l) = 0.2, 0.4, 0.6, 0.8 and 1.0

Operating reserve: As percentage of load, hourly load = 10%

As percentage of renewable output, solar power output = 5%

### **Wind turbines**

Wind turbine sizes considered (kW) = 0, 600, 600\*2, 600\*3

Cost of wind turbine (US\$/turbine) = 1 000 000

Cost of replacement of wind turbine (US\$/turbine) = 800 000

Operation and maintenance cost (US\$/turbine/year) = 12 000

Operation life of the wind turbine (Years) = 20

### **Photovoltaic modules**

Photovoltaic sizes considered (kW) = 0 and 1 000

Cost of photovoltaic array (US\$/kW) = 3 500

Replacement cost of photovoltaic array (US\$/kW) = 3 500

Operation and maintenance cost of PV array (US\$/kW/year) = 25

Photovoltaic modules were considered as fixed

Working life of photovoltaic panels (years) = 20

### **Power converter**

Power converter sizes considered (kW) = 0 and 500

Cost of power converter (US\$/kW) = 900

Replacement cost of power converter (US\$/kW) = 900

Operation and maintenance cost of power converter (US\$/kW/year) = 0

Working lifespan of power converter (years) = 15

Inverter efficiency (%) = 90

### **Diesel generators**

Generator 1 sizes considered (kW) = 0 and 1 120

Generator 2 sizes considered (kW) = 0 and 1 120

Generator 3 sizes considered (kW) = 0 and 1 120

Generator 4 sizes considered (kW) = 0 and 1 120

Generator 5 sizes considered (kW) = 0 and 1 120

Lifetime operating hours (hours) = 20 000

Minimum load ratio (%) = 30

Capital cost (US\$/kW) = 1 521

Replacement cost (US\$/kW) = 1 521

Operation and maintenance cost (US\$/hour) = 0.012

## **8.5 DISCUSSION AND SPECIFICATIONS**

Based on the above input, a total of 276 480 runs were made, which consisted of 540 sensitivities and 512 simulations for each sensitivity run. A high-speed computer, Pentium D, with 3.2GHz speed and 2GB ram took 40 minutes and 27 seconds to complete the required simulation. The HOMER suggested an optimal wind-pv-diesel hybrid power system for the village with three wind turbines each of 600kW (26% wind penetration), 1 000kWp pv panels (9% solar energy penetration); five generators with rated power of 1 120 each, and 500kW-sized power converter. The suggested optimal hybrid power system was found to have a capital cost of US\$13 764 080 with an annual operating cost of US\$2 408 521, total net present cost (NPC) of US\$41 389 628 and levelised cost of energy (COE) of 0.212US\$/kWh, as shown in Table 8.1. The diesel-only power system was found to be the most uneconomical power system (COE 0.232US\$/kWh) even at a diesel price 0.2US\$/l. The energy output and

the economic analysis of the proposed hybrid systems and the related sensitivity analysis are provided in the following paragraphs.

Table 8.1 Optimal wind-pv-diesel hybrid power system for the village

	PV (kW)	D4/48	G1 (kW)	G2 (kW)	G3 (kW)	G4 (kW)	G5 (kW)	Conv. (kW)	Initial Capital	Operating Cost (\$/yr)	Total NPC	COE (\$/kWh)	Ren. Frac.	Diesel (L)	G1 (hrs)	G2 (hrs)	G3 (hrs)
		3	1120	1120	1120	1120			\$ 9,814,080	2,605,263	\$ 39,696,244	0.203	0.27	4,907,834	8,571	6,718	2,98
		3	1120	1120	1120		1120		\$ 9,814,080	2,605,263	\$ 39,696,244	0.203	0.27	4,907,834	8,571	6,718	2,98
		3	1120	1120		1120	1120		\$ 9,814,080	2,691,583	\$ 40,686,324	0.208	0.27	4,907,834	8,571	6,718	
		3	1120		1120	1120	1120		\$ 9,814,080	2,691,583	\$ 40,686,324	0.208	0.27	4,907,834	8,571		6,71
		3		1120	1120	1120	1120		\$ 9,814,080	2,691,583	\$ 40,686,324	0.208	0.27	4,907,834		8,571	6,71
		3	1120	1120	1120	1120	1120		\$ 11,517,600	2,565,658	\$ 40,945,496	0.209	0.27	4,914,286	8,571	6,718	2,98
		2	1120	1120	1120	1120			\$ 8,814,080	2,817,480	\$ 41,130,352	0.210	0.18	5,339,599	8,756	7,271	3,41
		2	1120	1120	1120		1120		\$ 8,814,080	2,817,480	\$ 41,130,352	0.210	0.18	5,339,599	8,756	7,271	3,41
	1000	3	1120	1120	1120	1120		500	\$ 13,764,080	2,408,521	\$ 41,389,628	0.212	0.36	4,485,265	8,427	6,082	2,75
	1000	3	1120	1120	1120		1120	500	\$ 13,764,080	2,408,521	\$ 41,389,628	0.212	0.36	4,485,265	8,427	6,082	2,75
		2	1120	1120		1120	1120		\$ 8,814,080	2,916,170	\$ 42,262,316	0.216	0.18	5,339,599	8,756	7,271	
		2	1120		1120	1120	1120		\$ 8,814,080	2,916,170	\$ 42,262,316	0.216	0.18	5,339,599	8,756		7,27
		2		1120	1120	1120	1120		\$ 8,814,080	2,916,170	\$ 42,262,316	0.216	0.18	5,339,599		8,756	7,27
	1000	3	1120	1120		1120	1120	500	\$ 13,764,080	2,488,035	\$ 42,301,648	0.216	0.36	4,485,265	8,427	6,082	
	1000	3	1120		1120	1120	1120	500	\$ 13,764,080	2,488,035	\$ 42,301,648	0.216	0.36	4,485,265	8,427		6,08
	1000	3		1120	1120	1120	1120	500	\$ 13,764,080	2,488,035	\$ 42,301,648	0.216	0.36	4,485,265		8,427	6,08
		2	1120	1120	1120	1120	1120		\$ 10,517,600	2,778,991	\$ 42,392,412	0.217	0.18	5,347,125	8,756	7,271	3,41
	1000	3	1120	1120	1120	1120	1120	500	\$ 15,467,600	2,362,492	\$ 42,565,192	0.218	0.36	4,485,533	8,427	6,082	2,75
	1000	2	1120	1120	1120	1120		500	\$ 12,764,080	2,611,454	\$ 42,717,252	0.219	0.27	4,907,984	8,709	6,596	3,17
	1000	2	1120	1120	1120		1120	500	\$ 12,764,080	2,611,454	\$ 42,717,252	0.219	0.27	4,907,984	8,709	6,596	3,17
	1000	2	1120		1120	1120	1120	500	\$ 12,764,080	2,703,348	\$ 43,771,268	0.224	0.27	4,907,984	8,709	6,596	
	1000	2	1120		1120	1120	1120	500	\$ 12,764,080	2,703,348	\$ 43,771,268	0.224	0.27	4,907,984	8,709	6,596	
	1000	2		1120	1120	1120	1120	500	\$ 12,764,080	2,703,348	\$ 43,771,268	0.224	0.27	4,907,984		8,709	6,59
	1000	2	1120	1120	1120	1120	1120	500	\$ 12,764,080	2,703,348	\$ 43,771,268	0.224	0.27	4,907,984		8,709	6,59
		1	1120	1120	1120	1120	1120		\$ 9,517,600	2,991,013	\$ 43,824,288	0.224	0.09	5,819,484	8,759	7,914	3,76
	1000	2	1120	1120	1120	1120	1120	500	\$ 14,467,600	2,565,424	\$ 43,892,808	0.225	0.27	4,909,253	8,709	6,596	3,17

### 8.5.1 Energy yield analysis

The proposed wind-pv-diesel hybrid system was able to meet the energy requirement of the village with 35% of renewable energy penetration (wind power = 26% and solar power = 9%) into the existing diesel-only power system with average wind speed of 5.85m/s and global solar radiation of 5.75kWh/m<sup>2</sup>/d. Table 8.2 summarises the energy contribution by wind, solar-pv system and the existing four generators. As can be seen from this table, 65% of the energy is supplied by the diesel generators and the remaining 35% by the wind and solar-pv system. The proposed 35% wind and solar-pv hybrid power penetration system was found to be optimal in terms of excess energy, i.e. only 4.1% or 734 606kWh of the energy was in excess.

Table 8.2 Energy contribution of different energy sources at annual mean wind speed and global solar radiation of 5.85m/s and 5.75kWh/m<sup>2</sup>/d, respectively

Item description	Wind	PV	Diesel generating units			
			G1	G2	G3	G4
Rated capacity, kW	1,800	1,000	1,120	1,120	1,120	1,120
Percentage contribution, %	26	9.7	64.3			
Capacity factor, %	29.9	18.9	69.8	34.9	10.9	2.0
Mean output power, kW	538	189	813	564	387	337
Annual energy output, (MWh)	4,713.7	1,653.5	6,851.2	3,427.7	1,066.4	197.3
Annual hours of operations	8,310	4,382	8,427	6,082	2,758	585

The monthly mean power contribution of pv systems to the hybrid power system remains almost the same with a slight variation of maximum and minimum of 194.7kW and 173.8kW in September and December, respectively, as shown in Figure 8.10. However, the wind power contribution varied between a maximum of 805kW in April and a minimum of 387kW in September. The wind power contribution during February to April was almost the same as that of diesel. The total power generated by all the generators (Gen) was found to be the maximum in August and the minimum in March.

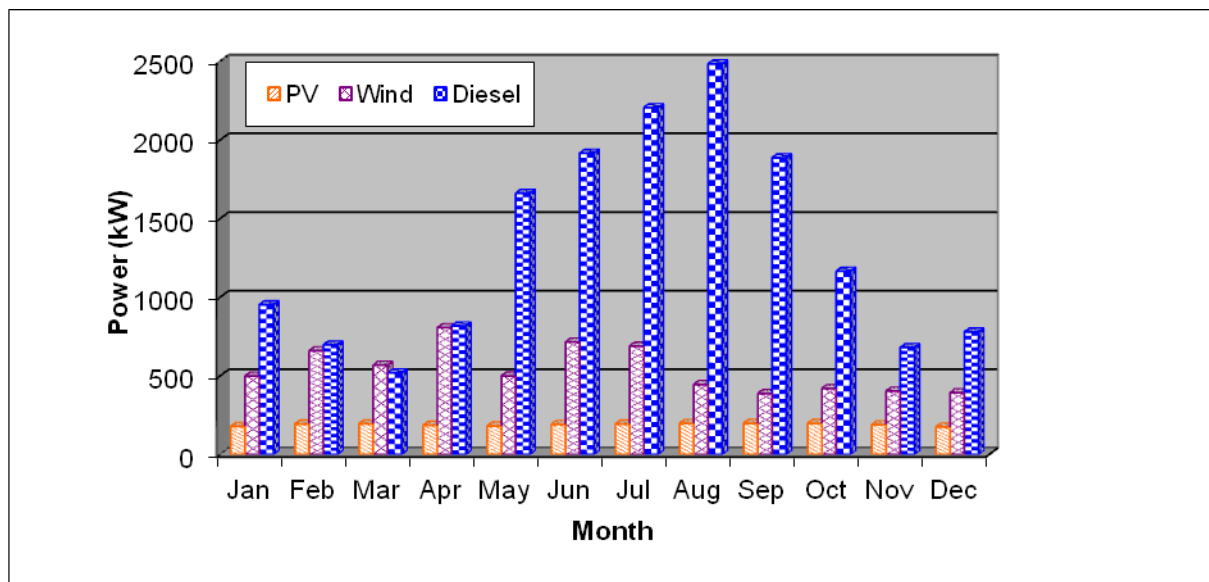


Figure 8.10 Monthly mean power contribution by wind, solar-pv and diesel systems

### 8.5.2 Greenhouse gas (GHG) emissions

The proposed wind-pv-diesel hybrid power system with 35% renewable energy penetration could avoid addition of 4 976.8 tons of GHG equivalent of CO<sub>2</sub> annually into the local atmosphere of the village under consideration. Furthermore, during the lifetime of the hybrid power plant, a total of 99 536 tons of GHG could be avoided from entering into the atmosphere of the village, which will further improve the health of the local inhabitants and result in reduction of their medical bills. The reduction in the quantity of different air pollutants for 35% renewable energy penetration compared with that of diesel-only power plant is given in Table 8.3. A 29% decrease in each pollutant is noticed for a 35% RE penetration into the existing diesel-only power system.

Table 8.3 Annual GHG emissions from diesel-only and hybrid power systems

Pollutant	Emissions (kg/yr)	
	Diesel only	35% RE Penetration
Carbon dioxide	16,657,316	11,811,177
Carbon monoxide	41,116	29,154
Unburnt hydrocarbons	4,554	3,229
Particulate matter	3,100	2,198
Sulphur dioxide	33,451	23,719
Nitrogen oxides	366,883	260,145
<b>Total GHG</b>	<b>17,106,420</b>	<b>12,129,622</b>

### 8.5.3 Economic analysis

The total cost of each component of the hybrid power systems, including the wind turbines, pv panels, four generators, and a power converter, is shown in Figure 8.11 and the breakup is of capital, replacement, operation and maintenance, fuel and salvage costs is given in Table 8.4 and the corresponding annualised costs are summarised in Table 8.5. It is evident that diesel generating sets account for bulk of the total net present cost (NPC) and the converter accounts for the least. The capital cost of the proposed hybrid power system was worked out to be US\$13 764 080 with replacement, operation and maintenance, and fuel cost of US\$15 233 948, US\$3 451 656 and US\$10 289 131, respectively. The annualised capital cost of wind turbines was US\$266 154, for pv panels it was US\$305 146 while that for diesel units, it was US\$594 084. However, the corresponding operation and maintenance costs were

US\$36 000, US\$25 000 and US\$239 931. Furthermore, the annualised fuel cost for diesel sets was US\$897 053 and zero in the case of wind and pv systems.

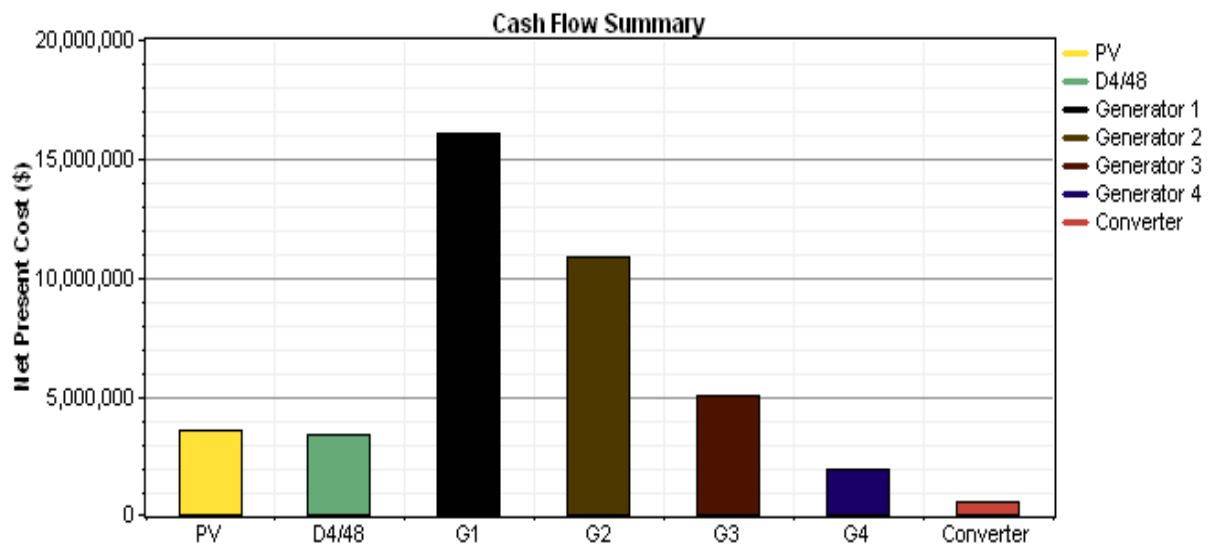


Figure 8.11 Cash flow summary of various components of the hybrid power system

Table 8.4 Summary of various costs related to the wind-pv-diesel hybrid system

Component	Capital (\$)	Replacement (\$)	O&M (\$)	Fuel (\$)	Salvage (\$)	Total (\$)
PV	3,500,000	0	286,748	0	-218,264	3,568,485
D4/48	3,000,000	0	412,917	0	0	3,412,917
Generator 1	1,703,520	7,686,923	1,299,071	5,661,295	-304,358	16,046,451
Generator 2	1,703,520	5,511,115	937,576	3,215,963	-487,610	10,880,563
Generator 3	1,703,520	1,848,143	425,162	1,178,456	-128,542	5,026,739
Generator 4	1,703,520	0	90,181	233,416	-116,857	1,910,261
Converter	450,000	187,769	0	0	-93,542	544,228
System	13,764,080	15,233,948	3,451,656	10,289,131	-1,349,172	41,389,640

Table 8.5 Summary of annualised cost of the hybrid power system

Component	Capital (\$/yr)	Replacement (\$/yr)	O&M (\$/yr)	Fuel (\$/yr)	Salvage (\$/yr)	Total (\$/yr)
PV	305,146	0	25,000	0	-19,029	311,117
D4/48	261,554	0	36,000	0	0	297,554
Generator 1	148,521	670,181	113,259	493,578	-26,535	1,399,003
Generator 2	148,521	480,484	81,742	280,382	-42,512	948,617
Generator 3	148,521	161,130	37,068	102,743	-11,207	438,254
Generator 4	148,521	0	7,862	20,350	-10,188	166,545
Converter	39,233	16,371	0	0	-8,155	47,448
System	1,200,015	1,328,165	300,931	897,053	-117,627	3,608,538

Furthermore, each MWh of electricity produced from renewable sources results in conservation of about 1.7 barrels of fuel, which means a revenue earning of US\$136 at US\$80, per barrel price of the fossil fuel. In the present case, the wind-pv system contributes 6 367.2MWh electricity, which means a saving of 10 824 barrels of fuel and hence a foreign earning of US\$865 939 annually. In 20 year's time, the integration of the wind-pv system into the existing diesel-only system can result in revenue savings of more than US\$17 million. Additionally, the utilization of renewable energy sources will also result in earning carbon credits of around US\$20 for each ton of GHG being avoided from entering into the atmosphere. In the present scenario, a total of US\$99 536 could be earned annually as a result of avoidance of 4 976.8 tons of GHG from entering into the local atmosphere. Over the lifetime of the hybrid power plant, around two million dollars could be collected as part carbon credit benefit.

#### 8.5.4 Sensitivity analysis

The contribution of wind and solar energy to the hybrid energy system depends on the intensity and the duration of availability of the respective sources of energy. For annual mean GSR of 5.75kWh/m<sup>2</sup>/d and annual solar energy contribution of 9%, i.e. 1 653.5MWh, the wind energy contribution at a wind speed of 4.5m/s was 13% while at 5.0m/s it was 18%, as given in Table 8.6. It is evident from this table that for every 0.5m/s increase in wind speed, there is an increase of 5% in wind energy contribution to the hybrid power system. Similarly, the COE decreased linearly and the overall achievable renewable energy fraction (REF) increased linearly as observed from Columns 5 and 7 of Table 8.6.

Table 8.6 Effect of annual mean wind speed (WS) on wind energy (WE) contribution, excess energy, COE, diesel consumed, REF achieved and total running hours for annual mean GSR of 5.75kWh/m<sup>2</sup>/d, annual mean solar energy of 1 653.48MWh and 9% contribution of solar energy in the wind-pv-diesel hybrid power system.

WS	WE	Excess Energy		COE	Diesel	REF	Running
(m/s)	(%)	(MWh/y)	(%)	(\$/kWh)	(1000L)	(%)	(Hours)
4.50	13	297.72	1.7	0.232	5168.9	22	19852
5.00	18	433.02	2.5	0.225	4934.8	27	19202
5.50	23	596.17	3.4	0.217	4671.2	32	18397
<b>5.85</b>	<b>26</b>	<b>734.61</b>	<b>4.1</b>	<b>0.212</b>	<b>4485.3</b>	<b>36</b>	<b>17852</b>
6.00	28	794.59	4.4	0.209	4400.2	37	17565
6.50	33	1008.15	5.6	0.201	4132.4	42	16734

The contribution of solar energy to the hybrid system with change in GSR was found to be minimal because for a change of 0.5kWh/m<sup>2</sup>/d in GSR intensity, only 1% increase in solar energy contribution was observed as can be seen from Table 8.7 and at higher values of GSR (>6.0 kWh/m<sup>2</sup>/d), no additional energy could be achieved. At lower values of GSR, the solar energy fraction contributed more towards the excess energy compared with wind energy contribution at lower wind speeds as can be cross-checked from Columns 3 and 4 in Tables 8.6 and 8.7 and vice versa. The diesel consumption and diesel generating set's running hours at designed GSR of 5.75kWh/m<sup>2</sup>/d were more at lower WS values and higher at WS greater than the designed WS of 5.85m/s as can be seen from Columns 6 and 8 of Tables 8.6 and 8.7. This simply means that wind energy contributes more efficiently to the proposed hybrid power system than solar energy.

The cost of the fuel, diesel in the present case, has a direct impact on the COE of a hybrid power system, as can be seen from Figure 8.12. It is evident that the wind-pv-diesel hybrid power system is always feasible compared with a diesel-only system for all price ranges of diesel fuel considered in the present study. The COE of a diesel-only system increases more rapidly than the COE of a hybrid power system with an increase in diesel price.

Table 8.7 Effect of annual mean global solar radiation (GSR) on solar energy (SE) contribution, excess energy, COE, diesel consumed, REF achieved and total running hours for a diesel price of 0.2US\$/l, annual mean WS of 5.85 m/s, annual mean wind energy of 1 653.48MWh and 27% contribution of wind energy in the wind-pv-diesel hybrid power system.

GSR (kWh/m <sup>2</sup> /d)	SE (%)	Excess Energy		COE (\$/kWh)	Diesel (1000L)	REF (%)	Running (Hours)
		(MWh/y)	(%)				
4.50	7	593.3	3.3	0.214	4565.8	34	18123
5.00	8	634.1	3.6	0.213	4528.7	34	18011
5.50	9	695.9	3.9	0.212	4498.1	35	17905
<b>5.75</b>	<b>9</b>	<b>734.6</b>	<b>4.1</b>	<b>0.212</b>	<b>4485.3</b>	<b>36</b>	<b>17852</b>
6.00	10	775	4.3	0.211	4473.8	36	17804
6.50	10	858.8	4.8	0.211	4455.5	36	17737

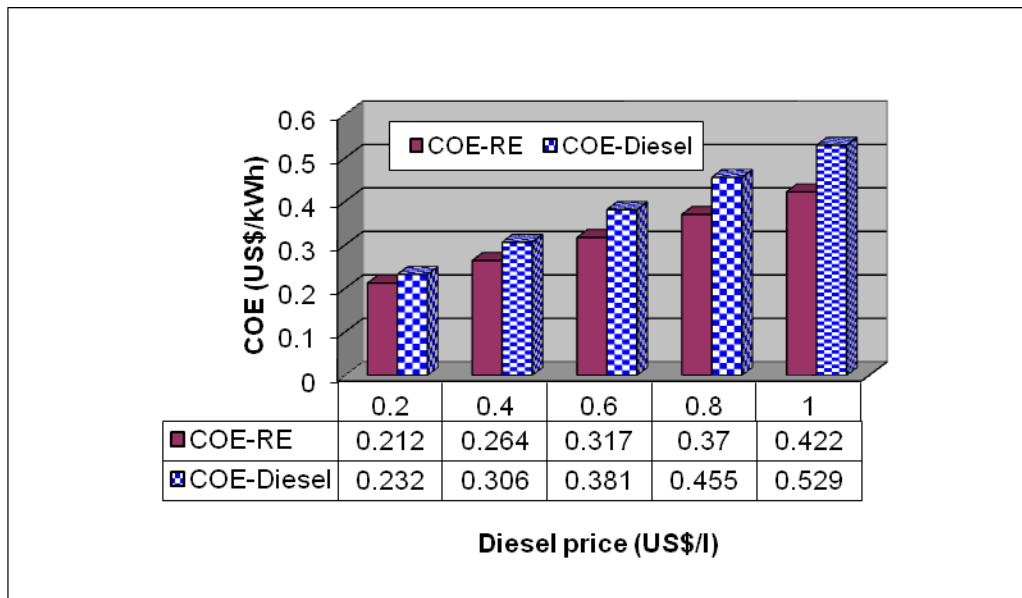


Figure 8.12 Effect of diesel price on COE of hybrid power system at annual average wind speed of 5.85m/s and global solar radiation of 5.75kWh/m<sup>2</sup>/d

## 8.6 SUMMARY

An attempt was made to explore the possibility of utilizing the power of the wind and sun to reduce the dependence on fossil fuel for power generation to meet the energy requirement of a small village, Rawdat Ben Habbas, located in the north-eastern part of Saudi Arabia. The wind-pv-diesel hybrid system with 35% renewable energy penetration (26% wind and 9% solar) and 65% diesel power contribution (five units of 1 120kW each) was found to be the most economical power system with COE of 0.212US\$/kWh at a diesel price of 0.2US\$/l. The COE for a diesel-only system at the same diesel price was found to be 0.232US\$/kWh, i.e. around 9.4% more than the hybrid system. The sensitivity analysis showed that for every 0.5m/s increase in wind speed, there was an increase of 5% in wind energy contribution to the hybrid power system and the COE decreased linearly and the overall achievable renewable energy fraction (REF) also increased linearly. Furthermore, the wind energy contributed more efficiently to the proposed hybrid power system than the solar-pv energy. Lastly, the COE of the diesel-only power system was found to be more sensitive to diesel price than the COE of the hybrid power system.

The proposed system will consist of three wind turbines each of 600kW, 1 000kW of pv panels, and four diesel generating sets each of 1 120kW rated power. The proposed system was able to meet the energy requirements (AC primary load of 17 043.4MWh/y) of the

village with 4.1% energy in excess. The annual contributions of wind, solar-pv and the diesel-generating sets were 4 713.7, 1 653.5, and 11 542.6MWh, respectively. The proposed hybrid power system will result in avoiding the addition of 4 976.8 tons of GHG equivalent of CO<sub>2</sub> gas into the local atmosphere of the village and will conserve 10 824 barrels of fossil fuel annually.

## CHAPTER 9

### WIND SPEED DATA ANALYSIS THROUGH WAVELETS AND FAST FOURIER TRANSFORM

Usually, most of the signals contain numerous non-stationary or transitory characteristics such as drift, trends, abrupt changes, and beginnings and ends of events. These characteristics are often the most important part of the signal and are needed to be analysed to understand physical phenomena hidden behind the signal. To study these characteristics, wavelets have been developed since the early eighties. Wavelet analysis methods allow the use of long time intervals where more precise low-frequency information is required, and shorter regions where high-frequency information is required. One major advantage afforded by wavelets is the ability to perform local analysis, that is, to analyse a localised area of a larger signal.

A plot of wavelet coefficients clearly shows the exact location at the time of the discontinuity. Wavelet analysis is capable of revealing aspects of data that other signal analysis techniques miss, aspects such as trends, breakdown points, discontinuities in higher derivatives, and self-similarity. Wavelet analysis can compress or denoise a signal without appreciable degradation. Wavelet analysis is the breaking up of a signal into shifted and scaled versions of the mother wavelet. Scaling a wavelet simply means stretching (or compressing) it. The wavelet transforms (wavelet coefficients) are functions of scale and position.

In plots, the  $x$ -axis represents a position along the signal (time), the  $y$ -axis represents scale, and the colour at each point represents the magnitude of the coefficient. Inspection of the continuous wavelet coefficient plot reveals patterns among scales and shows the signal's possibly fractal nature. Calculating wavelet coefficients at every possible scale is a fair amount of work, and it generates an awful lot of data. It turns out that if we choose scales and positions are chosen based on powers of two, so-called dynamic scales and positions, then analysis becomes much more efficient and accurate. The low-frequency content is the most important part. It is what gives the signal its identity. The high-frequency content, on the other hand, imparts flavour or nuance. Any signal (function) can be decomposed into two parts called approximation and details. The approximations are the high-scale, low-frequency components of the signal. The details are the low-scale, high-frequency components. In this chapter, MATLAB TOOL BOX is applied to detect discontinuities and breakdown points,

long-term evolution and self-similarity of the signals of meteorological parameters of nine meteorological stations of the kingdom.

The first- and second-level details show the discontinuity most clearly, because the rupture contains the high-frequency part. The presence of noise, which is fairly common in signal processing, makes identification of discontinuities more complete. If the first levels of the decomposition can be used to eliminate a large part of the noise, the rupture is sometimes visible at deeper levels in the decomposition. In order to detect a singularity, the selected wavelet must be sufficiently regular, which implies a longer filter impulse response.

The signals of meteorological parameters of the Kingdom of Saudi Arabia have so much noise that their overall shape is not apparent upon visual inspection but trends become clearer with each approximation. Thus, wavelet analysis is useful in revealing signal trends, a goal that is complementary to revealing a signal hidden in noise. If the signal itself includes sharp changes, then successive approximations look less and less similar to the original signal. A repeating pattern in the wavelet coefficient plots is characteristic of a signal that looks similar on many scales. If a signal is similar to itself at different scales, then the wavelet coefficients will also be similar at different scales. In the coefficient plot, which shows scale on the vertical axis, this self-similarity generates a characteristic pattern.

## 9.1 MATHEMATICAL DESCRIPTION OF WAVELET METHODOLOGY

The term wavelet means small waves, and in brief, a wavelet is an oscillation that decays quickly. The equivalent mathematical conditions are as follows:

$$\int_{-\infty}^{\infty} |\psi(t)|^2 dt < \infty \quad (9.1)$$

$$\int_{-\infty}^{\infty} \psi(t) dt = 0 \quad (9.2)$$

Where  $\int_{-\infty}^{\infty} \frac{|\psi(\xi)|^2}{|\xi|} d\xi < \infty$  is the admissibility condition and  $\psi(\xi)$  is the admissibility constant. In wavelet theory a function is represented by infinite series expansion in terms of a dilated and translated version of a basis function and called mother wavelet satisfying the above conditions:

$$\psi_{a,b} = a^{-1/2} \psi\left(\frac{t-b}{a}\right), \text{ where } a > 0 \quad (9.3)$$

$$T_{\psi}f(a, b) = a^{-1/2} \int_{-\infty}^{\infty} f(t)\psi\left(\frac{t-b}{a}\right) dt = \langle f, \psi_{a,b} \rangle \quad (9.4)$$

Where  $\langle f, \psi_{a,b} \rangle$  is the inner product of  $f$  and  $\psi_{a,b}$  and  $T_{\psi}f(a, b)$  is called the wavelet function of  $f(t)$ . A wavelet transform  $T_{\psi}$  decomposes a signal into several groups of coefficients. Different coefficient vectors contain information about characteristics of the sequence at different scales. It may be observed that the wavelet transform is a prism, which exhibits properties of signal such as points of abrupt changes, seasonality or periodicity. The wavelet transform is a function of the scale of frequency (a) and is the spatial position or time (b).

The plane defined by the variables (a, b) is called the scale-space or time frequency plane.

The wavelet transform  $T_{\psi}f(a, b)$  measures the variation of  $f$  in a neighbourhood of b. For a compactly supported wavelet (for a wavelet vanishing outside a closed and bounded interval), the value of  $T_{\psi}f(a, b)$  depends upon the value of  $f$  in a neighbourhood of b of size proportional to the scale a. At small scales,  $T_{\psi}f(a, b)$  provides localised information such as localised regularity (smoothness) of f. The local regularity of a function (or signal) is often measured with Lipschitz exponent (Hurst parameter also fractal dimension). The global and local Lipschitz regularity can be characterised by the asymptotic decay of wavelet transformation at small scales. For example, if  $f$  is differentiable at  $b$ , then  $T_{\psi}f(a, b)$  has the order  $a^{3/2}$  as  $a \rightarrow 0$ .

## 9.2 WAVELET-BASED DECOMPOSITION OF WIND SPEED DATA

The discrete wavelet analysis of meteorological parameters is performed in terms of decomposition, approximation, compression, and denoising of the original signal. The decomposition analysis of wind speed data for Abha, Dhahran, Gizan, Guryat, Hail, Jeddah, Riyadh, Turaif and Yanbo is shown in Figures 9.1 to 9.9, respectively. In these figures, the x-axis shows the number of days of the entire data period used in this study. Each of these figures has seven parts. The first part “S” represents the signal or raw data and the second part “a<sub>5</sub>” corresponds to the amplitude of the signal for wavelet Daubechies (db) at level 5.

The last five parts, i.e.  $d_1$ ,  $d_2$ ,  $d_3$ ,  $d_4$  and  $d_5$  of these figures represent details of the signal or raw data at five different levels.

Wind speed is a highly random meteorological phenomenon and changes with the time of the day and geographical location. It is very difficult to predict the trend of wind speed both in time and especially domains. The discrete wavelet analysis of daily mean values of wind speed at nine locations was performed using db 5 and is shown in Figures 9.1 to 9.9. The comparison of signal strength  $S$  or  $S/d$  in the first part of these figures shows that the minimum value of 0-15 correspond to Gizan and Riyadh (Figures 9.3 and 9.7) while the maximum of 0 – 30 to Guryat and Dhahran (Figures 4 and 9). Figures 4 and 9 also show that the amplitude  $a_5$  ranges from 4 – 14 for Guryat and 5 – 10 for Yanbo. The  $d_5$  values of wind speed data at these two locations were the same, i.e. -2 to +2. The second group, Dhahran, Jeddah and Turaif with signal strength between 0-20, looks another group with similar wind speed characteristics, as seen from Figures 9.2, 9.6 and 9.8, respectively. The amplitude  $a_5$  at these locations was observed as 5-10, 5-10 and 6-12, which look similar. The values of Daubechies coefficients  $d_5$  were found to be the same as -2 to +2 for all three locations. Similarly, Gizan and Riyadh show almost the same values of  $S$ ,  $a_5$  and  $d_5$  and hence can be said to be having similar wind speed characteristics. Abha and Hail seem to be also similar to each other where wind speed characteristics at these two locations are concerned.

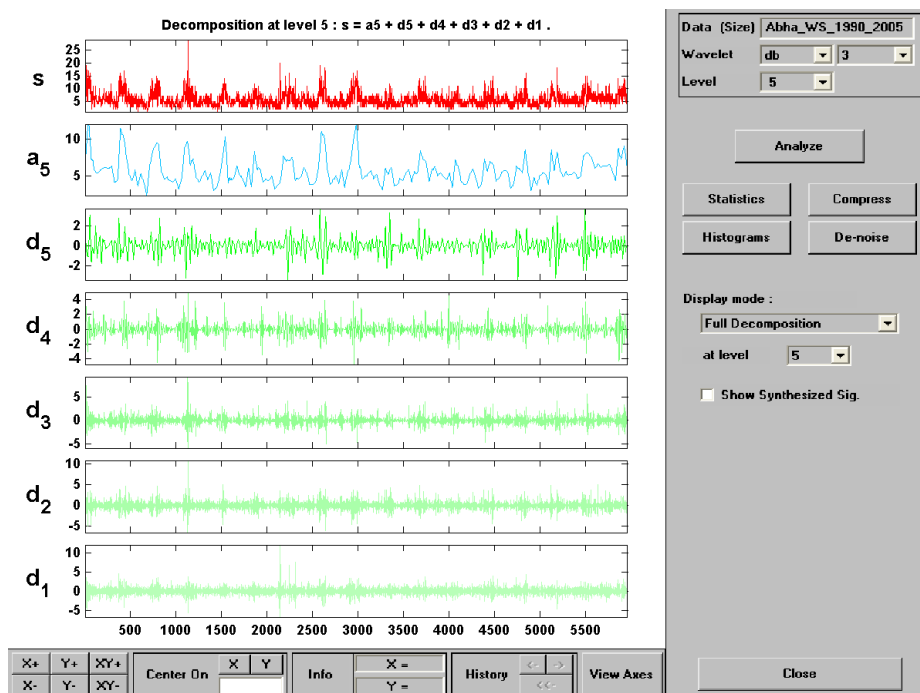


Figure 9.1 Decomposition of wind speed time series data for Abha using DB5

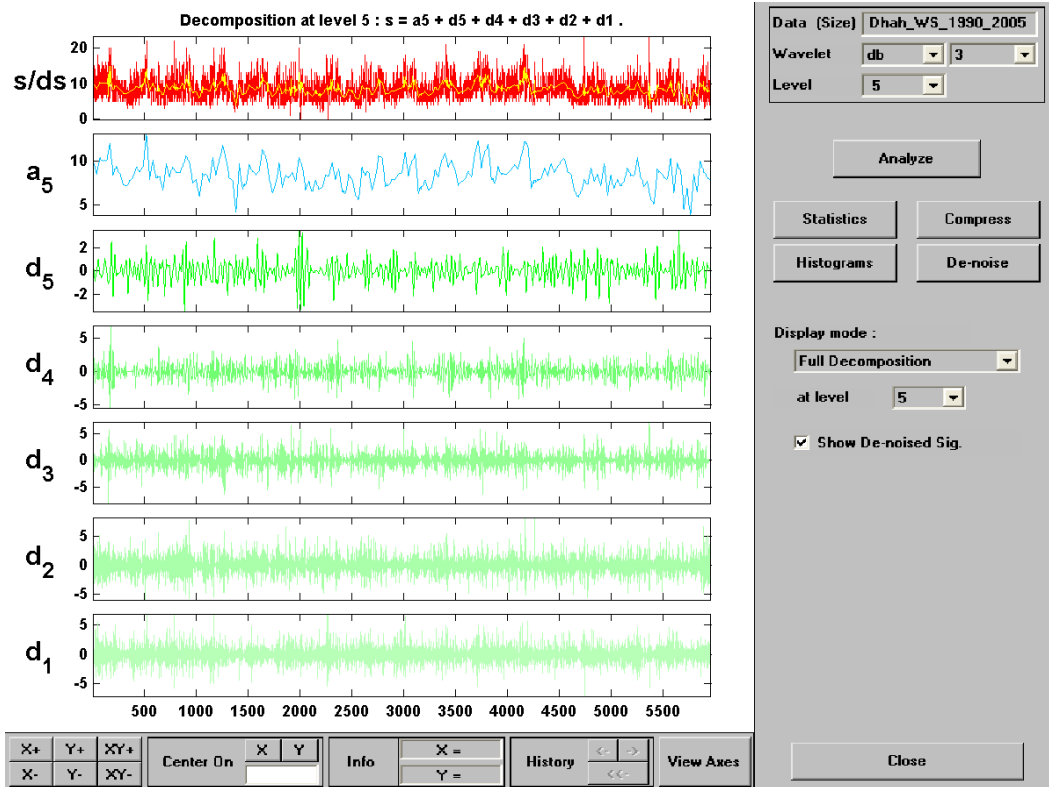


Figure 9.2 Decomposition of wind speed time series data for Dhahran using DB5

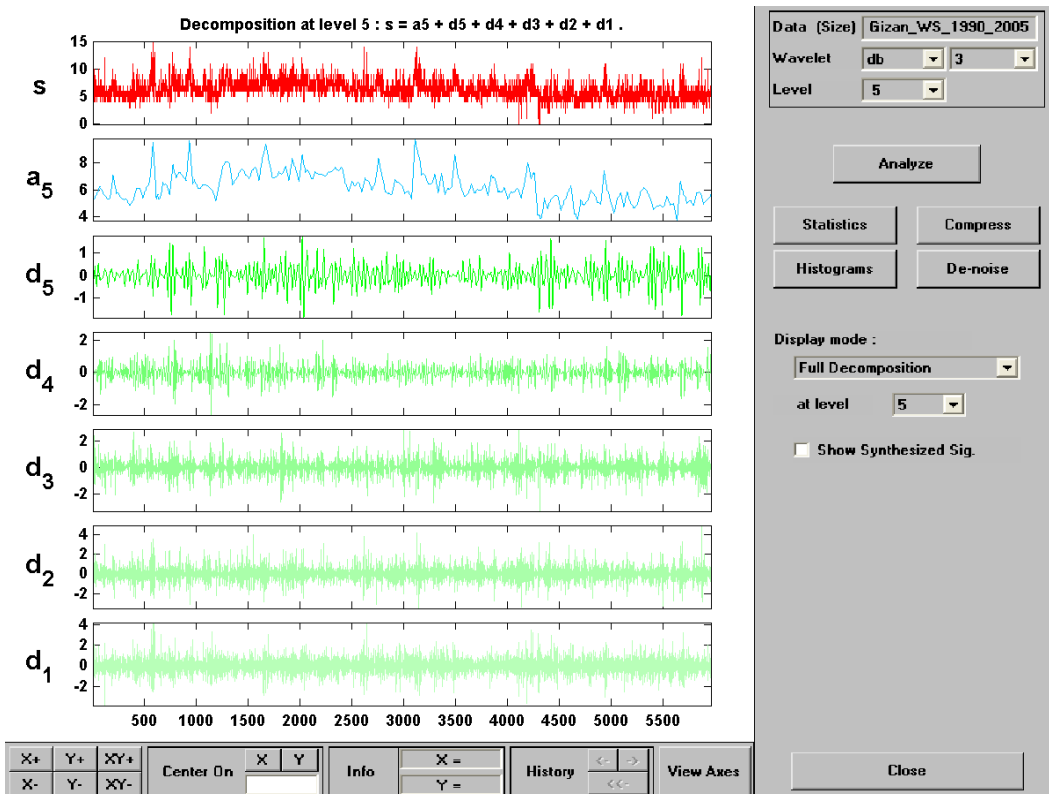


Figure 9.3 Decomposition of wind speed time series data for Gizan using DB5

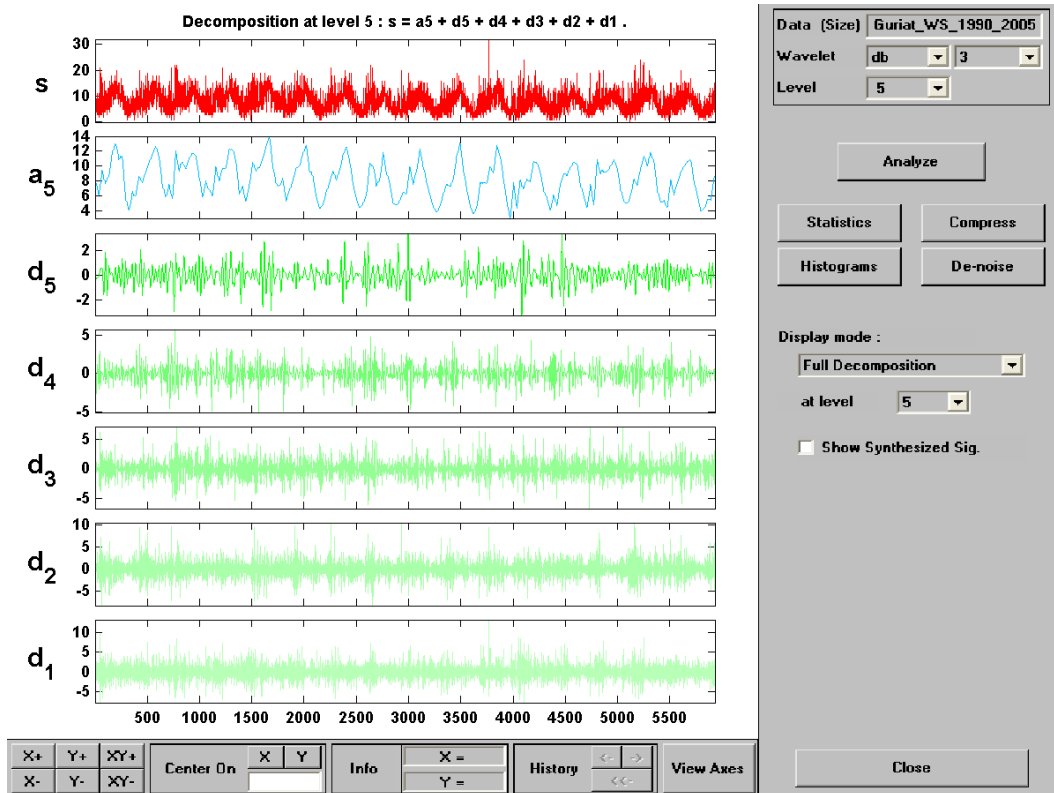


Figure 9.4 Decomposition of wind speed time series data for Guryat using DB5

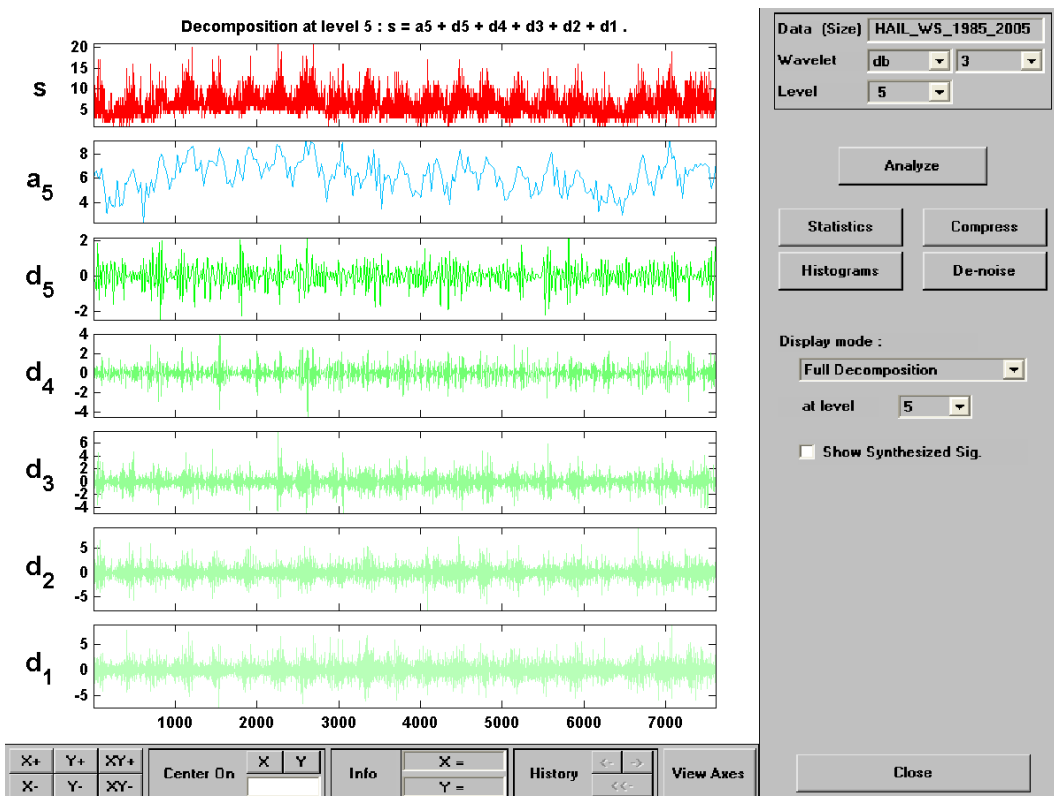


Figure 9.5 Decomposition of wind speed time series data for Hail using DB5

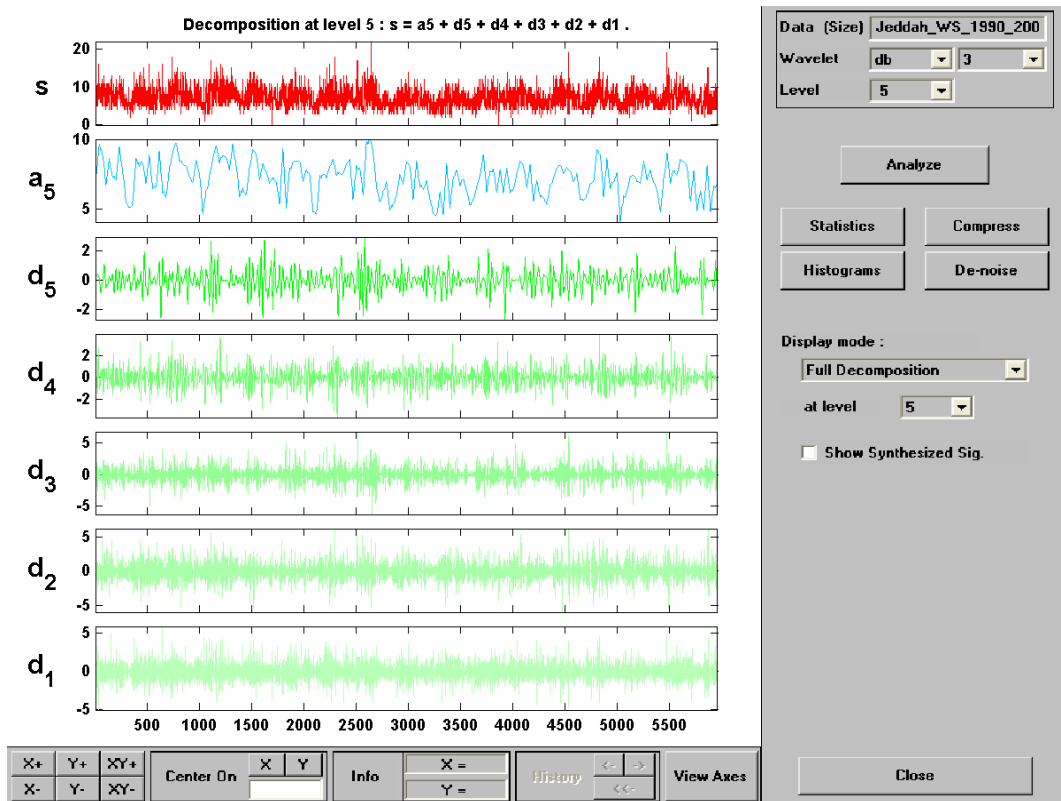


Figure 9.6 Decomposition of wind speed time series data for Jeddah using DB5

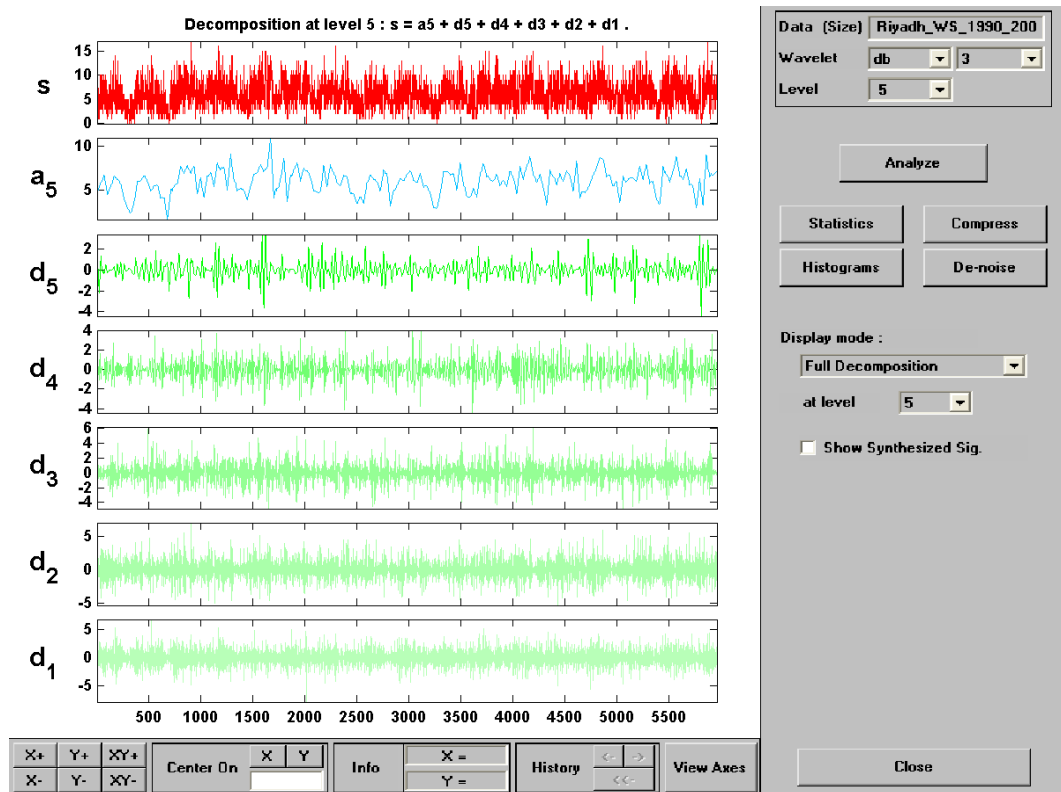


Figure 9.7 Decomposition of wind speed time series data for Riyadh using DB5

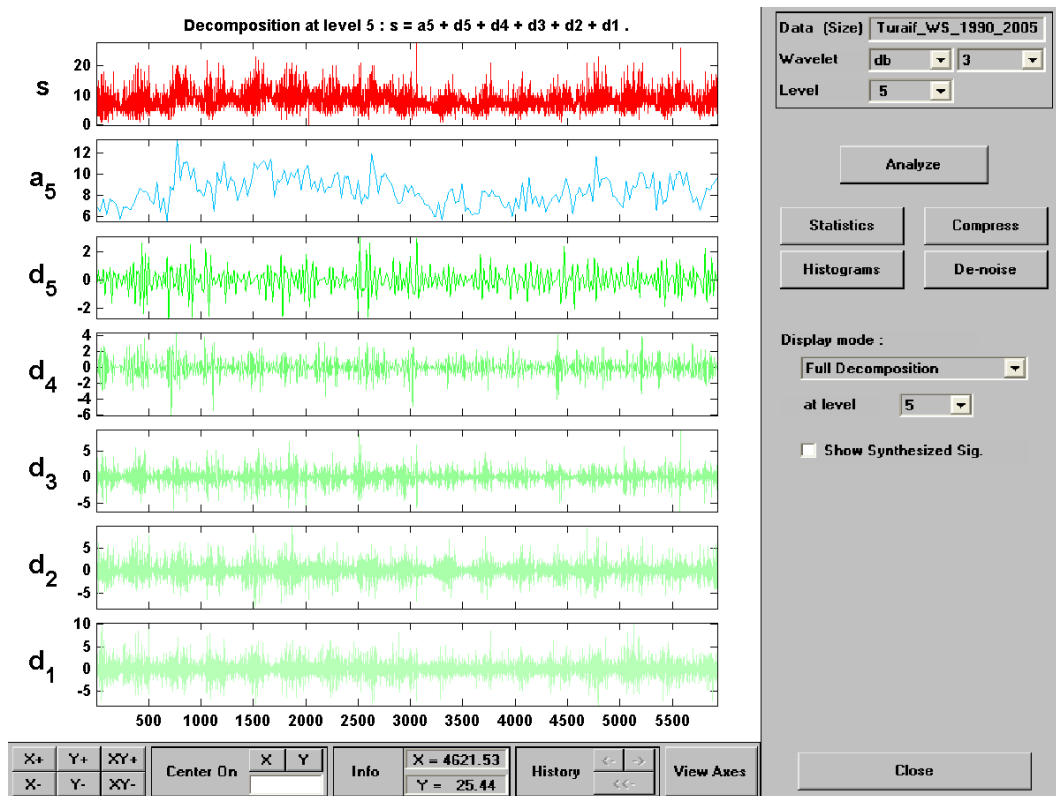


Figure 9.8 Decomposition of wind speed time series data for Turaif using DB5

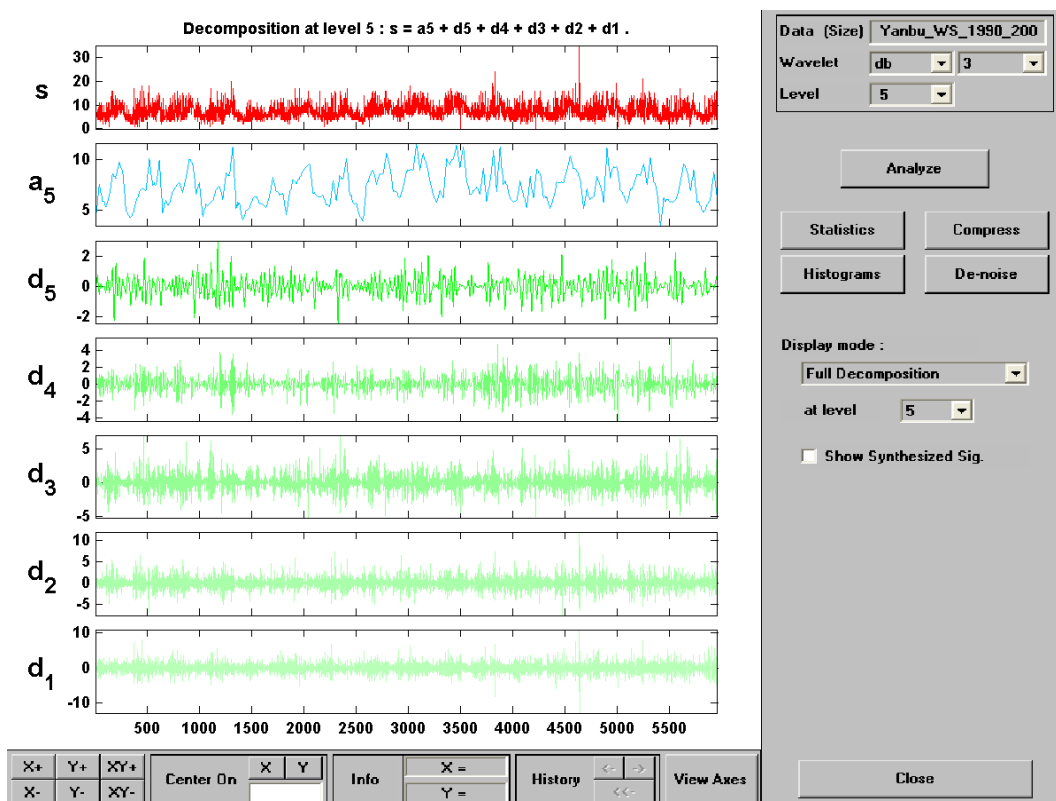


Figure 9.9 Decomposition of wind speed time series data for Yanbu using DB5

### 9.3 FAST FOURIER TRANSFORM POWER SPECTRUM OF WIND SPEED DATA

In this chapter, a study on the effects of transforming wind speed data, from a time series domain into a frequency domain via fast Fourier transform (FFT) is presented. The wind data is first transformed into a stationary pattern from a non-stationary pattern of time series data using statistical software. This set of time series is then transformed using FFT for the main purpose of the chapter. The analysis is done through MATLAB software, which provides a very useful function in FFT algorithm. Parameters of engineering significance such as hidden periodicities, frequency components, absolute magnitude and phase of the transformed data, power spectral density and cross-spectral density can be obtained. Results obtained using data from case studies involving nine weather stations in Saudi Arabia show great potential for application in verifying the current criteria used for design practices.

Abha is a hill station and there are many hills around. Due to having many hills, possibly of different scales, the power spectral energy is mostly concentrated on low-frequency range 0.02-0.007. The high-frequency energies ( $f > 0.03$ ) are low, as shown in Figure 9.10. Dhahran is a coastal site 3km inland from sea. There is a small single-storey airport building in the vicinity of the meteorological station. The station level is most possibly higher than sea level (17m above mean sea level) and wind direction is mostly from the sea to the station. When the wind flows from the sea to the station, the wind confronts hurdles producing large eddies of  $f = 0.0039\text{Hz}$  and small eddies, which are connected with the high-frequency energies ( $f > 0.03$ ). The high-frequency energies at Dhahran (Figure 9.11) are larger than those at Abha (Figure 9.10).

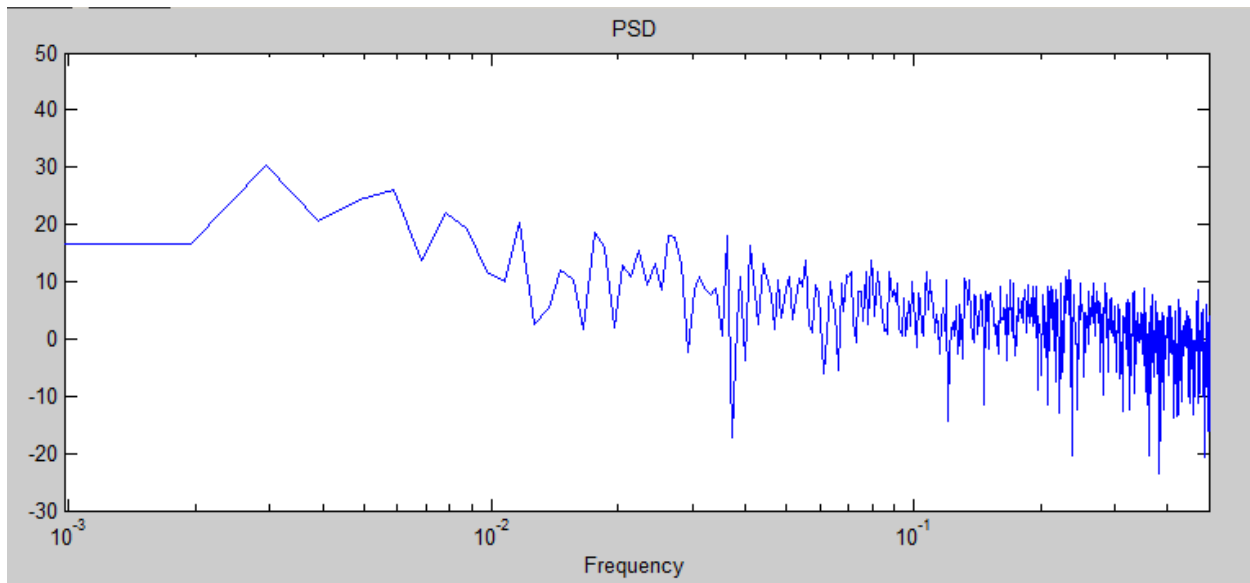


Figure 9.10 FFT power spectrum of wind speed data for Abha.

Gizan is a coastal station just on the west coast of Saudi Arabia, a few 100metres inland. There is one small single-storey airport building and some trees around. This station is only 5metres above mean sea level. The Red Sea is a bit more turbulent than the Arabian Gulf on the east coast (Dhahran) and is wide open. This geographical situation results in higher winds from the seafront due to water and land interaction and produces much higher eddies of  $f = 0.0052$ , as shown in Figure 9.12. The eddies are higher than the eddies at Dhahran. That is why both the low- and high-frequency energies are low. There are no large-scale eddies. Guryat is an inland station with high land and small hills with gentle topographical features. Since the station is high, large-scale eddies of  $f=0.0031$  exist and the small hills generate high-frequency, small-scale eddies, see Figure 9.4 for more information. Hail is a high land plateau in the north central area of KSA. Here the large-scale eddies are not regular as energy is not concentrated at any specific  $f$  but at  $f < 0.004$ . Energies at the high frequencies are smaller than those at Dhahran and Guryat, as can be seen from Figure 9.14 for Hail.

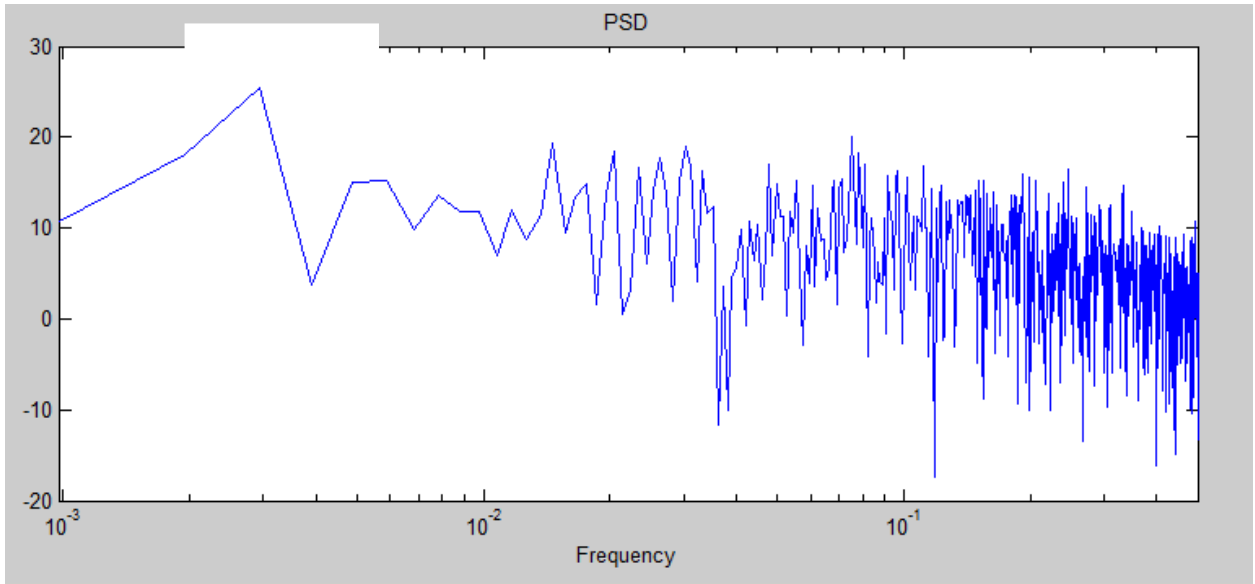


Figure 9.11 FFT power spectrum of wind speed data for Dhahran

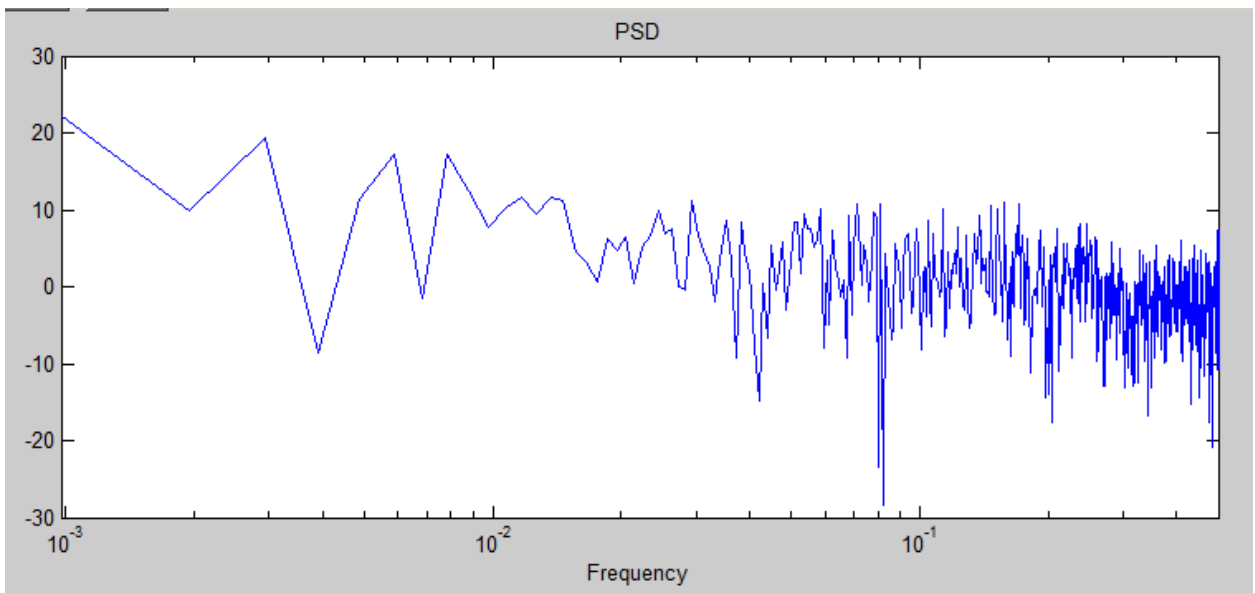


Figure 9.12 FFT power spectrum of wind speed data for Gizan

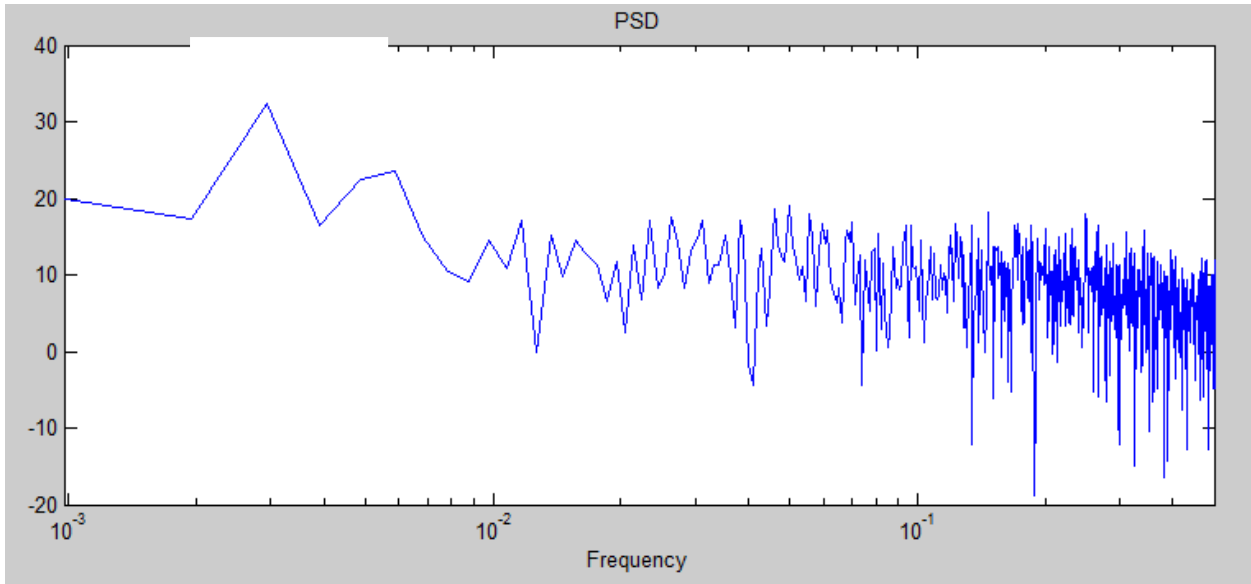


Figure 9.13 FFT power spectrum of wind speed data for Guryat

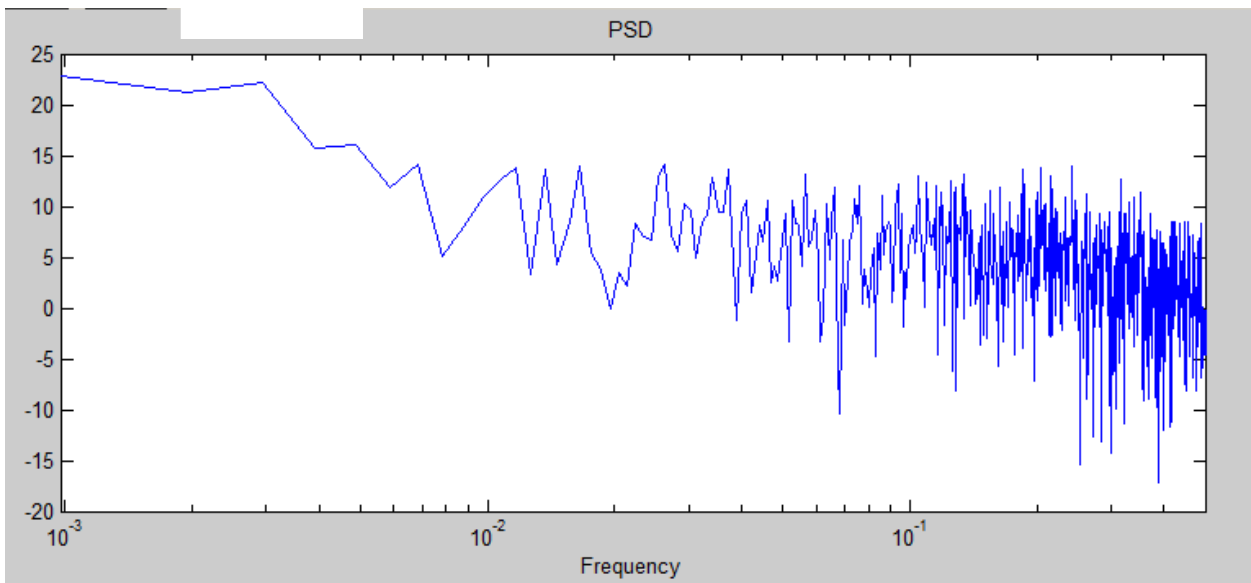


Figure 9.14 FFT power spectrum of wind speed data for Hail

Jeddah station is around 10km inland from the Red Sea. The FFT power spectrum for this station is shown in Figure 9.15. There are many buildings around and this is an urban area. The wind blows from the sea inwards and is intercepted by high-rise buildings and structures such as bridges and other industrial installations. Due to this confrontation of wind with structures, larger eddies of magnitude  $f=0.0046$  are produced. The FFT power spectrum obtained using long-term mean wind speed data for Riyadh is shown in Figure 9.16. Riyadh station is on the mainland and is around 450km above mean sea level. Riyadh is the capital of Saudi Arabia, hence it is a very developed region and surrounded by high-rise buildings,

bridges and various industrial installations. The winds are prevalent from the north and north-west directions in this region. These winds are intercepted by tall structures and result in larger eddies of magnitude of  $f=0.0038$  but smaller than those in Jeddah and Gizan.

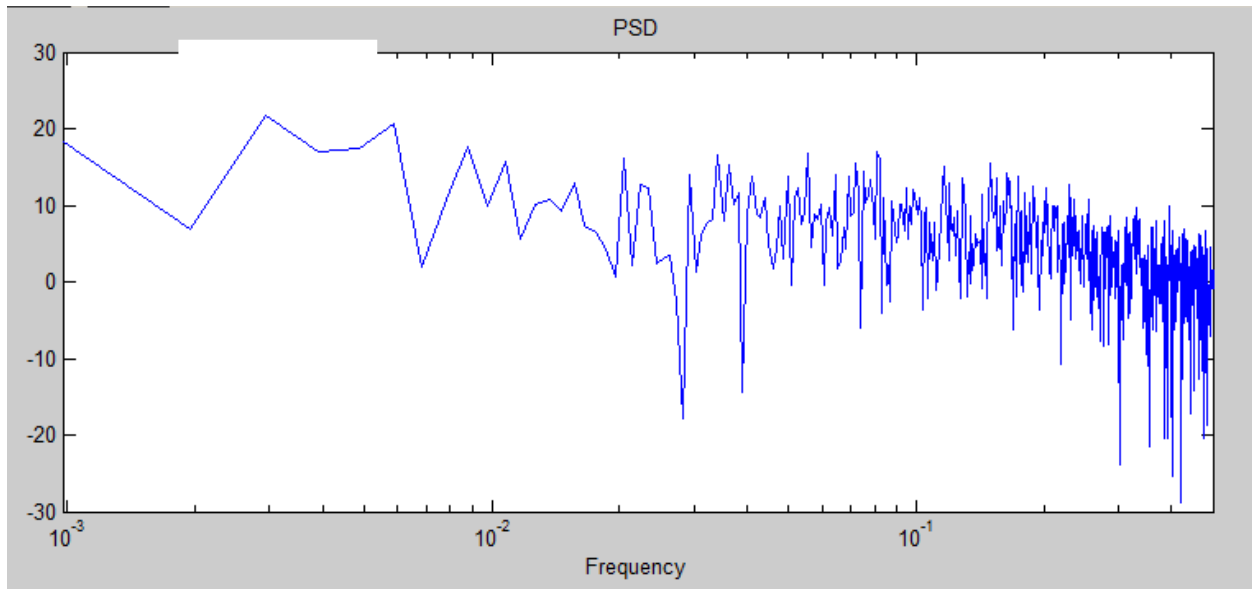


Figure 9.15 FFT power spectrum of wind speed data for Jeddah

The FFT power spectrum obtained using long-term wind speed values for Turaif is shown in Figure 9.17. Turaif is a small city in the northern most part of Saudi Arabia and is a hillock inland area. The wind blows mostly from the north in this area and accelerates due to topographical features. This is reflected by higher magnitude of eddies with  $f=0.0044$ . Yanbo is a coastal site on the Red Sea in the north-west of Saudi Arabia. It is an industrial area and is surrounded by a range of hills on the northern side and exposed to the sea on its west. The station is 10metres above mean sea level. The winds are blocked while blowing from north but blow from the west or seaside. The higher eddies of magnitude  $f=0.0036$  are due to geographical situation, as seen from Figure 9.18. The magnitude of  $f$  at Yanbo is the least compared with other coastal locations on the west coast such as Jeddah ( $f=0.0046$ , Figure 9.15) and Gizan ( $f=0.0052$ , Figure 9.12).

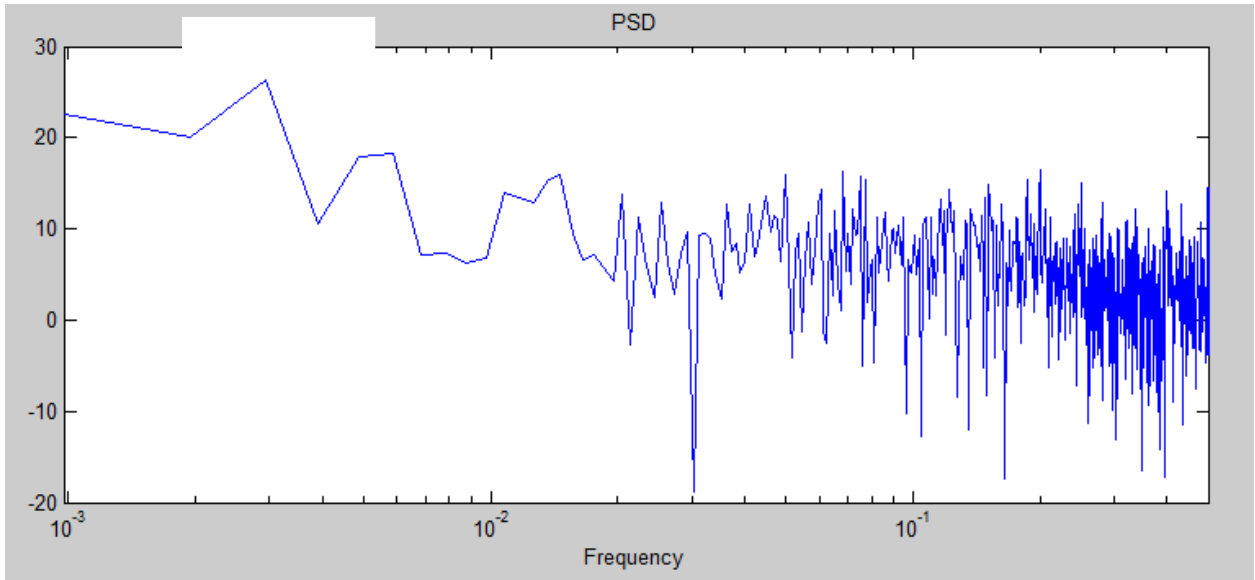


Figure 9.16 FFT power spectrum of wind speed data for Riyadh

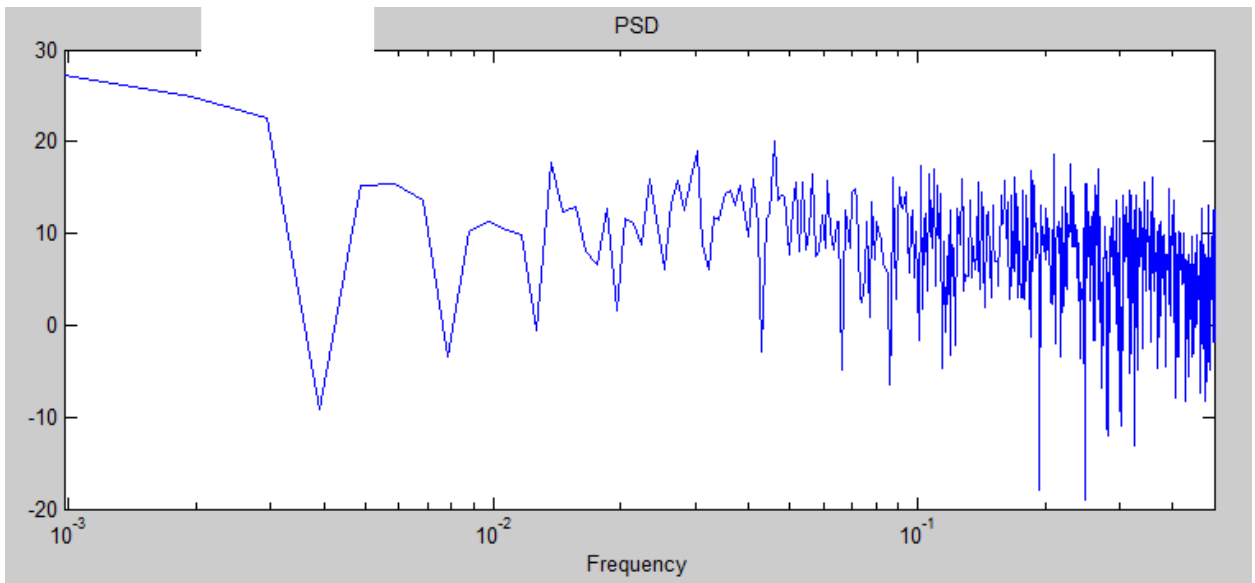


Figure 9.17 FFT power spectrum of wind speed data for Turaif

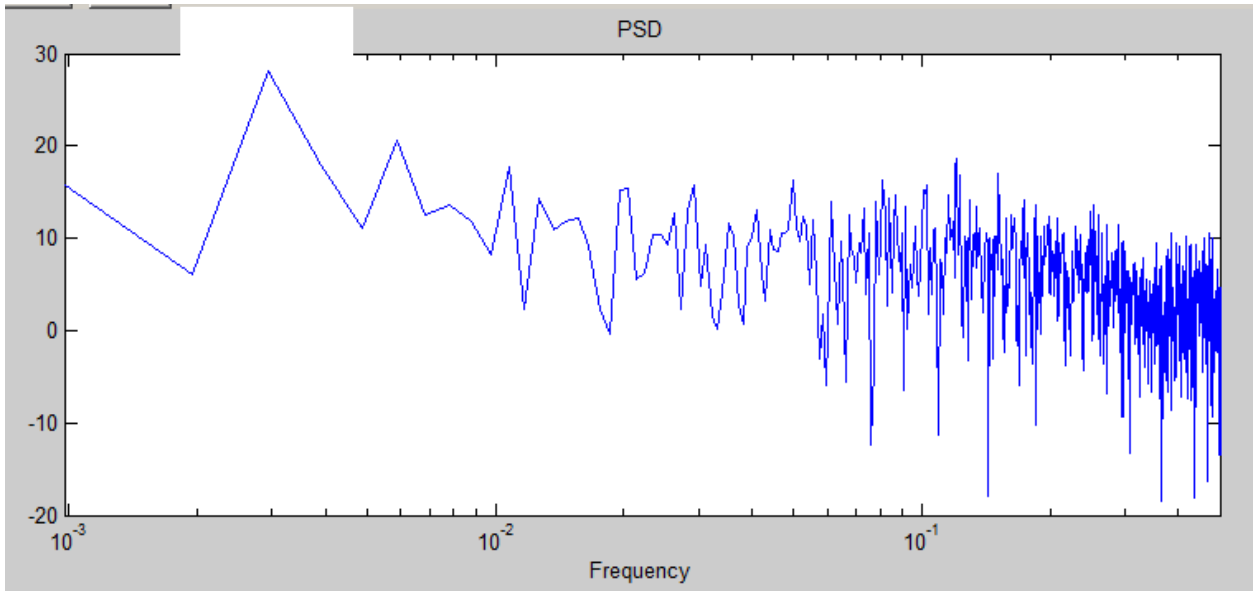


Figure 9.18 FFT power spectrum of wind speed data for Yanbo

## CHAPTER 10

### CONCLUSIONS AND RECOMMENDATIONS

The growing global population and more rapidly increasing energy demands have become a matter of challenge for governments to provide energy to all people and the industry according to their requirement. The design and development of fossil-fuel-based power plants require huge investments and relatively longer time periods in its realisation. In this modern world, there are more than 2 billion people who do not have access to electricity. The utilisation of renewable sources of energy requires more initial investment, but can reach to both remote and urban populations. Saudi Arabia is the major fossil fuel supplier. It meets around 25 to 28% of the global needs of the fossil fuel energy of the world. The Kingdom of Saudi Arabia has always been among the front-runners where promotion and utilisation of clean sources of energy are concerned. The present study is an indicator of the kingdom's ambitions towards wind power utilisation for both grid-connected and hybrid power systems.

The study utilised daily average wind speed data over a period of 37 years from 28 meteorological stations and wind speed measurements at 20, 30 and 40m AGL from seven stations for wind resource assessment of various regions of the kingdom. The outcome of the present study and possibility of future work are summarised in the following sub-sections of this chapter.

#### 10.1 SUMMARY OF FINDINGS

- More than 300 research papers and documents available on the internet were reviewed for knowledge building on the wind speed and wind power-related issues and technological development around the globe. As of December 2009, the global wind power installed capacity reached more than 157GW and China alone installed a maximum capacity in 2009. The other major global players in the wind power sectors are the United States, Germany, Denmark, China and India. The European Union led the way where regional share of wind power is concerned.
- In Saudi Arabia, the per capita energy consumption has reached 20kWh/day in 2008 compared with 19.4kWh/day in 2007, i.e. a net increase of 3.1% in one year. On an average over the 25-year period from 1984 to 2008, a 4.1% annual increase in per capita energy per day has been observed, which is significant and needs to be resolved immediately.

- From the analysis of 28 meteorological stations, the highest annual average wind speed (at 10m AGL) of 4.4m/s was observed at Dhahran while the lowest of 1.59m/s at Makkah as can be seen from Figure 5.1. Promising long-term annual means of more than 4m/s were observed at Al-Wejh, Guriat, Turaif and Yanbo.
- A clear seasonal effect was noticed in wind speed intensities and spread of the higher wind speed values in larger areas. For example, during the winter months, the higher wind speed values were observed over a wide area in the northern and western parts of the kingdom while further higher wind intensities were confined only to a few areas in the eastern, northern and western parts.
- Based on regression line analysis, decreasing trends of annual mean wind speed were found at Al-Ahsa, Al-Baha, Bisha, Dhahran, Gizan, Guriat, Hail, Khamis-Mushait, Madina, Makkah, Nejran, Qasumah, Riyadh, Sharourah, Tabouk, Taif, Wadi Al-Dawasser and Yanbo and increasing trends at the remaining locations, i.e. Abha, Al-Jouf, Al-Wejh, Gassim, Hafr Al-Batin, Jeddah, Rafha, Sulayel, Turaif and Wadi Al-Dawasser. Overall, a decreasing trend of 0.01852m/s per year was observed in annual mean wind speed values based on the algebraic average of the trend coefficient ( $a$ ) of all the stations used in the present work.
- At Sharourah, in southern Saudi Arabia, a significantly high rate of decrease of 0.0999m/s in annual mean wind speed values was observed from 1990 to 2006. Al-Ahsa was the next station where an annual decrease of 0.0876m/s was estimated and similar magnitude of rate of decrease was followed at Al-Baha (0.0656m/s per year), Qaisumah (0.0513 m/s per year), Nejran (0.0495m/s per year), Guriat (0.0477m/s per year), and Yanbo (0.0405m/s per year). At Hafr Al-Batin, Taif, Turaif and Al-Wejh, the rate of increase of annual wind speed of 0.0391, 0.0154, 0.0151 and 0.014 m/s respectively was observed. These trends need to be verified using more accurate wind speed measurements but could be used as preliminary indicators of the future wind regime in Saudi Arabia.
- The annual  $k$  values were found to be decreasing at Bisha, Guriat, Madinah, Taif and Yanbo and increasing for the rest of the stations. On the other hand, the scale parameter regression lines for Abha, Al-Ahsa, and Al-Baha showed decreasing trends of 0.0004, 0.0988 and 0.0688 m/s.
- The annual scale parameter trends were found to be decreasing for most of the station with the exception of Al-Jouf, Gassim, Hafr-Al-Batin, Jeddah, Rafha, Sulayel, Turaif and

Wadi Al-Dawasser with an increasing rate of 0.0117, 0.0065, 0.0442, 0.0036, 0.0297, 0.001, 0.0125 and 0.0161 m/s, respectively.

- The highest values of long-term annual temperatures ( $\geq 30^{\circ}\text{C}$ ) were observed at Gizan and Makkah and lowest of  $12.2^{\circ}\text{C}$  at Abha. The knowledge of temperature magnitude and its frequency of occurrence in different temperature bins are important from wind turbine energy output and the functioning of different components of wind turbine.
- The long-term air density was observed to be more than 1.0 at all the stations except at Abha, Al-Baha and Khamis-Mushait where it was a little less than 1.0. The lower values of air density at these locations could be attributed to low air pressure at high altitudes.
- The highest wind was observed at Dhulom while the lowest in Gassim with good wind regimes at Rawdat Ben Habbas, Juaymah and Dhahran with more than 5 m/s annual average wind speed. The local wind shear exponent (WSE) was highest for Gassim and lowest for Yanbo. The overall mean temperature was found to be highest at Yanbo and lowest in Arar. The prevailing wind direction at all of these sites was found to be from North with some seasonal variation.
- In general, the wind frequency analysis indicated lesser rated power yield at most of these stations but higher yields. Finally, the wind data collection sites can be prioritized as first, second etc. best in order as Juaymah, Rawdat Ben Habbas, Dhulom, Arar, Dhahran, Yanbo, and Gassim with having wind frequencies of around 75%, 74%, 72%, 71%, 68%, 55%, and 52% above 4 m/s at 40m AGL, respectively.
- The highest WSE value of 0.286 was obtained for Rawdat Ben Habbas while the lowest of 0.081 for Yanbo. Following WSE values should be used to extrapolate the wind speed above measurement heights to get accurate wind speed values at higher altitudes.

Rawdat Ben Habbas	0.286
Juaymah	0.274
Dhahran	0.151
Arar	0.182
Gassim	0.241
Yanbo	0.081
Dhulom	0.193

- According to roughness value classification, Rawdat Ben Habbas and Gassim were classified as suburban areas while Gassim and Dhulom as areas having few trees in the surroundings. Juaymah, Dhahran and Yanbo were classified as areas having many trees, crops, and smooth, respectively.

- Based on energy yield from a single machine it is recommended that wind machines of sizes ranging between 600 and 1000 kW should be used for wind farm development if commercially available. In case of unavailability, WECS of 1300 or 1500 may be considered.
- Based on hub-height effect on energy production, it is recommended that a maximum of 60 metres of hub-height should be used for wind farm development. The maximum increase of about 8% was obtained for a change of hub-height from 50 to 60 metres while further increase in hub-height from 60 to 70 metres produced only 4% more of electricity. The increase in energy production was found to be only 3% for further increase of 10 metres in hub-height.
- As a first attempt, an empirical correlation was developed for the estimation of near optimal hub height ( $HH = 142.035 * (\alpha) + 40.33$ ) with coefficient of correlation of 97% as a function of local wind shear exponent ( $\alpha$ ). This correlation was developed using energy yield from a wind turbine of 1000kW rated power and wind speed and local exponent for seven locations in Saudi Arabia.
- Relatively higher values of PCF were obtained for WECS of smaller sizes. The plant capacity analysis also showed that maximum increase of 2.12% in PCF was found for an increase in hub-height from 50 to 60 metres while less than 1% in other cases except for 60 to 70metre increase in hub-height where it was 1.17%.
- The net annual energy yield from the chosen wind turbine at a hub height of 100m was more than 7,000MWh at Al-Wejh, Guriat, Qaisumah, Turaif, Dhahran, and Yanbo. At Al-Jouf, Arar, Rafha and Jeddah the net annual energy yield was little more than 6,000MWh. At Al-Ahsa, Gizan, Hafr, Sulayel, Taif and Wadi Al-Dawasser the annual energy yield was found to be between 5,000 and 6,000MWh.
- The plant capacity factor (PCF) was found to vary between a minimum of 4% and a maximum of 35% corresponding to Makkah and Dhahran, respectively. At Al-Wejh, Guriat, Turaif and Yanbo the annual mean PCF was between 30 and 35% while it varied from 25 to 30% at Al-Jouf, Arar, Jeddah, Qaisumah and Rafha. The PCF was found to vary from 20 to 25% at Al-Ahsa, Gizan, Hafr Al-Batin, Riyadh, Sulayel, Taif, and Wadi Al-Dawasser.
- The wind-pv-diesel hybrid system with 35% renewable energy penetration (26% wind and 9% solar) and 65% diesel power contribution (five units of 1120kW each) was found to be the most economical power system with COE of 0.212US\$/kWh at a diesel price of 0.2US\$/l. The COE for diesel only system at same diesel price was found to be 0.232US\$/kWh i.e. around 9.4% more than the hybrid system.

- The proposed system will be comprised of 3 wind turbines each of 600kW, 1000kW of PV panels, and four diesel generating sets each of 1120kW rated power. The proposed system was able to meet the energy requirements (AC primary load of 17,043.4MWh/y) of the village with 4.1% energy in excess. The annual contributions of wind, solar pv and the diesel generating sets were 4,713.7, 1,653.5, and 11,542.6MWh, respectively. The proposed hybrid power system will result in avoiding addition of 4,976.8 tons of GHG equivalent of CO<sub>2</sub> gas in to the local atmosphere of the village and will conserve 10,824 barrels of fossil fuel annually.

## **10.2 FUTURE WORK**

- It is recommended that hub height optimization study should be conducted further using multi-megawatt wind turbines and wind measurements made at more than one height.
- Preliminary wind resource assessment should be conducted using re-analysis data and WAsP tool and verification of the resulting frequency distributions should be made for site where measurements are available at more than one height above ground level.
- Wind masts of 80 to 100 metres tall should be installed along west and east coasts and some inland locations in the Kingdom and wind speed and direction measurements should be made at different heights for at least one complete year.
- The laser anemometers should be installed at some locations along the 80 – 100metre tall wind masts and the measured values should be verified with cup anemometer based wind speed measurements. This will be helpful in developing confidence on the laser anemometer based wind measurements. Once tested and found accurate, laser anemometers could be moved easily and installed without much civil work within a short time and least effort. The advantage of such equipment is that it can measure the wind speed up to 150m and more above the ground level.
- A wind-diesel and wind-pv-diesel hybrid power systems should be developed in real practice to partially replace the diesel power dependence and reduce the addition of green house gases in the local clean environment of the remotely located populations.
- Last but not the least, a grid-connected wind farm of around 40MW installed capacity should be brought into existence at some windy location in the Kingdom to demonstrate the wind at work to the people from all walks of life. This wind farm will create awareness among common people; provide avenues for master and doctoral level research opportunities.
- The high prevailing temperatures and presence of dust in the local atmosphere are the two challenges which can affect adversely the performance of the wind turbine and the

working life of the moving parts of the turbine. These issues could be addressed only when the wind turbines are in place in Saudi Arabia.

## REFERENCES

1. IPCC (2007-05-04). "Summary for Policymakers" (PDF). *Climate Change 2007: The Physical Science Basis. Contribution of Working Group I to the Fourth Assessment Report of the Intergovernmental Panel on Climate Change*. <http://www.ipcc.ch/pdf/assessment-report/ar4/wg1/ar4-wg1-spm.pdf>. Retrieved 2009-07-03.
2. Lu, Jian; Vecchi, Gabriel A.; Reichler, Thomas (2007). "Expansion of the Hadley cell under global warming" (PDF). *Geophysical Research Letters* **34**: L06805. doi:10.1029/2006GL028443. [http://www.atmos.berkeley.edu/~jchiang/Class/Spr07/Geog257/Week10/Lu\\_Hadley06.pdf](http://www.atmos.berkeley.edu/~jchiang/Class/Spr07/Geog257/Week10/Lu_Hadley06.pdf).
3. IPCC (2007). *Climate Change 2007: Synthesis Report. Contribution of Working Groups I, II and III to the Fourth Assessment Report of the Intergovernmental Panel on Climate Change*. [Core Writing Team, Pachauri, R.K and Reisinger, A. (eds.)]. Geneva, Switzerland: IPCC. [http://www.ipcc.ch/publications\\_and\\_data/publications\\_ipcc\\_fourth\\_assessment\\_report\\_synthesis\\_report.htm](http://www.ipcc.ch/publications_and_data/publications_ipcc_fourth_assessment_report_synthesis_report.htm).
4. Winter C. J., "Solar Cities", *Renewable Energy*, 4(1) (1994), p. 15.
5. Sadik N., Weltbevölkerungsbericht -1991- Freie Ent - Scheidung oder Schicksal? Deutsche Gesellschaft für Die Vereinten Nationen e.v., Bonn,(1991).
6. Presidency Meteorology and Environment (PME), Jeddah, Saudi Arabia, [www.pme.gov.sa](http://www.pme.gov.sa).
7. [U.S. Census Bureau - World POPClock Projection](http://www.census.gov/ipeds/data/states/2005/popclock/)
8. [Cities in Nigeria: 2005 Population Estimates — MongaBay.com](http://www.mongabay.com/igapo/2005_world_city_populations/Nigeria.html). [http://www.mongabay.com/igapo/2005\\_world\\_city\\_populations/Nigeria.html](http://www.mongabay.com/igapo/2005_world_city_populations/Nigeria.html). Retrieved 1 July 2008.
9. [Country Profile: Nigeria](http://news.bbc.co.uk/2/hi/africa/country_profiles/1064557.stm). *BBC News*. 24 December 2009. [http://news.bbc.co.uk/2/hi/africa/country\\_profiles/1064557.stm](http://news.bbc.co.uk/2/hi/africa/country_profiles/1064557.stm). Retrieved 1 July 2008.
10. As graphically illustrated by [population since 10,000BC](http://www.bbc.co.uk/1/hi/world/south_asia/4994590.stm) and [population since 1000AD](http://www.bbc.co.uk/1/hi/world/south_asia/4994590.stm)
11. [The end of India's green revolution?](http://news.bbc.co.uk/1/hi/world/south_asia/4994590.stm). *BBC News*. 29 May 2006. [http://news.bbc.co.uk/1/hi/world/south\\_asia/4994590.stm](http://news.bbc.co.uk/1/hi/world/south_asia/4994590.stm). Retrieved 29 November 2009.
12. United Nations Population Division (13 March 2007). ["World population will increase by 2.5 billion by 2050; people over 60 to increase by more than 1 billion"](http://www.un.org/News/Press/docs/2007/pop952.doc.htm). Press release. <http://www.un.org/News/Press/docs/2007/pop952.doc.htm>. Retrieved 14 March 2007. "The world population continues its path towards population ageing and is on track to surpass 9 billion persons by 2050.
13. Growth in world electric power generation and total energy consumption, 1990-2035 (index, 1990 = 1), Department of Energy (DOE)/EIA-0484(2009), Released on July 27, 2010.
14. Unless otherwise specified, the population data used here, including the projections, come from the UN, <http://www.un.org/esa/population/unpop.htm>. Remarkably similar projections are available from the U.S. Census Bureau, <http://www.census.gov/ipc/www/idbsprd.html>.
15. Demographics of Africa and the Middle East continue to explode, [http://www.terradaily.com/reports/Demographics Of Africa And The Middle East Continue To Explode.html](http://www.terradaily.com/reports/Demographics_Of_Africa_And_The_Middle_East_Continue_To_Explode.html), (Accessed on September 24, 2010).

16. <http://www.nytimes.com/2007/01/18/news/18iht-oxan.0118.4250941.html> (Accessed on 24 September 2010).
17. An EU-GCC Dialogue for Energy Stability and Sustainability, Task 4: Development of Renewable Energies, Promotion of the Rational Use of Energy and Reduction of CO<sub>2</sub> Emissions in the GCC Region, 4.1041/D/02-008-S07 21089, The Commission of the European Communities.
18. [http://en.wikipedia.org/wiki/Demographics\\_of\\_Saudi\\_Arabia](http://en.wikipedia.org/wiki/Demographics_of_Saudi_Arabia), Accessed on September 24, 2010.
19. Ministry of Water and Electricity (MOWE), Saudi Arabia, Annual Report 2008, <http://www.mowe.gov.sa>
20. Global Wind Energy Council (GWEC): Global wind power boom continues despite economic woes [http://www.gwec.net/index.php?id=30&no\\_cache=1&tx\\_ttnews\[tt\\_news\]=247&tx\\_tnews\[backPid\]=4&cHash=1196e940a0](http://www.gwec.net/index.php?id=30&no_cache=1&tx_ttnews[tt_news]=247&tx_tnews[backPid]=4&cHash=1196e940a0) (Accessed on February 12 2010)
21. Tennis MW., Clemmer S., Howland J. Assessing Wind Resources: A Guide for Landowners, Project Developers, and Power Suppliers, Union of Concerned Scientist, (2002).
22. Potts JR, Pierson SW, Mathisen PP, Hamel JR, Babau VC. Wind Energy Assessment of Western and Central Massachusetts. AIAA-2001-0060, (2001).
23. Brower M. New Maxico Wind Resources: AGIS Approach, New Maxico Energy, Minerals, and Natural Resources Department, Final Report, September, (1997).
24. Rehman S. Prospects of wind farm development in Saudi Arabia. *Renewable Energy* 2004(a);30(3):447-463.
25. Rehman S. Wind energy resource assessment for Yanbo, Saudi Arabia. *Energy Conversion and Management* 2004(b);45(13-14):2019–2032.
26. Rehman S. Aftab A. Assessment of wind energy potential for coastal locations of the Kingdom Saudi Arabia. *Energy – The International Journal* 2004;29:1105–1115.
27. Rehman S, Halawnai TO, Mohandes M. Wind power cost assessment at twenty locations in the Kingdom of Saudi Arabia. *Renewable Energy* 2003;28:573-583.
28. Al-Abbadi N. M., Wind energy resource assessment for five locations in Saudi Arabia, *Renewable Energy* 30 (2005) 1489–1499.
29. Al-Abbadi N. M., Alawaji S. H. and Eugenio N. N., Wind Energy Resource Assessment: A three year Experience, *Windpower1997 Proceedings, Annual Conference of the American Wind Energy Association, AWEA, Austin, Texas, June 15-18, pp 533-541, 1996.*
30. Alawaji S. H., Wind Energy Resource Assessment in Saudi Arabia-I Network Design and Description, *Renewable Energy* 1996;7(4):319-328.
31. Rehman S, Halawani TO. Statistical characteristics of wind in Saudi Arabia. *Renewable Energy* 1994;4(8):949-956.
32. Rehman S, Halawani TO, Husain T. Weibull parameters for wind speed distribution in Saudi Arabia. *Solar Energy* 1994;3(6):473-479.
33. Jaramillo OA, Borja MA. Wind speed analysis in La Ventosa, Mexico: A Bimodal probability distribution case. *Renewable Energy* 2004;29:1613–1630.
34. Kainkwa, RMR. Wind speed pattern and the available wind power at Basotu, Tanzania. *Renewable Energy* 2000;21:289–295.
35. Ali Naci Celik, Energy output estimation for small-scale wind power generators using Weibull-representative wind data. *Journal of Wind Engineering and Industrial Aerodynamics* 2003;91.
36. Ackermann T, Soder L. Wind energy technology and current status: A review. *Renewable and Sustainable Energy Reviews* 2000;4.

37. Jebraj S. InivanS., A review of energy model.: *Renewable & Sustainable Energy Reviews* 2006;10(4):281-311.
38. Perez IA, Garcia MA, Sanchez MN. Et al Autocorrelation analysis of meteorological data from a RASS.: *Journal of Applied Meteorology* 2004;43(8):1213-1223.
39. Akpinar KE, Akpinar S. An assessment on seasonal analysis of wind energy characteristics and wind turbine characteristics. *Energy Conversion and Management* 2005;46:1848-1867.
40. Acker TL, Williams SK, Duque EPN, Brummels G, Buechler J. Wind resource assessment in the state of Arizona: Inventory, capacity factor and cost. *Renewable Energy* 2007;2:1453-1466.
41. Shata ASA, Hanitsch R, The potential of electricity generation on the east coast of Red Sea in Egypt. *Renewable Energy* 2006;31(10):1597-1615.
42. Shata A.S.A. and Hanitsch R., Electricity generation and wind potential assessment at Hurghada, Egypt, *Renewable Energy* 2007
43. Hrayshat ES. Wind resource assessment of the Jordanian southern region. *Renewable Energy* 2007;32:1948–1960.
44. Bagiorgas HS, Assimakopoulos MN, Theoharopoulos D, Matthopoulos D, Mihalakakou GK. Electricity generation using wind energy conversion systems in the area of Western Greece. *Energy Conversion and Management* 2007;48:1640–1655.
45. Jiang Yingni, Yuan Xiuling, Feng Jianmei and Cheng Xiaojun. Wind power density statistics using the Weibull model for inner Mongolia, China. *Wind Engineering*, 2006;30(2):161–168.
46. Ulgen K., Genc A., Hepbasli A., et al., Assessment of wind characteristics for energy generation. *Energy Sources* 2004;26(13):1227-1237.
47. Eskin N., Artar H., and Tolun S., Wind energy potential of Gokceada Island in Turkey, *Renewable and Sustainable Energy Reviews*
48. El-Osta W. and Kalifa Y., Prospects of wind power plants in Libya: a case study, *Renewable Energy* 28 (2003), pp. 363–371.
49. Omer A.M., On the wind energy resources of Sudan, *Renewable and Sustainable Energy Reviews*
50. Himri Y., Rehman S., Draoui B., and Himri S., Wind power potential assessment for three locations in Algeria, *Renewable and Sustainable Energy Reviews*
51. Chang Tsang-Jung and Tu Yi-Long, Evaluation of monthly capacity factor of WECS using chronological and probabilistic wind speed data: A case study of Taiwan, *Renewable Energy* 32 (2007) 1999–2010.
52. Mabel M. C and Fernandez E., Growth and future trends of wind energy in India, *Renewable and Sustainable Energy Reviews*
53. Ngala G.M., Alkali B., and Aji M.A., Viability of wind energy as a power generation source in Maiduguri, Borno state, Nigeria, *Renewable Energy* 32 (2007) 2242–2246.
54. Elamouri M. and Ben Amar F., Wind energy potential in Tunisia, *Renewable Energy*
55. Mostafaeipour A. and Abarghoeei H., Harnessing wind energy at Manjil area located in north of Iran, *Renewable and Sustainable Energy Reviews*
56. Mirza U. K., Ahmad N., Majeed T., and Harijan K., Wind energy development in Pakistan, *Renewable and Sustainable Energy Reviews*, 11 (2007) 2179–2190.
57. Tar Ka'roly, Some statistical characteristics of monthly average wind speed at various heights, *Renewable and Sustainable Energy Reviews*
58. Radics K. and Bartholy J., Estimating and modeling the wind resource of Hungary, *Renewable and Sustainable Energy Reviews*
59. Dua M., Manwell J.F., and McGowan J.G., Utility scale wind turbines on a grid-connected island: A feasibility study, *Renewable Energy*

60. Dhanju A., Whitaker P., and Kempton W., Assessing offshore wind resources: An accessible methodology, *Renewable Energy*
61. Marciukaitis M., Katinas V., and Kavaliauskas A. Wind power usage and prediction prospects in Lithuania, *Renewable and Sustainable Energy Reviews*, 12 (2008) 265–277.
62. Gong Li, Jing Shi, and Junyi Zhou, Bayesian adaptive combination of short-term wind speed forecasts from neural network models, *Renewable Energy* 2011;36:352–359.
63. Sfetsos A. A comparison of various forecasting techniques applied to mean hourly wind speed time series. *Renewable Energy* 2000;21(1):23-35.
64. Monfared M, Rastegar H, Kojabadi H. A new strategy for wind speed forecasting using artificial intelligent methods. *Renewable Energy* 2009;34(3):845-848.
65. Ma L, Luan S, Jiang C, Liu H, Zhang Y. A review on the forecasting of wind speed and generated power. *Renewable and Sustainable Energy Reviews* 2009;13(4):915-920.
66. Jones MS, Colle BA, Tongue JS. Evaluation of a mesoscale short-range ensemble forecast system over the northeast United States. *Weather and Forecasting* 2007;22(1):36-55.
67. Kamal L, Jafri YZ. Time series models to simulate and forecast hourly averaged wind speed in Quetta, Pakistan. *Solar Energy* 1997;61(1):23-32.
68. Torres J, Garcia A, Deblas M, Defrancisco A. Forecast of hourly average wind speed with arma models in navarre (Spain). *Solar Energy* 2005;79(1):65-77.
69. Kavasseri R, Seetharaman K. Day-ahead wind speed forecasting using f-ARIMA models. *Renewable Energy* 2009;34(5):1388-93.
70. Shamshad A, Bawadi MA, Wan Hussin WMA, Majid TA, Sanusi SAM. First and second order Markov chain models for synthetic generation of wind speed time series. *Energy* 2005;30:693-708.
71. Costa A, Crespo A, Navarro J, Lizcano G, Madsen H, Feitosa E. A review on the young history of the wind power short-term prediction. *Renewable and Sustainable Energy Reviews* 2008;12(6):1725-44.
72. Alexiadis M, Dokopoulos P, Sahsamanoğlu H, Manousaridis I. Short term forecasting of wind speed and related electrical power. *Solar Energy* 1998;63(1):61-8.
73. More A, Deo MC. Forecasting wind with neural networks. *Marine Structures* 2003;16(1):35-49.
74. Maqsood I, Khan MR, Huang GH, Abdalla R. Application of soft computing models to hourly weather analysis in southern Saskatchewan, Canada. *Engineering Applications of Artificial Intelligence* 2005;18(1):115-25.
75. Kariniotakis G, Stavrakakis G, Nogaret E. Wind power forecasting using advanced neural network models. *IEEE Trans Energy Conversion* 1996;11(4):762-7.
76. Barbounis TG, Theocharis JB. Locally recurrent neural networks for long-term wind speed and power prediction. *Neurocomputing* 2006;69(4-6):466-96.
77. Burnham KP, Anderson DR. *Model selection and multi-model inference*. 2<sup>nd</sup> ed., New York: Springer; 2002.
78. Sánchez I. Adaptive combination of forecasts with application to wind energy y. *International Journal of Forecasting* 2008;24(4):679-93.
79. I. G. Damousis, M. C. Alexiadis, and J. B. Theocharis, “A fuzzy model for wind speed prediction and power generation in wind parks using spatial correlation,” *IEEE Trans. on Energy Conversion*, vol. 19, no. 2, pp. 352-361. June 2004.
80. M. C. Alexiadis, P. S. Dokopoulos, and H. S. Sahsamanoğlu, “Wind speed and power forecasting based on spatial correlation models,” *IEEE Trans. Energy Conversion*, vol. 14, pp. 836–842, Sept. 1999.

81. R. Corotis, A. Sigl, and M. Cohen, "Variance analysis of wind characteristics for energy conversion," *J. Appl. Meteorology*, vol. 16, pp. 1149–1157, Nov. 1977.
82. H. G. Beyer, J. Luther, and R. Steinbergerwillms, "Power fluctuations in spatially dispersed wind turbine systems," *Sol. Energy*, vol. 64, no. 4, pp. 297–305, 1993.
83. I. Palomino and F. Martin, "A simple method for spatial interpolation of the wind in complex terrain," *J. Appl. Meteorology*, vol. 34, no. 7, pp. 1678–1693, 1995.
84. D. A. Bechrakis and P. D. Sparis, Correlation of Wind Speed Between Neighboring Measuring Stations, *IEEE Trans. on Energy Conversion*, vol. 19, no. 2, JUNE 2004.
85. A. Öztopal, "Artificial neural network approach to spatial estimation of wind velocity data", *Energy Conversion and Management*, vol. 47, pp. 395–406, 2006.
86. E. Cadenas and W. Rivera, "Wind speed forecasting in the South Coast of Oaxaca, Mexico", *Renewable Energy*, vol. 32, pp. 2116–2128, 2007.
87. M. Bilgili, B. Sahin and A. Yasar, "Application of artificial neural networks for the wind speed prediction of target station using reference stations data", *Renewable Energy*, vol. 32, pp. 2350–2360, 2007.
88. A. Lapedes and R. Farber, "Nonlinear signal processing using neural networks: prediction and system modeling. Technical report LA-UR-87-2662." Los Alamos, NM: Los Alamos National Laboratory; 1987.
89. Y. D. Song, A new approach for wind speed prediction", *Wind Engineering*, 2000; 24(1):35–47.
90. M. Alexiadis, I. Dokopoulos, H. Sahsamanoglou and I. Manousardis, "Short term forecasting of wind speed and related power", *Solar Energy*, vol. 63, no. 1, pp. 61–8, 1988.
91. D. A. Bechrakis and P. D. Sparis, "Wind Speed Prediction Using Artificial Neural Networks", *Journal of Wind Engineering*, vol. 22, No 6, 1998.
92. P. Lopez, R. Velo and F. Maseda, "Effect of direction on wind speed estimation in complex terrain using neural networks", *Renewable Energy*, vol. 33, pp. 2266–2272, 2008.
93. Krishnamurti TN, Kishtawal CM, LaRow TE, Bachiochi DR, Zhang Z, Williford CE, et al. Improved weather and seasonal climate forecasts from multimodel superensemble. *Science* 1999;285(5433):1548-50.
94. Georgakakos KP, Seo DJ, Gupta H, Schake J, Butts MB. Characterizing stream flow simulation uncertainty through multimodel ensembles. *Journal of Hydrology* 2004;298(1-4):222 - 41.
95. Hoeting JA, Madigan D, Raftery AE, Volinsky CT. Bayesian model averaging: a tutorial. *Statistical Science* 1999;14(4):382-417.
96. Raftery AE, Gneiting T, Balabdaoui F, Polakowski M. Using Bayesian model averaging to calibrate forecast ensembles. *Monthly Weather Review* 2005;133(5):1155-74.
97. Duan Q, Ajami N, Gao X, Sorooshian S. Multi-model ensemble hydrologic prediction using Bayesian model averaging. *Advances in Water Resources* 2007;30(5):1371e86.
98. Slughter JM, Gneiting T, Raftery AE. Probabilistic wind speed forecasting using ensembles and Bayesian model averaging. Technical report no. 544;2008. <http://www.stat.washington.edu/research/reports/2008/tr544.pdf>.
99. Li G, Shi J. Application of Bayesian model averaging in modeling long-term wind speed distributions. *Renewable Energy* 2010;35(6):1192-202.
100. Sancho Salcedo-Sanz, Angel M. Perez-Bellido, Emilio G. Ortiz-García, Antonio Portilla-Figueras, Luis Prieto, and Daniel Paredes, Hybridizing the fifth generation mesoscale model with artificial neural networks for short-term wind speed prediction, *Renewable Energy* 34 (2009) 1451–1457.

101. Lazar Lazic, Goran Pejanovic, Momcilo Zivkovic, Wind forecasts for wind power generation using the Eta model, *Renewable Energy* 35 (2010) 1236–1243
102. Lei M, Shiyang L, Chuanwen J, Hongling L, Yan Z. A review on the forecasting of wind speed and generated power. *Renewable and Sustainable Energy Reviews* 2009;1:915–20.
103. Landberg L, Giebel G, Nielsen HA, Nielsen T, Madsen H. Short-term prediction and overview. *Wind Energy* 2003;6(3):273–80.
104. Landberg L. Short-term prediction of the power production from wind farms. *Journal of Wind Engineering and Industrial Aerodynamics* 1999;80:207–20.
105. Ramirez-Rosado IJ, Fernandez-Jimenez A, Monteiro C, Sousa J, Bessa R. Comparison of two new short-term wind-power forecasting systems. *Renewable Energy* 2009;34:1848–54.
106. Nutter P, Manobianco J. Evaluation of the 29-km Eta model. Part I: Objective verification at three selected stations. *Weather and Forecasting* 1999;14:5–17.
107. O'Connor WP, Schwab DJ, Lang GA. Forecast verification for Eta model winds using Lake Erie storm surge water levels. *Weather and Forecasting* 1999;14:119–33.
108. Chou SC, Marengo JA, Dereczynski CP, Waldheim PV, Manzi AO. Comparison of CPTEC GCM and Eta model results with observational data from the Rondonia LBA reference site, Brazil. *Journal of the Meteorological Society of Japan* 2007;85A:25–42.
109. Elmore KL, Baldwin ME, Schultz DM. Field significance revisited: Spatial bias errors in forecasts as applied to the Eta model. *Monthly Weather Review* 2006;134:519–31.
110. Elmore KL, Schultz DM, Baldwin ME. The behavior of synoptic-scale errors in the Eta model. *Monthly Weather Review* 2006;134:3355–66.
111. Cheng WYY, Steenburgh WJ. Evaluation of surface sensible weather forecasts by the WRF and the Eta models over the Western United States. *Weather and Forecasting* 2005;20:812–21.
112. Rajagopal EN, Iyengar GR. Mesoscale forecasts with Eta model over Indian region. *Current Science* 2005;88(6):906–12.
113. Chou SC, Tanajura CAS, Xue Y, Nobre CA. Validation of the Eta/SSiB over South America. *Journal of Geophysical Research* 2002;107. D20, 8088.
114. Monobianco J, Nutter PA. Evaluation of the 29-km Eta model. Part II: Subjective verification over Florida. *Weather and Forecasting* 1999;14:18–37.
115. Kavasseri RG and Seetharaman K. Day-ahead wind speed forecasting using f-ARIMA models, *Renewable Energy* 34 (2009) 1388–1393.
116. Daniel AR, Chen AA. Stochastic simulation and forecasting of hourly average wind speed sequences in Jamaica. *Solar Energy* 1991;46(1):1–11.
117. Nielsen TL, Madsen H, Tofting J. Experience with statistical methods for wind power prediction. In: *Proceedings of the European wind energy conversion*; 1999. p. 1066–9. Nice, France.
118. Milligan M, Schwartz M, Wan Y. Statistical wind power forecasting models: results for U.S. wind farms. NREL-CP-500-33956; May 2003. <http://www.nrel.gov/docs/fy03osti/33956.pdf>.
119. Bossanyi EA. Short term stochastic prediction and possible control applications. In: *Proceedings of the Delphi workshop on wind energy applications*, Greece; May 1985. p. 66–79.
120. Kariniotakis GN, Nogaret EF, Stavrakakis GS. Advanced short-term forecasting of wind power production. In: *Proceedings of the European wind energy conference*; 1997. p. 751–4.
121. Hui Liu, Hong-Qi Tian, Chao Chen, Yan-Fei Li, A hybrid statistical method to predict wind speed and wind power, *Renewable Energy* 35 (2010) 1857–1861.

122. Negnevitsky M, Johnson P, Santoso S. Short term wind power forecasting using hybrid intelligent systems. in: IEEE proceedings of the power engineering general meeting; 2007. p. 1–4.
123. Miranda MS, Dunn RW. One-hour-ahead wind speed prediction using a Bayesian methodology, in: IEEE power engineering society general meeting; 2006. p. 1–6.
124. Flores P, Tapia A, Tapia G. Application of a control algorithm for wind speed prediction and active power generation. *Renewable Energy* 2005;30:523–36.
125. Barbounis TG, Theocharis JB. A locally recurrent fuzzy neural network with application to the wind speed prediction using spatial correlation. *Neurocomputing* 2007;70(7/9):1525–42.
126. Palomares-Salas JC, DelaRosa JJG, Ramiro JG, Melgar J, Aguilera A, Moreno A. ARIMA vs. Neural Networks for wind speed forecasting. In: IEEE international conference on computational intelligence for measurement systems and applications; 2009. p. 129–133.
127. Louka P, Galanis G, Siebert N, Kariniotakis G, Katsafados P, Pytharoulis I, et al. Improvements in wind speed forecasts for wind power prediction purposes using Kalman filtering. *Journal of Wind Engineering and Industrial Aerodynamics* 2008;96:2348–62.
128. Sideratos G, Hatzigiorgiou ND. An advanced statistical method for wind power forecasting. *Power Systems* 2007;22(1):258–65.
129. Erasmo Cadenas and Wilfrido Rivera, Wind speed forecasting in three different regions of Mexico, using a hybrid ARIMA-ANN model, *Renewable Energy* 35 (2010) 2732-2738.
130. Negnevitsky M and Potter CW. Innovative short-term wind generation prediction techniques. In: Proceedings of the power systems conference and exposition; 2006. p. 60-5.
131. Focken U, Lange M, Monnich K, Waldl H-P, Georg Beyer H, Luig A. Short-term prediction of the aggregated power output of wind farms e a statistical analysis of the reduction of the prediction error by spatial smoothing effects. *Journal of Wind Engineering and Industrial Aerodynamics* 2002;90(3):231-46.
132. Barbounis TG, Theocharis JB. A locally recurrent fuzzy neural network with application to the wind speed prediction using spatial correlation. *Neurocomputing* 2007;70(7/9):1525-42.
133. Lalarukh K, Yasmin ZJ. Time series models to simulate and forecast hourly averaged wind speed in Quetta, Pakistan. *Solar Energy* 1997;61(1):23-32.
134. Sfetsos A. A novel approach for the forecasting of mean hourly wind speed time series. *Renewable Energy* 2002;27(2):163-74.
135. Hamzaç C. Improving artificial neural networks' performance in seasonal time series forecasting. *Information Sciences* 2008;178:4550-9.
136. Kalogirou SA. Artificial neural networks in renewable energy systems applications: a review. *Renewable and Sustainable Energy Reviews* 2001;5:273-401.
137. Hwam H. Insights into neural-network forecasting of time series corresponding to ARMA (p,q) structures, *Omega. The International Journal of Management Science* 2001;29:273-89.
138. Balkin SD. The value of nonlinear models in the M3-competition. *International Journal of Forecasting* 2001;17:545-6.
139. Nelson M, Hill T, Remus W, O'Connor M. Time series forecasting using neural networks: should the data be deseasonalized first? *Journal of Forecasting* 1999;18:359-67.

140. Ray ML, Rogers AL, McGowan JG. Analysis of wind shear models and trends in different terrain. In: Proceedings of American Wind Energy Association Windpower 2006, Pittsburgh, PA, USA; June 2006.
141. Rehman S, Al-Abbadi NM. Wind shear coefficient, turbulence intensity and wind power potential assessment for Dhulom, Saudi Arabia. *Renew Energy* 2008;33:2653-60.
142. Bailey BH. Predicting vertical wind profiles as a function of time of the day and surface wind speed. In: Proceedings of an international colloquium on wind energy. Brighton, UK: BWEA; 1981.
143. Irwin JS. A theoretical variation of the wind profile power law exponent as a function of surface roughness length and stability. *Atmos Environ* 1979;13:191-4.
144. Bechrakis DA, Sparis PD. Simulation of the wind speeds at different heights using artificial neural networks. *Wind Eng* 2000;24(2):127-36.
145. Farrugia RN. The wind shear exponent in a Mediterranean island climate. *Renew Energy* 2003;28:647-53.
146. Rehman S, Al-Abbadi NM. Wind shear coefficients and energy yield for Dhahran, Saudi Arabia. *Renew Energy* 2007;32:738-49.
147. Smith K, Randall G, Malcolm D, Kelley N, Smith B. Evaluation of wind shear patterns at midwest wind energy facilities. NREL/CP-500-32492, Wind Power Conference. Portland, Oregon: National Renewable Energy Laboratory; 2002.
148. Sandia National Laboratories. New Mexico wind resource assessment. Global Energy Concepts, LLC, USA, February 2003.
149. Minnesota Department of Commerce. Wind resource analysis program 2002. St. Paul, Minnesota, USA: Minnesota Department of Commerce; October 2002.
150. Rogers AL. SODAR shear measurements at Brewster, Massachusetts. Massachusetts Technology Collaborative, FSRP0040-B; June 2008.
151. Schwartz M, Elliott D. Wind shear characteristics at central plains tall towers. National Renewable Energy Laboratory, NREL/CP-500-40019, Wind Power 2006 Conference, Pittsburgh, Pennsylvania.
152. Rehman S, El-Amin IM, Shaahid S, Ahmad A, Ahmad F, Thabit T. Wind measurements and energy potential for a remote village in Saudi Arabia. IEEE PES PowerAfrica 2007 Conference and Exposition, Johannesburg, South Africa, 16-20 July 2007.
153. Jaramillo OA, Borja MA. Wind speed analysis in La Ventosa, Mexico: a bimodal probability distribution case. *Renew Energy* 2004;29:1613-30.
154. Tar K. Some statistical characteristics of monthly average wind speed at various heights. *Renew Sustain Energy Rev* 2008;12:1712-24.
155. Gualtieri, G and Secci, S, Wind shear coefficients, roughness length and energy yield over coastal locations in Southern Italy, *Renewable Energy* 36(3):2011:1081-1094.
156. Rehman S. and Al-Abbadi N.M., Wind shear coefficients and its effect on energy production, *Energy Conversion and Management* 46 (2005) 2578–2591.
157. Al-Abbadi N.M. and Rehman S., Wind speed and wind power characteristic for Gassim, Saudi Arabia, *International Journal of Green Energy* 6(2):(2009):201-217.
158. Rehman S. and Al-Abbadi, N. M. (2010). Wind Power Characteristics on the North West Coast of Saudi Arabia, *Energy & Environment*, 20(8)/21(1), pp. 1257 - 1270.
159. Hall T. and Smith B. U.S. (2000). DOE-EPRI Wind turbine verification program. TVP News Bulletin, Issue 5.
160. Oklahoma Wind Power Initiative, Wind summary Hobart's KTJS sensors tower at 40, 70 and 100 metres, May 2002.

161. Smith K., Randall G., Malcolm D., Kelley N. and Smith B. (2002). Evaluation of wind shear patterns at Midwest wind energy facilities, National Renewable energy Laboratory, NREL/CP-500-32492, WINDPOWER Conference 2002, Portland Oregon.
162. Sisterton D. L., Hicks B. B., Coulter R. L., and Wesely M. L. (1983). Difficulties in using power laws for wind energy assessment. *Solar Energy* 31(2):201–204.
163. Michael W. T, Steven C., and Jonathan H., Assessing wind resources, A guide for landowners, project developers, and power suppliers, Union of Concern Scientists.
164. Michael Brower, Iowa wind resource maps – A GIS approach, February 1997.
165. Tar K. Some statistical characteristics of monthly average wind speed at various heights. *Renewable and Sustainable Energy Reviews* 2008;12:1712-24.
166. Weisser D. A wind energy analysis of Grenada: an estimation using the Weibull density function. *Renewable Energy* 2003;28:1803-12.
167. Dorvlo Atsu SS. Estimating wind speed distribution. *Energy Conversion and Management* 2002;43:2311-8.
168. Ramirez P, Carta JA. Influence of the data sampling interval in the estimation of the parameters of the Weibull wind speed probability density distribution: a case study. *Energy Conversion and Management* 2005;46:2419-38.
169. Lun IYF, Lam JC. A study of Weibull parameters using long-term wind observations. *Renewable Energy* 2000;20:145-53.
170. Stevens MJM, Smulders PT. The estimation of the parameters of the Weibull wind speed distribution for wind energy utilisation purposes. *Wind Engineering* 1979;3(2):132-45.
171. Gupta BK. Weibull parameters for annual and monthly wind speed distributions for five locations in India. *Solar Energy* 1986;37(6):469-71.
172. Justus CG, Hargraves WR, Yalcin A. National assessment of potential output from wind powered generators. *Journal of Applied Meteorology* 1976;15(7):673-8.
173. Corotis RB, Sigl AB, Klein J. Probability models of wind velocity magnitude and persistence. *Solar Energy* 1978;20:483-93.
174. Hennessey Jr. JP. Some aspects of wind power statistics. *Journal of Applied Meteorology*, 1977;16(2):119-28.
175. Hennessey Jr. JP. A comparison of the Weibull and Rayleigh distributions for estimating wind power potential. *Wind Engineering* 1978;2(3):156-64.
176. Garcia A, Torres JL, Prieto E, De Francisco A. Fitting wind speed distributions: a case study. *Solar Energy* 1998;62(2):139-44.
177. Lysen H. (1983). Introduction to wind energy. Consultancy Services, Wind Energy, Developing Countries (CWD), 82-1, May, 2nd Edition, The Netherlands 36–47.
178. Justus C. G., Mikhail A. (1976). Height variation of wind speed and wind distributions statistics. *Geophysical Research Letters* 3(5):261–264.
179. Darwish A.S.K. and Sayigh A.A.M. (1988). Wind energy potential in Iraq. *Solar and Wind Technology* 5(3):215–22.
180. Nfaoui H., Bahraui J., Darwish A.S.K. and Sayigh A.A.M. (1991). Wind energy potential in Morocco. *Renewable Energy* 1(1):1–8.
181. Jamil M., Parsa S. and Majidi M. (1995). Wind power statistics and evaluation of wind energy density. *Renewable Energy* 6(5):623–628.
182. Khogali A., Albar O.F. and Yousif B. (1991). Wind and solar energy potential in Makkah (Saudi Arabia)—comparison with Red Sea coastal sites. *Renewable Energy* 1(3):435–40.
183. Celik A. N. (2003). Energy output estimation for small-scale wind power generators using Weibull-representative wind data, *Journal of Wind Engineering and Industrial Aerodynamics* 91:693–707

184. Vogiatzis N., Kotti K., Spanomitsios S., Stoukides M. (2004). Analysis of wind potential and characteristics in North Aegean, Greece. *Renewable Energy* 29:1193–1208.
185. Essa K.S.M. and Mubarak F. (2006). Survey and Assessment of Wind-speed and Windpower in Egypt, including Air Density Variation. *Wind Engineering* 30(2):95–106.
186. Rehman S. (2004). Prospects of wind farm development in Saudi Arabia. *Renewable Energy* 30(3):447-463.
187. Rehman S. and Aftab A. (2004). Assessment of wind energy potential for coastal locations of the Kingdom Saudi Arabia. *Energy* 29:1105–1115.
188. Rehman, S. and Halawani, T. O. (1994). Statistical characteristics of wind in Saudi Arabia. *Renewable Energy* 4(8):949-956.
189. Rehman, S., Halawani, T. O., and Husain, T. (1994). Weibull parameters for wind speed distribution in Saudi Arabia. *Solar Energy* 53(6):473-479.
190. Rehman S. (2004). Wind energy availability and capacity factor analysis. Proceedings of the 2nd BSME-ASME International Conference on Thermal Engineering, BUET, Dhaka, Bangladesh, January 02 to 04, Vol. 2:900–905.
191. Rehman S. (2000). Renewable energy education – Its Need and Global Status. Proceedings of The Workshop on Energy Conservation, pp. 389-392, King Fahd University of Petroleum and Minerals, Dhaharn, Saudi Arabia.
192. Alawaji S. H. (1996). Wind energy resource assessment in Saudi Arabia-I Network Design and Description. *Renewable Energy* 7(4):319-328.
193. Al-Abbadi N. M., Alawaji S. H. and Eugenio N. N. (1997). Wind energy resource assessment: A three year Experience, Windpower1997 Proceedings, Annual Conference of the American Wind Energy Association, AWEA, Austin, Texas, June 15-18:533-541.
194. Al-Abbadi N. M. (2005). Wind energy resource assessment for five locations in Saudi Arabia. *Renewable Energy* 30:1489–1499.
195. Safari B. and Gasore J., A statistical investigation of wind characteristics and wind energy potential based on the Weibull and Rayleigh models in Rwanda, *Renewable Energy* 35 (2010) 2874-2880.
196. A.W. Dahmouni, M. Ben Salah, F. Askri, C. Kerkeni, S. Ben Nasrallah, Wind energy in the Gulf of Tunis, Tunisia, *Renewable and Sustainable Energy Reviews* 14 (2010) 1303–1311.
197. Carta J.A. and Ramirez P., Analysis of two-component mixture Weibull statistics for estimation of wind speed distributions, *Renewable Energy* 32 (2007) 518–531.
198. Ettoumi F.Y., Sauvageot H. and Adane A.E.H., Statistical bivariate modelling of wind using first-order Markov chain and Weibull distribution, *Renewable Energy* 28 (2003) 1787–1802.
199. Tuller SE, Brett AC. The characteristics of wind velocity that favor the fitting of a Weibull distribution in wind speed analysis. *Journal of Applied Meteorology*, 1984;23:124–34.
200. Weibull W. A statistical distribution function of wide applicability. *J Appl Mech* 1951;18:293–7.
201. Khogali A, Albar OF, Yousif B. Wind, solar energy potential in Makkah (Saudi Arabia). Comparison with Red Sea coastal sites. *Renewable Energy* 1991;1(3/4):435–40.
202. Hasan A. Wind energy in West Bank and Gaza Strip. *Renewable Energy* 1992;2(6):637–40.

203. Morgan VT. Statistical distributions of wind parameters at Sydney, Australia. *Renewable Energy* 1995;6(1):39–48.
204. Eskin N., Artar H. and Tolun S., Wind energy potential of Gokceada Island in Turkey, *Renewable and Sustainable Energy Reviews* 12 (2008) 839–851.
205. Wind Power Technology, Renewable Energy House, 26, rue du Trône, B-1000 Brussels, Belgium
206. Wind Power: News and Information about wind Power Technology <http://www.alternative-energy-news.info/technology/wind-power/> (Accessed on November 20, 2010)
207. Tom Kraeutler, May 16th 2010 at 12:00PM, <http://www.walletpop.com/blog/2010/05/16/new-wind-power-technology-offers-savings-at-home/> (Accessed on November 20, 2010)
208. Drouilhet SM. Power Flow Management in a High Penetration Wind-Diesel Hybrid Power System with Short-Term Energy Storage, National Wind Technology Center, NREL/CP-500-26827, Windpower '99, June 20–23, 1999, Burlington, Vermont.
209. Baring-Gould I. Hybrid systems architecture and control. Handbook on hybrid power systems. Golden, Colorado: National Renewable Energy Laboratory; March, 1998.
210. Yang H, Wei Z, Chengzhi L. Optimal design and techno-economic analysis of a hybrid solar-wind power generation system. *Applied Energy* 2009;86:163.
211. Yang H, Zhou W, Lu L, Fang Z. Optimal sizing method for stand-alone hybrid solar-wind system with LPSP technology by using genetic algorithm. *Solar Energy* 2008;82:354.
212. Wichert B et al. Development of a test facility for photovoltaic-diesel hybrid energy systems. *Renewable Energy* 2001;22(1):311–319.
213. Hunter R, Elliot G. Wind-diesel system options: A guide to the technology. Wind-diesel systems. Cambridge: Cambridge University Press; 1998.
214. Mahmoud MM, Ibrik IH. Techno-economic feasibility of energy supply of remote villages in Palestine by PV-systems, diesel generators and electric grid. *Renewable and Sustainable Energy Reviews* 2006;10:128–138.
215. Bagen BR. Evaluation of different operating strategies in small stand-alone power systems. *IEEE Trans Energy Conversion* 2005;20(3):654–660.
216. Bakos GC, Soursos M. Techno-economic assessment of a stand-alone PV/hybrid installation for low-cost electrification of a tourist resort in Greece. *Applied Energy* 2002;73:183–193.
217. Colle S, Abreu SL, Ruther R. Economic evaluation and optimization of hybrid diesel/photovoltaic systems integrated to electricity grid. *Solar Energy* 2004;76:295–299.
218. Schmid AL, Hoffmann CAA. Replacing diesel by solar in the Amazon: short-term economic feasibility of PV-diesel hybrid systems. *Energy Policy* 2004;32:881–898.
219. Wies RW, Johnson RA, Agrawal AN, Chubb TJ. Simulink model for economic analysis and environmental impacts of a PV with Diesel battery system for remote villages. *IEEE Trans Power Systems* 2005;20(2):692–700.
220. Dufo-Lo'pez R, Bernal-Agusti'n JL. Design and control strategies of PV-Diesel systems using genetic algorithms. *Solar Energy* 2005;79(1):33–46.
221. Nfah EM, Ngundam JM, Tchinda R. Modelling of solar/diesel/battery hybrid power systems for far-north Cameroon. *Renewable Energy* 2007;32:832–844.
222. Bala BK, Siddique SA. Optimal design of a PV-diesel hybrid system for electrification of an isolated island—Sandwip in Bangladesh using genetic algorithm. *Energy for Sustainable Development* 2009;13:137–142.

223. Hrayshat ES. Techno-economic analysis of autonomous hybrid photovoltaic-diesel-battery system. *Energy for Sustainable Development* 2009;13:143–150.
224. Dihrab SS, Sopian K. Electricity generation of hybrid PV/wind systems in Iraq. *Renewable Energy* 2010;35:1303–1307.
225. Barley CD. Optimal dispatch strategy in remote hybrid power systems. *Solar Energy* 1996;58:165–79.
226. Bryne J, Shen B, Wallace B. The economics of sustainable energy for rural development: a study of renewable energy in China. *Energy Policy* 1998;26:45–54.
227. Celik AN. A simplified model for estimating yearly wind fraction. *Renewable Energy* 2006;31:105–18.
228. Cavello AJ, Grubb AM. *Renewable energy sources for fuels and electricity*. London: Earthscan; 1993.
229. Ekren O, Ekren BY, Ozerdem B. Break-even analysis and size optimization of a PV/wind hybrid energy conversion system with battery storage – a case study. *Applied Energy* 2009;86(7–8):1043–54.
230. Saheb-Koussa D, Haddadi M, Belhamel M. Economic and technical study of a hybrid system (wind–photovoltaic–diesel) for rural electrification in Algeria. *Applied Energy* 86 (2009) 1024–1030.
231. Jose L, Bernal-Agustin, Dufo-Lopez R. Techno-economical optimization of the production of hydrogen from PV-Wind systems connected to the electrical grid. *Renewable Energy* 35 (2010) 747–758.
232. Arribas L, Cano L, Cruz I, Mata M, Llobet E. PV–wind hybrid system performance: A new approach and a case study. *Renewable Energy* 35 (2010) 128–137.
233. Sopian K, Ibrahim MZ, Daud WRW, Othman MY, Yatim B, Amin N. Performance of a PV–wind hybrid system for hydrogen production. *Renewable Energy* 34 (2009) 1973–1978.
234. Mahmoudi H, Abdul-Wahab SA, Goosen MFA, Sablani SS, Perret J, Ouagued A, et al. Weather data and analysis of hybrid photovoltaic-wind power generation systems adapted to a seawater greenhouse desalination unit designed for arid coastal countries. *Desalination* 2008;222:119.
235. Dufo-Lopez R, Jose L, Bernal-Agustin. Multi-objective design of PV– wind– diesel–hydrogen– battery systems. *Renewable Energy* 33 (2008) 2559– 2572.
236. Shakya BD, Aye L, Musgrave P. Technical feasibility and financial analysis of hybrid wind-photovoltaic system with hydrogen storage for Cooma. *International Journal of Hydrogen Energy* 2005;30:9.
237. Tina G, Gagliano S, Raiti S. Hybrid solar/wind power system probabilistic modeling for long-term performance assessment. *Solar Energy* 2006;80:578.
238. Kalantar M. and Mousavi S.M.G., Dynamic behavior of a stand-alone hybrid power generation system of wind turbine, microturbine, solar array and battery storage, *Applied Energy* 87 (2010) 3051–3064.
239. Lau K.Y., Yousof M.F.M., Arshad S.N.M., Anwari M., and Yatim A.H.M., Performance analysis of hybrid photovoltaic/diesel energy system under Malaysian conditions, *Energy* 35 (2010) 3245-3255.
240. Diaf S., Notton G., Belhamel M., Haddadi M., and Louche A., Design and techno-economical optimization for hybrid PV/wind system under various meteorological conditions, *Applied Energy* 85 (2008) 968–987.
241. Ekren O. and Ekren B.Y., Size optimization of a PV/wind hybrid energy conversion system with battery storage using response surface methodology, *Applied Energy* 85 (2008) 1086–1101.

242. Dalton G.J., Lockington D.A., and Baldock T.E., Feasibility analysis of renewable energy supply options for a grid-connected large hotel, *Renewable Energy* 34 (2009) 955–964.
243. Iqbal M.T., A feasibility study of a zero energy home in Newfoundland, *Renewable Energy* 29 (2004) 277–289.
244. Kamel S. and Dahl C., The economics of hybrid power systems for sustainable desert agriculture in Egypt , *Energy* 30(8), (2004),1271-1281.
245. Parker DS, Dunlop JP, Barkaszi SF, Sherwin JR, Anello MT, Sonne JK. Towards zero energy demand: evaluation of super efficient building technology with photovoltaic power for new residential housing. In: *Proceedings ACEEE Summer Study on Energy Efficiency in Buildings*, vol 1; 2000, pp. 1207–23.
246. Reijenga TH. Energy efficient and zero-energy building in the Netherlands. In: *International Workshop on Energy Efficiency in Buildings in China for the 21st Century*, CBEEA, Beijing; December 2000.
247. Gilijamse W. Zero-energy houses in the Netherlands. In: *Proceedings of Building Simulation '95*. Madison, Wisconsin, USA, August 14–16; 1995, pp. 276–83.
248. Merrigan T. On the path to zero energy homes. NREL/BR-550-29915, National Renewable Energy Laboratory, Golden, CO, US, Mar 2001 ([www.nrel.gov/docs/fy01osti/29915.pdf](http://www.nrel.gov/docs/fy01osti/29915.pdf))
249. Kadam S. Zero net energy buildings: are they economically feasible? In: *Sustainable Energy Proceedings*. Spring 2001. (<http://web.mit.edu/energylab/www/se/proceedings/Kadam2001.pdf>)
250. Zero energy homes: combining energy efficiency and solar energy technologies. NREL report #NREL/BR-550-27809. National Renewable Energy Laboratory. Golden, CO, March 2000. (<http://www.osti.gov/gpo/servlets/purl/754722-pxampg/native/>)
251. Ashraf I, Chandra A, Sodha MS. Techno-economic and environmental analysis for grid interactive solar photovoltaic power system of Lakshadweep islands. *International Journal of Energy Research* 2004;28(12):1033–42.
252. Chokmaviroj S, Wattanapong R, Suchart Y. Performance of a 500 kWp grid connected photovoltaic system at Mae Hong Son Province, Thailand. *Renewable Energy* 2006;31(1):19–28.
253. Zahedi A. Solar photovoltaic (PV) energy; latest developments in the building integrated and hybrid PV systems. *Renewable Energy* 2006;31(5):511–8.
254. Fernandez-Infantes A, Contreras J, Bernal-Agustin JL. Design of grid connected PV systems considering electrical, economical and environmental aspects: a practical case. *Renewable Energy* 2006;31(13):2042–62.
255. Gong X, Kulkarni M. Design optimization of a large scale rooftop photovoltaic system. *Solar Energy* 2005;78(3):362–74.
256. Yang D. Local photovoltaic wind hybrid system with battery storage or grid connection. NREL. Available from: [http://www.chem.jyu.fi/ue/frame\\_left/UEsem2005-Yang.pdf](http://www.chem.jyu.fi/ue/frame_left/UEsem2005-Yang.pdf); 2004.
257. Muir-Harmony A. Obstacles to the widespread use of grid-connected small WECS. *Sustainable Energy*. Available from: <http://www.mit.edu/afs/athena/course/10/10.391j/www/proceedings/Muir-Harmony2001.pdf> 2001.
258. Ubeda JR, Rodriguez Garcia MAR. Reliability and production assessment of wind energy production connected to the electric network supply. *IEE Proceedings-Generation, Transmission and Distribution* 1999;146(2):169–75.

259. Forsyth T, Tu P, Gilbert J. Economics of grid-connected small wind turbines in the domestic market. National Renewable Energy Laboratory (NREL). Available from: <<http://www.nrel.gov/docs/fy00osti/26975.pdf>>; 2002.
260. Underwood CP, Ramachandran J, Giddings RD, Alwan Z. Renewable-energy clusters for remote communities. *Applied Energy* 2007;84(6):579–98.
261. Mitchell K, Rizk J, Nagrial M. Balanced renewable energy system. In: power electronics and motion control conference. Available from: <<http://ieeexplore.ieee.org/iel5/7087/19127/00884619.pdf>>; 2000.
262. Kaldellis JK, Koronakis P, Kavadias K. Energy balance analysis of a stand-alone photovoltaic system, including variable system reliability impact. *Renewable Energy* 2004;29(7):1161–80.
263. Kaldellis JK, Kavadias KA. Optimal wind-hydro solution for Aegean Sea islands' electricity-demand fulfilment. *Applied Energy* 2001;70(4):333–54.
264. Lew D, Barley CD, Flowers LT. Wind/PV for households in Inner Mongolia. In: International Conference on village electrification through renewable energy. NREL. Available from: <[http://www.nrel.gov/international/china/pdfs/hybrid\\_wind\\_photovoltaic\\_systems\\_for\\_households\\_in\\_inner\\_mongolia.pdf](http://www.nrel.gov/international/china/pdfs/hybrid_wind_photovoltaic_systems_for_households_in_inner_mongolia.pdf)>; 1997.
265. Lambert T and Lilienthal P. HOMER: the micro-power optimization model. Software Developed by NREL. Available from: <[www.nrel.gov/HOMER](http://www.nrel.gov/HOMER)>; 2004 <http://www.mistaya.ca/homer/MicropowerSystemModelingWithHOMER.pdf>
266. Rhoads-Weaver H, Grove J. Exploring joint green tag financing and marketing models for energy independence. In: Conference proceedings of global windpower. NREL, [http://www.ourwind.org/windcoop/pdfs/AWEA\\_Paper.pdf](http://www.ourwind.org/windcoop/pdfs/AWEA_Paper.pdf).
267. Yang D. Local photovoltaic wind hybrid system with battery storage or grid connection. NREL, [http://www.chem.jyu.fi/ue/frame\\_left/UEsem2005-Yang.pdf](http://www.chem.jyu.fi/ue/frame_left/UEsem2005-Yang.pdf).
268. Borowy BS, Salameh ZM. Optimum photovoltaic array size for a hybrid wind–PV system. *IEEE Trans Energy Conversion* 1994;9(3):482–8.
269. Borowy BS, Salameh ZM. Methodology for optimally sizing the combination of a battery bank and PV array in a wind–PV hybrid system. *IEEE Trans Energy Conversion* 1996;11(2):367–75.
270. Markvart T. Sizing of hybrid photovoltaic-wind energy systems. *Sol Energy* 1996;57(4):277–81.
271. Bagul AD, Salameh ZM, Borowy BS. Sizing of stand-alone hybrid wind–PV system using a three event probability density approximation. *Sol Energy* 1996;56(4):323–35.
272. Ashok S. Optimised model for community-based hybrid energy system. *Renewable Energy* 2007;32(7):1155–64.
273. Bakos GC, Tsagas NF. Techno-economic assessment of a hybrid solar/wind installation for electrical energy saving. *Energy Build* 2003;35(2):139–45.
274. Zhou W, Lu L, Yang H. A novel optimization sizing model for hybrid solar-wind power generation system. *Sol Energy* 2007;81(1):76–84.
275. Protegeropoulos C, Brinkworth BJ, Marshall RH. Sizing and techno-economical optimization for hybrid solar photovoltaic/wind power systems with battery storage. *Int J Energy Res* 1997;21(6):465–79.
276. Seeling-Hochmuth GC. A combined optimization concept for the design and operation strategy of hybrid-PV energy systems. *Sol Energy* 1997;61(2):77–87.
277. Kellog W, Nehrir MH, Venkataramanan G, Gerez V. Optimal unit sizing for a hybrid wind/photovoltaic generating system. *Elect Power Syst Res* 1996;39(1):35–8.
278. Eke R, Kara O, Ulgen K. Optimization of a wind/PV hybrid power generation system. *Int J Green Energy* 2005;2(1):57–63.

279. Carlos GVL, Carlos AAS. Economic analysis of a diesel/photovoltaic hybrid for decentralized power generation in Northern Brazil. *Energy* 1998;23(4):317-23.
280. Sopian K, Othman MY, Rahman MAA. Performance of a photovoltaic diesel hybrid system in Malaysia. *ISESCO Sci Technol Vision* 2005;1:37-9.
281. Abdullah MO, Yung VC, Anyi M, Othman AK, Ab. Hamid KB, Tarawe J. Review and comparison study of hybrid diesel/solar/hydro/fuel cell energy schemes for a rural ICT Telecenter. *Energy*; 2009. doi:10.1016/j.energy.2009.10.035.
282. M. Bolinger and R. Wiser, Analysis of Utility-Scale Wind Turbines and Projects in the US, Ernest Orlando Lawrence Berkeley National Laboratory, Environmental Energy Technologies Division, 1 Cyclotron Rd., MS 90-4000, Berkeley, CA 94720, August 9, 2002. <http://eetd.lbl.gov/ea/ems/reports/47705.pdf>
283. Nordex Publication, N80 technical description document, Rev. 5.0, 2001. [http://www.nordex-online.com/e/produkte\\_und\\_service/index.html](http://www.nordex-online.com/e/produkte_und_service/index.html)
284. Nordex Publication, N60 technical description document, Rev. 5.0, 2001. [http://www.nordex-online.com/e/produkte\\_und\\_service/index.html](http://www.nordex-online.com/e/produkte_und_service/index.html)
285. Nordex Publication, N50 technical description document, Rev. 5.0, 2001. [http://www.nordex-online.com/e/produkte\\_und\\_service/index.html](http://www.nordex-online.com/e/produkte_und_service/index.html)
286. Nordex Publication, N43 technical description document, Rev. 5.0, 2001. [http://www.nordex-online.com/e/produkte\\_und\\_service/index.html](http://www.nordex-online.com/e/produkte_und_service/index.html)
287. Nordex Publication, S70 technical description document, Rev. 5.0, 2001. [http://www.nordex-online.com/e/online\\_service/download/dateien/S70\\_77.pdf](http://www.nordex-online.com/e/online_service/download/dateien/S70_77.pdf)
288. Nordex Publication, N90 technical description document, Rev. 5.0, 2001. [http://www.nordex-online.com/pdf/produktbroschueren/n80\\_en.pdf](http://www.nordex-online.com/pdf/produktbroschueren/n80_en.pdf)
289. Nordex Publication, N54 technical description document, Rev. 5.0, 2001. [http://www.nordex-online.com/pdf/produktbroschueren/n54\\_en.pdf](http://www.nordex-online.com/pdf/produktbroschueren/n54_en.pdf)
290. Vestas, Publication, V47 660 kW wind machine technical description, [http://www.vestas.com/produkter/V47/v47\\_UK.html](http://www.vestas.com/produkter/V47/v47_UK.html)
291. Vestas, Publication, V47 850 kW wind machine technical description, [http://www.vestas.com/produkter/V52/v52\\_UK.html](http://www.vestas.com/produkter/V52/v52_UK.html)
292. Vestas, Publication, V80 1800 kW wind machine technical description, [http://www.vestas.com/produkter/v80/v80\\_1\\_8\\_UK.html](http://www.vestas.com/produkter/v80/v80_1_8_UK.html)
293. DeWind, Publication, D4 600 kW wind machine technical description, <http://www.dewind.de/en/downloads/D4-600-100-eng.pdf>
294. DeWind, Publication, D6 1000 kW wind machine technical description, <http://www.dewind.de/en/downloads/D6-1000-100-eng.pdf>
295. DeWind, Publication, D8 2000 kW wind machine technical description, <http://www.dewind.de/en/downloads/D8-2000-100-eng.pdf>
296. GE Power Systems, Publication 900 kW wind machine technical information, [http://www.gepower.com/prod\\_serv/products/wind\\_turbines/en/900kw/index.htm](http://www.gepower.com/prod_serv/products/wind_turbines/en/900kw/index.htm)
297. GE Power Systems, Publication 1500 kW wind machine technical information, [http://www.gepower.com/prod\\_serv/products/wind\\_turbines/en/15mw/index.htm](http://www.gepower.com/prod_serv/products/wind_turbines/en/15mw/index.htm)
298. GE Power Systems, Publication 2300, 2500, and 2700 kW wind machine technical information, [http://www.gepower.com/prod\\_serv/products/wind\\_turbines/en/2xmw/index.htm](http://www.gepower.com/prod_serv/products/wind_turbines/en/2xmw/index.htm)
299. Bonus, Publication, 600 kW wind machine technical description, [http://www.bonus.dk/uk/produkter/tekbe\\_600\\_spec.html](http://www.bonus.dk/uk/produkter/tekbe_600_spec.html)
300. Bonus, Publication, 1000 kW wind machine technical description, [http://www.bonus.dk/uk/produkter/tekbe\\_1mv\\_spec.html](http://www.bonus.dk/uk/produkter/tekbe_1mv_spec.html)
301. Bonus, Publication, 1300 kW wind machine technical description, [http://www.bonus.dk/uk/produkter/tekbe\\_1300\\_spec.html](http://www.bonus.dk/uk/produkter/tekbe_1300_spec.html)

302. Morthorst P. E., Costs and prices: Wind energy – The Facts, Volume 2, [http://www.ewea.org/fileadmin/ewea\\_documents/documents/publications/WETF/Facts\\_Volume\\_2.pdf](http://www.ewea.org/fileadmin/ewea_documents/documents/publications/WETF/Facts_Volume_2.pdf) (Accessed 22 August 2011)
303. Lambert T and Lilienthal P. HOMER: the micro-power optimization model. Software Developed by NREL. Available from: <www.nrel.gov/HOMER>; 2004 <http://www.mistaya.ca/homer/MicropowerSystemModelingWithHOMER.pdf>
304. Rhoads-Weaver H, Grove J. Exploring joint green tag financing and marketing models for energy independence. In: Conference proceedings of global windpower. NREL, [http://www.ourwind.org/windcoop/pdfs/AWEA\\_Paper.pdf](http://www.ourwind.org/windcoop/pdfs/AWEA_Paper.pdf) .
305. Yang D. Local photovoltaic wind hybrid system with battery storage or grid connection. NREL, [http://www.chem.jyu.fi/ue/frame\\_left/UEsem2005-Yang.pdf](http://www.chem.jyu.fi/ue/frame_left/UEsem2005-Yang.pdf) .
306. Edwards JL, Wisser R, Bolinger M, Forsyth T. Building a market for small wind: the break-even turnkey cost of residential wind systems in the United States. Berkeley, CA (US): Ernest Orlando Lawrence Berkeley National Laboratory, [http://www.osti.gov/energycitations/product.biblio.jsp?osti\\_id=4823465](http://www.osti.gov/energycitations/product.biblio.jsp?osti_id=4823465)
307. Forsyth T, Tu P, Gilbert J. Economics of grid-connected small wind turbines in the domestic market. National Renewable Energy Laboratory (NREL). Available from: <http://www.nrel.gov/docs/fy00osti/26975.pdf>.

## **APPENDICES**

**APPENDIX A**

**TECHNICAL INFORMATION RELATED TO WIND ENERGY CONVERSION  
SYSTEM FROM SELECTED MANUFACTURERS**

Table A-1 Information on 600kW wind machine

S.No.	Name	Type	Rotor Dia, m	Cut-in Speed, m/s	Cut-out Speed, m/s	Rated, rpm	Hub Heights m	PCRv	TCRV	C <sub>T</sub>	Cost
1.	Get	41	41.0	4.0	25.0	27.8	50, 70	A	A	A	
2.	Vestas	V42	42.0	5.0	25.0	30.0	35, 40, 45, 50, 55	A	A	A	
3.	Nordtank		43.0	3.0	25.0	27.0	44.5, 50, 60	A	A	A	
4.	NegMicon	NM600/43	44.0	4.0	25.0	27.0	40, 45, 46, 56.5	A	A	A	
5.	Bonus		41.0	5.0	25.0	29.1	35	A	A	A	
6.	Dewind	D4/46	46.0	3.0	22.0	29.2	70, 40, 55, 60	A	A	A	
7.	Enercon	E-40/6.44	44.0	3.0	25.0	34.5	78, 46, 50, 58	A	A	A	
8.	Nordex	N-43	43.0	3.0	25.0	27.2	40, 50, 78	A	NA	NA	
9.	Micon	M1500	43.0	4.0	25.0	27.0	40, 46, 57, 50	A	A	A	
10.	Markham	VS45	45.9	3.0	35.0	32.0	52, 62	A	A	A	
11.	Jacobs	48/600	48.4	3.0	20.0	22.3	65, 50, 75	A	A	A	
12.	Windtec	WT641	40.6	4.0	25.0	35.0	52, 42	A	A	A	
13.	Wincon	W600/45	45.0	4.6	25.0	22.5	45	A	A	A	
14.	Tacke	TW 600	43.0	4.0	25.0	27.0	50, 60	A	A	A	
15.	Izar-Bonus	MK IV	44.0	4.0	25.0	27.0	40, 45, 50	A	A	A	
16.	Genesys	600	45.9	3.0	25.0	32.0	60, 50, 70	A	A	A	
17.	Anbonus	AN 600kW/41	41.0	5.0	25.0	29.0	50, 42	A	A	A	

Table A-2 Information on 750kW wind machine

S.No.	Name	Type	Rotor Dia, m	Cut-in Speed, m/s	Cut-out Speed, m/s	Rated, rpm	Hub Heights m	PCR V	TCRV	C <sub>T</sub>	Cost
1.	Lagerway	LW 50/750	51.5	4.0	25.0	27.0	75, 50	A	A	A	
2.	Wincon	W755/48 (755kW)	48.0	3.1	25.0	22.5	45	A	A	A	

Table A-3 Information on 800kW wind machine

S.No.	Name	Type	Rotor Dia, m	Cut-in Speed, m/s	Cut-out Speed, m/s	Rated, rpm	Hub Heights m	PCRv	TCRv	C <sub>T</sub>	Cost
1.	Nordex	N-50	50.0	3.0	25.0	23.75	46, 50, 70	NA	NA	NA	
2.	Made	AE-52	52.0	4.0	25.0	25.7	50	A	A	A	
3.	Fuhrlander	FL 800/48	48.0	3.0	25.0	22.0	60, 70	A	A	A	

Table A-4 Information on 1 000kW wind machine

S.No.	Name	Type	Rotor Dia, m	Cut-in Speed, m/s	Cut-out Speed, m/s	Rated , rpm	Hub Heights m	PCRv	TCRv	C <sub>T</sub>	Cost
1.	NegMicon	NM60/1000	60.0	1.7	20.0	18.0	45, 50, 70, 80	A	A	A	
2.	Enercon	E-58/10.58	58.0	2.6	25.0	24.0	70.5, 89	A	A	A	
3.	Nordex	N-54/1000	54.0	3.6	25.0	21.5	60, 70	A	A	A	
4.	GE (GE Wind Energy 900s)	<b>(900 kW)</b>	55.0	3.0	25.0	15-28		NA	NA	NA	
5.	Jacobs	<b>1050 kW</b>	57.0	3.5	25.0	22.9	55, 60, 70	A	A	A	
6.	HSW	1000/54	54.0	5.0	28.0	24.4					
7.	Izar-Bonus	1.0 MW	54.2	4.0	25.0	22.0	45, 50, 60	A	A	A	

Table A-5 Information on 1 300kW wind machine

S.No.	Name	Type	Rotor Dia, m	Cut-in Speed, m/s	Cut-out Speed, m/s	Rated, rpm	Hub Heights m	PCRv	TCRv	C <sub>T</sub>	Cost
1.	NegMicon	NM60/1000	60.0	3.0	20.0	18.0	45, 50, 70, 80	A	A	A	
2.	Bonus	1.3MW	62.0	4.0	25.0	19.0		A	A	A	
3.	Dewind	D6/60-1,250MW	60.0	3.0	28.0	23.9	60	A	A	A	
4.	Nordex	N-54/1000	54	3.6	25.0		60, 70	A	A	A	
5.	Izar-Bonus	1.3MW	62.0	4.0	25.0	19.0	45, 49, 60, 68	A	A	A	

Table A-6 Information on 1 500kW wind machine

S.No.	Name	Type	Rotor Dia, m	Cut-in Speed, m/s	Cut-out Speed, m/s	Rated , rpm	Hub Heights m	PCRv	TCRv	C <sub>T</sub>	Cost
1.	Lagerway	LW 70/1500	71.2	4.0	25.0	18.0	80, 65	A	A	A	
2.	Vestas	V63	63.0	4.5	25.0	21.0	60, 58	A	A	A	
3.	Nordtank		60.0	5.0	25.0	19.0	59.5	A	A	A	
4.	NegMicon	NM72C/1500	72.0	3.0	25.0	17.3	62, 78	A	A	A	
5.	Enercon	E-66/15.66	66.0	3.0	25.0	22.0	67, 85	A	A	A	
6.	GE	GE Wind Energy 1.5s	70.5	3.0	22.0	11-22	65, 80, 85, 100	NA	NA	NA	
7.	Jacobs	MD 70	70.0	3.5	25.0	19.0	65, 80, 85	A	A	A	
8.	Fuhrlander	FL MD 70	70	3.5	25.0	19.0	65, 85, 100	A	A	A	
9.	Gamesa	G80/1500	80.0	4.0	25.0	19.0	78, 67, 100	A	A	A	

Table A-7 Information on 2 000kW wind machine

S.No.	Name	Type	Rotor Dia, m	Cut-in Speed, m/s	Cut-out Speed, m/s	Rated, rpm	Hub Heights m	PCRv	TCRV	C <sub>T</sub>	Cost
1.	Lagerway	LW 70/2000	71.2	4.0	25.0	24.0	65, 80	A	A	A	
2.	Vestas	V80-2.0MW	80.0	4.0	25.0	16.7	78, 60, 67, 100	A	A	A	
3.	Dewind	D8/80-2MW	80.0	3.0	25.0	18.0	80, 95	A	A	A	
4.	Enercon	E-66/18.7 (1800kW)	70.0	2.5	25.0	22.0	65, 85, 98	A	A	A	
5.	Gamesa	G80/200	80.0	4.0	25.0	19.0	67, 60, 78, 100	A	A	A	
6.	Anbonus	AN 2MW/76	76.0	3.0	25.0	17.0	80, 60, 90	A	A	A	

Table A-8 Information on 2 500kW wind machine

S.No.	Name	Type	Rotor Dia, m	Cut-in Speed, m/s	Cut-out Speed, m/s	Rated, rpm	Hub Heights m	PCRv	TCRV	C <sub>T</sub>	Cost
1.	Nordex	N80/2500 kW	80.0	4.0	25.0	19.1	60, 80, 100	A	NA	NA	

## **APPENDIX B**

### **DETAILED TECHNICAL INFORMATION ON WIND ENERGY CONVERSION SYSTEM FROM NORDEX, VESTAS, DEWIND, GE AND BONUS**

**NORDEX**

[WECS – N43 -600 kW](#)

[WECS – N50 -800 kW](#)

[WECS – N60 -1300 kW](#)

[WECS – S70 -1500 kW](#)

[WECS – N80 -2300 kW](#)

[WECS – N90 -2500 kW](#)

**VESTAS**

[WECS – V47 – 660 kW](#)

[WECS – V52 – 850 kW](#)

[WECS – V80 – 1800 kW](#)

[WECS – V80 – 2000 kW](#)

**DEWIND**

[WECS – D4 – 600 kW](#)

[WECS – D6 – 1000 kW](#)

[WECS – D8 – 2000 kW](#)

**GE**

[WECS – GE900S – 900 kW](#)

[WECS – GE1.5SL – 1500 kW](#)

[WECS – GE2.3 – 2300 kW](#)

[WECS – GE2.5 – 2500 kW](#)

**BONUS**

[WECS – BONUS – 600 kW](#)

[WECS – BONUS – 1000 kW](#)

[WECS – BONUS – 1300 kW](#)

**ENERCON**

[WECS – ENERCON – 600 kW](#)

[WECS – ENERCON – 1000 kW](#)

[WECS – ENERCON – 1500 kW](#)

[WECS – ENERCON – 1800 kW](#)

**APPENDIX C**  
**ENERGY CALCULATIONS FROM SINGLE WIND MACHINES**

Table C-1 Wind energy output from single Nordex WECSs using wind data at 10metres for Yanbo

WS (m/s)	Frequency No. of hours	Wind power curve for Nordex wind machines (kW)							Wind energy output from single wind machine (kWh)						
		2500	2300	1500	1300	1000	800	600	2500	2300	1500	1300	1000	800	600
0	236	0	0	0	0	0	0	0	0	0	0	0	0	0	0
1	315	0	0	0	0	0	0	0	0	0	0	0	0	0	0
2	1173	0	0	0	0	0	0	0	0	0	0	0	0	0	0
3	1332	0	0	0	0	0	0	0	0	0	0	0	0	0	0
4	1196	15	70	24	29	14	23	17	17940	83720	28704	34684	16744	27508	20332
5	1241	120	183	86	73	51	57	45	148920	227103	106726	90593	63291	70737	55845
6	887	248	340	188	131	105	90	72	219976	301580	166756	116197	93135	79830	63864
7	638	429	563	326	241	179	165	124	273702	359194	207988	153758	114202	105270	79112
8	542	662	857	728	376	297	257	196	358804	464494	394576	203792	160974	139294	106232
9	448	964	1225	1006	536	427	359	277	431872	548800	450688	240128	191296	160832	124096
10	379	1306	1607	1271	704	548	470	364	494974	609053	481709	266816	207692	178130	137956
11	149	1658	1992	1412	871	697	572	444	247042	296808	210388	129779	103853	85228	66156
12	92	1984	2208	1500	1016	749	668	534	182528	203136	138000	93472	68908	61456	49128
13	66	2269	2300	1500	1124	885	747	584	149754	151800	99000	74184	58410	49302	38544
14	33	2450	2300	1500	1247	999	805	618	80850	75900	49500	41151	32967	26565	20394
15	24	2470	2300	1500	1301	1082	838	619	59280	55200	36000	31224	25968	20112	14856
16	4	2500	2300	1500	1344	1090	842	618	10000	9200	6000	5376	4360	3368	2472
17	1	2500	2300	1500	1364	1086	840	619	2500	2300	1500	1364	1086	840	619
18	2	2500	2300	1500	1322	1033	827	620	5000	4600	3000	2644	2066	1654	1240
19	0	2500	2300	1500	1319	1025	808	610	0	0	0	0	0	0	0
20	1	2500	2300	1500	1314	1021	785	594	2500	2300	1500	1314	1021	785	594
21	1	2500	2300	1500	1312	1011	757	592	2500	2300	1500	1312	1011	757	592
22	0	2500	2300	1500	1307	1000	728	590	0	0	0	0	0	0	0
23	0	2500	2300	1500	1299	990	743	580	0	0	0	0	0	0	0
24	0	2500	2300	1500	1292	980	742	575	0	0	0	0	0	0	0
25	0	2500	2300	1500	1292	970	745	570	0	0	0	0	0	0	0
		<b>Total:</b>							<b>2,688,142</b>	<b>3,397,488</b>	<b>2,383,535</b>	<b>1,487,788</b>	<b>1,146,984</b>	<b>1,011,668</b>	<b>782,032</b>

Table C-2 Wind energy output from single Nordex WECSs at 40-metre hub height for Yanbo wind data

WS (m/s)	Frequency No. of hours	Wind power curve for NORDEX wind machines (kW)							Wind energy output from single wind machine (kWh)						
		2500	2300	1500	1300	1000	800	600	2500	2300	1500	1300	1000	800	600
0	236	0	0	0	0	0	0	0	0	0	0	0	0	0	0
1	315	0	0	0	0	0	0	0	0	0	0	0	0	0	0
2	274	0	0	0	0	0	0	0	0	0	0	0	0	0	0
3	1236	0	0	0	0	0	0	0	0	0	0	0	0	0	0
4	1134	15	70	24	29	14	23	17	17010	79380	27216	32886	15876	26082	19278
5	1057	120	183	86	73	51	57	45	126840	193431	90902	77161	53907	60249	47565
6	1241	248	340	188	131	105	90	72	307768	421940	233308	162571	130305	111690	89352
7	89	429	563	326	241	179	165	124	38181	50107	29014	21449	15931	14685	11036
8	895	662	857	728	376	297	257	196	592490	767015	651560	336520	265815	230015	175420
9	681	964	1225	1006	536	427	359	277	656484	834225	685086	365016	290787	244479	188637
10	402	1306	1607	1271	704	548	470	364	525012	646014	510942	283008	220296	188940	146328
11	448	1658	1992	1412	871	697	572	444	742784	892416	632576	390208	312256	256256	198912
12	27	1984	2208	1500	1016	749	668	534	53568	59616	40500	27432	20223	18036	14418
13	374	2269	2300	1500	1124	885	747	584	848606	860200	561000	420376	330990	279378	218416
14	144	2450	2300	1500	1247	999	805	618	352800	331200	216000	179568	143856	115920	88992
15	74	2470	2300	1500	1301	1082	838	619	182780	170200	111000	96274	80068	62012	45806
16	66	2500	2300	1500	1344	1090	842	618	165000	151800	99000	88704	71940	55572	40788
17	7	2500	2300	1500	1364	1086	840	619	17500	16100	10500	9548	7602	5880	4333
18	30	2500	2300	1500	1322	1033	827	620	75000	69000	45000	39660	30990	24810	18600
19	22	2500	2300	1500	1319	1025	808	610	55000	50600	33000	29018	22550	17776	13420
20	3	2500	2300	1500	1314	1021	785	594	7500	6900	4500	3942	3063	2355	1782
21	5	2500	2300	1500	1312	1011	757	592	12500	11500	7500	6560	5055	3785	2960
22	0	2500	2300	1500	1307	1000	728	590	0	0	0	0	0	0	0
23	0	2500	2300	1500	1299	990	743	580	0	0	0	0	0	0	0
24	0	2500	2300	1500	1292	980	742	575	0	0	0	0	0	0	0
25	0	2500	2300	1500	1292	970	745	570	0	0	0	0	0	0	0
<b>Total:</b>									<b>4,776,823</b>	<b>5,611,644</b>	<b>3,988,604</b>	<b>2,569,901</b>	<b>2,021,510</b>	<b>1,717,920</b>	<b>1,326,043</b>

Table C-3 Wind energy output from single Nordex WECS at 50-metre hub height for Yanbo wind data

WS (m/s)	Frequency No. of hours	Wind power curve for Nordex wind machines (kW)							Wind energy output from single wind machine (kWh)						
		2500	2300	1500	1300	1000	800	600	2500	2300	1500	1300	1000	800	600
0	236	0	0	0	0	0	0	0	0	0	0	0	0	0	0
1	315	0	0	0	0	0	0	0	0	0	0	0	0	0	0
2	274	0	0	0	0	0	0	0	0	0	0	0	0	0	0
3	1236	0	0	0	0	0	0	0	0	0	0	0	0	0	0
4	995	15	70	24	29	14	23	17	14925	69650	23880	28855	13930	22885	16915
5	1196	120	183	86	73	51	57	45	143520	218868	102856	87308	60996	68172	53820
6	1241	248	340	188	131	105	90	72	307768	421940	233308	162571	130305	111690	89352
7	89	429	563	326	241	179	165	124	38181	50107	29014	21449	15931	14685	11036
8	895	662	857	728	376	297	257	196	592490	767015	651560	336520	265815	230015	175420
9	541	964	1225	1006	536	427	359	277	521524	662725	544246	289976	231007	194219	149857
10	542	1306	1607	1271	704	548	470	364	707852	870994	688882	381568	297016	254740	197288
11	58	1658	1992	1412	871	697	572	444	96164	115536	81896	50518	40426	33176	25752
12	417	1984	2208	1500	1016	749	668	534	827328	920736	625500	423672	312333	278556	222678
13	352	2269	2300	1500	1124	885	747	584	798688	809600	528000	395648	311520	262944	205568
14	149	2450	2300	1500	1247	999	805	618	365050	342700	223500	185803	148851	119945	92082
15	17	2470	2300	1500	1301	1082	838	619	41990	39100	25500	22117	18394	14246	10523
16	105	2500	2300	1500	1344	1090	842	618	262500	241500	157500	141120	114450	88410	64890
17	43	2500	2300	1500	1364	1086	840	619	107500	98900	64500	58652	46698	36120	26617
18	26	2500	2300	1500	1322	1033	827	620	65000	59800	39000	34372	26858	21502	16120
19	24	2500	2300	1500	1319	1025	808	610	60000	55200	36000	31656	24600	19392	14640
20	1	2500	2300	1500	1314	1021	785	594	2500	2300	1500	1314	1021	785	594
21	8	2500	2300	1500	1312	1011	757	592	20000	18400	12000	10496	8088	6056	4736
22	0	2500	2300	1500	1307	1000	728	590	0	0	0	0	0	0	0
23	0	2500	2300	1500	1299	990	743	580	0	0	0	0	0	0	0
24	0	2500	2300	1500	1292	980	742	575	0	0	0	0	0	0	0
25	0	2500	2300	1500	1292	970	745	570	0	0	0	0	0	0	0
<b>Total:</b>									<b>4,972,980</b>	<b>5,765,071</b>	<b>4,068,642</b>	<b>2,663,615</b>	<b>2,068,239</b>	<b>1,777,538</b>	<b>1,377,888</b>

Table C-4 Wind energy output from single Nordex WECSs at 60-metre hub height for Yanbo wind data

WS (m/s)	Frequency No. of hours	Wind power curve for Nordex wind machines (kW)							Wind energy output from single wind machine (kWh)						
		2500	2300	1500	1300	1000	800	600	2500	2300	1500	1300	1000	800	600
0	236	0	0	0	0	0	0	0	0	0	0	0	0	0	0
1	315	0	0	0	0	0	0	0	0	0	0	0	0	0	0
2	274	0	0	0	0	0	0	0	0	0	0	0	0	0	0
3	1236	0	0	0	0	0	0	0	0	0	0	0	0	0	0
4	995	15	70	24	29	14	23	17	14925	69650	23880	28855	13930	22885	16915
5	1196	120	183	86	73	51	57	45	143520	218868	102856	87308	60996	68172	53820
6	111	248	340	188	131	105	90	72	27528	37740	20868	14541	11655	9990	7992
7	1219	429	563	326	241	179	165	124	522951	686297	397394	293779	218201	201135	151156
8	798	662	857	728	376	297	257	196	528276	683886	580944	300048	237006	205086	156408
9	638	964	1225	1006	536	427	359	277	615032	781550	641828	341968	272426	229042	176726
10	140	1306	1607	1271	704	548	470	364	182840	224980	177940	98560	76720	65800	50960
11	460	1658	1992	1412	871	697	572	444	762680	916320	649520	400660	320620	263120	204240
12	390	1984	2208	1500	1016	749	668	534	773760	861120	585000	396240	292110	260520	208260
13	379	2269	2300	1500	1124	885	747	584	859951	871700	568500	425996	335415	283113	221336
14	22	2450	2300	1500	1247	999	805	618	53900	50600	33000	27434	21978	17710	13596
15	144	2470	2300	1500	1301	1082	838	619	355680	331200	216000	187344	155808	120672	89136
16	74	2500	2300	1500	1344	1090	842	618	185000	170200	111000	99456	80660	62308	45732
17	67	2500	2300	1500	1364	1086	840	619	167500	154100	100500	91388	72762	56280	41473
18	7	2500	2300	1500	1322	1033	827	620	17500	16100	10500	9254	7231	5789	4340
19	30	2500	2300	1500	1319	1025	808	610	75000	69000	45000	39570	30750	24240	18300
20	20	2500	2300	1500	1314	1021	785	594	50000	46000	30000	26280	20420	15700	11880
21	9	2500	2300	1500	1312	1011	757	592	22500	20700	13500	11808	9099	6813	5328
22	0	2500	2300	1500	1307	1000	728	590	0	0	0	0	0	0	0
23	0	2500	2300	1500	1299	990	743	580	0	0	0	0	0	0	0
24	0	2500	2300	1500	1292	980	742	575	0	0	0	0	0	0	0
25	0	2500	2300	1500	1292	970	745	570	0	0	0	0	0	0	0
<b>Total:</b>									<b>5,358,543</b>	<b>6,210,011</b>	<b>4,308,230</b>	<b>2,880,489</b>	<b>2,237,787</b>	<b>1,918,375</b>	<b>1,477,598</b>

Table C-5 Wind energy output from single Nordex WECSs at 70-metre hub height for Yanbo wind data

WS (m/s)	Frequency No. of hours	Wind power curve for Nordex wind machines (kW)							Wind energy output from single wind machine (kWh)						
		2500	2300	1500	1300	1000	800	600	2500	2300	1500	1300	1000	800	600
0	236	0	0	0	0	0	0	0	0	0	0	0	0	0	0
1	315	0	0	0	0	0	0	0	0	0	0	0	0	0	0
2	274	0	0	0	0	0	0	0	0	0	0	0	0	0	0
3	1236	0	0	0	0	0	0	0	0	0	0	0	0	0	0
4	995	15	70	24	29	14	23	17	14925	69650	23880	28855	13930	22885	16915
5	1196	120	183	86	73	51	57	45	143520	218868	102856	87308	60996	68172	53820
6	111	248	340	188	131	105	90	72	27528	37740	20868	14541	11655	9990	7992
7	1218	429	563	326	241	179	165	124	522522	685734	397068	293538	218022	200970	151032
8	798	662	857	728	376	297	257	196	528276	683886	580944	300048	237006	205086	156408
9	96	964	1225	1006	536	427	359	277	92544	117600	96576	51456	40992	34464	26592
10	681	1306	1607	1271	704	548	470	364	889386	1094367	865551	479424	373188	320070	247884
11	402	1658	1992	1412	871	697	572	444	666516	800784	567624	350142	280194	229944	178488
12	448	1984	2208	1500	1016	749	668	534	888832	989184	672000	455168	335552	299264	239232
13	28	2269	2300	1500	1124	885	747	584	63532	64400	42000	31472	24780	20916	16352
14	374	2450	2300	1500	1247	999	805	618	916300	860200	561000	466378	373626	301070	231132
15	127	2470	2300	1500	1301	1082	838	619	313690	292100	190500	165227	137414	106426	78613
16	92	2500	2300	1500	1344	1090	842	618	230000	211600	138000	123648	100280	77464	56856
17	31	2500	2300	1500	1364	1086	840	619	77500	71300	46500	42284	33666	26040	19189
18	43	2500	2300	1500	1322	1033	827	620	107500	98900	64500	56846	44419	35561	26660
19	26	2500	2300	1500	1319	1025	808	610	65000	59800	39000	34294	26650	21008	15860
20	24	2500	2300	1500	1314	1021	785	594	60000	55200	36000	31536	24504	18840	14256
21	9	2500	2300	1500	1312	1011	757	592	22500	20700	13500	11808	9099	6813	5328
22	0	2500	2300	1500	1307	1000	728	590	0	0	0	0	0	0	0
23	0	2500	2300	1500	1299	990	743	580	0	0	0	0	0	0	0
24	0	2500	2300	1500	1292	980	742	575	0	0	0	0	0	0	0
25	0	2500	2300	1500	1292	970	745	570	0	0	0	0	0	0	0
<b>Total:</b>									<b>5,630,071</b>	<b>6,432,013</b>	<b>4,458,367</b>	<b>3,023,973</b>	<b>2,345,973</b>	<b>2,004,983</b>	<b>1,542,609</b>

Table C-6 Wind energy output from single Nordex WECSs at 80-metre hub height for Yanbo wind data

WS (m/s)	Frequency No. of hours	Wind power curve for Nordex wind machines (kW)							Wind energy output from single wind machine (kWh)						
		2500	2300	1500	1300	1000	800	600	2500	2300	1500	1300	1000	800	600
0	236	0	0	0	0	0	0	0	0	0	0	0	0	0	0
1	315	0	0	0	0	0	0	0	0	0	0	0	0	0	0
2	274	0	0	0	0	0	0	0	0	0	0	0	0	0	0
3	1236	0	0	0	0	0	0	0	0	0	0	0	0	0	0
4	995	15	70	24	29	14	23	17	14925	69650	23880	28855	13930	22885	16915
5	139	120	183	86	73	51	57	45	16680	25437	11954	10147	7089	7923	6255
6	1168	248	340	188	131	105	90	72	289664	397120	219584	153008	122640	105120	84096
7	1130	429	563	326	241	179	165	124	484770	636190	368380	272330	202270	186450	140120
8	887	662	857	728	376	297	257	196	587194	760159	645736	333512	263439	227959	173852
9	96	964	1225	1006	536	427	359	277	92544	117600	96576	51456	40992	34464	26592
10	681	1306	1607	1271	704	548	470	364	889386	1094367	865551	479424	373188	320070	247884
11	402	1658	1992	1412	871	697	572	444	666516	800784	567624	350142	280194	229944	178488
12	448	1984	2208	1500	1016	749	668	534	888832	989184	672000	455168	335552	299264	239232
13	28	2269	2300	1500	1124	885	747	584	63532	64400	42000	31472	24780	20916	16352
14	352	2450	2300	1500	1247	999	805	618	862400	809600	528000	438944	351648	283360	217536
15	149	2470	2300	1500	1301	1082	838	619	368030	342700	223500	193849	161218	124862	92231
16	17	2500	2300	1500	1344	1090	842	618	42500	39100	25500	22848	18530	14314	10506
17	105	2500	2300	1500	1364	1086	840	619	262500	241500	157500	143220	114030	88200	64995
18	36	2500	2300	1500	1322	1033	827	620	90000	82800	54000	47592	37188	29772	22320
19	33	2500	2300	1500	1319	1025	808	610	82500	75900	49500	43527	33825	26664	20130
20	4	2500	2300	1500	1314	1021	785	594	10000	9200	6000	5256	4084	3140	2376
21	29	2500	2300	1500	1312	1011	757	592	72500	66700	43500	38048	29319	21953	17168
22	0	2500	2300	1500	1307	1000	728	590	0	0	0	0	0	0	0
23	0	2500	2300	1500	1299	990	743	580	0	0	0	0	0	0	0
24	0	2500	2300	1500	1292	980	742	575	0	0	0	0	0	0	0
25	0	2500	2300	1500	1292	970	745	570	0	0	0	0	0	0	0
<b>Total:</b>									<b>5,784,473</b>	<b>6,622,391</b>	<b>4,600,785</b>	<b>3,098,798</b>	<b>2,413,916</b>	<b>2,047,260</b>	<b>1,577,048</b>

Table C-7 Wind energy output from single Vestas WECSs using wind data at 10metres for Yanbo

s

WS (m/s)	Frequency No. of hours	Wind power curve for wind machines (kW)				Wind energy output from single wind machine (kWh)			
		WECS SIZE (kW) ▶▶	600	850	1500	2000	600	850	1500
0	236	0	0	0	0	0	0	0	0
1	315	0	0	0	0	0	0	0	0
2	1173	0	0	0	0	0	0	0	0
3	1332	0	0	0	0	0	0	0	0
4	1196	0	25.5	0	44.1	0	30498	0	52743.6
5	1241	22	67.4	55	135	27302	83643.4	68255	167535
6	887	65	125	145	261	57655	110875	128615	231507
7	638	120	203	266	437	76560	129514	169708	278806
8	542	188	304	421	669	101896	164768	228182	362598
9	448	268	425	613	957	120064	190400	274624	428736
10	379	356	554	836	1279	134924	209966	316844	484741
11	149	440	671	1065	1590	65560	99979	158685	236910
12	92	510	759	1267	1823	46920	69828	116564	167716
13	66	556	811	1407	1945	36696	53526	92862	128370
14	33	582	836	1474	1988	19206	27588	48642	65604
15	24	594	846	1495	1998	14256	20304	35880	47952
16	4	598	849	1500	2000	2392	3396	6000	8000
17	1	600	850	1500	2000	600	850	1500	2000
18	2	600	850	1500	2000	1200	1700	3000	4000
19	0	600	850	1500	2000	0	0	0	0
20	1	600	850	1500	2000	600	850	1500	2000
21	1	600	850	1500	2000	600	850	1500	2000
22	0	600	850	1500	2000	0	0	0	0
23	0	600	850	1500	2000	0	0	0	0
24	0	600	850	1500	2000	0	0	0	0
25	0	600	850	1500	2000	0	0	0	0
<b>Total:</b>						<b>706,431</b>	<b>1,198,535</b>	<b>1,652,361</b>	<b>2,671,219</b>

Table C-8 Wind energy output from single Vestas WECSs using wind data at 40metres for Yanbo

WS (m/s)	Frequency No. of hours	Wind power curve for wind machines (kW)				Wind energy output from single wind machine (kWh)			
		600	850	1500	2000	600	850	1500	2000
WECS SIZE (kW)	▶▶								
0	236	0	0	0	0	0	0	0	0
1	315	0	0	0	0	0	0	0	0
2	274	0	0	0	0	0	0	0	0
3	1236	0	0	0	0	0	28917	0	50009.4
4	1134	0	25.5	0	44.1	23254	71241.8	58135	142695
5	1057	22	67.4	55	135	80665	155125	179945	323901
6	1241	65	125	145	261	10680	18067	23674	38893
7	89	120	203	266	437	168260	272080	376795	598755
8	895	188	304	421	669	182508	289425	417453	651717
9	681	268	425	613	957	143112	222708	336072	514158
10	402	356	554	836	1279	197120	300608	477120	712320
11	448	440	671	1065	1590	13770	20493	34209	49221
12	27	510	759	1267	1823	207944	303314	526218	727430
13	374	556	811	1407	1945	83808	120384	212256	286272
14	144	582	836	1474	1988	43956	62604	110630	147852
15	74	594	846	1495	1998	39468	56034	99000	132000
16	66	598	849	1500	2000	4200	5950	10500	14000
17	7	600	850	1500	2000	18000	25500	45000	60000
18	30	600	850	1500	2000	13200	18700	33000	44000
19	22	600	850	1500	2000	1800	2550	4500	6000
20	3	600	850	1500	2000	3000	4250	7500	10000
21	5	600	850	1500	2000	0	0	0	0
22	0	600	850	1500	2000	0	0	0	0
23	0	600	850	1500	2000	0	0	0	0
24	0	600	850	1500	2000	0	0	0	0
25	0	600	850	1500	2000	0	0	0	0
<b>Total:</b>						<b>1,234,745</b>	<b>1,977,951</b>	<b>2,952,007</b>	<b>4,509,223</b>

Table C-9 Wind energy output from single Vestas WECSs using wind data at 50metres for Yanbo

WS (m/s)	Frequency No. of hours	Wind power curve for wind machines (kW)				Wind energy output from single wind machine (kWh)			
		WECS SIZE (kW) ▶▶	600	850	1500	2000	600	850	1500
0	236	0	0	0	0	0	0	0	0
1	315	0	0	0	0	0	0	0	0
2	274	0	0	0	0	0	0	0	0
3	1236	0	0	0	0	0	0	0	0
4	995	0	25.5	0	44.1	0	25372.5	0	43879.5
5	1196	22	67.4	55	135	26312	80610.4	65780	161460
6	1241	65	125	145	261	80665	155125	179945	323901
7	89	120	203	266	437	10680	18067	23674	38893
8	895	188	304	421	669	168260	272080	376795	598755
9	541	268	425	613	957	144988	229925	331633	517737
10	542	356	554	836	1279	192952	300268	453112	693218
11	58	440	671	1065	1590	25520	38918	61770	92220
12	417	510	759	1267	1823	212670	316503	528339	760191
13	352	556	811	1407	1945	195712	285472	495264	684640
14	149	582	836	1474	1988	86718	124564	219626	296212
15	17	594	846	1495	1998	10098	14382	25415	33966
16	105	598	849	1500	2000	62790	89145	157500	210000
17	43	600	850	1500	2000	25800	36550	64500	86000
18	26	600	850	1500	2000	15600	22100	39000	52000
19	24	600	850	1500	2000	14400	20400	36000	48000
20	1	600	850	1500	2000	600	850	1500	2000
21	8	600	850	1500	2000	4800	6800	12000	16000
22	0	600	850	1500	2000	0	0	0	0
23	0	600	850	1500	2000	0	0	0	0
24	0	600	850	1500	2000	0	0	0	0
25	0	600	850	1500	2000	0	0	0	0
<b>Total:</b>						<b>1,278,565</b>	<b>2,037,132</b>	<b>3,071,853</b>	<b>4,659,073</b>

Table C-10 Wind energy output from single Vestas WECSs using wind data at 60metres for Yanbo

WS (m/s)	Frequency No. of hours	Wind power curve for wind machines (kW)				Wind energy output from single wind machine (kWh)			
		600	850	1500	2000	600	850	1500	2000
WECS SIZE (kW)	▶▶								
0	236	0	0	0	0	0	0	0	0
1	315	0	0	0	0	0	0	0	0
2	274	0	0	0	0	0	0	0	0
3	1236	0	0	0	0	0	0	0	0
4	995	0	25.5	0	44.1	0	25372.5	0	43879.5
5	1196	22	67.4	55	135	26312	80610.4	65780	161460
6	111	65	125	145	261	7215	13875	16095	28971
7	1219	120	203	266	437	146280	247457	324254	532703
8	798	188	304	421	669	150024	242592	335958	533862
9	638	268	425	613	957	170984	271150	391094	610566
10	140	356	554	836	1279	49840	77560	117040	179060
11	460	440	671	1065	1590	202400	308660	489900	731400
12	390	510	759	1267	1823	198900	296010	494130	710970
13	379	556	811	1407	1945	210724	307369	533253	737155
14	22	582	836	1474	1988	12804	18392	32428	43736
15	144	594	846	1495	1998	85536	121824	215280	287712
16	74	598	849	1500	2000	44252	62826	111000	148000
17	67	600	850	1500	2000	40200	56950	100500	134000
18	7	600	850	1500	2000	4200	5950	10500	14000
19	30	600	850	1500	2000	18000	25500	45000	60000
20	20	600	850	1500	2000	12000	17000	30000	40000
21	9	600	850	1500	2000	5400	7650	13500	18000
22	0	600	850	1500	2000	0	0	0	0
23	0	600	850	1500	2000	0	0	0	0
24	0	600	850	1500	2000	0	0	0	0
25	0	600	850	1500	2000	0	0	0	0
<b>Total:</b>						<b>1,385,071</b>	<b>2,186,748</b>	<b>3,325,712</b>	<b>5,015,475</b>

Table C-11 Wind energy output from single Vestas WECSs using wind data at 70metres for Yanbo

WS (m/s)	Frequency No. of hours	Wind power curve for wind machines (kW)				Wind energy output from single wind machine (kWh)			
		600	850	1500	2000	600	850	1500	2000
WECS SIZE (kW)	▶▶								
0	236	0	0	0	0	0	0	0	0
1	315	0	0	0	0	0	0	0	0
2	274	0	0	0	0	0	0	0	0
3	1236	0	0	0	0	0	0	0	0
4	995	0	25.5	0	44.1	0	25372.5	0	43879.5
5	1196	22	67.4	55	135	26312	80610.4	65780	161460
6	111	65	125	145	261	7215	13875	16095	28971
7	1218	120	203	266	437	146160	247254	323988	532266
8	798	188	304	421	669	150024	242592	335958	533862
9	96	268	425	613	957	25728	40800	58848	91872
10	681	356	554	836	1279	242436	377274	569316	870999
11	402	440	671	1065	1590	176880	269742	428130	639180
12	448	510	759	1267	1823	228480	340032	567616	816704
13	28	556	811	1407	1945	15568	22708	39396	54460
14	374	582	836	1474	1988	217668	312664	551276	743512
15	127	594	846	1495	1998	75438	107442	189865	253746
16	92	598	849	1500	2000	55016	78108	138000	184000
17	31	600	850	1500	2000	18600	26350	46500	62000
18	43	600	850	1500	2000	25800	36550	64500	86000
19	26	600	850	1500	2000	15600	22100	39000	52000
20	24	600	850	1500	2000	14400	20400	36000	48000
21	9	600	850	1500	2000	5400	7650	13500	18000
22	0	600	850	1500	2000	0	0	0	0
23	0	600	850	1500	2000	0	0	0	0
24	0	600	850	1500	2000	0	0	0	0
25	0	600	850	1500	2000	0	0	0	0
<b>Total:</b>						<b>1,446,725</b>	<b>2,271,524</b>	<b>3,483,768</b>	<b>5,220,912</b>

Table C-12 Wind energy output from single Vestas WECSs using wind data at 80metres for Yanbo

WS (m/s)	Frequency No. of hours	Wind power curve for wind machines (kW)				Wind energy output from single wind machine (kWh)			
		600	850	1500	2000	600	850	1500	2000
WECS SIZE (kW)	▶▶								
0	236	0	0	0	0	0	0	0	0
1	315	0	0	0	0	0	0	0	0
2	274	0	0	0	0	0	0	0	0
3	1236	0	0	0	0	0	0	0	0
4	995	0	25.5	0	44.1	0	25372.5	0	43879.5
5	139	22	67.4	55	135	3058	9368.6	7645	18765
6	1168	65	125	145	261	75920	146000	169360	304848
7	1130	120	203	266	437	135600	229390	300580	493810
8	887	188	304	421	669	166756	269648	373427	593403
9	96	268	425	613	957	25728	40800	58848	91872
10	681	356	554	836	1279	242436	377274	569316	870999
11	402	440	671	1065	1590	176880	269742	428130	639180
12	448	510	759	1267	1823	228480	340032	567616	816704
13	28	556	811	1407	1945	15568	22708	39396	54460
14	352	582	836	1474	1988	204864	294272	518848	699776
15	149	594	846	1495	1998	88506	126054	222755	297702
16	17	598	849	1500	2000	10166	14433	25500	34000
17	105	600	850	1500	2000	63000	89250	157500	210000
18	36	600	850	1500	2000	21600	30600	54000	72000
19	33	600	850	1500	2000	19800	28050	49500	66000
20	4	600	850	1500	2000	2400	3400	6000	8000
21	29	600	850	1500	2000	17400	24650	43500	58000
22	0	600	850	1500	2000	0	0	0	0
23	0	600	850	1500	2000	0	0	0	0
24	0	600	850	1500	2000	0	0	0	0
25	0	600	850	1500	2000	0	0	0	0
<b>Total:</b>						<b>1,498,162</b>	<b>2,341,044</b>	<b>3,591,921</b>	<b>5,373,399</b>

Table C-13 Wind energy output from single Ge WECSs using wind data at 10metres for Yanbo

WS (m/s)	Frequency No. of hours	Wind power curve for wind machines (kW)				Wind energy output from single wind machine (kWh)			
		WECS SIZE (kW) ▶▶	900	1500	2300	2500	900	1500	2300
0	236	0	0	0	0	0	0	0	0
1	315	0	0	0	0	0	0	0	0
2	1173	0	0	0	0	0	0	0	0
3	1332	0	4	8	0	0	5328	10656	0
4	1196	15	35	71	53	17940	41860	84916	63388
5	1241	61	116	187	153	75701	143956	232067	189873
6	887	137	235	363	304	121519	208445	321981	269648
7	638	229	395	609	517	146102	252010	388542	329846
8	542	329	595	934	800	178318	322490	506228	433600
9	448	472	890	1352	1156	211456	398720	605696	517888
10	379	638	1210	1480	1616	241802	458590	560920	612464
11	149	797	1400	2113	2061	118753	208600	314837	307089
12	92	868	1500	2259	2366	79856	138000	207828	217672
13	66	898	1500	2295	2477	59268	99000	151470	163482
14	33	900	1500	2300	2498	29700	49500	75900	82434
15	24	900	1500	2300	2500	21600	36000	55200	60000
16	4	900	1500	2300	2500	3600	6000	9200	10000
17	1	900	1500	2300	2500	900	1500	2300	2500
18	2	900	1500	2300	2500	1800	3000	4600	5000
19	0	900	1500	2300	2500	0	0	0	0
20	1	900	1500	2300	2500	900	1500	2300	2500
21	1	900	1500	2300	2500	900	1500	2300	2500
22	0	900	1500	2300	2500	0	0	0	0
23	0	900	1500	2300	2500	0	0	0	0
24	0	900	1500	2300	2500	0	0	0	0
25	0	900	1500	2300	2500	0	0	0	0
<b>Total:</b>						<b>1,310,115</b>	<b>2,375,999</b>	<b>3,536,941</b>	<b>3,269,884</b>

Table C-14 Wind energy output from single Ge WECSs using wind data at 40metres for Yanbo

WS (m/s)	Frequency No. of hours	Wind power curve for wind machines (kW)				Wind energy output from single wind machine (kWh)			
		900	1500	2300	2500	900	1500	2300	2500
WECS SIZE (kW)	▶▶								
0	236	0	0	0	0	0	0	0	0
1	315	0	0	0	0	0	0	0	0
2	274	0	0	0	0	0	0	0	0
3	1236	0	4	8	0	0	4944	9888	0
4	1134	15	35	71	53	17010	39690	80514	60102
5	1057	61	116	187	153	64477	122612	197659	161721
6	1241	137	235	363	304	170017	291635	450483	377264
7	89	229	395	609	517	20381	35155	54201	46013
8	895	329	595	934	800	294455	532525	835930	716000
9	681	472	890	1352	1156	321432	606090	920712	787236
10	402	638	1210	1480	1616	256476	486420	594960	649632
11	448	797	1400	2113	2061	357056	627200	946624	923328
12	27	868	1500	2259	2366	23436	40500	60993	63882
13	374	898	1500	2295	2477	335852	561000	858330	926398
14	144	900	1500	2300	2498	129600	216000	331200	359712
15	74	900	1500	2300	2500	66600	111000	170200	185000
16	66	900	1500	2300	2500	59400	99000	151800	165000
17	7	900	1500	2300	2500	6300	10500	16100	17500
18	30	900	1500	2300	2500	27000	45000	69000	75000
19	22	900	1500	2300	2500	19800	33000	50600	55000
20	3	900	1500	2300	2500	2700	4500	6900	7500
21	5	900	1500	2300	2500	4500	7500	11500	12500
22	0	900	1500	2300	2500	0	0	0	0
23	0	900	1500	2300	2500	0	0	0	0
24	0	900	1500	2300	2500	0	0	0	0
25	0	900	1500	2300	2500	0	0	0	0
<b>Total:</b>						<b>2,176,492</b>	<b>3,874,271</b>	<b>5,817,594</b>	<b>5,588,788</b>

Table C-15 Wind energy output from single Ge WECSs using wind data at 50metres for Yanbo

WS (m/s)	Frequency No. of hours	Wind power curve for wind machines (kW)				Wind energy output from single wind machine (kWh)			
		900	1500	2300	2500	900	1500	2300	2500
WECS SIZE (kW)	▶▶								
0	236	0	0	0	0	0	0	0	0
1	315	0	0	0	0	0	0	0	0
2	274	0	0	0	0	0	0	0	0
3	1236	0	4	8	0	0	4944	9888	0
4	995	15	35	71	53	14925	34825	70645	52735
5	1196	61	116	187	153	72956	138736	223652	182988
6	1241	137	235	363	304	170017	291635	450483	377264
7	89	229	395	609	517	20381	35155	54201	46013
8	895	329	595	934	800	294455	532525	835930	716000
9	541	472	890	1352	1156	255352	481490	731432	625396
10	542	638	1210	1480	1616	345796	655820	802160	875872
11	58	797	1400	2113	2061	46226	81200	122554	119538
12	417	868	1500	2259	2366	361956	625500	942003	986622
13	352	898	1500	2295	2477	316096	528000	807840	871904
14	149	900	1500	2300	2498	134100	223500	342700	372202
15	17	900	1500	2300	2500	15300	25500	39100	42500
16	105	900	1500	2300	2500	94500	157500	241500	262500
17	43	900	1500	2300	2500	38700	64500	98900	107500
18	26	900	1500	2300	2500	23400	39000	59800	65000
19	24	900	1500	2300	2500	21600	36000	55200	60000
20	1	900	1500	2300	2500	900	1500	2300	2500
21	8	900	1500	2300	2500	7200	12000	18400	20000
22	0	900	1500	2300	2500	0	0	0	0
23	0	900	1500	2300	2500	0	0	0	0
24	0	900	1500	2300	2500	0	0	0	0
25	0	900	1500	2300	2500	0	0	0	0
<b>Total:</b>						<b>2,233,860</b>	<b>3,969,330</b>	<b>5,908,688</b>	<b>5,786,534</b>

Table C-16 Wind energy output from single Ge WECSs using wind data at 60metres for Yanbo

WS (m/s)	Frequency No. of hours	Wind power curve for wind machines (kW)				Wind energy output from single wind machine (kWh)			
		900	1500	2300	2500	900	1500	2300	2500
WECS SIZE (kW)	▶▶								
0	236	0	0	0	0	0	0	0	0
1	315	0	0	0	0	0	0	0	0
2	274	0	0	0	0	0	0	0	0
3	1236	0	4	8	0	0	4944	9888	0
4	995	15	35	71	53	14925	34825	70645	52735
5	1196	61	116	187	153	72956	138736	223652	182988
6	111	137	235	363	304	15207	26085	40293	33744
7	1219	229	395	609	517	279151	481505	742371	630223
8	798	329	595	934	800	262542	474810	745332	638400
9	638	472	890	1352	1156	301136	567820	862576	737528
10	140	638	1210	1480	1616	89320	169400	207200	226240
11	460	797	1400	2113	2061	366620	644000	971980	948060
12	390	868	1500	2259	2366	338520	585000	881010	922740
13	379	898	1500	2295	2477	340342	568500	869805	938783
14	22	900	1500	2300	2498	19800	33000	50600	54956
15	144	900	1500	2300	2500	129600	216000	331200	360000
16	74	900	1500	2300	2500	66600	111000	170200	185000
17	67	900	1500	2300	2500	60300	100500	154100	167500
18	7	900	1500	2300	2500	6300	10500	16100	17500
19	30	900	1500	2300	2500	27000	45000	69000	75000
20	20	900	1500	2300	2500	18000	30000	46000	50000
21	9	900	1500	2300	2500	8100	13500	20700	22500
22	0	900	1500	2300	2500	0	0	0	0
23	0	900	1500	2300	2500	0	0	0	0
24	0	900	1500	2300	2500	0	0	0	0
25	0	900	1500	2300	2500	0	0	0	0
<b>Total:</b>						<b>2,416,419</b>	<b>4,255,125</b>	<b>6,482,652</b>	<b>6,243,897</b>

Table C-17 Wind energy output from single Ge WECSs using wind data at 70metres for Yanbo

WS (m/s)	Frequency No. of hours	Wind power curve for wind machines (kW)				Wind energy output from single wind machine (kWh)			
		900	1500	2300	2500	900	1500	2300	2500
WECS SIZE (kW)	▶▶								
0	236	0	0	0	0	0	0	0	0
1	315	0	0	0	0	0	0	0	0
2	274	0	0	0	0	0	0	0	0
3	1236	0	4	8	0	0	4944	9888	0
4	995	15	35	71	53	14925	34825	70645	52735
5	1196	61	116	187	153	8479	16124	25993	21267
6	111	137	235	363	304	160016	274480	423984	355072
7	1218	229	395	609	517	258770	446350	688170	584210
8	798	329	595	934	800	291823	527765	828458	709600
9	96	472	890	1352	1156	45312	85440	129792	110976
10	681	638	1210	1480	1616	434478	824010	1007880	1100496
11	402	797	1400	2113	2061	320394	562800	849426	828522
12	448	868	1500	2259	2366	388864	672000	1012032	1059968
13	28	898	1500	2295	2477	25144	42000	64260	69356
14	374	900	1500	2300	2498	316800	528000	809600	879296
15	127	900	1500	2300	2500	134100	223500	342700	372500
16	92	900	1500	2300	2500	15300	25500	39100	42500
17	31	900	1500	2300	2500	94500	157500	241500	262500
18	43	900	1500	2300	2500	32400	54000	82800	90000
19	26	900	1500	2300	2500	29700	49500	75900	82500
20	24	900	1500	2300	2500	3600	6000	9200	10000
21	9	900	1500	2300	2500	26100	43500	66700	72500
22	0	900	1500	2300	2500	0	0	0	0
23	0	900	1500	2300	2500	0	0	0	0
24	0	900	1500	2300	2500	0	0	0	0
25	0	900	1500	2300	2500	0	0	0	0
<b>Total:</b>						<b>2,512,144</b>	<b>4,435,760</b>	<b>6,564,762</b>	<b>6,521,143</b>

Table C-18 Wind energy output from single Ge WECSs using wind data at 80metres for Yanbo

WS (m/s)	Frequency No. of hours	Wind power curve for wind machines (kW)				Wind energy output from single wind machine (kWh)			
		WECS SIZE (kW)	900	1500	2300	2500	900	1500	2300
0	236	0	0	0	0	0	0	0	0
1	315	0	0	0	0	0	0	0	0
2	274	0	0	0	0	0	0	0	0
3	1236	0	4	8	0	0	4944	9888	0
4	995	15	35	71	53	14925	34825	70645	52735
5	139	61	116	187	153	8479	16124	25993	21267
6	1168	137	235	363	304	160016	274480	423984	355072
7	1130	229	395	609	517	258770	446350	688170	584210
8	887	329	595	934	800	291823	527765	828458	709600
9	96	472	890	1352	1156	45312	85440	129792	110976
10	681	638	1210	1480	1616	434478	824010	1007880	1100496
11	402	797	1400	2113	2061	320394	562800	849426	828522
12	448	868	1500	2259	2366	388864	672000	1012032	1059968
13	28	898	1500	2295	2477	25144	42000	64260	69356
14	352	900	1500	2300	2498	316800	528000	809600	879296
15	149	900	1500	2300	2500	134100	223500	342700	372500
16	17	900	1500	2300	2500	15300	25500	39100	42500
17	105	900	1500	2300	2500	94500	157500	241500	262500
18	36	900	1500	2300	2500	32400	54000	82800	90000
19	33	900	1500	2300	2500	29700	49500	75900	82500
20	4	900	1500	2300	2500	3600	6000	9200	10000
21	29	900	1500	2300	2500	26100	43500	66700	72500
22	0	900	1500	2300	2500	0	0	0	0
23	0	900	1500	2300	2500	0	0	0	0
24	0	900	1500	2300	2500	0	0	0	0
25	0	900	1500	2300	2500	0	0	0	0
<b>Total:</b>						<b>2,600,705</b>	<b>4,578,238</b>	<b>6,778,028</b>	<b>6,703,998</b>

Table C-19 Wind energy output from single DeWind WECSs using wind data at 10metres for Yanbo

WS (m/s)	Frequency No. of hours	Wind power curve for wind machines (kW)			Wind energy output from single wind machine (kWh)		
		600	1000	2000	600	1000	2000
WECS SIZE (kW) ▶▶		600	1000	2000	600	1000	2000
0	236	0	0	0	0	0	0
1	315	0	0	0	0	0	0
2	1173	0	0	0	0	0	0
3	1332	7	12	11	9324	15984	14652
4	1196	22	34	73	26312	40664	87308
5	1241	52	80	164	64532	99280	203524
6	887	93	158	295	82491	140146	261665
7	638	158	271	480	100804	172898	306240
8	542	244	413	720	132248	223846	390240
9	448	354	586	1010	158592	262528	452480
10	379	489	781	1345	185331	295999	509755
11	149	590	971	1715	87910	144679	255535
12	92	600	1000	1890	55200	92000	173880
13	66	600	1000	1985	39600	66000	131010
14	33	600	1000	2000	19800	33000	66000
15	24	600	1000	2000	14400	24000	48000
16	4	600	1000	2000	2400	4000	8000
17	1	600	940	2000	600	940	2000
18	2	600	840	2000	1200	1680	4000
19	0	600	750	2000	0	0	0
20	1	600	650	2000	600	650	2000
21	1	600	560	2000	600	560	2000
22	0	600	475	2000	0	0	0
23	0	600	390	2000	0	0	0
24	0	600	390	2000	0	0	0
25	0	600	390	2000	0	0	0
<b>Total:</b>					<b>981,944</b>	<b>1,618,854</b>	<b>2,918,289</b>

Table C-20 Wind energy output from single DeWind WECSs using wind data at 40metres for Yanbo

WS (m/s)	Frequency No. of hours	Wind power curve for wind machines (kW)			Wind energy output from single wind machine (kWh)		
		600	1000	2000	600	1000	2000
WECS SIZE (kW) ▶▶		600	1000	2000	600	1000	2000
0	236	0	0	0	0	0	0
1	315	0	0	0	0	0	0
2	274	0	0	0	0	0	0
3	1236	7	12	11	8652	14832	13596
4	1134	22	34	73	24948	38556	82782
5	1057	52	80	164	54964	84560	173348
6	1241	93	158	295	115413	196078	366095
7	89	158	271	480	14062	24119	42720
8	895	244	413	720	218380	369635	644400
9	681	354	586	1010	241074	399066	687810
10	402	489	781	1345	196578	313962	540690
11	448	590	971	1715	264320	435008	768320
12	27	600	1000	1890	16200	27000	51030
13	374	600	1000	1985	224400	374000	742390
14	144	600	1000	2000	86400	144000	288000
15	74	600	1000	2000	44400	74000	148000
16	66	600	1000	2000	39600	66000	132000
17	7	600	940	2000	4200	6580	14000
18	30	600	840	2000	18000	25200	60000
19	22	600	750	2000	13200	16500	44000
20	3	600	650	2000	1800	1950	6000
21	5	600	560	2000	3000	2800	10000
22	0	600	475	2000	0	0	0
23	0	600	390	2000	0	0	0
24	0	600	390	2000	0	0	0
25	0	600	390	2000	0	0	0
<b>Total:</b>					<b>1,589,591</b>	<b>2,613,846</b>	<b>4,815,181</b>

Table C-21 Wind energy output from single DeWind WECSs using wind data at 50metres for Yanbo

WS (m/s)	Frequency No. of hours	Wind power curve for wind machines (kW)			Wind energy output from single wind machine (kWh)		
		600	1000	2000	600	1000	2000
WECS SIZE (kW) ▶▶		600	1000	2000	600	1000	2000
0	236	0	0	0	0	0	0
1	315	0	0	0	0	0	0
2	274	0	0	0	0	0	0
3	1236	7	12	11	8652	14832	13596
4	995	22	34	73	21890	33830	72635
5	1196	52	80	164	62192	95680	196144
6	1241	93	158	295	115413	196078	366095
7	89	158	271	480	14062	24119	42720
8	895	244	413	720	218380	369635	644400
9	541	354	586	1010	191514	317026	546410
10	542	489	781	1345	265038	423302	728990
11	58	590	971	1715	34220	56318	99470
12	417	600	1000	1890	250200	417000	788130
13	352	600	1000	1985	211200	352000	698720
14	149	600	1000	2000	89400	149000	298000
15	17	600	1000	2000	10200	17000	34000
16	105	600	1000	2000	63000	105000	210000
17	43	600	940	2000	25800	40420	86000
18	26	600	840	2000	15600	21840	52000
19	24	600	750	2000	14400	18000	48000
20	1	600	650	2000	600	650	2000
21	8	600	560	2000	4800	4480	16000
22	0	600	475	2000	0	0	0
23	0	600	390	2000	0	0	0
24	0	600	390	2000	0	0	0
25	0	600	390	2000	0	0	0
<b>Total:</b>					<b>1,616,561</b>	<b>2,656,210</b>	<b>4,943,310</b>

Table C-22 Wind energy output from single DeWind WECSs using wind data at 60metres for Yanbo

WS (m/s)	Frequency No. of hours	Wind power curve for wind machines (kW)			Wind energy output from single wind machine (kWh)		
		600	1000	2000	600	1000	2000
WECS SIZE (kW) ▶▶		600	1000	2000	600	1000	2000
0	236	0	0	0	0	0	0
1	315	0	0	0	0	0	0
2	274	0	0	0	0	0	0
3	1236	7	12	11	8652	14832	13596
4	995	22	34	73	21890	33830	72635
5	1196	52	80	164	62192	95680	196144
6	111	93	158	295	10323	17538	32745
7	1219	158	271	480	192602	330349	585120
8	798	244	413	720	194712	329574	574560
9	638	354	586	1010	225852	373868	644380
10	140	489	781	1345	68460	109340	188300
11	460	590	971	1715	271400	446660	788900
12	390	600	1000	1890	234000	390000	737100
13	379	600	1000	1985	227400	379000	752315
14	22	600	1000	2000	13200	22000	44000
15	144	600	1000	2000	86400	144000	288000
16	74	600	1000	2000	44400	74000	148000
17	67	600	940	2000	40200	62980	134000
18	7	600	840	2000	4200	5880	14000
19	30	600	750	2000	18000	22500	60000
20	20	600	650	2000	12000	13000	40000
21	9	600	560	2000	5400	5040	18000
22	0	600	475	2000	0	0	0
23	0	600	390	2000	0	0	0
24	0	600	390	2000	0	0	0
25	0	600	390	2000	0	0	0
<b>Total:</b>					<b>1,741,283</b>	<b>2,870,071</b>	<b>5,331,795</b>

Table C-23 Wind energy output from single DeWind WECSs using wind data at 70metres for Yanbo

WS (m/s)	Frequency No. of hours	Wind power curve for wind machines (kW)			Wind energy output from single wind machine (kWh)		
		600	1000	2000	600	1000	2000
WECS SIZE (kW) ▶▶		600	1000	2000	600	1000	2000
0	236	0	0	0	0	0	0
1	315	0	0	0	0	0	0
2	274	0	0	0	0	0	0
3	1236	7	12	11	8652	14832	13596
4	995	22	34	73	21890	33830	72635
5	1196	52	80	164	62192	95680	196144
6	111	93	158	295	10323	17538	32745
7	1218	158	271	480	192444	330078	584640
8	798	244	413	720	194712	329574	574560
9	96	354	586	1010	33984	56256	96960
10	681	489	781	1345	333009	531861	915945
11	402	590	971	1715	237180	390342	689430
12	448	600	1000	1890	268800	448000	846720
13	28	600	1000	1985	16800	28000	55580
14	374	600	1000	2000	224400	374000	748000
15	127	600	1000	2000	76200	127000	254000
16	92	600	1000	2000	55200	92000	184000
17	31	600	940	2000	18600	29140	62000
18	43	600	840	2000	25800	36120	86000
19	26	600	750	2000	15600	19500	52000
20	24	600	650	2000	14400	15600	48000
21	9	600	560	2000	5400	5040	18000
22	0	600	475	2000	0	0	0
23	0	600	390	2000	0	0	0
24	0	600	390	2000	0	0	0
25	0	600	390	2000	0	0	0
<b>Total:</b>					<b>1,815,586</b>	<b>2,974,391</b>	<b>5,530,955</b>

Table C-24 Wind energy output from single DeWind WECSs using wind data at 80metres for Yanbo

WS (m/s)	Frequency No. of hours	Wind power curve for wind machines (kW)			Wind energy output from single wind machine (kWh)		
		600	1000	2000	600	1000	2000
WECS SIZE (kW) ▶▶		600	1000	2000	600	1000	2000
0	236	0	0	0	0	0	0
1	315	0	0	0	0	0	0
2	274	0	0	0	0	0	0
3	1236	7	12	11	8652	14832	13596
4	995	22	34	73	21890	33830	72635
5	139	52	80	164	7228	11120	22796
6	1168	93	158	295	108624	184544	344560
7	1130	158	271	480	178540	306230	542400
8	887	244	413	720	216428	366331	638640
9	96	354	586	1010	33984	56256	96960
10	681	489	781	1345	333009	531861	915945
11	402	590	971	1715	237180	390342	689430
12	448	600	1000	1890	268800	448000	846720
13	28	600	1000	1985	16800	28000	55580
14	352	600	1000	2000	211200	352000	704000
15	149	600	1000	2000	89400	149000	298000
16	17	600	1000	2000	10200	17000	34000
17	105	600	940	2000	63000	98700	210000
18	36	600	840	2000	21600	30240	72000
19	33	600	750	2000	19800	24750	66000
20	4	600	650	2000	2400	2600	8000
21	29	600	560	2000	17400	16240	58000
22	0	600	475	2000	0	0	0
23	0	600	390	2000	0	0	0
24	0	600	390	2000	0	0	0
25	0	600	390	2000	0	0	0
<b>Total:</b>					<b>1,866,135</b>	<b>3,061,876</b>	<b>5,689,262</b>

Table C-25 Wind energy output from single Bonus WECSs using wind data at 10metres for Yanbo

WS (m/s)	Frequency No. of hours	Wind power curve for wind machines (kW)			Wind energy output from single wind machine (kWh)		
WECS SIZE (kW) ▶▶		600	1000	1300	600	1000	1300
0	236	0	0	0	0	0	0
1	315	0	0	0	0	0	0
2	1173	0	0	0	0	0	0
3	1332	0	0	0	0	0	0
4	1196	0	24.1	32.1	0	28823.6	38391.6
5	1241	4.74	69.3	91.6	5882.34	86001.3	113675.6
6	887	45.46	130	172.5	40323.02	115310	153007.5
7	638	103.18	219.1	291.2	65828.84	139785.8	185785.6
8	542	171.97	333.5	439.3	93207.74	180757	238100.6
9	448	249.68	463.1	604.3	111856.64	207468.8	270726.4
10	379	338.39	598.1	770.6	128249.81	226679.9	292057.4
11	149	417.09	730	928.7	62146.41	108770	138376.3
12	92	483.29	846.5	1072.2	44462.68	77878	98642.4
13	66	534.55	928.8	1183.1	35280.3	61300.8	78084.6
14	33	573.71	972.6	1250.1	18932.43	32095.8	41253.3
15	24	599.84	990.8	1281.7	14396.16	23779.2	30760.8
16	4	620.11	997.2	1294	2480.44	3988.8	5176
17	1	628.74	1000	1298.2	628.74	1000	1298.2
18	2	628.63	1000	1299.5	1257.26	2000	2599
19	0	630.48	1000	1299.8	0	0	0
20	1	621.19	1000	1300	621.19	1000	1300
21	1	620	1000	1300	620	1000	1300
22	0	600	1000	1300	0	0	0
23	0	600	1000	1300	0	0	0
24	0	600	1000	1300	0	0	0
25	0	600	1000	1300	0	0	0
<b>Total:</b>					<b>626,174</b>	<b>1,297,639</b>	<b>1,690,535</b>

Table C-26 Wind energy output from single Bonus WECSs using wind data at 40metres for Yanbo

WS (m/s)	Frequency No. of hours	Wind power curve for wind machines (kW)			Wind energy output from single wind machine (kWh)		
WECS SIZE (kW) ▶▶		600	1000	1300	600	1000	1300
0	236	0	0	0	0	0	0
1	315	0	0	0	0	0	0
2	274	0	0	0	0	0	0
3	1236	0	0	0	0	0	0
4	1134	0	24.1	32.1	0	27329.4	36401.4
5	1057	4.74	69.3	91.6	5010.18	73250.1	96821.2
6	1241	45.46	130	172.5	56415.86	161330	214072.5
7	89	103.18	219.1	291.2	9183.02	19499.9	25916.8
8	895	171.97	333.5	439.3	153913.15	298482.5	393173.5
9	681	249.68	463.1	604.3	170032.08	315371.1	411528.3
10	402	338.39	598.1	770.6	136032.78	240436.2	309781.2
11	448	417.09	730	928.7	186856.32	327040	416057.6
12	27	483.29	846.5	1072.2	13048.83	22855.5	28949.4
13	374	534.55	928.8	1183.1	199921.7	347371.2	442479.4
14	144	573.71	972.6	1250.1	82614.24	140054.4	180014.4
15	74	599.84	990.8	1281.7	44388.16	73319.2	94845.8
16	66	620.11	997.2	1294	40927.26	65815.2	85404
17	7	628.74	1000	1298.2	4401.18	7000	9087.4
18	30	628.63	1000	1299.5	18858.9	30000	38985
19	22	630.48	1000	1299.8	13870.56	22000	28595.6
20	3	621.19	1000	1300	1863.57	3000	3900
21	5	620	1000	1300	3100	5000	6500
22	0	600	1000	1300	0	0	0
23	0	600	1000	1300	0	0	0
24	0	600	1000	1300	0	0	0
25	0	600	1000	1300	0	0	0
<b>Total:</b>					<b>1,140,438</b>	<b>2,179,155</b>	<b>2,822,514</b>

Table C-27 Wind energy output from single Bonus WECSs using wind data at 50metres for Yanbo

WS (m/s)	Frequency No. of hours	Wind power curve for wind machines (kW)			Wind energy output from single wind machine (kWh)		
WECS SIZE (kW) ▶▶		600	1000	1300	600	1000	1300
0	236	0	0	0	0	0	0
1	315	0	0	0	0	0	0
2	274	0	0	0	0	0	0
3	1236	0	0	0	0	0	0
4	995	0	24.1	32.1	0	23979.5	31939.5
5	1196	4.74	69.3	91.6	5669.04	82882.8	109553.6
6	1241	45.46	130	172.5	56415.86	161330	214072.5
7	89	103.18	219.1	291.2	9183.02	19499.9	25916.8
8	895	171.97	333.5	439.3	153913.15	298482.5	393173.5
9	541	249.68	463.1	604.3	135076.88	250537.1	326926.3
10	542	338.39	598.1	770.6	183407.38	324170.2	417665.2
11	58	417.09	730	928.7	24191.22	42340	53864.6
12	417	483.29	846.5	1072.2	201531.93	352990.5	447107.4
13	352	534.55	928.8	1183.1	188161.6	326937.6	416451.2
14	149	573.71	972.6	1250.1	85482.79	144917.4	186264.9
15	17	599.84	990.8	1281.7	10197.28	16843.6	21788.9
16	105	620.11	997.2	1294	65111.55	104706	135870
17	43	628.74	1000	1298.2	27035.82	43000	55822.6
18	26	628.63	1000	1299.5	16344.38	26000	33787
19	24	630.48	1000	1299.8	15131.52	24000	31195.2
20	1	621.19	1000	1300	621.19	1000	1300
21	8	620	1000	1300	4960	8000	10400
22	0	600	1000	1300	0	0	0
23	0	600	1000	1300	0	0	0
24	0	600	1000	1300	0	0	0
25	0	600	1000	1300	0	0	0
<b>Total:</b>					<b>1,182,435</b>	<b>2,251,617</b>	<b>2,913,099</b>

Table C-28 Wind energy output from single Bonus WECSs using wind data at 60metres for Yanbo

WS (m/s)	Frequency No. of hours	Wind power curve for wind machines (kW)			Wind energy output from single wind machine (kWh)		
WECS SIZE (kW) ▶▶		600	1000	1300	600	1000	1300
0	236	0	0	0	0	0	0
1	315	0	0	0	0	0	0
2	274	0	0	0	0	0	0
3	1236	0	0	0	0	0	0
4	995	0	24.1	32.1	0	23979.5	31939.5
5	1196	4.74	69.3	91.6	5669.04	82882.8	109553.6
6	111	45.46	130	172.5	5046.06	14430	19147.5
7	1219	103.18	219.1	291.2	125776.42	267082.9	354972.8
8	798	171.97	333.5	439.3	137232.06	266133	350561.4
9	638	249.68	463.1	604.3	159295.84	295457.8	385543.4
10	140	338.39	598.1	770.6	47374.6	83734	107884
11	460	417.09	730	928.7	191861.4	335800	427202
12	390	483.29	846.5	1072.2	188483.1	330135	418158
13	379	534.55	928.8	1183.1	202594.45	352015.2	448394.9
14	22	573.71	972.6	1250.1	12621.62	21397.2	27502.2
15	144	599.84	990.8	1281.7	86376.96	142675.2	184564.8
16	74	620.11	997.2	1294	45888.14	73792.8	95756
17	67	628.74	1000	1298.2	42125.58	67000	86979.4
18	7	628.63	1000	1299.5	4400.41	7000	9096.5
19	30	630.48	1000	1299.8	18914.4	30000	38994
20	20	621.19	1000	1300	12423.8	20000	26000
21	9	620	1000	1300	5580	9000	11700
22	0	600	1000	1300	0	0	0
23	0	600	1000	1300	0	0	0
24	0	600	1000	1300	0	0	0
25	0	600	1000	1300	0	0	0
<b>Total:</b>					<b>1,291,664</b>	<b>2,422,515</b>	<b>3,133,950</b>

Table C-29 Wind energy output from single Bonus WECSs using wind data at 70metres for Yanbo

WS (m/s)	Frequency No. of hours	Wind power curve for wind machines (kW)			Wind energy output from single wind machine (kWh)		
WECS SIZE (kW) ▶▶		600	1000	1300	600	1000	1300
0	236	0	0	0	0	0	0
1	315	0	0	0	0	0	0
2	274	0	0	0	0	0	0
3	1236	0	0	0	0	0	0
4	995	0	24.1	32.1	0	23979.5	31939.5
5	1196	4.74	69.3	91.6	5669.04	82882.8	109553.6
6	111	45.46	130	172.5	5046.06	14430	19147.5
7	1218	103.18	219.1	291.2	125673.24	266863.8	354681.6
8	798	171.97	333.5	439.3	137232.06	266133	350561.4
9	96	249.68	463.1	604.3	23969.28	44457.6	58012.8
10	681	338.39	598.1	770.6	230443.59	407306.1	524778.6
11	402	417.09	730	928.7	167670.18	293460	373337.4
12	448	483.29	846.5	1072.2	216513.92	379232	480345.6
13	28	534.55	928.8	1183.1	14967.4	26006.4	33126.8
14	374	573.71	972.6	1250.1	214567.54	363752.4	467537.4
15	127	599.84	990.8	1281.7	76179.68	125831.6	162775.9
16	92	620.11	997.2	1294	57050.12	91742.4	119048
17	31	628.74	1000	1298.2	19490.94	31000	40244.2
18	43	628.63	1000	1299.5	27031.09	43000	55878.5
19	26	630.48	1000	1299.8	16392.48	26000	33794.8
20	24	621.19	1000	1300	14908.56	24000	31200
21	9	620	1000	1300	5580	9000	11700
22	0	600	1000	1300	0	0	0
23	0	600	1000	1300	0	0	0
24	0	600	1000	1300	0	0	0
25	0	600	1000	1300	0	0	0
<b>Total:</b>					<b>1,358,385</b>	<b>2,519,078</b>	<b>3,257,664</b>

Table C-30 Wind energy output from single Bonus WECSs using wind data at 80metres for Yanbo

WS (m/s)	Frequency No. of hours	Wind power curve for wind machines (kW)			Wind energy output from single wind machine (kWh)		
WECS SIZE (kW) ▶▶		600	1000	1300	600	1000	1300
0	236	0	0	0	0	0	0
1	315	0	0	0	0	0	0
2	274	0	0	0	0	0	0
3	1236	0	0	0	0	0	0
4	995	0	24.1	32.1	0	23979.5	31939.5
5	139	4.74	69.3	91.6	658.86	9632.7	12732.4
6	1168	45.46	130	172.5	53097.28	151840	201480
7	1130	103.18	219.1	291.2	116593.4	247583	329056
8	887	171.97	333.5	439.3	152537.39	295814.5	389659.1
9	96	249.68	463.1	604.3	23969.28	44457.6	58012.8
10	681	338.39	598.1	770.6	230443.59	407306.1	524778.6
11	402	417.09	730	928.7	167670.18	293460	373337.4
12	448	483.29	846.5	1072.2	216513.92	379232	480345.6
13	28	534.55	928.8	1183.1	14967.4	26006.4	33126.8
14	352	573.71	972.6	1250.1	201945.92	342355.2	440035.2
15	149	599.84	990.8	1281.7	89376.16	147629.2	190973.3
16	17	620.11	997.2	1294	10541.87	16952.4	21998
17	105	628.74	1000	1298.2	66017.7	105000	136311
18	36	628.63	1000	1299.5	22630.68	36000	46782
19	33	630.48	1000	1299.8	20805.84	33000	42893.4
20	4	621.19	1000	1300	2484.76	4000	5200
21	29	620	1000	1300	17980	29000	37700
22	0	600	1000	1300	0	0	0
23	0	600	1000	1300	0	0	0
24	0	600	1000	1300	0	0	0
25	0	600	1000	1300	0	0	0
<b>Total:</b>					<b>1,408,234</b>	<b>2,593,249</b>	<b>3,356,361</b>

Table C-31 Wind energy output from single Enercon WECSs using wind data at 10metres for Yanbo

WS (m/s)	Frequency No. of hours	Wind power curve for wind machines (kW)				Wind energy output from single wind machine (kWh)			
		WECS SIZE (kW)	600	1000	1500	1800	600	1000	1500
0	236	0	0	0	0	0	0	0	0
1	315	0	0	0	0	0	0	0	0
2	1173	0	0	0	0	0	0	0	0
3	1332	1.7	2.6	1.8	15.3	2264.4	3463.2	2397.6	20432.88
4	1196	14.74	25.6	30.1	51.8	17629.04	30617.6	35999.6	61976.72
5	1241	40.8	75.8	89.3	117	50632.8	94067.8	110821.3	144899.16
6	887	79.64	140.3	174	209	70640.68	124446.1	153894.5	185170.12
7	638	134.8	232.8	296	339	86002.4	148526.4	188848	216116.12
8	542	207.1	366.6	445	510	112248.2	198697.2	241190	276479.62
9	448	292.8	516.2	653	726	131174.4	231257.6	292364.8	325068.8
10	379	403.4	680.8	877	991	152888.6	258023.2	332383	375589
11	149	508.1	854.8	1122	1275	75706.9	127365.2	167178	189969.04
12	92	554.8	952.4	1338	1549	51041.6	87620.8	123077.6	142547.56
13	66	613.2	1000	1469	1729	40471.2	66000	96940.8	114139.08
14	33	600	1000	1522	1817	19800	33000	50222.7	59966.28
15	24	600	1000	1540	1847	14400	24000	36957.6	44337.12
16	4	600	1000	1541	1866	2400	4000	6164	7462.92
17	1	600	1000	1541	1867	600	1000	1541.4	1867.27
18	2	600	1000	1540	1867	1200	2000	3080	3733.9
19	0	600	1000	1539	1866	0	0	0	0
20	1	600	1000	1500	1800	600	1000	1500	1800
21	1	600	1000	1500	1800	600	1000	1500	1800
22	0	600	1000	1500	1800	0	0	0	0
23	0	600	1000	1500	1800	0	0	0	0
24	0	600	1000	1500	1800	0	0	0	0
25	0	600	1000	1500	1800	0	0	0	0
<b>Total:</b>						<b>830,300</b>	<b>1,436,085</b>	<b>1,846,061</b>	<b>2,173,356</b>

Table C-32 Wind energy output from single Enercon WECSs using wind data at 40metres for Yanbo

WS (m/s)	Frequency No. of hours	Wind power curve for wind machines (kW)				Wind energy output from single wind machine (kWh)			
		WECS SIZE (kW)	600	1000	1500	1800	600	1000	1500
0	236	0	0	0	0	0	0	0	0
1	315	0	0	0	0	0	0	0	0
2	274	0	0	0	0	0	0	0	0
3	1236	1.7	2.6	1.8	15.3	2101.2	3213.6	2224.8	18960.24
4	1134	14.74	25.6	30.1	51.8	16715.16	29030.4	34133.4	58763.88
5	1057	40.8	75.8	89.3	117	43125.6	80120.6	94390.1	123415.32
6	1241	79.64	140.3	174	209	98833.24	174112.3	215313.5	259071.16
7	89	134.8	232.8	296	339	11997.2	20719.2	26344	30147.86
8	895	207.1	366.6	445	510	185354.5	328107	398275	456548.45
9	681	292.8	516.2	653	726	199396.8	351532.2	444420.6	494133.6
10	402	403.4	680.8	877	991	162166.8	273681.6	352554	398382
11	448	508.1	854.8	1122	1275	227628.8	382950.4	502656	571182.08
12	27	554.8	952.4	1338	1549	14979.6	25714.8	36120.6	41834.61
13	374	613.2	1000	1469	1729	229336.8	374000	549331.2	646788.12
14	144	600	1000	1522	1817	86400	144000	219153.6	261671.04
15	74	600	1000	1540	1847	44400	74000	113952.6	136706.12
16	66	600	1000	1541	1866	39600	66000	101706	123138.18
17	7	600	1000	1541	1867	4200	7000	10789.8	13070.89
18	30	600	1000	1540	1867	18000	30000	46200	56008.5
19	22	600	1000	1539	1866	13200	22000	33858	41059.04
20	3	600	1000	1500	1800	1800	3000	4500	5400
21	5	600	1000	1500	1800	3000	5000	7500	9000
22	0	600	1000	1500	1800	0	0	0	0
23	0	600	1000	1500	1800	0	0	0	0
24	0	600	1000	1500	1800	0	0	0	0
25	0	600	1000	1500	1800	0	0	0	0
<b>Total:</b>						<b>1,402,236</b>	<b>2,394,182</b>	<b>3,193,423</b>	<b>3,745,281</b>

Table C-33 Wind energy output from single Enercon WECSs using wind data at 50metres for Yanbo

WS (m/s)	Frequency No. of hours	Wind power curve for wind machines (kW)				Wind energy output from single wind machine (kWh)			
		WECS SIZE (kW)	600	1000	1500	1800	600	1000	1500
0	236	0	0	0	0	0	0	0	0
1	315	0	0	0	0	0	0	0	0
2	274	0	0	0	0	0	0	0	0
3	1236	1.7	2.6	1.8	15.3	2101.2	3213.6	2224.8	18960.24
4	995	14.74	25.6	30.1	51.8	14666.3	25472	29949.5	51560.9
5	1196	40.8	75.8	89.3	117	48796.8	90656.8	106802.8	139644.96
6	1241	79.64	140.3	174	209	98833.24	174112.3	215313.5	259071.16
7	89	134.8	232.8	296	339	11997.2	20719.2	26344	30147.86
8	895	207.1	366.6	445	510	185354.5	328107	398275	456548.45
9	541	292.8	516.2	653	726	158404.8	279264.2	353056.6	392549.6
10	542	403.4	680.8	877	991	218642.8	368993.6	475334	537122
11	58	508.1	854.8	1122	1275	29469.8	49578.4	65076	73947.68
12	417	554.8	952.4	1338	1549	231351.6	397150.8	557862.6	646112.31
13	352	613.2	1000	1469	1729	215846.4	352000	517017.6	608741.76
14	149	600	1000	1522	1817	89400	149000	226763.1	270756.84
15	17	600	1000	1540	1847	10200	17000	26178.3	31405.46
16	105	600	1000	1541	1866	63000	105000	161805	195901.65
17	43	600	1000	1541	1867	25800	43000	66280.2	80292.61
18	26	600	1000	1540	1867	15600	26000	40040	48540.7
19	24	600	1000	1539	1866	14400	24000	36936	44791.68
20	1	600	1000	1500	1800	600	1000	1500	1800
21	8	600	1000	1500	1800	4800	8000	12000	14400
22	0	600	1000	1500	1800	0	0	0	0
23	0	600	1000	1500	1800	0	0	0	0
24	0	600	1000	1500	1800	0	0	0	0
25	0	600	1000	1500	1800	0	0	0	0
<b>Total:</b>						<b>1,439,265</b>	<b>2,462,268</b>	<b>3,318,759</b>	<b>3,902,296</b>

Table C-34 Wind energy output from single Enercon WECSs using wind data at 60metres for Yanbo

WS (m/s)	Frequency No. of hours	Wind power curve for wind machines (kW)				Wind energy output from single wind machine (kWh)			
		600	1000	1500	1800	600	1000	1500	1800
WECS SIZE (kW)	▶▶								
0	236	0	0	0	0	0	0	0	0
1	315	0	0	0	0	0	0	0	0
2	274	0	0	0	0	0	0	0	0
3	1236	1.7	2.6	1.8	15.3	2101.2	3213.6	2224.8	18960.24
4	995	14.74	25.6	30.1	51.8	14666.3	25472	29949.5	51560.9
5	1196	40.8	75.8	89.3	117	48796.8	90656.8	106802.8	139644.96
6	111	79.64	140.3	174	209	8840.04	15573.3	19258.5	23172.36
7	1219	134.8	232.8	296	339	164321.2	283783.2	360824	412924.06
8	798	207.1	366.6	445	510	165265.8	292546.8	355110	407067.78
9	638	292.8	516.2	653	726	186806.4	329335.6	416358.8	462932.8
10	140	403.4	680.8	877	991	56476	95312	122780	138740
11	460	508.1	854.8	1122	1275	233726	393208	516120	586481.6
12	390	554.8	952.4	1338	1549	216372	371436	521742	604277.7
13	379	613.2	1000	1469	1729	232402.8	379000	556675.2	655435.02
14	22	600	1000	1522	1817	13200	22000	33481.8	39977.52
15	144	600	1000	1540	1847	86400	144000	221745.6	266022.72
16	74	600	1000	1541	1866	44400	74000	114034	138064.02
17	67	600	1000	1541	1867	40200	67000	103273.8	125107.09
18	7	600	1000	1540	1867	4200	7000	10780	13068.65
19	30	600	1000	1539	1866	18000	30000	46170	55989.6
20	20	600	1000	1500	1800	12000	20000	30000	36000
21	9	600	1000	1500	1800	5400	9000	13500	16200
22	0	600	1000	1500	1800	0	0	0	0
23	0	600	1000	1500	1800	0	0	0	0
24	0	600	1000	1500	1800	0	0	0	0
25	0	600	1000	1500	1800	0	0	0	0
<b>Total:</b>						<b>1,553,575</b>	<b>2,652,537</b>	<b>3,580,831</b>	<b>4,191,627</b>

Table C-35 Wind energy output from single Enercon WECSs using wind data at 70metres for Yanbo

WS (m/s)	Frequency No. of hours	Wind power curve for wind machines (kW)				Wind energy output from single wind machine (kWh)			
		WECS SIZE (kW) ▶▶	600	1000	1500	1800	600	1000	1500
0	236	0	0	0	0	0	0	0	0
1	315	0	0	0	0	0	0	0	0
2	274	0	0	0	0	0	0	0	0
3	1236	1.7	2.6	1.8	15.3	2101.2	3213.6	2224.8	18960.24
4	995	14.74	25.6	30.1	51.8	14666.3	25472	29949.5	51560.9
5	1196	40.8	75.8	89.3	117	48796.8	90656.8	106802.8	139644.96
6	111	79.64	140.3	174	209	8840.04	15573.3	19258.5	23172.36
7	1218	134.8	232.8	296	339	164186.4	283550.4	360528	412585.32
8	798	207.1	366.6	445	510	165265.8	292546.8	355110	407067.78
9	96	292.8	516.2	653	726	28108.8	49555.2	62649.6	69657.6
10	681	403.4	680.8	877	991	274715.4	463624.8	597237	674871
11	402	508.1	854.8	1122	1275	204256.2	343629.6	451044	512533.92
12	448	554.8	952.4	1338	1549	248550.4	426675.2	599334.4	694144.64
13	28	613.2	1000	1469	1729	17169.6	28000	41126.4	48422.64
14	374	600	1000	1522	1817	224400	374000	569190.6	679617.84
15	127	600	1000	1540	1847	76200	127000	195567.3	234617.26
16	92	600	1000	1541	1866	55200	92000	141772	171647.16
17	31	600	1000	1541	1867	18600	31000	47783.4	57885.37
18	43	600	1000	1540	1867	25800	43000	66220	80278.85
19	26	600	1000	1539	1866	15600	26000	40014	48524.32
20	24	600	1000	1500	1800	14400	24000	36000	43200
21	9	600	1000	1500	1800	5400	9000	13500	16200
22	0	600	1000	1500	1800	0	0	0	0
23	0	600	1000	1500	1800	0	0	0	0
24	0	600	1000	1500	1800	0	0	0	0
25	0	600	1000	1500	1800	0	0	0	0
<b>Total:</b>						<b>1,612,257</b>	<b>2,748,498</b>	<b>3,735,312</b>	<b>4,384,592</b>

Table C-36 Wind energy output from single Enercon WECSs using wind data at 80metres for Yanbo

WS (m/s)	Frequency No. of hours	Wind power curve for wind machines (kW)				Wind energy output from single wind machine (kWh)			
		600	1000	1500	1800	600	1000	1500	1800
WECS SIZE (kW)	▶▶								
0	236	0	0	0	0	0	0	0	0
1	315	0	0	0	0	0	0	0	0
2	274	0	0	0	0	0	0	0	0
3	1236	1.7	2.6	1.8	15.3	2101.2	3213.6	2224.8	18960.24
4	995	14.74	25.6	30.1	51.8	14666.3	25472	29949.5	51560.9
5	139	40.8	75.8	89.3	117	5671.2	10536.2	12412.7	16229.64
6	1168	79.64	140.3	174	209	93019.52	163870.4	202648	243831.68
7	1130	134.8	232.8	296	339	152324	263064	334480	382776.2
8	887	207.1	366.6	445	510	183697.7	325174.2	394715	452467.57
9	96	292.8	516.2	653	726	28108.8	49555.2	62649.6	69657.6
10	681	403.4	680.8	877	991	274715.4	463624.8	597237	674871
11	402	508.1	854.8	1122	1275	204256.2	343629.6	451044	512533.92
12	448	554.8	952.4	1338	1549	248550.4	426675.2	599334.4	694144.64
13	28	613.2	1000	1469	1729	17169.6	28000	41126.4	48422.64
14	352	600	1000	1522	1817	211200	352000	535708.8	639640.32
15	149	600	1000	1540	1847	89400	149000	229445.1	275259.62
16	17	600	1000	1541	1866	10200	17000	26197	31717.41
17	105	600	1000	1541	1867	63000	105000	161847	196063.35
18	36	600	1000	1540	1867	21600	36000	55440	67210.2
19	33	600	1000	1539	1866	19800	33000	50787	61588.56
20	4	600	1000	1500	1800	2400	4000	6000	7200
21	29	600	1000	1500	1800	17400	29000	43500	52200
22	0	600	1000	1500	1800	0	0	0	0
23	0	600	1000	1500	1800	0	0	0	0
24	0	600	1000	1500	1800	0	0	0	0
25	0	600	1000	1500	1800	0	0	0	0
<b>Total:</b>						<b>1,659,280</b>	<b>2,827,815</b>	<b>3,836,746</b>	<b>4,496,335</b>